Synthetic, architectural and bonding aspects of carboranyl assemblies.

Lynne Ahfeld Boyd

Synthetic, Architectural and Bonding Aspects of Carboranyl Assemblies

by

Lynn Ahlfeld Boyd, B.Sc.

Graduate Society, University of Durham

A thesis submitted in part fulfilment of the requirements for the degree of Doctor of Philosophy at the University of Durham

October 1997

to my family

Declaration

The work described in this thesis was carried out at the University of Durham between October 1994 and September 1997. All the work is my own, unless stated to the contrary, and it has not been submitted previously for a degree at this or any other university.

Statement Of Copyright

Financial Support

The University of Durham is gratefully acknowledged for providing a studentship for the work described herein.

Abstract

Synthetic, Architectural and Bonding Aspects of Carboranyl Assemblies

This thesis describes the syntheses, structures, bonding characteristics and degradation reactions of carborane containing compounds. Systems containing one, two and three carborane units are considered.

Chapter One outlines the general chemistry of icosahedral carborane compounds, reviewing their contributions to bonding theory and highlighting their specific properties and potential applications.

Chapter Two describes the syntheses of one cage carborane derivatives. Of specific interest are *closo*-derivatives of general formula $RCB_{10}H_{10}CX$ (X=OH, F, CO_2H, CO_2^-), which have the potential to form an *exo*-π bond (a multiple bond between the cage carbon atom and the X substituent). General synthetic techniques are explored with regard to hydroxy, carboxy, halo and heteroaryl derivatives. New and novel routes to fluorinated and sulfonylated carboranes are also discussed.

Chapter Three discusses how substitution at the carboranyl cage carbon atoms affects the bonding characteristics of the derivative. NMR spectroscopic and X-ray crystallographic data are used to illustrate *exo*-π bonding, with particular reference to carboranes of general formula $RCB_{10}H_{10}CX$, (X=OH, F, CO_2H, CO_2^-). Hydrogen bonding interactions within one-cage systems containing a pyridyl or thiophenyl group, are also investigated, with reference to IR spectroscopic and X-ray crystal diffraction studies.

Chapter Four examines the chemistry of multi-carboranyl assemblies, with particular reference to 2,4,6-tri-(carboranyl)-1,3,5-triazines. The synthesis of these derivatives is shown to be more facile than for the 1,3,5-tri-(carboranyl)-benzene analogues. X-ray powder and crystal diffraction studies illustrate the structural similarities between the triazine derivatives and their benzene counterparts. The relative chemical and thermal stabilities of the 2,4,6-tri-(carboranyl)-1,3,5-triazines are also discussed.

Chapter Five examines the deboronation reactions of one and three-cage carborane derivatives. Fluoride ion deboronation reactions of one cage systems containing heteroaryl substituents are discussed. In 1,7-di-(2'-thiophenyl)- and 1,7-di-(3'-pyridyl)-*meta*-carboranes cage B-F fluorination is observed. Degradation by standard deboronation methods of the 2,4,6-tri-(*ortho*, *meta* and *para*-carboranyl)-1,3,5-triazines discussed in Chapter Four is also discussed.

Lynn Ahlfeld Boyd (October 1997)

Acknowledgements

Firstly I would like to thank my supervisor, Professor Ken Wade, for all his advice and support during the course of my PhD. I am also very grateful to Hugh MacBride and Mark Fox for their advice and many helpful discussions throughout my project.

All the support staff at Durham are gratefully acknowledged for their help, particularly Ian McKeag, Alan Kenwright and Julia Say of the NMR service. Thanks must also go to Dave Apperley of the Mountjoy Research Centre, Durham for solid state NMR spectra and to Simon Hutton for XPS measurements. I would also like to express my thanks to Angus MacKinnon, Roy Copley, Vanessa Hoy, Judith Howard and Bill Clegg of the crystallography departments at Durham and Newcastle Universities for all the X-ray data and pretty pictures, and to Christian Lehmann for X-ray powder diffraction data.

A big thank you goes to all members of the Wade group and the "inorganic posse and hangers on", namely Andy J, Andy K, Tom, Brian, Patrick, Marky, Simon P, Simon C, Nikki, Graham, Pete, Dave, Rob, Sarah M, Sarah L, Richard Peace, Richard Price, Leela, Mark, Hugh, Wendy and the ex-Lab 19 boys for keeping me sane and making the last three years in Durham so enjoyable.

Finally, I would like to thank Robin for all his love and encouragement, and my family for their continued love and support throughout my student years.

Abbreviations

IR	Infrared Spectroscopy
	Band intensity : s - strong, m - medium, w - weak, br. - broad
m.p.	melting point
b.p.	boiling point
NMR	Nuclear Magnetic Resonance Spectroscopy
	Multiplicity : m - multiplet, s - singlet, d - doublet, t - triplet, tt - triplet of triplets *etc.*, br. -broad
COSY	Correlation Spectroscopy
UV	Ultraviolet Spectroscopy
m/z	mass/charge ratio (mass spectroscopy)
EI^+	Electron Ionisation
CI^+/CI^-	Chemical Ionisation
FAB	Fast Atom Bombardment
TLC	Thin Layer Chromatography
Prep. TLC	Preparative Thin Layer Chromatography
GC	Gas Chromatography
GCMS	Gas Chromatographic Mass Spectroscopy
XPD	X-ray Powder Diffraction
XPS	X-ray Photoelectron Spectroscopy
ortho-carborane	1,2-dicarbadodecaborane, *o*-$HCB_{10}H_{10}CH$
meta-carborane	1,7-dicarbadodecaborane, *m*-$HCB_{10}H_{10}CH$
para-carborane	1,12-dicarbadodecaborane, *p*-$HCB_{10}H_{10}CH$
NFBS	*N*-fluorobenzenesulfonimide
F-TEDA	1-(chloromethyl)-4-fluoro-1,4diazoniabicyclo[2.2.2]octanebis(tetrafluoroborate)
pyF^+	1-fluoro-2,6-dichloro-pyridinium as the tetrafluoroborate salt
DME	Dimethylethoxyether, monoglyme
Ether	Diethyl ether
THF	Tetrahydrofuran
Proton Sponge	1,8-N,N,N',N'-tetramethylnapthalenediamine
VSEPR	Valence Shell Electron Pair Repulsion
e.d.	electron density
NLO	Non-linear optics
BNCT	Boron Neutron Capture Therapy

Table of Contents

Appendices

Chapter One

Carboranes - A General Introduction

1.1 INTRODUCTION

Cluster compounds of the main group elements have long been the subject of study for those interested in meeting the challenges set by electronically diverse compounds. Clusters are of many types, from homonuclear charged or uncharged species such as Zintl ions (e.g. Sn_5^{2-}), buckminsterfullerenes (e.g. C_{60}), or phosphorus (P_4), to heteroatomic species like the boron hydrides (e.g. $B_6H_6^{2-}$), where a central core of boron atoms is surrounded by bound hydrogen atoms. Many cluster compounds are electron deficient species, and the study of such compounds has led to the advancement of bonding theories and to the discovery of novel molecular architectures.

The cluster compounds of interest in this thesis are the icosahedral carboranes, $C_2B_{10}H_{12}$, and their derivatives. This chapter will give an overview of the interesting peculiarities of this group of compounds, discussing their history and what has led to the development of the field of study, and the rationalisation of their structures. Their properties and some applications are also reviewed.[1]

1.2 STRUCTURE AND BONDING IN BORON HYDRIDES AND CARBORANES - AN OVERVIEW

a) Cluster Bonding

Between 1912 and 1936, Stock made and isolated many boron hydrides, including those of formulae B_2H_6, B_4H_{10}, B_5H_9, B_5H_{11}, B_6H_{10} and $B_{10}H_{14}$.[2] Although he knew the molecular formulae of these compounds, the structures were unknown. Later, Longuet-Higgins deduced the structure of diborane[3] and through the concept of three-centre-two-electron (3c2e) bonds, the bonding of diborane, B_2H_6, could be rationalised. In diborane each boron atom donates two of its three electrons to form two σ bonds with its attached protons. This leaves each boron with two orbitals and one electron. The two borons and two bridging hydrogen atoms use four electrons (one from each boron, one from each hydrogen) and six orbitals (two from each boron, one from each hydrogen) to form two three-centre-two-electron bonds.

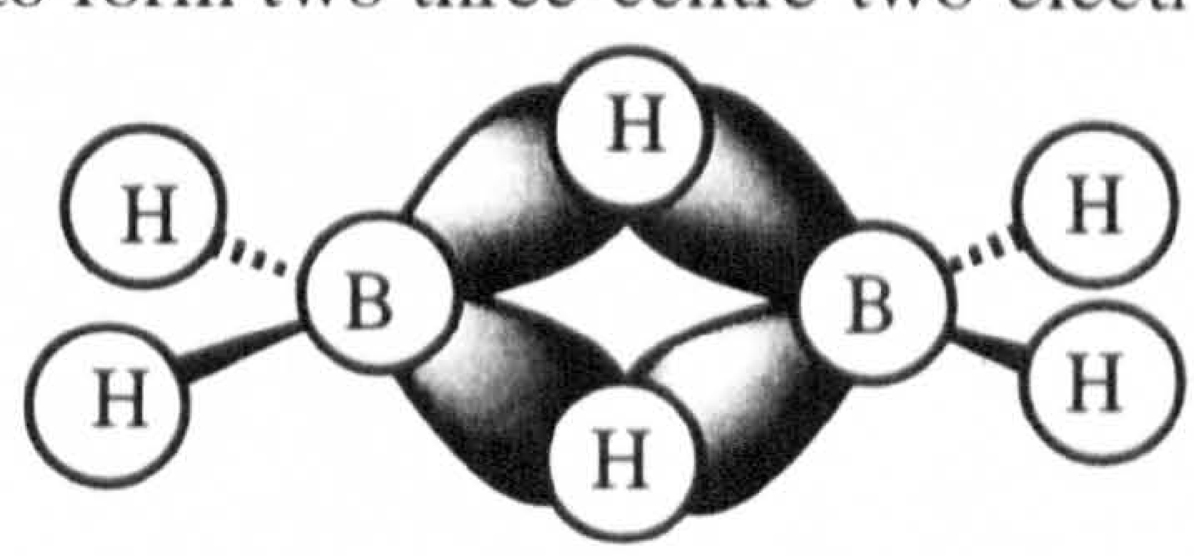

figure 1.1: bonding in diborane

An extension of this theory led to the development of "styx" rules by W.N. Lipscomb, which could be used to rationalise the bonding of cluster boron hydrides.[4]

Each styx solution gave a unique "code" to describe the number and type of each bond present in the structure; *s* being the number of B-H-B bonds, *t* referring to three-centre BBB bonds, *y* to 2c2e B-B bonds and *x* to the number of extra terminal hydrogen atoms, usually in the form of BH_2 groups. The structures rationalised by these rules had been confirmed by X-ray crystallographic studies by Lipscomb for many of the larger boron hydrides including compounds such as decaborane, $B_{10}H_{14}$.[5] With many clusters, however, so many possible combinations of 3c2e BHB and BBB and 2c2e BH and BB bonds exist (e.g. figure 1.2), that localised bonding descriptions are of limited value. A molecular orbital approach may be used instead.[6,7]

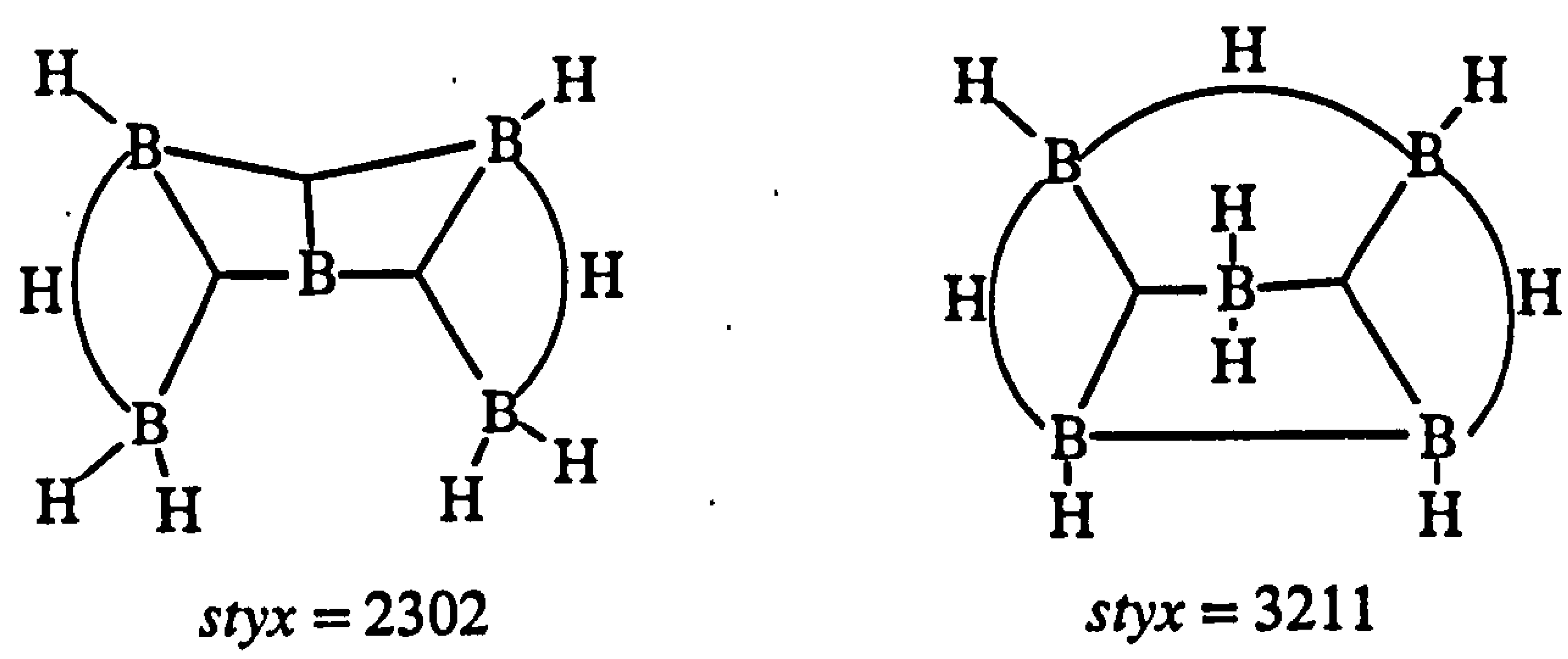

figure 1.2: possible solutions to the bonding in B_5H_9

As more structures of the boron hydrides were elucidated, it became apparent that the boron hydrides (and carboranes) were deltahedral fragments, originating from a closed deltahedral (i.e. all the faces are triangular) parent compound. For example, the *arachno* species, decaborane, $B_{10}H_{14}^{2-}$, can be viewed as a fragment of *nido*-$B_{11}H_{13}^{2-}$, which is in turn a fragment of the parent deltahedral icosahedron dodecaborane, *closo*-$B_{12}H_{12}^{2-}$. A pattern was acknowledged to exist between the classes of cluster fragments, namely *closo* (cage-like), *nido* (nest-like), *arachno* (web-like) and *hypho* (net-like), and a consideration of the electrons within these species related the skeletal structures to the number of skeletal electron pairs the compound contained.

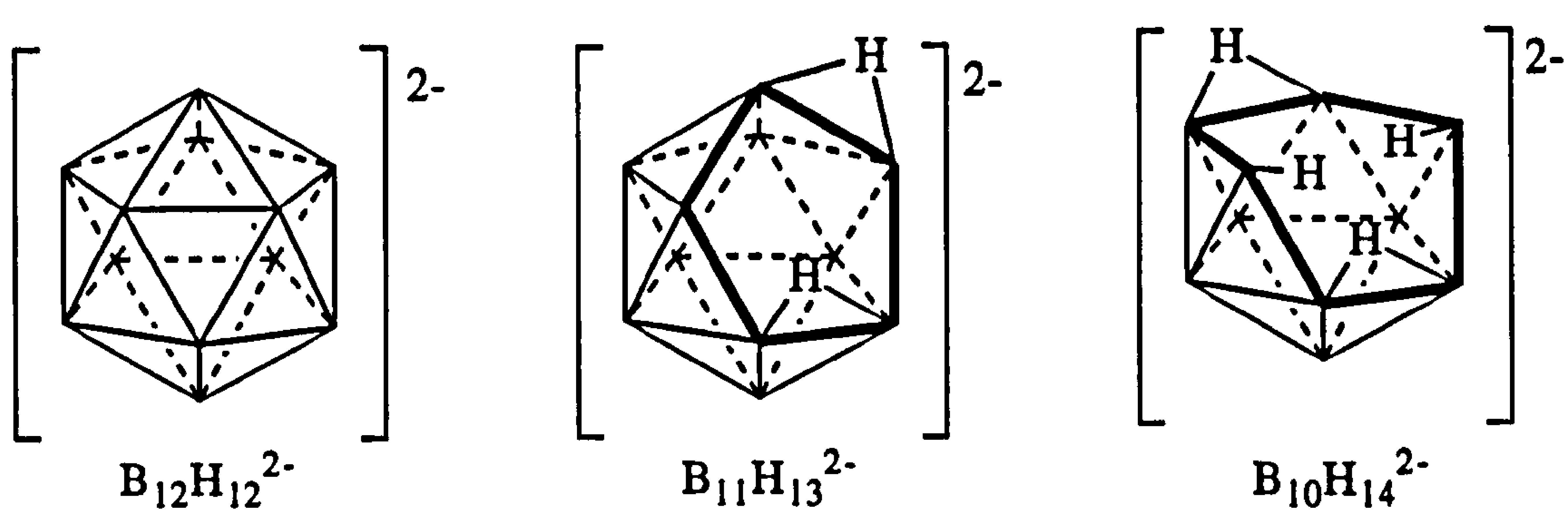

figure1.3: closo, nido and arachno boranes formed by successive removal of an icosahedral vertex

The icosahedral carboranes, $C_2B_{10}H_{12}$, with which this thesis is concerned are formally derived from the icosahedral dodecaborate anionic species, $B_{12}H_{12}^{2-}$. The bonding in both compounds, and indeed in many heteroboranes, can be treated in the same manner due to the isoelectronic relationship between $\{BH^-\}$ and $\{CH\}$ units.

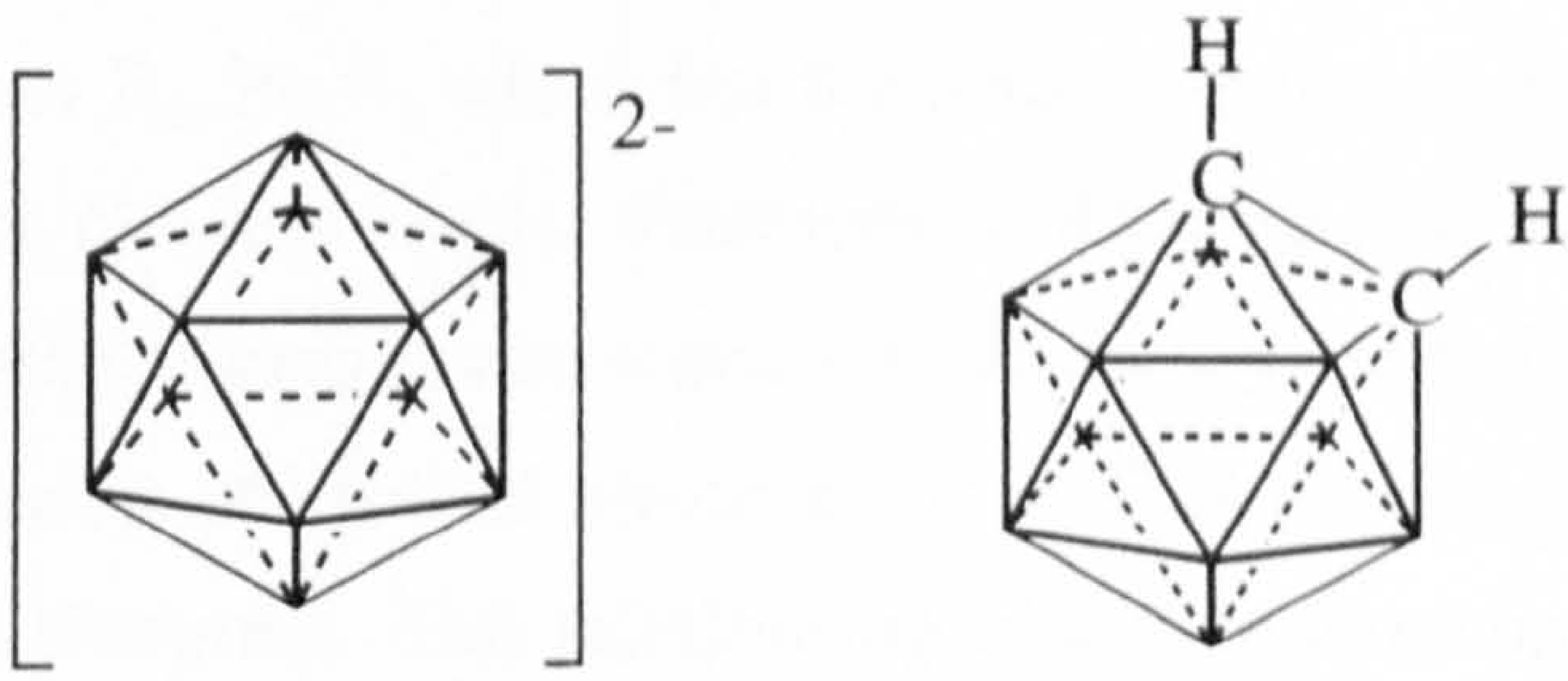

$B_{12}H_{12}^{2-}$ $C_2B_{10}H_{12}$

figure 1.4: dodecaborate anion and icosahedral dicarbadodecaborane are electronically equivalent (isoelectronic)

Each carbon and boron atom of the "C_2B_{10}" cluster contains one *s* and three *p* orbitals. To bond the protons to the cluster, a hybrid sp_z orbital, radial to each core atom on the cage surface, donates one electron to form a σ bond. The remaining 24 *p* (p_x,p_y) orbitals which lie tangential to the cage surface are available for cluster bonding together with the inward facing sp_z hybrid orbital.

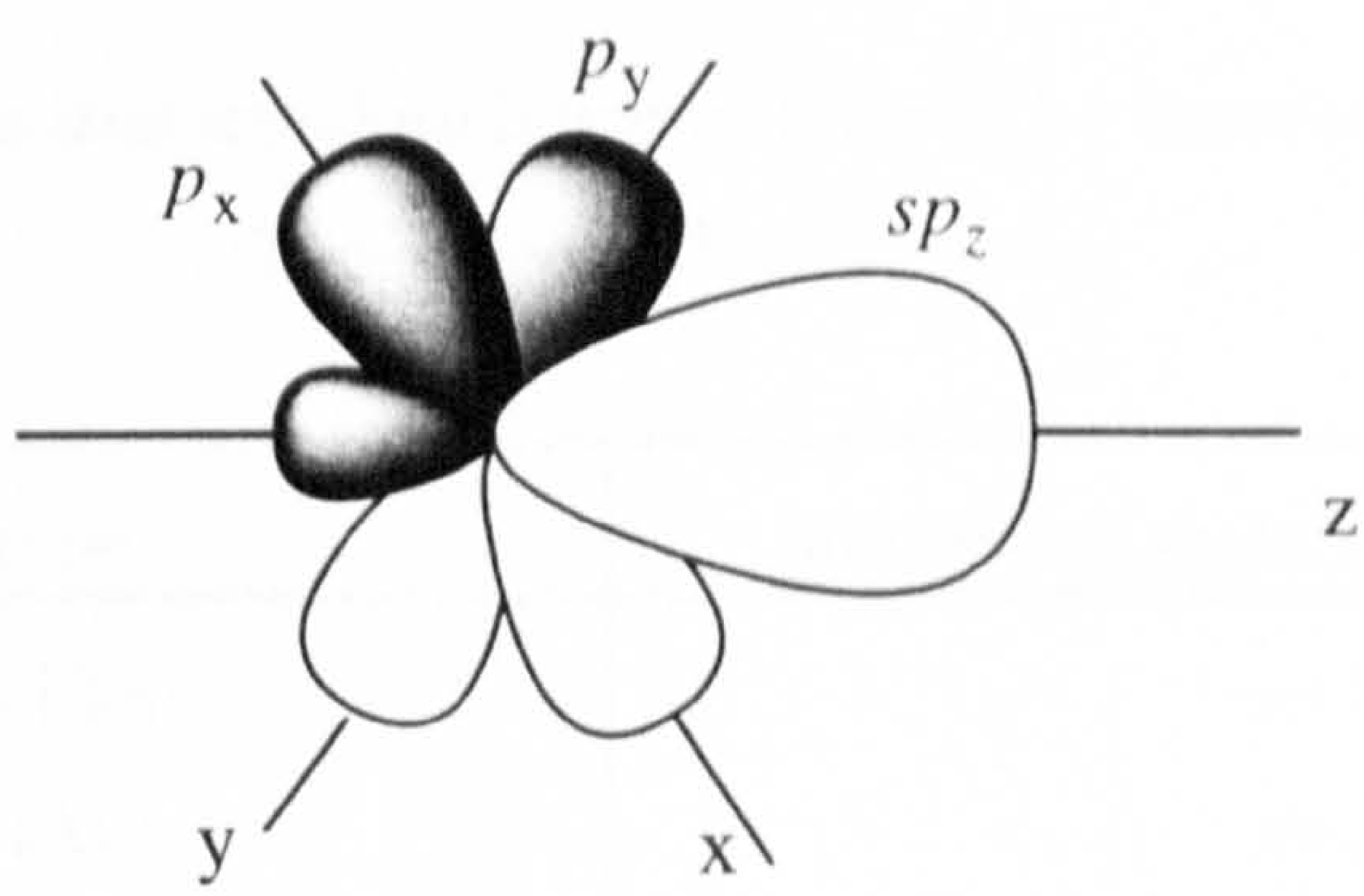

figure 1.5: orbital hybridisation at each icosahedral vertex

For skeletal bonding of the icosahedron, each boron atom can donate two electrons and each carbon, three electrons. Including any charge on the compound, this equates to a total of 26 electrons (13 pairs) which can contribute to binding the 12 vertex *closo* $B_{12}H_{12}^{2-}$ or $C_2B_{10}H_{12}$ cage together through 13 bonding molecular orbitals. For the 12 vertex icosahedron there are always 13 bonding molecular orbitals, although their symmetry and degeneracies are dependant upon the symmetry of the compound.

This relationship holds true for all n vertex polyhedra; the atoms of a closed cluster are assumed to occupy the vertices of an n vertex deltahedron and supply $(n + 1)$ pairs of skeletal electrons to the $(n + 1)$ skeletal bonding orbitals.[6] If each open cage structure is treated as a fragment of the *closo* $B_mH_m^{2-}$ (or *closo*-$C_aB_mH_{m+2}$ (a=0-2)), removal of a $\{BH^{2+}\}$ unit (or $\{CH^+\}$ unit) from the parent compound leaves a compound of formula $B_mH_m^{4-}$, which has the same number of bonding electron pairs and as the parent, but one less vertex. Protonation of this species with a combination of *exo*, *endo* and bridging hydrogens converts it to $B_mH_{m+2}^{2-}$ (*c.f.* figure 1.3), which still retains the same number of skeletal electron pairs. This gives a *nido* n vertex residue with $(n + 2)$ pairs of electrons. This relationship applies to more open structures as well and is summarised for carboranes in table 1.1.

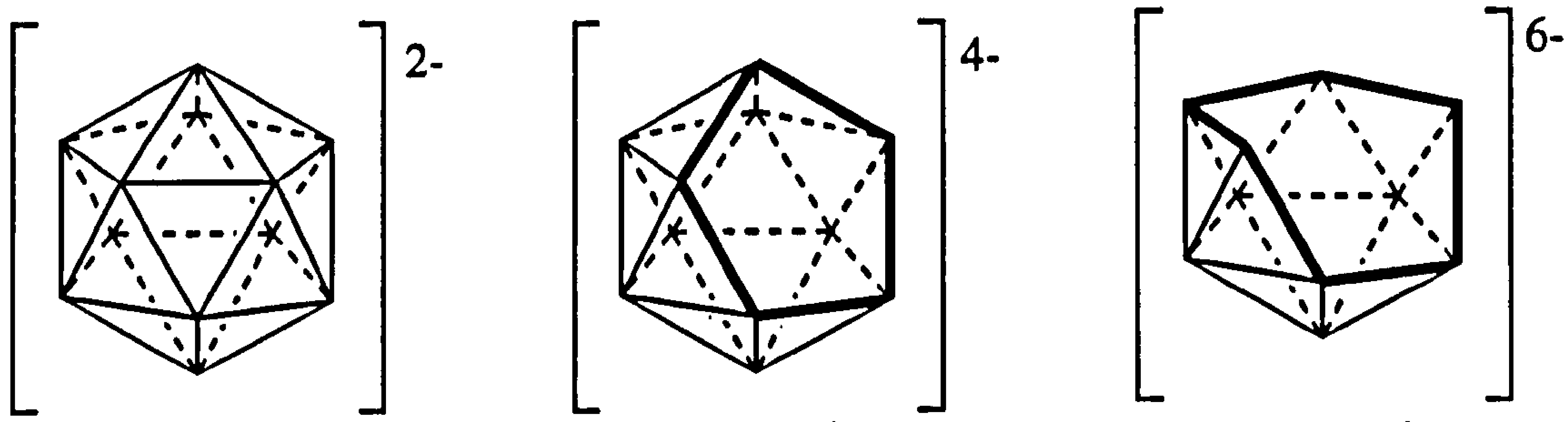

$B_{12}H_{12}^{2-}$	$B_{11}H_{11}^{4-}$	$B_{10}H_{10}^{6-}$
26 skeletal electrons	26 skeletal electrons	26 skeletal electrons
13 electron pairs	13 electron pairs	13 electron pairs

figure1.6: closo, nido and arachno boranes formed by successive removal of BH^{2+} from an icosahedral vertex

structure type	number of skeletal electron pairs
closo (cage-like)	n+1
nido (nest-like)	n+2
arachno (web-like)	n+3
hypho (net-like)	n+4

table 1.1: relationship between skeletal electron pairs and cage geometry in carboranes[6]

b) Electronic Distribution

In the closed polyhedral structures, the electrons populate the skeletal bonding orbitals, effectively forming a pseudo-spherical distribution of electron density over the atoms which define the twelve vertex icosahedron (figure 1.5).

In the icosahedral $B_{12}H_{12}^{2-}$ unit, electron density can be assumed to be relatively evenly spread over the deltahedral surface. However, when heteroatoms, such as carbon, are incorporated into the cage structure, the electron distribution is altered. The protons attached to the carbon sites of the carborane are more electropositive than the boron-attached protons. It is for this reason that when a metallating reagent is introduced to the parent carborane system, $C_2B_{10}H_{12}$, the protons of the carbon atoms, being the most acidic, are metallated preferentially. Following this reasoning, the boron atom of the BH vertex most highly connected to a CR (R=H, alkyl or aryl) vertex is the most electropositive boron, and this explains its preferential removal by a strong nucleophile during deboronation reactions. These features will be discussed further in later chapters.

The twelve vertex "B_{12}" icosahedron has maximum symmetry (I_h), however, as the icosahedron is altered to incorporate heteroatoms, two carbons in the case of the icosahedral carboranes, $C_2B_{10}H_{12}$, the cage symmetry is reduced. The differing electronegativities of the cluster atoms, leads to distortions in the cage geometry as a result of redistribution of electron density. As the carbons are further substituted, more distortions arise, the nature of which is dependent upon the substituent. As well as theoretical studies, such as ab initio and IGLO calculations[8], X-ray crystallographic studies quantify these distortions, and nuclear magnetic resonance spectroscopy also aids the analysis of such changes.[9]

1.3 NOMENCLATURE[10]

The principal systems which will be discussed in this thesis are the 12-vertex-*closo* and the 11-vertex-*nido* species. In altering the cage type, the cage numbering scheme also changes. The degree of cage opening is described by a prefix *closo, nido, arachno* or *hypho* as in table 1.1. In the borane and carborane structures, an apical atom is labelled atom 1. Successive belts of cage atoms are numbered in a clockwise manner, with carbon atoms having priority over boron vertices.

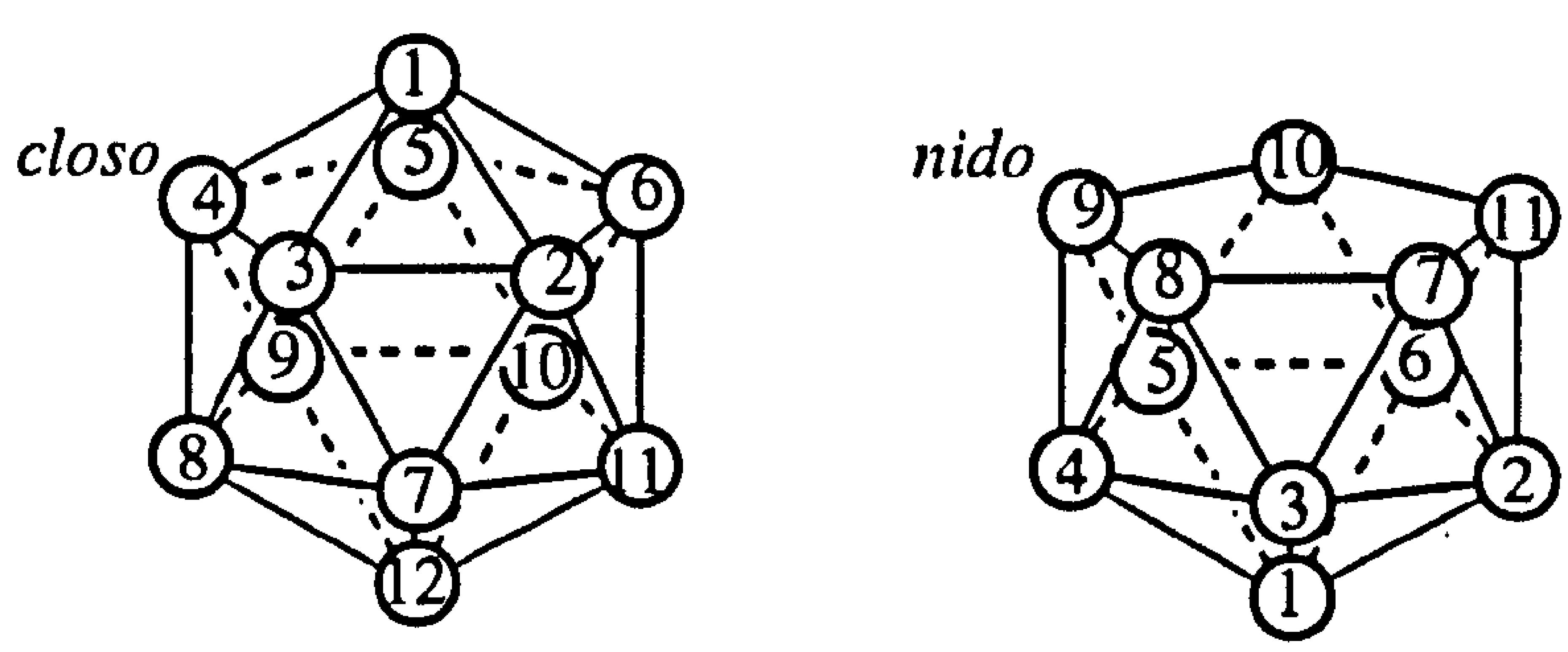

figure 1.7: cage numbering scheme for closo and nido cage systems

1.4 PROPERTIES AND APPLICATIONS[11]

Neutral carboranes containing two carbon atoms are derived from the polyhedral boron hydride species, $B_nH_n^{2-}$, and have the general formula $C_2B_nH_{(n+2)}$ (n=5-12). The carborane of interest in this thesis is dicarbadodecaborane, $C_2B_{10}H_{12}$, (and derivatives thereof) which exists as an icosahedron with twenty deltahedral faces. Three isomers are possible and all are known. These are 1,2-, 1,7- and 1,12-dicarbadodecaborane or *ortho*-, *meta*- and *para*-carborane respectively. In figure 1.8, the connectivities which would illustrate a two-centre two-electron bond in a "normal" compound, are not indicative of a formal bond. They simply illustrate the shape and connectivities within the cluster. Unmarked vertices represent a BH group.

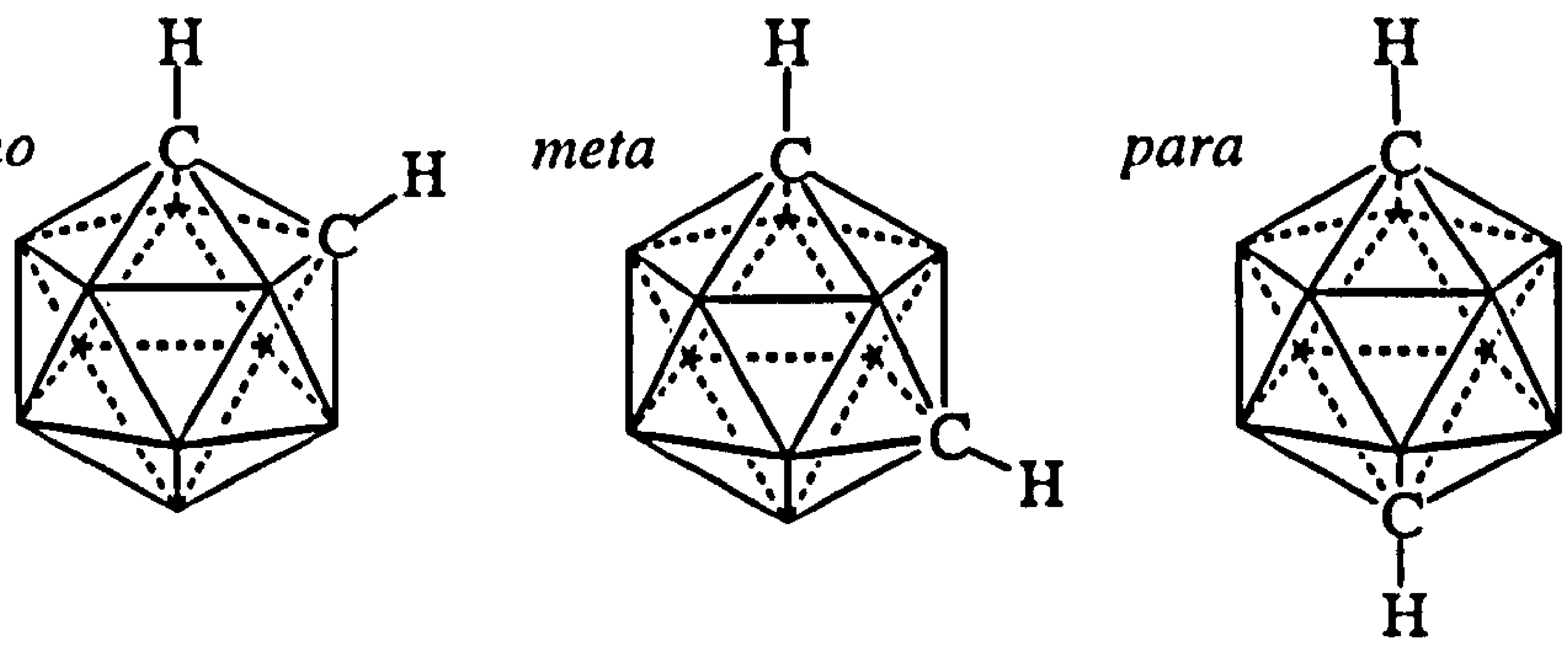

figure 1.8: ortho-, meta- and para-carborane

The discovery that the boron hydrides produced a lot of energy when burned, led to their investigation as rocket fuels during the 1960's. Decaborane, $B_{10}H_{14}$, was produced on a multi-ton scale for this purpose. As will be discussed further in Chapter Two, the icosahedral carboranes $C_2B_{10}H_{12}$ are readily accessible from decaborane.

The carboranes can undergo substitution reactions at cage carbon and boron sites without cage degradation occurring, however the predominant feature of the carboranes is their remarkable chemical and thermal stability. *Ortho*-carborane is stable up to *c*.400°C and remains intact in the presence of oxidising agents, alcohols and strong acids. Above *c*.400°C however, isomerisation can occur to the *meta* and then *para*-isomer. The *ortho*- to *meta*- transformation is quantitative (460°C), but isomerisation to *para*-carborane (620°C) is not very efficient. Various mechanisms have been postulated for the rearrangement.[12] The diamond-square-diamond mechanism (scheme 1.1) can explain the isomerisation *ortho* to *meta*-carborane but cannot be used for isomerisation to *para*. Alternative mechanistic rearrangements include rotation of a triangular face and rotation of two pentagonal faces (figure 1.9). Both these methods explain both isomerisations in the icosahedral carborane. The driving force for the isomerisation is proposed to be the reduction in the overall dipole of the carborane upon increased separation of the carbon atoms.

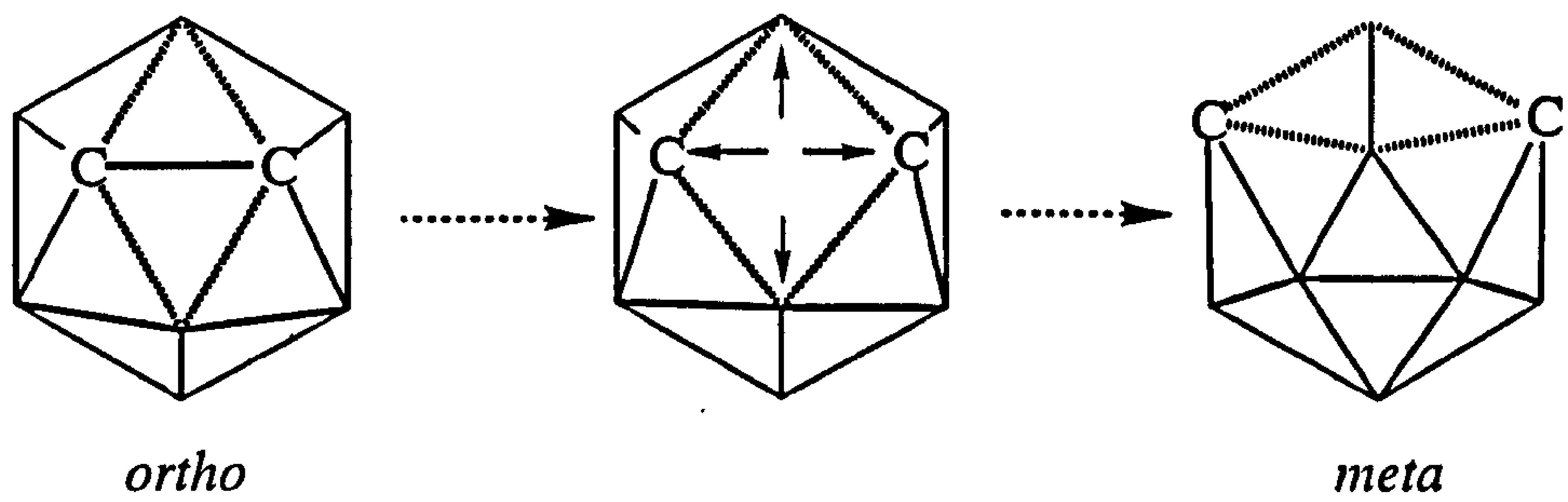

scheme 1.1: thermal isomerisation of ortho- to meta-carborane via a diamond-square-diamond mechanism

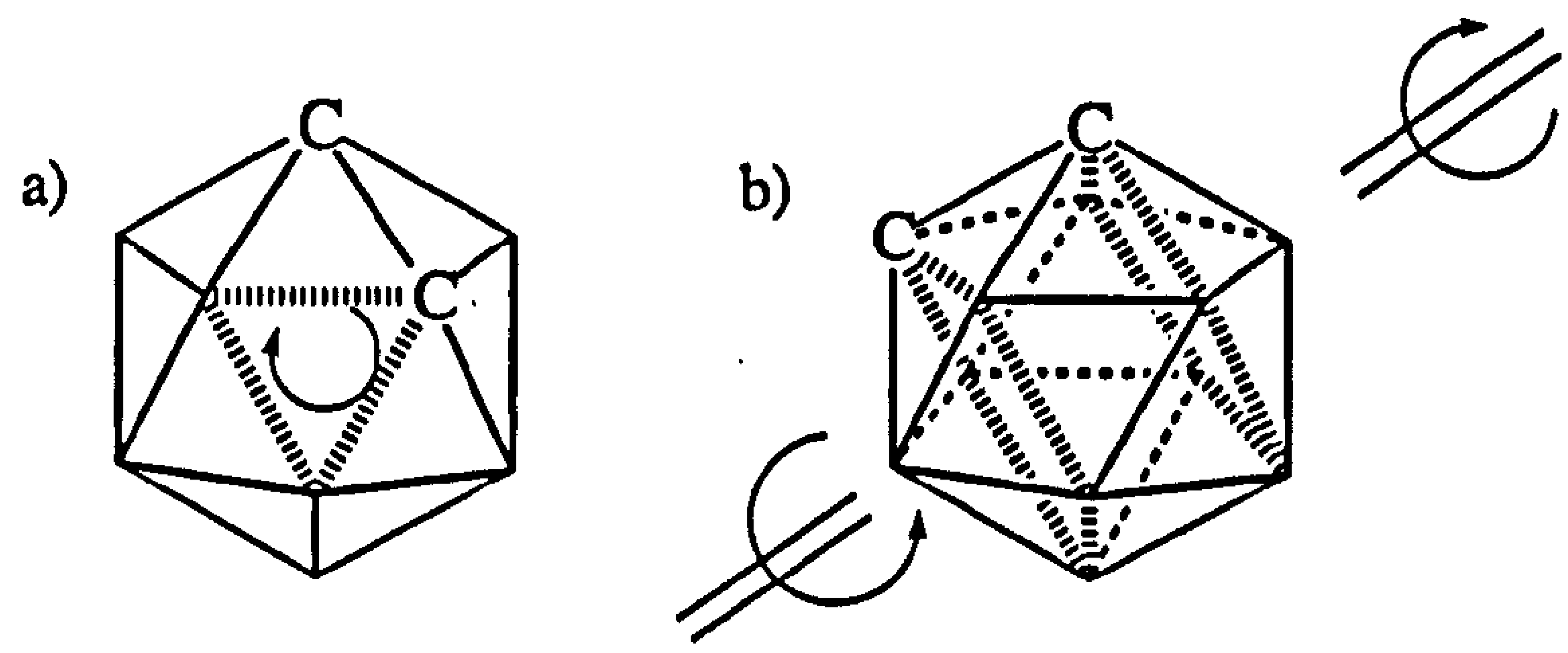

figure 1.9: isomerisation through triangular face rotation and by rotation of a pentagonal pyramid

Reverse isomerisation from *meta* to *ortho*-carborane has also been achieved by isomerisation of the *meta*-carboranyl dianion, followed by oxidation of the *ortho*-carborane dianion to the neutral *closo* species.[13]

The carborane cage has a strong electron withdrawing effect and tends to withdraw any available electron density into its delocalised electronic system. This electron-withdrawing effect decreases as the isomers are progressed from *ortho* through to *para*, in both *closo* and *nido* species.

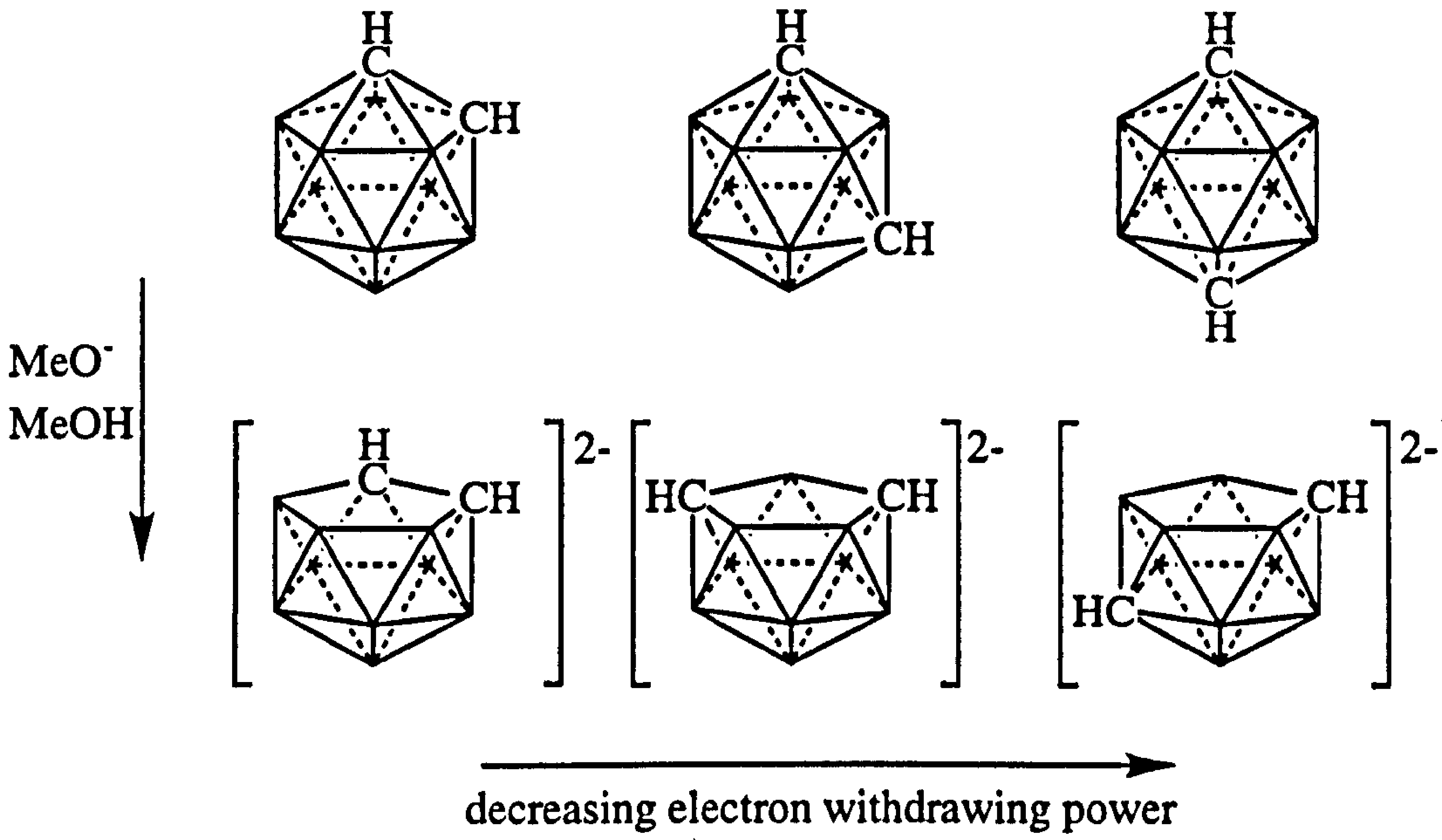

figure 1.10: relative electron withdrawing potential of unsubstituted closo and nido carboranes

The electron withdrawing power of the *ortho*-carboranyl moiety is considerably greater than that of its aryl counterparts. This is illustrated by a comparison of pK_a values (figure 1.11). The same is true of the *meta* and *para* isomers.

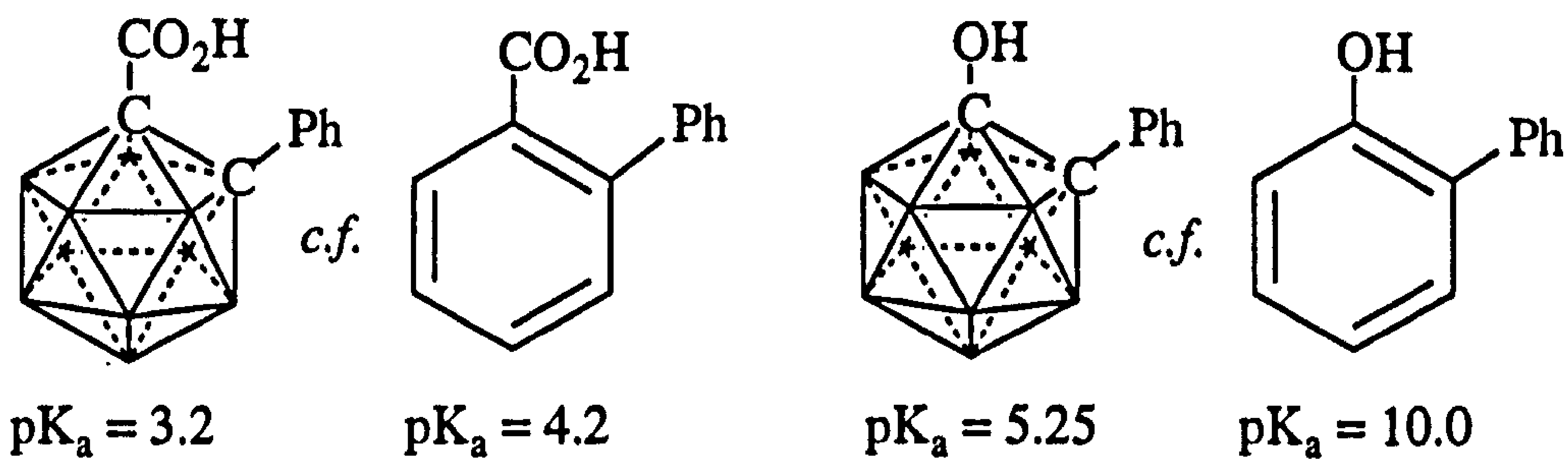

figure 1.11: comparison of pK_a values between aryl and carboranyl systems

The chemical and thermal stability associated with carboranes has led to their incorporation into polymeric[14], macrocyclic[15] and dendritic[16] species. The field of carboranyl polymers has been the most widely explored, leading to the synthesis of polymers (primarily incorporating *meta* and *para*-carboranyl units for geometric considerations) which are stable to diverse chemical environments, to elevated temperatures and which are of high strength. Although the "Dexsils", polymers in which carborane polyhedra are linked through short siloxy $(R_2SiO)_n$ chains, have found commercial application[17], many of these multi-carboranyl assemblies have yet to find practical application, as adequate properties are often achievable by organic systems at lower cost.

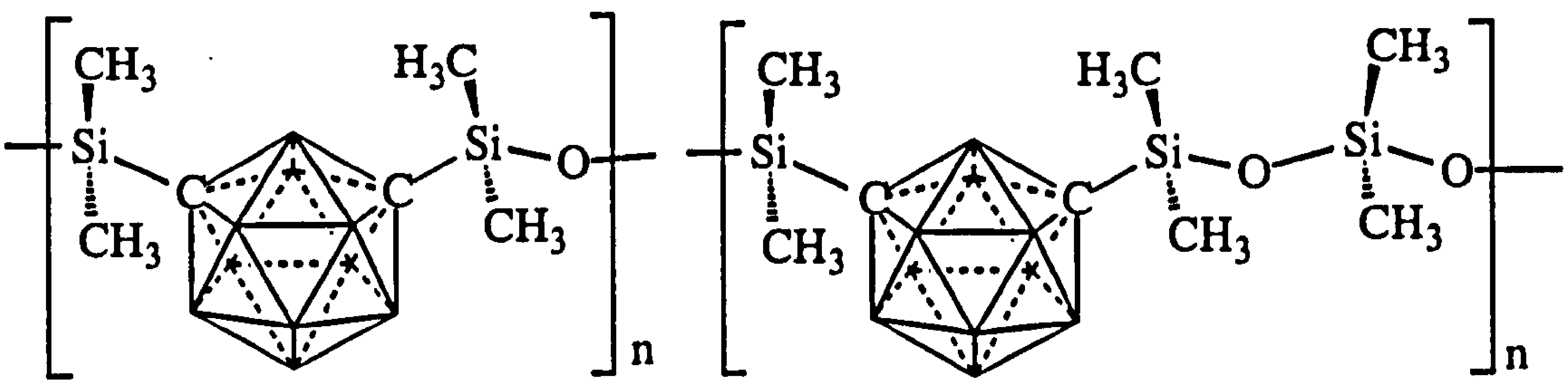

Dexsil 100 crystalline polymer   Dexsil 200 elastomer

figure 1.12: carborane containing polymers

Pyrolysis of carborane (or boron) containing polymers can lead to the formation of thermally stable coatings[18] and ceramic materials.[19] As carborane compounds contain the elements required for the formation of thin boron carbide films, they have potential as source materials for chemical vapour deposition (CVD) techniques.[20] Synchrotron radiation has been used to prepared a B_5C boron carbide/Si(III) heterojunction diode by the radiation induced decomposition of *ortho*-carborane.[21]

Boron compounds have found application in the field of medicine, as a treatment for tumours. Boron Neutron Capture Therapy (BNCT) relies upon the decay of the ${}^{10}_{5}B$ nucleus when bombarded with a neutron, to give an *in situ* dose of α radiation to the tumour. Compounds with a high boron content which are stable under physiological conditions and which have tumour targeting selectivity are required for this treatment, and much effort is being expended in this field.[22]

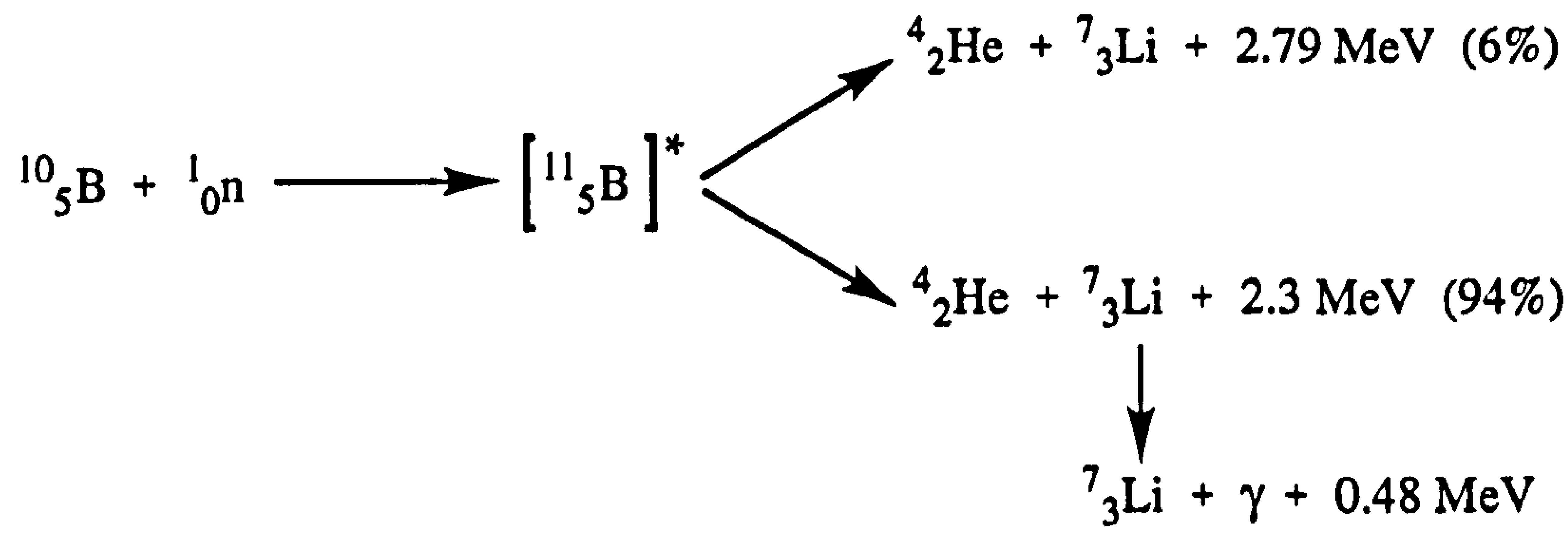

scheme 1.2: ^{10}B neutron capture process

Metallacarborane complexes have been proven to possess catalytic activity. In particular, rhodacarborane catalysts[23], prepared from the reaction of a rhodium(I) cation with a *nido*-$C_2B_9H_{12}^-$ residue, have shown activity as homogeneous hydrogenation, isomerisation and hydrosilylation catalysts.

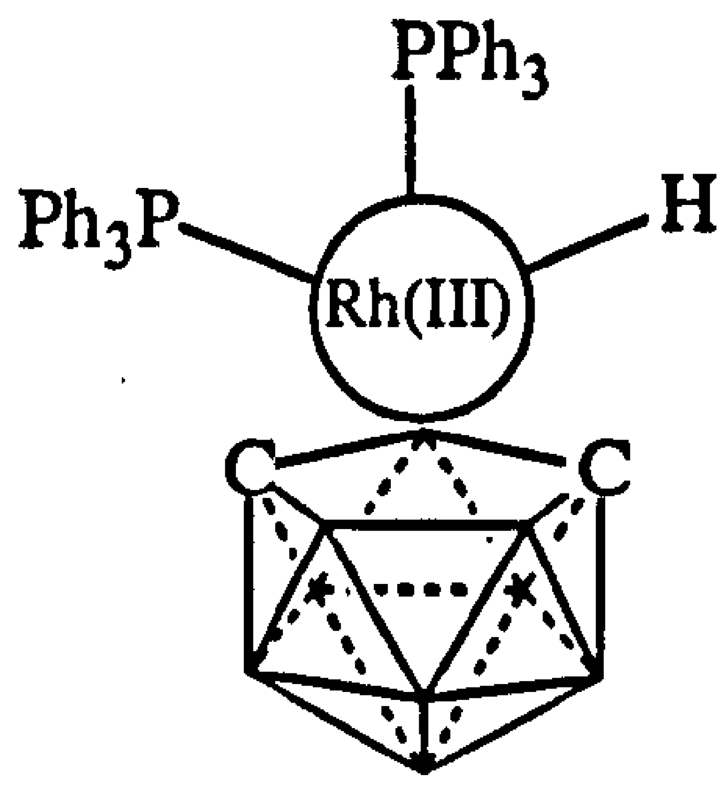

figure 1.13: rhodacarboranes have proven to be successful catalysts for specific reactions

The synthesis of compounds which have a large difference between the ground and excited state dipole moments, which are not highly coloured, and which crystallise in a non-centrosymmetric space group leads to materials which are of interest in the field of non-linear optics. *Ortho*-carborane has a ground state dipole moment of 4.45D, and derivatives of this and other carborane isomers have been investigated as potential non-linear optical materials.[24]

Unlike many salts of organic and inorganic acids, salts of polyborates dissolve readily in organic solvents. This allows their extraction from the aqueous to the organic phase. Using this principle, metallacarboranes of the type $[(C_2B_9H_{11})_2\text{-}3\text{-}M^{III})]^-$ have been used to aid the extraction of metals including radionuclides from spent nuclear fuels.

The dicarbollide anion, $[C_2B_9H_{11}]^{2-}$, is known to stabilise metals in high oxidation states by forming sandwich complexes $M(C_2B_9H_{11})_2{}^{e-}$. Salts of these anions are generally oxygen and moisture stable and so relatively easy to handle. For this reason, the dicarbollides of formula $M(C_2B_9H_{11})_2{}^{n-}$ have been investigated as charge transfer devices.[25]

1.5 AIMS AND OBJECTIVES

This chapter has outlined the general chemistry of icosahedral carborane cluster compounds, reviewing their contributions to bonding theory and highlighting their superb chemical and thermal stability. The following chapters will look in detail at specific carborane derivatives together with their chemical, bonding and structural characteristics.

Chapter Two will discuss primarily the synthesis of one cage carborane derivatives relevant to this study. In particular, aryl and heteroaryl, carboxy and hydroxy derivatives are discussed and new synthetic routes to fluorinated and sulfonylated carboranes are described.

Chapter Three will examine how substitution of a carboranyl carbon atom affects the bonding characteristics of the derivative. *Exo*-π bonding, where the *exo*-substituent donates electron density back into the carborane cage, is discussed with particular reference to carboxy, hydroxy and fluoro-carboranes. Hydrogen bonding interactions within one-cage systems substituted with a heteroaryl functionality, are also of interest.

Chapter Four will consider the chemistry of multi-carboranyl assemblies, looking at the syntheses of two and three-carborane cage assemblies. Of particular interest are the 2,4,6-tri-(carboranyl)-1,3,5-triazine derivatives and their structures and chemical and thermal stabilities are discussed.

Deboronation reactions of one and three cage carborane containing compounds are explored in Chapter Five. Deboronation by fluoride ion of one cage hetero-aryl carboranes are discussed, and cage fluorination observed in several instances. The degradation reactions of the 2,4,6-tri-(carboranyl)-1,3,5-triazine derivatives discussed in Chapter Four are also of interest in this chapter.

1.6 REFERENCES

1 For more complete reviews, see Carboranes, R.N. Grimes, Academic Press, Inc. (London) Ltd., 1970; V.I. Bregadze, Chem. Rev., 1992, **92**, 209; J. Plesek, Chem. Rev., 1992, **92**, 269

2 A. Stock, Hydrides of Boron and Silicon, Cornell Univ. Press, Ithaca, New York, 1933

3 H.C. Longuet-Higgins, J. Chem. Phys., 1949, **46**, 275

4 W.N. Lipscombe, Adv. Inorg. Chem. Radiochem., 1950, **117**, 1

5 W.N. Lipscombe, Boron Hydrides, 1965, Benjamin, New York; W.N. Lipscombe, Science, 1977, **196**, 1047

6 K. Wade, Chem. Commun., 1971, 792

7 R.E. Williams, Inorg. Chem., 1971, **10**, 210; K. Wade, Nature Physical Science, 1972, **240**, 71; D.M.P. Mingos, Nature Physical Science, 1972, **236**, 99 and **239**, 16; R.W. Rudolph, Acc. Chem. Res., 1976, **9**, 446; R.W. Rudolph, W.R. Pretzer, Inorg. Chem., 1972, **11**, 1974; K. Wade, Adv. Inorg. Chem. Radiochem., 1976, **18**, 1; R.E. Williams, Adv. Inorg. Chem. Radiochem., 1976, **18**, 67; A.J. Stone, Inorg. Chem., 1981, **20**, 563A.J. Stone, M.J. Alderton, Inorg. Chem., 1982, **21**, 2297

8 e.g. M. Diaz, J. Jaballas, J. Arias, H. Lee, T. Onak, J. Am. Chem. Soc., 1996, **118**, 4405; A.M. Mebel, O.P. Charkin, M. Bühl, P. v.R. Schleyer, Inorg. Chem., 1993, **32**, 463; T. Onak, D. Tran, J. Tseng, M. Diaz, J. Arias, S.

Herrera, J. Am. Chem. Soc., 1993, **115**, 9210; P.v.R. Schleyer, M. Bühl, U. Fleischer, W. Koch, Inorg. Chem., **29**, 153

9 F. Teixidor, C. Vinas, R.W. Rudolph, Inorg. Chem., 1986, **25**, 3339; A.R. Siedle, G.M. Bodner, A.R. Garber, D.C. Beer, L.J. Todd, Inorg. Chem., 1974, **13**, 2321; S. Hermanek, J. Plesek, V. Gregor, B. Stibr, J. Chem. Soc., Chem. Commun., 1972, 561

10 R. Adams, Inorg. Chem, 1963, **2**, 1087

11 J. Plesek, Chem. Rev., 1992, **92**, 269

12 S.-h. Wu, M. Jones Jnr., J. Am. Chem., Soc., 1989, **111**, 5373; G.M. Edvenson, D.F. Gaines, Inorg. Chem., 1990, **29**, 1210; D.J. Wales, J. Am. Chem. Soc., 1993, **115**, 1557; B.F.G. Johnson, Y.V. Roberts, E. Parsini, Inorganica Chimica Acta, 1993, **211**, 17; Y.V. Roberts, B.F.G. Johnson, J. Chem. Soc., Dalton Trans., 1994, 759

13 L.I. Zakharkin, V.N. Kalinin, L.S. Podvisotskaya, Bull. Acad. Sci. USSR, 1967, 2212

14 e.g. D.A. Brown, H.M. Colquhoun, J.A. Daniels, J.A.H. MacBride, I.R. Stephenson, K. Wade, J. Mater. Chem., 1992, **2**, 793; R.M. Harrison, T. Brotin, B.C. Noll, J. Michl, Organometallics, 1997, **16**, 3401; U. Schöberl, T.F. Magnera, R.M. Harrison, F. Fleischer, J.L. Pflug, P.F.H. Schwab, X. Meng, D. Lipiak, B.C. Noll, V.S. Allured, T. Rudalevige, S. Lee, J. Michl, J. Am. Chem. Soc., 1997, **119**, 3907; H.M. Colquhoun, D.F. Lewis, J.A. Daniels, P.L. Herbertson, J.A.H. MacBride, I.R. Stephenson, K. Wade, Polymer, 1997, **38**, 2447

15 e.g. Z. Zheng, X. Yang, C.B. Knobler, M.F. Hawthorne, J. Am. Chem. Soc., 1993, **115**, 5320; X. Yang, C.B. Knobler, M.F. Hawthorne, J. Am. Chem. Soc., 1993, **115**, 4904; M.F. Hawthorne, X. Yang, Z. Zheng, Pure and Appl. Chem., 1994, **66**, 245; W. Jiang, C.B. Knobler, M.F. Hawthorne, Inorg. Chem., 1996, **35**, 3056; W. Jiang, I.T. Chizhevsky, M.D. Mortimer, W. Chen, C.B. Knobler, S.E. Johnson, F.A. Gomez, M.F. Hawthorne, Inorg. Chem., 1996, **35**, 5417; W. Clegg, W.R. Gill, J.A.H. MacBride, K. Wade, Angew. Chem., Int. Ed. Engl., 1993, **32**, 1328; R.C. Haushalter, R.W. Rudolph, J. Amer. Chem. Soc., 1978, **100**, 4628

16 e.g. D. Armspach, M. Cattalini, E.C. Constable, C.E. Housecroft, D. Philips, Chem. Commun., 1996, 1823; G.R. Newkome, C.N. Moorefield, J.M. Keith, G.R. Baker, G.H. Escamilla, Angew. Chem., Int. Ed. Engl., 1994, **33**, 666

17 H. Schroeder, Inorg. Macromol. Rev., 1970, **1**, 45

18 S. Packirisamy, D. Schwam, M.H. Litt, J. Materials Science, 1995, **30**, 308

19 e.g. D. Bucca, T.M. Keller, J. Polymer Sci. A, Polym. Chem., 1997, **35**, 1033; L.G. Sneddon, M.G.L. Mirabelli, A.T. Lynch, P.J. Fazen, K. Su, J.S. Beck, Pure and Appl. Chem., 1991, **63**, 407

20 A.P. Hitchcock, S.G. Urquhart, A.T. Wen, A.L.D. Kilcoyne, T. Tyliszczak, E. Rühl, N. Kosugi, J.D. Bosek, J.T. Spencer, D.N. McIlroy, P.A. Dowben, J. Phys. Chem. B, 1997, **101**, 3483

21 D. Byun, S-d. Hwang, P.A. Dowben, F.K. Perkins, F.Filips, N.J. Ianno, Appl. Phys. Lett., 1994, **64**, 1968

22 e.g. W.V. Dahlhoff, J. Bruckmann, K. Angermund, C. Krüger, Liebigs Ann. Chem., 1993, 831; R.C. Reynolds, T.W. Trask, W.D. Sedwick, J. Org. Chem., 1991, **56**, 2391; M.F. Hawthorne, Pure and Appl. Chem., 1991, **63**, 327; B.F. Spielvogel, A. Sood, B.R. Shaw, I.H. Hall, Pure and Appl. Chem., 1991, **63**, 415; Y. Yamamoto, Pure and Appl. Chem., 1991, **63**, 423; J.H. Morris, Chemistry in Britain, 1991, **27**, 331

23 e.g. A.K. Saxena, N.S. Hosmane, Chem. Rev., 1993, **93**, 1081; T.E. Paxson, M.F. Hawthorne, J. Am. Chem. Soc., 1974, **96**, 4674; E.L. Hoel, M.F. Hawthorne, J. Am. Chem. Soc., 1974, **96**, 4676; L.I. Zakharkin, T.B. Agakhanova, J. Gen. Chem. USSR, 1977, **47**, 2191; L.I. Zakharkin, T.B. Agakhanova, Bull. Acad. Sci. USSR, 1978, **27**, 1900; E.S. Chandrasekaran, D.A. Thompson, R.W. Rudolph, Inorg. Chem., 1978, **17**, 760; R.T. Baker, R.E. King III, C. Knobler, C.A. O'Con, M.F. Hawthorne, J. Am. Chem. Soc., 1978, **100**, 8266; R.T. Baker, M.S. Delaney, R.E. King III, C.B. Knobler, J.A. Long, T.B. Marder, T.E. Paxson, R.G. Teller, P.E. Behnken, E.A. Mizusawa, M.F. Hawthorne, J. Am. Chem. Soc., 1984, **106**, 2965

24 e.g. D.M. Murphy, D.M.P. Mingos, J.M. Forward, J. Mater. Chem., 1993, **3**, 67; D.M. Murphy, D.M.P. Mingos, J.L. Haggitt, H.R. Powell, S.A. Westcott, T.B. Marder, N.J. Taylor, D.R. Kanis, J. Mater. Chem., 1993, **3**, 139

25 e.g. P.A. Chetcuti, W. Hofherr, A. Liégard, G. Rihs, G. Rist, Organometallics, 1995, **14**, 666

Chapter Two

Synthetic Strategies For Icosahedral Carborane Derivatisation

2.1 INTRODUCTION

Although there are many carboranes, only the chemistry of icosahedral dicarbadodecaboranes, *ortho-*, *meta-* and *para-*$C_2B_{10}H_{12}$, and their deboronated anionic fragments, dicarbaundecaborane, $C_2B_9H_{11}^{2-}$, are discussed in this thesis. This chapter deals primarily with *closo*-monocarboranyl derivatives; compounds containing two or more cages will be discussed in Chapter Four and *nido* systems in Chapter Five.

The chemistry of icosahedral carboranes has been extensively developed and an overview of this will be given in the initial part of this chapter. The main focus of the experimental work will be on systems capable of *exo*-π bonding to the carborane cage, namely hydroxide, carboxylic acid and fluorine derivatives. Pyridyl and thiophenyl derivatives are also of interest as systems which exhibit intra- and inter-molecular hydrogen bonding. A novel route to sulfonylated carboranes has also been devised.

2.2 CARBORANE DERIVATISATION - AN OVERVIEW

2.2.1 Acetylenes and Decaborane

Closo icosahedral carboranes are formed from the reaction of the *nido* species decaborane, $B_{10}H_{14}$ with a suitably derivatised acetylene.[1,2] The most simple carborane, *ortho*-carborane is produced in high yield when the decaborane adduct, $B_{10}H_{12}L_2$ (where L represents a Lewis base and is generally either CH_3CN, $(CH_3)_2S$ or $(CH_3)_2N.C_6H_5$), is reacted with acetylene gas, yielding *closo*-1,2-dicarbadodecaborane(12) as a white crystalline solid. Derivatisation of the acetylene gives easy access to many *mono-* and *di-* C-substituted *ortho*-carboranes.

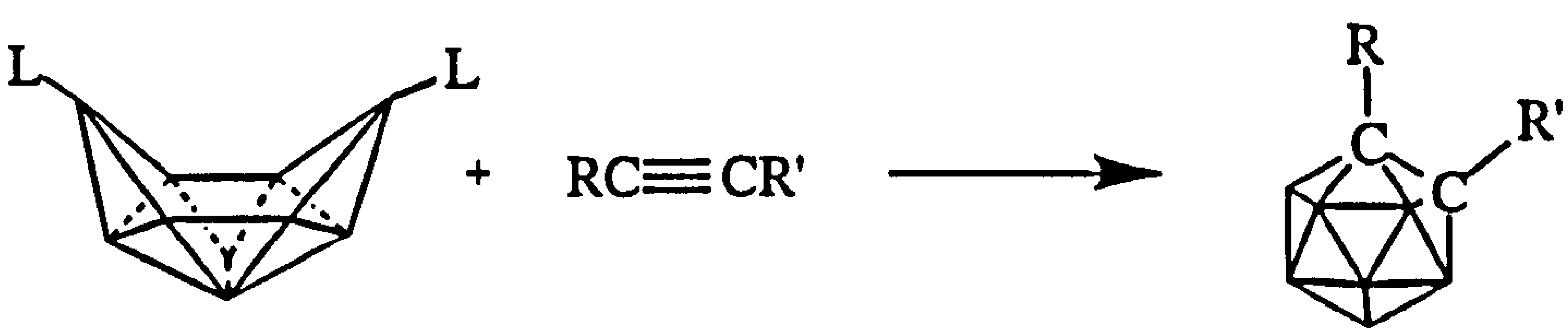

scheme 2.1: reaction of decaborane as the arachno adduct $B_{10}H_{12}L_2$ and acetylene

From these compounds, often the *meta* and occasionally the *para* isomers can be formed through thermal isomerisation[3] of the *ortho*-carboranyl starting material. There are of course limitations to this strategy in that not all functional groups can be made to form an acetylene, for example, functionalities containing a hydroxide or a carboxylic acid group. Equally, the *ortho*-carboranyl derivative from which we may wish to form the *meta-* or *para-* isomer may not be suitably stable to heat and subsequently degrade when thermal isomerisation is attempted. Alternative synthetic routes must therefore be employed.

2.2.2 Derivatisation Through Metallation

a) Alkali Metal Derivatives

As the hydrogen atoms attached to the carborane cage carbon atoms are acidic[4], they are prone to nucleophilic attack. This property allows the dilithiation of all three carborane isomers to be achieved readily by means of reagents such as butyl lithium, to produce air and moisture sensitive salts which can be further reacted with an appropriate halo-compound to give the required derivative.[2,5,6]

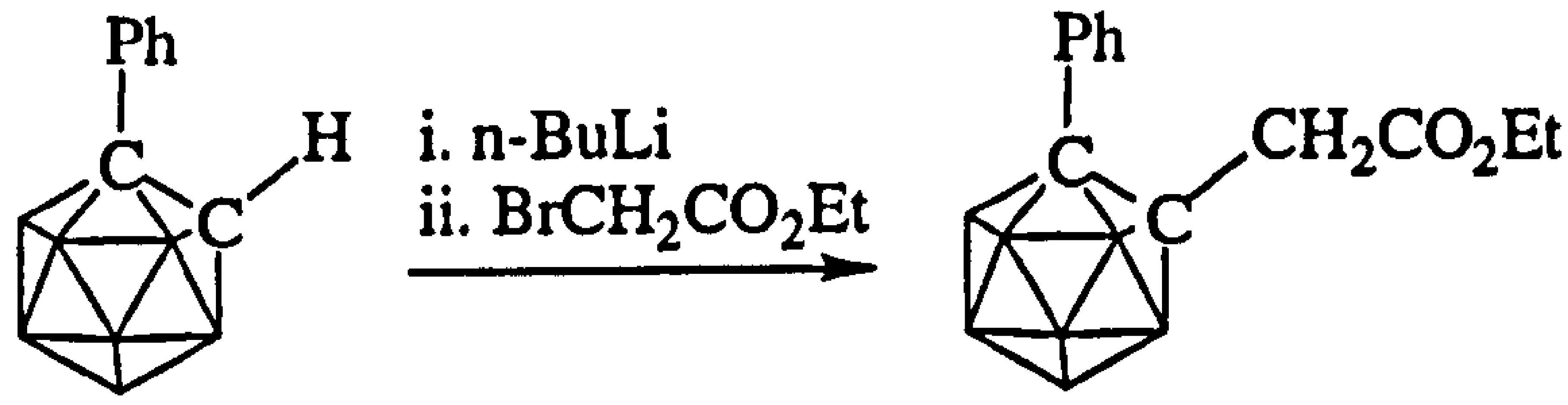

scheme 2.2: substitution via carborane lithiation

Monolithiation is also achieved with relative ease, however, a degree of disproportionation, often solvent dependent, is observed in many cases due to the solution equilibrium of the intermediates formed.

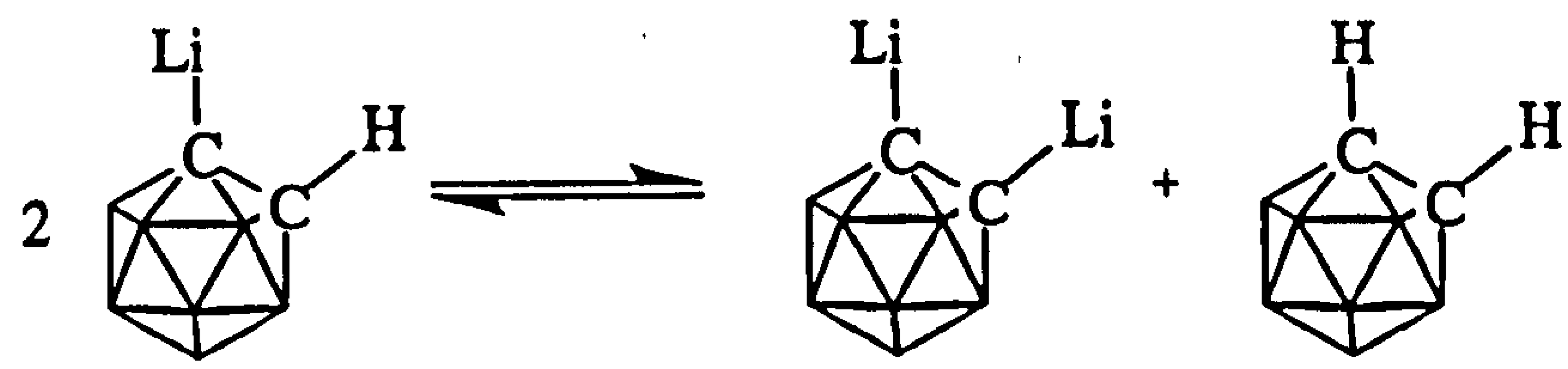

scheme 2.3: solution equilibrium of lithio-carborane

This method of derivatisation has proven successful in the synthesis of many compounds which form the subject matter of this thesis. Specific examples and reaction conditions will be discussed in section 2.2.3.

Other, less widely exploited, metal salts of carboranes include sodium, potassium and calcium.[7,8,9] These are prepared from the relevant metal amide in liquid ammonia at low temperature, but given the ease with which lithium salts can be prepared, these other salts have not been widely developed as precursors to carborane derivatives.

b) Magnesium and Grignard Reagents

On an equal footing with lithiation is the derivatisation of carboranes through a Grignard intermediate.[5,10] The carboranyl Grignard reagent is formed through reaction of the carborane with the appropriate alkyl magnesium halide, or by reaction of a suitable halocarborane with magnesium metal. Further reaction with a suitably chosen reagent yields the required product.

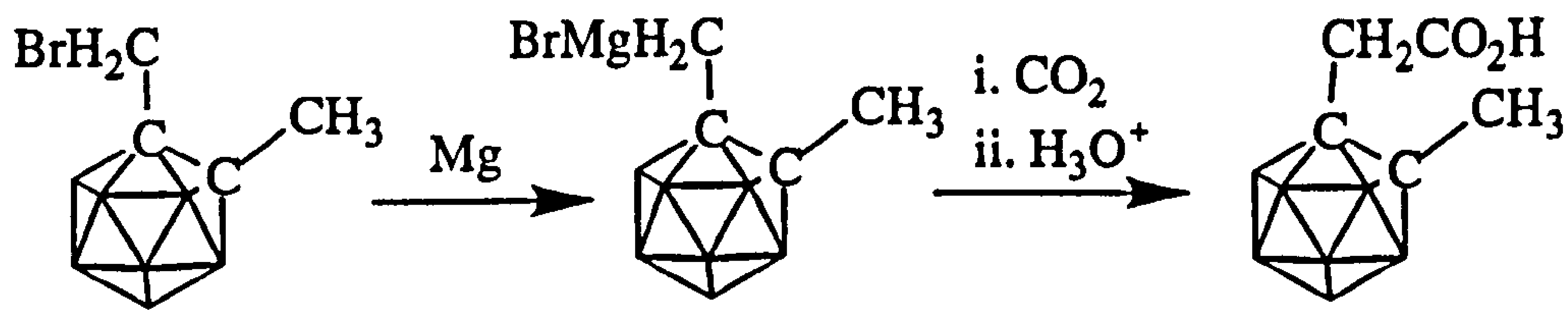

scheme 2.4: carborane derivatisation through a Grignard intermediate

As with lithiation, the metallated intermediate of the parent carboranes, $C_2B_{10}H_{12}$, may disproportionate giving mono-, di- and unsubstituted carboranyl products. With Grignard reagents, however, there is an added complication in that they can rearrange and often mixtures of products are observed.[11]

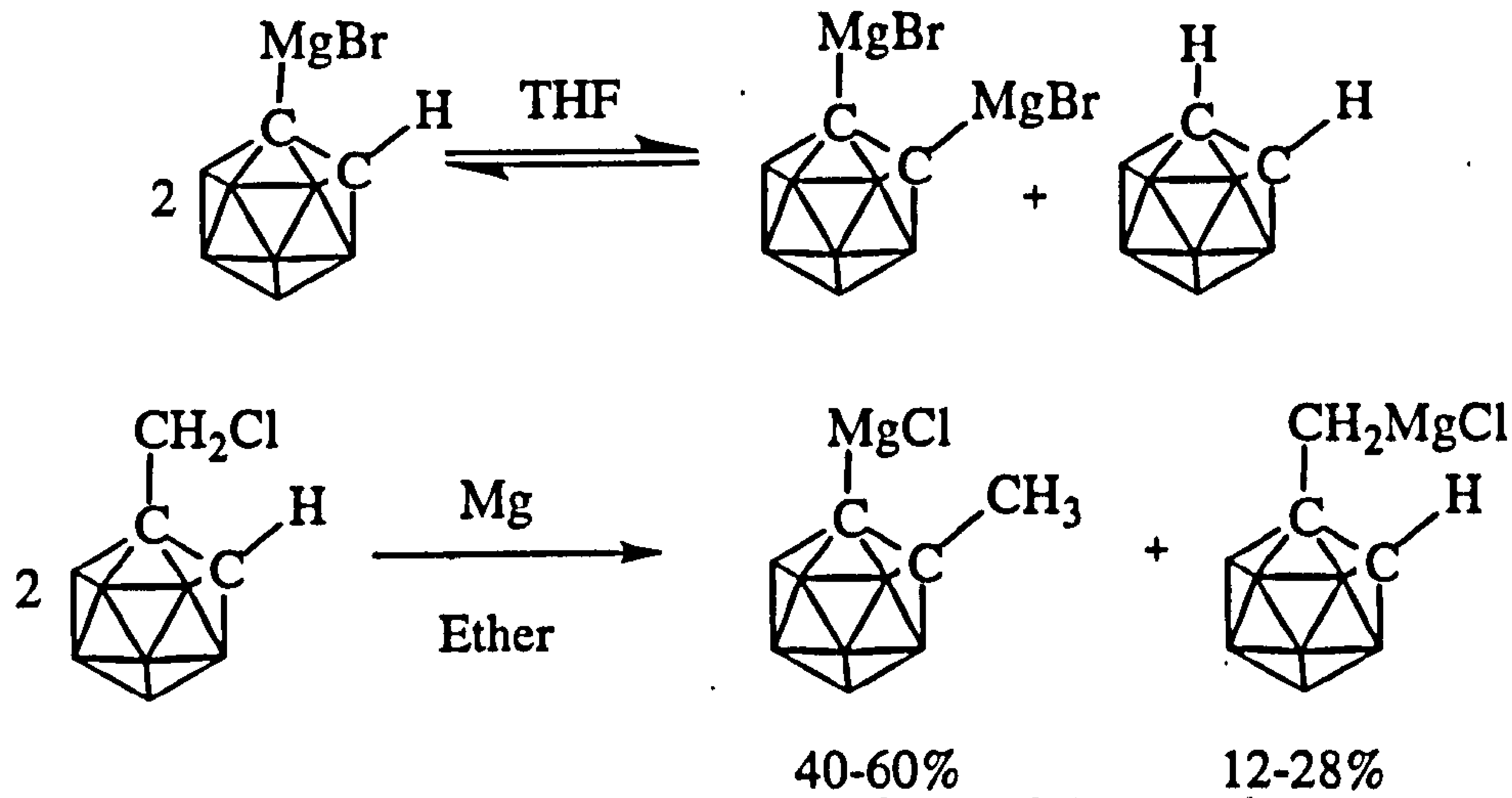

scheme 2.5: solution equilibria of carboranyl Grignard reagents.
Top: disproportionation, bottom: rearrangement

The balance of this equilibrium is solvent and halide dependent. The varying electronegativities of the respective halides lead to differences in acidity of the cage proton explaining why chloride derivatives rearrange to a greater extent than bromide derivatives.

c) Copper and Palladium

If the prospective substituent is incompatible with the lithiated carborane intermediate, substitution can be effected via a copper coupling reaction using copper(I).[12,13,14] This method is commonly used to obtain mono and diaryl substituted *meta-* and *para-*carboranes and monoarylated *ortho-*carboranes which are otherwise unavailable by means of lithiation or thermal isomerisation, or whose yields are low by these means.

Literature published on this method of coupling varies between research groups. Some claim that palladium is required for a successful carborane-aryl coupling reaction[15], however, work within this research group has led to continued success with the use of copper(I) chloride and pyridine to effect the coupling in both aryl and heteroaryl substitution reactions. For example:

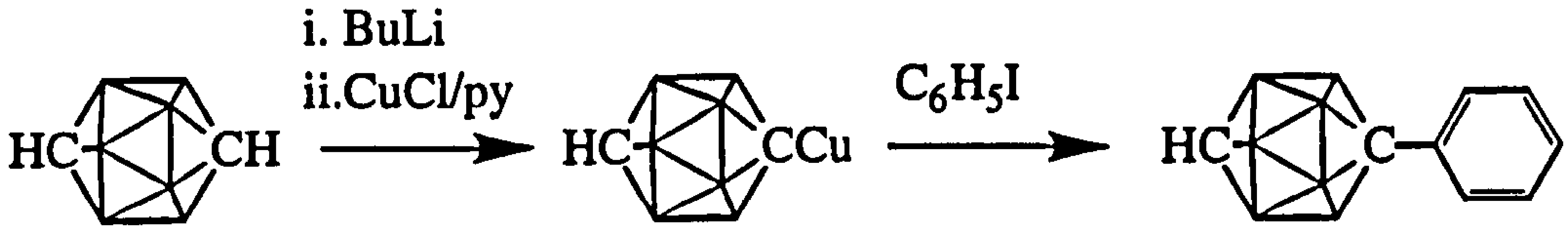

scheme 2.6: carborane substitution through a copper intermediate

As with other carborane metallations, some disproportionation is observed, and often the disubstituted carborane is isolated as a minor product.

2.2.3 Synthesis Of Particular One-Cage *Closo*-Carborane Derivatives

a) Hydroxides and Ketones

We were interested in synthesising hydroxy carboranes, $RCB_{10}H_{10}COH$, and their oxy anions, $RCB_{10}H_{10}CO^-$, in order to look for *exo*-π bonding effects in this type of system. Deprotonation of the hydroxide functionality, discussed in part c), leaves an electron pair on the oxygen, which can delocalise back into the cage system, causing the cage C-C bond to lengthen and the C-O bond *exo* to the cage to shorten significantly and to gain π-character in the *ortho*-carboranyl system[16] (scheme 2.7). A study of the parent compounds is obviously required to highlight the effect of *exo*-π bonding.

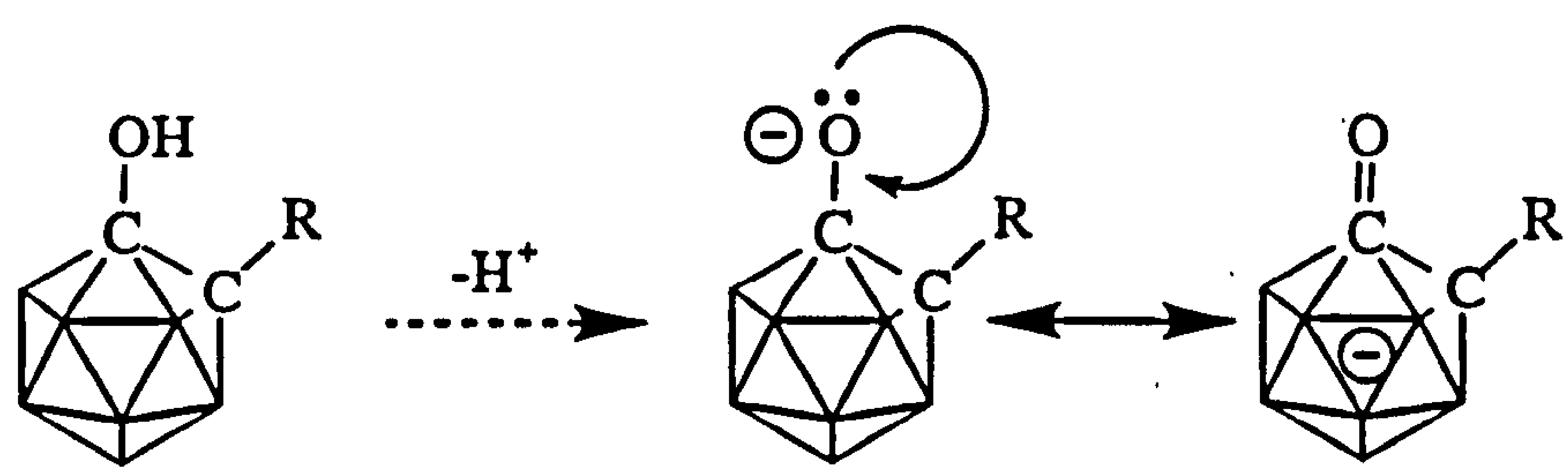

scheme 2.7: back donation of electron density in deprotonated hyroxy carboranes

Hydroxy-carboranes cannot be synthesised directly from the reaction of decaborane and acetylenic hydroxide due to the extended delocalisation in the acetylene, but one possible method for their preparation is to pass molecular oxygen or dry air over the lithio carborane salt, which once acidified will yield the appropriate hydroxycarborane.[17] Yields by this method are in the range 30-40%. An alternative method is to use peroxides[18], in the ratio carborane:peroxide 2:1, where the hydroxy carborane can be achieved in up to 50% yield. This yield cannot be increased as the peroxide splits, one half generating the relevant ketone, the other the hydroxide.

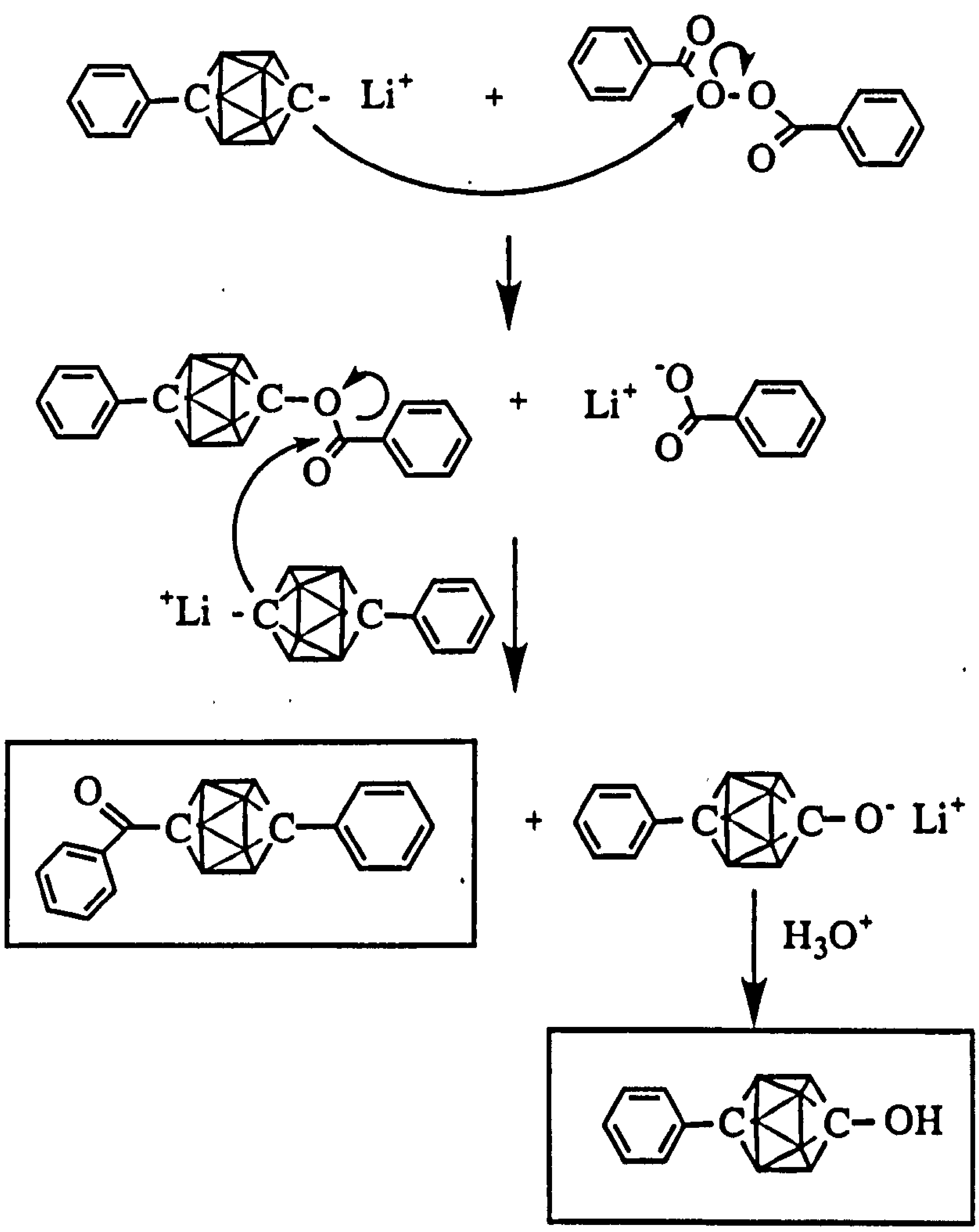

scheme 2.8: mechanism of the reaction between lithio-carborane and benzoyl peroxide

An alternative route to carboranyl ketones, $RCB_{10}H_{10}CCOR$, is via carboxylic acid chlorides.[19] Through reaction of lithiocarborane and the chloride of the appropriate carboxylic acid, a range of carboranyl ketones can be synthesised with relative ease.

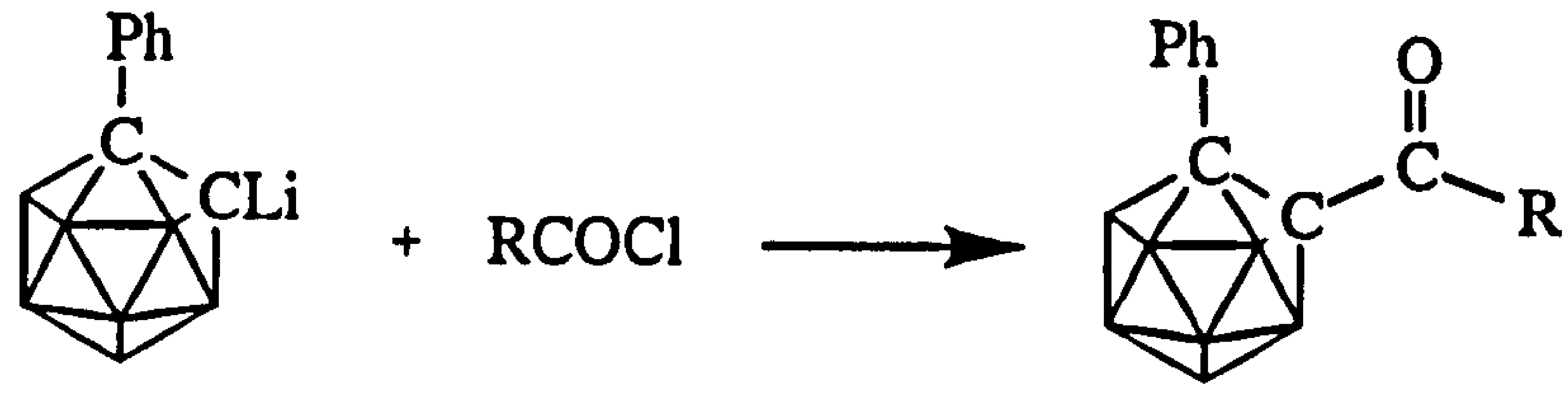

scheme 2.9: formation of a carboranyl ketone

Organic chemists have also looked to carboranes as protecting groups in the syntheses of aldehydes and ketones.[20] Protecting groups that have been employed in the synthesis of such compounds include acetals and ketals, however these are of limited use as they are easily cleaved by acid hydrolysis and Lewis acid co-ordination - conditions in which carboranes are, conversely, very stable. The carborane can be removed by the action of base which leaves the desired aldehyde or ketone intact.

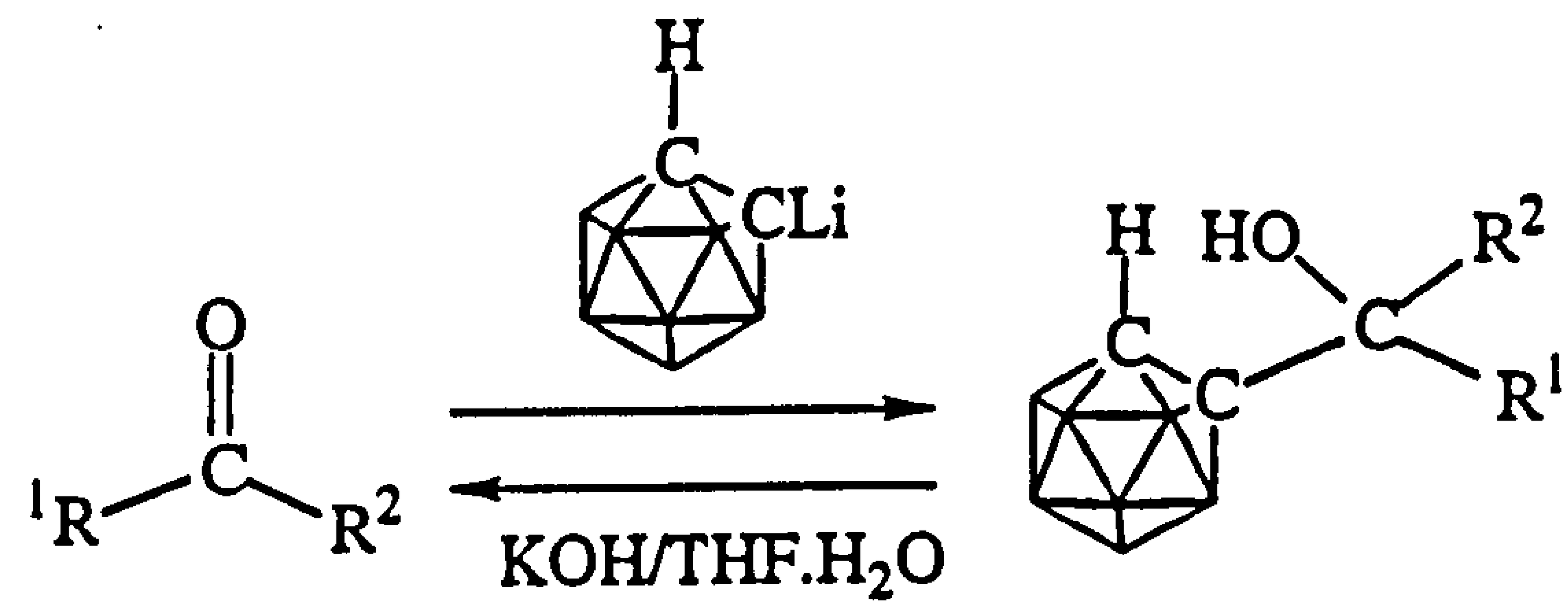

scheme 2.10: carboranyl protection of a ketone

b) Carboxylic Acids

The family of carboranyl carboxylic acids, $RCB_{10}H_{10}CCO_2H$, were of interest to us, again as subjects for the study of *exo*-π bonding effects in carboranyl compounds. Upon deprotonation of the acid, an extra pair of electrons from the *exo*-functionality becomes available to the cage system (scheme 2.11). The carborane cage has the ability to attract electron density away from the carboxylate carbon atom, creating a pseudo CO_3^{2-} system. The synthesis of the parent carboxylic acids gives an in-road to such systems which should mimic the carbonate anion and create an *exo*-π bond between the carbonyl and cage carbon atoms.

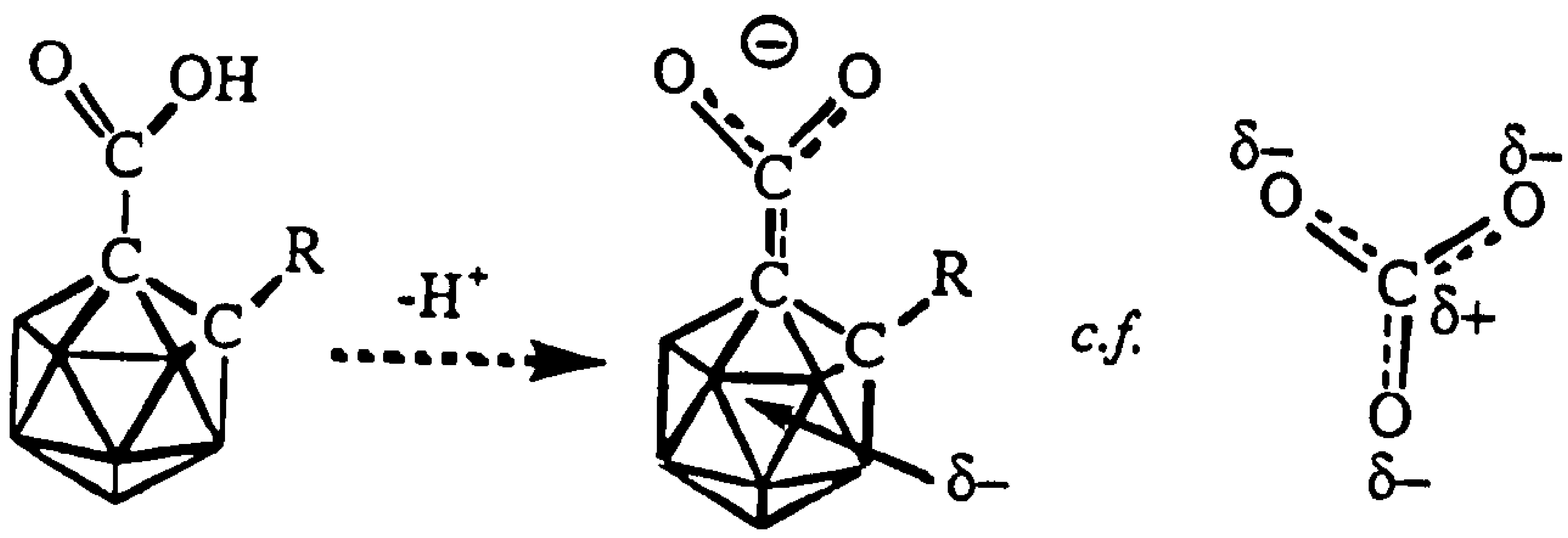

scheme 2.11: the proposed similarity between the carborane cage and the O$^-$ anion

Like their hydroxy analogues, carboranyl-carboxylic acids cannot be synthesised from an acetylene, however, their synthesis is straightforward and high yielding if the lithio-carborane is taken as the reaction intermediate.[21] In several literature examples solid carbon dioxide is poured directly into the reaction vessel, but the use of dried gaseous CO_2 gives higher yields, as any moisture present will hydrolyse the lithiocarborane. Carboxylic acid derivatives can be synthesised from carboranyl-Grignard intermediates but the reaction is less efficient, requiring longer reaction times, and a higher gas pressure.[22]

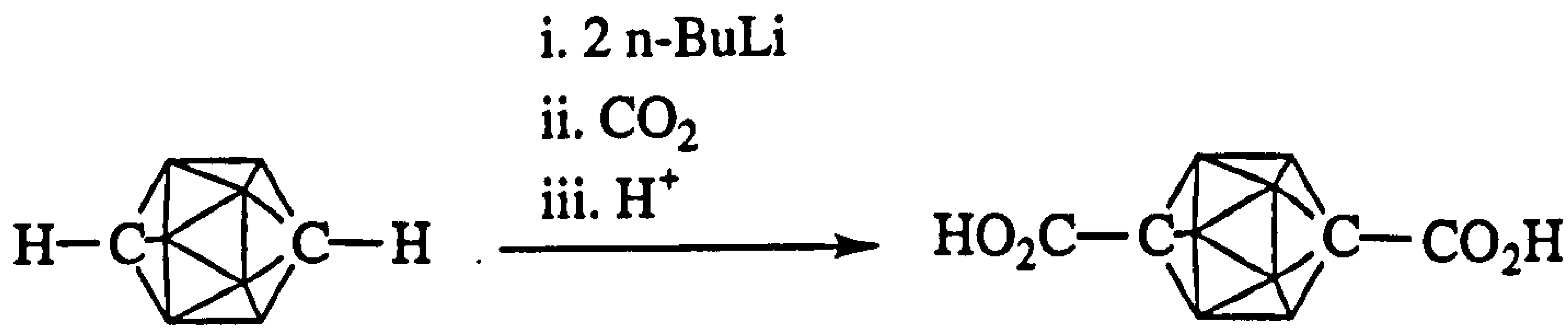

scheme 2.12: formation of a carboranyl carboxylic acid

Carboxylic acid derivatives can also be made indirectly, for example by hydrolysis of an acid chloride, or by oxidation of a hydroxide if there is a funtionality between the carborane and the carboxylic acid group.[23]

c) Deprotonation of Hydroxide and Carboxylic Acid Derivatives

The purpose of synthesising carboranyl hydroxide and carboxylic acid derivatives was to examine the effect of the *exo*-substitutent on electron density and distribution within the *closo* cage structure as outlined in the preceeding section. By deprotonating the hydroxide compounds, an electron rich O^- substituent is generated, and for comparison, a CO_2^- functionality when the carboxylic acid derivative is deprotonated. As the protons of the hydroxides and carboxylic acids are suitably acidic, their deprotonation is achieved readily by the action of an appropriate base. Studies of this sort have been conducted in the past on hydroxides, thiols and amine substituents[16,24,25] - we aim to extend the study to carboxylic acids.

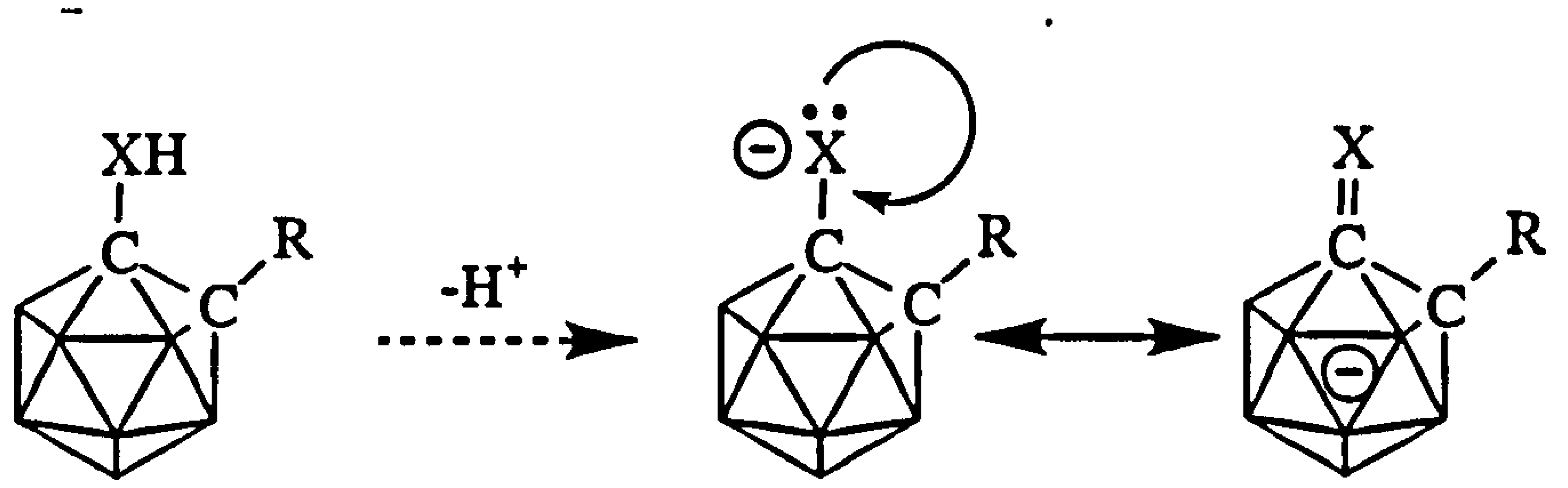

scheme 2.13: formation of an exo-π bond through deprotonation of a carboranyl substituent. X=O, S, NR, CO_2

i) Proton Sponge - 1,8-*bis*-(dimethylamino)-naphthalene

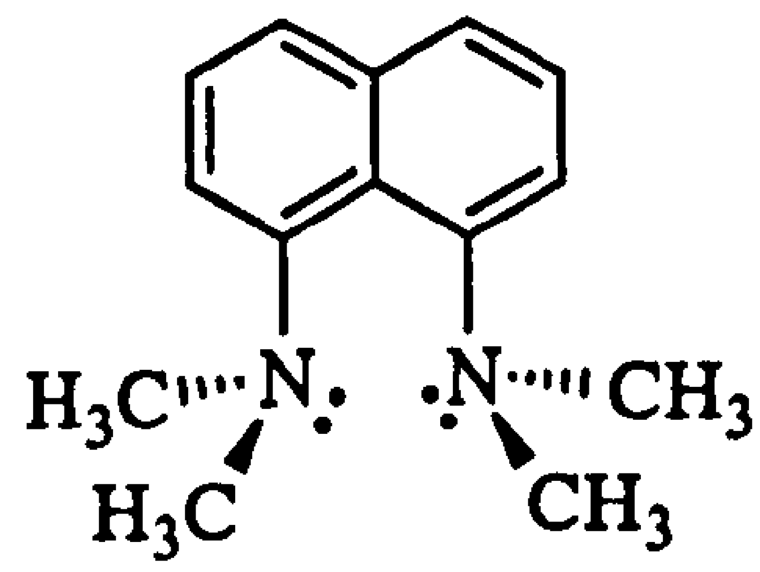

figure 2.1: proton sponge

Proton sponge, like other 1,8-diaminonaphthalene derivatives, is an extremely strong protic base (pK_a = 12.34)[26] and can efficiently deprotonate carboranyl hydroxide and carboxylic acid derivatives (e.g. $pK_a(PhCB_{10}H_{10}COH)$ = 5.25, $pK_a(PhCB_{10}H_{10}CCO_2H)$ = 3.2). Adding to its basicity and its deprotonation ability is its strained ring configuration.[27] The lone pairs on the pendant dimethylamino groups of the naphthalene ring system cause the naphthalene to adopt an unfavoured, non-planar configuration. When a proton is "captured" by the nitrogen lone pairs of the amine groups, causing a N···H···N intramolecular hydrogen bond to form, the ring strain is relieved, and the naphthalene group becomes planar.[28] In doing this, the acidic proton is drawn away from the O^- or CO_2^- entity and electron density on the substituent becomes localised.

Past studies[16] on the deprotonation of hydroxy-carboranes have shown this particular naphthalene derivative to be the most effective, causing the greatest shift in the infrared spectrum between the parent hydroxide and the prepared hydroxy salt. Other amine bases such as trimethylamine, triethylamine, TMEDA and pyridine also give the deprotonated product[29,30] but the effect is less dramatic, in that hydrogen bonding persists to the oxygen atom which is therefore not completely deprotonated.

ii) Ammonia

Aqueous ammonia has been reported to efficiently remove the acidic proton from carboranyl hydroxides.[18] There are, however, conflicts of opinion which claim this same procedure causes degradation of this, and other systems, to the dicabaundecaborate anion[31], and not deprotonation.

iii) Metallation

Many metal salts of carboranyl hydroxides and carboxylic acids[32] are known and are in fact intermediates in the formation of such carboranyl derivatives. Obviously the metal salt of such a derivative influences the electron density on the O^- or CO_2^- substituent, however, the relationship between the two ions is electrostatic and there is still a degree of interaction between the species. The effect of deprotonation subsequently appears less than with amine bases, in particular proton sponge, where the acidic proton is held at a considerable distance from the *exo-* substituent.

d) Halogenation of Carboranes

There are various methods by which a halogen atom can be substituted onto a carboranyl cage atom, attaching itself to either a boron or to a carbon. As the scope of this thesis is the dicarbadodecaboranyl system, let us consider the halogenation of the *ortho*, *meta*, and *para*-carboranes, in particular, substitution of a halogen at the carbon sites.

As in strictly organic systems, fluorination is also a special case for carboranes, and subsequently will be treated separately. When the halogen concerned is either chlorine, bromine or iodine, the same general procedures and conditions apply to each and these will be considered together.

i) Fluorination

Interest in synthesising carboranyl fluorides arose as the fluorine atom is isoelectronic with the O^- ion and the OH group, and if prepared, these subjects for comparison of *exo*-π bonding effects become available.

There are numerous examples of cage boron atom fluorination occurring in icosahedral carboranes, effected by a variety of means. The first reported example is by Russian workers[33], who employed HF to convert a diazotised cage boron to a BF functionality.

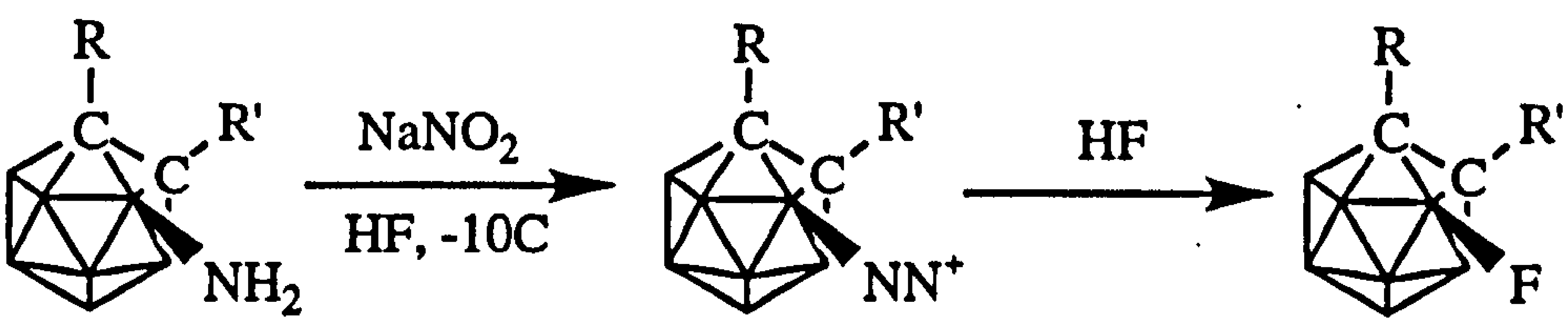

scheme 2.14: fluorination of cage boron atoms

Similarly harsh conditions, where antimony pentafluoride acts as the fluorinating agent have been used to effectively synthesise BF connectivities in uncharged *closo ortho-* and *meta*-carboranes.[34] In charged species, namely $CB_{11}H_{12}^-$ and $B_{10}H_{10}^{2-}$ and substituted derivatives thereof, other reagents have been used such as $BF_3.OEt_2$[35], liquid anhydrous hydrogen fluoride (LAHF)[36], and the N-F reagent, 1-(chloromethyl)-4-fluoro-1,4-diazoniabicyclo-[2.2.2]-octane-*bis*-(tetrafluoroborate) (F-

TEDA)[37]. Fluorination at boron has also been achieved by insertion of BF into a *nido* cage residue.[38]

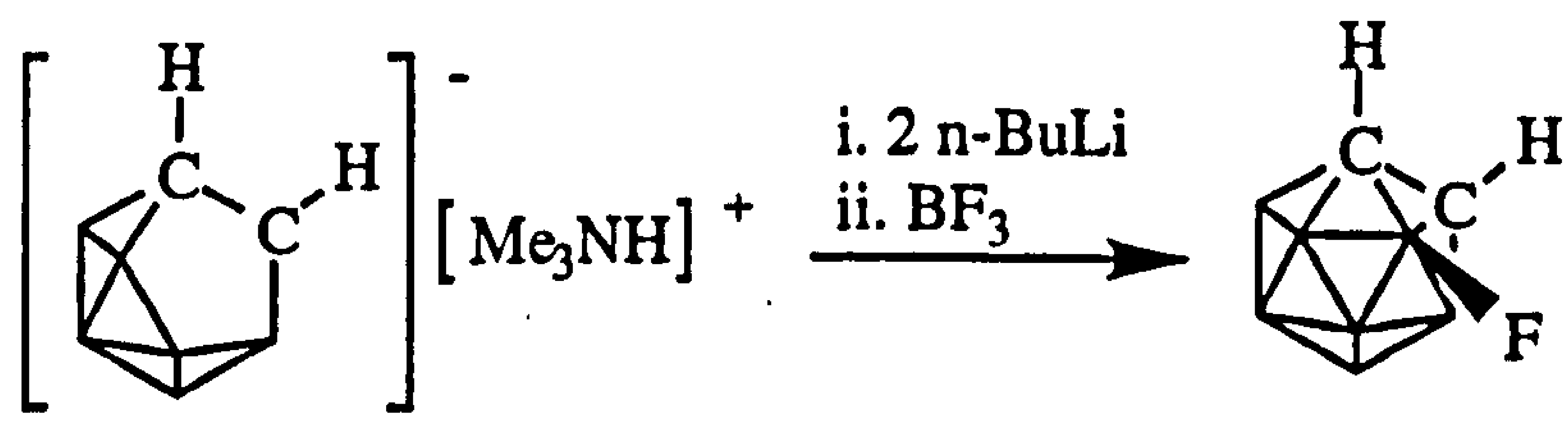

scheme 2.15: formation of fluorinated carboranes through insertion reactions

B-F bond formation in *nido*-RR'-$C_2B_9H_{10}$ systems, occurring during the use of fluoride ion to effect deboronation, will be discussed separately in Chapter Five.

Cage fluorination on boron has also been observed in smaller carboranes e.g. *closo*-2,4-$C_2B_5H_7$[39,40,41], where fluoride ion displaces previously substituted higher halogens. It is proposed that any attacking halogen smaller than that already substituted on the carborane will replace the original halogen, for example:

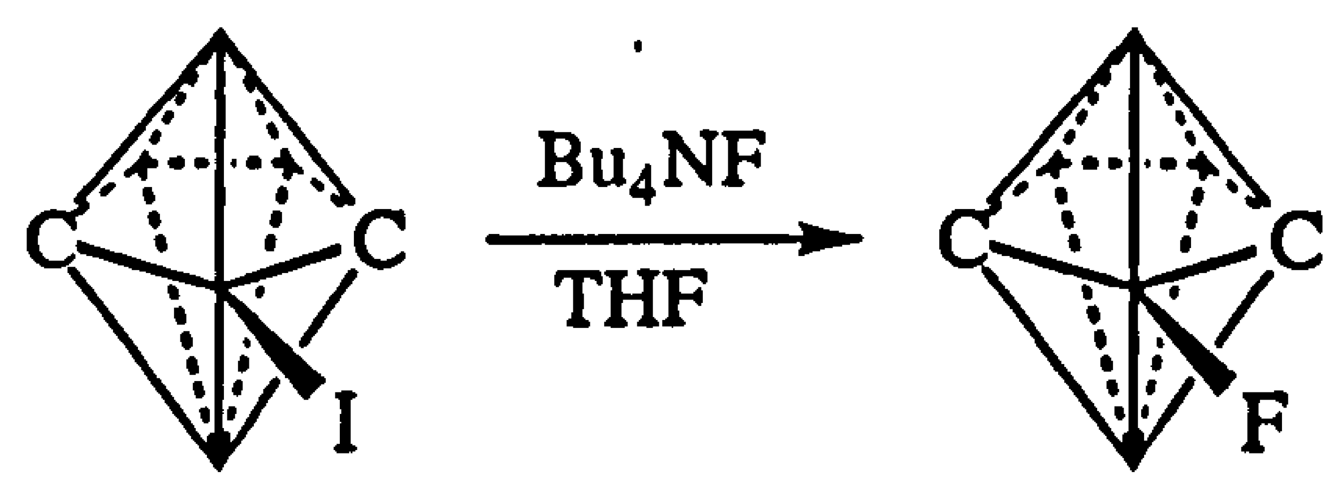

scheme 2.16: cage fluorination of small carboranes by fluoride ion

None of the above methodologies have been employed in the synthesis of C-F functionalised icosahedral carboranes, and to date only one paper has been published on carboranyl carbon fluorination, highlighting the fluorination of the cage system of the *ortho*, *meta* and *para*-$C_2B_{10}H_{12}$ icosahedra.[42] The fluorination of carboranyl carbons was reported for the *meta*-carboranyl isomer. 1,7-difluoro-*meta*-carborane was synthesised using perchloryl fluoride as the fluorinating agent, however, no structural or NMR spectroscopic data were presented. When fluorination of the *ortho*- isomer was attempted using this reagent, the reaction mixture exploded. No data were given for the *para*- system. In this previous study, it was also found that the use of elemental fluorine fluorinated only the cage boron atoms, leaving the carbons unreacted.

$$\left.\begin{matrix}o\\m\\p\end{matrix}\right\}HCB_{10}H_{10}CH + 10\,ClF \xrightarrow[HF,\,0C]{} \left.\begin{matrix}o\\m\\p\end{matrix}\right\}HCB_{10}Cl_{10}CH + 10\,HF$$

$$\left.\begin{matrix}o\\m\\p\end{matrix}\right\}HCB_{10}H_{10}CH \xrightarrow[HF,\,0C]{ClF_3} \left.\begin{matrix}o\\m\\p\end{matrix}\right\}HCB_{10}Cl_xH_{10-x}CH + \left.\begin{matrix}o\\m\\p\end{matrix}\right\}HCB_{10}FCl_xH_{9-x}CH \quad x=1\text{-}6$$

$$\left.\begin{matrix}o\\m\\p\end{matrix}\right\}HCB_{10}H_{10}CH + 10\,F_2 \xrightarrow[HF,\,0C]{} \left.\begin{matrix}o\\m\\p\end{matrix}\right\}HCB_{10}F_{10}CH + 10\,HF$$

$$m\text{-}LiCB_{10}H_{10}CLi \xrightarrow[-\,2LiClO_3]{2ClO_3F} m\text{-}FCB_{10}H_{10}CF \xrightarrow[-\,10\,HF]{10\,F_2} m\text{-}FCB_{10}F_{10}CF$$

scheme 2.17: fluorination reactions of ortho, meta and para-carboranes

It is interesting to note the differences in the reaction between *ortho*-carborane and elemental fluorine, where decafluoro-*ortho*-carborane is the dominant product and no selectivity is observed, and the insertion reaction of BF_3 into the *nido*-$Li_2C_2B_9H_{11}$ where the 3-F isomer is produced exclusively. A degree of selectivity is also available through other fluorination agents mentioned earlier.

ii) Chlorination, Bromination and Iodination

There are various methods by which a Cl, Br or I moiety can be introduced on to the cage carbon atoms. The starting point is generally either the lithio or Grignard derivative of the appropriate carborane. Each method has its relative merits for each isomer.

Generally, chlorination is achieved by the action of elemental chlorine or CCl_4 on the lithio- or halomagnesio-carborane.[43,44,45,46] For example:

$$p\text{-}RCB_{10}H_{10}CLi \quad + \quad X_2 \longrightarrow p\text{-}RCB_{10}H_{10}CX \quad + \quad LiX$$

$$X = Cl, Br, I;\ R = H, CH_3$$

scheme 2.18: reaction of lithio-carborane with elemental halogen

Problems are sometimes encountered in chlorination reactions.[44,47,48] Halogenation of both cage carbon and boron atoms is sometimes observed, and if the starting Grignard has X=Br or I, often brominated or iodinated products are isolated.

For example,

$$o\text{-}HCB_{10}H_{10}CMgBr \xrightarrow[THF\ +\ C_6H_6]{Cl_2\ \text{or}\ CCl_4} o\text{-}ClCB_{10}H_{10}CCl + o\text{-}HCB_{10}H_9ClCCl$$

$$\underset{X\,=\,Br,\,I}{o\,(m)\text{-}RCB_{10}H_{10}CMgX} \xrightarrow[THF]{Cl_2} \underset{\sim 95\%}{o\,(m)\text{-}RCB_{10}H_{10}CX} + \underset{\sim 5\%}{o\,(m)\text{-}RCB_{10}H_{10}CCl}$$

scheme 2.19: side reactions encountered in chlorination reactions using elemental chlorine

As a preferred alternative to elemental chlorine, sulfuryl chloride, sulfur sesquichloride and *p*-tolyl-sulfonyl chloride can effect chlorination.[44] In the first two instances, both B and C positions are attacked by the chlorine, however the use of *p*-tolyl-sulfonyl chloride leads uniquely to C substituted carboranes.

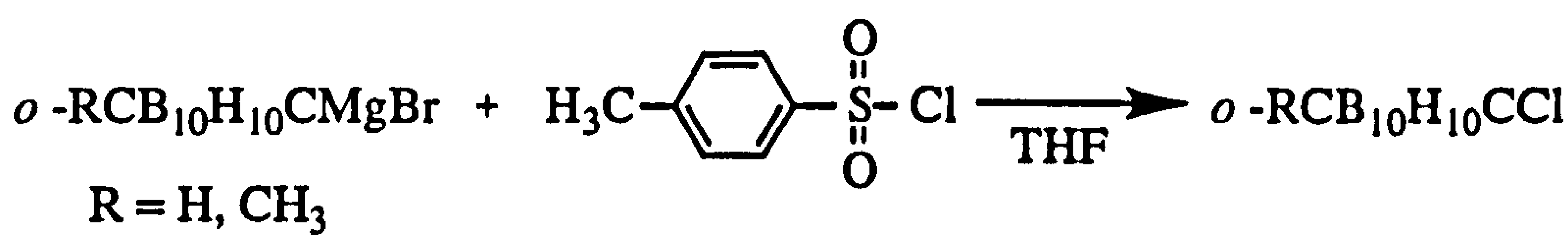

scheme 2.20: chlorination of para-carborane with p-tolyl-sulfonyl chloride

<u>Bromination</u> of the Grignard derivative is effected by the use of elemental bromine. This gives yields of *c*.40% for *ortho*-carborane[44] and the bromo-carborane derivatives are more efficiently prepared from the lithio-carborane derivatives.

<u>Iodination</u> of *ortho*-carborane is facile, both from lithio- and Grignard carboranes, giving a good yield of product from the reaction with ICl.[44]

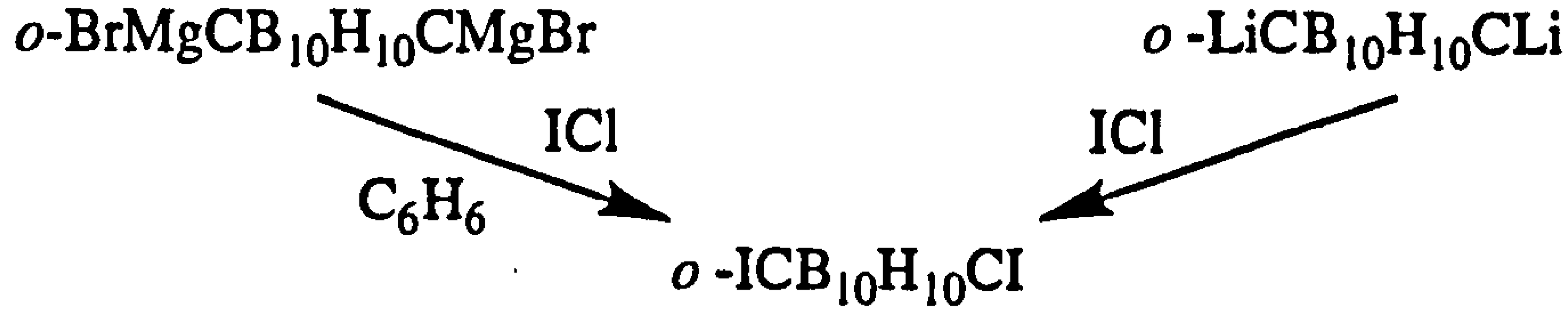

scheme 2.21: iodination of carborane derivatives

Iodination of *meta*-carborane works best with lithio-carborane and ICl, as the Grignard starting material gives chlorinated products with this reagent. The chlorinated products are more readily available from the reaction of elemental chlorine on the *meta*-carboranyl Grignard.

e) Sulfonylation of Carboranes

Sulfur moieties can be attached with relative ease to a carboranyl carbon atom through reactions[49] such as

$$RCB_{10}H_{10}CNa + S \xrightarrow{H^+} RCB_{10}H_{10}CSH$$

$$NaSCB_{10}H_{10}CSNa + 2CH_3I \longrightarrow CH_3SCB_{10}H_{10}CSCH_3$$

scheme 2.22: synthesis of carboranyl sulfides

The introduction of a sulfur-oxygen moiety however, be it a sulfoxide, a sulfone or a sulfinic acid function has always been achieved through the oxidation of the appropriate sulfide, by oxidants such as hydrogen peroxide[49], *p*-nitroperbenzoic acid[50], sodium hypochlorite[51] and peracetic acid[52]; no SO functionality reported has been immediately incorporated into the carborane cage. For example:

$$m\text{-}RCB_{10}H_{10}CSCH_3 + H_2O_2 \longrightarrow m\text{-}RCB_{10}H_{10}CSO_2CH_3$$

$$R{=}H, CH_3$$

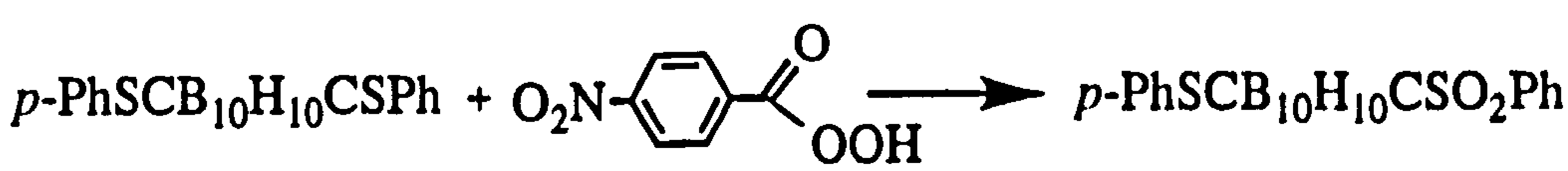

$$m\text{-}HSCB_{10}H_{10}CSH \xrightarrow[CCl_4]{Cl_2} m\text{-}ClSCB_{10}H_{10}CSCl$$

$$m\text{-}ClSCB_{10}H_{10}CSCl \xrightarrow[H_2O,\ CCl_4]{NaOCl} m\text{-}ClO_2SCB_{10}H_{10}CSO_2Cl$$

$$m\text{-}HO_3SCB_{10}H_{10}CSO_3H \xleftarrow[H^+]{2AlCl_3} m\text{-}ClO_2SCB_{10}H_{10}CSO_2Cl$$

scheme 2.23: indirect synthesis of sulfonylated carboranes

There is only one exception to date, and that is sulfonylation through reaction of lithio-carborane with sulfur dioxide, followed by hydrolysis.[49]

$$m\text{-}RCB_{10}H_{10}CLi \xrightarrow[R=H,\ CH_3]{i.\ SO_2 \quad ii.\ H_3O^+} m\text{-}RCB_{10}H_{10}CSO_2H$$

scheme 2.24: direct sulfonylation of carboranes

2.3 RESULTS AND DISCUSSION

Hydroxide and carboxylic acid derivatives, $RCB_{10}H_{10}COH$ and $RCB_{10}H_{10}CCO_2H$, were the initial synthetic subjects in the study of *exo-π* bonding effects. From this starting point, the synthesis of fluoro-carboranes, $RCB_{10}H_{10}CF$, was investigated giving interesting results. Subsequent synthetic targets were the sulfonlyated carboranes, $RCB_{10}H_{10}CSO_2R$, and the development of a one-pot synthesis for such compounds. Heterocyclic carboranes, (2-thiophenyl)-$CB_{10}H_{10}CH$ and (3-pyridyl)-$CB_{10}H_{10}CH$, have also been synthesised and illustrate *intra-* and *inter-*molecular hydrogen bonding.

General synthetic information and analytical data are reported in the following discussion, whilst specific synthetic procedures and analytical data (infrared spectroscopy, elemental analysis, mass spectroscopy, melting point, multi-nuclear FT-NMR spectroscopy) are detailed at the end of this chapter.

2.3.1 Starting Materials

When evaluating the effect of an *exo* substituent on the carborane cage, a reference compound is required. The synthesis of basic carboranes, namely 1-bromomethyl-, 1-methyl- and 1-phenyl-*ortho*-carborane, and mono- and di-phenyl *meta-* and *para*-carboranes by standard literature methods detailed earlier, has provided such reference materials.

2.3.2 Carboranyl Hydroxides and Ketones

Earlier work had illustrated that deprotonation of the hydroxide functionality of *ortho*-carboranes gives a short C-O bond and a lengthened cage C-C bond[16], however, although *exo-π* bonding is obviously present, the structural determination of the parent hydroxide had not been carried out. In the current study, 1-phenyl-2-hydroxy-*ortho*-carborane has been resynthesised and X-ray quality crystals grown from hexane.

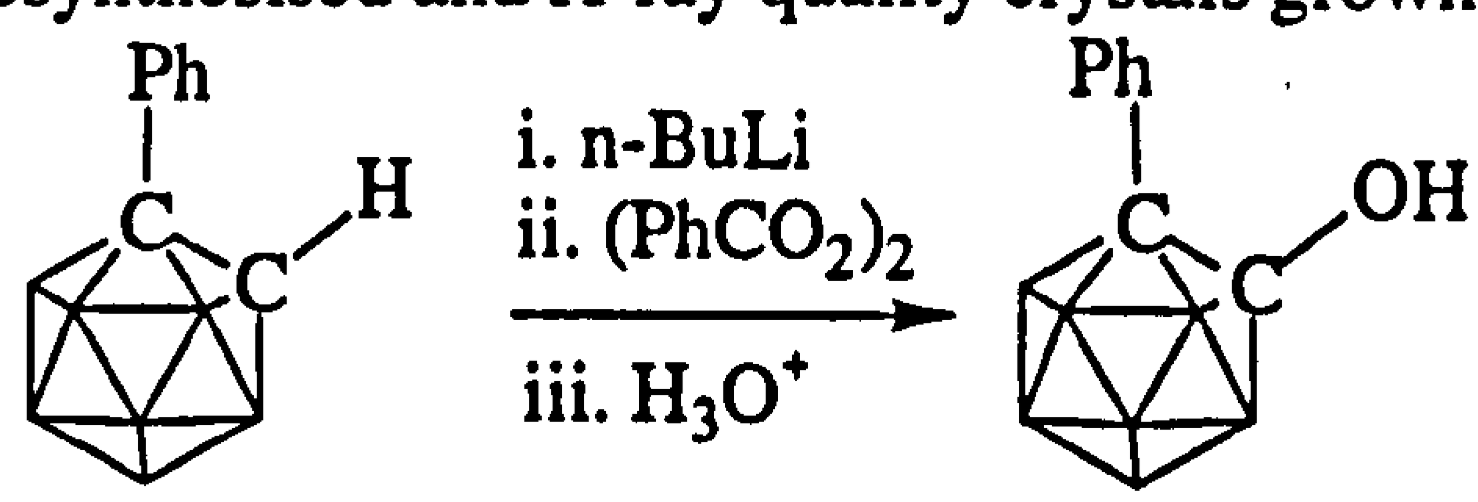

scheme 2.25: synthesis of 1-phenyl-2-hydroxy-ortho-carborane

Other hydroxides isolated, following literature preparations are the 1-hydroxy-*meta*-carborane and 1-hydroxy-*para*-carborane. The 1-(benzoyloxy)-*para*-carborane was also isolated from the latter reaction (*c.f.* scheme 2.8).

Synthesis of di-hydroxy-*ortho-*, *meta-* and *para-* carboranes was also attempted, but without success. When substitution of one position is required, using a peroxide, two products are obtained. With di-substitution the synthesis becomes less clean, giving a large mixture of similar products.

2.3.3 Carboranyl Carboxylic Acids

The synthesis of carboxylic acids according to literature methods, from reaction of lithio-carborane and carbon dioxide has been followed for the large part in this study. The only change made was that the carbon dioxide gas employed, either from a cylinder, or from the evaporation of solid carbon dioxide, was passed through a P_2O_5 drying column before reaction with the lithio-carborane. 1-phenyl-2-carboxy-*ortho*-carborane has been synthesised and structurally characterised, the crystals having been grown from 40-60° petroleum ether. Other carboxylic acid derivatives synthesised for this study were 1,7-dicarboxy-*meta*-carborane, 1-phenyl-12-carboxy-*para*-carborane and 1,12-di-carboxy-*para*-carborane.

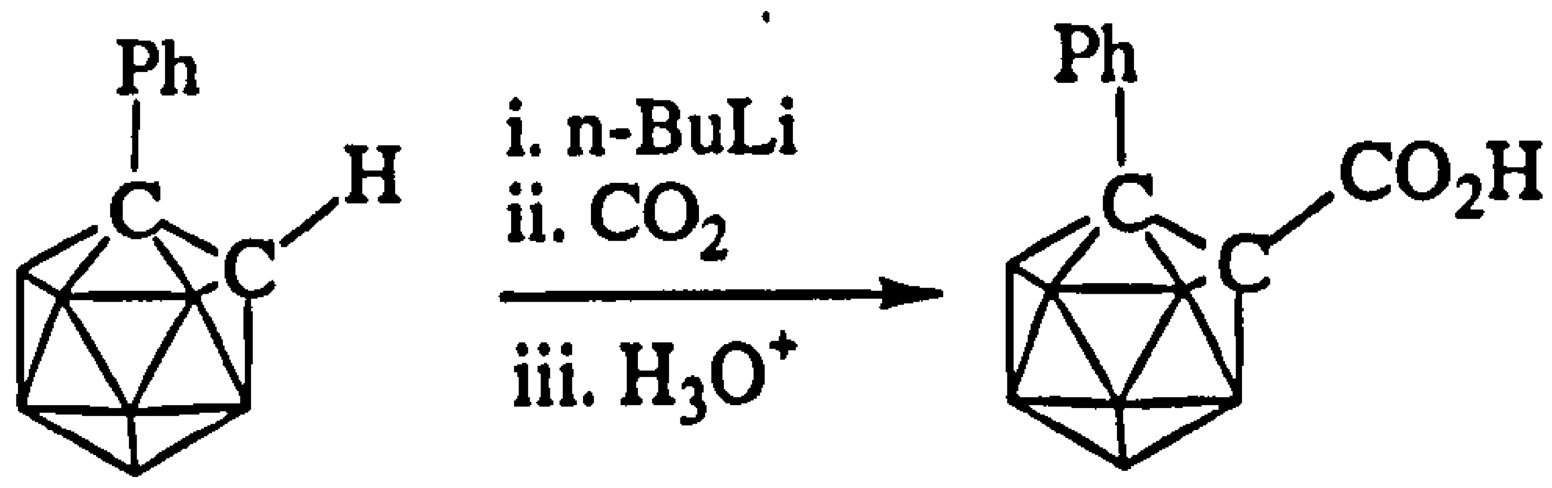

scheme 2.26: synthesis of 1-phenyl-2-carboxy-ortho-carborane

2.3.4 Deprotonation of hydroxides and carboxylic acids

The earlier study of *exo*-π bonding in hydroxy-carboranes has been extended here to the carboxylic acid functionality for the reasons described in the earlier text. Various methods of deprotonation were employed.

a) Proton Sponge

This amine base was found to be the most successful deprotonating agent for the hydroxy carboranes.[16] It is also successful in removing the proton from the carboxylic acid functionality, allowing some electron density of the CO_2^- to be delocalised into the cage system (see Chapter Three). As well as 1-phenyl-2-carboxy-*ortho*-carborane, 1,7-dicarboxy-*meta*- and 1,12-dicarboxy-*para*-carborane have been deprotonated using this base.

b) Ammonia

Early workers claimed that aqueous ammonia could remove an acidic proton from a carboranyl hydroxide, whilst later work suggested that this in fact led to cage degradation. Attempted deprotonation of 1-phenyl-2-carboxy-*ortho*-carborane with aqueous ammonia in the current study, resulted in a mixture of deprotonated and deboronated materials. Given the lack of selectivity of this base, it cannot be considered an ideal candidate for successful deprotonation and was not used in further deprotonation reactions.

c) Metallation

Although metal salts form ionic bonds with carboxylate "ligands", when combined with the 18-crown-6 cyclic ether the metal is held further from the CO_2^- group. X-ray quality crystals have been grown of the deprotonated 1-phenyl-2-carboxy-*ortho*-carborane derivative but have proven to be disordered. The 1,7-di-carboxy-*meta*-carborane was also deprotonated by this method. The proton was initially removed by the action of KOH, then 18-crown-6 ether added to form the salt. Reaction conditions must be controlled to minimise cage deboronation by KOH. Copper (II) sulfate was used to deprotonate the 1,12-di-carboxy-*para*-carborane with the aim of creating a polymeric deprotonated carboxylic acid system.

2.3.5 Fluorination

The discussion in section 2.2.3d) has illustrated that electrophilic fluorinating agents are capable of causing a degree of boron fluorination in icosahedral carboranes, however, there have been no instances noted of them leading to carboranyl C-F halogenated species. In contrast, electrophilic NF reagents, where the fluorine carries a δ^+ polarisation, have been used successfully to fluorinate wholly organic aromatic species.[53,54]

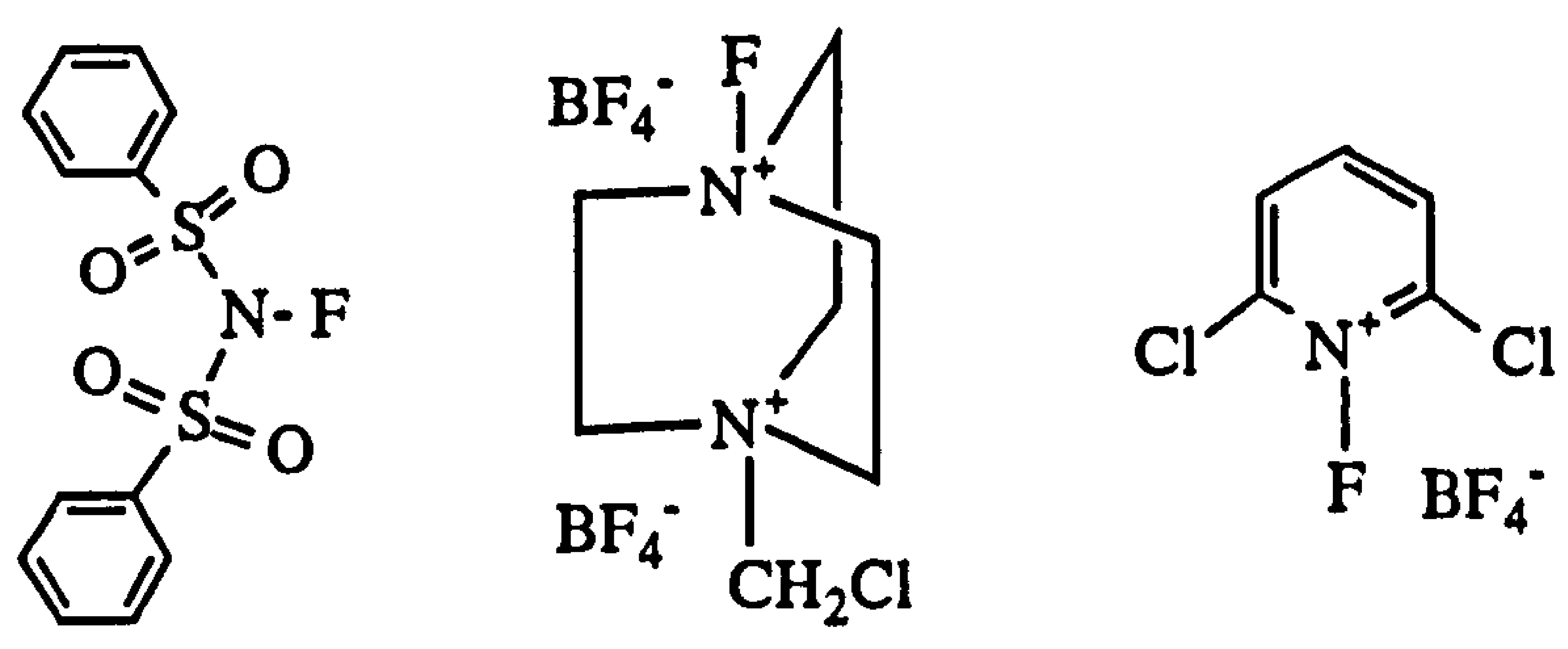

NFBS F-TEDA pyF+

figure 2.2: examples of electrophilic fluorinating agents; N-Fluorobenzenesulfonimide (NFBS), 1-(chloromethyl)-4-fluoro-1,4-diazoniabicyclo[2.2.2]octane bis(tetrafluoroborate) (F-TEDA, or F-TEDA-BF4), and 1-fluoro-2,6-dichloro-pyridinium tetrafluoroborate (pyF+).

In particular, *N*-Fluorobenzenesulfonimide (NFBS)[54], reacts with lithio-aromatics, effecting fluorination under relatively mild conditions and in reasonable yield. For example,

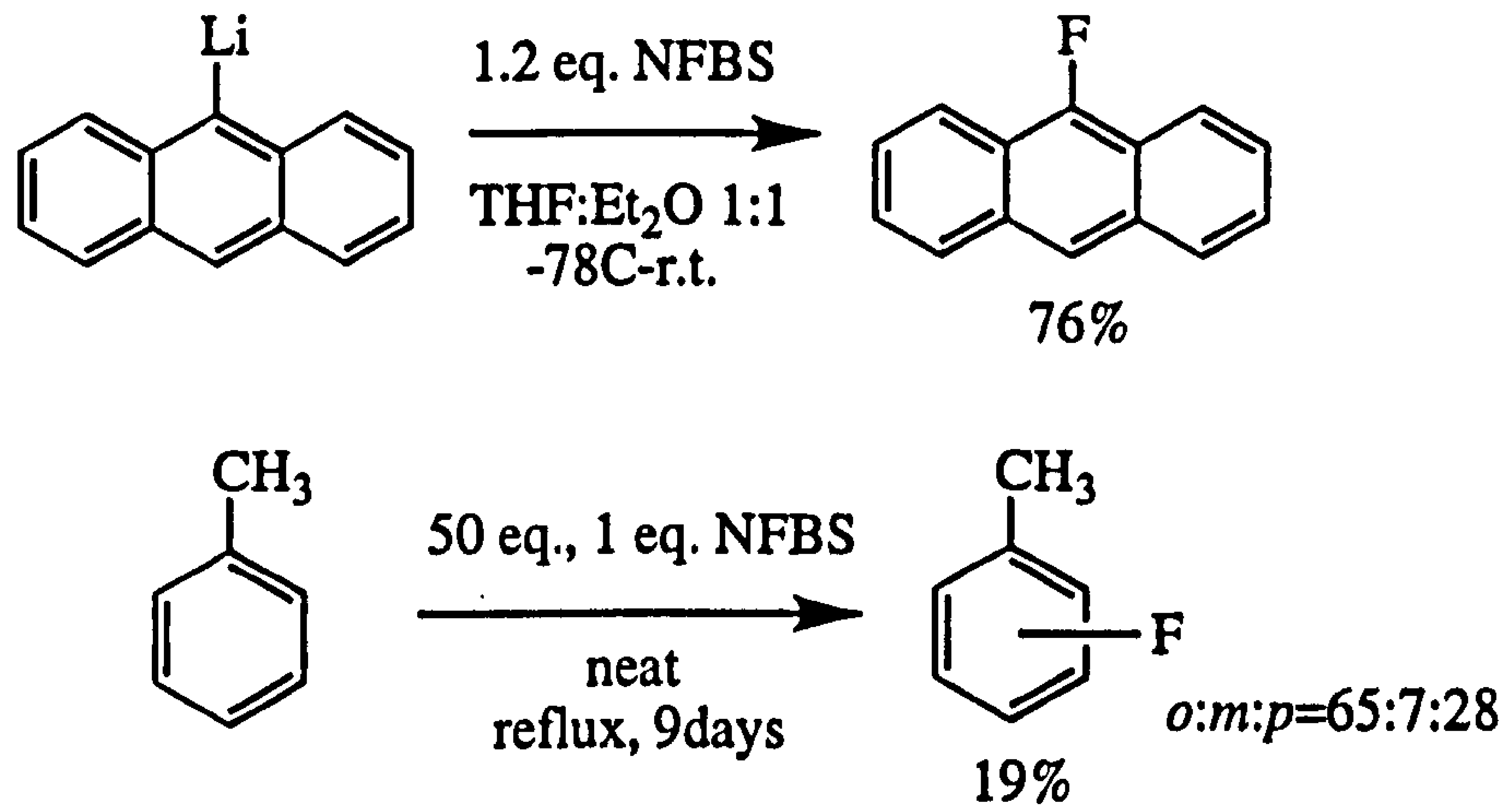

scheme 2.27: fluorination of aromatic systems by NFBS

Given the relative similarities of the lithio-aromatic and lithio-carboranyl systems, we decided to examine the possibility of fluorinating a carboranyl carbon, *via* the lithio-carborane intermediate, using the reagent NFBS. 1-fluoro-12-(phenylsulfonyl)-*para*-carborane and 1-phenyl-2-fluoro-*ortho*-carborane were successfully isolated (scheme 2.28), and NMR evidence indicated that this reagent also C-fluorinated other carborane derivatives, such as methyl-*ortho*-carborane and phenyl-*meta*- and *para*-carboranes (table 2.1).

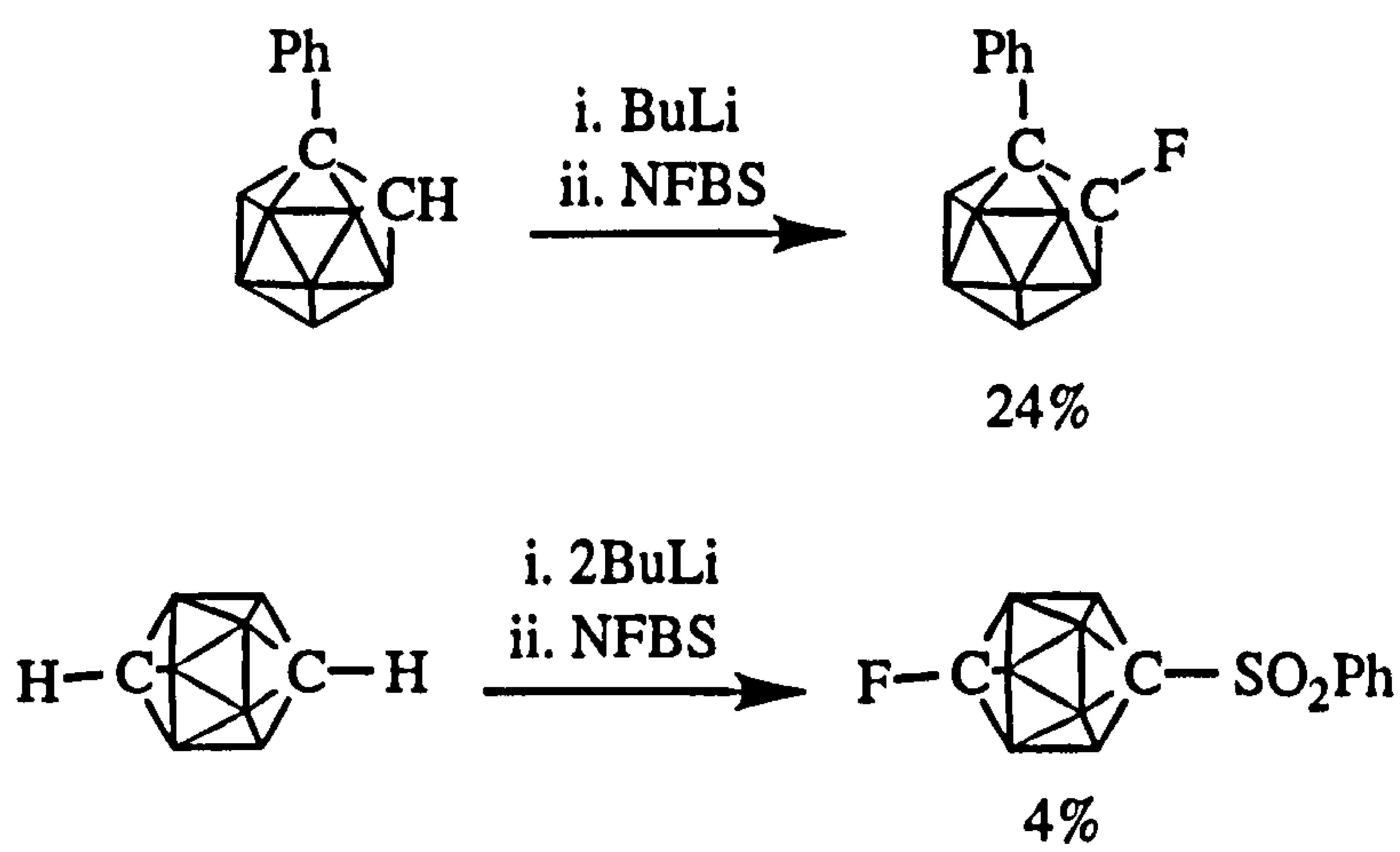

scheme 2.28: fluorination of carboranyl systems by NFBS

NFBS + R	δ ^{19}F / ppm	reaction product
o-$LiCB_{10}H_{10}CLi$	-154*	$B(OH)_3$
o-$MeCB_{10}H_{10}CLi$	-152	*o*-$MeCB_{10}H_{10}CF$ (not isolated)
o-$PhCB_{10}H_{10}CLi$	-149	*o*-$PhCB_{10}H_{10}CF$ (24%)
m-$LiCB_{10}H_{10}CLi$	-157	not isolated
m-$PhCB_{10}H_{10}CLi$	-157	*m*-$PhCB_{10}H_{10}CF$ (not isolated)
p-$LiCB_{10}H_{10}CLi$	-147.5	*p*-$PhSO_2CB_{10}H_{10}CF$ (4%)
p-$PhCB_{10}H_{10}CLi$	-150.64	*p*-$PhCB_{10}H_{10}CF$
n-BuLi	-220.1 (t of t, $^1J_{HF}$=48Hz, $^2J_{HF}$=24Hz)	$H_3CCH_2CH_2CH_2F$

* this peak is not observed in the final product

table 2.1: reaction summary of NFBS with lithio-carboranes

^{19}F NMR spectra showed a sharp singlet in the range -147 to -157ppm for the carboranyl C-F compounds, values typically seen for C-fluorinated aromatic systems. $^{13}C\{^1H\}$ NMR spectra showed the carboranyl fluorinated carbon as a doublet due to the C-F splitting. Coupling constants of 312.5Hz and 302.5Hz were observed for 1-phenyl-2-fluoro-*ortho*-carborane (figure 2.3) and 1-fluoro-12-(phenyl-sulfonyl)-*para*-carborane respectively. Some work has suggested that the C-F coupling constant is indicative of bond length.[55] If this obtains here, the carboranyl C-F bond would be short implying a degree of *exo*-π bonding between the cage carbon and the fluorine. This idea will be developed in Chapter Three.

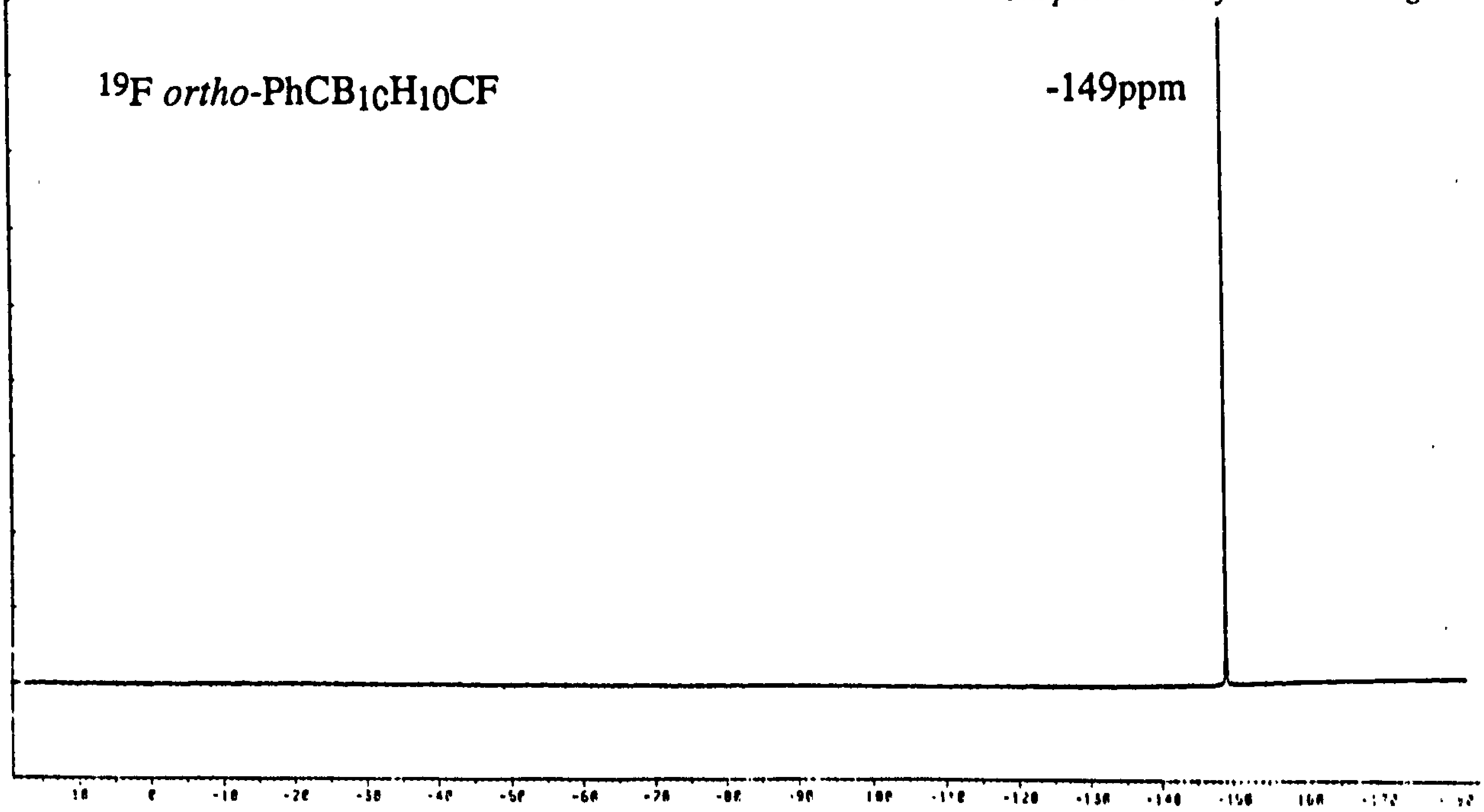

figure 2.3a: ^{19}F NMR spectrum of 1-fluoro-2-phenyl-ortho-carborane

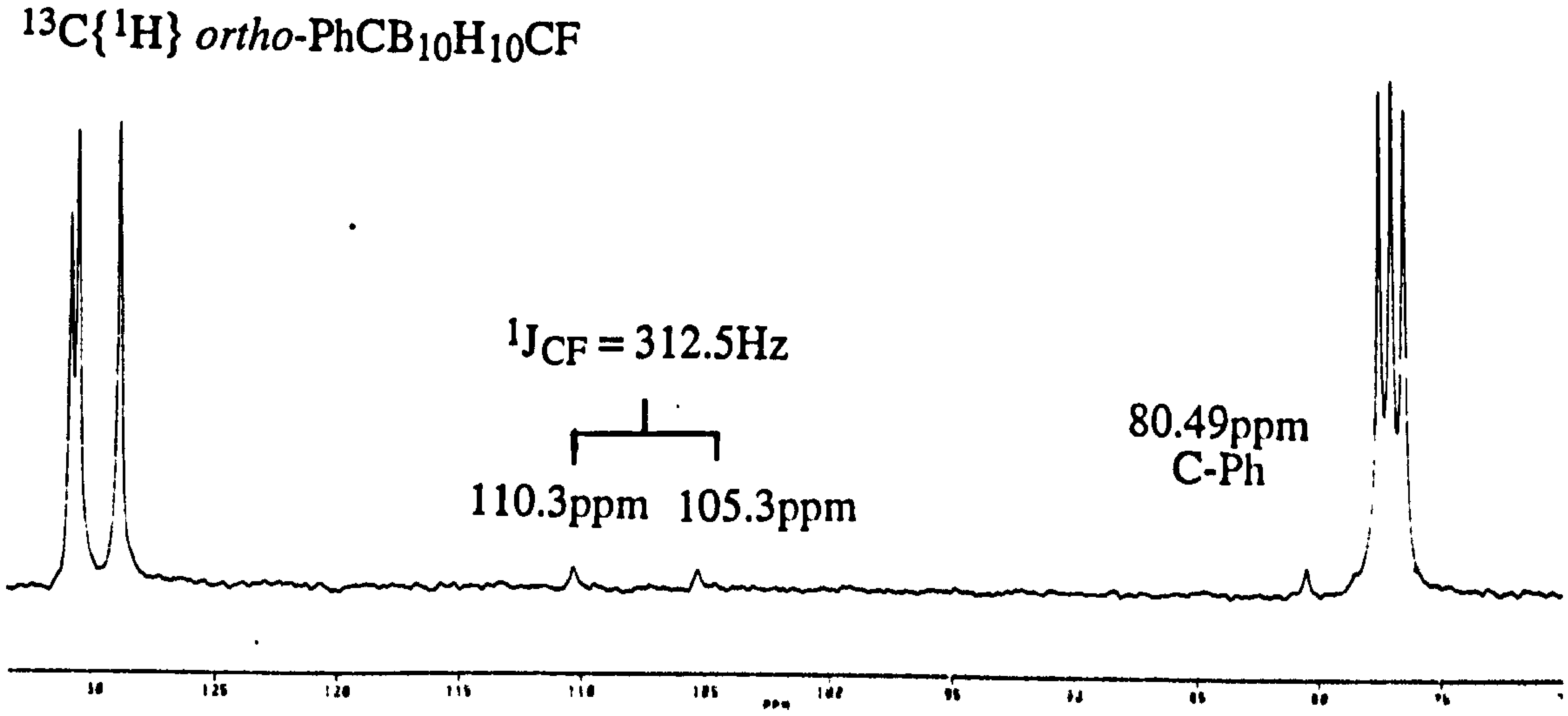

figure 2.3b: $^{13}C\{^1H\}$ NMR spectrum of 1-fluoro-2-phenyl-ortho-carborane

Increasing the reaction time, executing the reaction at a variety of temperatures and changing the reaction solvent did not augment the yields. However, although the yields of these fluoro-carboranes were not high, typically less than 25%, the reagents were safe, relatively easy to handle, and the reaction conditions were mild. Through NFBS, we have shown that fluorination of the carboranyl carbon atoms can be achieved, without the need for the specialised equipment required to handle other fluorinating agents such as HF, F_2 and perchloryl fluoride.

The reagent had a drawback however, and this was apparent in the reaction between dilithio-*ortho*-carborane and NFBS. The stability of the fluoro-carborane compounds was unknown, although the two isolated products named above appeared stable to air and moisture. It is known that the decafluoro-*ortho*- and *meta*-carboranes hydrolyse with cage degradation, in the presence of water or moist air, the *meta*-being the more stable and consequently taking longer to degrade. Ultimately both degrade to boric acid. The *para*-carborane derivative, *p*-$C_2H_2B_{10}F_{10}$ is stable to moisture, although refluxing with water in acetonitrile solution again results in complete degradation to boric acid.[42] In other C-halogenated system, generally C-halogenated carboranes are stable in the order *para* > *meta* > *ortho*, with the order of halogen stability being I>Br>Cl.[44,45] If this sequence were to continue, obviously the fluorinated derivatives would be the most labile, although this appeared to be disproven by the apparent stability of the above mentioned C-F carboranes.

In the reaction between dilithio-*ortho*-carborane and NFBS, the $C_2B_{10}H_{12}$ cage was degraded ultimately to boric acid (*c.f.* table 2.1), although initially some degree of fluorination did occur. Following the above stability scheme and given that fluoride ion is known to cause degradation in icosahedral cages (see Chapter Five), decomposition of difluoro-*ortho*-carborane ultimately to boric acid is a likely result.

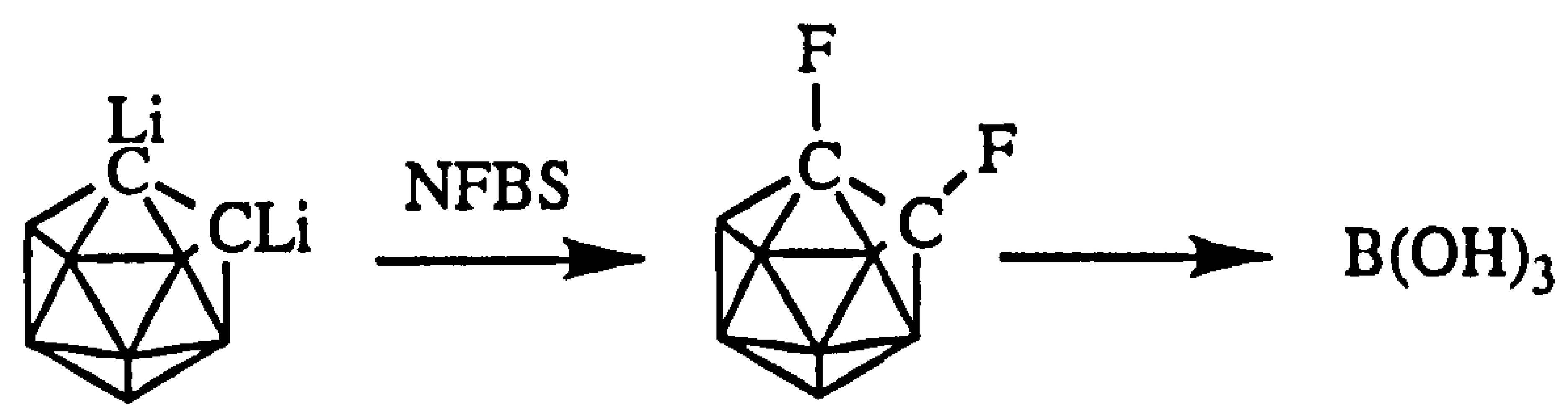

scheme 2.29: reaction between NFBS and di-lithio-ortho-carborane

Another drawback of NFBS was the production of sulfonylated side products. The serendipitous product, 1-phenyl-12-(phenylsulfonyl)-*para*-carborane (scheme 2.28), obtained from the reaction of dilithio*para*-carborane with NFBS, showed that perhaps this was not the ideal electrophilic fluorinating agent for carboranes. In the unisolated reaction products of a variety of lithio-carboranes with NFBS, infrared spectroscopic bands in the range 1350 -1440cm^{-1} indicated the presence of the S=O functionality. This led us to consider other electrophilic fluorinationg agents and pyF$^+$ as its tetrafluoroborate salt, was chosen as it seemed unlikely to lead to a variety of substitution products on the carborane.

The reaction between di-lithio-*ortho*-carborane and pyF$^+$ was followed by ^{19}F NMR spectroscopy and the formation of a variety of peaks in the aromatic C-F region noted, the same region in which we would observe carboranyl C-F species.

There was obviously a degree of fluorination occurring, perhaps the formation of mono- and di-fluoro-*ortho*-carboranes. However, with this particular NF reagent there was a side reaction which interfered with and in fact appeared to dominate the desired reaction pathway, and that was the migration of the F^+ to a ring position.

$$(PhSO_2)_2NF + n\text{-}BuLi \longrightarrow CH_3CH_2CH_2CH_2F + (PhSO_2)_2NLi$$

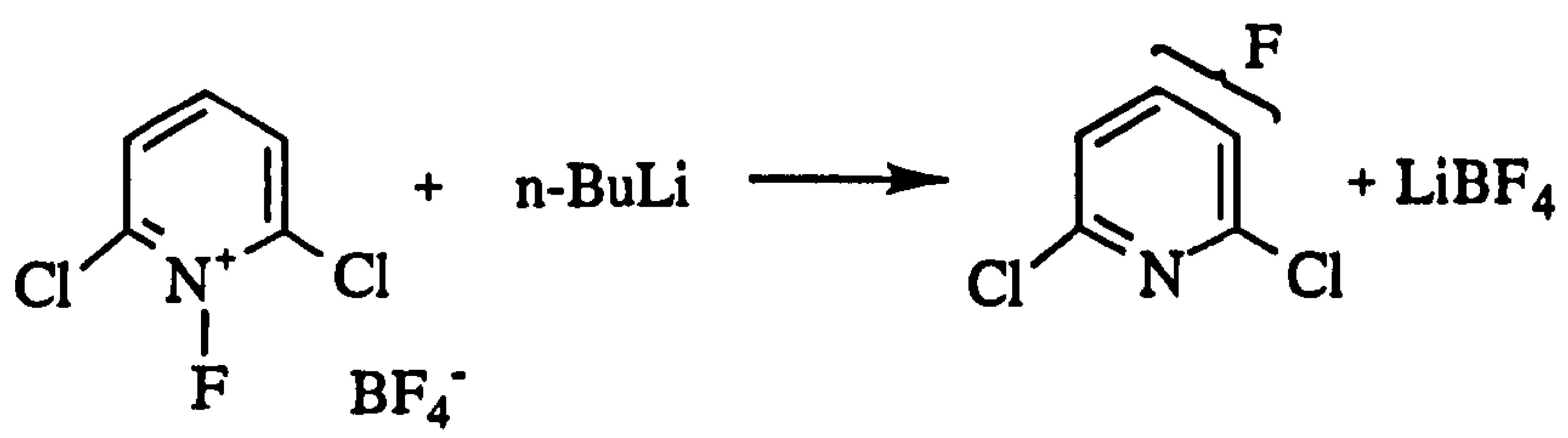

scheme 2.30: control reactions of NF reagents with butyl lithium

In the syntheses discussed earlier, as a control reaction for the identification of side products, NFBS was reacted with Li^+ (in the form of BuLi). The product was found to be 1-fluorobutane, evident as a triplet of triplets at -220ppm in the ^{19}F NMR spectrum. This chemical shift was not observed in any reaction between a lithio-carborane and NFBS, indicating that the fluorine of NFBS formed the fluoro-carborane and not lithium fluoride. However, where the NF reagent was pyF^+, there was a problem in that pyF^+ rearranged in the presence of Li^+ (from BuLi) to give a strong fluorine signal at -157ppm indicating the fluorine had migrated to a carbon ring position.

This same signal was observed in reactions between dilithio-*ortho*-carborane and pyF^+ ($\delta(^{19}F)$ = -157ppm), and lithiated phenyl-*ortho*-carborane and pyF^+($\delta(^{19}F)$ = -158ppm). At this stage it was unclear whether the carborane was being fluorinated or if the pyF^+ was simply rearranging. However, on working up the reaction of phenyl *ortho*-carborane and pyF^+, the major product was found to be 1-phenyl-*ortho*-carborane. Obviously ring substitution of the pyridyl group was taking place, and any carboranyl C-F substitution was a minor side reaction.

Of the two NF reagents tried, NFBS proved to be the more successful at effecting cage carbon fluorination, although it did lead to a degree of sulfonylated side-products. In order to evaluate the electronic effects the fluorine and sulfonyl entities independently exert on the carborane cage, the synthesis of sulfonylated carboranes was investigated.

2.3.6 Sulfonylation

On investigation of the reaction between lithio-carboranes and the sulfonyl halides, RSO_2Cl and RSO_2F, we discovered that, most probably as a result of the differing electronegativities of the respective halogens, we could achieve either chlorination (with $PhSO_2Cl$) or sulfonylation (with $PhSO_2F$) of the carboranyl carbon atoms using these reagents. On reaction of lithio-carborane with benzene sulfonyl chloride, the sulfonylated carboranyl product was anticipated. However, only the chlorinated product was formed. Reviewing earlier work[44], a similar observation had been made where *p*-tolyl-sulfonyl chloride led to C-chlorinated carboranes. The reaction worked well for *para*-carboranyl isomers but unfortunately, was not so successful for *ortho* and *meta* derivatives.

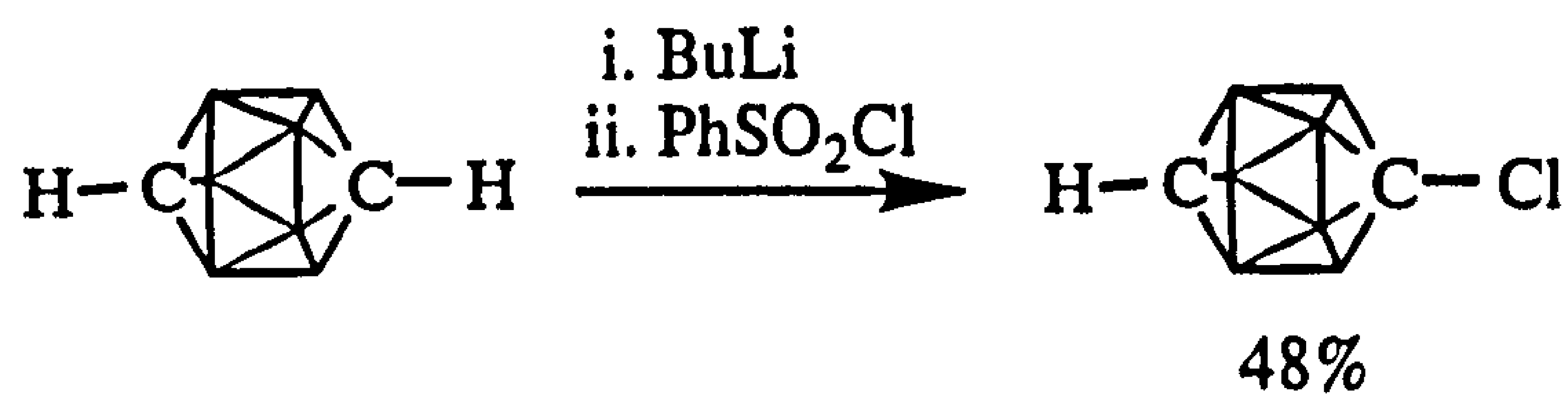

scheme 2.31: reaction of lithio-carboranes with benzene sulfonyl chloride

Following on from this result, benzenesulfonyl fluoride would be expected to be the ideal reagent to effect fluorination, and so improve drastically the efficiency with which fluorinated carboranes could be produced. However, as has been noted for the reaction of aryl sulfonyl fluorides with metallo-aryl species,[56] no fluorination was observed and sulfonylated carborane was the unique product. This result led to the development of a simple one-pot method involving safe, readily available reagents which avoided the use of the more hazardous oxidising agents and forcing conditions which have been used previously (section 2.2.5).

In the example of *para*-carborane, monolithiated with BuLi, only disulfonylated carborane was produced - no mono substituted carborane was found, and unreacted carborane was recovered by sublimation .

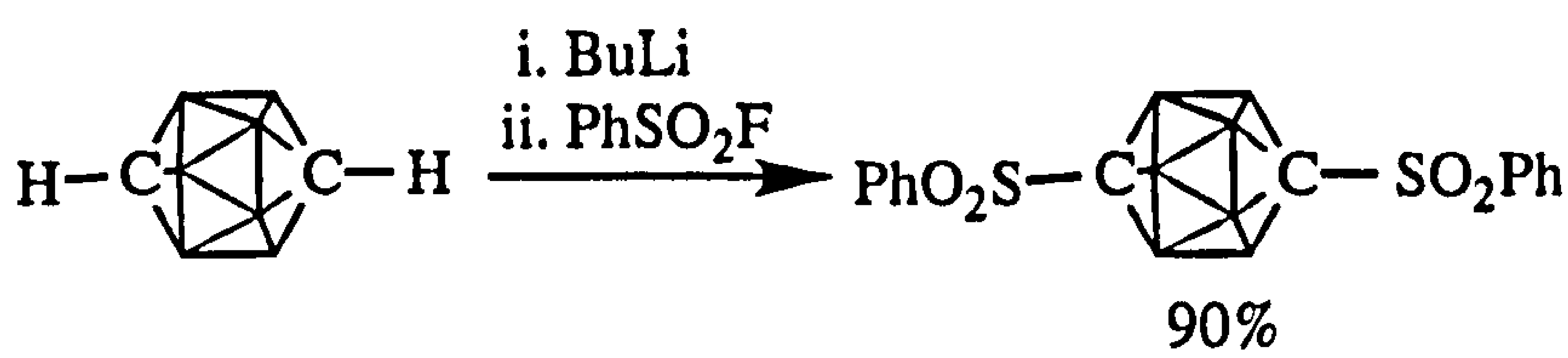

scheme 2.32: reaction of lithio-carborane and benzene sulfonyl fluoride

Similar results have been observed in wholly aromatic systems.[56,57] In these systems direct sulfonylation methods are again rare, however this disulfonylation effect with arenesulfonyl fluorides has been found in reactions involving alkyl organometallic reagents possessing an α-proton.

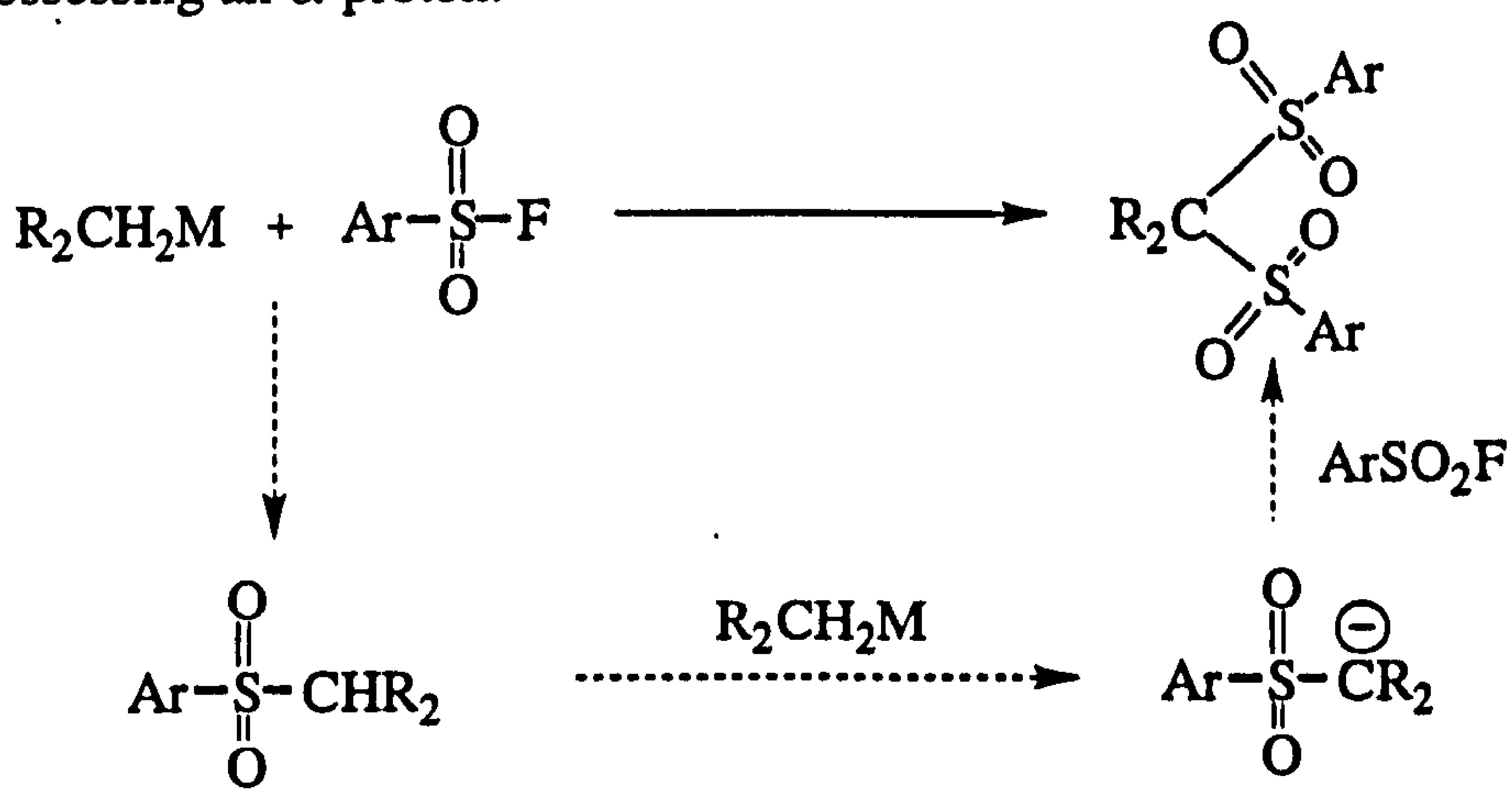

scheme 2.33: mechanism of disulfonylation of alkyl groups with aryl sulfonyl fluoride

This mechanism is easily transferred to the *para*-carboranyl system, and also supports the argument of disulfonylation in *ortho*-carboranes being prevented by steric hindrance.

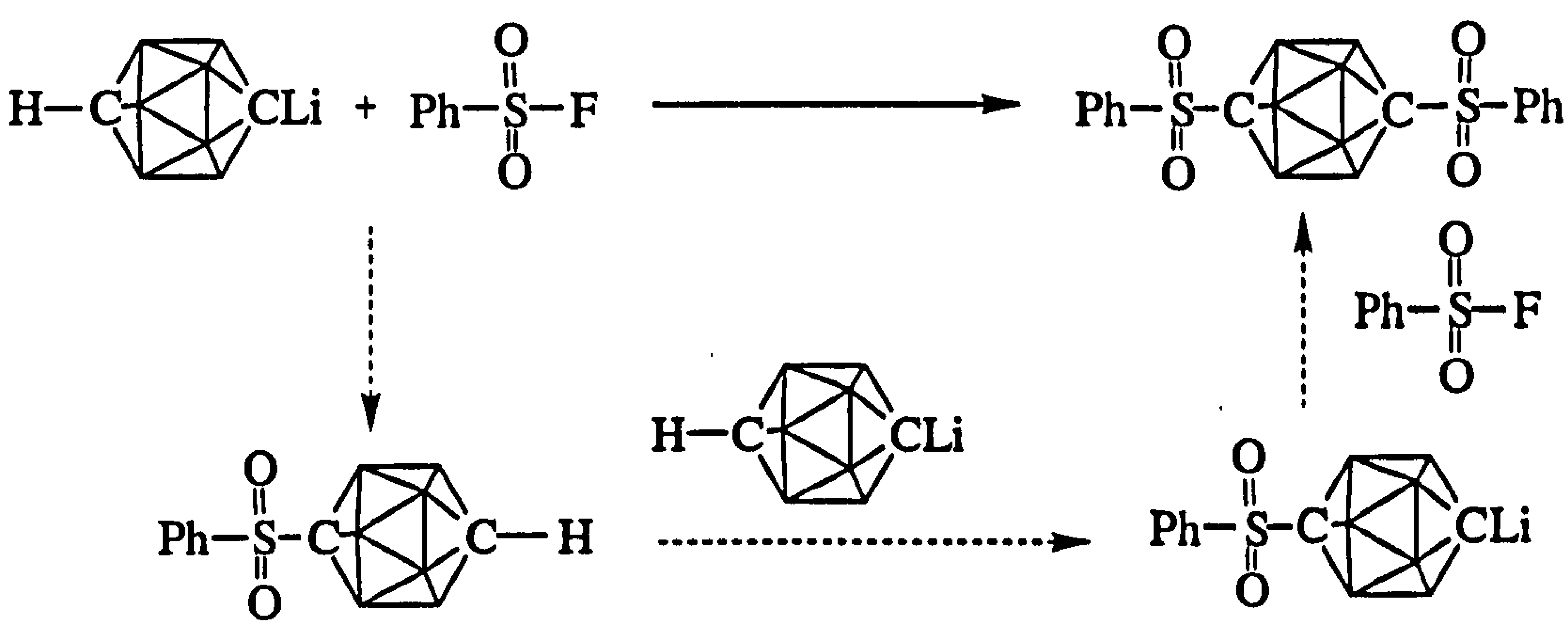

scheme 2.34: mechanism of di-sulfonylation of para-carborane with benzene sulfonyl fluoride

Where the second carbon was previously substituted, mono-sulfonylated products were obtained. Apart from examples in which the second carbon was protected with a silyl group, where the silyl functionality was cleaved by F^- and left the carborane unreacted, this reagent worked well for all three carborane isomers, in yields of 33%, 72% and 97% for the mono-phenyl-*ortho*, *meta* and *para*-isomers respectively. The yield of the *ortho*-isomer may have been hampered as a result of the bulky $-SO_2Ph$ group attacking the already sterically hindered C(2) position of the 1-phenyl-*ortho*-carborane.

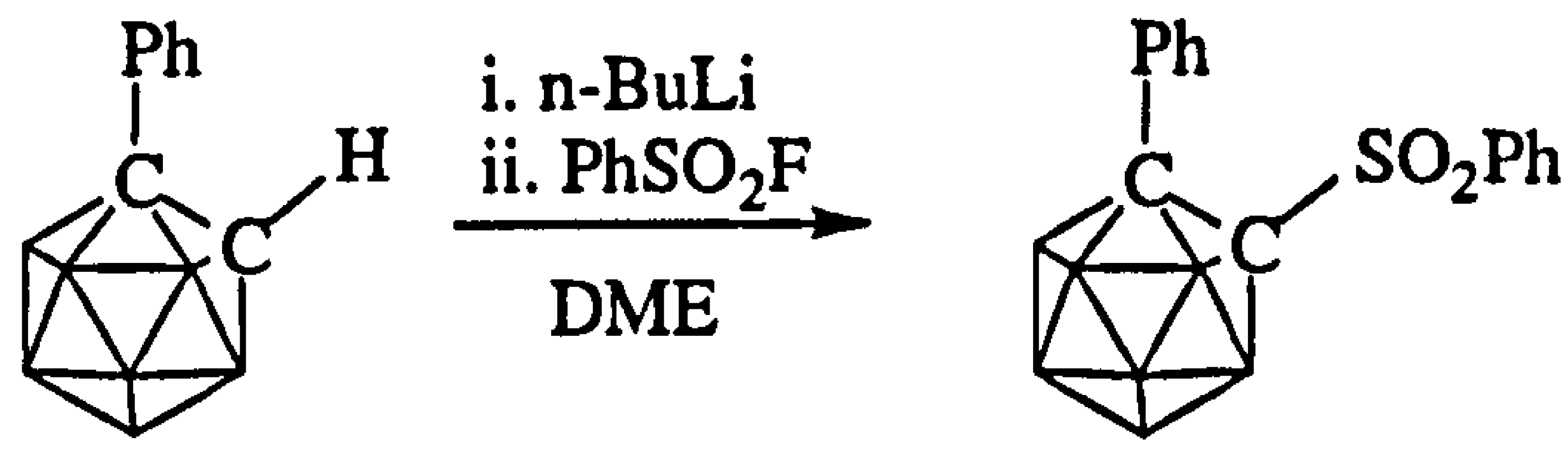

scheme 2.35: sulfonylation of substituted carboranes

$PhSO_2F$ + Cb	product	yield
o-$HCB_{10}H_{10}CLi$	*o*-$HCB_{10}H_{10}CSO_2Ph$	27%
o-$PhCB_{10}H_{10}CLi$	*o*-$PhCB_{10}H_{10}CSO_2Ph$	33%
m-$PhCB_{10}H_{10}CLi$	*m*-$PhCB_{10}H_{10}CSO_2Ph$	72%
p-$HCB_{10}H_{10}CLi$	*p*-$PhSO_2CB_{10}H_{10}CSO_2Ph$	90%
p-$LiCB_{10}H_{10}CLi$	*p*-$PhSO_2CB_{10}H_{10}CSO_2Ph$	90%
p-$PhCB_{10}H_{10}CLi$	*p*-$PhCB_{10}H_{10}CSO_2Ph$	97%
p-$R_3SiCB_{10}H_{10}CLi$	*p*-$HCB_{10}H_{10}CH$	100%

table 2.2: reaction summary of benzene sulfonyl fluoride with lithio-carboranes

The carborane substitution reaction is analogous to the reaction between a metallated aryl ring, (where there is no possible second metallation position), and aryl sulfonyl fluoride where no disulfonylated products are observed.[57]

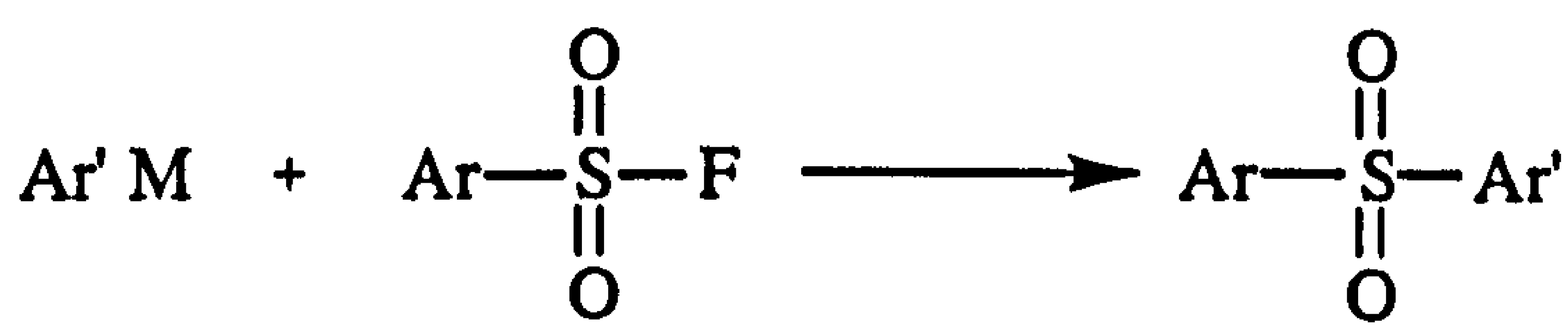

scheme 2.36: sulfonylation of an aryl ring with arylsulfonyl fluoride

Previous work in the field of polymer chemistry has investigated, amongst others, poly-(arylene sulfones)[58] and poly-(arylene ether sulfones)[59], aromatic systems which contain SO_2 linkages. Carboranes themselves have been studied within the context of polymer chemistry and found to produce durable, high strength, high quality materials. With this simple synthesis of sulfonylated carboranes, there is no obvious reason why functionality cannot be incorporated into the aryl ring of the arylsulfonyl fluoride to give further derivatisation options, including perhaps a system suitable for polymerisation (scheme 2.37).

$$Ar(OM)_2 + Ar'X_2 \longrightarrow [Ar\text{-}O\text{-}Ar'\text{-}O] + 2MX$$

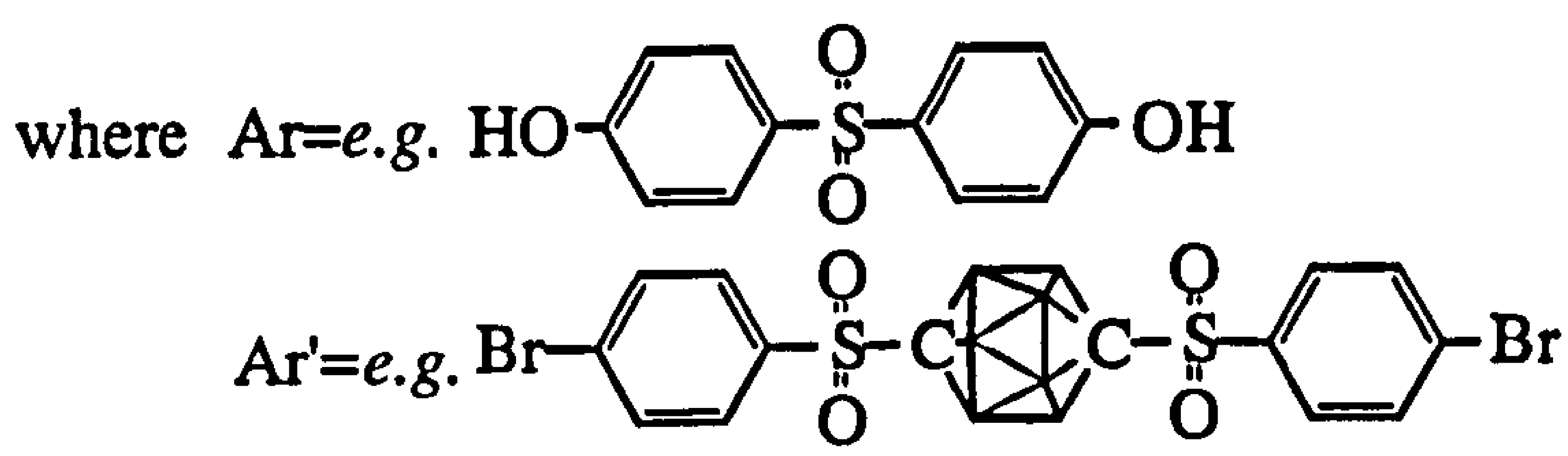

M=alkali metal
X=halogen

scheme 2.37: possible monomers for polymerisation of sulfonylated carboranes following the given reaction scheme

2.3.7 Aryl and Heteroaryl Carboranes

a) *ortho*-carboranes

Mono-aryl-*ortho*-carboranes can be prepared from the aryl-alkyne derivative and decaborane, or from the carboranyl copper derivative and aryl iodide or bromide as described in section 2.2.2. For specific cases, certain routes are preferred depending on the ease with which the relevant acetylene can be prepared. Where we wish to substitute an aryl or heteroaryl functionality onto both carbons, there is the factor of steric bulk to consider. For example, di-(phenyl)-*ortho*-carborane is preferentially prepared from 1,2-di-(phenyl)-acetylene.

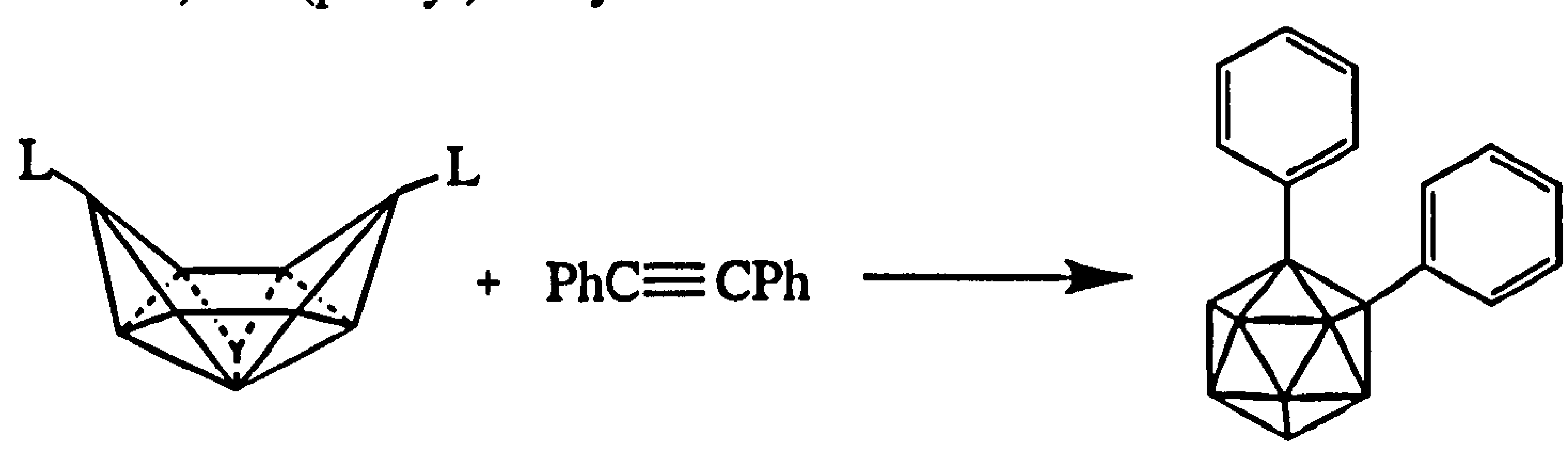

scheme 2.38: synthesis of 1,2-di-(phenyl)-ortho-carborane

As in many examples of organic chemistry, heterocycles show subtle differences in chemical reactivity. In the known reaction of 2-bromo-pyridine with *ortho*-carborane via the copper coupling reaction[13], di-(2'-pyridyl)-*ortho*-carborane is the unique product, possibly as a result of intramolecular hydrogen bonding causing activation of the second carboranyl carbon position. To further examine hydrogen bonding effects in heteroaryl-carboranes, the syntheses of 3'-pyridyl and 2'-thiophenyl-*ortho*-carboranes were carried out.

The reaction of 3-bromopyridyl and cuprocarborane was found to give only mono-substituted product irrespective of reactant quantities. Crystallographic data on crystals grown from ethanol/water showed this pyridyl derivative to exhibit inter-molecular hydrogen bonding. Unlike the 2'-pyridyl analogue, there was no intra-molecular hydrogen bonding effect and the carborane remained mono-substituted as the pyridine ring was sufficiently bulky to hinder disubstitution. If the di-3'-pyridyl system were required, the acetylene would need to be prepared then reacted with decaborane.[60]

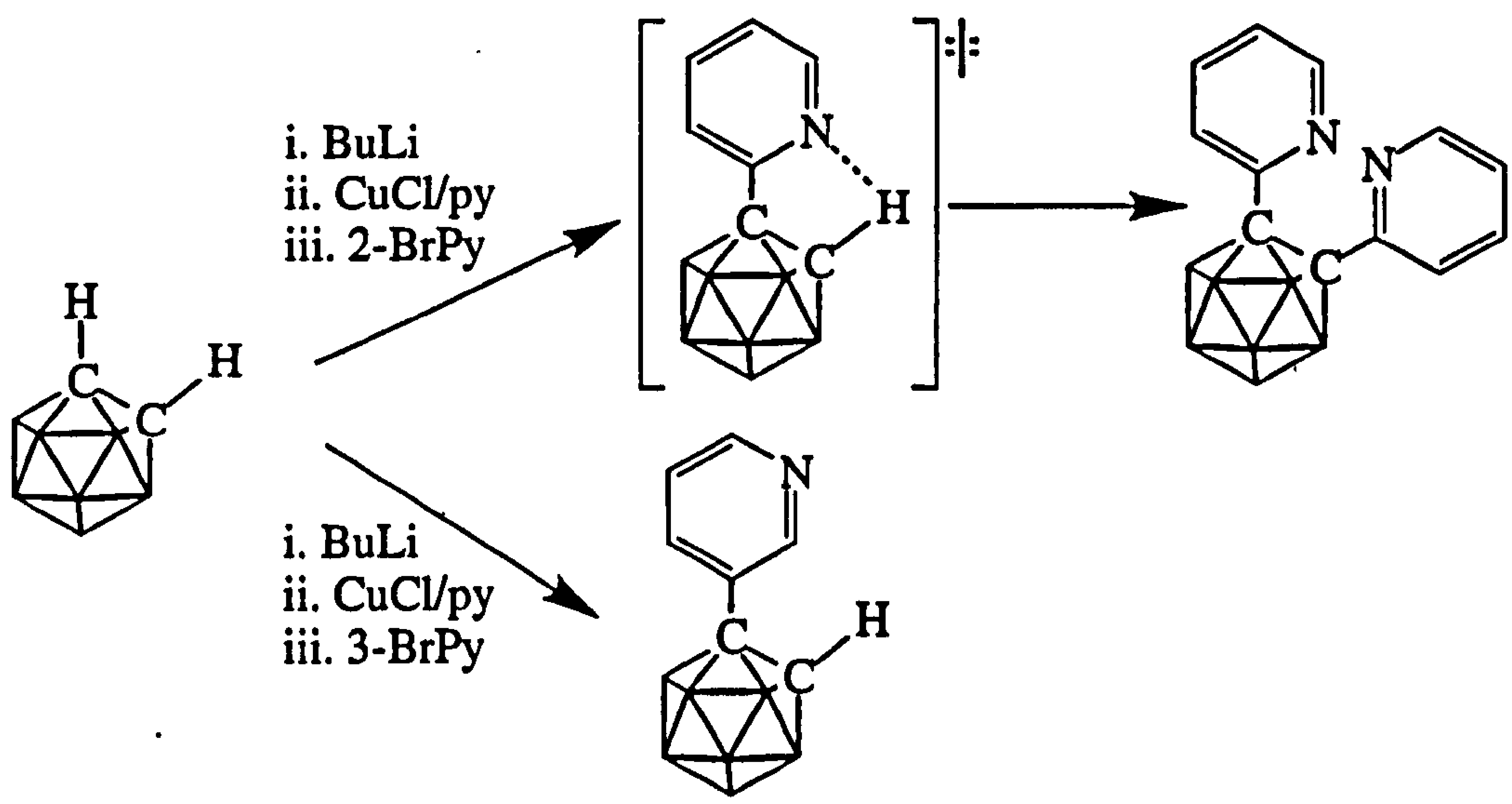

scheme 2.39: syntheses of 2'- and 3'-pyridyl ortho-carboranes

Reaction of lithio-*ortho*-carborane with 2-iodo-thiophene gave mono-thiophenyl *ortho*-carborane[61] as the unique product. Crystallisation from chloroform yielded X-ray quality crystals which although disordered, showed some intramolecular hydrogen bonding to be present. Infrared spectroscopy conversely showed intermolecular hydrogen bonding to be present. (This will be discussed further in Chapter Three.) This hydrogen bonding interaction between the ring sulfur and the carboranyl proton might have been expected to give di-substituted product as in the 2'-pyridyl example, however, sulfur is considerably larger than nitrogen so the second carboranyl carbon is quite heavily protected from substitution by the sheer bulk of the thiophenyl ring.

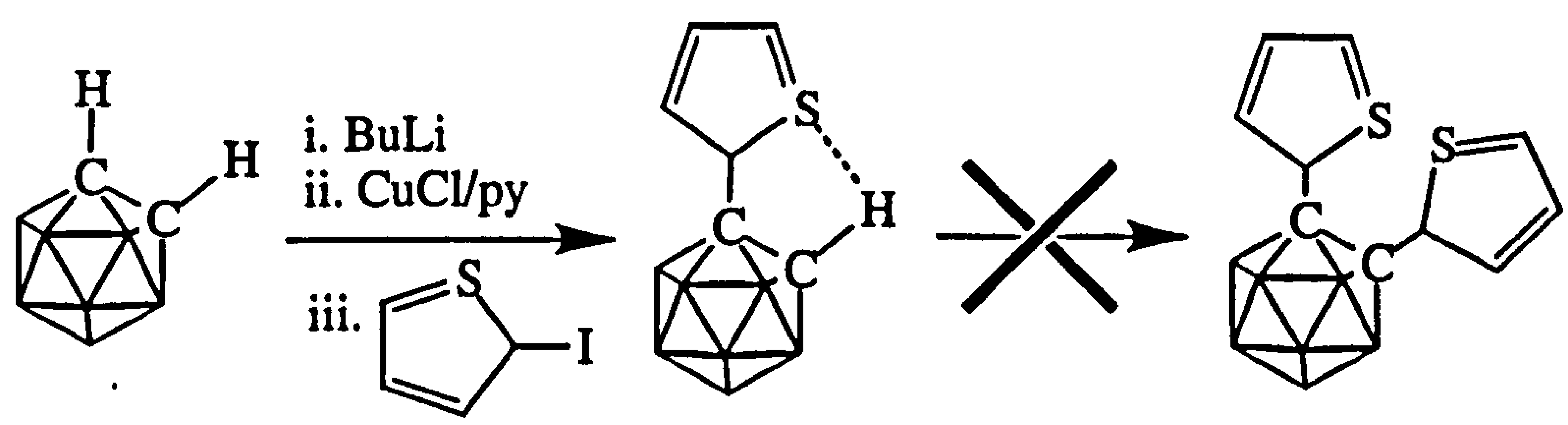

scheme 2.40: synthesis of thiophenyl ortho-carboranes

b) *meta*-carboranes

To form the *meta*-carboranyl analogues of the above compounds, the synthetic strategy was to go via the carboranyl copper intermediate. To form the mono-substituted derivatives, the reaction was straightforward and high yielding, however, when the appropriate quantities to form the di-substituted derivatives were reacted, mono-arylated carborane was the predominant product, with the desired di-arylated carborane only being obtained in low yield.

The reaction of lithio-*meta*-carborane with 3-bromopyridine in the presence of Cu(I) and pyridine gave mono-substituted product in 54% yield with only a trace amount of di-substituted product being recovered. The same was true of the reaction between 2-iodo-thiophene and *meta*-carborane where 1-(2'-thiophenyl)-*meta*-carborane was the major product.

Why this should be is unclear, although there may a problem in that the copper forms a stable or insoluble complex with the mono-pyridyl or mono-thiophenyl *meta*-carborane which hinders reaction at the second carbon position.

2.4 EXPERIMENTAL DETAILS

1-Bromomethyl-*ortho*-carborane[62]

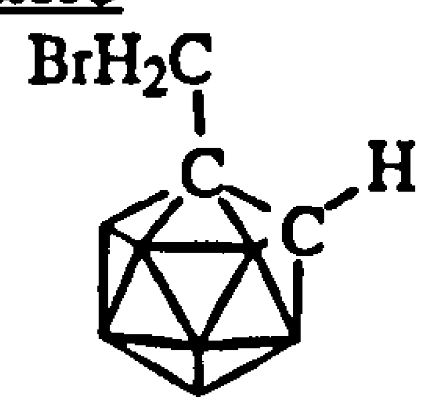

1-bromomethyl-*ortho*-carborane was prepared according to literature methods from the reaction of decaborane (23.92g, 0.2mmol) with propargyl bromide (15mL, 0.23mol). The crude product was isolated as a yellow oil which distilled (83.5 - 86°C, 0.01mm Hg) to give a clear liquid distillate which solidified to a white crystalline solid on standing (37.5g).

Yield : 78% *IR*: 3065 m (carboranyl C-H); 3032 m; 2979 m; 2840 w; 2617 br. s (carboranyl B-H); 1849 w; 1426 s; 1249 s; 1185 s; 1122 s; 1060 s; 1015 s; 1002 s; 972 w; 935 m; 914 s; 882 s; 820 s; 782 m; 761 w; 721 s; 682 s; 665 s; 633 s; 595 w; 556 m; 500 m; 450 m cm^{-1} *m/z*(EI$^+$): 472 (dimer); 392; 237 ($C_3B_{10}H_{13}Br$) *Elemental analysis* ($C_3B_{10}H_{13}Br$): C 15.27% (15.19%), H 5.50% (5.53%), Br 33.74% (33.70%) *m.p.*: 33.3°C

NMR ($CDCl_3$)/ppm: ^{1}H: 4.01(1H, br. s, carboranyl C-*H*), 3.97(2H, s, methyl C-*H*), 3.6-1.1(10H, br., carboranyl B-*H*); $^{13}C\{^1H\}$: 71.63 (carboranyl *C*-CH_2Br), 61.65 (carboranyl *C*-H), 32.92 (*C*H_2Br)

1-methyl-*ortho*-carborane[63]

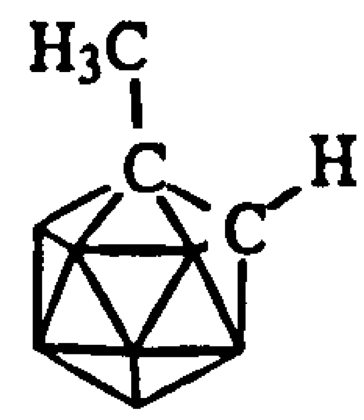

1-methyl-*ortho*-carborane was prepared according to literature methods from the reaction of 1-bromomethyl-*ortho*-carborane (25.26g, 0.11mol) with magnesium filings (3.1g, 0.13mol, 20% excess) and subsequent hydrolysis of the resulting Grignard. (A few drops of dibromoethane were added to help initiation of the Grignard reaction). The crude product was recrystallised from methanol (gave a sticky white solid), then sublimed under dynamic vacuum giving the desired product as a white crystalline solid (7.81g).

Yield : 45% *IR* : 3061 s (carboranyl C-H); 2999 w; 2944 s (methyl CH_3); 2871 s; 2635 br.,s (carboranyl B-H); 1851 m; 1444 s; 1389 s; 1261 w; 1228 m; 1131 s; 1095 s; 1081 s; 1033 s; 1015 s; 996 s; 974 m; 934 m; 915 m; 901 m; 881 m; 785 s; 768 m; 720 s; 675 m; 655 m; 591 w; 495 m; 459 w cm^{-1} *m/z*(EI^+): 316 ($(CH_3C_2B_{10}H_{10})_2$); 158 ($C_3B_{10}H_{14}$)
NMR ($CDCl_3$)/ppm: ^1H: 3.57 (1H, br. s, carboranyl CH), 2.02 (3H, s, methyl CH), 3.5-0.8 (10H, br., carboranyl BH)

1-phenyl-*ortho*-carborane[1]

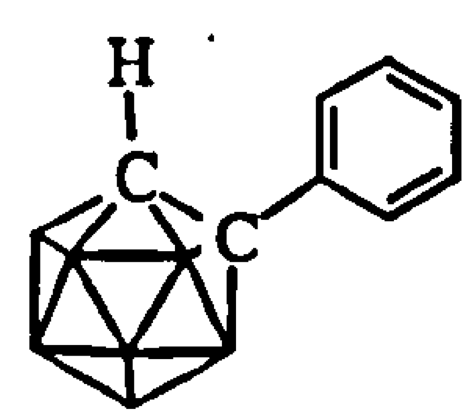

1-phenyl-*ortho*-carborane was prepared according to literature methods from the reaction of decaborane dimethylsulfide (24.9g, 0.1mol) with phenyl acetylene (11.5mL, 0.1mol). The crude product was distilled under dynamic vacuum (0.01mm Hg, 92-98°C) giving a white solid residue which was recrystallised from acetic acid, then sublimed under dynamic vacuum (75°C) to give a white crystalline solid (14.87g).

Yield : 68% *IR* : 3110 w (phenyl CH); 3082 s (carboranyl CH); 3038 m (phenyl CH); 2642 m, 2605 s, 2565 s (carboranyl BH); 1581 w; 1494 s; 1473 w; 1446 s; 1337 w; 1160 m; 1067 s; 1037 m; 1017 m; 1001 s; 913 w; 874 w; 799 m; 749 m; 734 m; 724 m, 685 s; 667 m; 601 w; 561 m; 487 m cm^{-1} *m/z* (EI^+): 220 ($C_8B_{10}H_{16}$) *Elemental analysis* ($C_8B_{10}H_{16}$): C 43.48% (43.61%), H 7.46% (7.32%) *m.p.*: 68.4°C

NMR ($CDCl_3$)/ppm: ^1H: 7.51, 7.47, 7.36 (5H, m, phenyl CH); 3.97 (1H, br. s, carboranyl CH); 4.0-1.0 (10H, br., carboranyl BH); $^{13}C\{^1H\}$: 130.6, 129.5, 128.2 (phenyl CH), 60.86 (carboranyl CH)

1-phenyl-*meta*-carborane and 1,7-di-phenyl-*meta*-carborane[13]

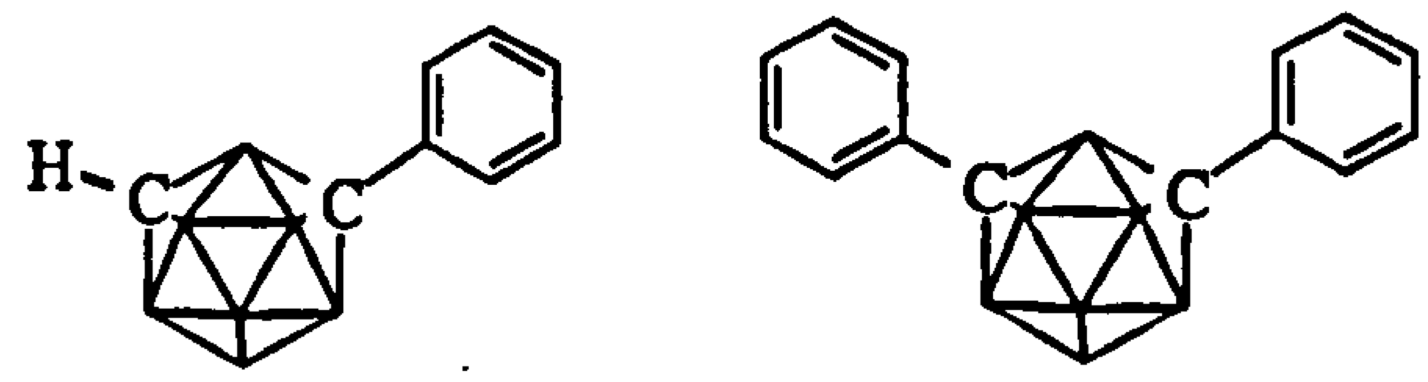

Meta-carborane (2.86g, 20mmol) was dissolved in DME (100mL) monolithiated with a solution of n-BuLi (2.38M in hexanes, 8.6mL, 20mmol) and left to equilibrate at room temperature under N_2 for 20 minutes. Against a flow of N_2, CuCl (1.98g, 20mmol) was added then pyridine (14mL) and the resulting cloudy brown solution refluxed for 30 minutes. Iodobenzene (2.5mL, 22mmol) was added and the solution left to reflux for a further 48 hours. The refluxing solution was cooled to room temperature, and stirred with diethyl ether (150mL) at room temperature for several hours to destroy the copper-pyridine complex. The solution was filtered and the filtrate transferred to a separating funnel, washed with 2M HCl (2 x 75mL), then with distilled water (2 x 75mL). The organic layers were dried over $MgSO_4$, filtered, and the solvent removed under reduced pressure to give a brown solid which was sublimed under dynamic vacuum (62°C) to give a white solid (1.59g). This identified as 1-phenyl-*meta*-carborane. The nonsublimed residue was dissolved in diethyl ether, decolourised with activated charcoal and filtered. The solvent was allowed to evaporate slowly to give a crystalline solid (0.46g) which analysed as 1,7-diphenyl-*meta*-carborane.

1-phenyl-meta-carborane

Yield : 36% *IR*: 3092 w, 3062 m (carboranyl C-H), 3054 m (phenyl C-H); 2604 br., s (carboranyl B-H); 1495 s; 1447 s; 1261 m; 1133 w; 1080 s; 1047 m; 875 m; 835 w; 806 m; 740 s; 691 s; 663 w; 605 w; 577 w; 527 w; 491 m cm^{-1} *m/z* (EI^+): 220 ($C_8H_{16}B_{10}$), 143 ($C_2H_{11}B_{10}$) *m.p.*: 42-43°C

NMR ($CDCl_3$)/ppm: ^1H: 7.4 (2H, m, phenyl CH), 7.3 (3H, m, phenyl C-*H*), 3.08 (1H, s, carboranyl C-*H*), 4.4-0.8 (10H, br., carboranyl B-*H*); $^{13}C\{^1H\}$: 135.6 (*ipso C*), 129.2, 128.8, 128.2 (phenyl *C*-H), 78.9 (carboranyl *C*-phenyl), 55.5 (carboranyl *C*-H); $^{11}B\{^1H\}$: -4.19 (1B), -9.01 (1B), -10.69 (4B), -13.68 (2B), -15.41 (2B)

1,7-diphenyl meta carborane

Yield: 0.46g, 2mmol *IR*: 3092 w, 3062 w, 3040 w, 3024 w (phenyl CH); 2622 m, 2604 s, 2586 s (carboranyl BH); 1495 w; 1445 w; 1385 w; 1261 s; 1099 s; 1083 s; 1023 s; 874 w; 851 w; 801 s; 743 w; 690 m cm^{-1} *m/z*(EI^+): 296 ($C_{14}B_{10}H_{20}$), 220 ($C_7B_{10}H_{15}$) *m.p.*: 117-118.5°C

NMR ($CDCl_3$)/ppm: ^1H: 7.48 (4H, m, phenyl CH), 7.2 (6H, m, phenyl CH), 4-1 (10H, br., carboranyl BH)

1-phenyl-*para*-carborane and 1,12-di-phenyl-*para*-carborane

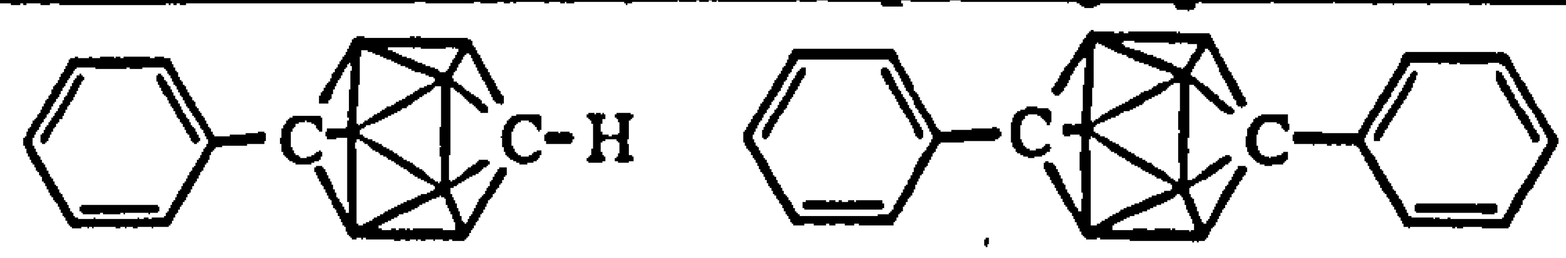

Para-carborane (5.78g, 40mmol) was dissolved in dry DME (200mL) and monolithiated with a solution of butyl lithium (2.38M in hexanes, 16.9mL, 40mmol) to give a pale yellow solution after 20 minutes equilibration at room temperature. CuCl (3.98g, 40mmol) was added against a flow of N_2, followed by pyridine (26mL) giving a dark brown cloudy solution which was refluxed for 30 minutes. Iodobenzene (5mL, 44mmol) was added and the solution left to reflux for 3 days.

The resulting cloudy red solution was cooled to room temperature, diethyl ether (150mL) added and the solution stirred for 3 hours at room temperature to destroy the copper-pyridine complex. The resulting precipitate was filtered off and the filtrate transferred to a separating funnel where it was washed firstly with 2M HCl (2 x 75mL) then with distilled water (2 x 75mL). The aqueous layers were re-extracted with diethyl ether, then the combined organic layers dried over $MgSO_4$, filtered, and the solvent removed under reduced pressure. The resulting residue was sublimed (50°C) to give 1-phenyl-*para*-carborane as a white solid. Unsublimed residue was 1,12-diphenyl-*para*-carborane.

1-phenyl-para-carborane

Yield : 60% *IR*: 3092 w (phenyl C-H); 3057 s (carboranyl C-H); 3024 w (phenyl C-H); 2598 s (carboranyl B-H); 1494 s; 1475 w; 1446 s; 1138 m; 1083 s; 1021 w; 1003 m; 909 w; 893 w; 830 m; 773 s; 741 s; 691 s; 672 m; 607 m; 582 w; 489 s cm^{-1} *m/z* (EI^+): 220 ($C_8B_{10}H_{16}$) *Elemental analysis* ($C_8B_{10}H_{16}$): C 43.76% (43.61%), H 7.29% (7.32%) *m.p.*: 99-100°C *b.p.*: 327-330°C

NMR ($CDCl_3$)/ppm: $^1H\{^{11}B\}$: 7.21 (3H, d, J_{HH} *c.* 7.5Hz; t, J_{HH} *c.* 7.5Hz, *ortho* and *para* C-*H*); 7.18(2H, t, J_{HH} *c.* 7.5Hz, *meta* C-*H*); 2.78 (1H, sextet, J_{HH} *c.* 3.5Hz, carboranyl C-*H*); 2.53 (5H, B(2)-B(6)); 2.29 (5H, B(7)-B(11)); $^{13}C\{^1H\}$: 136.7 (*ipso*

C), 128.2 (*para C*), 128.0 (*meta C*), 126.9 (*ortho C*), 86.4 (carboranyl *C*-phenyl), 59.7 (carboranyl *C*-H); $^{11}B\{^{1}H\}$: -9.16 (5B, d, J_{BH}=163Hz, B(2)-B(6)), -11.85 (5B, d, J_{BH}=171Hz: B(7)-B(11))

1,12-di-phenyl-para-carborane

Yield : 0.10g, 0.4mmol *IR*: 3106 w, 3092 w, 3056 m, 3040 w (phenyl C-H); 2604 s (carboranyl B-H); 1597 m; 1579 m; 1498 s; 1445 s; 1261 m; 1187 w; 1108 w; 1085 s; 1029 m; 1002 m; 913 m; 790 s; 755 m; 729 s; 691 s; 646 s; 602 s; 485 s cm^{-1} *m/z* (EI^{+}): 296 ($C_{14}B_{10}H_{20}$), 220 ($C_8B_{10}H_{16}$) *Elemental analysis* ($C_{14}B_{10}H_{20}$): C 55.75% (56.73%), H 6.93% (6.80%) *m.p.*: 214.2°C

NMR ($CDCl_3$)/ppm: ^{1}H: 7.2 m (10H, phenyl C-*H*), 4.0-1.2 br. (10H, carboranyl B-*H*); $^{13}C\{^{1}H\}$: 136.97 (*ipso* C), 129.06, 128.77, 127.81 (phenyl CH), 83.48 (carboranyl C); $^{11}B\{^{1}H\}$: -9.27 (10B, d, J_{BH}=163Hz)

CARBORANYL HYDROXIDES AND KETONES

Benzoyl Peroxide

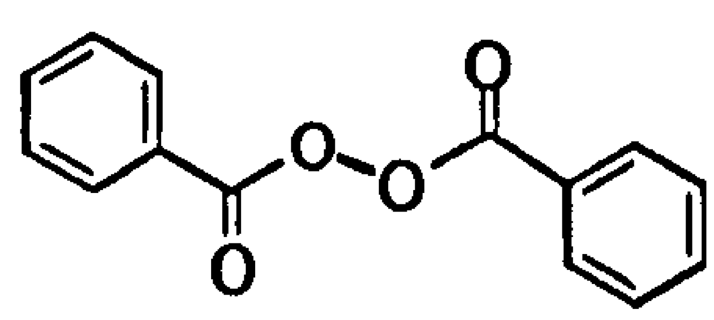

Dry benzoyl peroxide is shock sensitive and so is stored with 30% water by weight. The benzoyl peroxide therefore must be dried before being used in these reactions as lithium carboranyl salts are moisture sensitive. To do this 1.74g of benzoyl peroxide (5 mmole) was dissolved in toluene then dried over $MgSO_4$, before being filtered and further dried over 4A molecular sieves.

1-hydroxy-*ortho*-carborane[18]

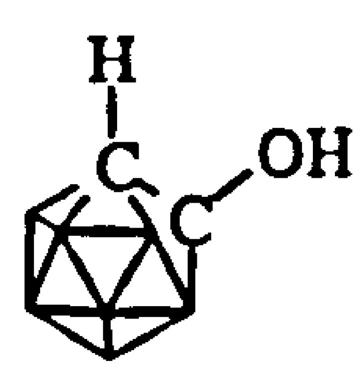

Ortho-carborane (2.89g, 20mmol) was dissolved in DME (20mL) and dilithiated with a solution of n-BuLi (2.52M in hexanes, 16mL, 40mmol). After 20 minutes stirring at room temperature, the solution was cooled in an ice bath and dry benzoyl peroxide (5mmol in 63mL of toluene) added dropwise over a 30 minute period. The solution was refluxed for 24 hours. After cooling to room temperature, 2M HCl (40mL) and water (100mL) were added with vigorous stirring. The solution was transferred to a separating funnel, washed with 10% NaOH, the organic layer isolated and washed a further twice with NaOH. The combined aqueous layers were acidfied with conc. HCl and extracted into ether. This organic layer was washed with $NaHCO_3$ and tested for peroxides before removing the solvent under reduced pressure. The resulting orange oil was purified by column chromatography on silica ($CHCl_3$) giving the hydroxide as a pale yellow solid (0.38g).

Yield : 24% (based on 50% conversion) *IR*: 3520 br. (OH); 3063 m (carboranyl CH); 2963 m; 2599 s (carboranyl BH); 1685 w; 1604 w; 1412 w; 1261 s; 1095 s; 1017 s; 942 w; 864 m; 800 s; 721 m; 695 m; 678 m; 662 m; 545 w, 499 w cm^{-1}
NMR($CDCl_3$)/ppm: ^1H: 4.30 (1H, s, OH); 3.97 (1H, s, carboranyl CH), 4.2-0.8 (10H, br., carboranyl BH); $^{13}C\{^1H\}$: 100.18 (s, carboranyl C-OH), 63.91 (d, J_{CH}=192Hz, carboranyl CH)

1-phenyl-2-hydroxy-*ortho*-carborane[18]

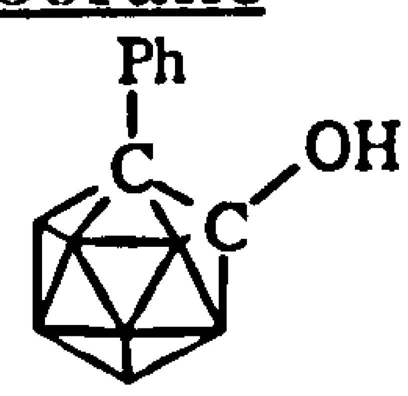

1-phenyl-*ortho*-carborane (2.20g, 10 mmole) was dissolved in dry toluene (20mL) and lithiated with a solution of n-BuLi (4mL, 2.5M in hexanes, 10 mmol). After stirring under reflux for two hours, the solution was cooled in an ice bath before dry ether (20mL) was added. Over a period of twenty minutes, benzoyl peroxide solution was added dropwise to the yellow solution whilst still in the ice bath. This resulted in a cloudy orange solution which reverted back to yellow at the end of the addition. The solution was left to reflux for a further two hours. After cooling to room temperature, distilled water (30mL) was added dropwise followed by 10% sodium hydroxide solution (50mL) giving two layers which were transferred to a separating funnel. The organic layer was isolated and washed with the sodium hydroxide solution a further twice. The combined aqueous layers were acidified with HCl giving a white precipitate. This solution was washed with three portions of ether and the organic layers washed with potassium bicarbonate solution (3 x 50mL). The organic layers were dried over $MgSO_4$, filtered and the solvent removed giving a viscous yellow oil which solidified after two hours drying on a vacuum line. The resulting yellow solid was recrystallised from hexane to give clear colourless needles.

Yield: 21% (based on 50% conversion) *IR*: 3644 s, 3484 s (O-H); 2594 s (carboranyl B-H); 1616 m; 1489 m; 1439 m; 1226 s (C-O); 1067 m; 1030 m; 939 w; 883 w; 800 w;

726 m; 687 m; 572 m; 410 m cm^{-1} <u>*m/z*</u> (EI^+): 236 ($C_8B_{10}H_{16}O$) <u>*Elemental analysis*</u> ($C_8B_{10}H_{16}O.{}^1/_2H_2O$): C 38.83% (39.16%), H 7.01% (6.98%) <u>*m.p.*</u>: 71.1°C
<u>*NMR*</u> ($CDCl_3$)/ppm: ^1H: 1-4 (10H, br., carboranyl B-*H*); 1.25 (1H, s, O-H); 7.7 (2H, m, phenyl CH), 7.4 (3H, m, phenyl C-*H*); $^{13}C\{^1H\}$: 131.1, 130.5, 129.9 (*ipso C*), 128.7 (phenyl *C*-H); 102.7 (carboranyl *C*-OH); 83.7 (carboranyl *C*-Ph); $^{11}B\{^1H\}$: -6.19 (1B, d, J_{BH}=149Hz, B12); -10.65 (1B, d, J_{BH}=*c.*160Hz, B9); -12.5 (6B, d, J_{BH}=164Hz); -16.37 (2B, d, J_{BH}=151Hz)

1-hydroxy-*meta*-carborane[64]

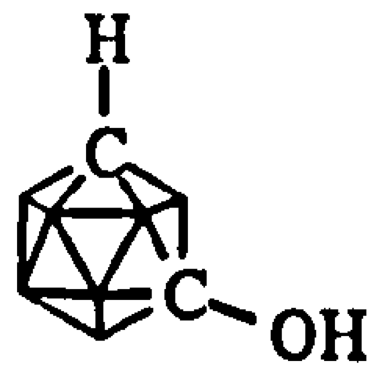

Meta-carborane (1.47g, 10mmol) was dissolved in DME (25mL) and dilithiated with a solution of n-BuLi (2.52M in hexanes, 8.5mL, 20mmol). After stirring for 20 minutes at ambient temperature, the solution was cooled in an icebath and a solution of dry benzoyl peroxide (2.5mmol in 32 mL toluene) added dropwise over a 20 minute period. The solution was refluxed for 48 hours. Once cool, water (100mL) and ether (250mL) were added, and the solution washed with 20% NaOH solution. The combined aqueous layers were acidified with conc. HCl and the hydroxy-carborane extracted into ether. The organic layer was washed with $NaHCO_3$, and tested for peroxides before the solvent was removed under reduced pressure. Column chromatography (silica, CH_2Cl_2: cyclohexane 1:1, R_F=0.91) yielded the product as fine white needles.

<u>*Yield*</u>: 14% <u>*IR*</u>: 3245 br. (OH); 3057 m (carboranyl CH); 2607 s (carboranyl BH); 1399 s; 1262 w; 1208 s; 1131 m; 1068 m; 1003 s; 932 m; 905 m; 834 w; 807 w; 779 w; 726 s; 603 w; 521 w; 496 w; 469 w cm^{-1} <u>*m/z*</u>: (EI^+) 161, (CI^-) 159 ($C_2B_{10}H_{12}0$) <u>*Elemental analysis*</u> ($C_2B_{10}H_{12}O$): C 15.57% (14.99%), H 7.69% (7.55%)
<u>*NMR*</u> ($CDCl_3$)/ppm: ^1H: 3.39 (1H, s, OH), 2.85 (1H, s, carboranyl CH), 4.2-0.9 (10H, br., carboranyl BH)

1-hydroxy-*para*-carborane and 1-(benzoyloxy)-*para*-carborane[18]

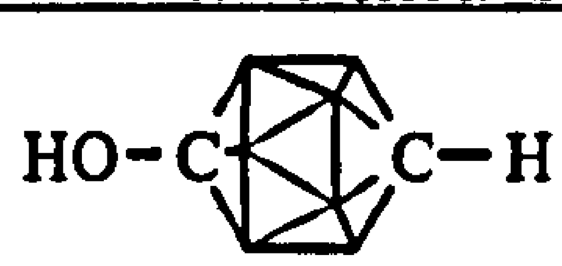

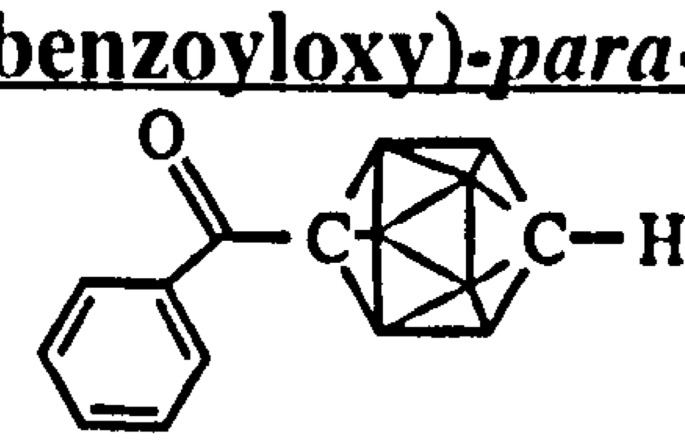

Para-carborane (1.47g, 10mmol) was dissolved in DME (20mL) and monolithiated with a solution of n-butyl lithium (2.52M in hexanes, 4mL, 10mmol).

This solution was left stirring at room temperature for 20 minutes to equilibrate before being cooled in an ice bath and diluted with dry diethyl ether (15mL). A solution of dry benzoyl peroxide in toluene (5mmol in 62.5mL toluene) was added dropwise over 30 minutes. The solution was warmed slowly to room temperature then refluxed for 48 hours. The resulting solution was cooled, hydrolysed with H_2O (30mL), transferred to a separating funnel and washed with a cold solution of 10% sodium hydroxide. The combined aqueous layers were acidified with HCl, and the resulting white precipitate extracted into ether.

The organic layers were kept separately from each other. Each was dried over $MgSO_4$, filtered and the solvent removed under reduced pressure. Sublimation of the residue from the first organic layer at 40°C isolates the hydroxy carborane. At 80°C unreacted *para*-carborane was recovered. The orange oily residue from the second organic layer solidified on standing. Sublimation of this solid under dynamic vacuum (50°C) gave a white powdery solid (0.91g) which identified as 1-(benzoyloxy)-*para*-carborane.

1-hydroxy-para-carborane

Yield: 20% *IR*: 3568 m, 3354 br. m (O-H); 3059 m (carboranyl C-H); 2923 s; 2853 m; 2611 s (carboranyl B-H); 1687 m (C-O); 1377 w; 1317 w; 1257 s; 1195 m; 1165 m; 1127 m; 1089 s; 1065 s; 1011 m; 899 m; 877 w; 826 w; 801 m; 755 m; 715 s; 695 s; 670 m; 626 m cm^{-1} *m/z*(EI^+): 160 ($C_2B_{10}H_{12}O$)

NMR ($CDCl_3$)/ppm: $^1H\{^{11}B\}$: 3.32 (1H, br., OH), 2.46 (5H, s, BH), 2.44 (1H, s, CH), 2.06 (5H, s, BH); $^{11}B\{^1H\}$: -9.89 (5B, d, J_{BH}=167Hz), -14.12 (5B, d, J_{BH}=165Hz)

1-(benzoyloxy)-para-carborane

Yield: 73% (based on 50% conversion) *IR*: 3500-2200 br.; 3071 m (carboranyl C-H); 2834 m; 2608 m, 2562 m (carboranyl B-H); 2089 w; 1915 w; 1792w; 1685 s (C=O); 1618 w; 1601 m; 1583 m; 1496 w; 1453 s; 1424 s; 1326 s; 1291 s; 1209 w; 1179 m; 1127 m; 1099 w; 1071 m; 1026 m; 999 w; 934 s; 804 m; 707 s; 683 m; 667 s; 551 m cm^{-1} *m.p.*: 103-105°C

NMR ($CDCl_3$)/ppm: $^1H\{^{11}B\}$: 8.1 (2H, d, *ortho* phenyl CH), 7.6 (1H, m, *para* phenyl CH), 7.5 (2H, m, *meta* phenyl CH), 2.47 (5H, br. s, carboranyl BH), 2.44 (1H, s, carboranyl CH), 2.07 (5H, br. s, carboranyl BH); $^{13}C\{^1H\}$: 173.0 (*C*=O); 134.5 (*ipso* *C*-H), 129.9, 130.9, 129.2 (phenyl*C*-H); $^{11}B\{^1H\}$: -13.27 (5B, d, J_{BH}=165Hz), -17.50 (5B, d, J_{BH}=166Hz)

CARBORANYL CARBOXYLIC ACIDS

1-phenyl-2-carboxy-*ortho*-carborane[10,65,66]

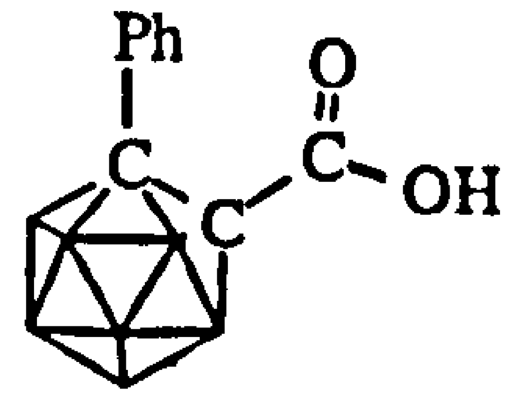

1-phenyl-2-carboxy-*ortho*-carborane was prepared by a modification of literature methods from the reaction of lithiated monophenyl-*ortho*-carborane (2.20g, 10mmol) with gaseous carbon dioxide. The carbon dioxide gas, evolved from solid carbon dioxide, was passed through a diphosphorus pentoxide drying column before being bubbled through the solution overnight. The resultant solution was hydrolysed with dilute HCl solution (5%). The crude product was isolated as a yellow oil (3.00g) which was recrystallised from 40-60° Petroleum Ether to give a white crystalline solid (1.48g).

Yield : 56% IR: 2867 br. m; 2651 s, 2592 s, 2586 s, 2570 s (carboranyl B-H); 1723 s (C=O); 1494 m; 1448 m; 1415 s; 1284 s; 1132 w; 1065 w; 1021 w; 1003 w; 922 w; 792 w; 756 m; 721 m; 704 w; 687 s cm^{-1} m/z (EI$^+$): 528 (dimer), 483 (dimer - CO_2), 264 ($B_{10}C_9H_{16}O_2$, single compound), 220 (mono-phenyl-*ortho*-carborane) m.p.: 146.2°C Elemental analysis ($C_9B_{10}H_{16}O_2$): C 40.58% (40.90%); H 6.07% (6.10%) NMR (in $CDCl_3$)/ppm: ^{1}H: 1-4 (10H, br. m, B-*H*); 7.3, 7.6 (5H, m, aromatic C-*H*); 10.2 (1H, br., CO_2*H*); $^{13}C\{^1H\}$: 75.3 (carboranyl*C*-CO_2H); 83.7 (carboranyl *C*-Ph); 128.6, 130.2 (*ipso C*), 130.7, 130.8 (aromatic *C*-H); 163.7ppm (*C*O_2H); $^{11}B\{^1H\}$: 2.93 (1B, d, J_{BH}=136Hz); -0.25 (1B, d, J_{BH}=149Hz); -6.44 (4B, d, J_{BH}=141Hz); -7.36 (4B, d, $J_{B\text{-}H}$=143Hz) [$^{11}B\{^1H\}$ (250MHz Bruker): -0.40 (1B), -3.58(1B), -9.76(8B)]

Reactions of 1-phenyl-2-carboxy-*ortho*-carborane

a. deprotonation with proton sponge

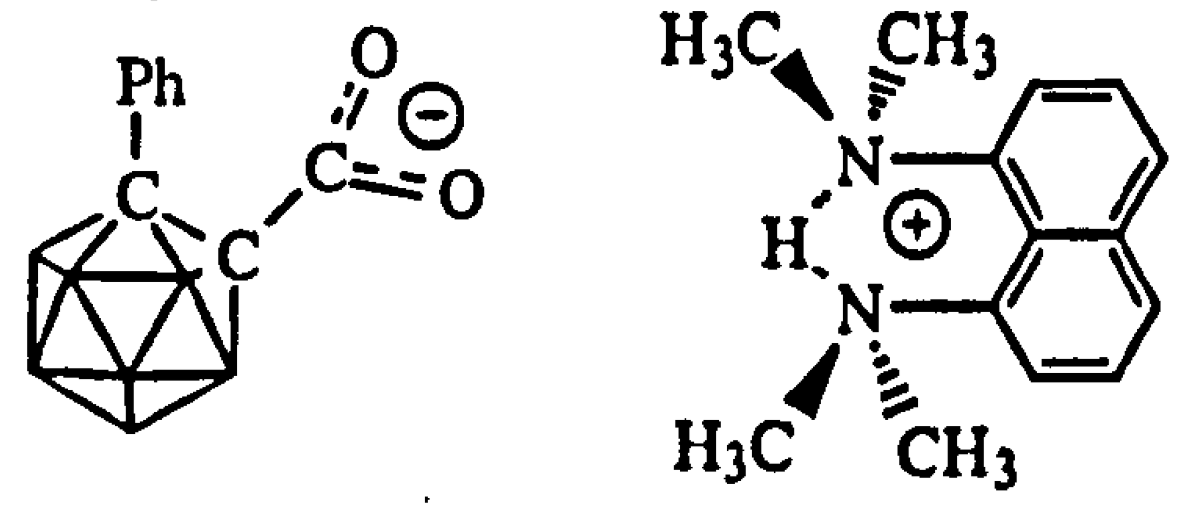

1-phenyl-2-carboxy-*ortho*-carborane (0.26g, 1mmol) was dissolved in diethyl ether and a solution of 1,8-*bis*--(dimethylamino)-naphthalene (0.21g, 1mmol) in diethyl ether added dropwise. A white precipitate of 1-phenyl-2-carboxy-*ortho*-carboranyl anion as its salt with proton sponge (0.44g) formed instantly.

Yield : 92% *IR*: 3064 w, 3001 w, 2962 m, 2875 w (proton sponge, carboranyl phenyl); 2643 s, 2598 s, 2573 s (carboranyl B-H); 1670 s (carboxylate C=O), 1626 m, 1605 m, 1579 w; 1517 w; 1463 s; 1445 m; 1430 m; 1389 m; 1303 s; 1219 m; 1194 w; 1177 m; 1161 m; 1092 m; 1032 m; 1005 m; 896 w; 833 s; 797 m; 768 s; 781 m; 758 s; 725 m; 714 m; 693 s; 621 m; 490 s cm^{-1} *Elemental analysis* ($C_{23}B_{10}H_{34}N_2O_2$): C 57.08% (57.72%); H 7.17% (7.16%); N 5.22% (5.85%)

NMR (CD_3CN): ^1H: 7.2, 7.1, 6.9, 6.7 (10H, m, aromatic CH), 4.41 (1H, s br., NH), 3.5-1.5 (10H, br., carboranyl BH), 1.6 (12H, m, CH_3); $^{13}C\{^1H\}$: 134.0, 130.8, 129.8, 128.0, 126.3, 122.1, 113.3 (aromatic C); 107.9, 92.8, 77.9 (carboranyl C-phenyl), 61.5 (carboranyl C-CO_2^-), 44.4 (CH_3); $^{11}B\{^1H\}$: -2.46 (1B, d, J_{BH}=147Hz), -4.43 (1B, d, J_{BH}=163Hz), -8,75 (2B, d, J_{BH}=151Hz), -10.44 (4B, d, J_{BH}=171Hz), -12.34 (2B, d, J_{BH}=160Hz) [minor product is deboronated, -13.28 (1B, d, J_{BH}=177Hz), -16.33 (1B, d, J_{BH}=130Hz), -17.64 (1B, d, J_{BH}=144Hz), -19.28 (1B, d, J_{BH}=145Hz), -22.18 (3B, d, J_{BH}=154Hz), -32.36 (1B, dd, $^1J_{BH}$=*c*.128Hz, $^2J_{BH}$=*c*.48Hz), -35.51 (1B, d, J_{BH}=135Hz)]

b. reaction with ammonia

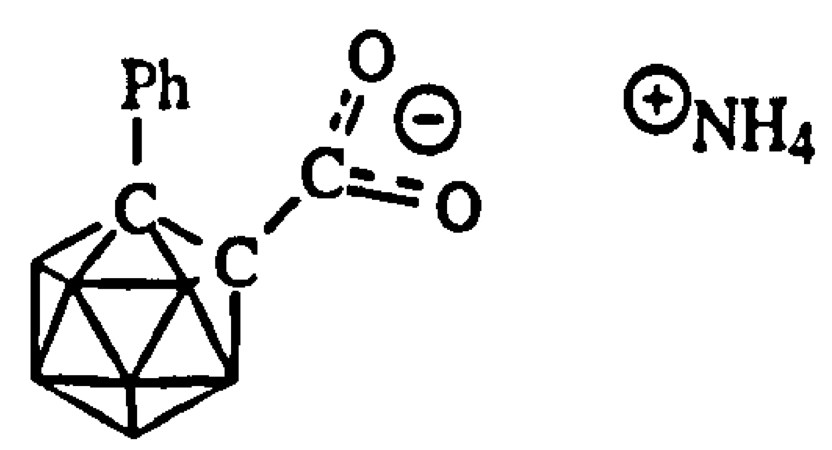

1-phenyl-2-carboxy-*ortho*-carborane (0.26g, 1mmol) was dissolved in diethyl ether (25mL) and left to stir overnight with a solution of aqueous ammonia (0.88 sp. gr., 100mL). The layers were separated, and the aqueous layer evaporated to give a white solid residue (0.30g) which was a mixture of the ammonium salt of the carboxy anion (major) and deboronated carborane (minor product - cf. IR, $^{11}B\{^1H\}$).

IR: 3321 s (NH_4^+); 3156 w, 3134 w (phenyl C-H); 3004 br. m; 2797 m; 2671 m, 2645 m, 2617 s, 2595 s, 2576 s, 2559 s, 2538 s (carboranyl B-H, *closo* and *nido* species); 1678 m; 1623 s (C=0); 1485 s; 1445 s; 1418 s; 1345 s; 1109 s; 1067 s; 799 w; 771 m; 755 w; 696 m cm^{-1}

NMR (D_2O)/ppm: ^1H: 6.78 (3H, m, phenyl CH), 6.74 (2H, m, phenyl CH); $^{13}C\{^1H\}$: 162.25 (CO_2^-); 131.57, 130.07, 128.37, 126.03 (phenyl CH); 83.83 (carboranyl C-Ph), 82.11 (carboranyl C-CO_2^-); $^{11}B\{^1H\}$: -0.18 (1B), -1.28 (1B), -7.57 (8B) [minor product (*nido* species): -14.08, -15.19, -16.37, -30.03, -33.07]

c. reaction with potassium 18-crown-6 hydroxide

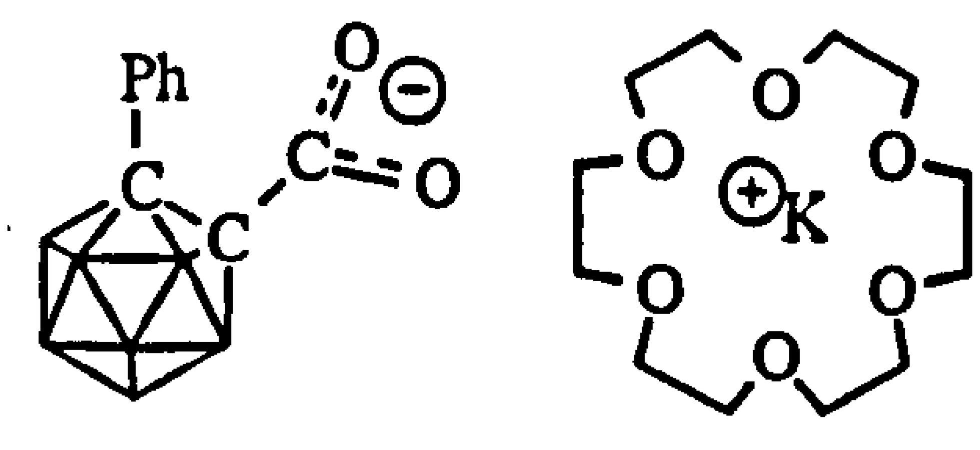

To a solution of potassium hydroxide (0.14g, 2.5mmol) in distilled water (20mL), 1-phenyl-2-carboxy-*ortho*-carborane (0.13g, 0.5mmol) was added. This gave a slightly misty solution. On the addition of 18-crown-6 (0.13g, 0.5mmol) a white precipitate (0.22g) was formed and subsequently isolated by filtration. Long, clear colourless needles were grown by recrystallisation from ethanol/water.

Yield : 82% *IR*: 3379 br (H_2O); 3047 w (phenyl C-H); 2908 s; 2825 m; 2527 s (carboranyl B-H); 1593 s (C=O); 1493 m; 1472 s; 1454 m; 1431 m; 1350 s; 1284 m; 1249 m; 1133 s; 1103 s; 1026 m; 961 s; 915 m; 837 m; 777 w; 700 m cm^{-1} *Elemental analysis* ($C_{21}B_{10}H_{39}O_8K$): C 43.66% (44.51%); H 6.79% (6.94%)
NMR ($CDCl_3$)/ppm: ^1H: 7.3 m, 7.1 m (5H, phenyl C-*H*); 1-4 (10H, br., carboranyl B-*H*); 3.62 s (20H, 18-crown-6 C*H2*); $^{13}C\{^1H\}$: 167.16 (CO_2^-), 146.25 (*ipso* C); 127.99, 127.65, 125.30 (phenyl *C*-H), 83.2 (carboranyl C-Ph); 70.81 (18-crown-6 CH_2); $^{11}B\{^1H\}$: -2.44 (1B, d, J_{BH}=152Hz), -4.72 (1B, d, J_{BH}=143Hz), -9.51 (4B, d, J_{BH}=139Hz), -10.89 (4B, d, J_{BH}=129Hz) [on standing in solution, the *closo* species was deboronated to the *nido* species: $^{13}C\{^1H\}$: 130.5, 129.3, 128.2 (phenyl CH); $^{11}B\{^1H\}$: -11.4 (1B, d, J_{BH}=*c*.120Hz), -13.12 (1B, d, J_{BH}=*c*.130Hz), -13.80 (1B, d, J_{BH}=*c*.120Hz), -17.02 (1B, d, J_{BH}=131Hz), -19.19 (2B, d, J_{BH}=121Hz), -22.89 (1B, d, J_{BH}=147Hz), -33.12 (1B, dd, $^1J_{BH}$=*c*.144Hz, $^2J_{BH}$=*c*.64Hz), -36.40 (1B, d, J_{BH}=138Hz)]

1,7-dicarboxy-*meta*-carborane

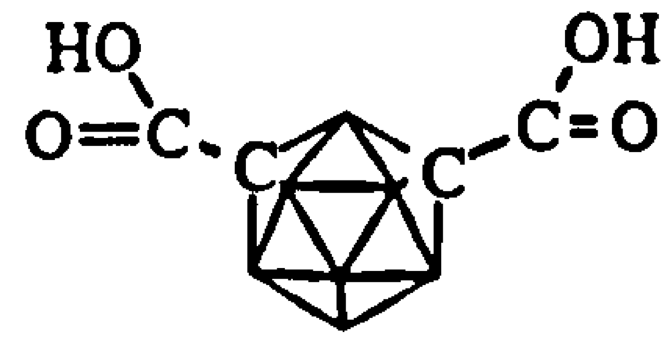

Meta-carborane (2.20g, 15mmol) was dissolved in DME (100mL) and dilithiated with a solution of n-BuLi (2.42M in hexanes, 14mL, 34mmol). After being allowed to equilibrate, gaseous carbon dioxide (produced from the reaction between sodium carbonate and hydrochloric acid) was passed through the reaction solution resulting in a cloudy white solution. Once the addition of carbon dioxide was judged to be complete, the lithio-carboxy-salt was transformed to the di-carboxylic acid by the addition of HCl (2M, 60mL). The solution became clear as the diacid was produced. Diethyl ether was added to the solution, the reaction solution transferred to a separating funnel where the organic layer was isolated, and the aqueous layer extracted a further twice with ether. The combined organic layers were dried over $MgSO_4$, filtered, and the solvent removed under dynamic vacuum to yield a yellow oil which crystallised on standing.

Yield: 65% *IR*: 3520 br. m (H_2O); 3446 br, m; 3068 w; 2963 w; 2621 s (carboranyl BH); 1994 br, m; 1747 s (carbonyl CO); 1437 m; 1262 s; 1035 s; 843 w; 801 m; 706 m; 621 w; 506 w; 413 w cm^{-1} *Elemental analysis* ($C_4H_{12}B_{10}O_4$): C 21.03% (20.69%), H 5.59% (5.17%)
NMR (CD_3CN)/ppm: $^{13}C\{^1H\}$: 161.75 (CO_2H), 68.69 (carboranyl C)

Single deprotonation of 1,7-dicarboxy-*meta*-carborane with KOH/18-crown-6-ether

1,7-dicarboxy-*meta*-carborane (0.60g, 3mmol) was added to an aqueous solution of KOH (0.30g, 5mmol, in 40mL H_2O) giving a misty solution and some undissolved sticky solid. The solution was decanted from undissolved residue and 18-crown-6 ether (0.68g, 3mmol) in H_2O (*c.* 5mL) added dropwise. Solvent was removed under reduced pressure leaving a yellow solid which left clear colourless flat platelets on recystallisation from ethanol. The NMR solutions became pink with time, and in fact the compound deboronated on standing in solution.

IR: 3455 br. (H_2O); 2952 m, 2900 s (methyl CH_2); 2622 s, 2589 s, 2558 s (carboranyl BH); 1639 (carboxylate CO); 1569 m (CO crown ether); 1476 m; 1455 m; 1352 s; 1325 s; 1287 m; 1253 m; 1106 s; 965 s; 839 s; 769 m; 755 m; 735 m; 530 w cm^{-1}

Deprotonation of 1,7-di-carboxy-*meta*-carborane with proton sponge

a) 1:1 carborane:proton sponge

1,7-di-carboxy-*meta*-carborane (0.12g, 0.5mmol) was dissolved in acetonitrile (*c.*5mL) and a solution of proton sponge (0.11g, 0.5mmol) in ether (*c.*5mL) added. The product (doubly deprotonated) dropped out of solution as a white precipitate and was removed by filtration. No singly deprotonated species was observed.

Yield: 80% ; *IR*: 3447 br. s (NH); 3098 m, 3058 m, 3024 m, 3000 (naphthalene CH); 2960 m, 2926 m (methyl CH); 2620 s, 2609 s, 2600 s, 2576 s (carboranyl BH); 1684 m (CO), 1653 s (CO); 1472 m; 1458 m; 1340 s; 1262 m; 1222 w; 1099 m; 838 m; 774 m; 623 m; 486 m; 419 m cm^{-1}; *Elemental analysis* ($C_4B_{10}H_{10}O_4.2C_{14}H_{19}N_2$): C 57.00% (58.16%), H 7.36% (7.32%), N 8.30% (8.48%)

NMR (D_2O)/ppm: ^{1}H: 7.33 (2H, d, J_{CH}=8.3Hz, *o* or *p*-CH), 7.27 (2H, d, J_{CH}=7.8Hz, *p* or *o*-CH), 7.04 (2H, t, J_{CH}=7.5Hz, *m*-CH), 2.50 (12H, s, CH_3); $^{13}C\{^1H\}$: 169.57 (CO_2^-); 146.24, 137.53, 132.73, 130.45, 128.12, 124.84, 122.50, 121.14 (naphthalene C); 81.59 (carboranyl C)

b) carborane:proton sponge 1:2

1,7-di-carboxy-*meta*-carborane (0.13g, 0.5mmol) was dissolved in acetonitrile (*c*.10mL) and a solution of proton sponge (0.21g, 1.0mmol) in ether (*c*.5mL) added. The product (doubly deprotonated carboxylic acid) dropped out of solution as a white precipitate and was removed by filtration.

Yield: 75%; *IR*: 3447 br. s (H_2O); 3058 m, 3924 m (naphthalene CH); 2958 m, 2924 m, 2882 m (methyl CH_3); 2622 s, 2608 s, 2598 s, 2588 s, 2574 s, 2548 s (carboranyl BH); 1654 s, 1646 s, 1637 s, 1628 s, 1618 s (CO); 1459 m; 1332 m; 1304 m; 1262 m; 1174 m; 1099 m; 1029 m; 831 m; 774 m; 748 m; 635 m; 487 m cm^{-1}; *Elemental analysis* ($C_4B_{10}H_{10}O_4.2C_{14}H_{19}N_2$): C 57.28% (58.16%), H 7.40%, (7.32%), N 8.36% (8.48%); *NMR* (D_2O)/ppm: ^{1}H: 7.17 (4H, d, JCH=7.2Hz, *o* or *p*-CH), 7.09 (4H, d, J_{CH}=7.8Hz, *p* or *o*-CH), 6.90 (4H, t, J_{CH}=7.7Hz, *m*-CH), 5.2 (2H, br., NH), 2.39 (24H, s, CH_3); $^{13}C\{^1H\}$: 169.15 (CO_2^-); 146.14 (*m*-CH), 137.38 (CH), 130.42 (CH), 124.89, 122.63, 120.93; 81.79 (carboranyl C); 48.32, 47.89 (CH_3); $^{11}B\{^1H\}$: 6.75 (br.), -11.67 (d, J_{BH}=*c*.120Hz), -14.5 (br.)

1-phenyl-12-carboxy-*para*-carborane

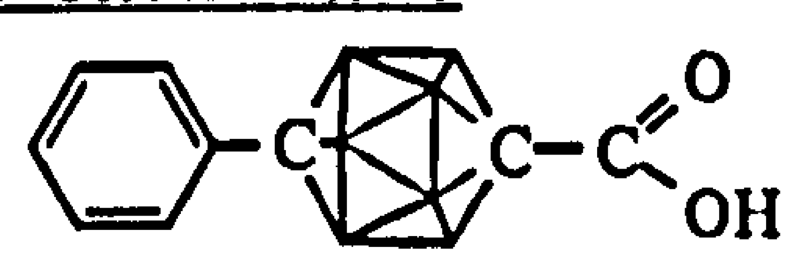

1-phenyl-*para*-carborane (0.24g, 2mmol) was dissolved in DME (80mL) and lithiated with a solution of n-BuLi (2.59M in hexanes, 1.4mL, 3.6mmol). After equilibrating for 1 hour at room temperature, carbon dioxide (evolved from solid carbon dioxide) was bubbled through the lithiocarborane solution for 4 hours. The resultant cloudy solution was acidified with 2M HCl then extracted into ether. The organic layer was washed with H_2O, then the solvent removed under reduced pressure leaving a pale yellow solid (0.32g) which was recrystallised from hexane.

Yield: 12%
NMR ($CDCl_3$)/ppm: $^1H\{^{11}B\}$: 7.2 (2H, m, *m*-CH), 7.1 (3H, m, *o*- and *p*-CH), 5.3 (br., CO_2H), 3.31 (5H, s, carboranyl BH), 2.52 (5H, s, carboranyl BH); $^{13}C\{^1H\}$: 164.52 (CO_2H), 136.70 (*ipso* C), 129.40, 127.45, 126.23 (phenyl CH), 86.35 (carboranyl C-Ph?), 78.63 (carboranyl C-CO_2H?); $^{11}B\{^1H\}$: -9.64 (5B, d, J_{BH}=*c*.170Hz), -10.45 (5B, d, J_{BH}=*c*.165Hz)

1,12-di-carboxy-*para*-carborane

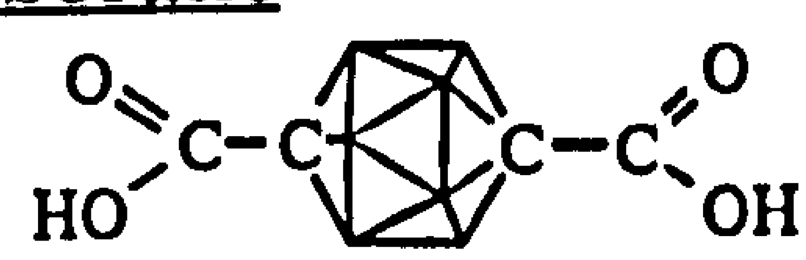

Para-carborane (1.44g, 10mmol) was dissolved in DME (200mL) and dilithiated with a solution of n-BuLi (2.59M in hexanes, 9mL, 23mmol) giving a slightly cloudy white solution. After one hour at room temperature, CO_2 (from the evaporation of solid carbon dioxide) was bubbled through this solution for *c*.8hours giving an intensely white cloudy solution. The addition of 2M HCl dissolved most of the product and extraction into ether followed by washing with H_2O left the dicarboxylic acid in the organic layer. The product was dried with anhydrous magnesum sulfate, filtered and the solvent removed under reduced pressure to leave a white powder (1.50g).

Yield: 65% _IR_: 3450-2000 br; 2627 s (carboranyl BH); 2534 m; 1717 s (carbonyl CO); 1414 s; 1281 s; 1137 m; 1087 m; 1059 w; 985 m; 926 m; 839 w; 803 w; 760 w; 738 w; 717 s; 453 m; 435 m cm^{-1} _m/z_(EI^+): 232 ($C_4B_{10}H_{12}O_2$)
NMR (CD_3CN)/ppm: $^{13}C\{^1H\}$: 162.42 (CO_2H), 78.85 (carboranyl C); $^{11}B\{^1H\}$: -13.49 (10B, d, J_{BH}=172Hz) [sample contained an impurity of 1-carboxy-*para*-carborane: $^{13}C\{^1H\}$: 162.52 (CO_2H), 71.35 (C-CO_2H), 57.83 (carboranyl CH); $^{11}B\{^1H\}$: -13.04 (d, J_{BH}=*c*.160Hz), -14.79 (d, J_{BH}=*c*.164Hz)]

Deprotonation of 1,12-di-carboxy-*para*-carborane with proton sponge

a) carborane:proton sponge 1:1

1,12-di-carboxy-*para*-carborane (0.12g, 0.5mmol) was dissolved in ether (*c*5mL) and a solution of proton sponge (0.11g, 0.5mmol in *c*.5mL ether) added. A white precipitate formed instantly. The solution was washed with acetonitrile, ether and water and the product (singly deprotonated) was isolated as a white precipitate by filtration.

Yield: 85% *IR*: 3448 m br. (NH); 3048 w, 3002 w (naphthalene CH); 2964 w, 2888 w, 2814 w (CH3); 2626 s, 2614 s (carboranyl BH); 1732 m, 1718 m (CO_2H impurity); 1684 s (CO_2^-); 1617 (CO_2^-) m; 1463 s; 1367 m; 1261 m; 1221 m; 1163 m; 1097 m; 1030 m, 1022 m; 805 m; 781 m; 768 m; 721 s; 581 m cm^{-1} *Elemental analysis* ($C_{18}B_{10}H_{30}O_4N_2$): C 46.96% (46.99%), H 6.63% (6.96%), N 6.05% (6.45%)
NMR (D_2O)/ppm: ^1H: 7.5, 7.4, 7.2 (m, naphthalene CH), 5.0 (br., NH), 2.56 (m, CH_3), 4-1ppm (br., carboranyl BH); $^{11}B\{^1H\}$: -13.68 (d, J_{BH}=161Hz)

b) carborane:proton sponge 1:2

1,12-di-carboxy-*para*-carborane (0.12g, 0.5mmol) was dissolved in ether (or acetonitrile, *c*5mL) and a solution of proton sponge (0.21g, 1.0mmol in *c*.5mL ether) added. A white precipitate formed instantly. The solution was extracted with acetonitrile and water then washed with ether. Removal of the solvent from the aqueous layer left the product (doubly deprotonated) as a white crystalline solid.

Yield: 90% *IR*: 3448 s, br. (NH); 3020 m, 3000 m (naphthalene CH); 2886 w, 2846 w, 2810 w (methyl CH_3); 2638 s, 2621 s, 2604 s, 2592 s (carboranyl BH); 1617 s (CO_2^-), 1465 s, 1365 s, 1332 s, 1276 m, 1221 m, 1194 m, 1165 m, 1119 m, 1029 m, 1007 m, 896 w, 841 m, 780 s, 739 m, 584 m, 488 m cm^{-1} *Elemental analysis* ($C_4B_{10}H_{10}O_4.2C_{14}H_{19}N_2$): C 52.20% (58.16%), H 7.44% (7.32%), N 7.62% (8.48 %)
NMR (D_2O)/ppm: ^1H: 7.25 (2H, d, J_{CH}=4.5Hz, *o* or *p*-CH), 7.22 (2H, d, J_{CH}=3.4Hz, *p* or *o*-CH), 6.99 (2H, t, J_{CH}=8Hz, *m*-CH); 2.45 (24H, s, CH_3), 3.5-1.0 (10H, br., carboranyl BH) $^{13}C\{^1H\}$: 170.56 (CO_2^-); 146.13, 137.44, 131.56, 129.29, 123.61, 121.02 (naphthalene C); 86.22 (carboranyl C-CO_2^-), 47.98 (CH_3); $^{11}B\{^1H\}$: -13.79 (d, J_{BH}=159Hz)

Deprotonation of 1,12-di-carboxy-*para*-carborane with copper(II) sulfate

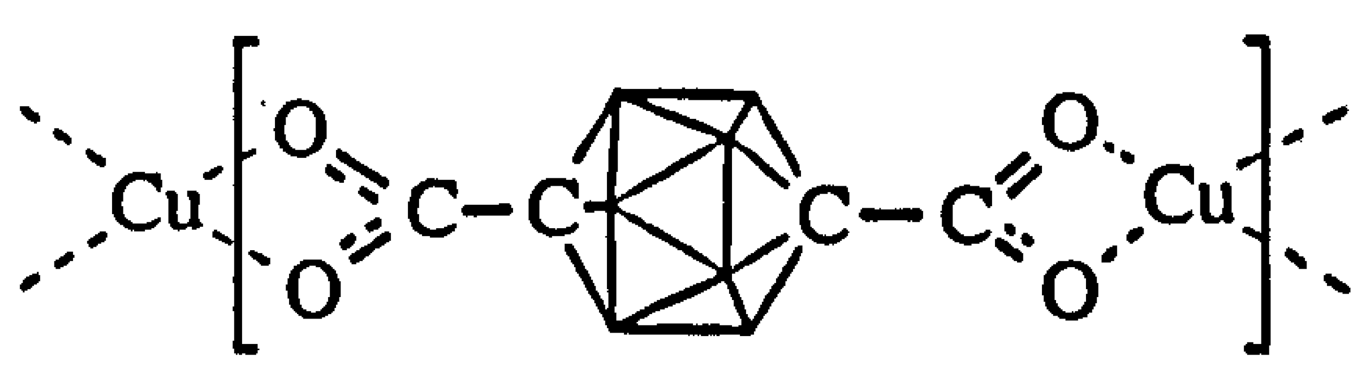

1,12-dicarboxy-*para*-carborane (0.13g, 0.56mmol) was dissolved in ethanol (*c*. 20mL) and neutralised by the addition of 1N NaOH. A solution of $CuSO_4.5H_2O$ (0.15g, 0.6mmol in 3mL H_2O) was added, instantly turning the solution bright blue.

This solution was left stirring overnight at room temperature, with no change. Solvent was removed on a vacuum line leaving a pale blue solid. Washing this with THF gave a blue precipitate which was removed by filtration. Upon standing, the THF washings evaporated to leave a green solid. The blue solid turned slowly green upon standing in solvent (THF, acetone), suggesting different copper salts or adducts were being formed.

IR: (blue solid) 3421 br. s; 2985 w; 2893 w; 2617 s (carboranyl BH); 1667 (CO^-); 1395 s; 1143 s; 1112 s; 1039 s; 996 m; 888 w; 847 w; 792 s; 741 m; 623 m; 499 m cm^{-1} (green solid) 3444 br. m; 3066 w; 2963 m; 2615 s (carboranyl BH); 1664 s, 1655 s (CO^-); 1399 s; 1261 s; 1097 s; 1021 s; 869 w; 801 s; 732 w; 668 w; 644 w; 465 w cm^{-1}
note - blue solid was insoluble. Green solid was sparingly soluble in chloroform. but went off to a blue solid which then precipitated out of solution.

NOTE: all deprotonated carboxylic acids were destroyed by dichloromethane and chloroform solutions.

REACTIONS WITH ELECTROPHILIC FLUORINATING AGENTS

Two electrophilic fluorinating agents were investigated as possible fluorinating agents for carboranyl carbons, N-Fluorobenzenesulfonimide (NFBS), and 1-fluoro-2,6-dichloropyridinium tetrafluoroborate (pyF^+).

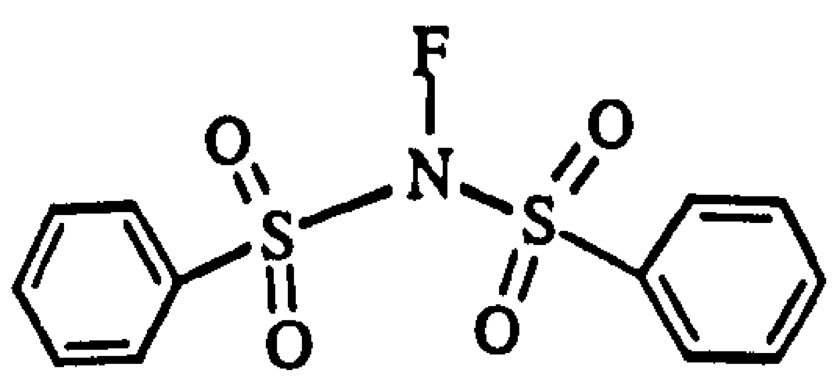

NFBS

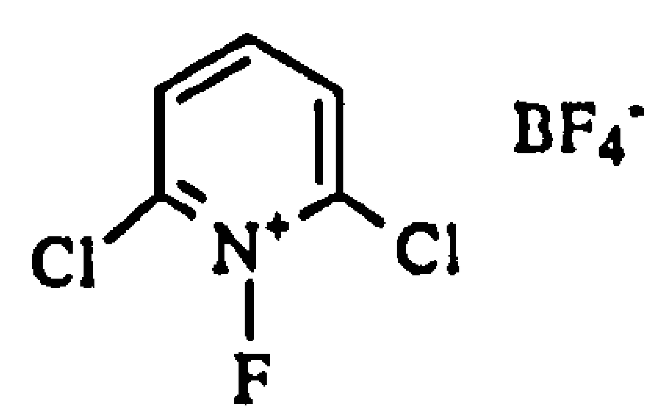

pyF^+

N-Fluorobenzenesulfonimide[54]

This is a commercially available electrophilic fluorinating agent which effects the fluorination of a wide variety of neutral and carbanionic nucleophiles in a one-step procedure. In the experiments conducted within the scope of this thesis, NFBS has proven mildly successful in the fluorination of dicarbadodecaboranes from their lithio intermediates. Before use, the reagent was recrystallised from diethyl ether.

IR: 3095 m, 3072 m (phenyl CH); 1998 w; 1978 w; 1917 w; 1819 w; 1781 w; 1581 s (S=O); 1476 s, 1451 s, 1394 s, 1343 s, 1313 s (S=O); 1290 m; 1197 s; 1081 s; 1023 w; 999 w; 924 m; 848 s; 793 s; 752 s; 727 s; 719 s; 679 s; 623 m; 589 m cm^{-1} *Elemental* *analysis* ($C_{12}H_{10}NS_2O_4F$): C 45.40% (45.71%); H 3.20% (3.19%); N 4.33% (4.44%); S 19.51 (20.33%) *m.p.*: 111-113.4°C (lit. 114-116°C)[54]

NMR ($CDCl_3$)/ppm: ^{1}H: 8.0 (4H, d, *ortho* CH), 7.78 (4H, t, *meta* CH), 7.61 (2H, t, *para* CH); $^{13}C\{^1H\}$: 136.65 (*para* CH), 135.33 (*ipso* C), 130.57, 130.24 (*ortho, meta* CH); ^{19}F: -37.89

Control Reactions

Reaction between NFBS and BuLi

$$\mathrm{BuLi} + (\mathrm{PhSO_2})_2\mathrm{NF} \longrightarrow \mathrm{CH_3CH_2CH_2CH_2F} + (\mathrm{PhSO_2})_2\mathrm{NLi}$$

NFBS (0.3g, 1mmol) was dissolved in sodium dried diethyl ether (40mL) under a dry dinitrogen atmosphere. The addition of a solution of n-BuLi (2.5M in hexanes, 0.4mL, 1mmol) changed the solution from clear and colourless to a cloudy pale yellow colour. The solution was analysed by ^{19}F NMR spectroscopy after stirring at room temperature for 1hour.

NMR ($CDCl_3$)/ppm: ^{19}F: -220.31 (tt, $^2J_{HF}$=48Hz, $^3J_{HF}$=24Hz)

Reaction between pyF$^+$ and BuLi

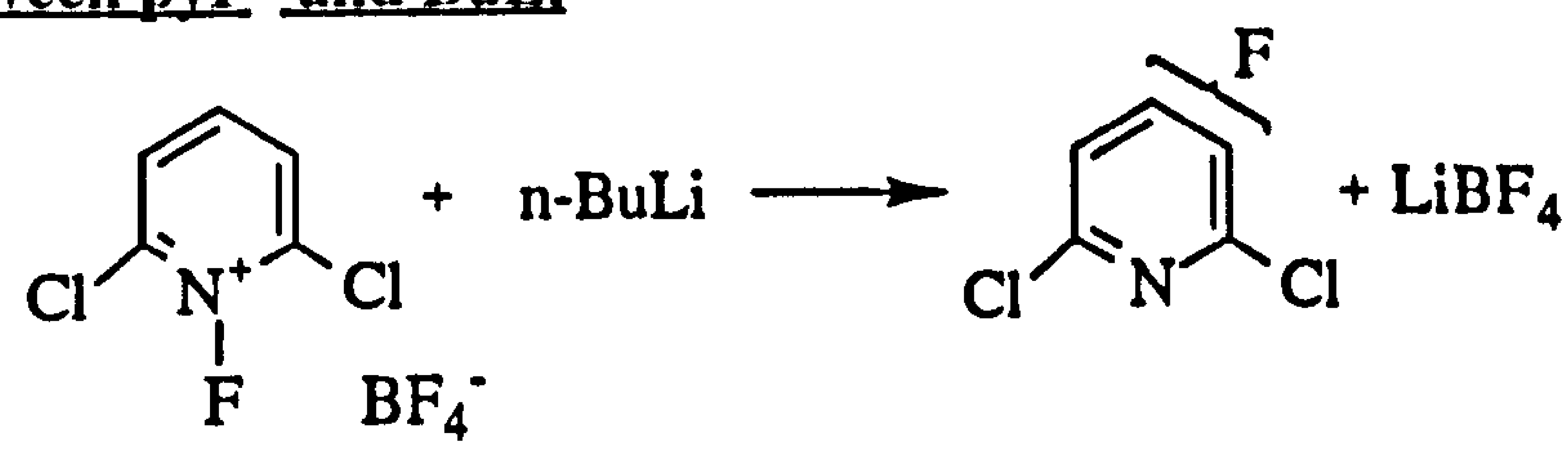

PyF$^+$ (0.38g, 1.5mmol) was suspended in sodium dried ether, cooled in an ice-bath and lithiated with a solution of n-BuLi (2.42M in hexanes, 0.6mL, 1.5mmol). As the solution warmed slowly to room temperature the solution changed from clear yellow to orange to deep red to orange with ppt and finally to a clear yellow solution with a white ppt. The organic solvent was removed to leave an orange solid (0.41g).

NMR ($CDCl_3$)/ppm: ^{19}F: -148.4 (minor), -150.16 (major), -153.56 (minor)

Reaction of *ortho*-carborane with NFBS

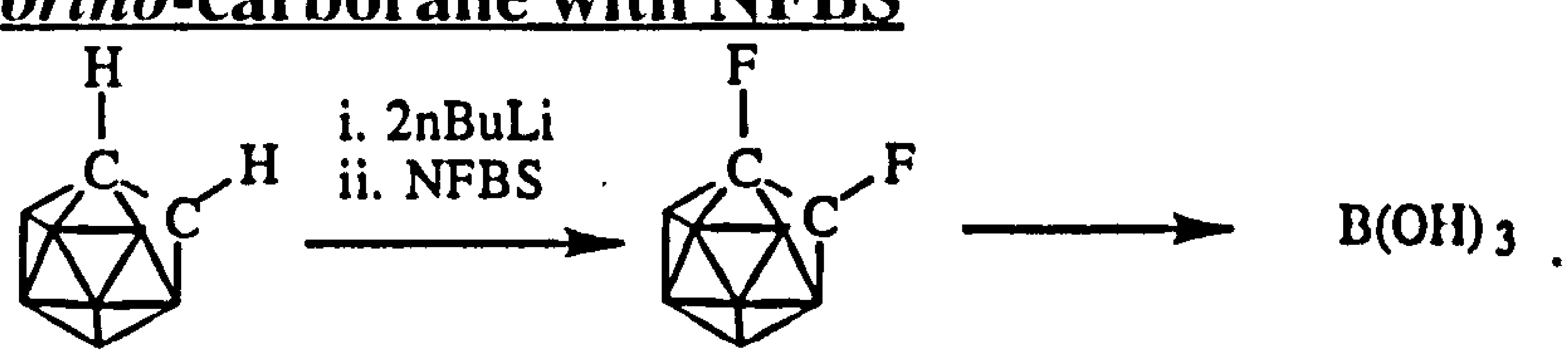

Ortho-carborane (0.36g, 2.5mmol) was dissolved in DME (25mL) and dilithiated with a solution of n-BuLi (1.61M in hexanes, 4.5mL, 7mmol). After 20 minutes at room temperature, NFBS (4.96g, 15mmol) was added giving a clear orange solution immediately. The reaction was followed by ^{19}F NMR spectroscopy. After 2 days stirring at room temperature, ^{19}F NMR spectroscopy showed peaks at -39ppm and at -154ppm, corresponding to unreacted NFBS and to carboranyl CF respectively. Ether was added to the solution and the solution washed with distilled water. The organic layer was dried over anhydrous $MgSO_4$, filtered and the solvent removed to leave an orange solid. Sublimation of this solid gave a sticky white residue which, when washed with acetonitrile appeared to degrade to a *nido* cage (IR 2526cm^{-1}) then ultimately to boric acid. Unsublimed residue was identified as $(PhSO_2)_2NH$.

Reaction of *ortho*-carborane with pyF^+

Ortho-carborane (0.43g, 3mmol) was dissolved in DME (20mL) and dilithiated with a solution of n-BuLi (2.5mL, 2.52M in hexanes, 6mmol). After 20 minutes stirring at room temperature, pyF^+ (1.52g, 6mmol) was added to the lithio-carborane suspension resulting in a highly exothermic reaction. ^{19}F NMR spectroscopy showed 1 peak at -154ppm after 15 minutes of reaction. The solution was left to reflux for 3 hours, cooled, washed with ether and water and the solvent removed from the organic layer. Column chromatography (silica, 1:4 $CHCl_3$:cyclohexane) of the resulting brown oil gave four fractions. Fractions 2-5 showed fluorinated products, but no clean fluorinated carborane was isolated.

fractions 2-5 ^{19}F NMR (Et_2O)/ppm: -76.47 (pyF^+), -149.80, -151.26, -184.14

Reaction of 1-methyl-*ortho*-carborane with NFBS

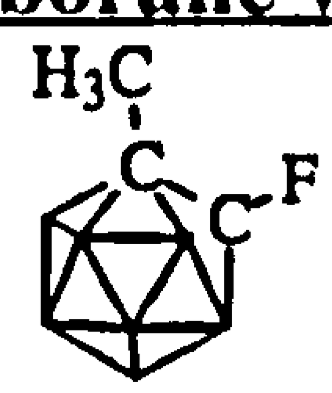

1-methyl-*ortho*-carborane (0.80g, 5mmol) was dissolved in dry ether and lithiated with a solution of n-BuLi (2.52M in hexanes, 2.5mL, 6mmol). After 1 hour stirring at room temperature, NFBS (1.57g. 5mmol) was added, changing the resulting clear, colourless solution instantly to bright yellow. The reaction was followed by ^{19}F NMR spectroscopy. The solution was refluxed for 4 hours giving a yellow solution and precipitate. (Even when the reflux period was extended, only $^1/_3$ of the NFBS added reacted). The solid was removed by filtration and the organic layer washed with distilled water. The organic layer was dried over $MgSO_4$, filtered, and the solvent removed under reduced pressure to leave a brown oil (1.32g). Purification of this oil by column chromatography (1:2 CH_2Cl_2:cyclohexane) was unsuccessful as the product decomposed on the column, although traces of carboranyl C-F were seen in fractions 3-

decomposed on the column, although traces of carboranyl C-F were seen in fractions 3-4 (^{19}F : -152.04ppm). (Fractions 15-20 have ^{19}F peak at -129.09ppm). Other reaction products were unreacted 1-methyl-*ortho*-carborane and 1-methyl-2-(phenylsulfonyl)-*ortho*-carborane (IR: 1495, 1447cm^{-1})

data for oil :

NMR (Et_2O)/ppm: ^{19}F: -39.19 (unreacted NFBS), -109.45 (F^-), -152.25 (carboranyl C-F)

Reaction of 1-phenyl-*ortho*-carborane with NFBS

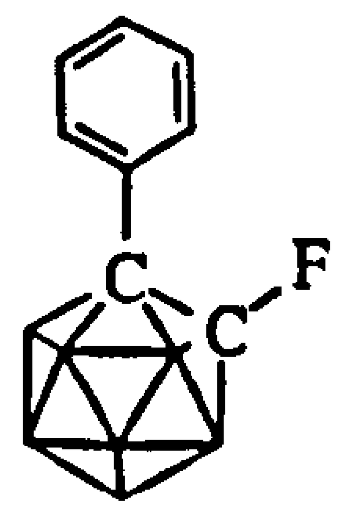

1-phenyl-*ortho*-carborane (0.66g, 3mmol) was dissolved in dry ether, cooled in an ice bath and lithiated with a solution of n-butyl lithium (2.5M in hexanes, 1.6mL, 3mmol) giving a clear yellow solution which was allowed to warm slowly to room temperature. The solution was cooled again in an icebath before the addition of NFBS (0.95g, 3mmol) to give a brown solid in a clear yellow solution. The solid was removed by filtration, and the liquid transferred to a separating funnel and washed with distilled water. The organic layer was isolated and the solvent removed under reduced pressure to give a yellow oil. This oil was sublimed under dynamic vacuum giving a white solid which was a mixture of 1-phenyl-2-fluoro-*ortho*-carborane and unreacted 1-phenyl-*ortho*-carborane. These were separated by preparative TLC (cyclohexane) to isolate the white crystalline product (0.17g).

Yield : 24% *IR*: 3090 w; 3070 w; 2962 w; 2924 w; 2645 m, 2576 s (carboranyl B-H); 1494 m; 1447 m; 1250 m; 1232 s (C-F?); 1193 m; 1106 w; 1070 s; 1029 s; 1002 m; 980 w; 933 m; 880 w; 783 m; 750 m; 723 s; 683 s; 596 w; 571 s; 495 w; 479 s cm^{-1} *m/z* (EI^+): 239 ($C_8B_{10}H_{15}F$) *Elemental analysis* ($C_8B_{10}H_{15}F$): C 40.67% (40.32%), H 6.52% (6.34%) *m.p.*: 87.2 - 88.2 °C

NMR ($CDCl_3$)/ppm: ^{1}H: 7.71 (2H, d, *meta* phenyl CH), 7.4 (3H, m, *ortho, para* phenyl CH), 4.1 - 0.9 (10H, br., carboranyl BH); $^{1}H\{^{11}B\}$: as ^{1}H, with BH region 2.95 (1H, s), 2.94 (1H, s), 2.65 (2H, s), 2.44 (2H, s), 2.30 (1H, s), 2.22 (1H, s), 2.12 (2H, s); $^{13}C\{^{1}H\}$: 80.5 (carboranyl C-Phenyl); 105.2, 110.3 (d, J_{CF} = 312.5Hz, carboranyl CF); $^{11}B\{^{1}H\}$: -5.83 (1B, J_{BH}=149Hz), -10.50 (1B, J_{BH}= 151Hz), -11.87 (4B, J_{BH}=221Hz), -12.76 (2B, J_{BH}=148Hz), -13.78 (2B, J_{BH}=156Hz); ^{19}F: -149

[$^{11}B\{^1H\}$ (250MHz Bruker): -5.88 (1B), -10.73 (1B), -11.94 (4B), -12.73 (2B), -13.71 (2B)]

Reaction of 1-phenyl-*ortho*-carborane with pyF^+

1-phenyl-*ortho*-carborane(1.13g, 5mmol) was dissolved in dry ether (40mL), cooled in an ice-bath, and lithiated with a solution of n-BuLi (2.4mL, 2.42M in hexanes, 5mmol). After warming to room temperature, pyF^+ (1.28g, 5mmol) was added giving a cloudy red solution which quickly changed to cloudy yellow with the evolution of heat. ^{19}F NMR spectroscopy showed only one peak at -158ppm (cf. reaction between pyF^+ and n-BuLi). The reaction was left stirring overnight at room temperature giving an almost clear yellow solution. Remaining precipitate was removed by filtration and the solvent removed leaving a yellow oil which solidified on standing. NMR spectroscopy suggested this was primarily unconverted starting material, with the pyF^+ having rearranged giving ring substitution.

IR: 3065 m (carboranyl CH), 2597 s (carboranyl BH) cm^{-1} (*cf.* 1-phenyl-*meta*-carborane 3062, 2604 cm^{-1})
NMR($CDCl_3$)/ppm: ^1H: 7.79, 7.58, 7.43, 7.35 (m, phenyl CH), 4.22 (s, carboranyl CH), 4.2-1.2 (s, carboranyl BH); $^{13}C\{^1H\}$: 60.31 (carboranyl CH), 69.5 (carboranyl C-phenyl), 127.42, 1128.86, 129.92 (phenyl CH), 133.28 (*ipso* C)

Reaction of 1-phenyl-*meta*-carborane with NFBS

1-phenyl-*meta*-carborane (0.27g, 1.3mmol), dissolved in toluene was lithiated with a solution of n-BuLi (2.71M in hexanes, 0.5mL, 1.3mmol) and left to equilibrate for 1hour at ambient temperature. NFBS (0.5g, 1.6mmol) was added and the solution left stirring at room temperature for 5 days, resulting in a cloudy orange solution which settled to a clear orange solution and precipitate. The precipitate was removed by filtration and the solvent removed from the filtrate under reduced pressure. The resulting brown oil was washed with pentane, yielding more precipitate which in turn was filtered off. The solvent was again removed leaving a yellow oil containing the desired product. The oil was separated using prep. TLC (2:1 CH_2Cl_2:cyclohexane) and the product isolated from the top band as a white powder (0.07g). (Previous attempts of this prep. revealed that the compound was unstable to alumina and silica column chromatography.)

Yield : 24% IR: 3070 w, 3058 w (phenyl CH); 2605 s (carboranyl BH); 1494 m, 1446 m; 1261 m; 1224 m; 1079 s; 1046 s; 1023 s; 1002 m; 874 m, 863 m; 799 s; 739 s; 689 s; 661 m; 603 w; 576 w; 529 w; 490 w cm^{-1}

NMR ($CDCl_3$)/ppm: ^{19}F: -157 (carboranyl CF)

Reaction of *meta*-carborane with NFBS

Meta-carborane (0.38g, 2.6mmol) was dissolved in DME and a solution of n-BuLi (1.47M in hexanes, 4.5mL, 6.6mmol) added against a flow of dinitrogen to dilithiate the carborane. After 20 minutes equilibration at room temperature, NFBS (3.96g, 12.6mmol) was added producing an exothermic reaction resulting in a cloudy orange solution. The reaction was followed by ^{19}F NMR spectroscopy and after 48 hours reaction, peaks at -39.2 (NFBS), -110 (F^-), -155.5 and -157.0 (intensities *c.* 3:1) were noted. The reaction solution was diluted with diethyl ether, washed with distilled water and the aqueous layers re-extracted with ether. The combined organic layers were dried over anhydrous $MgSO_4$, filtered and the solvent removed under reduced pressure. The resulting solid decomposed on silica.

organic layer : ^{19}F NMR (Et_2O)/ppm: -39.2 (NFBS), -157.1 (carboranyl C-F)

Reaction of 1-phenyl-*para*-carborane with NFBS

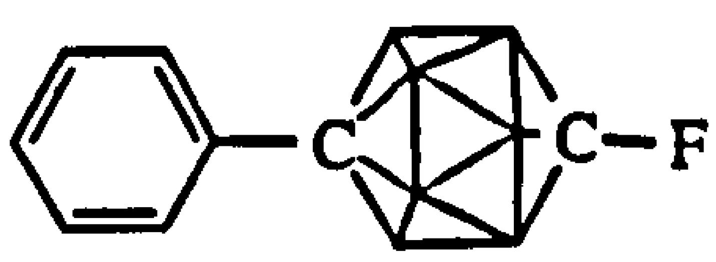

1-phenyl-*para*-carborane (0.12g, 0.5mmol) was dissolved in DME (40mL) and lithiated with a solution of BuLi (2.59M in hexanes, 1mL, 2.2mmol) to give a slightly cloudy solution. After stirring this solution for 30 minutes at room temperature, NFBS (0.52g, 1.6mmol) was added giving an intense yellow solution instantly. The reaction was followed by ^{19}F NMR spectroscopy and after 2 hours stirring at ambient temperature, no NFBS was detected in the reaction solution. The solution was diluted with diethyl ether and washed with distilled water. The aqueous layers were re-extracted with ether and the combined organic layers dried over $MgSO_4$, filtered. The solvent was removed under reduced pressure. The resulting yellow oil contained unreacted phenyl-*para*-carborane and 1-phenyl-12-fluoro-*para*-carborane.

NMR ($CDCl_3$)/ppm: ^{19}F : -150.64 (carboranyl C-F)

Reaction of *para*-carborane with NFBS

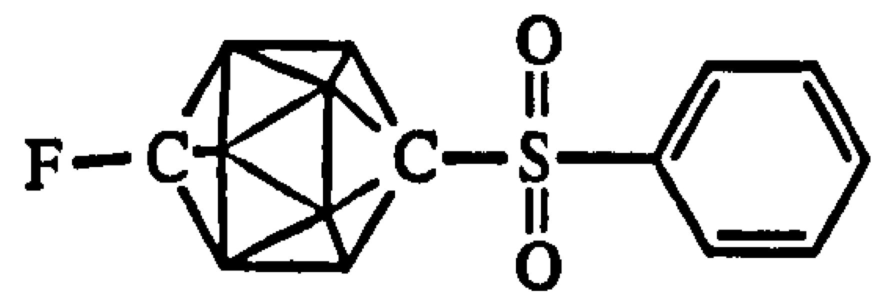

Para-carborane (0.40g, 2.8 mmole) was dissolved in DME (20mL) and lithiated with a solution of n-BuLi (4.5mL, 6.6 mmole - excess reagent was used to try to prevent starting material being an impurity in the final product mixture). After stirring at room temperature for 90 minutes, NFBS (4.77g, 15 mmole) was added, instantly turning the solution dark orange. The solution was left stirring at room temperature and the reaction was followed by ^{19}F NMR spectroscopy. After three days the reaction was deemed to be complete. The reaction solution was diluted with ether (150mL) and washed with water (4 x 150mL) to remove DME. The aqueous layers were extracted into ether and the combined organic layers dried over $MgSO_4$ and filtered. The volume of ether was reduced and a white solid, $PhSO_2Li$, dropped out of solution. The excess unused reagent proved extremely difficult to remove. The residue was transferred to sublimation apparatus and sublimed under dynamic vacuum (62°C) to give a red oily residue on the cold finger. This was washed into a conical flask with acetone and the acetone left to evaporate. After a few days, clear colourless crystals had grown which analysed as 1-fluoro-12-(phenylsulfonyl)-*para*-carborane.

Yield: 4% *IR*: 3068 w (phenyl C-H); 2962 w; 2631 s (carboranyl B-H); 1581 w; 1476 w; 1450 s (S=O); 1339 s (C-F or C-S); 1312 m; 1290 w; 1232 s (C-F?); 1181 m; 1154 s; 1087 s; 1072 m; 998 w; 986 w; 939 w; 879 m; 862 w; 761 s; 731 m; 720 s; 687 s; 602 s; 592 s; 539 s; 504 w; 454 w cm^{-1} *m/z*(EI$^+$): 302 ($C_8B_{10}H_{15}SO_2F$), 238, 141 ($C_2B_{10}H_{10}$), 77 (C_6H_5) *Elemental analysis* ($C_8B_{10}H_{15}SO_2F$): C 30.96% (31.80%), H 4.83% (5.00%) *m.p.*: 365°C

NMR ($CDCl_3$)/ppm : ^1H: 7.74, 7.55 (m, phenyl CH), 7.74; $^{13}C\{^1H\}$: 135.7 (*ipso* C), 135.1 (C6), 129.6 (C5), 129.1 (C4); 122.90, 118.09 (d, J_{CF}=302.5Hz, C1), 84.35 (C3); $^{11}B\{^1H\}$(250MHz Bruker): -14.61 (5B, J_{BH} = 159Hz), -15.63 (5B, J_{BH} = 195Hz); ^{19}F: -147.5 (s)

REACTIONS WITH BENZENESULFONYL FLUORIDE

1-(phenylsulfonyl)-*ortho*-carborane

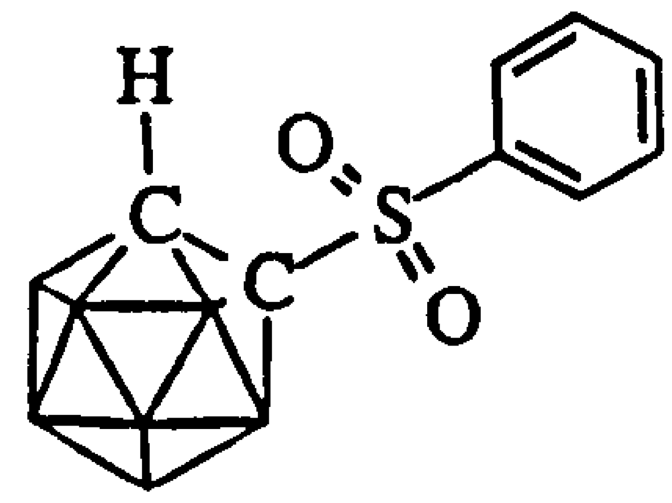

Ortho-carborane (0.72g, 5mmol) was dissolved in DME (60mL) under a dry dinitrogen atmosphere and monolithiated with a solution of n-BuLi (2.5M in hexanes, 2mL, 5mmol). After 20 minutes stirring at room temperature, benzenesulfonyl fluoride (0.7mL, 5.5mmol) was added giving a cloudy white solution instantly. After 4 hours at room temperature, the solution was diluted with diethyl ether and washed with distilled water. The isolated organic layer was dried over $MgSO_4$, filtered and the solvent removed under reduced pressure. Washing the resulting brown solid with a small quantity of ethanol yielded a white insoluble powdery solid (0.38g).

Yield : 27% IR: 3420 br.,s, 3376 br., s, 3284 br., s; 3068 s (carboranyl CH); 2600 s, 2574 s (carboranyl BH); 1685 w, 1655 w; 1447 s, 1419 s (sulfonyl SO); 1237 s; 1187 s; 11131 s; 1039 s; 1019 s 997 m; 884 w; 799 w; 756 m; 735 m; 717 m; 688 m; 627 m; 611 m; 572 m; 492 w cm^{-1}

1-phenyl-2-(phenylsulfonyl)-*ortho*-carborane

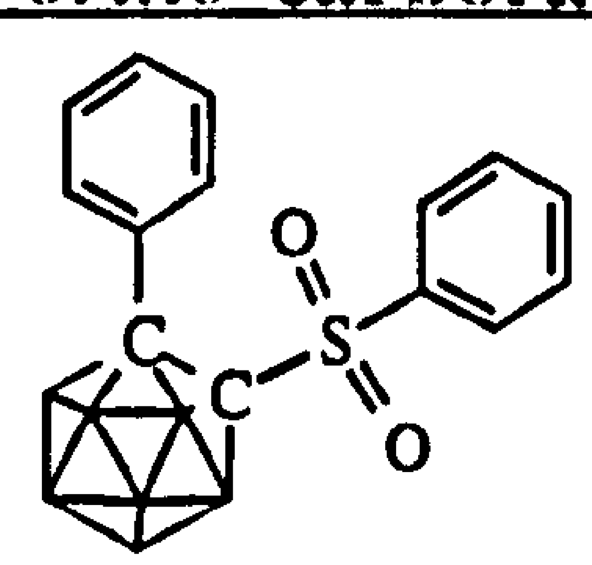

1-pheny-*ortho*-carborane (0.22g, 1mmol) was dissolved in DME (45mL) and lithiated with a solution of nBuLi (2.59M in hexanes, 0.6mL, 1.5mmol). After equilibrating at room temperature for 1.5 hours, benzenesulfonyl fluoride (0.15mL, 1.3mmol) was added yielding a yellow solution. This was diluted with diethyl ether, washed with distilled water, and the organic layers dried over $MgSO_4$. Solvent was removed from the subsequent filtrate under reduced pressure to leave a pale brown oily solid. Washing this oil with a small quantity of ethanol yielded the product as fine white crystals (0.12g).

Yield : 33% IR: 3090 w, 3068 w, 3030 w (phenyl CH); 2962 w, 2934 w; 2634 m, 2600 s, 2590 s, 2566 s, 2556 s (carboranyl BH); 1447 s (sulfonyl SO), 1354 s (sulfonyl SO or CS), 1315 w; 1261 w; 1187 s; 1161 s; 1082 s; 938 m; 883 m; 801 m; 750 m; 713 w; 684 s; 632 m; 589 m; 571 s; 528 m; 489 w; 455 w cm^{-1} m/z (EI^+): 360 ($C_{14}B_{10}H_{20}SO_2$), 296 ($C_{14}B_{10}H_{20}$)

NMR ($CDCl_3$)/ppm: ^1H: 7.9 (d), 7.6-7.3 (10H, m, phenyl CH); 4-1 (10H, br., carboranyl BH)

1-phenyl-7-(phenylsulfonyl)-*meta*-carborane

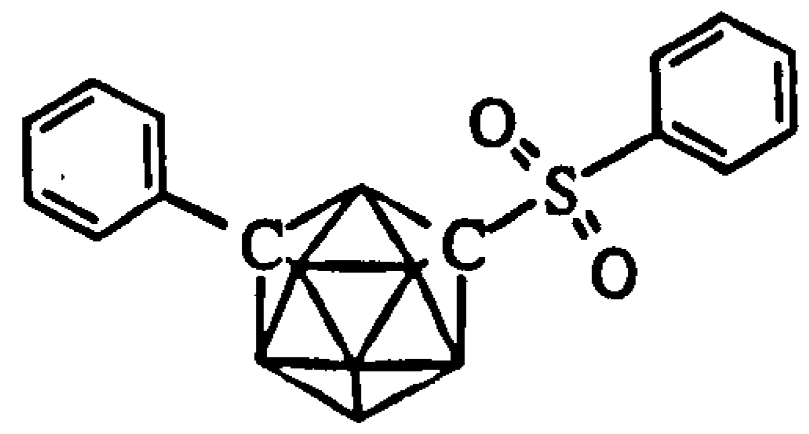

1-phenyl-*meta*-carborane (0.22g, 1mmol) was dissoved in DME (40mL) and lithiated with a solution of n-BuLi (2.59M in hexanes, 0.5mL, 1.3mmol). After stirring at room temperature for two hours, benzenesulfonyl fluoride (0.15mL, 1.3mmol) was added and the solution left stirring at room temperature for a further hour. The final reaction solution was diluted with ether, transferred to a separating funnel and washed with distilled water. The aqueous layers were re-extracted with ether, and the combined organic layers dried over $MgSO_4$ then filtered. The solvent was removed under reduced pressure. Purification of the resulting oil was achieved by column chromatography on silica (1:1 CH_2Cl_2:cyclohexane) to yield the product as a pale yellow solid (R_F=0.48).

Yield : 72% IR: 3090 w, 3064 w, 3042 w (phenyl C-H); 2963 m; 2642 m, 2632 m, 2612 s, 2590 s, 2578 s (carboranyl B-H); 1582 w; 1492 w; 1447 m (sulfonyl S=O); 1345 m; 1310 w; 1261 s; 1169 m; 1153 m; 1089 s; 1021 s; 872 w; 799 s; 762 w; 745 w; 718 w; 694 w; 683 m; 635 m; 576 s; 540 w cm^{-1} m/z : 355, 296, 220 ($C_{14}B_{10}H_{20}SO_2$ requires 360) Elemental analysis : C 41.94% (46.65%), H 5.79% (5.59%) m.p.: 120-123°C

NMR($CDCl_3$)/ppm: ^1H: 7.9 (2H, m, phenylsulfonyl CH, *ortho*), 7.7 (1H, m, phenylsulfonyl CH, *para*), 7.6 (2H, m, phenylsulfonyl CH, *meta*), 7.4 (2H, m, phenyl CH, *meta*), 7.3 (3H, m, phenyl CH, *ortho, para*), 4-1 (10H, br., carboranyl BH); $^{13}C\{^1H\}$: 136.55 (phenyl C, *ipso*), 135.96 (phenylsulfonyl *para* CH), 134.73 (phenyl sulfonyl C, *ipso*), 130.82 (phenylsulfonyl CH, *ortho*), 129.90 (phenylsulfonyl CH, *meta*), 129.86 (phenyl CH, *para*), 129.28 (phenyl CH, *ortho*), 128.41 (phenyl CH, *meta*), 88.89 (carboranyl C-sulfonyl), 78.5 (carboranyl C-phenyl)

1-phenyl-12-(phenylsulfonyl)-*para*-carborane

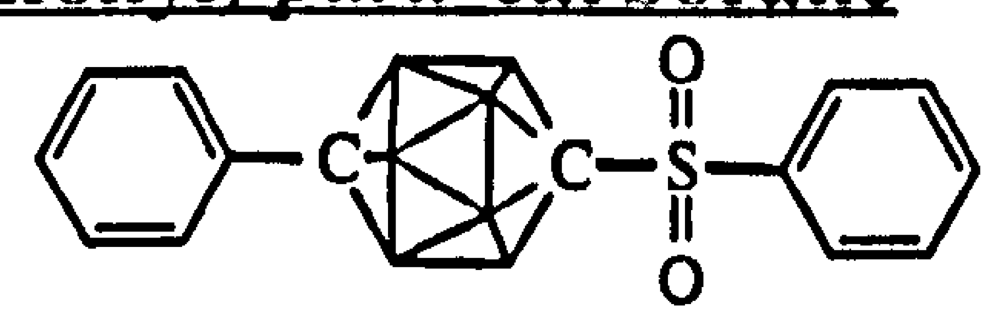

1-phenyl-*para*-carborane (0.22g, 1mmol) was dissolved in DME and lithiated with a solution of nBuLi (2.59M in hexanes, 0.5mL, 1.3mmol). After stirring for 2 hours at room temperature, benzenesulfonyl fluoride (0.14mL, 1.2mmol) was added, and after 30 minutes at room temperature a slightly cloudy solution was produced. This was diluted with diethyl ether, washed with distilled water, and the organic layers dried over $MgSO_4$ before being filtered and the solvent removed under reduced pressure. The resulting sticky white solid was washed with a small amount of ethanol to remove unreacted benzenesulfonyl fluoride, yielding a powdery white solid (0.26g). Clear colourless crystals (0.09g) formed in the ethanol washings which also analysed as the product.

Yield : 97% IR: 3164 w, 3096 w, 3064 w, 3030 w (phenyl CH); 2615 s (carboranyl BH); 1581 m; 1497 m, 1477, 1447 s (sulfonyl SO); 1336 s; 1313 s; 1262 m; 1166 s, 1154 s; 1087 s; 1023 m; 918 w; 849 m; 787 m; 759 m; 741 s; 721 s; 687 s; 631 s; 601 m; 578 s; 541 s; 490 m; 450 m cm^{-1} *m/z* (EI^+): 360 ($C_{14}B_{10}H_{20}SO_2$), 296 ($C_{14}B_{10}H_{20}$), 249, 236, 219 Elemental analysis : C 46.48% (46.65%), H 5.50% (5.59%) m.p.: 177.5-178.5°C

NMR ($CDCl_3$)/ppm: ^1H: 7.9 m, 7.7 m (5H, phenyl CH), 7.3 m (5H, phenyl CH), 4-1 (10H, br., carboranyl BH); $^1H\{^{11}B\}$: 7.7 (2H, m, phenyl*ortho* CH), 7.6 (1H, m, phenyl *para*CH), 7.5 (2H, m, phenyl *meta*CH), 7.2 (1H, m, phenyl *para*CH), 7.1 ((4H, m, phenyl*o,m*CH), 2.53 (5H, s, carboranyl BH), 2.48 (5H, s, carboranyl BH); $^{13}C\{^1H\}$: 136.32, 135.94, 135.64, 130.70, 129.67, 129.49, 128.90, 127.45 (phenyl C's); 92.17, 86.10 (carboranyl C's); $^{11}B\{^1H\}$: -13.04 (5B, J_{BH}=167Hz), -14.13 (5B, J_{BH}=169Hz)

1,12 -di-(phenylsulfonyl)-*para*-carborane

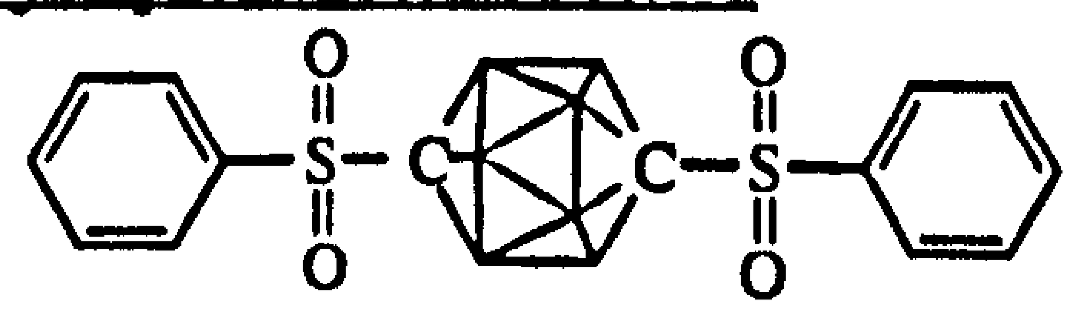

Para-carborane (0.72g, 5mmol) was dissolved in DME (75mL) and lithiated with a solution of n-butyl lithium (2.38M in hexanes, 2.5mL, 6mmol) giving a pale yellow cloudy solution. Against a flow of dinitrogen, benzenesulfonyl fluoride (0.60mL, 5mmol) was added. After stirring for 20 minutes at room temperature, the cloudy yellow solution was diluted, transferred to a separating funnel, washed with distilled water (2x50mL), then the combined aqueous layers were re-extracted with diethyl ether. The insoluble precipitate which formed at the aqueous/organic interface was removed by filtration and dried under vacuum yielding a white powder (0.76g) identified as the desired product. A second crop (0.19g) was obtained from the organic residue, which was washed with acetone to remove impurities, and the product was recrystallised from toluene, yielding clear colourless crystals. Unreacted *para*-carborane was removed from the organic residue by sublimation under dynamic vacuum.

Yield : 90% *IR*: 3091 w, 3062 m (phenylC-H); 2636 s, 2625 s, 2609 s (carboranyl B-H); 1581 s; 1475 m; 1447 s; 1340 s; 1316 s; 1288 m; 1168 s; 1157.14(s); 1083.18(s); 1023 m; 996 m; 941 w; 784 s; 763 s; 737 m; 713 s; 687 s; 670 m; 601 s; 584 s; 533 s; 461 m; 447 s cm^{-1} *m/z*(EI^+): 424 ($C_{14}H_{20}B_{10}S_2O_4$), 360 ($C_{14}H_{20}B_{10}S_2$), 284 ($C_8H_{16}B_{10}SO_2$) *Elemental analysis* : C 38.66% (39.61%), H 4.73% (4.75%) *m.p.*: 337-339°C
NMR ($CDCl_3$)/ppm: $^1H\{^{11}B\}$: 7.66 (3H, m, phenyl CH), 7.48 (2H, m, phenyl CH); 2.38 (10H, s, carboranyl BH); $^{13}C\{^1H\}$: 135.31, 135.09, 130.03, 129.15 (phenyl C), 67.0 (carboranyl C); $^{11}B\{^1H\}$: -11.11 (d, J_{BH} = 176.51Hz)

1-(trimethylsilyl)-*para*-carborane

A solution of *para*-carborane(1.42g, 10mmol) in dry DME (50mL) was monolithiated with a solution of n-butyl lithium (2.59M in hexanes, 3.9mL, 10mmol) giving a clear colourless solution after 1 hour stirring at room temperature. Trimethylsilylchloride (1.35mL, d=0.856, 11mmol) was added against a flow of dinitrogen to give a pale yellow solution which was left stirring overnight at room temperature. The resultant solution was diluted with diethyl ether (75mL) and toluene (100mL) and transferred to a separating funnel. The organic solution was washed with 2M HCl, distilled water, and the aqueous layer reextracted into toluene. Removal of the organic solvents from the combined organic layers yielded a yellow oil. Sublimation removed unreacted *para*-carborane (60°C) then the desired product (0.86g) at 70°C under dynamic vacuum.

Yield: 40% *IR*: 3061 m (carboranyl C-H); 2960 m (methyl CH_3); 2900 w; 2607 s (carboranyl B-H); 1408 w; 1253 s (Si-$(CH_3)_3$); 1142 w; 1099 s; 1045 w; 1015 w; 914 m; 846 s (Si-$(CH_3)_3$); 773 m (Si-$(CH_3)_3$) cm^{-1} *Elemental analysis* ($C_5B_{10}H_{20}Si$): C 25.60% (27.75%), H 9.23% (9.32%)

NMR ($CDCl_3$)/ppm: ^1H: 3.8-0.8 (10H, br., carboranyl B-*H*), 2.85 (1H, s, carboranyl C-*H*); 0.06 (12H, Si-(CH_3)$_3$); $^{13}C\{^1H\}$: 75.03 (carboranyl *C*-Si), 67.26 (carboranyl *C*-H), -0.60 (Si-(CH_3)$_3$)

Reaction between 1-(trimethylsilyl)-*para*-carborane and $PhSO_2F$

1-(trimethylsilyl)-*para*-carborane (0.5g, 2.3mmol) was dissolved in DME and lithiated with a solution of butyl lithium (2.59M in hexanes, 1.2mL, 3mmol). After 30 minutes stirring at room temperature, benzene sulfonyl fluoride (0.3ml, 2.6mmol) was added and the solution left to stir at room temperature for a further hour. The final reaction solution was diluted with ether and washed with distilled water. The organic layer was dried over anhydrous magnesium sulfate, filtered, and the solvent removed to leave *para*-carborane.

REACTIONS WITH BENZENE SULFONYL CHLORIDE

1-chloro-*para*-carborane

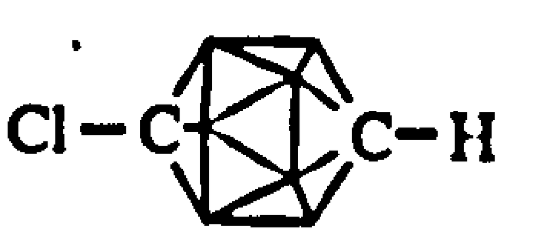

Para-carborane (0.74g, 5mmol) was dissolved in DME (75mL) and monolithiated with a solution of n-butyl lithium (2.5M in hexanes, 6.5mmol) giving a cloudy white solution. The addition of benzenesulfonyl chloride (0.7mL, d=1.384g cm^{-1}, 5mmol) instantly precipitated a white solid. The solution was diluted with ether and washed with distilled water. The organic layer was isolated and the solvent removed under reduced pressure to leave an off-white solid which sublimed under dynamic vacuum (25°C) to give a white solid (0.41g).

Yield : 48% *IR*: 3065 m (carboranyl C-H); 2942 w; 2875 w; 2615 s (carboranyl B-H); 2264 w; 2138 w; 2032 w; 1924 w; 1829 w; 1618 w; 1386 w; 1261 m; 1193 w; 1138 s; 1094 s; 1069 s; 1036 s; 1004 s; 936 w; 905 s; 823 m; 792 s; 775 w; 761 m; 727 s; 647 m; 535 w; 492 w; 403 w cm^{-1} *m/z*(EI$^+$): 196, 180 ($C_2B_{10}H_{11}Cl$), 152 *Elemental analysis* ($C_2B_{10}H_{11}Cl$): C 12.64% (13.45%), H 6.38% (6.21%), Cl 18.70% (19.84%) *m.p.*: 158°C (sublimes)
NMR ($CDCl_3$)/ppm: ^1H: 2.60 (1H, carboranyl C-H), 4-1 (10H, br., carboranyl B-H); $^{13}C\{^1H\}$: 81.35 (carboranyl C-Cl), 55.29 (carboranyl C-H); $^{11}B\{^1H\}$: -11.81 (5B, d, J_{BH} = 169Hz), -15.87 (5B, d, J_{BH} = 167Hz) [$^{11}B\{^1H\}$ (250MHz Bruker): -11.39, -15.41]

Note: The above reaction was repeated for *ortho*- and *meta*-carboranes, but in each case, unreacted carborane was the only recovered carborane product.

PYRIDYL AND THIOPHENYL CARBORANES

1-(3'-pyridyl)-*ortho*-carborane

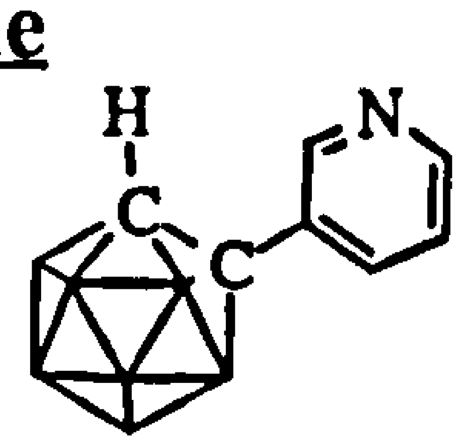

Ortho-carborane (1.44g, 10mmol) was dissolved in DME (100mL) and lithiated with a solution of n-butyl lithium (9.5mL, 24mmol) to give a cloudy white solution after 40 minutes stirring at room temperature under N_2. Copper(I) chloride (2.23g, 22mmol) was added to the reaction mixture together with pyridine (13mL) to give a black solution. After one hour at the reflux temperature, 3-bromo-pyridine (2mL, 21mmol) was added, and the solution left to reflux under a positive nitrogen pressure for 7 days. The resulting deep red cloudy solution was allowed to cool to room temperature, then stirred with diethyl ether (100mL) for four hours to destroy the copper/pyridine complex. The precipitate was filtered off, and the green filtrate transferred to a separating funnel where it was washed with 2M HCl (3x *c*.70mL) and distilled water (3x *c*.50mL). The combined aqueous layers were re-extracted with diethyl ether (2x c. 50mL). $MgSO_4$ was used to dry the combined organic layers, the solution filtered, and the solvent removed to leave a pale yellow solid.

The product was purified by column chromatography on silica (chloroform) collecting the fractions in 25mL aliquots. The product was collected in fractions 14 - 23 (R_F= 0.18) as a pale yellow solution. This was washed with activated charcoal, filtered and the solvent removed leaving a very pale yellow solid (0.74g) which analysed as 1-(3'-pyridyl)-*ortho*-carborane.

Yield: 33% *IR* (KBr disc): 3024 m (pyridyl CH); 2963 m; 2640 m, 2629 m, 2616 m, 2590 s; 2555 s (carboranyl B-H); 1476 m; 1420 m; 1261 s; 1097 s; 1075 s; 1020 s; 877 w; 800 s; 722 w; 704 m cm^{-1} *IR* (CCl_4 solution): 3086 w, 3070 w, 3042w (carboranyl C-H, pyridyl C-H); 2962 m; 2599 s (carboranyl B-H); 1569 s; 1549 s; 1480 m; 1419 m; 1260 s; 1216 m; 1097 s; 1076 s; 1013 s; 981 m; 794 s, 761 s (CCl_4); 704 m cm^{-1} *m/z* (EI^+): 221 ($C_7B_{10}H_{15}N$) *Elemental analysis* ($C_7B_{10}H_{15}N$): C 36.64% (37.99%), H 7.01% (6.80%), N 4.73% (6.33%) *m.p.*: 129.1°C

NMR ($CDCl_3$)/ppm: ^1H: 8.75 (1H, br. s), 8.73 (1H, br. s), 7.81 (1H, br. s), 7.28 (1H, br. s, pyridyl C-*H*); 3.96 (1H, s, carboranyl C-*H*); 4 - 1 (10H, br., carboranyl B-*H*); $^1H\{^{11}B\}$: as ^1H, with BH region as 2.62 (1H), 2.47 (4H), 2.35 (4H), 2.30 (1H); $^{13}C\{^1H\}$: 150.99, 148.25, 135.40, 129.58 (*ipso* C), 123.32 (pyridyl *C*-H), 73.60 (carboranyl C-pyridyl), 60.09 (carboranyl C-H); $^{11}B\{^1H\}$: 1.49 (1B, d, J_{BH}=149Hz), -0.59 (1B, d, J_{BH}=149Hz) (B9 and B12); -5.56 (2B, d, J_{BH}=153Hz), -7.74 (2B, d, J_{BH}=173Hz), -8.45 (2B, d, J_{BH}=165Hz), -9.37 (2B, d, J_{BH}=165Hz)

1-(3'-pyridyl)-*meta*-carborane and 1,7-di-(3'-pyridyl)-*meta*-carborane

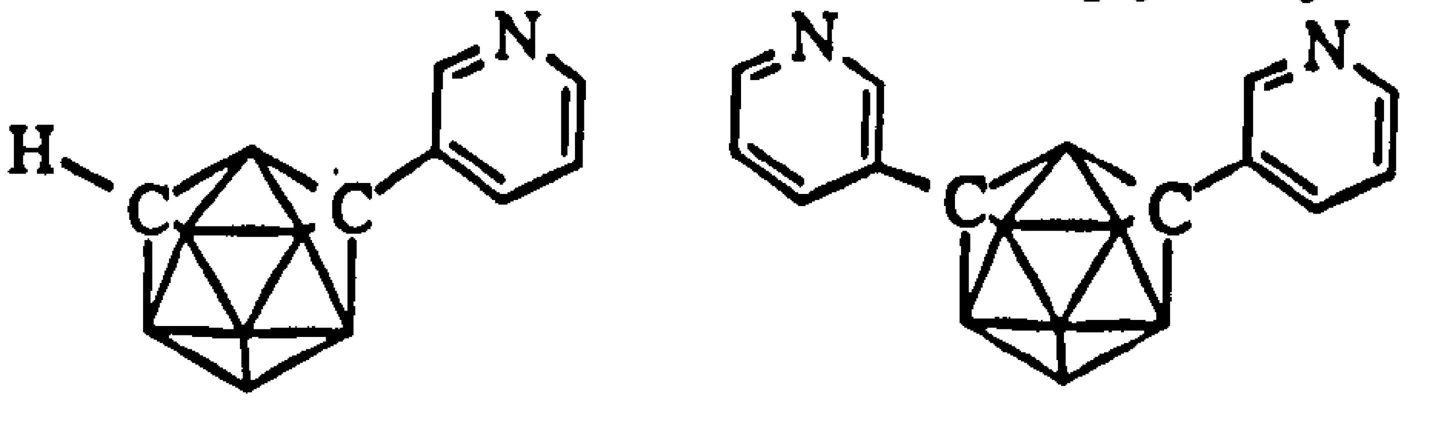

Following the same general procedure as above, *meta*-carborane (2.93g, 20mmol) was dissolved in DME (150mL) and dilithiated with a solution of n-BuLi (2.59M in hexanes, 41mmol). After being allowed to equilibrate for one hour at room temperature, copper(I) chloride (4.08g, 41mmol) and pyridine (24mL) were added and the solution refluxed for 1.5 hours to give a red-brown cloudy solution. To this, 3-bromo-pyridine (42mmol) was added and solution left to reflux for 3 further days. The solution was cooled to room temperature and treated with ether as before. The filtrate was washed with HCl, distilled H_2O and the aqueous layers re-extracted into ether. The combined organic layers were dried and the solvent removed to leave a brown crystalline solid. Unreacted *meta*-carborane (1.06g, 7mmol) was removed by sublimation under dynamic vacuum (40°C), followed by 1-(3'-pyridyl)-*meta*-carborane (90°C). The unsublimed residue, once decolourised with activated charcoal and recrystallised from ethanol gave 1,7-di-(3'-pyridyl)-*meta*-carborane as a pale yellow crystalline solid.

1-(3'-pyridyl) -meta-carborane

Yield : 54% IR (KBr disc): 3096 w (pyridyl C-H); 3042 w; 3022 s (carboranyl C-*H*); 2974 w; 2624 s, 2596 s, 2589 s, 2578 s (carboranyl B-H); 1573 m; 1482 s; 1417 s; 1341 m; 1198 m; 1132 m; 1083 m; 1057 m; 1031 m; 975 m; 923 w; 877 m; 838 w; 822 m; 731 m; 704 s; 684 m; 625 w cm^{-1} IR (CCl_4 solution): 3405 br.; 3090 w; 3068 w (carboranyl C-H); 3042 w; 2607 s (carboranyl B-H); 1549 s (pyridyl); 1480 m; 1417 m; 1253 m; 1217 m; 1085 w; 1031 w; 1007 m; 978 m; 876 w; 794 s, 763 s (CCl_4) cm^{-1} m/z(EI^+): 221 ($C_7H_{15}NB_{10}$) Elemental analysis ($C_7B_{10}H_{15}N$): C 37.90% (37.99%), H 7.47% (6.83%), N 5.91% (6.33%) m.p.: 90-92°C

<u>NMR</u> ($CDCl_3$)/ppm: ^{1}H: 8.66 (1H, s, C(2)-H), 8.50 (1H, d, J_{CH}=*c*.5Hz, C(4)-H), 7.68 (1H, d, J_{CH}=*c*.10Hz, C(6)-H), 7.18 (1H, m, C(5)-H); 4.2-1.2 (10H, br., carboranyl B-*H*); 3.28 (1H, carboranyl C-*H);* ^{1}H{^{11}B}: as ^{1}H, with BH region as 3.10 (1H, Cb CH), 2.94 (1H), 2.61 (1H), 2.46 (2H), 2.27 (4H), 2.20 (2H); ^{13}C{^{1}H}: 150.45, 149.09, 135.89, 131.76 (*ipso C*), 123.61 (pyridyl *C*); 75.65 (carboranyl *C*-pyridyl); 56.09 (carboranyl *C*-H); ^{11}B{^{1}H}: -4.29 (1B, d, J_{BH}=161Hz), -8.39 (1B, d, J_{BH}=165Hz), -10.51 (4B, d, J_{BH}=153Hz), -13.37 (2B, J_{BH}=167Hz), -15.387 (2B, J_{BH}=181Hz)

<u>1,7-di-(3'-pyridyl)-meta-carborane</u>

<u>Yield</u> : trace *<u>IR</u>*: 3088 w, 3048 w, 3038 w (pyridyl CH); 2635 s, 2599, 2575 s (carboranyl BH); 1567 m; 1476 s; 1417 s; 1260 m; 1194 m; 1130 m; 1083 m; 1022 s; 921 w; 889 w; 872 w; 855 m; 821 m; 738 m; 701 s; 619 m cm^{-1} *<u>m/z</u>*(EI$^+$) : 299 ($C_{12}B_{10}H_{18}N_2$) *<u>Elemental analysis</u>* ($C_{12}B_{10}H_{18}N_2$): C 47.27% (48.30%), H 6.19% (6.08%), N 8.90% (9.39%)

<u>NMR</u> ($CDCl_3$)/ppm: ^{1}H{^{11}B}: 8.72 (2H, s, pyridyl CH), 8.57 (2H, s, pyridyl CH), 7.7 (2H, m, pyridyl CH), 7.2 (2H, m, pyridyl CH); ^{11}B{^{1}H}: -5.66 (1B, d, J_{BH}=148Hz), -10.17 (4B, d, J_{BH}=149Hz), -10.65 (4B, d, J_{BH}=169Hz), -13.62 (1B, d, J_{BH}=178Hz)

<u>1-(2'-thiophenyl)-*ortho*-carborane</u>

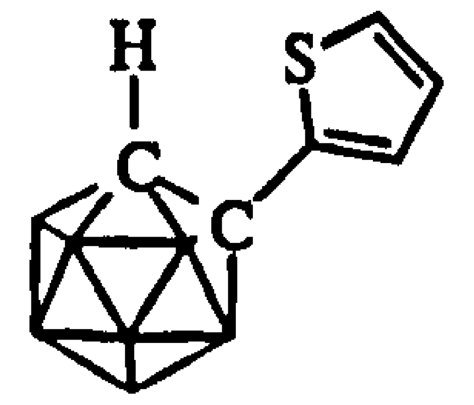

Ortho-carborane (2.88g, 20mmol) was dissolved in dry DME (200mL) and dilithiated with a solution of n-butyl lithium (2.59M in hexanes, 17mL, 44mmol). After stirring for 40 minutes at room temperature, a cloudy white solution was obtained. Copper(I) chloride (4.25g, 42mmol) and dry pyridine (12mL) were added, and the resulting solution heated to the reflux temperature and left to reflux for 1 hour before the addition of 2-iodo-thiophene (4.5mL, 41mmol). The resulting solution was refluxed for a further three days. After this time, TLC($CHCl_3$) indicated there was only one reaction product. The solution was allowed to cool to room temperature before being stirred with diethyl ether overnight to destroy the copper/pyridine complex. The resulting precipitate was removed by filtration, and the filtrate washed first with 2M HCl, then distilled H_2O. The aqueous washings were re-extracted with diethyl ether and the combined organic layers dried over $MgSO_4$. The solvent from the filtered solution was removed under reduced pressure, leaving a blood red oil, which was purified by column chromatography (silica, CH_2Cl_2, R_F= 0.90). The resulting product was further purified by distillation under dynamic vacuum yielding the product as a yellow oil (1.22g) which solidified on standing.

Yield: 27% *IR* (KBr disc): 3110 w, 3092 w, 3063 m (thiophenyl CH, carboranyl intramolecular C-H-S); 2596 s (carboranyl B-H); 1429 m; 1355 m; 1253 m; 1226 m; 1149 w; 1069 m; 1015 m; 859 w; 826 w; 719 s; 699 s cm^{-1} *IR* (CCl_4 solution): 3406 br; 3071 m (carboranyl C-H); 2600 s (carboranyl B-H); 1549 s; 1255 s; 1219 m; 1071 m; 1006 s; 979 s; 792 s, 761 s (CCl_4); 707 s cm^{-1} *m/z*(EI^+): 352 ($C_6B_{10}H_{13}SI$, 1% of baseline), 226 ($C_6B_{10}H_{14}S$) *Elemental analysis* ($C_6B_{10}H_{14}S$): C 31.48% (31.84%), H 6.13% (6.23%) *m.p.*: 69°C *b.p.*: 344°C
NMR ($CDCl_3$)/ppm: $^1H\{^{11}B\}$: 7.17(d), 7.12(d), 6.8(t) (3H, thiophenyl C-*H*); 3.75 (s, carboranyl C-*H*), 2.67(s), 2.40(s), 2.21(s), 4-1(11H, br., carboranyl B-*H*); $^{13}C\{^1H\}$: 137.4(*ipso* C); 130.6, 128.53, 127.9 (thiophenyl *C*-H); 72.65 (carboranyl *C*-thiophene); 63.9 (carboranyl *C*-H); $^{11}B\{^1H\}$: -1.77 (1B, d, J_{BH}=150Hz), -5.02 (1B, d, J_{BH}=149Hz), -9.65 (2B, d, J_{BH}=170Hz), -10.33 (2B, d, J_{BH}=*c*.150Hz), -11.59 (2B, d, J_{BH}=*c*. 180Hz), -12.89 (2B, d, J_{BH}=164Hz)

1-(2'-thiophenyl)-*meta*-carborane and 1,7-di-(2'-thiophenyl)-*meta*-carborane

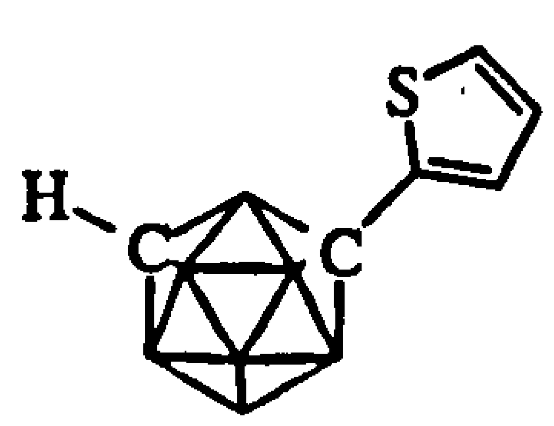

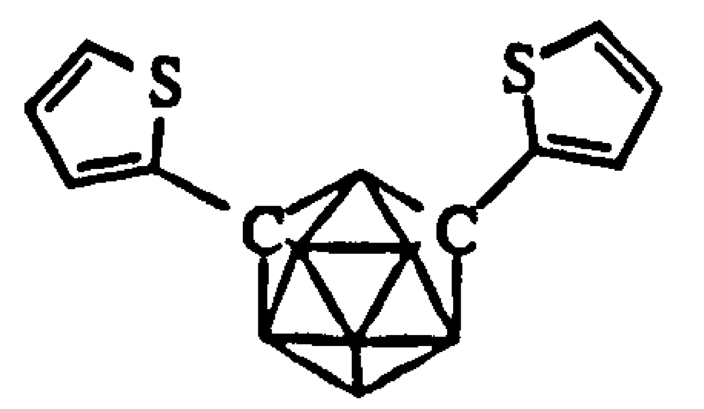

Following the same general procedure as before, *meta*-carborane (2.88g, 20mmol) was dissolved in DME (80mL) and mono-lithiated with a solution of n-BuLi (2.59M in hexanes, 8mL, 21mmol) giving a clear yellow solution. Copper(I) chloride (2.07g, 21mmol) and pyridine (12mL) were added, and after refluxing this solution for 2 hours, 2-iodothiophene (2.3mL, 20mmol) was added. The solution was left to reflux for 3 days. The solution was cooled to room temperature and stirred with ether overnight to destroy the copper/pyridine complex. Filtration left an orange solution which was washed with 2M HCl and distilled water. The aqueous layers were then re-extracted with ether and the combined organic layers dried over $MgSO_4$, filtered and the solvent removed under reduced pressure leaving an oily orange solid. Unreacted *meta*-carborane was recovered by sublimation and the remaining product was purified by distillation giving a yellow oil (1.5g). GC showed this to contain two products (mono 94%, di 6%). The undistilled residue crystallised and analysed satisfactorily for the disubstituted product.

1-(2'-thiophenyl)-meta-carborane

IR (KBr disc): 3058 m (carboranyl C-H); 2603 s (carboranyl B-H); 1431 m; 1245 m; 1215 m; 1128 w; 1084 m; 1022 m; 1008 m; 858 w; 843 s; 835 s; 815 m; 726 s; 702 s cm^{-1} IR (CCl_4 solution): 3405 br. w; 3068 w (carboranyl C-H); 2606 s (carboranyl B-H); 1549 s; 1249 m; 1217 m; 1084 m; 1008 m; 978 m; 793 s, 761 s (CCl_4); 701 s cm^{-1}
m/z (EI^+): 226 ($C_6H_{14}B_{10}S$) m.p.: 36-37°C
NMR ($CDCl_3$)/ppm: $^1H\{^{11}B\}$: 7.13 (1H, m), 6.98 (1H, m), 6.84 (1H, m) (thiophenyl C-*H*); 3.06 (1H, s, carboranyl C-*H*), 3.8-1 (10H, br., carboranyl B-*H*); $^1H\{^{11}B\}$: as for ^1H, with BH region as 3.06 (1H, s, carboranyl C-*H*), 3.01 (1H), 2.70 (1H), 2.65 (2H), 2.28 (4H), 2.21 (2H); $^{13}C\{^1H\}$: 139.59 (*ipso C*), 127.98, 127.53, 126.69 (thiophenyl *C*-H), 73.47 (carboranyl *C*-thiophene), 57.80 (carboranyl *C*-H); $^{11}B\{^1H\}$: -0.15 (1B, d, J_{BH}=163Hz); -5.96 (1B, d, J_{BH}=122Hz), -6.67 (2B, d, J_{BH}=138Hz), -7.43 (2B, d, J_{BH}=138Hz), -10.32 (2B, d, J_{BH}=179Hz), -11.51 (2B, d, J_{BH}=187Hz)

1,7-di-(2'-thiophenyl)-meta-carborane

IR (KBr disc): 3104 w, 3094 w, 3082 w (thiophenyl C-H); 2963 s; 2630 m, 2603 s, 2572 m (carboranyl B-H); 1430 m, 1412 m (thiophenyl C-S); 1352 w; 1261 s; 1215 w; 1097 s, 1020 s; 857 m; 799 s; 703 m cm^{-1} m/z (EI^+): 308 ($C_{10}B_{10}H_{16}S_2$) Elemental analysis ($C_{10}B_{10}H_{16}S_2$): C 38.33% (38.93%), H 5.56% (5.23%) m.p.: 119-121°C
NMR ($CDCl_3$)ppm: ^1H: 7.15 (2H, m), 7.03 (2H, m), 6.86 (2H, m) (thiophenyl C-*H*), 4-1ppm (10H, br., carboranyl B-*H*); $^1H\{^{11}B\}$: as ^1H with BH region as 3.36 (2H), 2.65 (6H), 2.30 (2H); $^{13}C\{^1H\}$: 139.34 (*ipso C*); 128.11, 127.60, 126.88 (thiophenyl *C*-H), 73.47 (carboranyl *C*-thiophene); $^{11}B\{^1H\}$: -2.48 (2B, d, J_{BH}=163Hz, antipodal *B*-H); -6.95 (4B, d, J_{BH}=159Hz); -7.45 (2B, d, J_{BH}=138Hz); -9.23 (2B, d, J_{BH}=183Hz)

2.5 SUMMARY

This chapter has concentrated on the synthetic methodologies employed in carborane derivatisation, including new synthetic routes to sulfonylated and fluoro-carboranes. Of particular interest have been hydroxide and carboxylic acid derivatives, together with their anions, synthesised following known preparative routes from the parent carboranes $RCB_{10}H_{10}CH$, where R is an aryl group. Electrophilic fluorinating agents NFBS (*N*-fluorobenzenesulfonimide) and pyF^+ (1-fluoro-2,6-dichloro-pyridinium tetrafluoroborate) have been explored as reagents suitable for carboranyl carbon fluorination, and NFBS has proven mildly successful. Investigations of the reactions of lithio-carboranes with the sulfonyl halide species, $PhSO_2Cl$ and $PhSO_2F$

has led to a novel route to sulfonylated carboranes. $PhSO_2Cl$ effected carborane C-chlorination whilst $PhSO_2F$ caused the $PhSO_2$ group to substitute onto the cage carbon atom. *Ortho-* and *meta*-carboranes substituted with the heteroaryl groups 3-pyridyl and 2-thiophenyl, have also been synthesised. Chapter Three will discuss the electronic influences these substituents exert on the *closo*-C_2B_{10}-icosahedra, and will also look at hydrogen bonding interactions between selected derivatives.

2.6 REFERENCES

1 V.I. Stanko, V.V. Kopylov, A.I. Klimova, J. Gen. Chem. USSR, 1965, **35**, 1437

2 T.L Heying, J.W. Ager, S.L. Clark, D.J. Mangold, H.L. Goldstein, M. Hillman, J. Polak, J.W. Szymanski, Inorg. Chem., 1963, **2**, 1097

3 D. Graftstein, J. Dvorak, Inorg. Chem., 1963, **2**, 1128

4 L.I. Zakharkin, A.V. Kazantsev, J. Gen. Chem. USSR, 1967, **37**, 1149

5 D. Grafstein, J. Bobinski, J. Dvorak, H. Smith, N. Schwartz, M.S. Cohen, M.M. Fein, Inorg. Chem., 1963, **2**, 1120

6 J. Cai, H. Nemoto, B. Singram, Y. Yamamoto, Tet. Lett., 1996, **37**, 3383

7 L.I. Zakharkin, V.I. Stanko, Y.A. Chapovskii, Bull. Acad. Sci. USSR, 1964, 547

8 L.I. Zakharkin, Bull. Acad. Sci. USSR, 1965, 138

9 L.I. Zakharkin, Tet. Lett., 1964, no. 33, 2255

10 T.L. Heying, J.W. Ager, S.L. Clark, R.P. Alexander, S. Papetti, J.A. Reid, S.I. Trotz, Inorg. Chem., 1963, **2**, 1097

11 L.I. Zakharkin, A.V. Grebennikov, L.E. Vinogradova, L.A. Leites, J. Gen. Chem. USSR, 1968, **38**, 1008

12 L.I. Zakharkin, A.I. Kovredov, Bull. Acad. Sci. USSR, Div. Chem. Sci., 1974, 710

13 R. Coult, M.A. Fox, W.R. Gill, P.L. Herbertson, J.A.H. MacBride, K. Wade, J. Organomet. Chem., 1993, **462**, 19

14 W.R. Gill, P.L. Herbertson, J.A.H. Macbride, K. Wade, J. Organomet. Chem., 1996, **507**, 249

15 U. Schöberl, T.F. Magnera, R.M. Harrison, F. Fleischer, J.L. Pflug, P.F.H. Schwab, X. Meng, D. Lipiak, B.C. Noll, V.S. Allured, T. Rudalevige, S. Lee, J. Michl, J. Am. Chem. Soc., 1997, **119**, 3907

16 D.A. Brown, W. Clegg, H.M. Colquhoun, J.A. Daniels, I.R. Stephenson, K. Wade, J. Chem. Soc., Chem Commun., 1987, 889

17 L.I. Zakharkin, G.G. Zhigareva, J. Gen. Chem. USSR, 1970, **40**, 2318

18 L.I. Zakharkin, G.G. Zhigareva, Bull. Acad. Sci. USSR, Div. Chem. Sci., 1970, 2153

19 L.I. Zakharkin, A.I. L'vov, Bull. Acad. Sci. USSR, Div. Chem. Sci., 1966, 128

20 H. Nakamura, K. Aoyagi, Y. Yamamoto, J. Org. Chem., 1997, 62, 780

21 L.I. Zakharkin, A.V. Grebennikov, Bull. Acad. Sci. USSR, Div. Chem. Sci., 1967, 1331

22 L.I. Zakharkin, A.V. Grebennikov, A.V. Kazantsev, A.I. L'vov, Bull. Acad. Sci. USSR, Div. Chem. Sci., 1967, 1994

23 L.I. Zakharkin, Y.A. Chapovskii, V.A. Brattsev, V.I. Stanko, J. Gen. Chem. USSR, 1966, 36, 892

24 R. Coult, M.A. Fox, W.R. Gill, K. Wade, Polyhedron, 1992, 11, 2717

25 R.J. Peace, PhD Thesis, 1996, Durham University

26 R.W. Alder, P.S.. Bowman, W.R.S. Steele, D.R. Winterman, Chem. Commun., 1968, 723

27 H. Einspahr, J.B. Robert, R.E. Marsh, J.D. Roberts, Acta Cryst., 1973, B29, 1611

28 R.W. Alder, J.E. Anderson, J. Chem. Soc., Perkin II, 1973, 2086

29 I.R. Stephenson, PhD Thesis, Durham, 1988

30 D.A. Brown, PhD Thesis, Durham, 1985

31 L.I. Zakharkin, A.V. Grebennikov, Bull. Acad. Sci. USSR, Div. Chem. Sci., 1966, 1952

32 e.g. O.Kríz, A.L. Rheingold, M. Shang, T.P. Fehlner, Inorg. Chem., 1994, 33, 3777

33 L.I. Zakharkin, V.I. Kalinin, B.A. Kvasov, É.I. Fedin, Bull. Acad. Sci. USSR, Div. Chem. Sci., 1968, 2295

34 V.N. Lebedev, E.V. Balagurova, A.V. Polyakov, A.I. Yanovsky, Y.T. Struchkov, L.I. Zakharkin, J. Organomet. Chem., 1990, 385, 307

35 F.C. Mair, J.H. Morris, D.F. Gaines, D. Powell, J. Chem. Soc., Dalton Trans., 1993, 135

36 S.V. Ivanov, A.J. Lupinetti, S.M. Miller, O.P. Anderson, K.A. Solntsev, S.H. Strauss, Inorg. Chem., 1995, 34, 6419

37 S.V. Ivanov, S.M. Ivanova, S.M. Miller, O.P. Anderson, K.A. Solntsev, S.H. Strauss, Inorg. Chem., 1996, 35, 6914

38 J.S. Roscoe, S. Kongpricha, S. Papetti, Inorg. Chem., 1970, 9, 1561

39 B. Ng, T. Onak, K. Fuller, Inorg. Chem., 1985, 24, 4371

40 B. Ng, T. Onak, J. Fluorine Chem., 1985, 27, 119

41 N.J. Maraschin, R.J. Lagow, Inorg. Chem., 1975, 14, 1855

42 S.Kongpricha, H. Schroeder, Inorg. Chem., 1969, 8, 2449

43 V.I. Stanko, G.A. Anorova, T.V. Klimova, J. Gen. Chem. USSR, 1969, 39, 2095

44 V.I. Stanko, G.A. Anarova, T.P. Klimova, J. Gen. Chem. USSR, 1969, 39, 1045

45 V.I. Stanko, G.A. Anorova, T.V. Klimova, T.P. Klimova, J.Gen. Chem. USSR, 1970, 40, 2418

46 H. Schroeder, T.L. Heying, J.R. Reiner, Inorg, Chem., 1963, 2, 1092

47 V.I. Stanko, G.A. Anorova, J. Gen. Chem. USSR, 1971, 41, 1526

48 L.I. Zakharkin, G.G. Zhigareva, L.S. Podvisotskaya, Bull. Acad. Sci., 1970, 413

49 L.I. Zakharkin, G.G. Zhigareva, J. Gen. Chem. USSR, 1975, 45, 777

50 R.N. Scott, H. Hooks Jnr., J.F. Sieckhaus, Inorg. Chem., 1971, 10, 2358

51 N.S. Semenuk, S. Papetti, H. Schroeder, Inorg. Chem., 1969, 8, 2441

52 A.R. Siedle, J. Inorg. Nucl. Chem., 1971, 33, 3677

53 M.R.C. Gerstenberger, A. Haas, Angew. Chem. Int. Ed. Engl., 1981, 20, 647; G. Resnati, D.D. DesMarteau, J. Org. Chem., 1991, 56, 4925; R.E. Banks, V. Murtagh, E. Tsiliopoulos, J. Fluorine Chem., 1991, 52, 389; G.S. Lal, J. Org. Chem., 1993, 58, 2791; S. Stavber, M. Zupan, J. Org. Chem., 1985, 50, 3609; L.J. Diorazio, D.A. Widdowson, J.M. Clough, Tetrahedron, 1992, 48, 8073

54 E. Differding, H. Ofner, Synlett, 1991, 187

55 N. Muller, D.T. Carr, J. Phys. Chem., 1963, 67, 112

56 L.L. Frye, E.L. Sullivan, K.P. Cusack, J.M. Funaro, J. Org. Chem., 1992, 57, 697

57 H. Fukuda, F.J. Frank, W.E. Truce, J. Org. Chem., 1963, 28, 1420

58 J.B. Rose, Chemistry and Industry, 1968, 461

59 T.E. Attwood, D.A. Barr, G.G. Feasey, V.J. Leslie, A.B. Newton, J.B. Rose, Polymer, 1977, 18, 354

60 K. Sonogashira, Y. Tohda, N. Hagihara, Tet. Lett., 1975, no. 50, 4467

61 This compound has been previously synthesised in 52% yield from the reaction of 2-ethynylthiophene with $B_{10}H_{10}(MeCN)_2$. Y.-K. Yan, D.M.P. Mingos, M. Kurmoo, W.-S. Li, I.J. Scowen, M. McPartlin, A.T. Coomber, R.H. Friend, J.Chem. Soc., Dalton Trans., 1995, 2851

62 M.F. Hawthorne, T.D. Andrews, P.M. Garrett, F.P. Olsen, M. Reintjes, F.N. Tebbe, L.F. Warren, P.A. Wegner, D.C. Young, Inorg. Chem., 1967, 10, p100

63 M.F. Hawthorne, T.D. Andrews, P.M. Garrett, F.P. Olsen, M. Reintjes, F.N. Tebbe, L.F. Warren, P.A. Wegner, D.C. Young, Inorg. Chem., 1967, **10**, p104

64 L.I. Zakharkin, G.G. Zhigareva, Bull. Acad. Sci. USSR, Div. Chem. Sci., 1970, 2153

65 L.I. Zakharkin, V.N. Kalinin, A.I. L'vov, Bull. Acad. Sci. USSR, Div. Chem. Sci, 1966, 1043

66 L.I. Zakharkin, Yu. A. Chapovskii, V.A. Brattsev, V.I. Stanko, J. Gen. Chem. USSR, 1966, 892

Chapter Three

Structure And Bonding In One-Cage Carboranyl Systems

3.1 INTRODUCTION

The synthesis of compounds such as the carboranyl hydroxides, $RCB_{10}H_{10}COH$, and carboxylic acids, $RCB_{10}H_{10}CCO_2H$, and their deprotonated anions, $RCB_{10}H_{10}CO^-$ and $RCB_{10}H_{10}CCO_2^-$, has been discussed in Chapter Two, together with fluoride derivatives, $RCB_{10}H_{10}CF$. Such compounds have the ability to effect a degree of π-bonding between the carboranyl carbon atom and the substituent *exo* to the carboranyl cage. In this chapter the manifestation of these *exo*-π bonding effects is discussed with reference to X-ray crystal data and multi-nuclear FT-NMR spectroscopy.

Also discussed are the intra- and inter-molecular hydrogen bonding interactions in carboxylic acid, thiophenyl and pyridyl derivatised carboranes. Crystal structures and solid and solution state infrared spectra are discussed.

The general principles of bonding in cluster compounds were introduced in Chapter One. In the present chapter, changes in the electronic distributions and cage structures of the carboranes brought about by various bonding interactions with substituents on cage carbon atoms will be considered.

3.2 STRUCTURE AND BONDING IN ICOSAHEDRAL CARBORANES - AN OVERVIEW

The general bonding principles of the carborane clusters has been described in Chapter One, with reference to three-centre two-electron bonding theories, and molecular orbital considerations. When the "perfect" $B_{12}H_{12}^{2-}$ icosahedron becomes modified to incorporate heteroatoms, two carbons in the case of $C_2B_{10}H_{12}$, it was noted that distortions occurred in the electronic distribution over the cage. When atoms of the cluster become further substituted as in species $RCB_{10}H_{10}CX$, the substituents R and X can cause further redistribution of electron density, depending upon their nature. Of particular interest in this study is the phenomenon of *exo*-π bonding between a carboranyl cage carbon atom and its attached substituent X, where X=O^-, S^-, NR^- or other electron rich substituent.

3.2.1 *Exo*-π bonding in carboranes

It has been shown that when a carboranyl carbon atom becomes substituted with an electron rich substituent, this substituent in some instances has the ability to donate electronic charge back into the cage bonding system. This effects an opening of the previously *closo* cage, manifested through a lengthening of the cage C-C bond, and a shortening of the cage carbon-substituent bond length[1,2,3], to give a bond with multiple bond character. This phenomenon has been reported for various *ortho*-carborane derivatives having the *exo* substituent O^-, S^- or NR^-. For a fuller explanation, the example of [1-phenyl-2-oxo-*ortho*-carborane]$^{1-}$ is examined here.[2]

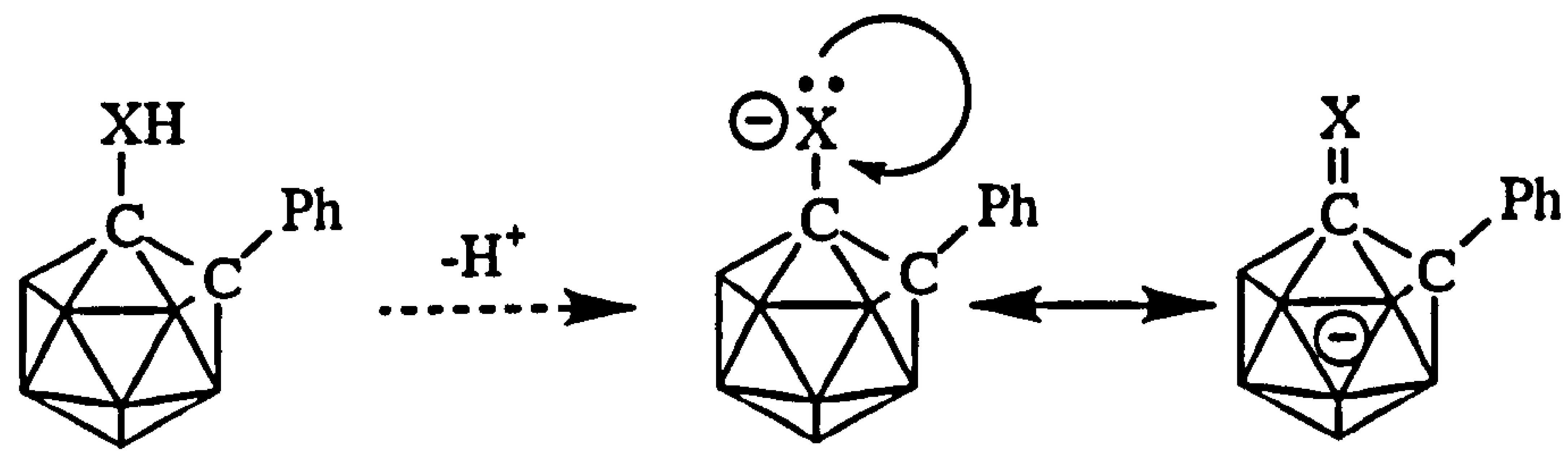

scheme 3.1: the principle of exo-π bonding in ortho-carboranes

1-phenyl-2-hydroxy-*ortho*-carborane has been deprotonated by the use of 1,8-*N,N,N',N'*-tetramethylnaphthalene-diamine (proton sponge) to give the oxo-anion. In doing this, the *exo*-substituent (oxygen) has become electron enriched. The crystal structure of this anion illustrated a long carboranyl cage C-C bond length of 2.001(3)Å, and a shortened C-O bond length of 1.245(3)Å, which suggested this connectivity had gained multiple bond character. (A C-O single bond would be *c.* 1.43Å). This structure has led to the interpretation of this species as a CO moiety capping a *nido*-cage residue as an extension of scheme 3.1. Comparisons can be made to the μ_5 bonding mode of a cyclopentadiene system.

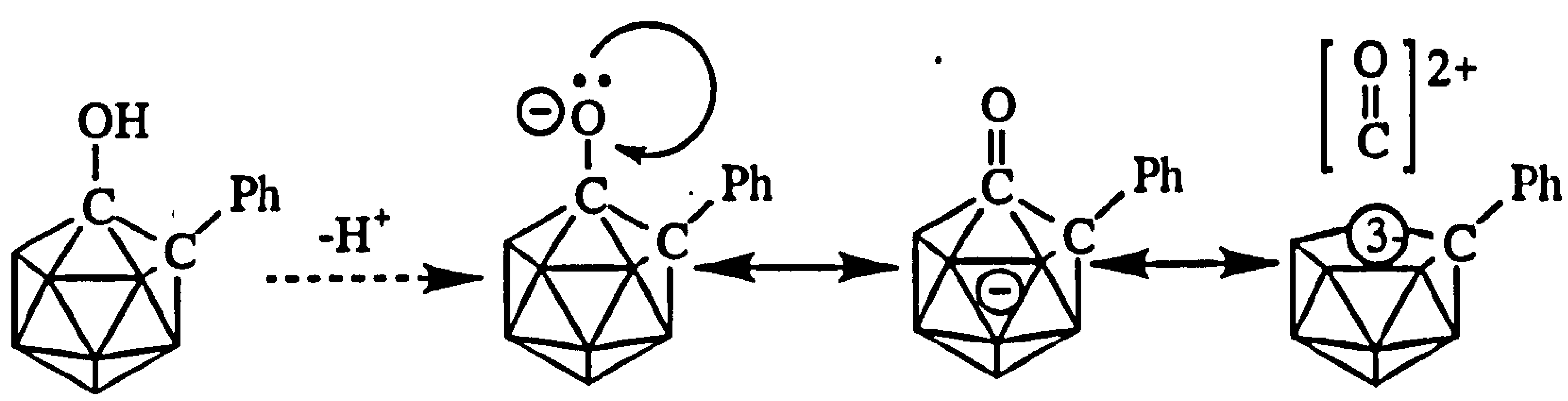

scheme 3.2: exo-π bonding in [1-phenyl-2-oxo-ortho-carborane]$^{1-}$

This *exo*-π bonding interaction has been rationalised by an investigation of the frontier orbitals. The 1-phenyl-2-oxo-*ortho*-carborane anion system has been considered as a CO "ligand" bonding to the open face of a *nido* $PhCB_{10}H_{10}C^-$ residue. The CO entity has three orbitals which it could use to bond to the open face of the *nido* residue, whilst the orbitals of the open face have been based on a study of the frontier orbitals of $B_{11}H_{11}^-$ and $CB_{10}H_{11}^-$ fragments.[4]

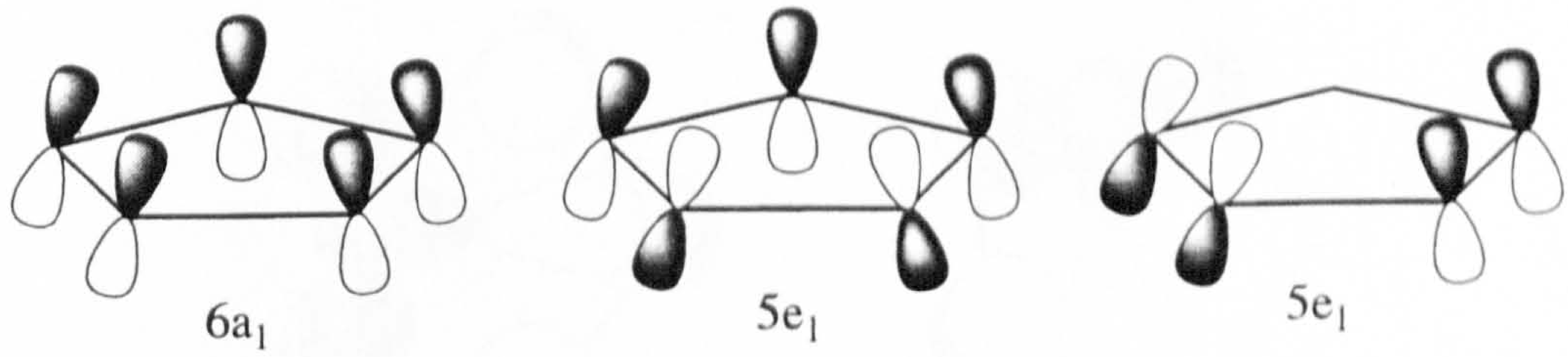

figure 3.1: frontier orbitals of $B_{11}H_{11}^-$

In the $B_{11}H_{11}^-$ fragment the $5e_1$ orbital set is degenerate, but on introducing one or two carbon atoms into the open face, the degeneracy is lost.

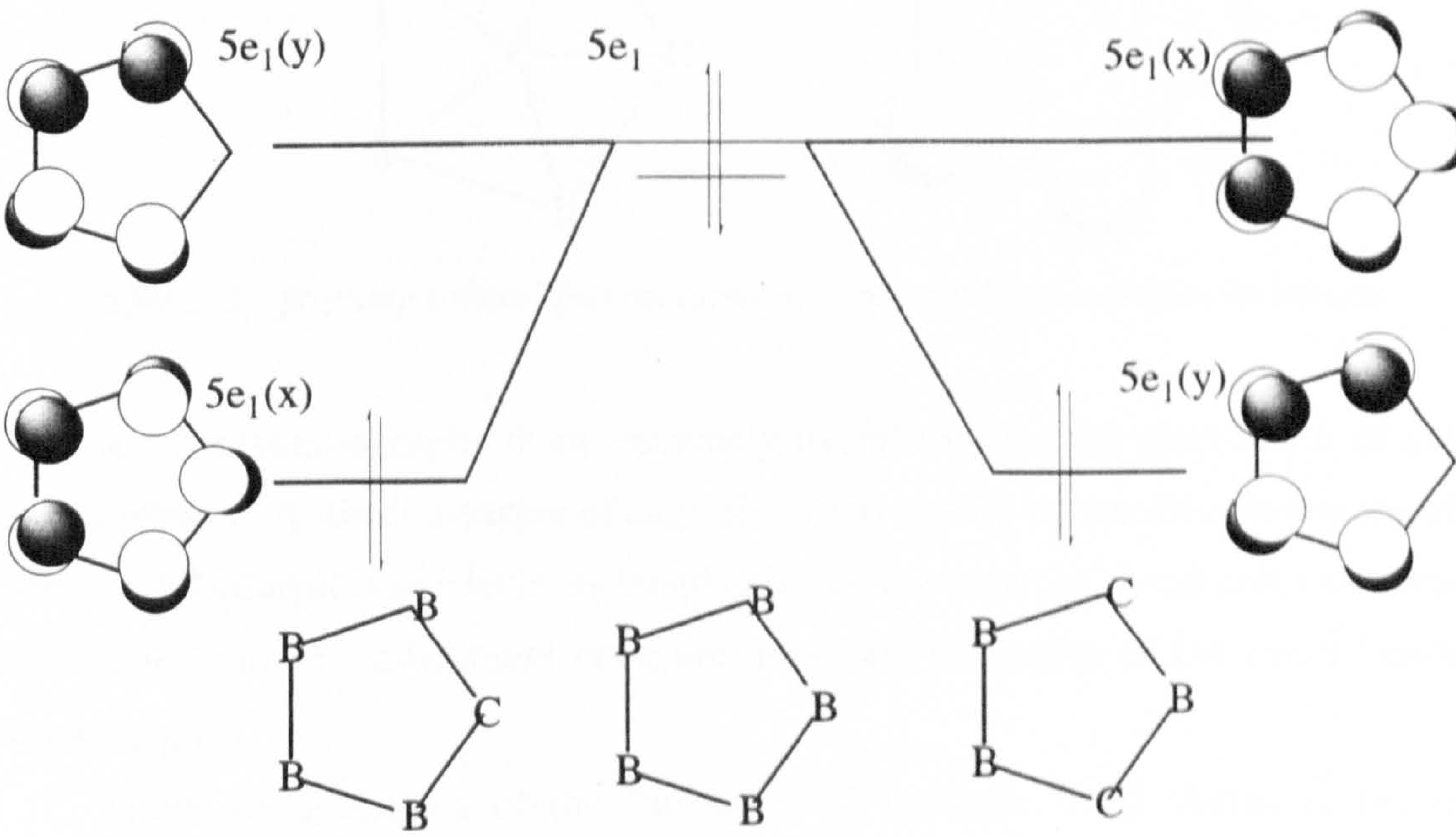

figure 3.2: substitution of carbon atoms into the $B_{11}H_{11}^-$ residue loses the degeneracy in the $5e_1$ levels

The $6a_1$ orbitals of the open face are aligned, leaning in towards the twelfth vertex, to accept back donation of electron density from the sp hybridised carbon of the CO moiety through a σ bond. The p_x and p_y orbitals of the carbon are aligned so as to interact with the $5e_1(x)$ and $5e_1(y)$ orbitals of the residue. The interaction between the $5e_1(y)$ and the p_y orbital is more efficient at back π-bonding than the $5e_1(x)$ and p_x interaction. The orientation of this preferred set of orbitals prompts the cage to open up, explaining the lengthening of the cage C-C bond.

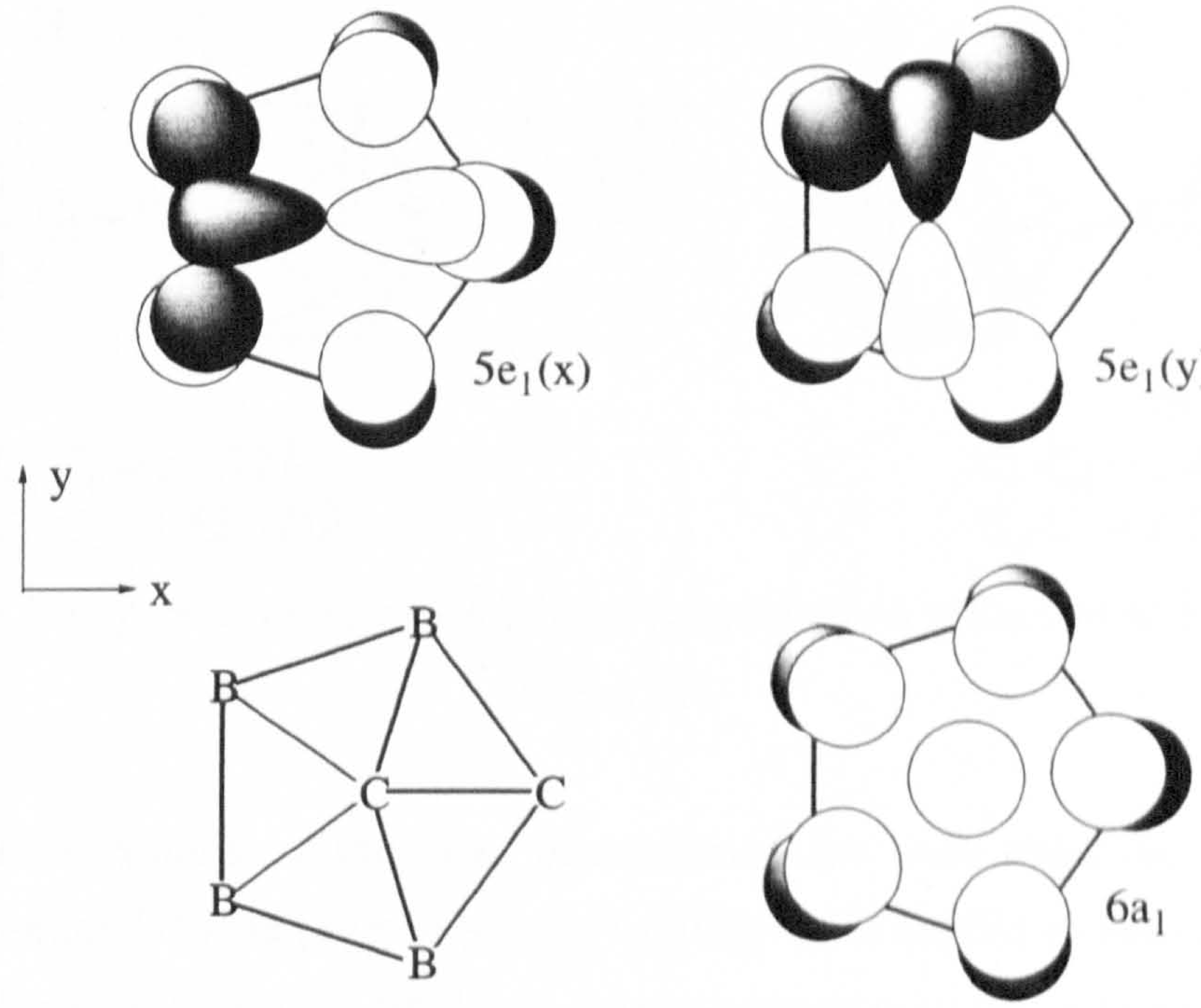

figure 3.3: frontier orbital interactions of 1-phenyl-2-oxo-ortho-carborane

X-ray crystallography is an extremely useful tool for the elucidation of *exo*-π bonding effects. A direct measure of cage distortion caused by the electronic properties of the *exo* substituent is available, as lengthening of the cage C-C bond and a shortening of the cage C to *exo* substituent bond are important indicators of the *exo*-π bonding phenomenon.

There are examples of the formation of multiple bond character between carborane substituents and the cage in systems outside of the one cage *ortho*-carborane system discussed above. A closely related example is that of *bis-ortho*-carborane.

The two electron reduction of *bis-ortho*-carborane led to the formation of two linked *nido* cages (scheme 3.3).[5] The crystal structure of the $[(C_6H_5)_3PCH_3^+]_2$ salt illustrated an intercage C-C bond length of 1.377(4)Å, revealing double bond character between the cages. (In *bis-ortho*-carborane an intercage C-C distance of 1.522(2)Å was reported.[6]) The cage C-C distance of 2.414(4)Å showed cage opening upon formation of the *exo* cage multiple bond.

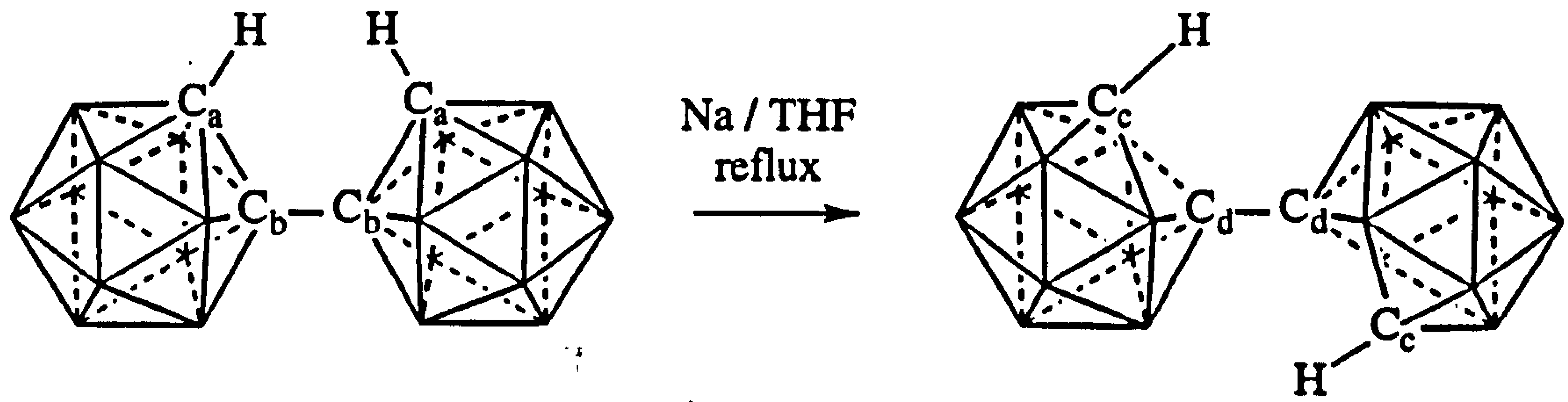

C_a-C_b = *c*.1.72Å
C_b-C_b =1.522(2)Å

C_c-C_d = 2.414(4)Å
C_d-C_d = 1.377(4)Å

scheme 3.3: formation of a multiple exo cage bond on reduction of bis-ortho-carborane

Another example of the same phenomenon has been observed for a smaller polyhedral borane.[7] In the [1-(η^5-C_5Me_5)-4-(NEt_2)-1-$RhB_{10}H_9$] an *exo* cage B-N bond of 1.427(8)Å showed multiple BN bond character through N->B π donation. A single BN bond would have been *c*.1.58Å.

In the above examples, X-ray crystallography has been used to give a quantitative measure of *exo*-π bonding in carborane systems. Theoretical methods can also be used to try to quantify redistributions of electron density, and so cage distortions and bond orders. Such effects are also evidenced by means of NMR spectroscopy.

3.2.2 NMR Spectroscopy And The Antipodal Effect

a) Boron NMR Spectroscopy[8]

Boron has two naturally ocurring isotopes ^{11}B ($I={}^3/_2$) and ^{10}B (I=3), both of which are NMR active. The ^{11}B nucleus is the more useful of the two; it has a high natural abundance (80.4%), a strong signal and resonates at a relatively high frequency (160MHz at 11.5T, cf. 500MHz for ^1H). Boron NMR signals tend to be broad, due to the electric quadrupole moment of the isotopes, which also results in broad signals in the proton NMR for boron attached protons. This is only a small effect, however, as is the peak widening caused by ^{11}B-^{11}B and ^{11}B-^{10}B couplings,[9] and the spectra obtained give valuable structural information.

The pattern of the boron NMR spectrum obtained is dependent upon the symmetry of the carborane, for example, *ortho*-R,R'-$C_2B_{10}H_{10}$ has six different boron environments whilst *para*-R,R'-$C_2B_{10}H_{10}$ has only two. Often the spectra can be assigned with the knowledge of similar compounds, however, where ambiguity arises, 2-D $^{11}B\{^1H\}$ NMR spectroscopy[10] is an invaluable aid to the elucidation of cage connectivities. Other methods which have been used to help assign boron spectra include selective cage deuteration, double resonance[11], line-narrowing[12] to separate overlapping peaks, and partial relaxation techniques.[13]

The boron chemical shift is governed by the coordination number of the cage vertex and by the concentration of electron density on it. It has been proposed that there are four principal influences on electronic distribution and by implication, on the boron chemical shift in *closo*-boranes and *closo*-heteroboranes[14], namely the neighbour, rhomboidal, butterfly and antipodal effects. These relate the position of cage substitution to a change in chemical shift, the magnitude of each effect varying with the coordination number of the concerned boron atom. For penta-coordinate atoms (excluding hydrogen atoms), including the C_2B_{10} icosahedra, the antipodal effect has the most significance.

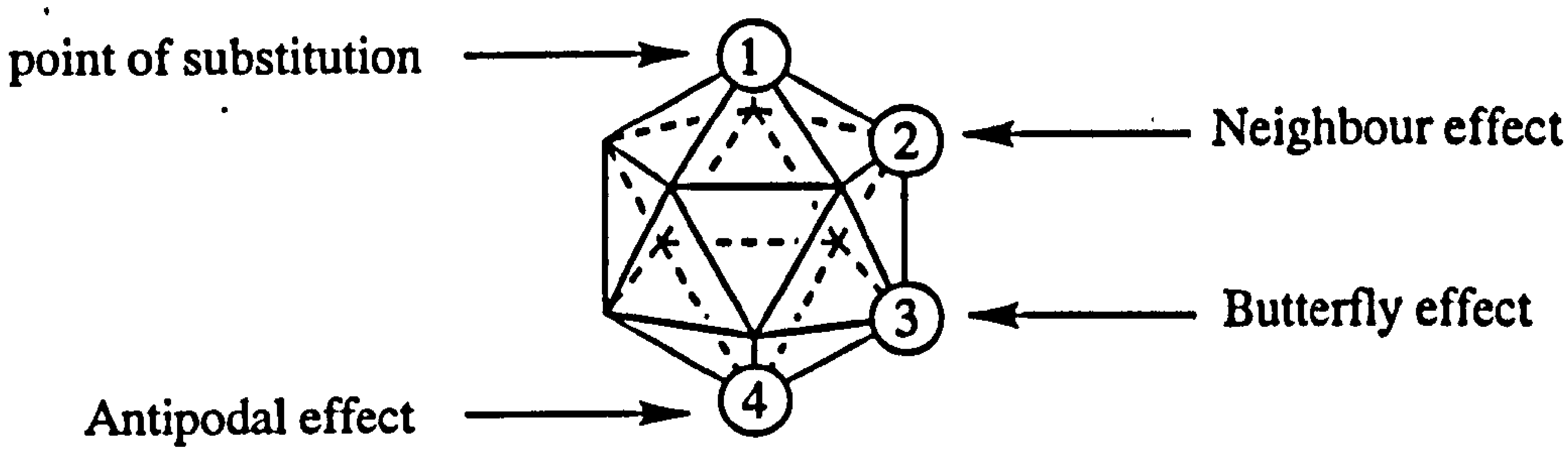

figure 3.4: substituent effects in the icosahedron

When a substituent X is introduced onto a carboranyl cage carbon (or boron) atom, it causes a change in the chemical shift of the cage atom diametrically opposite. This is the antipodal effect[15] and is noted for the $^{11}B\{^1H\}$ nuclear magnetic resonances of *ortho-*, and *meta-* C-substituted carboranes and for those of $^{13}C\{^1H\}$ for C-substituted *para*-carboranes. As less electron density becomes available to the cage from substituent X, the chemical shift of the antipodal atom tends to a lower field (a more positive δ), (a positive sign is used to indicate a shift at lower field than the standard trifluoroborane etherate), and *vice versa.* The effect has much in common with the mesomeric effect[16] of organic π-electron systems, where increased shielding of a particular atom gives a subsequent upfield shift (more negative δ).

The orbitals which are involved in producing this antipodal shift, the NMR active orbitals, have been proposed[17] to be the p_x and p_y orbitals which lie tangential to the cage surface. The electron density is decreased in these orbitals, whilst the density in the axial p_z orbital is increased, as less electron density is donated to the cage, and *vice versa.* Chemical reactivity is determined by the radial orbitals (electrophilic substitution at a position antipodal to an electron withdrawing substitutent is favoured even although NMR spectroscopic evidence suggests that electron density is decreased at such a position), whilst the tangential orbitals do not appear to influence chemical reactivity.

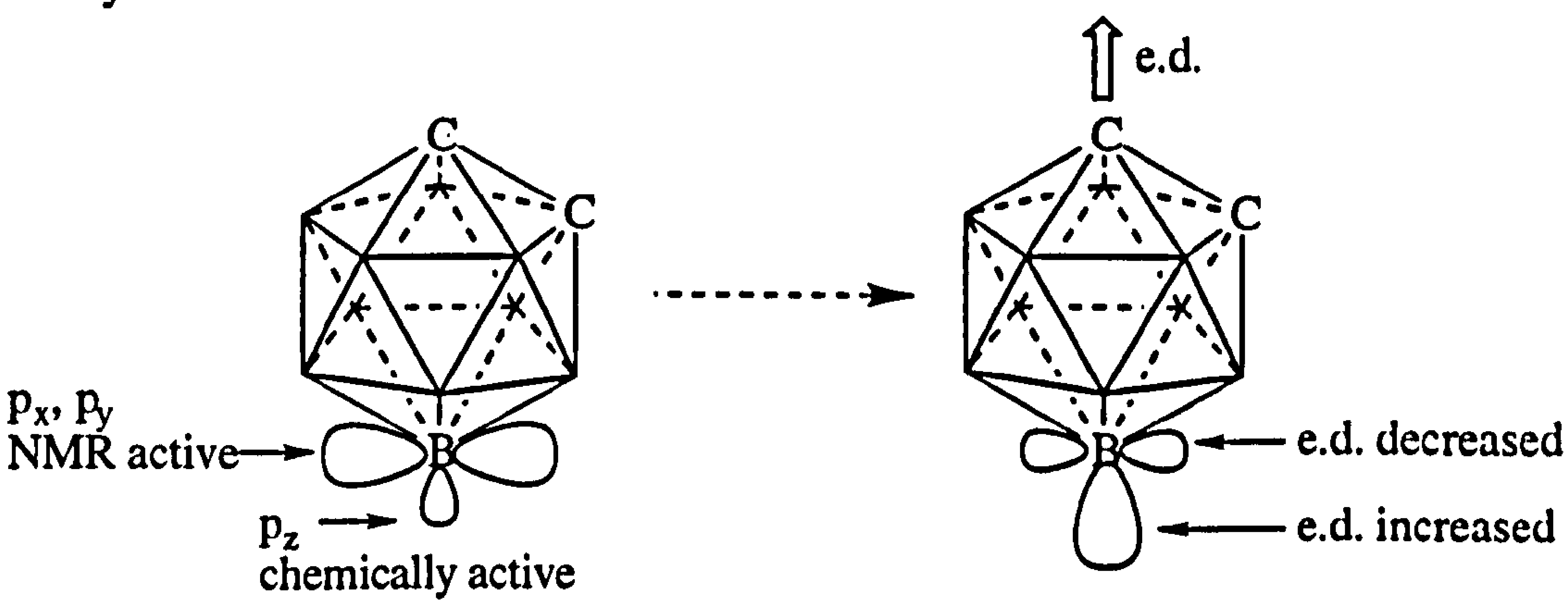

figure 3.5: as electron density is withdrawn from the cage system, electron densities in the antipodal orbitals are altered

For the example of 1-phenyl-2-hydroxy-*ortho*-carborane a significant antipodal shift is observed upon creation of the oxo anion.[1] This upfield shift results from increased electron density on the antipodal atom of the anion with respect to that found for the parent hydroxide. This example illustrates how NMR is indicative of *exo*-π bonding in carboranes.

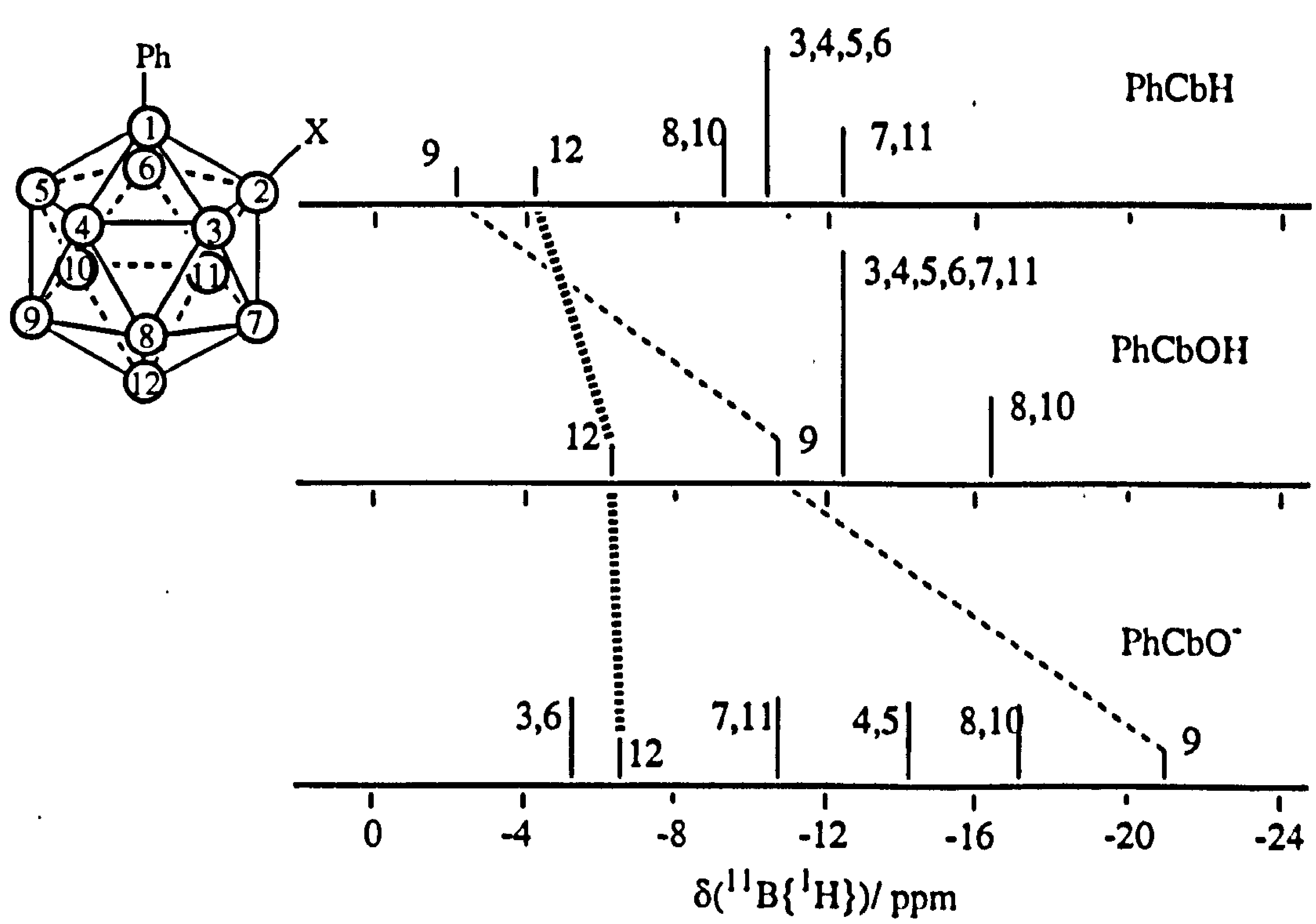

figure 3.6: increased electron density on the antipodal atom leads to an upfield antipodal shift

The antipodal effect has been used to detect *exo*-π bonding in hydroxy-[1,18], thio-[2], and amino-carboranes[3], where deprotonation of the *exo*-substituent results in a higher charge density in the NMR active orbitals of the antipodal atom. In section 3.3.1, this theme will be continued to the carboxylic acid and fluoro-derivatives.

b) Carbon NMR Spectroscopy

With respect to boron NMR spectroscopic studies, comparatively little carbon data has been presented for carboranes[19,20] with regard to electron density studies. In *ortho*-carboranes, the carbon position is classified by the neighbour effect and is proposed to be of only minor influence. In *para*-carboranes however, it is the carbon atoms which are the antipodal atoms, and the idea of antipodal carbon shifts will be explored in sections 3.3.1d) and 3.3.2.

3.2.3 Hydrogen Bonding in Carborane Systems

Hydrogen bonding is found in many naturally occurring and synthetic molecules and is of great importance in determining crystal geometries. This is a useful property in crystal engineering. Many compounds have been shown to hydrogen bond, but for carboranes, there are relatively few examples.

Hydrogen bonding of unsubstituted icosahedral *ortho*-, *meta*- and *para*-carboranes, $C_2B_{10}H_{12}$, with Lewis bases has been used to elucidate the structures of these compounds.[21] The interaction between the base and the acidic protons of the carboranyl carbon atom allowed the carbon and boron atoms of the cage to be distinguished by X-ray crystallography.

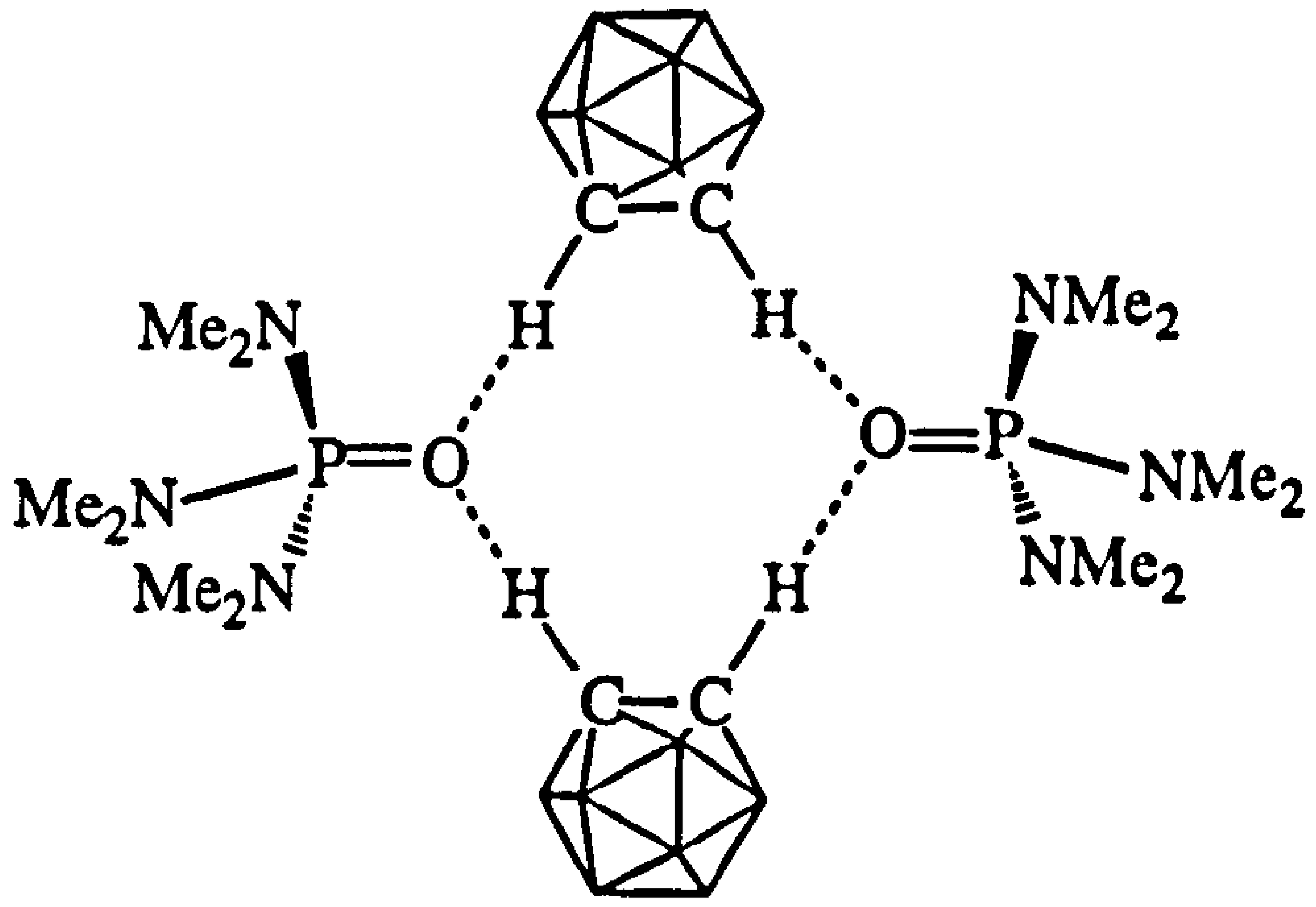

figure 3.7: hydrogen bonding interaction between ortho-carborane and HMPA (hexamethylphosphoramide)

Carboranes have also been shown to form supramolecular complexes, aided by hydrogen bonding.[22]

Hydrogen bonding can, in some cases, be responsible for altering the reactivity of a compound. In Chapter Two, the proton on the second carboranyl carbon was shown to be activated towards further substitution as a result of the intramolecular hydrogen bonding interaction between the proton and the pyridyl nitrogen.[23]

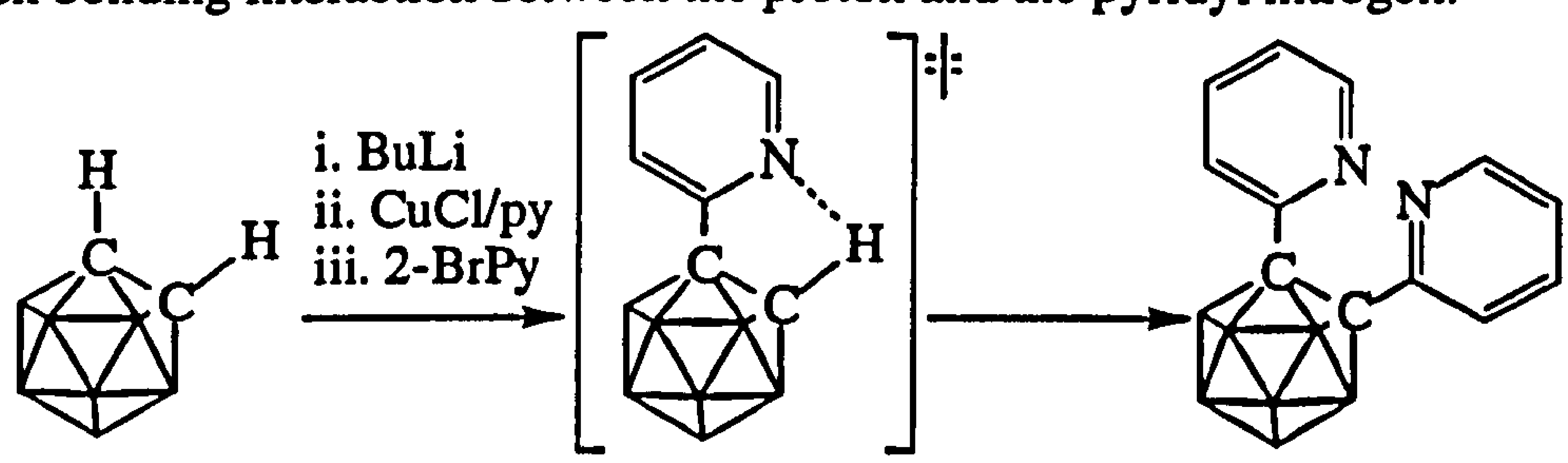

scheme 3.4: intramolecular hydrogen bonding in 1-(2'-pyridyl)-ortho-carborane leads to exclusively di-substituted product

3.3 RESULTS AND DISCUSSION

3.3.1 Exo-π bonding in *ortho*-carboranes

a) 1-phenyl-2-hydroxy-*ortho*-carborane

The structure of the 1-phenyl-2-oxo-*ortho*-carborane anion has been reported[1] and shown to have a C-O bond length of 1.245(3)Å, closer to that of a ketone C=O than a single CO bond. Combined with the ^{11}B antipodal shift of B9, from -10.65ppm ($CDCl_3$) for the hydroxide to -21.06ppm (C_6D_6) for the O^- anion, this is evidence of a π bond forming *exo* to the cage. The cage C-C distance of 2.001Å is also longer than expected for a *closo* cage, suggesting the CO^- residue takes the form of a CO fragment on a *nido* residue. For direct structural comparison, crystals of the 1-phenyl-2-hydroxide-*ortho*-carborane have been grown from hexane, and shown to crystallise as the hydrate, $PhCB_{10}H_{10}COH.{}^1/_2H_2O$.

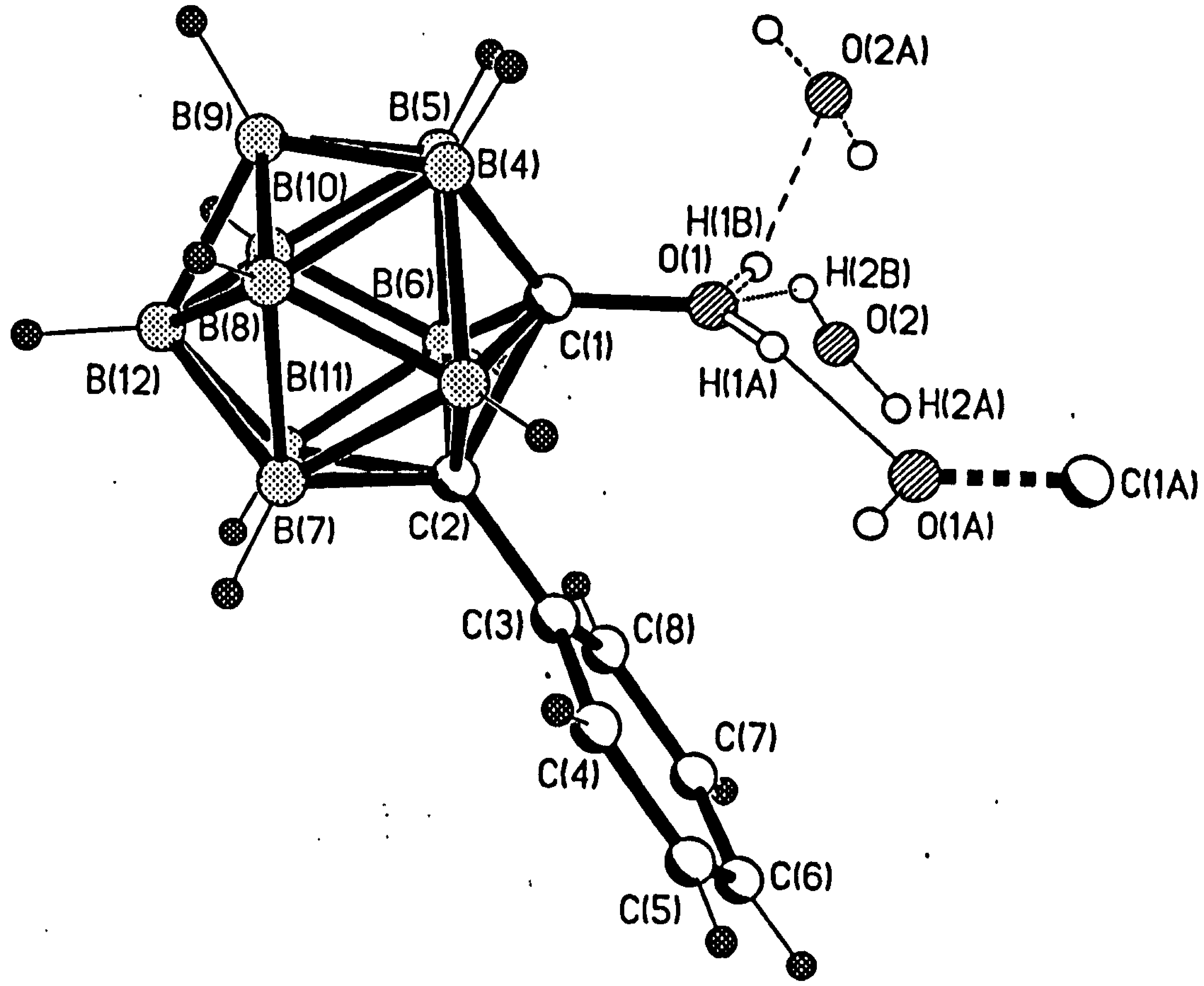

figure 3.8: crystal structure of 1-phenyl-2-hydroxy-ortho-carborane

bond	bond length / Å	bond	bond length / Å
O(1) - H(1A)	0.85(6)	O(1) - H(1B)	0.80(7)
O(1) - C(1)	1.366(2)	C(1) - C(2)	1.723(3)
C(1) - B(3)	1.711(3)	C(2) - B(3)	1.738(3)
C(1) - B(4)	1.704(3)	C(2) - B(6)	1.734(3)
C(1) - B(5)	1.697(3)	C(2) - B(7)	1.707(3)
C(1) - B(6)	1.722(3)	C(2) - B(11)	1.705(3)

table 3.1: selected bond lengths for 1-phenyl-2-hydroxy-ortho-carborane

atoms	bond angle/ °	atoms	bond angle/ °
H(1B)-O(1)-C(1)	123(5)	H(1A)-O(1)-C(1)	119(5)
O(1)-C(1)-C(2)	115.6(2)	C(3)-C(2)-C(1)	117.9(2)
O(1)-C(1)-B(3)	116.5(2)	C(3)-C(2)-B(3)	117.1(2)
O(1)-C(1)-B(4)	112.8(2)	C(3)-C(2)-B(6)	118.3(2)
O(1)-C(1)-B(5)	122.6(2)	C(3)-C(2)-B(11)	123.3(2)
O(1)-C(1)-B(6)	116.6(2)	C(3)-C(2)-B(7)	122.5(2)

table 3.2: selected bond angles for 1-phenyl-2hydroxy-ortho-carborane

A standard C-O single bond between four coordinate carbon and two coordinate oxygen, would be expected to be *c.* 1.43Å. The carboranyl *C-O*H distance is shorter (1.366(2)Å), showing that even in the protonated species, a degree of π interaction takes place between the cage and the OH functionality. The cage C-C distance of 1.723(2)Å is longer than that of 1-phenyl-*ortho*-carborane (1.640(5)Å) indicating that the OH group also causes a degree of cage opening, although obviously not to the same extent as the O^- which has significantly more electron density to donate back to the cage.

This structural data has confirmed the findings of the ^{11}B NMR spectroscopic data and quantifies the structural changes incurred upon deprotonation of the hydroxide to form the oxy anion.

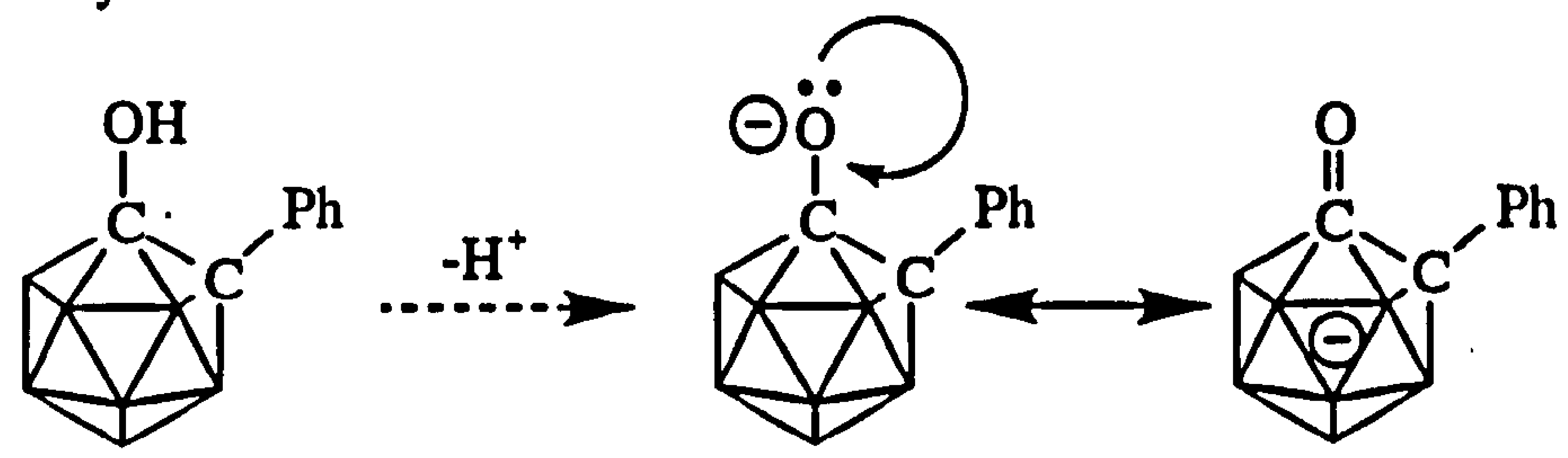

scheme 3.5: deprotonation of 1-phenyl-2-hydroxy-ortho-carborane

carborane	PhCbOH	PhCbO$^-$
cage C-C	1.723(3)Å	2.001(3)Å
exo C-O	1.366(2)Å	1.245(3)Å

table 3.3: comparison of bond lengths between the 1-phenyl-2-hydroxy and 2-oxo-ortho-carboranes

b) 1-phenyl-2-fluoro-*ortho*-carborane

The fluoride moiety is isolobal and isoelectronic with the OH and O^- functionalities, and like the O^- anion, the lone pairs on the F moiety are ideally aligned for π overlap. It was therefore of interest to see if this substituent would also *exo*-π bond to the cage. 1-phenyl-2-fluoro-*ortho*-carborane was synthesised, but unfortunately no X-ray quality crystals were grown. ^{11}B NMR spectroscopy has exhibited the degree of *exo*-π bonding in the OH/O^- system and the relevance of the observed chemical shifts has been confirmed by X-ray crystallography. By the same principles, the extent of the bonding interaction between the carboranyl cage carbon atom and the fluoride substituent should be evident from the NMR shifts of the antipodal cage atoms, assigned with the aid of 2D ^{11}B NMR spectroscopy, without the necessity for an X-ray structure.

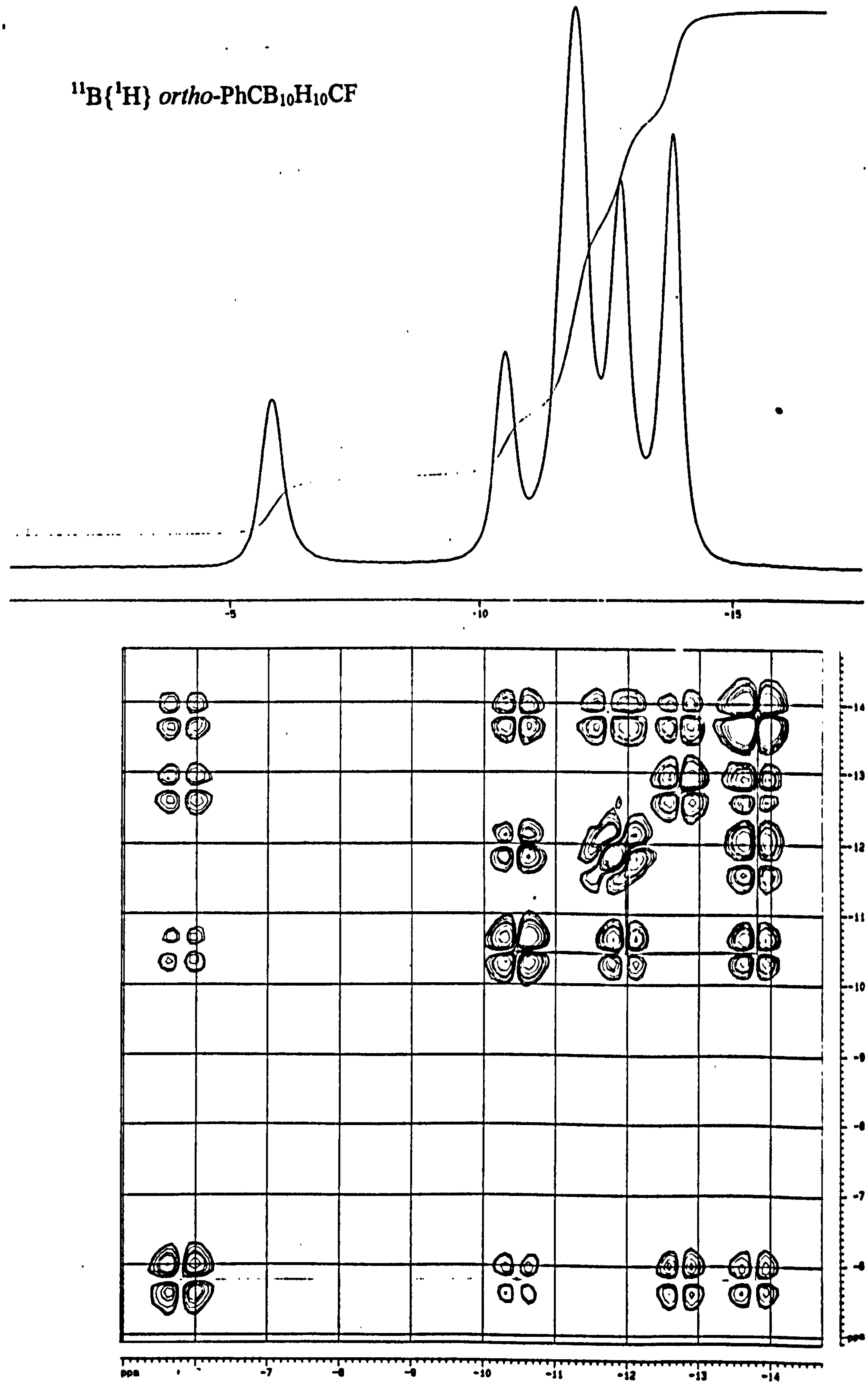

figure 3.9: $^{11}B\{^1H\}$ NMR spectrum (top) and $^{11}B\{^1H\}$-$^{11}B\{^1H\}$ COSY NMR spectrum (bottom) of 1-phenyl-2-fluoro-ortho-carborane

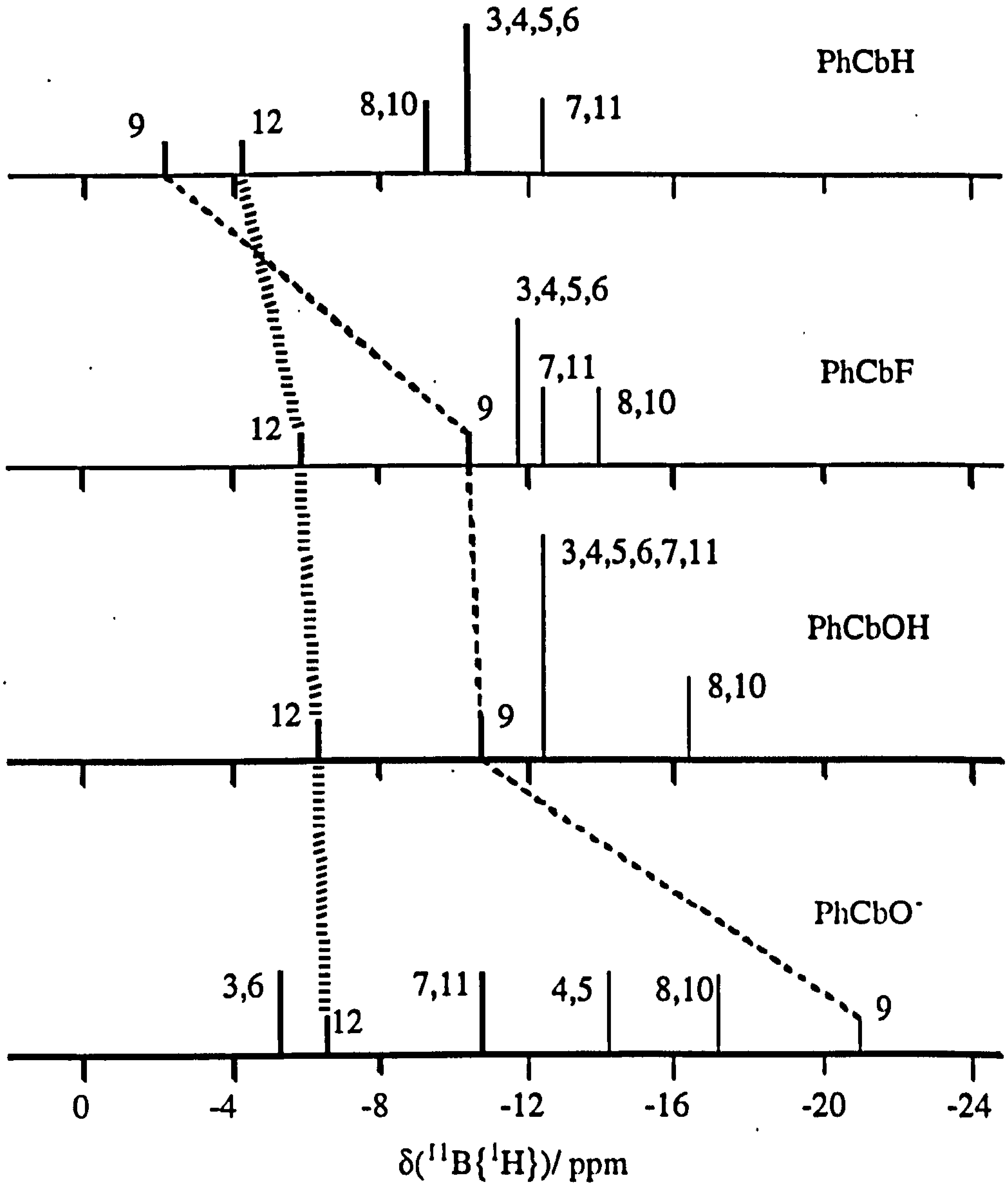

figure 3.10: schematic representation of the ^{11}B chemical shifts of 1-phenyl-ortho-carboranyl derivatives. B9 is antipodal to H, F, OH or O^- respectively, and B12 antipodal to Ph

Although a shorter, stronger bond had been anticipated as a result of the electronegativity of the fluoride entity, this NMR spectroscopic evidence suggested there was little difference in the degree of *exo*-π bonding between the F and OH substituted carboranes. *Exo*-π bonding to the extent of that observed for 1-phenyl-2-oxo-*ortho*-carborane can be ruled out.

Theoretical calculations conducted by Dr. Mark Fox on 1-phenyl-*ortho*-carborane and the OH and O^- derivatives[24], gave good agreement between the theoretical structure and the X-ray data obtained. His findings for 1-phenyl-2-fluoro-*ortho*-carborane showed a cage C-C bond length of 1.690Å (STO3G). The cage C-C bond of 1-phenyl-2-hydroxy-*ortho*-carborane was 1.723(3)Å, so as predicted by ^{11}B

NMR spectroscopy, the degree of π-bonding in these compounds was similar, and only small.

c) 1-phenyl-2-carboxy-*ortho*-carborane

As deprotonation of the hydroxide functionalised carborane has been proven to give an *exo*-π bonding substituent, it was of interest to see if carboxylic acid derivatives would display a similar phenomenon. It was hoped that the deprotonated carboxylic acid derivative would mimic a carboxylate anion, where the carborane would behave as a pseudo-oxygen atom.

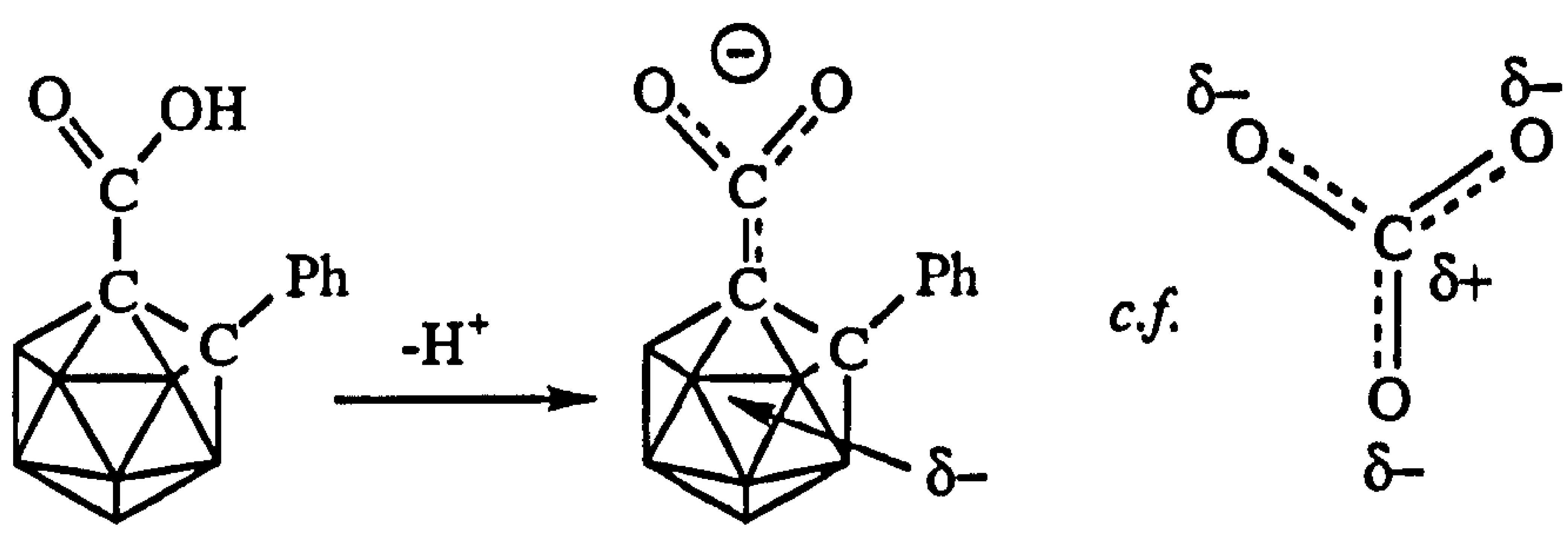

figure 3.11: deprotonation of a carboxylic acid derivative to give a pseudo-carboxylate anion

1-phenyl-2-carboxy-*ortho*-carborane has been synthesised and X-ray quality crystals grown from 40-60° petroleum ether as clear, colourless needles. The X-ray structure is interesting in that there are two orientations of the carboxylic acid functionality within the crystal lattice. In the first, the carboxy group lies roughly perpendicular to the phenyl group, in the second it is twisted off the perpendicular axis. This difference in orientations leads to differences in the bond lengths around the cage.

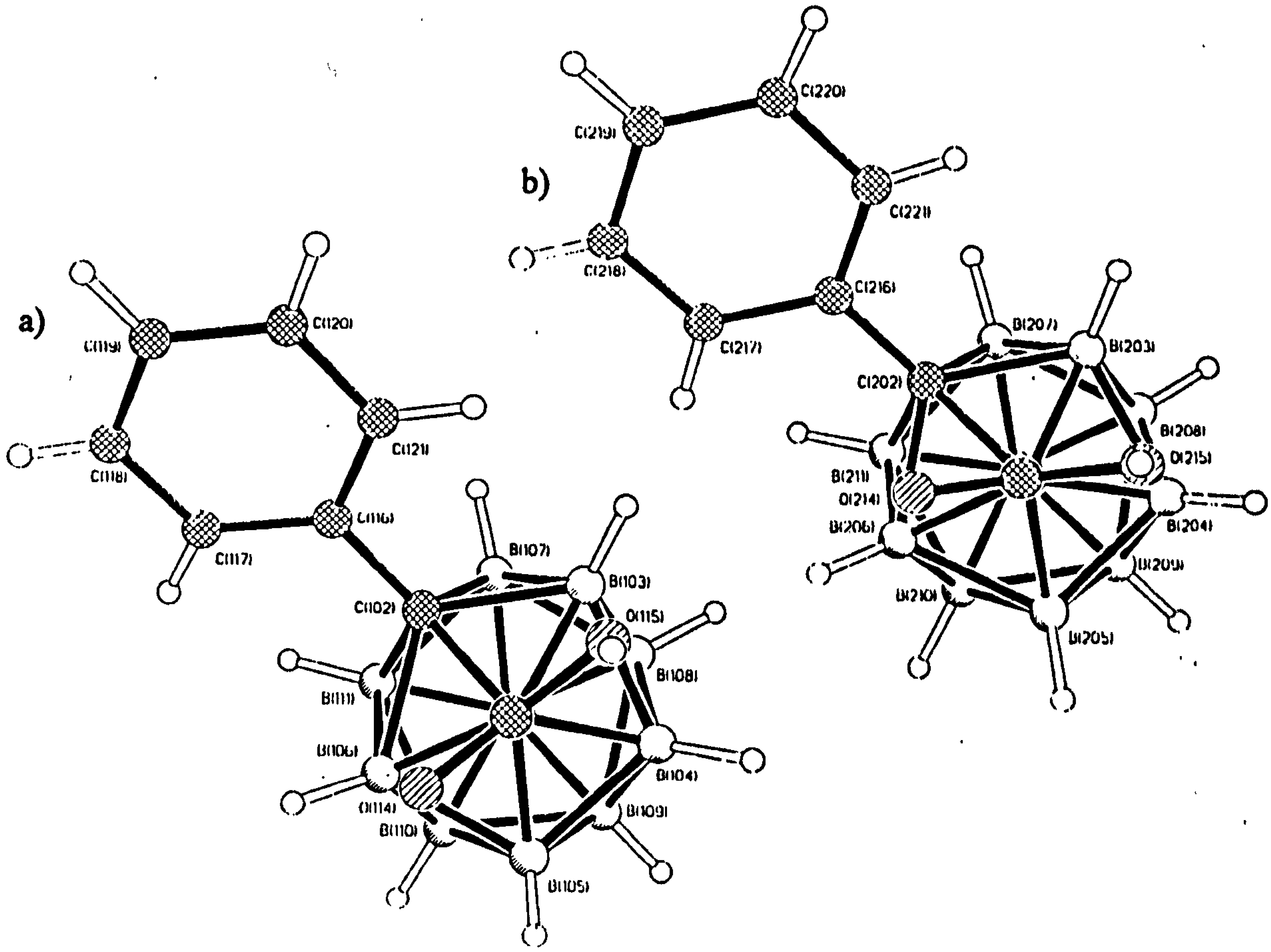

figure 3.12: the CO_2H group of 1-phenyl-2-carboxy-ortho-carborane has two crystallographic orientations

atoms	bond length (a)/ Å	bond length (b)/ Å
cage C-C	1.677(3)	1.693(3)
cage C-Ph	1.505(3)	1.505(3)
cage $C\text{-}CO_2H$	1.510(3)	1.510(4)
carboxy C=O	1.219(3)	1.194(3)
carboxy C-OH	1.277(3)	1.272(3)
carboxy O-H	0.95(3)	0.90(3)
C(2)-B(3)	1.745(4)	1.759(4)
B(3)-B(4)	1.782(5)	1.766(5)
B(4)-B(5)	1.787(5)	1.772(5)
B(5)-B(6)	1.780(5)	1.787(5)
B(6)-C(2)	1.755(4)	1.734(4)

table 3.4: bond lengths of 1-phenyl-2-carboxy-ortho-carborane, molecules (a) and (b)

Also of interest is the dimerisation of the compound into a Z-configuration through hydrogen bonds (O(14)···H(15')-O(15')=1.705Å). Dimerisation of carboxylic acids is a common feature of such compounds, and the Z-like orientation adopted here is possibly to minimise steric interactions between the phenyl rings of the carboranes. It is also interesting to note that the phenyl group is always directed towards the O and not the OH fragment of the carboxylic acid group. The distortion of the CO_2H groups observed in the individual molecules is seen in the dimers as well, and it may be that this preference of the carboxy groups to hydrogen bond has led to the observed twist.

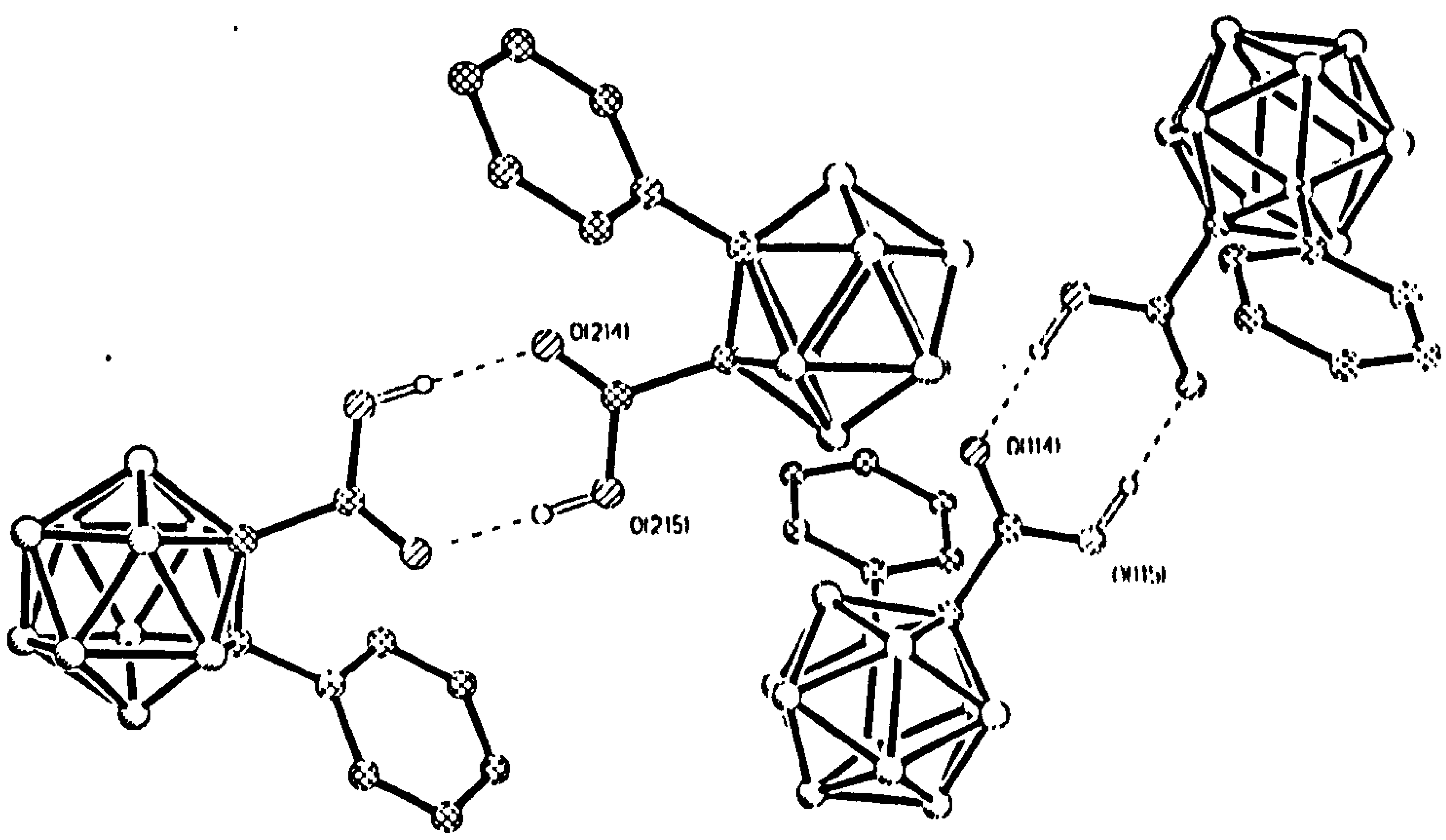

figure 3.13: Z-packing configuration of 1-phenyl-2-carboxy-ortho-carborane

The bond lengths of interest in the study of *exo*-π bonding were those of the cage C-C and the cage C-CO_2H functionality. These are 1.677(3)Å and 1.510(3)Å respectively (1.693(3)Å and 1.510(4)Å respectively in the second molecule). Comparison with the hydroxy and oxo compounds suggested there was no significant degree of π interaction between the cage carbon and the carboxylic acid function. The interatomic distances of 1.219(3)Å, (1.194(3)Å for molecule (b)), and 1.277(3)Å, (1.272(3)Å for (b)), for the carboxylic acid C=O and C-OH bonds show no deviation from standard carboxylic acid bond lengths. (The crystal structure of 1,12-di-(carboxy)-*para*-carborane shows a cage C-CO_2H bond of 1.515(1)Å and C-OH and C=O distances of 1.262(1)Å and 1.221(1)Å respectively.[25])

Deprotonation of this compound was achieved by proton sponge, ammonia and potassium 18-crown-6 ether. In all cases deprotonation was achieved (deboronation was also observed in some instances and this will be examined in Chapter Five.), and the subsequent change in the infrared spectroscopic stretch observed. The change was most marked with ammonia where ν(CO) of CO_2^- was noted at 1622cm^{-1} compared to 1724cm^{-1} for the parent compound. (The maximum change observed on deprotonation of *ortho*-$PhCB_{10}H_{10}COH$ to *ortho*-$PhCB_{10}H_{10}CO^-$, where the *exo*-π bonding interaction was strong, was 230cm^{-1} from 1690cm^{-1} to 1460cm^{-1}.)

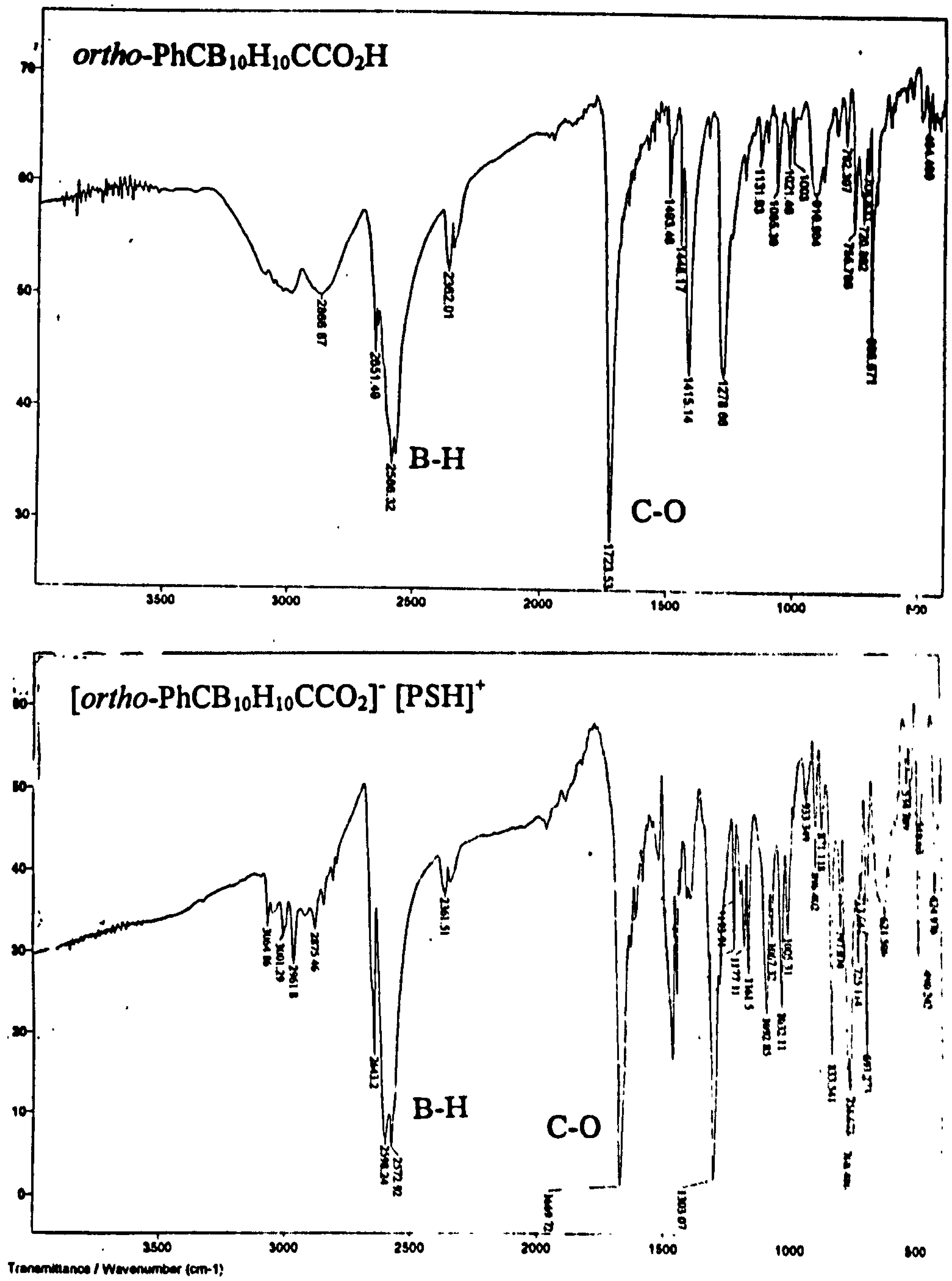

figure 3.14: IR spectra illustrating the change in CO stretching frequency upon deprotonation

Unfortunately, no X-ray quality crystals were obtained, however, as for 1-phenyl-2-fluoro-*ortho*-carborane, ^{11}B NMR spectroscopy was employed to monitor electronic changes within the icosahedral framework.

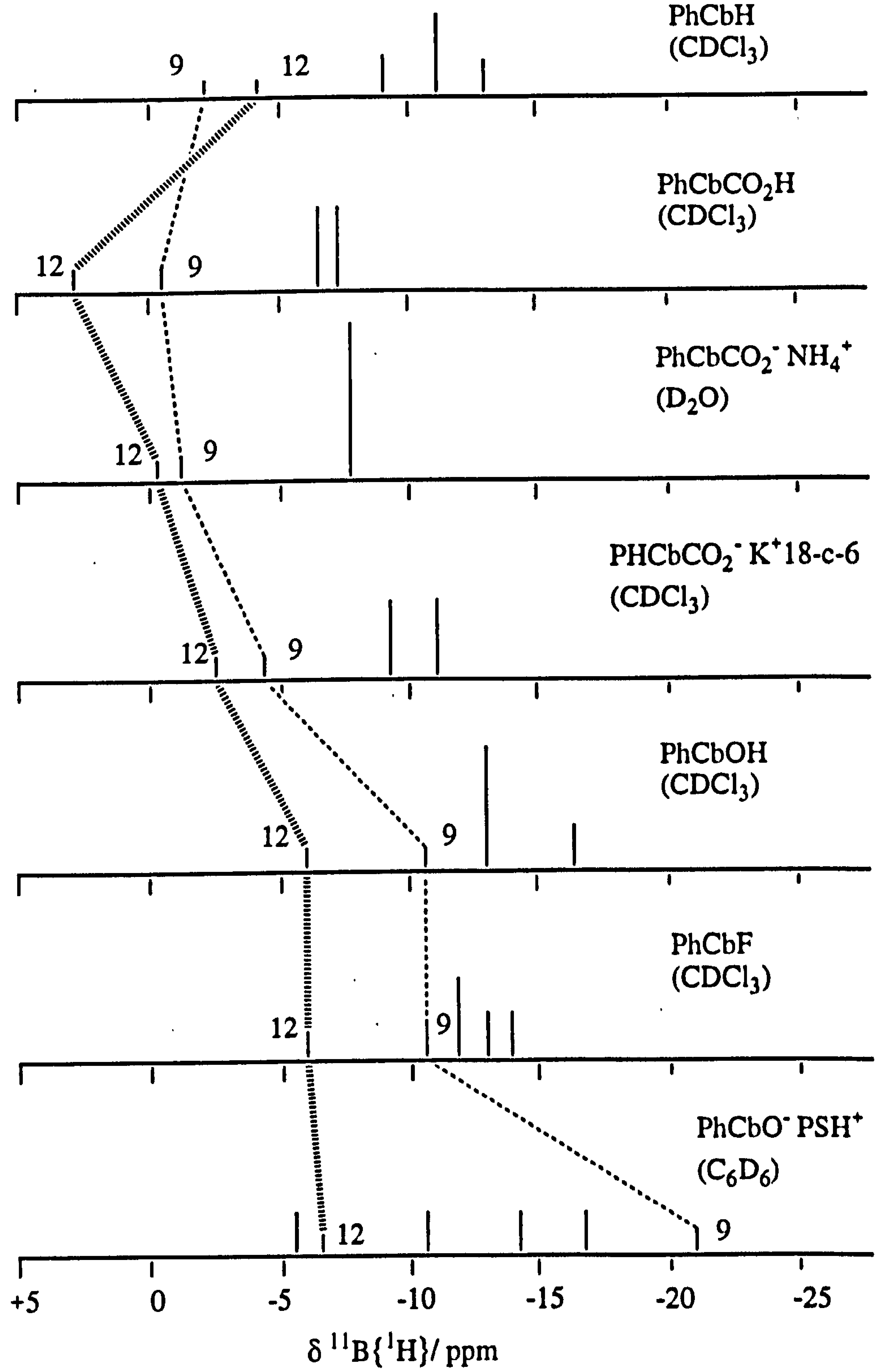

figure 3.15: $^{11}B\{^{1}H\}$ NMR shifts of ortho-carboranyl derivatives. B12 is antipodal to Ph, B9 is antipodal to X substituent

In carboranes o-$RCB_{10}H_{10}CX$, where X, (X=NR, O, S or PR), was the *exo*-substituent, it has been shown through theoretical calculations, X-ray and NMR data that the antipodal shift increased as π-bonding interactions between the cage and *exo*-substituent increased.[3] The antipodal atom shifts observed for the deprotonated carboxylic acid derivative ($X=CO_2^-$), suggested that very little, if any, π-bonding occured in this derivative. Conversely, theoretical calculations at the STO3G level, performed by Dr. Mark Fox, calculated the cage C-C distance to be 1.807Å.[24] This suggested an opening of the cage which would be indicative of *exo*-π bonding, although this result was not confirmed by NMR spectroscopy.

d) ^{13}C NMR spectroscopy

Other electronic effects are manifested through NMR spectroscopy as explained in the introduction to this chapter. For icosahedral carboranes, the antipodal effect is reportedly the most pronounced, followed by the butterfly effect, then the neighbour effect.[14] In icosahedral *ortho*-carborane derivatives, the substituted carbon, C(2), is the neighbouring atom. In a schematic representation of the $^{13}C\{^1H\}$ NMR spectra of $PhCB_{10}H_{10}CX$, little change was observed in the position of the atom neighbouring the electron rich X substituent. The position of the X substituted carbon conversely was shifted to a lower field (more positive δ) as the degree of *exo*-π bonding increased.

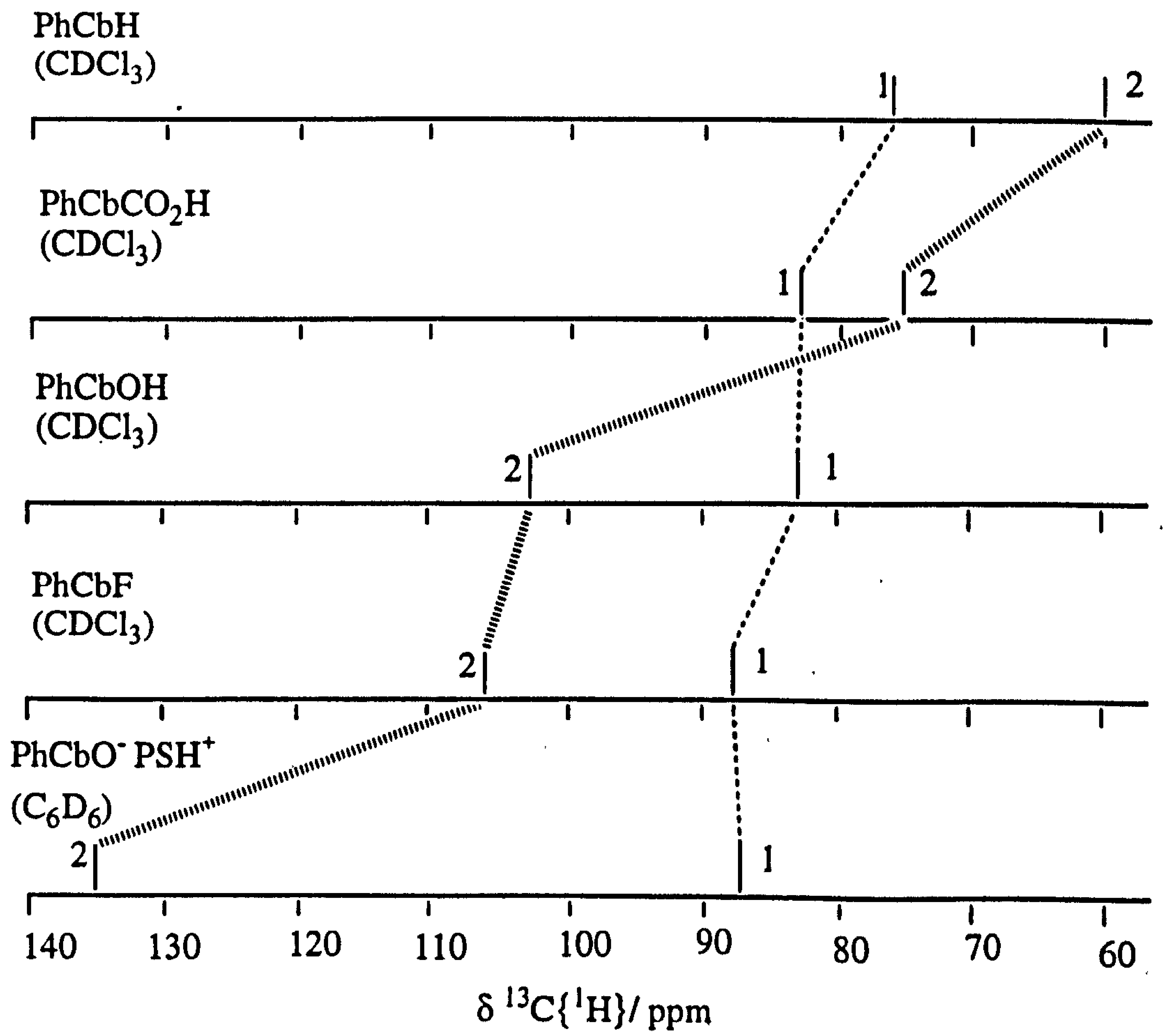

figure 3.16: $^{13}C\{^1H\}$ NMR shifts of ortho-carboranyl derivatives. 1=C-Ph, 2=C-X

This suggested that unlike the antipodal atom, where electron density (e.d.) increased in the NMR active orbitals as the degree of *exo*-π bonding increased, the electron density was decreased in the tangential, NMR active p_x and p_y orbitals and concentrated in the radial p_z orbital of the substituted carbon, C(2). This would explain the strengthened interaction between the cage carbon and the *exo* substituent.

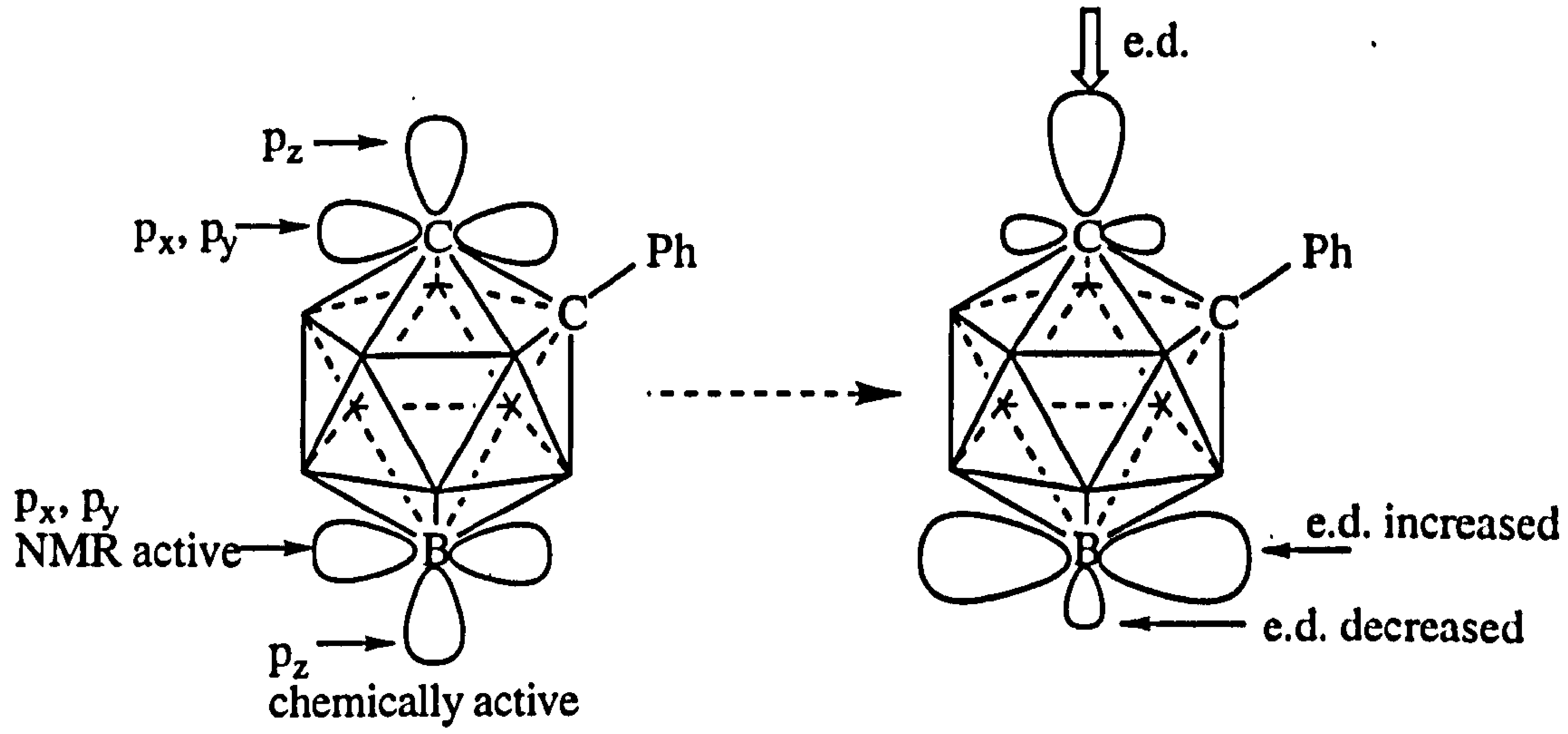

figure 3.17: electron distribution at the apical atoms alters as the degree of exo-π bonding increases

e) Summary of *exo*-π bonding in *ortho*-$PhCB_{10}H_{10}CX$

The results obtained in this study follow the observations of previous studies. Where X-ray structures are unavailable, theoretical methods can be used to predict the electronic distribution. Alternatively, the degree of *exo*-π bonding between a substituent X and the carboranyl cage atom can be predicted from the NMR shift of the atom antipodal to the point of substitution. *Exo*-π bonding increases as the antipodal shift becomes greater with the sole exception of *o*-$PhCB_{10}H_{10}CCO_2^-$, whose theoretical structure suggested *exo*-π bonding which was not substantiated by ^{11}B NMR spectroscopy. This has been illustrated in figure 3.15.

Placing the compounds in the order of increasing *exo*-π bonding as predicted by NMR spectroscopy, the increased cage C-C distance illustrates how the cage opens up as more density is donated by the *exo*-substituent. The non-conformity of the carboxylic acid is also illustrated in this table (table 3.5).

$PhCB_{10}H_{10}CX$ / X=	cage C-X / Å	cage C-C / Å
H	1.10	1.640(5)
CO_2H	1.510(3) and 1.510(4)	1.677(3) and 1.693(3)
CO_2^-	-	1.807(STO3G)
F	-	1.690(STO3G)
OH	1.366(2)	1.723(3)
O^-	1.245(3)	2.001(3)

table 3.5: bond lengths in ortho-$RCB_{10}H_{10}CX$

3.3.2 *Exo*-π bonding in *para*-carboranes

With regard to the investigations carried out with *ortho*- and *meta*-carboranyl systems, comparatively little work has been done on the *para*-carborane derivatives. With a view to looking at electronic effects within the highly symmetrical cage, a series of *para*-carborane derivatives have been synthesised, and their carbon and boron NMR spectra recorded.

In a manner similar to that used for the discussion of *ortho*-carborane derivatives, the NMR spectra give valuable information about electronic distributions within the cage. In the *para*-system, however, it is the carbon atoms which are antipodal, although it is anticipated that information may also be gleaned from the $^{11}B\{^1H\}$ NMR spectral data.

a) Carboxylic Acid Derivatives

A series of *para*-carboranyl carboxylic acid derivatives were synthesised and their NMR spectra recorded. Although only a few results were obtained, an initial survey of the results would suggest that as the *exo*- substituent becomes more electron rich, the cage carbon atom is shifted to a lower field (more positive δ) and the NMR signals produced by the cage boron atoms are shifted to higher field.

derivative	$^{11}B\{^1H\}$ / ppm	$^{13}C\{^1H\}$ cage carbon/ ppm
$HO_2CCB_{10}H_{10}CCO_2H$	-13.49	78.85
$HO_2CCB_{10}H_{10}CCO_2^-$	-13.68, -13.80	-
$^-O_2CCB_{10}H_{10}CCO_2^-$	-13.97	86.22

table 3.6: NMR spectroscopic shifts of para-carborane carboxylic acid derivatives

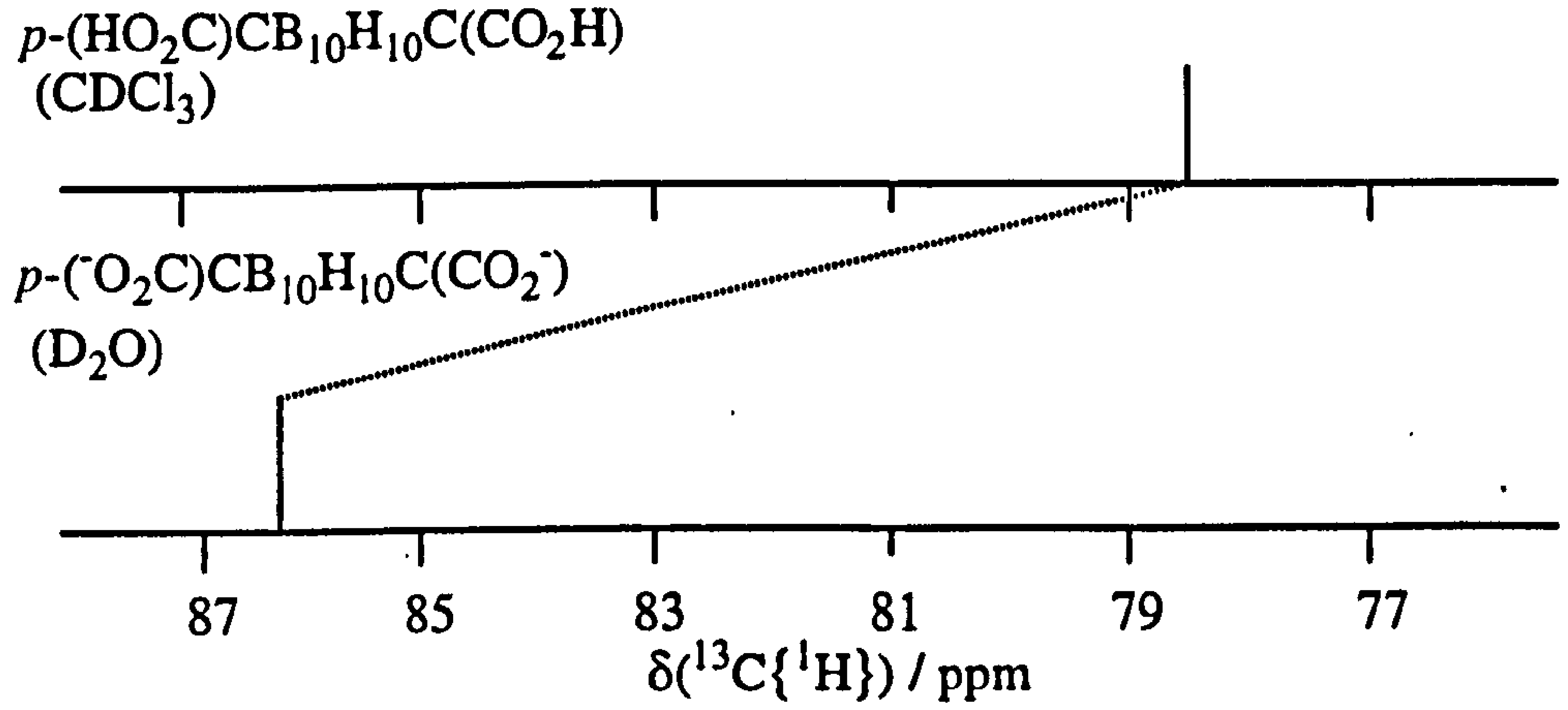

figure 3.18: schematic representation of the $^{13}C\{^1H\}$ NMR spectra of para-carborane carboxylic acid derivatives

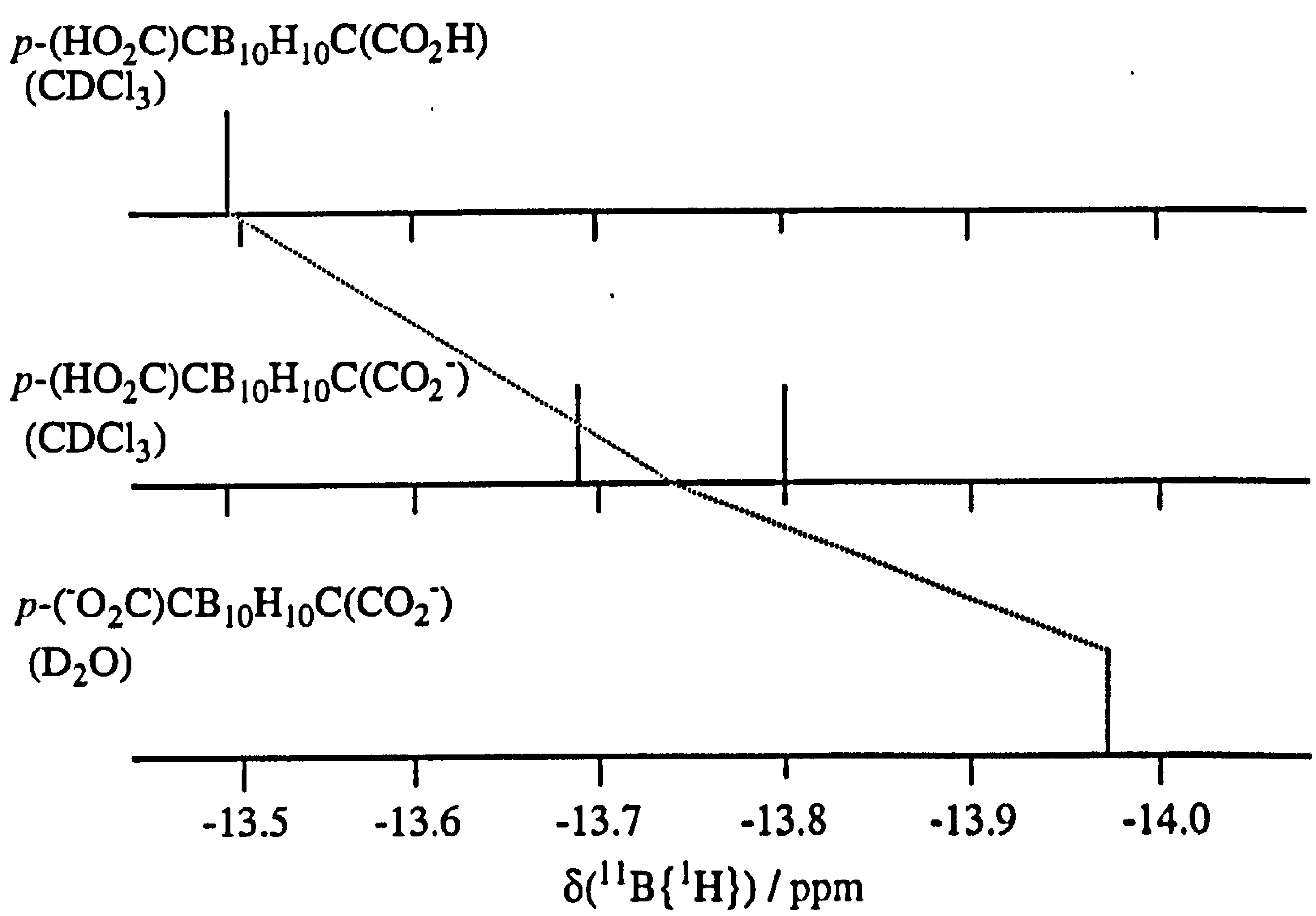

figure 3.19: schematic representation of the $^{11}B\{^1H\}$ NMR spectra of para-carborane carboxylic acid derivatives. Dotted line indicates average chemical shift.

With reference to figure 3.20, this would perhaps suggest that as more electron density is donated to the cage from the *exo* substituent, the NMR inactive radial orbitals of the carborane carbon atoms become filled with electron density, as the electron density in the NMR active p_x and p_y tangential orbitals of the cage boron atoms increases.

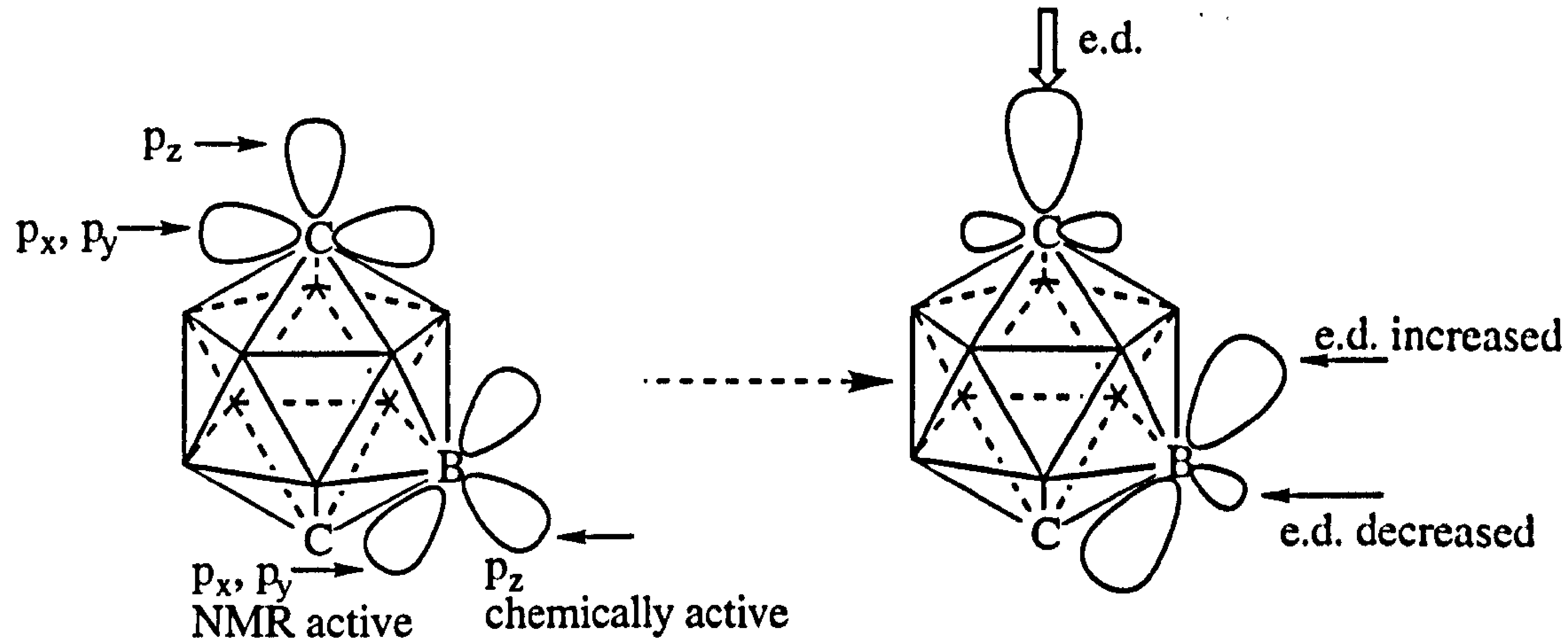

figure 3.20: proposed changes in electronic distribution as more electron density is donated to a para-carborane system. Illustrated C and B vertices are representative of each in the cage.

This proposed change would increase the electron density between the cage carbon and the *exo-* substituent leading to a multiple *exo*-bond as seen for *ortho-* carborane systems.

b) Benzene sulfonyl Derivatives

Several benzene-sulfonyl *para*-carborane derivatives were synthesised and again studied by NMR spectroscopy for changes in electronic distributions. The same trend observed for the carboxylic acid derivatives was observed for these compounds. As the substituent, X, on the carbon atom antipodal to C-$PhSO_2$ became more electron rich, the CX carbon shift moved to lower field as did the C-SO_2Ph carbon. The chemical shift values observed for the cage boron atoms were conversely shifted to higher field.

$PhSO_2CB_{10}H_{10}CR$ / R=	$^{11}B\{^1H\}$ / ppm	$^{13}C\{^1H\}$ / ppm
SO_2Ph	-11.11	67.0
Ph	-13.04, -14.13	86.10, 92.17
F	-14.61, -15.63	84.35 (C-SO_2Ph)
		120.5 (C-F)

table 3.7: chemical shifts for para-$PhSO_2CB_{10}H_{10}CR$

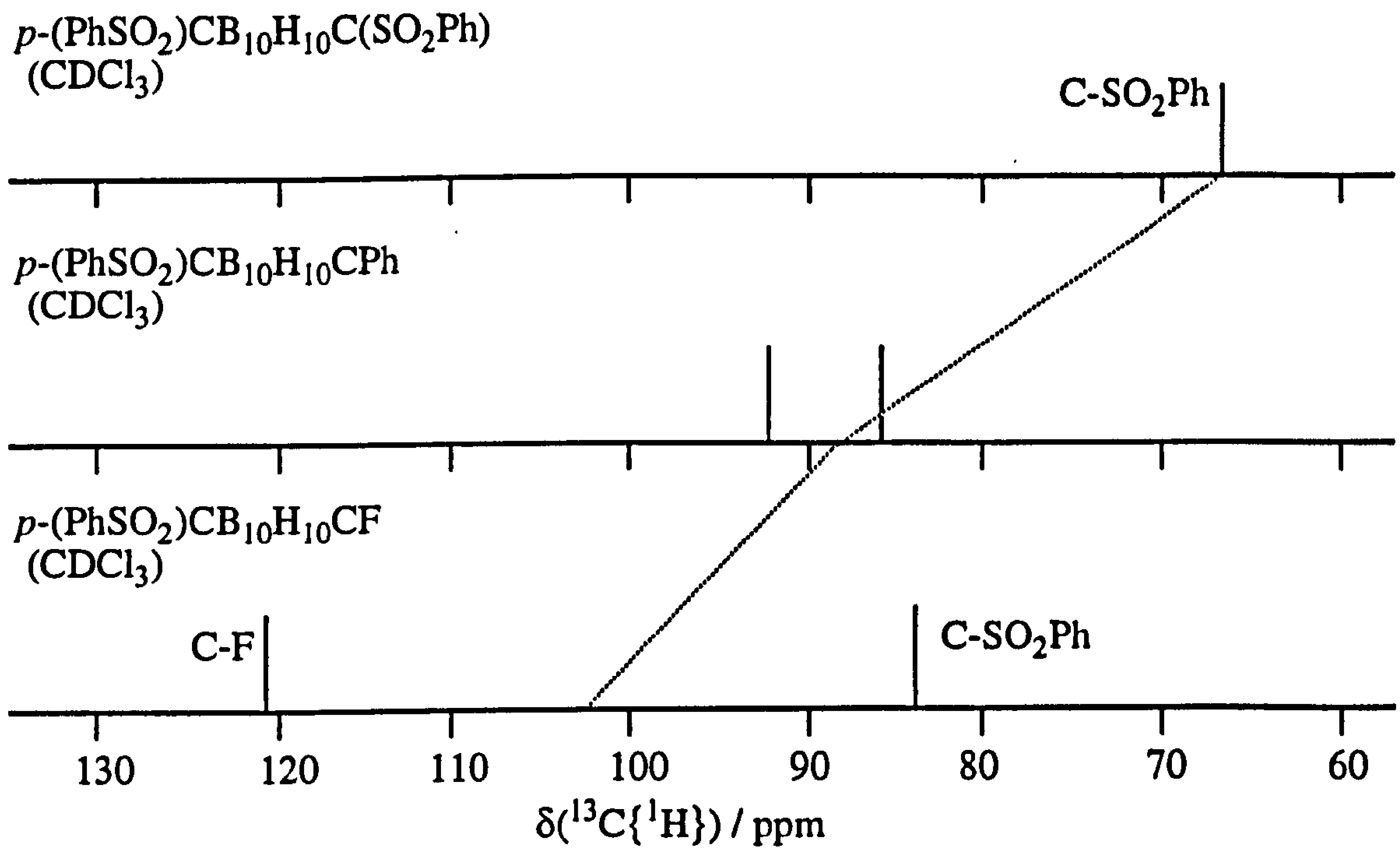

figure 3.21: schematic representation of $^{13}C\{^1H\}$ NMR spectra of para-$PhSO_2$-carborane derivatives. Dotted line shows average chemical shift.

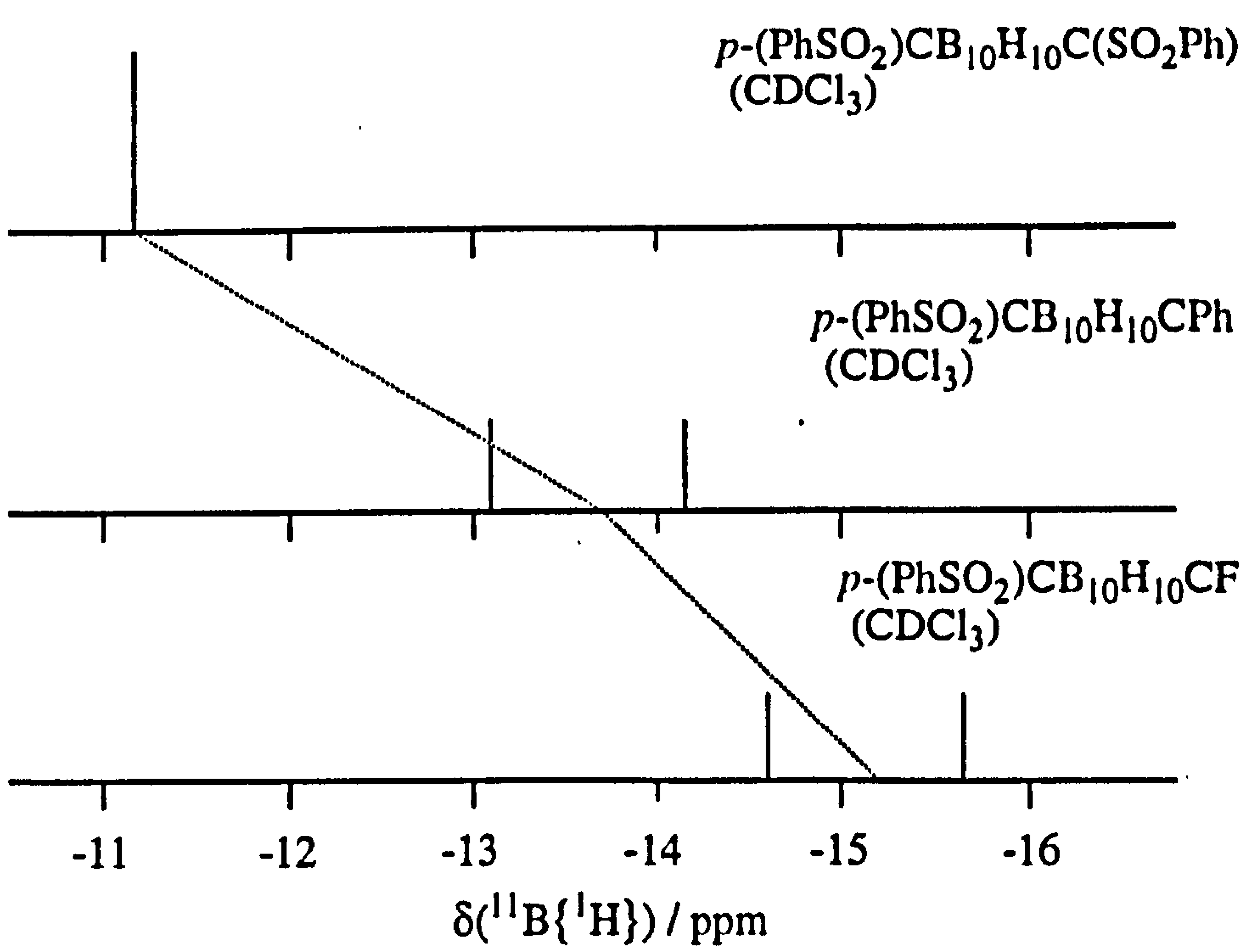

figure 3.22: schematic representation of $^{11}B\{^1H\}$ NMR spectra of para-$PhSO_2$-carborane derivatives. Dotted line represents average chemical shift

There is no evidence of an antipodal shift in the same sense as that seen for *ortho-* and *meta*-carborane derivatives with boron NMR spectroscopy, however, there does seem to be a redistribution of electron density away from the NMR active orbitals of the cage carbon atoms. As postulated above, this could mean the electron density has been increased in the radial p orbital, suggestive of *exo*-π bond formation.

X-ray quality crystals have been grown of 1,12-di-(phenyl-sulfonyl)-*para*-carborane, 1-(phenyl-sulfonyl)-12-phenyl-*para*-carborane, and 1-(phenyl-sulfonyl)-12-fluoro-*para*-carborane, however, only the latter structure has been solved.

X-ray structure of 1-(phenyl-sulfonyl)-12-fluoro-*para*-carborane

Clear, colourless, platelike crystals of this compound were grown by the slow evaporation of acetone. The fluorine moiety on C(12) lies on the axis of the cage within experimental error, whilst the SO_2Ph group is oriented at an angle to the cage (table 3.9).

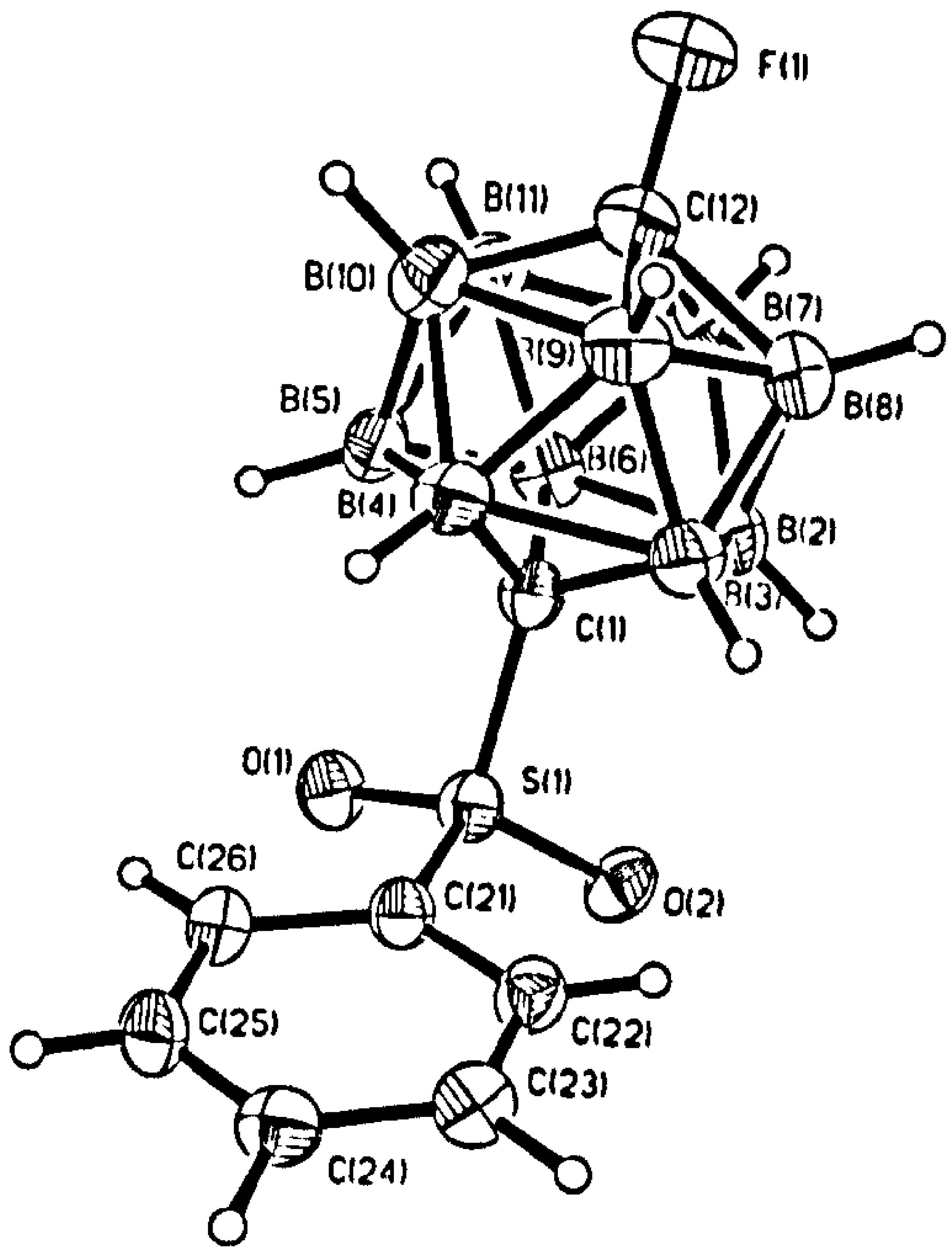

figure 3.23: crystal structure of 1-(phenyl-sulfonyl)-12-fluoro-para-carborane

atoms	bond length / Å	atoms	bond length / Å
C(1)-S(1)	1.821(3)	C(12)-F(1)	1.364(3)
S(1)-O(1)	1.435(2)	S(1)-O(2)	1.441(2)
S(1)-C(21)	1.758(3)	C(12)-B(7)	1.702(5)
C(1)-B(2)	1.732(4)	C(12)-B(8)	1.699(5)
C(1)-B(3)	1.713(4)	C(12)-B(9)	1.703(5)
C(1)-B(4)	1.719(4)	C(12)-B(10)	1.701(5)
C(1)-B(5)	1.719(4)	C(12)-B(11)	1.712(5)
C(1)-B(6)	1.719(4)		

table 3.8: bond lengths within 1-(phenyl-sulfonyl)-12-fluoro-para-carborane

atoms	bond angle / °	atoms	bond angle / °
S(1)-C(1)-B(2)	116.1(2)	F(1)-C(12)-B(7)	116.8(3)
S(1)-C(1)-B(3)	119.7(2)	F(1)-C(12)-B(8)	116.8(3)
S(1)-C(1)-B(4)	120.2(2)	F(1)-C(12)-B(9)	116.5(3)
S(1)-C(1)-B(5)	116.6(2)	F(1)-C(12)-B(10)	116.7(3)
S(1)-C(1)-B(6)	114.2(2)	F(1)-C(12)-B(11)	116.8(3)
C(1)-S(1)-O(1)	106.68(13)		
C(1)-S(1)-O(2)	106.59(13)		
C(1)-S(1)-C(21)	106.09(13)		

table 3.9: bond angles within 1-(phenyl-sulfonyl)-12-fluoro-para-carborane

This is the first structurally characterised example of a carboranyl C-F bond and as such no direct comparisons with analogous systems could be drawn. In organic aromatic systems containing the Ar-F fragment, bond lengths of 1.34-1.36Å are found to be typical[26], placing the observed carboranyl C-F bond distance of the carboranyl compound (1.364(3)Å) at the lengthier end of the scale. However, the high carbon coordination number cannot be ignored, implying that the CF bond is indeed short. A short bond would have been predicted as the fluorine is electron rich and has the potential to form an *exo*-π bond with the cage. Reference to the 1-phenyl-2-hydroxy-*ortho*-carborane and 1-phenyl-2-fluoro-*ortho*-carborane systems however, showed through NMR spectroscopy that the fluorine only *exo*-π bonded to a similar degree as the OH substituent. If this trend is continued in the *para*- system, no great degree of *exo*-π bonding is expected.

Within the sulfonyl group the S=O bond lengths of 1.435(2)Å and 1.441(2)Å are unextraordinary, as is the S-phenyl distance of 1.758(3)Å. For an aryl C-SO_2Ph fragment, a C-S bond of 1.75-1.76Å is usual, and with the *para*-carborane in place of the aryl group, a C-S connectivity of 1.758(3)Å is observed. No other *para*-carborane structures incorporating a sulfonyl group have been solved to our knowledge, so no direct comparisons can be drawn.

The NMR spectra recorded for this series of compounds suggested that electron density was directed away from the tangential orbitals of the carbon atoms. If this e.d. were redirected into the radial orbital, a short C-*exo*-substituent bond would be expected. This has been suggested by X-ray crystallography. An alternative explanation available from the NMR spectroscopic study is that the electron density has moved to fill the tangential orbitals of the cage boron atoms, accounting for the upfield shift observed for these atoms.

c) Other *para*-carborane derivatives

The above discussion has made a tentative suggestion that there may a relationship between the observed $^{11}B\{^1H\}$ and $^{13}C\{^1H\}$ chemical shifts of series of substituted *para*-carborane derivatives. When other compounds are considered a relationship is not so obvious as that proposed above which links $^{11}B\{^1H\}$ and $^{13}C\{^1H\}$ chemical shifts. A more detailed study is obviously required to elucidate any firm connection between the NMR spectra of such compounds.

$HCB_{10}H_{10}CR$ / R=	$^{11}B\{^1H\}$ / ppm	$^{13}C\{^1H\}$ / ppm
$C_3N_3(CB_{10}H_{10}CH)_2$	-13.26, -14.59	63.43 (C-H)
		82.78 ($C\text{-}C_3N_3(Cb)_2$)
$Si(CH_3)_3$	-	67.26 (C-H)
		75.03 (C-Si)
CO_2H	-13.04, -14.79	57.83 (C-H)
		71.35 ($C\text{-}CO_2H$)
Cl	-11.81, -15.87	55.29 (C-H)
		81.35 (C-Cl)
H	-12.8	64.26
BrPh	-12.71, -15.21	60.6 (C-H)
		86.1 (C-PhBr)
Ph	-9.16, -11.85	59.7 (C-H)
		86.4 (C-Ph)
OH	-9.89, -14.12	-

table 3.10: chemical shift values for para-$HCB_{10}H_{10}CR$

$PhCB_{10}H_{10}CR$ / R=	$^{11}B\{^1H\}$ / ppm	$^{13}C\{^1H\}$ / ppm
Ph	-9.27	83.48
H	-9.16, -11.85	59.7 (C-H)
		86.4 (C-Ph)
SO_2Ph	-13.04, -14.13	86.10, 92.17
CO_2H	-9.64, -10.45	-
$C_3N_3(CB_{10}H_{10}CPh)_2$	-12.79, -13.21	79.43 (C-Ph)
		85.43 ($C\text{-}C_3N_3(CbPh)_2$)

table 3.11: chemical shift values for para-$PhCB_{10}H_{10}CR$

3.3.3 Hydrogen Bonding In Heterocyclic Carboranes

Hydrogen bonding interactions are of interest in the field of crystal engineering. Two types of interaction are possible, either intermolecular or intramolecular. Both types of hydrogen bonding interaction have been observed in carborane systems, and here the study has been extended to the mono-substituted (2'-thiophenyl)- and (3'-pyridyl)-*ortho*- and *meta*-carboranes.

a) Pyridyl derivatives

In previous work[23], 1-(2'-pyridyl)-*ortho*-carborane has been shown to intramolecularly hydrogen bond to the acidic proton on C(2), (see Chapter Two, scheme 2.39). By contrast, the 3'-pyridyl analogue has been shown to intermolecularly hydrogen bond to give a dimer in the solid state. Crystals of the compound were grown from ethanol/water, and display an intermolecular C-H···N hydrogen bond of 2.514Å.

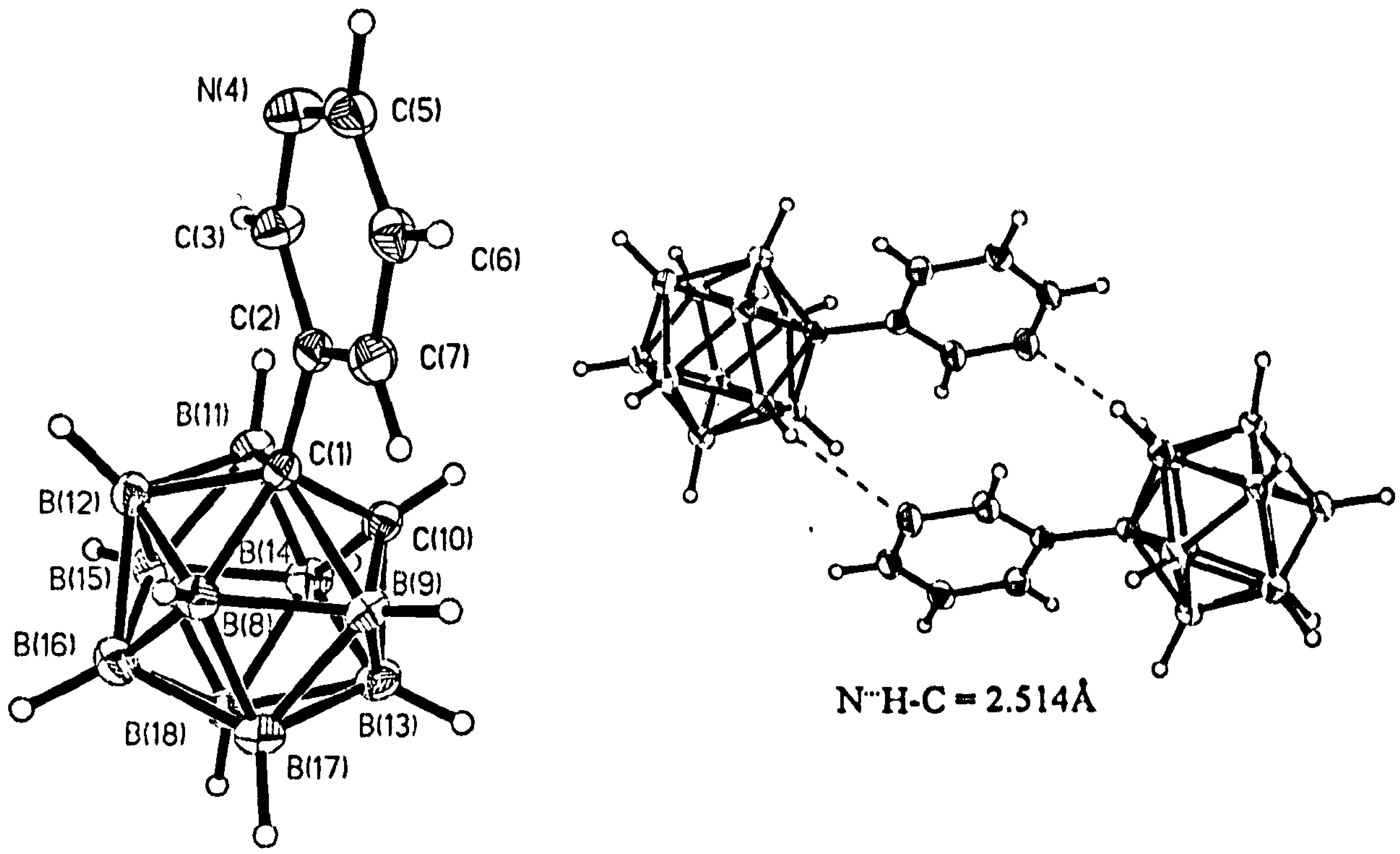

figure 3.24: crystal structure of 1-(3'-pyridyl)-ortho-carborane

atoms	bond length / Å	atoms	bond length / Å
C(1)-C(10)	1.664(2)	N(4)-H(10')	2.514
C(1)-C(2)	1.512(2)	C(2)-C(3)	1.395(2)
C(3)-N(4)	1.343(2)	N(4)-C(5)	1.340(2)
C(5)-C(6)	1.381(2)	C(6)-C(7)	1.391(2)
C(7)-C(2)	1.388(2)		

table 3.12: selected bond lengths of 1-(3'-pyridyl)-ortho-carborane

Where the 1-(2'-pyridyl)-*ortho*-carborane forms π-stacks, no evidence of π-stacking between the pyridyl rings of 1-(3'-pyridyl)-*ortho*-carborane is seen. It is assumed that hydrogen bonding controls the packing of the 3'-pyridyl derivative in the crystal lattice, preventing the formation of π-stacks.

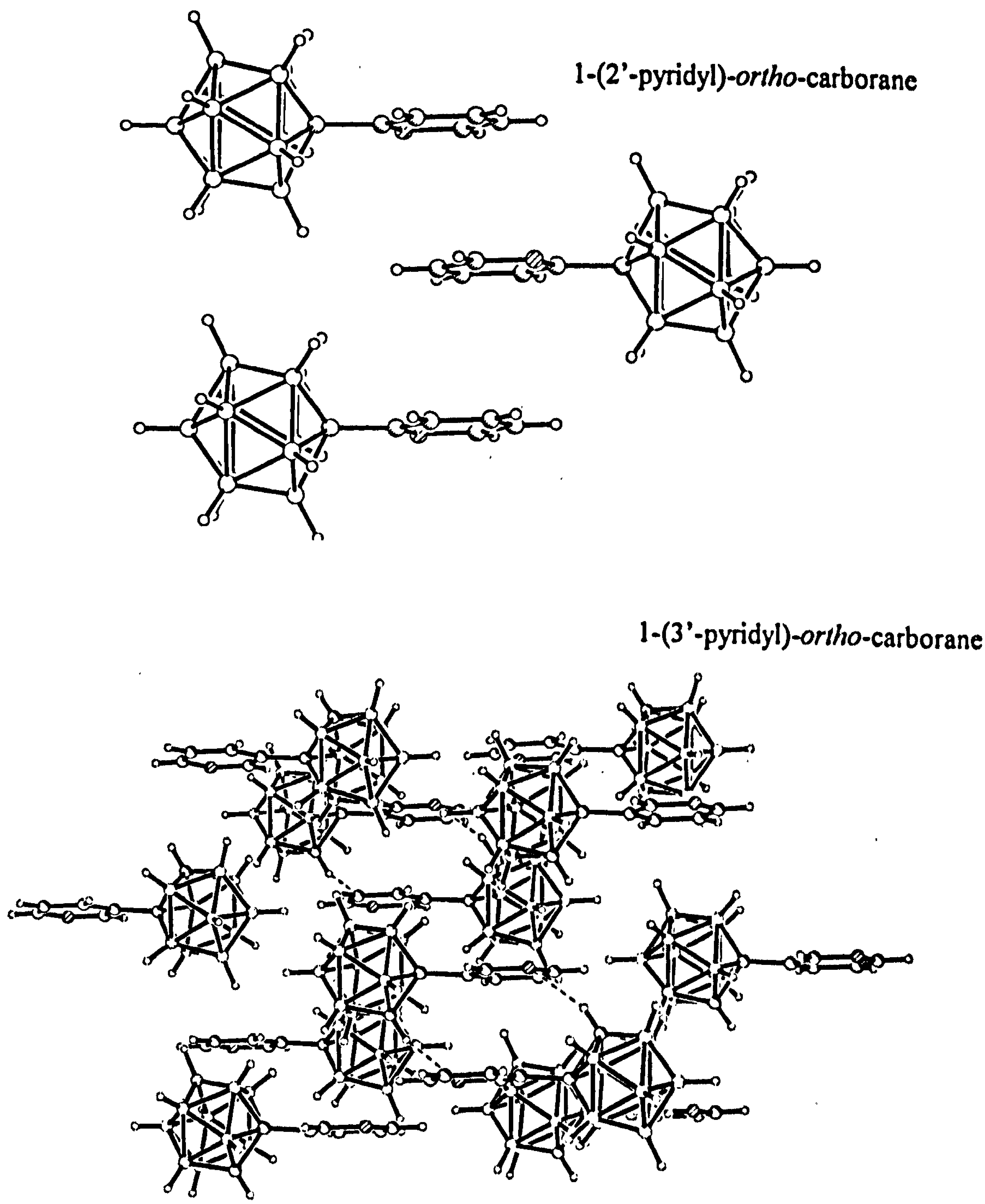

figure 3.25: packing diagrams of 1-(2'-pyridyl)-ortho-carborane (top) and 1-(3'-pyridyl)-ortho-carborane (bottom)

Infrared spectroscopy is a valuable tool in the elucidation of hydrogen bonding interactions. In the solid state, the molecules are not free to move as much as in solution, so by recording one sample in the solid state (KBr disc) and another in solution (CCl_4) the type of hydrogen bonding interaction can be deduced. If the bonding mode is intermolecular, the N···H interaction in this example, will be removed in solution, changing the stretching frequency of the CH bond. If it is intramolecular, the carboranyl CH stretching frequency will remain the same in both the solid and solution state. Dilution studies would also yield information about intermolecular hydrogen bonding interactions.

X-ray crystallography has been used to observe the hydrogen bonding in 1-(3'-pyridyl)-*ortho*-carborane, but it is also obvious by IR spectroscopy. The same type of intermolecular hydrogen bond is present in the *meta-* isomer as well, although the crystallographic structure has not been solved.

compound	υ(IR) carboranyl CH/ cm^{-1} KBr disc	CCl_4 solution
o-(2'-pyridyl)-$CB_{10}H_{10}CH$	3072	-
o-(3'-pyridyl)-$CB_{10}H_{10}CH$	3024	3042
m-(3'-pyridyl)-$CB_{10}H_{10}CH$	3022	3068

table 3.13: IR spectroscopic stretching frequencies of the carboranyl CH bond in pyridyl-ortho- and meta-carboranes

b) Thiophenyl derivatives

In 1-(2'-thiophenyl)-*ortho*-carborane an intramolecular hydrogen bonding interaction was anticipated as seen in the 2-pyridyl system. A possible intermolecular interaction was postulated for the *meta*-isomer. IR spectroscopy suggested, however, that both compounds should display intermolecular hydrogen bonds.

compound	υ(IR) carboranyl CH/ cm^{-1} KBr disc	CCl_4 solution
o-(2'-SC_4H_3)-$CB_{10}H_{10}CH$	3063	3071
m-(2'-SC_4H_3)-$CB_{10}H_{10}CH$	3058	3068

table 3.14: IR stretching frequencies of the carboranyl CH bond in 1-(2'-thiophenyl)-ortho- and meta-carborane

Crystals of 1-(2'-thiophenyl)-*ortho*-carborane were grown from chloroform as clear colourless square platelets. Like the 3-pyridyl analogue of this compound, no π-stacking is seen in the crystal lattice between thiophenyl rings.

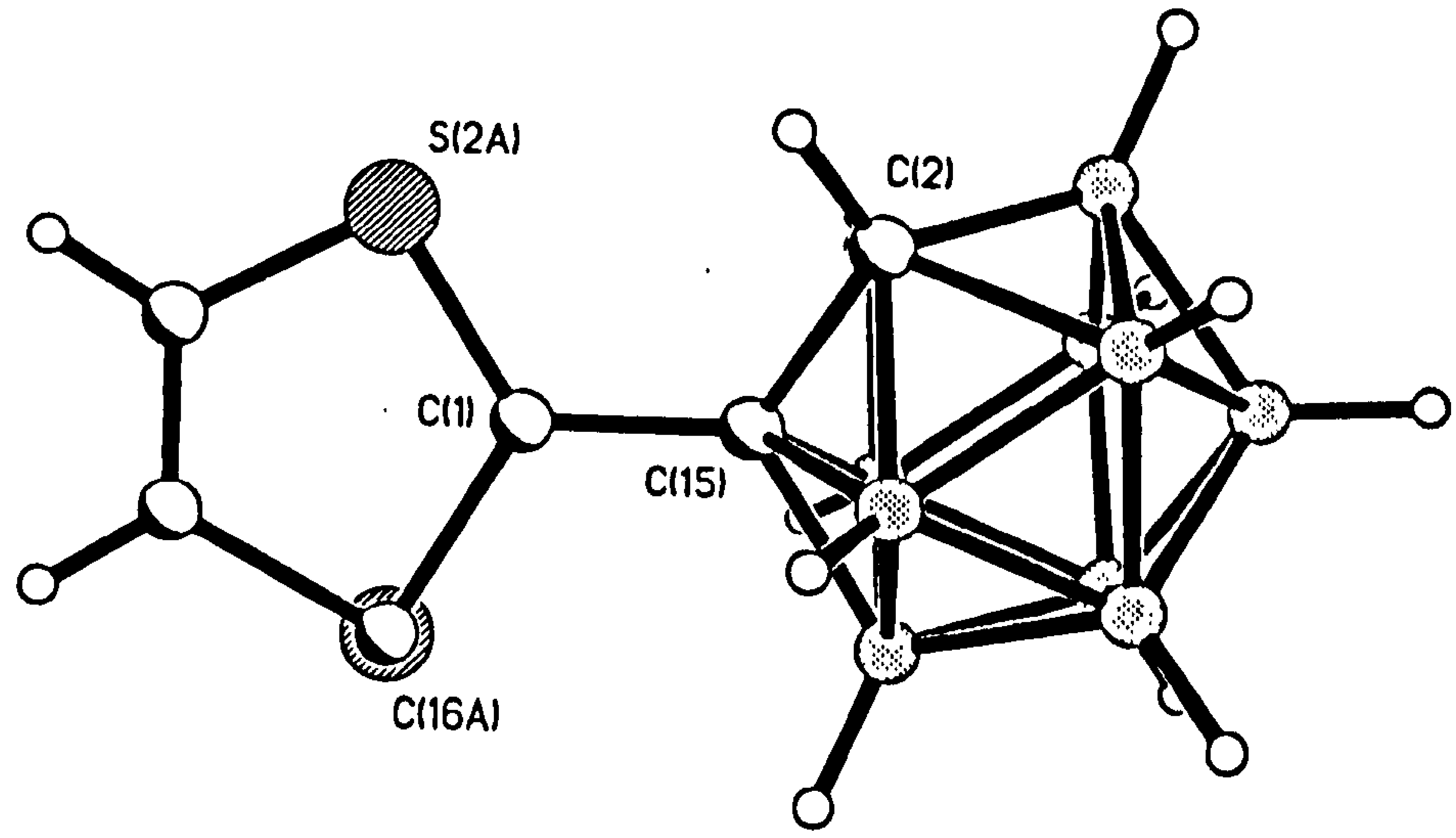

figure 3.26: crystal structure of 1-(2'-thiophenyl)-ortho-carborane

To lower the R factor of the crystal solution to a reasonable level (8.7%), the structure has been refined by modelling both S(2A) and C(16A) as sulfur atoms. The occupancy of the sulfur is actually 40% in position S(2A) and 60% in position C(16A). In reality the thiophenyl ring would not have the high symmetry of that in figure 3.26.

Preliminary results show that in the packing model of this compound, there are no interactions between S(2A) (or C(16A)) and the proton of C(2). This would suggest that, contrary to IR spectroscopic evidence, no intermolecular interactions are present in this compound. However, the structure is highly disordered, and given the majority of sulfur occupancy is calculated to be at C(16A), intermolecular interactions can be envisaged.

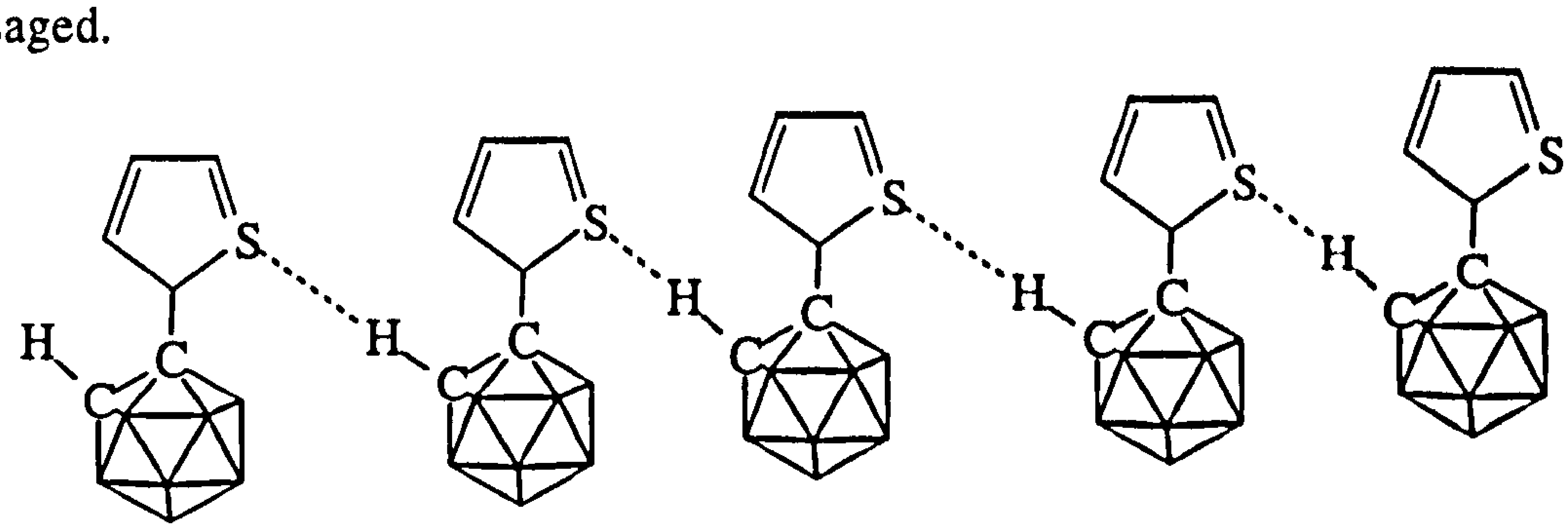

figure 3.27: possible intermolecular hydrogen bonding in 1-(2'-thiophenyl)-ortho-carborane

When the thiophenyl sulfur occupies position S(2A), a C(2)-H···S(2A) bond length of 2.79Å is indicative of a strong intramolecular hydrogen bonding interaction.

For the modelled compound, a cage C-C distance of 1.471Å is measured. This significant shortening of the cage C-C bond illustrates how cage distortion has been induced by the intramolecular hydrogen bond. This is a much shorter cage C-C bond than seen for any pyridyl derivative (*c.f.* table 3.15). This cage C-C bond shortening may be "real" or it may be a result of crystallographic compromise.

o-$RCB_{10}H_{10}CH$ / R=	cage C-C / Å	H bond length / Å
H[21]	1.630(6)	N/A
Ph[27]	1.640(5)	N/A
2'-pyridyl[28]	1.634(3)	2.41 (intramolecular)
2'-thiophenyl	1.47	2.79 (intra)
(2'-pyridyl)-CH_2[29]	1.624(4)	2.58 (intra) 2.41 (inter)

table 3.15: cage C-C distance variations resulting from intramolecular hydrogen bonding interactions

3.4 SUMMARY

Chapter Three has discussed the effect a substituent can exert on electronic distributions and structure within an icosahedral C_2B_{10} carborane system.

Exo-π bonding, where an electron rich substituent with appropriately oriented orbitals, is able to donate electron density back into the cage system and effectively form a multiple bond between the *exo* substituent and the cage has been investigated in previous years. The classic example of 1-phenyl-2-oxo-*ortho*-carborane anion is well known for this *exo*-π bonding phenomenon. Here, the parent compound, 1-phenyl-2-hydroxy-*ortho*-carborane, has been crystallised and its structure solved. The cage C-C distance of 1.723(3)Å quantifies the change between the hydroxy and oxo species resulting from *exo*-π bonding, although the C-OH distance of 1.366(2)Å suggests there may also be a small degree of *exo*-π bonding occurring in the parent compound.

As fluorine is isoelectronic and isolobal with OH and O^-, 1-phenyl-2-fluoro-*ortho*-carborane was studied with a view to detecting *exo*-π bonding. Unfortunately, no suitable crystals were obtained, although NMR spectroscopic data and theoretical calculations suggested the fluoro derivative only *exo*-π bonded to the same extent as the hydroxy compound.

Studies on carboxylic acid derivatives suggested that these compounds did not *exo*-π bond to the cage either. Upon deprotonation to the CO_2^- species, theoretical calculations suggested *exo*-π bonding should be detectable, but NMR evidence did not substantiate this.

A study of *para*-carboranyl derivatives was conducted to see if any *exo*-π bonding would be seen in these systems. Some carboxylic acid derivatives were synthesised and although no X-ray data were obtained, NMR evidence suggested that as the *exo* substituent became more electron rich, electron density on the cage boron atoms increased (^{11}B NMR shift to higher field) whilst that in the NMR active orbitals of the apical carbon atoms decreased ($^{13}C\{^{1}H\}$ NMR shift to lower field). The same trend was observed for $PhSO_2CB_{10}H_{10}CR$ derivatives. The structure of 1-fluoro-12-(phenylsulfonyl)-*para*-carborane was elucidated and showed a short CF bond of 1.364(3)Å, but otherwise no great degree of bond distortion. No similar compounds are available for direct comparison.

Hydrogen bonding in 3-pyridyl and 2-thiophenyl substituted carboranes was also investigated. 1-(3'-pyridyl)-*ortho* and *meta*-carboranes both exhibited intermolecular hydrogen bonding interactions. Infrared spectroscopy gave clear evidence of this, and the X-ray structure of the *ortho*-derivative illustrated an intermolecular C-H···N bond of 2.514Å.

Their IR spectra suggested that 1-(2'-thiophenyl)-*ortho* and *meta*-carboranes should both have intermolecular hydrogen bonds, although an intramolecular interaction would have been expected for the *ortho* derivative. Contrary to the IR spectroscopic evidence, the crystal structure of 1-(2'-thiophenyl)-*ortho*-carborane had an intramolecular C-H···S hydrogen bond interaction of 2.79Å.

3.5 REFERENCES

1 D.A. Brown, W. Clegg, H.M. Colquhoun, J.A. Daniels, I.R. Stephenson, K. Wade, J. Chem. Soc., Chem. Commun., 1987, 889

2 R. Coult, M.A. Fox, W.R. Gill, K. Wade, W. Clegg, Polyhedron, **11**, 2717

3 R.J. Peace, PhD Thesis, Durham, 1996

4 D.M.P. Mingos, J. Chem. Soc., Dalton Trans., 1977, 602

5 T.D. Getman, C.B. Knobler, M.F. Hawthorne, J. Am. Chem. Soc., 1990, **112**, 4593

6 L.H. Hall, A. Perloff, F.A. Mauer, S. Block, J. Chem. Phys., 1965, **43**, 3911

7 E.J. Ditzel, X.L.R. Fontaines, N.N. Greenwood, J.D. Kennedy, M. Thornton-Pett, J. Chem. Soc., Chem. Commun., 1989, 1115

8 S. Hermanek, Chem. Rev., 1992, **92**, 325

9 R. Weiss, R.N. Grimes, J. Am. Chem. Soc., 1978, **100**, 1401

10 T.L. Venable, W.C. Hutton, R.N. Grimes, J. Am. Chem. Soc., 1984, **106**, 29

11 B.E. Aufderheide, R.F. Sprecher, Inorg. Chem., 1974, **13**, 2286

12 A.O. Clouse, D.C. Moody, R.R. Rietz, T. Roseberry, R. Schaeffer, J. Am. Chem. Soc., 1973, **95**, 2496

13 A. Allerhand, A.O. Clouse, R.R. Rietz, T. Roseberry, R. Schaeffer, J. Am. Chem. Soc., 1972, **94**, 2445

14 F. Teixidor, C. Vinas, R.W. Rudolph, Inorg. Chem., 1986, **25**, 3339

15 A.R. Siedle, G.M. Bodner, A.R. Garber, D.C. Beer, L.J. Todd, Inorg. Chem., 1974, **13**, 2321

16 S. Hermanek, J. Plesek, V. Gregor, B. Stibr, J. Chem. Soc., Chem. Commun., 1977, 561

17 S. Hermanek, D. Hynk, Z. Havlas, J. Chem. Soc., Chem. Commun., 1989, 1859

18 I.R. Stephenson, PhD Thesis, Durham, 1988

19 B. Wrackmeyer, Progress in NMR Spectroscopy, 1979, **12**, 227

20 M. Diaz, J. Jaballas, J. Arias, H. Lee, T. Onak, J. Am. Chem. Soc., 1996, **118**, 4405

21 M.G. Davidson, T.G. Hibbert, J.A.K. Howard, A. MacKinnon, K. Wade, Chem. Commun., 1996, 2285

22 R.J. Blanch, M. Williams, G.D. Fallon, M.G. Gardiner, R. Kaddour, C.L. Raston, Angew. Chem., Int. Ed. Engl., 1997, **30**, 504

23 R. Coult, M.A. Fox, W.R. Gill, P.L. Herbertson, J.A.H. MacBride, K. Wade, J. Organomet. Chem., 1993, **462**, 19

24 M.A. Fox, K. Wade, unpublished results

25 R. Centore, M.R. Ciajolo, A. Tuzi, Acta Cryst., 1994, **C50**, 905

26 Cambridge Structural Database Survey

27 P.T. Brain, J. Cowie, D.J. Donohoe, D. Hnyk, D.W.H. Rankin, D. Reed, B.D. Reid, H.E. Robertson, A.J. Welch, M. Hofmann, P.v.R.Schleyer, Inorg. Chem., 1996, **35**, 1701

28 Z.G. Lewis, A.J. Welch, Acta Cryst., 1993, **C49**, 705

29 T.G. Hibbert, K. Wade, R. Copely, J.A.K. Howard, unpublished results

Chapter Four

Multicarboranyl Assemblies - The Chemistry Of Carboranyl Triazines And Related Systems

4.1 INTRODUCTION

This chapter will concentrate on the synthetic, structural and bonding aspects of multi-carboranyl assemblies, in particular, compounds where the carborane units are centred around a triazine (C_3N_3) moiety. Three-cage systems are the main focus of the following discussion but two-cage assemblies are also considered. An introduction to the field of multi-carboranyl chemistry is followed by a résumé of their syntheses. Difficulties encountered by centring the carboranes around a heterocycle, as opposed to the previously investigated aliphatic and benzene systems will be discussed, together with the subsequent stability and derivatisation potential of such compounds. Electron distributions, hydrogen bonding interactions and structural features of this novel group of compounds are also explored.

4.2 MULTI-CARBORANYL ASSEMBLIES - AN OVERVIEW

When looking for comparative systems to the multi-carboranyl assemblies which will be discussed here, we must look back a good number of years for the first example of a di-carboranyl assembly[1], and also for the first instance of a tri-carboranyl assembly.[2]

Dicarboranyl assemblies have manifested themselves primarily as *bis*-carboranes where two icosahedral cages are linked by means of a C-C[1,3,4,5], B-B[6] or a C-B[7] bond, but also as dicarbollides, where two cages are joined through an aliphatic[8] or aromatic[9,10] bridge. Such compounds can subsequently be deboronated and made to incorporate metal centres[8,11,12,13], so providing a route to compounds which exhibit NLO properties,[14] and which may also give a degree of success as catalysts.[15]

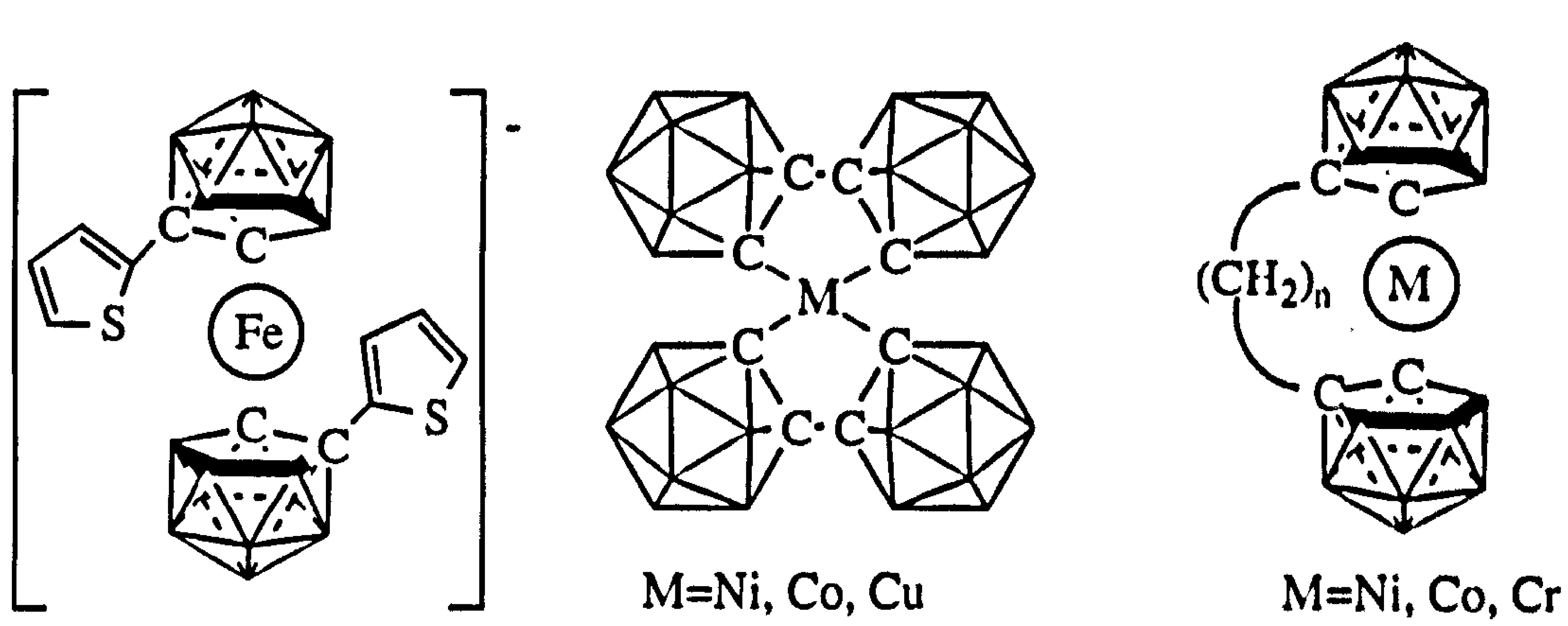

figure 4.1: incorporation of metals into two-cage carboranyl assemblies

As with many pieces of novel science, the first tri-carboranyl assembly, 1,2,4-tri-(1'-1',2'-carboranyl)-benzene, was an accidental discovery, the product being isolated from the reaction of a benzene solution of 1-ethynyl-*ortho*-carborane with a catalytic quantity of *bis*-(acrylonitrile)nickel(0).[2]

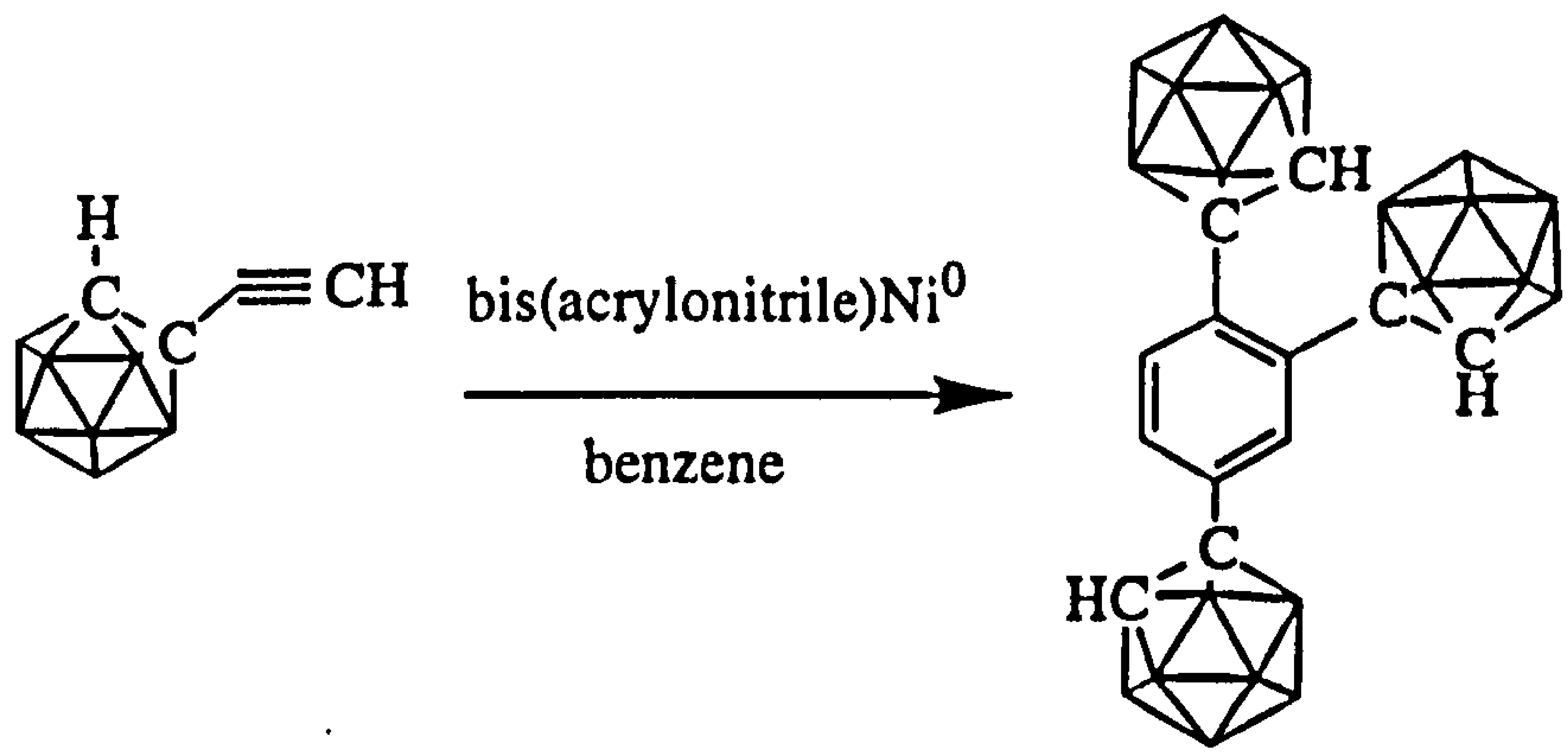

scheme 4.1: synthesis of 1,2,4-tri-carboranyl benzene

This reaction produced no 1,3,5-substituted product, the less sterically hindered isomer. However, later work yielded 1,3,5-tri-(*ortho*-carboranyl)-benzene derivatives[10,16] from the reaction between the appropriate 1,3,5-tri-(acetylenyl)-benzene and decaborane, and the 1,3,5-tri-(*meta*- and 1,3,5-tri-(*para*-carboranyl)-benzene derivatives[10] by means of copper coupling reactions.[17] These compounds give us excellent material for comparison to the current systems as they are the benzene analogues of the triazinyl species to be discussed within the scope of this chapter.

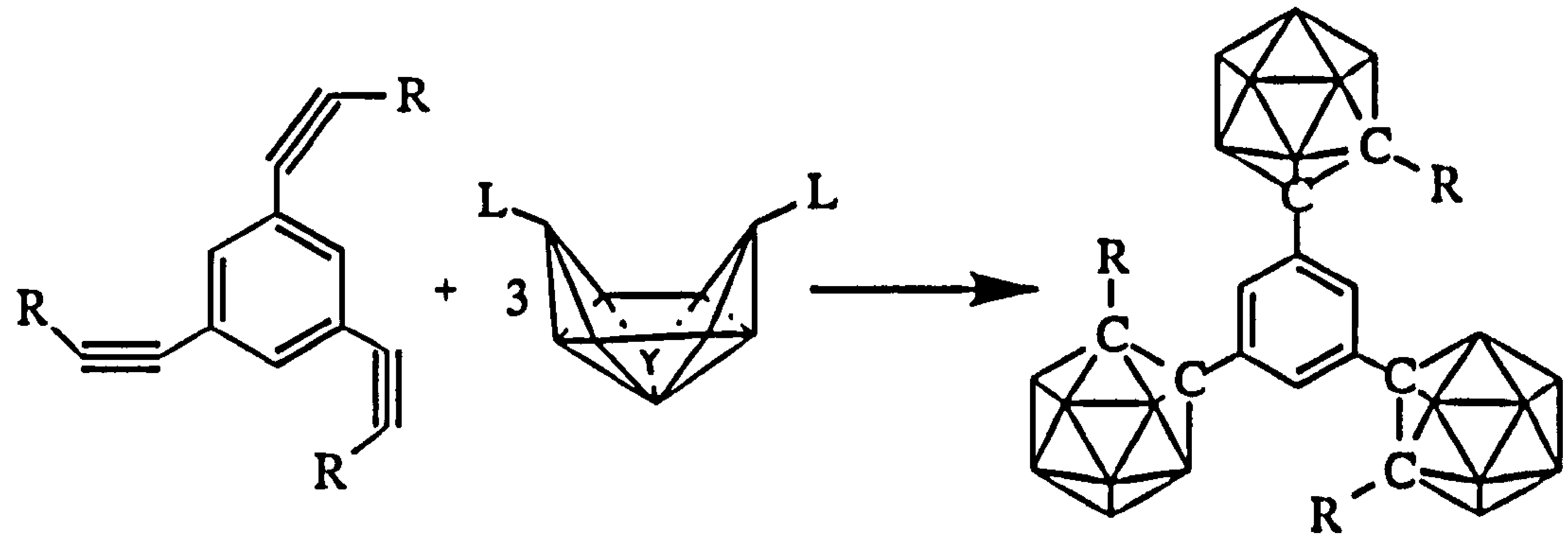

scheme 4.2: synthesis of 1,3,5-tri-(carboranyl)-benzene

The incorporation of more than one carborane cage into both organic and inorganic systems in recent years has been prevalent. Much attention has been paid to carboranyl polymers[18,19], but carboranes have also been incorporated into dendritic systems[20,21], and macrocyclic assemblies[9,10,22,23,24,25,26,27] and two to four unit linear[10,28,29] and stellated[30,31] organisations.

One example of a dendritic system is that of G.R. Newkome *et al.*[20], where an *ortho*-carboranyl moiety is incorporated into an organic dendrimer through an acetylenic functionality. By tailoring the termini of the dendritic branches the molecule's solubility can be altered to produce either a hydrophobic or, as in the case of a polysulfated dendrimer, a hydrophilic system, which is particularly unusual for a neutral carborane-containing compound. Carboranes have also been incorporated into metallodendrimers as end groups on a ruthenium-terpyridine tetranuclear complex[21] with the idea of creating a boron-rich metallo-dendrimer suitable for BNCT.

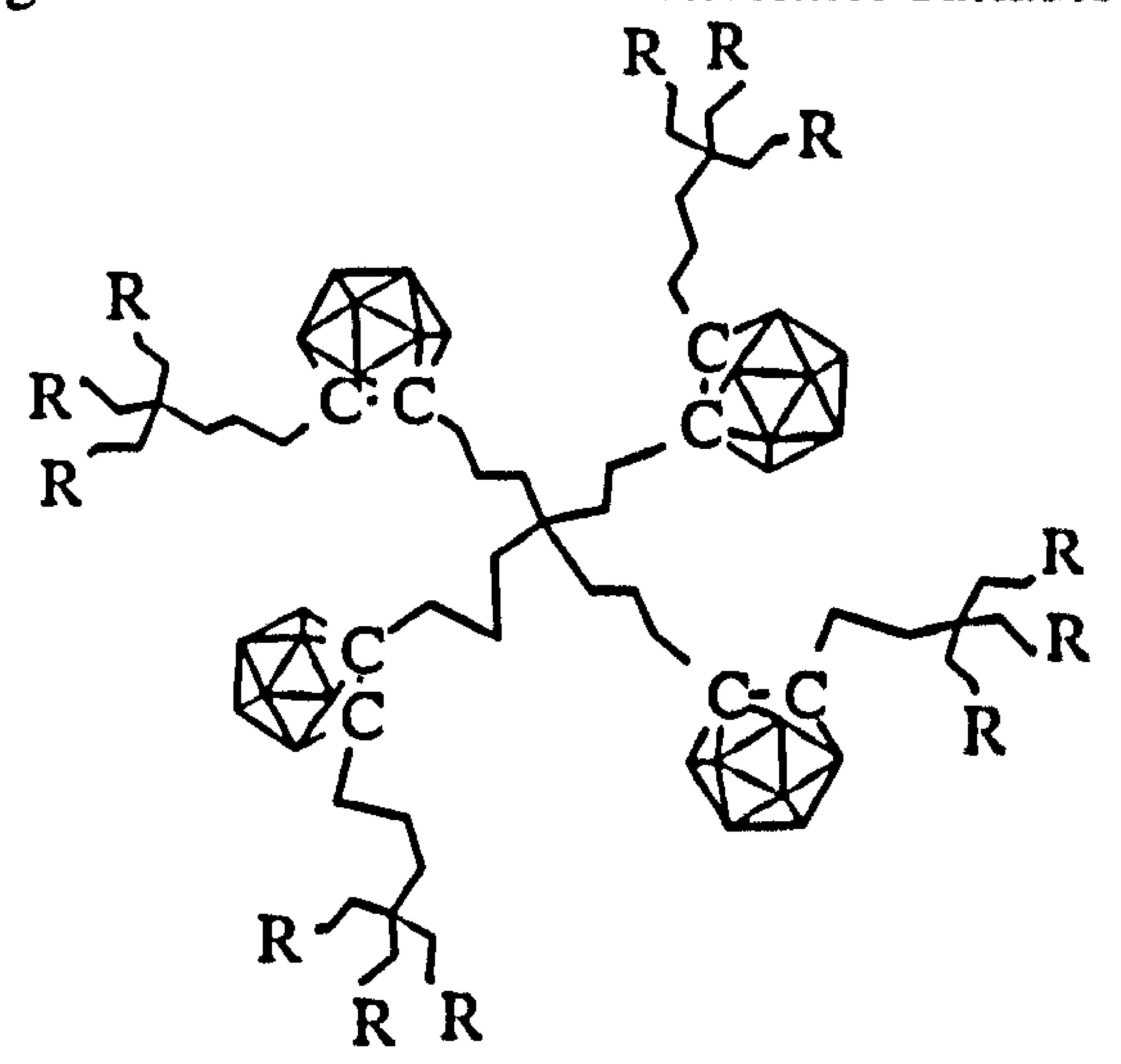

figure 4.2: carborane containing dendrimer

Cyclic and macrocyclic carboranyl assemblies have two forms. The first is where the carboranyl units, either *ortho* or *meta*, are linked by a wholly organic moiety, be it aromatic (*e.g.* benzene[9], pyridine[32]), aliphatic[24,25], or a combination of both.

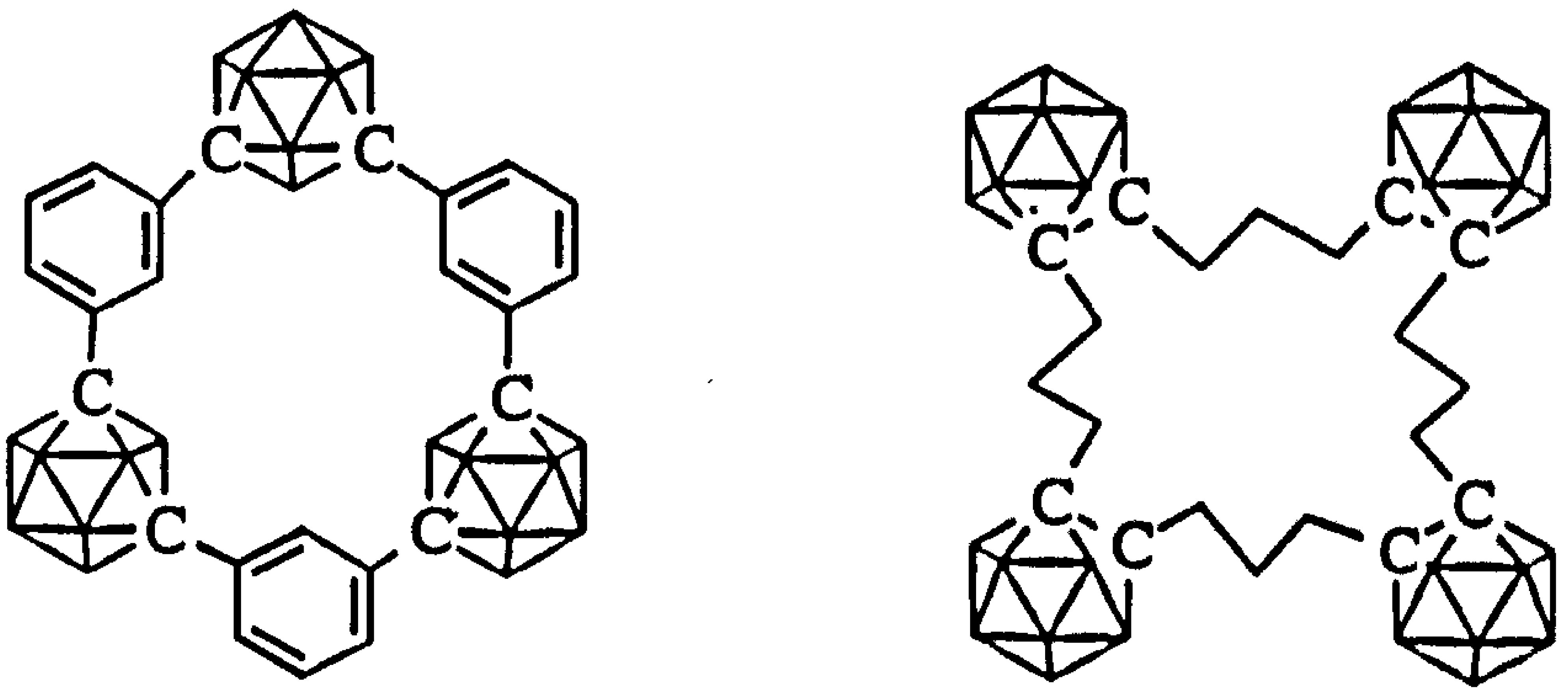

figure 4.3: carboranyl macrocycles with organic linkages

The rings reported to date contain two to four carborane units, the number of carboranes and by implication, ring size, often being determined by the geometry of the carborane, although obviously a degree of flexibility is available if the linking units are aliphatic. Other carboranacycles have inorganic linkages and include the sulfide and sulfoxide cycles[33,34] and the so called "anti-crowns", the pseudonym for the mercury-carboranyl systems developed by M.F. Hawthorne *et al.*.[22,23,27,35]

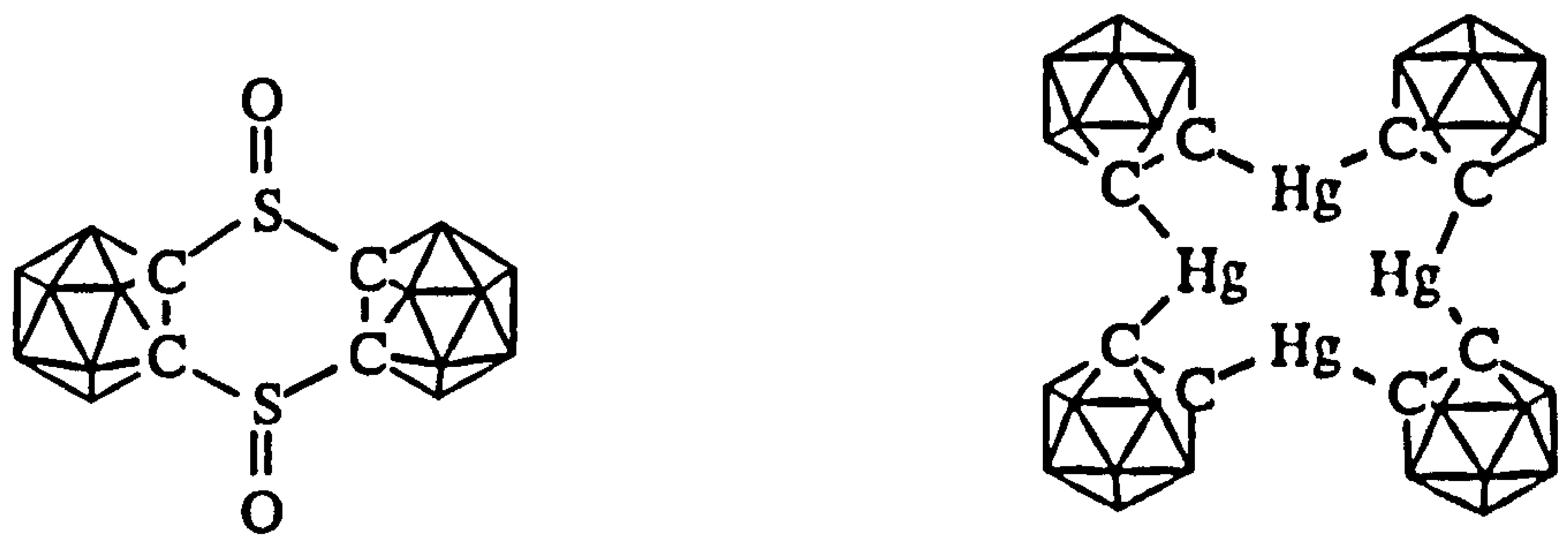

figure 4.4: carboranyl macrocycles with inorganic linkages

Three and four unit mercury-carborane assemblies have been reported and they have the ability to act as clathrates to incorporate halide ions and nucleophilic solvent molecules in the case of the three carborane ring. In the example of the macrocycle containing four mercury-linked *ortho*-carborane units, the macrocycle can play host to a *closo*-decaboranyl unit, forming a supramolecular aggregate.

No carboranyl or multi-carboranyl triazines have been reported before.

4.3 SYNTHESIS OF MULTI-CARBORANYL ASSEMBLIES

The synthetic strategies employed for multi-carboranyl assemblies are largely an extension of those described in Chapter Two. Some variations do arise however, particularly where the incorporation of a heterocycle is required, and the synthesis of such assemblies will be discussed here.

4.3.1 Synthesis Of *Bis*-Carboranes

Bis-carboranes are attainable either through reaction of a diacetylene with a decaborane adduct to give a di-*ortho*-carboranyl C-C linked *bis*-carborane[1,3] which can subsequently be isomerised to its *meta*- and *para*- isomers,[4] or alternatively through a copper coupling reaction to give *ortho*-, *meta*- and *para*- isomers directly.[5] Longer chains are also accessible by such coupling reactions.[28,29] Cages can alternatively be linked by a B-B[6] or a B-C[7] connection.

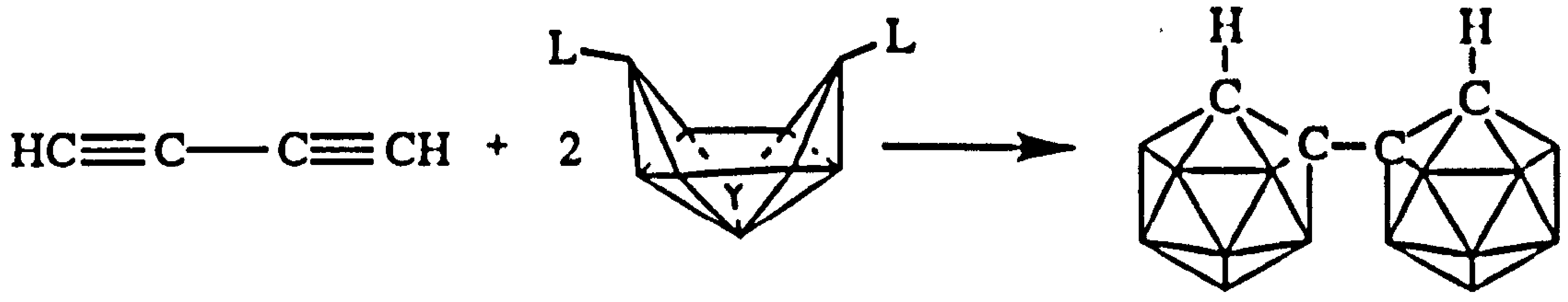

$$o, m, p\ HCB_{10}H_{10}CLi \xrightarrow{CuCl_2} {}^1/_2\ o, m, p\text{-}(HCB_{10}H_{10}C)_2$$

scheme 4.3: synthesis of bis-carboranes

Derivatisation of such compounds, for example lithiation or deboronation, can then be achieved by standard methods.

4.3.2 Synthesis Of Spaced Multicarboranyl Assemblies

Where the compound does not consist of directly-linked carborane cages, but contains carborane polyhedra linked through organic or inorganic moieties, similar strategies are applicable. For example, the tri-carboranyl benzenes, which are perhaps the closest analogues of the tricarboranyl triazines to be discussed here, are synthesised from either a tri-acetylenic benzene (*c.f.* scheme 4.2) or alternatively through a copper coupling[32] or palladium catalysed[30] reaction. The drawback of this coupling method is that a mixture of mono-, di- and tri-substituted products is always obtained. Di-substituted *ortho*-carboranyl benzenes are successfully substituted through reaction of a diacetylenic benzene to give the so-called "Z-compounds".[36]

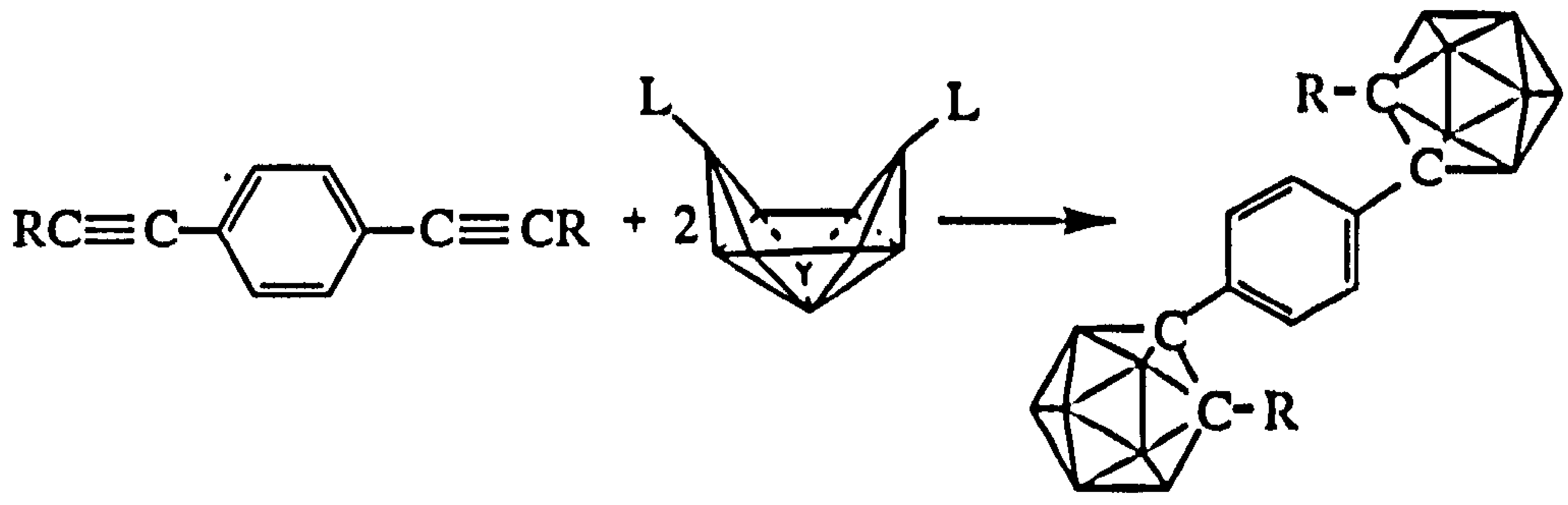

scheme 4.4: synthesis of linked di-carboranyl assemblies

Aliphatically linked multicarboranyl assemblies are synthesised from reaction of a chosen dihaloalkane, $X(CH_2)_nX$ where X=halogen, with lithio-carboranes. Such compounds can subsequently be deboronated and a metal incorporated to give dicarbollide species[8,14,34] (*cf.* figure 4.1). The coupling reaction of a metallocarborane and a dihalo-compound gives carboranyl macrocycles.[30] For polymer synthesis, linkage is achieved by a variety of means including coupling through triflic acid.[18,19]

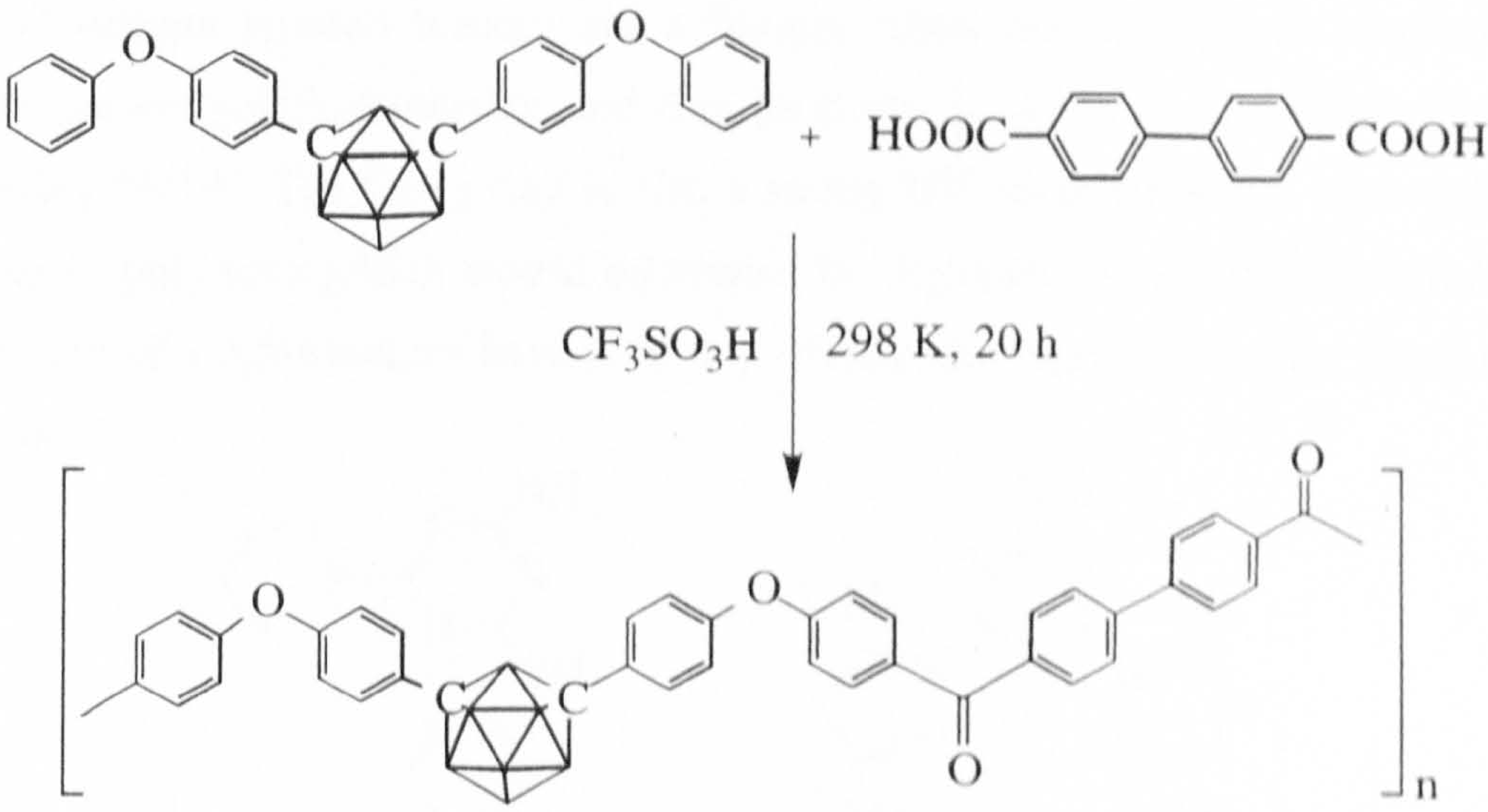

scheme 4.5: polymer synthesis via triflic acid coupling

4.4 TRIAZINES

4.4.1 Overview

Triazines have many applications, and 1,3,5-triazines are most commonly used as resins, herbicides and as constituents of dyestuffs. Certain derivatives are also explosive, whilst others are fire retardants.[37]

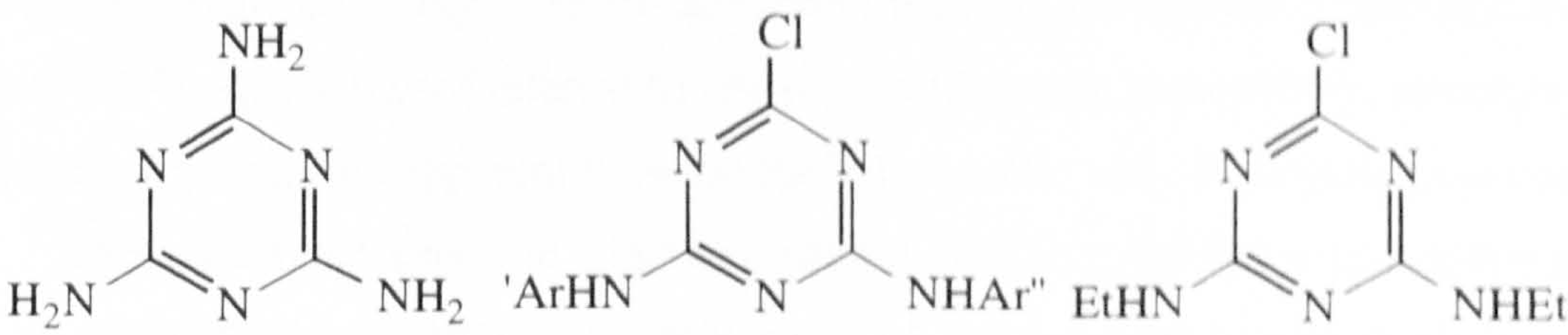

melamine (resin) — "reactive" dye — simazine (herbicide)

figure 4.5: varying applications of 1,3,5-triazine derivatives

Substituted triazines have also been shown to exhibit clathrate behaviour[38,39], forming a Piedfort-based host lattice to small molecules like 1,4-dioxane and isopropanol.

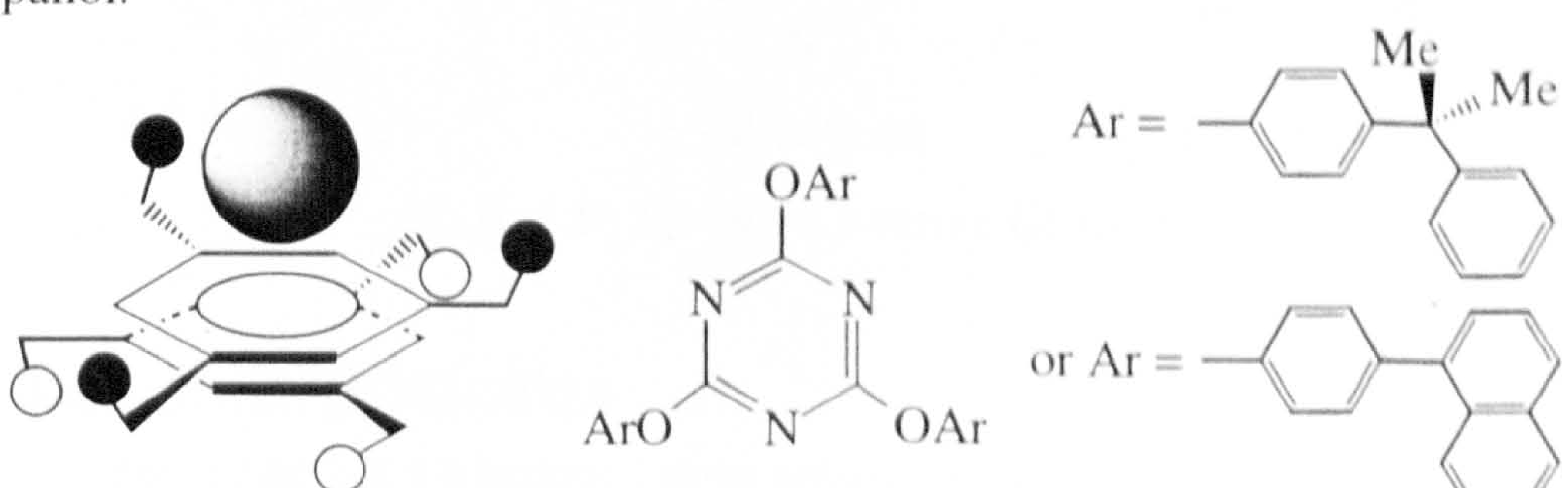

figure 4.6: Piedfort, hexahost clathrate where two tri-substituted aromatic rings (1,3,5-triazines) lie above each other and play host to a small solvent molecule.

Hydrogen bonded lattices are a feature often encountered in triazine (and nitrogen heterocyclic) chemistry and this property is useful in the field of crystal engineering.[40,41,42] The C_3N_3 ring is also a strong UV absorber and is often used as a stabiliser in polymers which would otherwise be degraded by ultraviolet radiation.[43] Another use of 1,3,5-triazines have is in terpyridine-like ligands[44] to give luminescent complexes.[45]

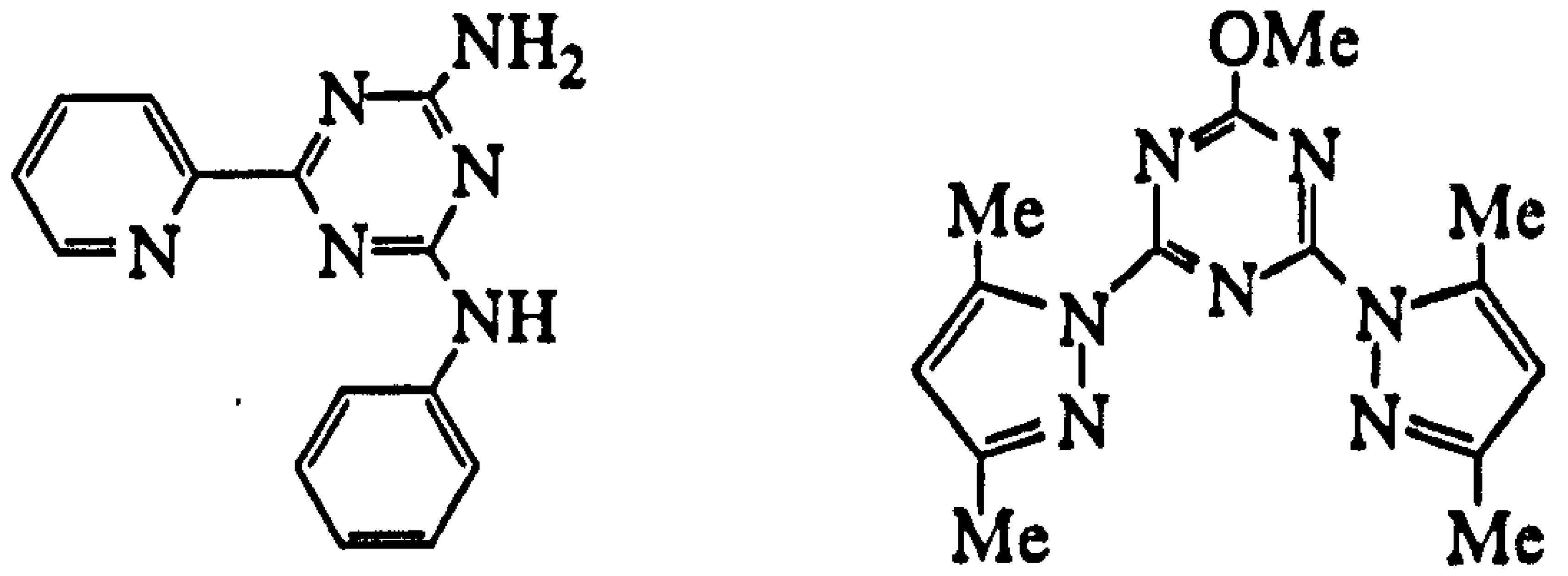

figure 4.7: triazine containing ligand systems

In common with icosahedral carboranes, 1,3,5-triazine derivatives exhibit second harmonic generation properties[46] making them suitable candidates for NLO materials and they have also found applications in charge transfer devices[47], and as catalyst supports.[48]

The principal multi-carboranyl system discussed in this chapter is the tri-carboranyl triazine assembly. The tri-carboranyl benzene systems have been previously studied[10,16,30], and it was of interest to see what differences in reactivity, structure and electronic properties are apparent between the heterocyclic and carbocyclic assemblies.

There are three possible triazine systems available, however considering the bulk of the carborane unit and as analogues of the 1,3,5-tri-(carboranyl)-benzene system are sought, the 1,3,5-triazine isomer was chosen as the most suitable. Of the three isomers it is also the most readily available, the most readily derivatised and, once derivatised, the most stable.[37]

figure 4.8: the three triazine isomers

4.4.2 Triazine Derivatisation

The family of 1,3,5-triazines, often referred to as *s*-triazines, can be synthesised by a variety of methods depending on what moieties are required in the ultimate triazine. For our purposes we have an ideal starting material in 2,4,6-trichloro-1,3,5-triazine, cyanuric chloride.

a) Symmetrically Substituted Triazines

Cyanuric chloride, $C_3N_3Cl_3$, is an obvious and convenient starting material from which to begin the derivatisation of the triazine ring. It is relatively inexpensive, and the chlorines can be substituted without too much difficulty, due to the activation of the carbons by the adjacent nitrogens. This activation is observed for all six-member ringed nitrogen heterocycles as all the carbons at positions *ortho-* and/or *para-* to the nitrogen atom are activated. This activation is attributed to a lowering of the energies in the π-orbitals that form the heterocycle, the energy decreasing by a larger amount as more nitrogens are incorporated into the six-membered ring. This makes nucleophilic attack on the carbons increasingly easier. Cyanuric chloride therefore readily loses its chlorine substituents, by way of nucleophilic substitution, to another substituent that may or may not help to stabilise the aromatic C_3N_3 ring, and the final triazine formed is dependent upon the nature of the introduced substituent.

Where the proposed substituent, R, is electron donating, mono substitution is favoured as electron density is pushed into the ring, stabilising the aromatic system and subsequently reducing the ability of the other chlorines to react further. If, on the other hand, R is electron withdrawing, the reverse is true and trisubstitution is favoured.

In summary:

- If R= electron donating,
  - mono-substitution = easy
  - di-substitution = possible
  - tri-substitution = difficult

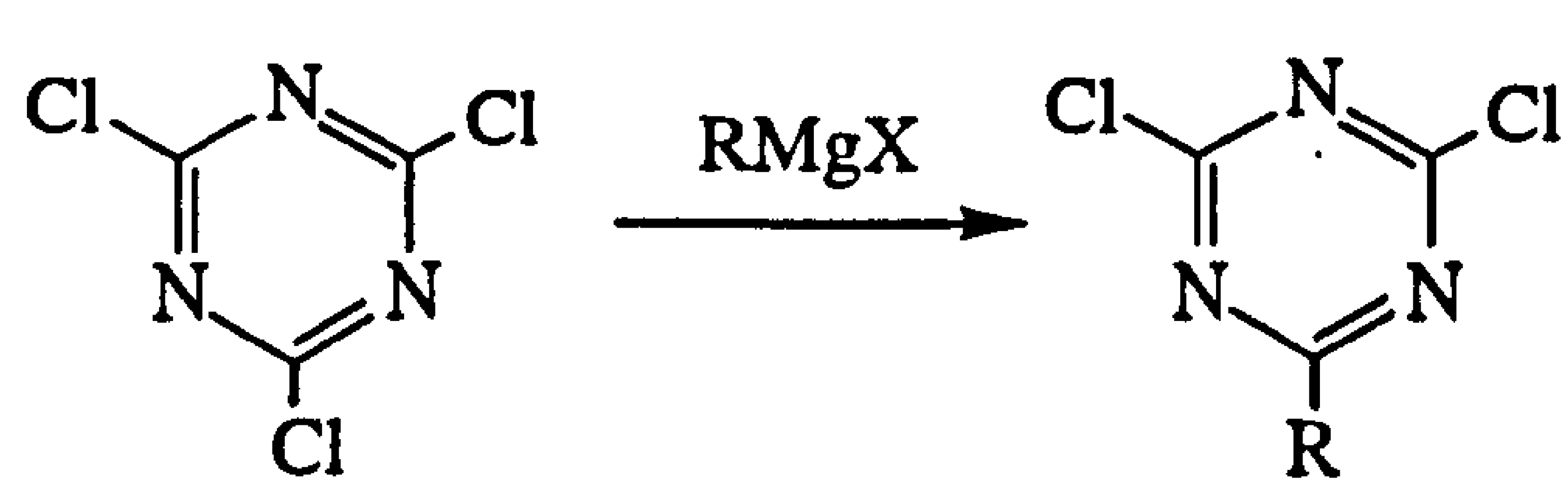

- If R= electron withdrawing,
  - mono-substitution = difficult
  - di-substitution = possible
  - tri-substitution = easy

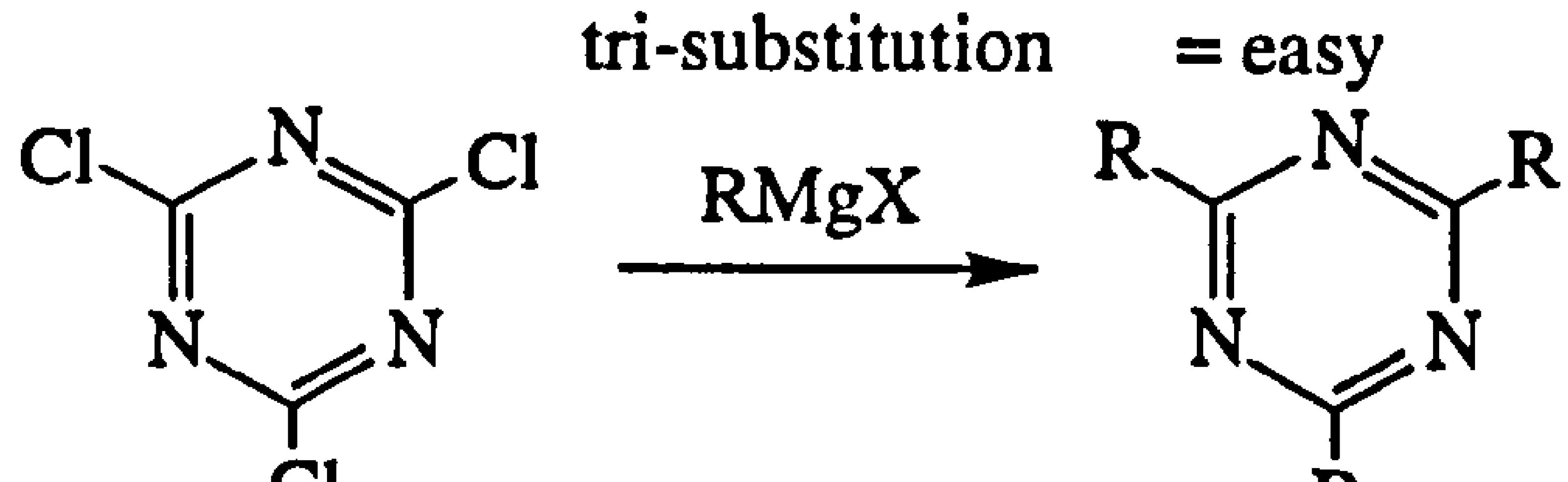

scheme 4.6: reaction summary of triazine reactivity

Disubstitution by comparison is difficult, although not impossible, to achieve from cyanuric chloride. The remaining chlorine can readily be substituted, and is obviously very susceptible to attack. If a disubstituted triazine is required, an alternative synthetic strategy is to build the triazine ring from its various constituent parts and this will be discussed in b). Alternatively, one of the chlorines can be substituted by an electron donating group, followed by the facile substitution of two electron withdrawing functions to give $RR'_2C_3N_3$.

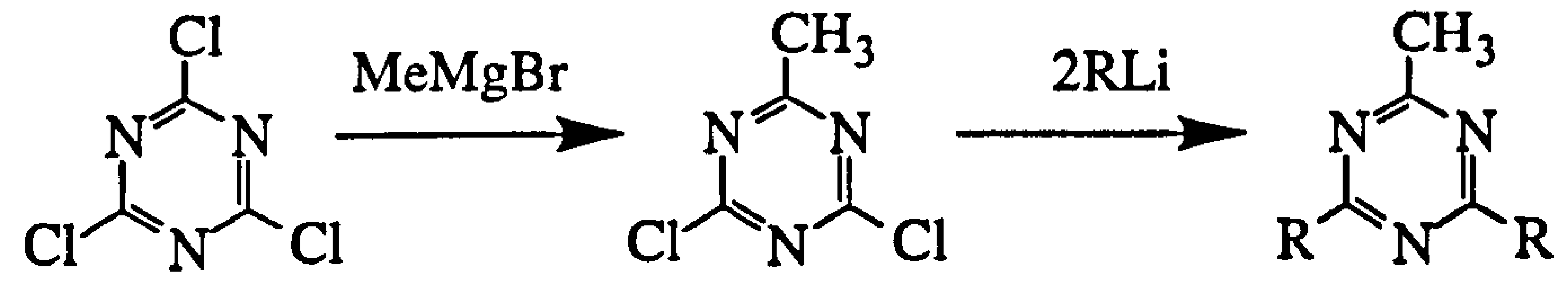

scheme 4.7: synthesis of a vari-substituted triazine

b) Assembly Of Vari-Substituted Triazines

Cyanuric chloride is an ideal starting point for tri-substituted 1,3,5-triazines with equal substituents, particularly when R is electron withdrawing. However, in order to synthesise mono- or di-functionalised triazines with either reactive sites for further substitution, or already usefully functionalised remaining carbons, the triazine needs to built, and there are various ways in which this can be done.

Unsubstituted positions can be created, before further reaction, by reduction using for example, $LiAlH_4$ to remove unwanted chlorines.[49]

Dialkyl triazines can be synthesised from cyanuric chloride, leaving one reactive chlorine free for further reaction. These dialkyl triazines are prepared from reaction of cyanuric chloride with the appropriate alkyl Grignard reagent.[50] The products, however, are of varying stability and the formation of desired product is often solvent and temperature dependent.

An alternative strategy to a vari-substituted triazine is to incorporate the desired substituent into a functionality which can be cyclised to give the triazine. For example, in the following reaction scheme[51] the ring is formed from acylamidines and amidines or guanidines (i). Alternatives include the reactions studied by E. Degner *et al* .[52,53] which involve the ring closure reactions of *N*-(*alpha*-chloroalkylidene)-carbamoyl chlorides (ii) or polychloroaza-alkenes (iii). Similar work[54] using *N*-aroylimidates and amidines (acetamimidine, benzamidine and guanidine) also yielded vari-substituted *s*-triazines (iv).

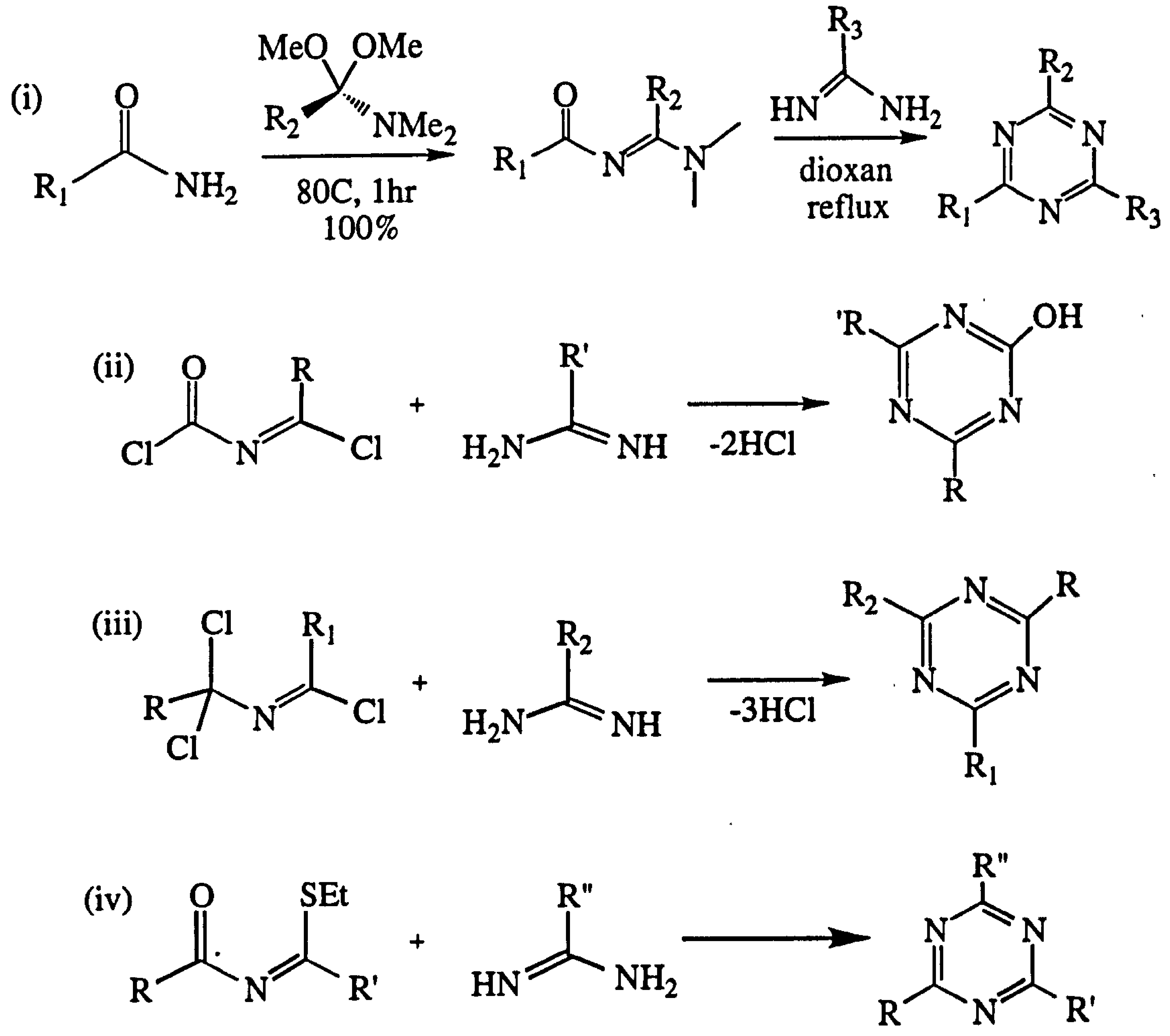

scheme 4.8: assembly of vari-substituted 1,3,5-triazines

The preparation of any carborane derivative fitting into the above type of compound, however, would be extremely complex and labour intensive so the value of attempting any such synthesis must be assessed first.

4.5 RESULTS AND DISCUSSION

4.5.1 Synthesis

a) *Bis*-carborane

Bis-carborane was synthesised, following literature methods[1,3], from the reaction of diacetylene gas and decaborane-acetonitrile adduct. The carbon-attached protons of the *bis*-carborane are still sufficiently acidic[11] to allow their lithiation by agents such as butyl lithium. From here, reaction with a suitable halo-derivative is known to give derivatised *bis*-carboranes[11] and following this methodology, the synthesis of methylene bridged-*bis*-carborane was attempted.

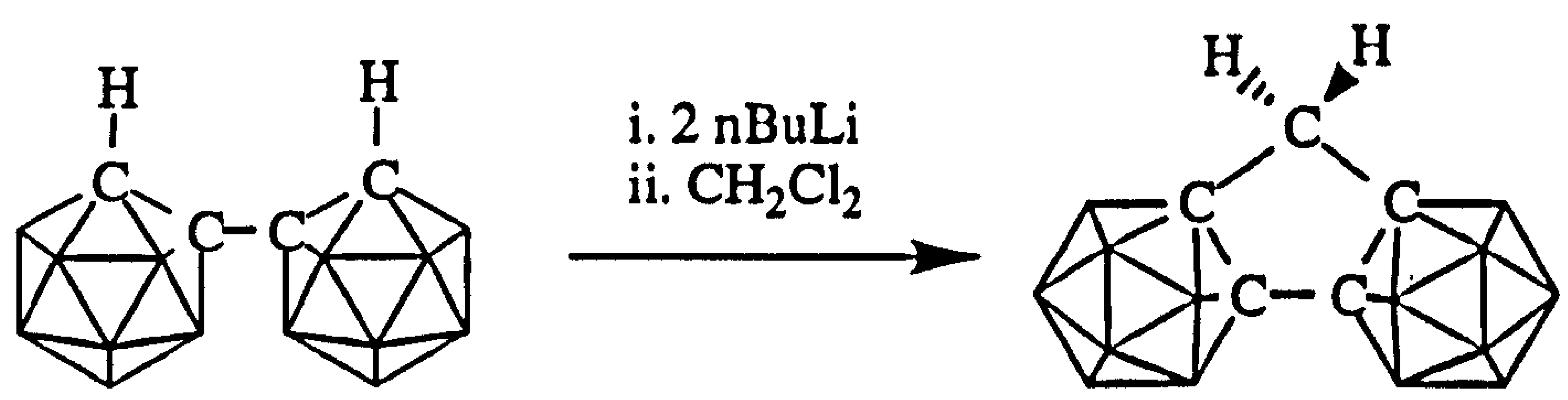

scheme 4.9: proposed synthesis of methylene-bridged-bis-ortho-carborane

The synthesis of such a compound was envisaged to provide, once deprotonated, a carboranyl fluorene analogue, with ligand potential.

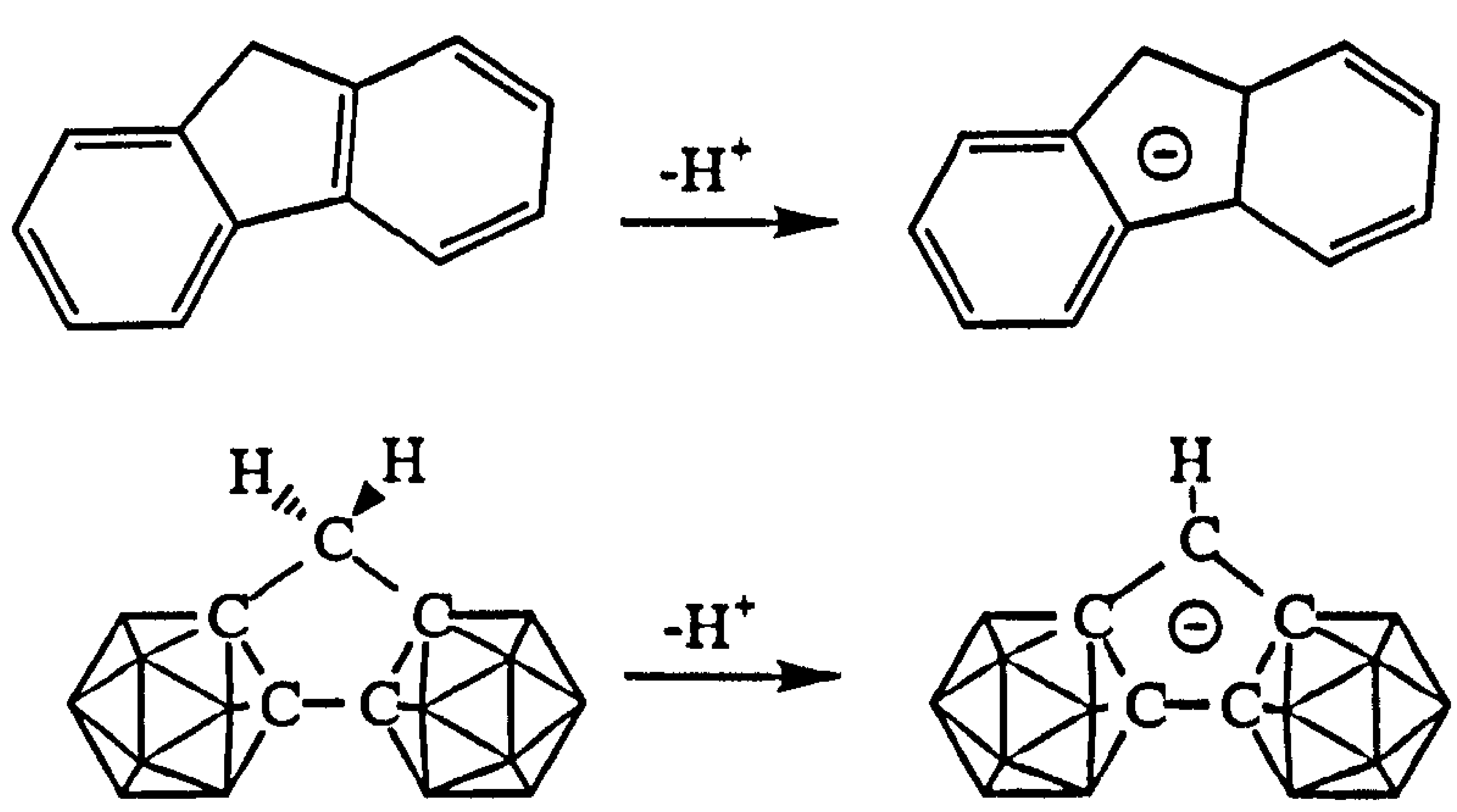

scheme 4.10: similarities between deprotonated fluorene and methylene bridged bis-carborane species

The reaction was conducted on a small scale, and mass spectroscopy showed a variety of products were obtained from the reaction of the above two compounds (figure 4.9). An alternative explanation for the mass ion peaks is fragmentation of a large multi-carborane assembly. This is not entirely unexpected, with linear combinations of molecules being formed preferentially over the strained *pseudo*-fluorene compound.

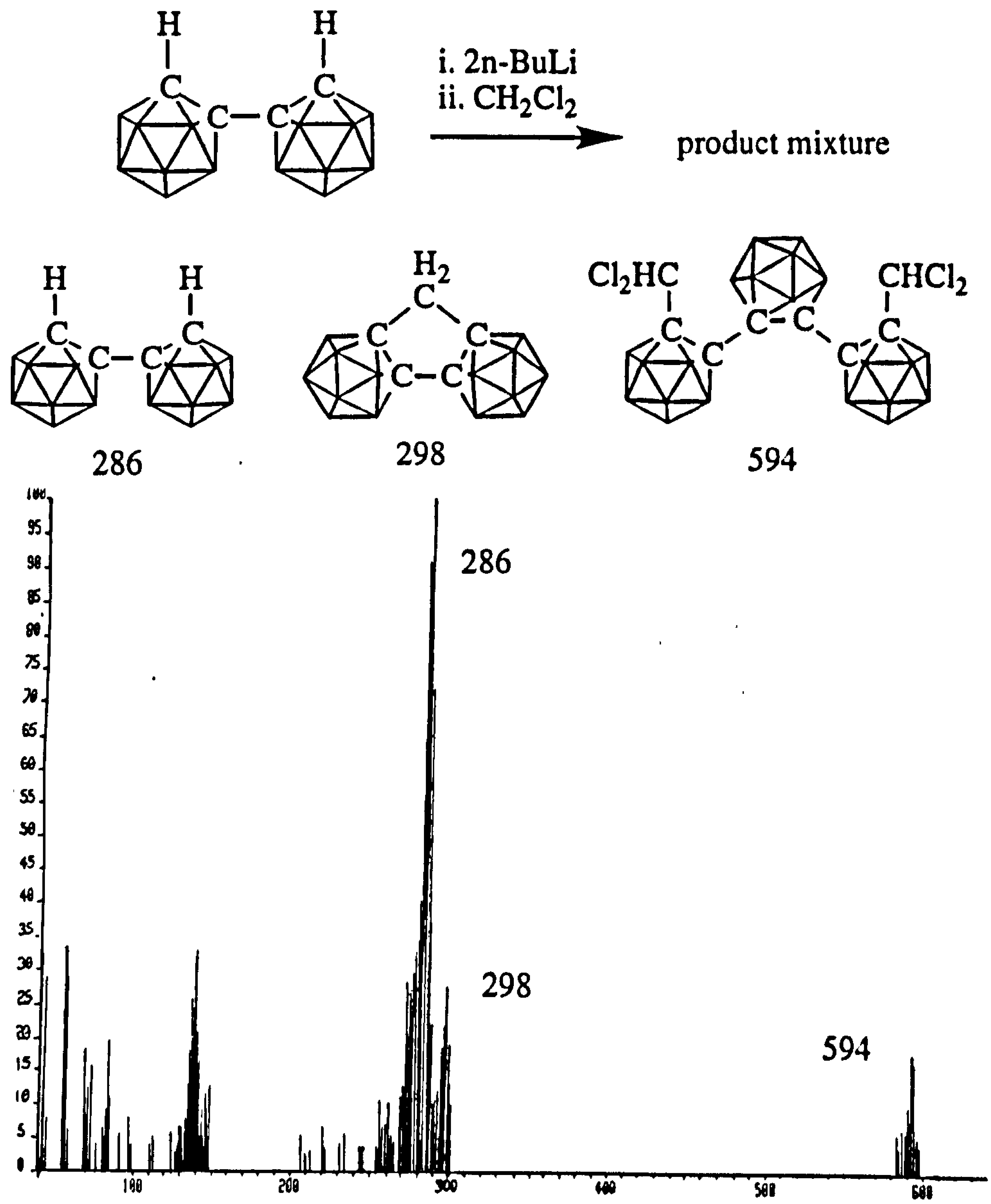

figure 4.9: proposed reaction products of the reaction between dilithio-bis-ortho-carborane and dichloromethane

b) Multi-carboranyl Triazines

The synthesis of tri-carboranyl benzenes has been discussed in the introduction to this chapter, however, in changing the chemistry of the central moiety from a carbocycle to a heterocycle, the synthetic strategies to such multi-carboranyl systems must be reviewed.

As has been highlighted earlier (4.4.2), substitution of 1,3,5-triazines is very much dependent on the nature of the introduced substitutent, with tri-substitution being favoured by electron withdrawing moieties. Carboranes are strongly electron-withdrawing groups, with *ortho*-carborane having the greatest electron withdrawing potential, followed by *meta*- and finally *para*-. Generally, the substitution of cyanuric chloride by R groups can be slowed to control or tailor the degree of substitution, to give for example, a mono-substituted product. However, where the R functionality is a carborane, tri-substituted triazine was found to be the unique multi-carboranyl product in the reaction between lithio-carborane and cyanuric chloride. This was independent of ratio of reagents, solvent, temperature, reaction time and whether the lithio-carborane was added to the cyanuric chloride or *vice versa*. Reaction was immediate, even when the reaction was conducted at -78°C. Although *para*-carborane is significantly less electron withdrawing than *ortho*-carborane, for all three isomers, either substituted or containing a carboranyl C-H functionality, trisubstituted triazine was the only new carboranyl product.

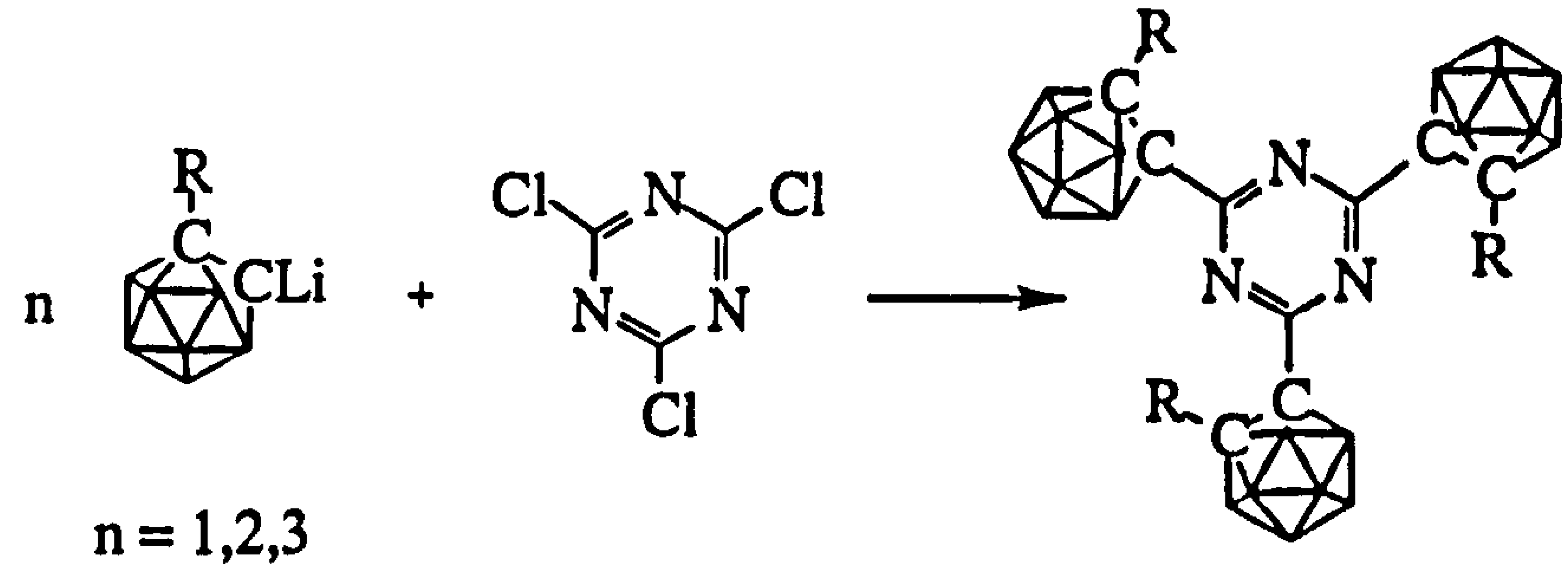

scheme 4.11: reaction of cyanuric chloride with lithio-carborane

Any unreacted carborane was recovered unchanged, generally by sublimation, and unreacted cyanuric chloride was converted into cyanuric acid, which is in equilibrium with its keto tautomer, in the aqueous work-up.[55]

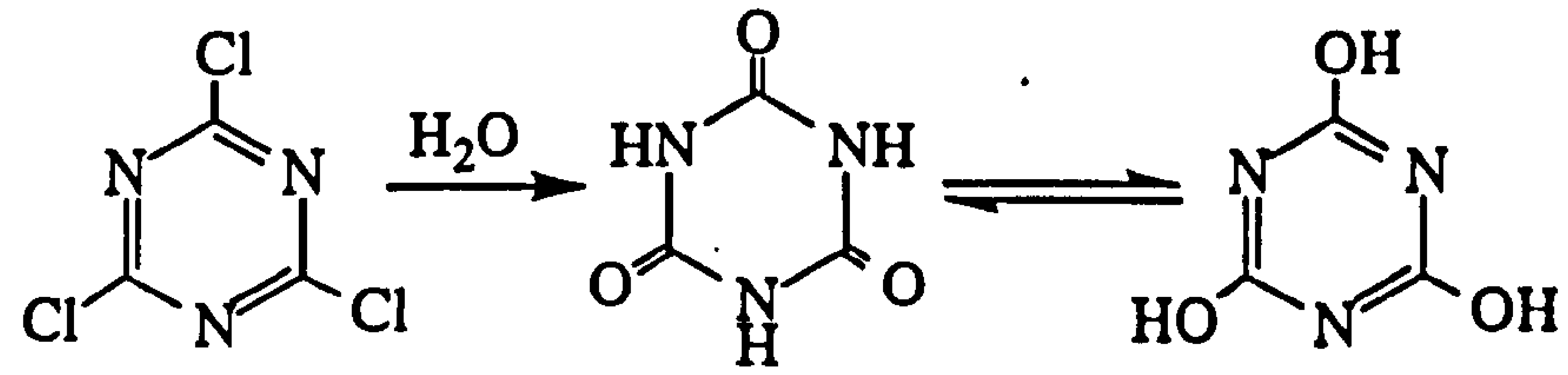

scheme 4.12: hydrolysis of cyanuric chloride to cyanuric acid

carborane	Cb:$C_3N_3Cl_3$	solvent	temperature	product	yield
o-HCbH	3:1	DME	0°C	tris	35%
o-HCbH	3:1	THF	0°C	tris	14%
o-MeCbH	3:1	DME	0°C	tris	19%
o-PhCbH	3:1	DME	0°C	tris	68%
o-PhCbH	2:1	DME	0°C	tris	16%
o-PhCbH	2:1	DME	r.t.	tris	35%
o-PhCbH	1:1	DME	0°C	tris	16%
o-PhCbH	1:1	DME	-78°C	tris	35%
m-Cb	2:1	DME	0°C	tris	47%
m-Cb	1:1	DME	0°C	tris	40%
m-PhCbH	3:1	DME	0°C	tris	60%
p-HCbH	3:1	DME	0°C	tris	70%
p-HCbH	2:1	DME	0°C	tris	87%
p-HCbH	1:1	DME	0°C	tris	98%
p-DCbD	3:1	DME	0°C	tris	95%
p-PhCbH	3:1	DME	0°C	tris	50%
p-PhCbH	5:1	DME	0°C	tris	58%
p-(4-BrPh)CbH	3:1	DME	r.t.	tris	40%

table 4.1: reaction details of the syntheses of tricarboranyl triazines

Solid State NMR spectroscopy has been an invaluable technique in the characterisation of products from the reactions between lithio-*meta*- and lithio-*para*-carborane and cyanuric chloride where the reactants were in the ratios 1:1, 2:1 and 3:1. When it was suspected that trisubstituted triazine was the unique carboranyl product, NMR studies (^{11}B, ^{13}C, ^{1}H) on these insoluble products provided evidence that this was indeed the case. Solid state nitrogen NMR spectroscopy was also attempted, but the lack of crystallinity in the samples, and the low concentration of nitrogen in the samples meant a small signal to noise ratio. If mono- and di-substituted carboranes were formed, more than one nitrogen environment would be present, but only one signal was detected in each instance tried, showing only one carboranyl-triazine product to be formed.

Conversely, when an excess (2 times) of cyanuric chloride was added to dilithio-*ortho*-, *meta*- or *para*-carborane, an insoluble pale yellow solid of undetermined composition resulted in each instance. 1,7-Di-(triazinyl)-*meta*-carborane was identified (solid state NMR) from the reaction of 2:1 $C_3N_3Cl_3$:*m*-LiCbLi. Where the proposed product was a di-triazinyl-carborane with four reactive chlorines for further substitution, in light of the above results, it is envisaged that a large triazine/carborane network was produced. Each carborane has two potential points of substitution, and each cyanuric chloride molecule, three. If the correct quantities of each reagent were combined (3:2 dilithio-carborane:cyanuric chloride), under the right reaction conditions, an interlocking sheet could perhaps be formed.

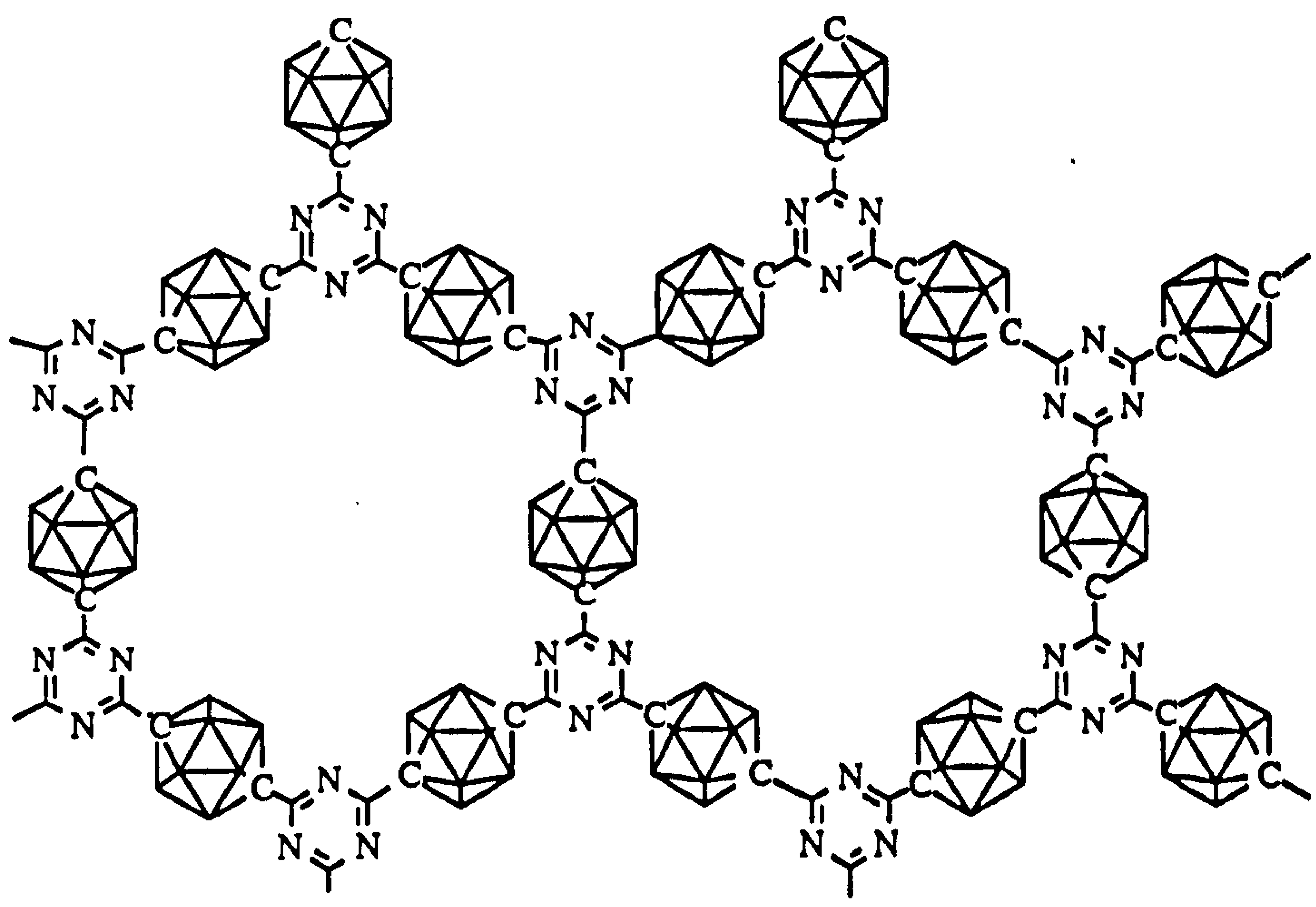

scheme 4.13: formation of a triazine-carborane network

c) Vari-Substituted Triazines

In organic systems, vari-substituted triazines can generally be synthesised with relative ease. However, given the extreme electron withdrawing potential of the carboranes, reaction conditions cannot simply be tailored to give mono- and di-carboranyl triazines, as illustrated above. To produce such a compound, the triazine must be derivatised before reaction with carborane.

Electron donating groups stabilise the C_3N_3 ring and substitution stops, under normal conditions, once one chlorine has been eliminated. From this, the remaining chlorines would be expected to be relatively unreactive and perhaps allow one carborane to be substituted and the second chlorine to be left unreacted. However, substitution of only one of these chlorines by a carborane, to give a product of the sort 2-R-4-($R'C_2B_{10}H_{10}$)-6-Cl-1,3,5-triazine, proved impossible, as the activating power of the carborane overthrew the deactivating power of the R group and both chlorines were easily substituted in the presence of lithio-carborane. Compounds of type 2-R-4,6-di-

(R'-carboranyl)-1,3,5-triazine were achieved *via* this comparatively facile synthesis, although yields were poor compared to those of tri-carboranyl triazines.

For example:

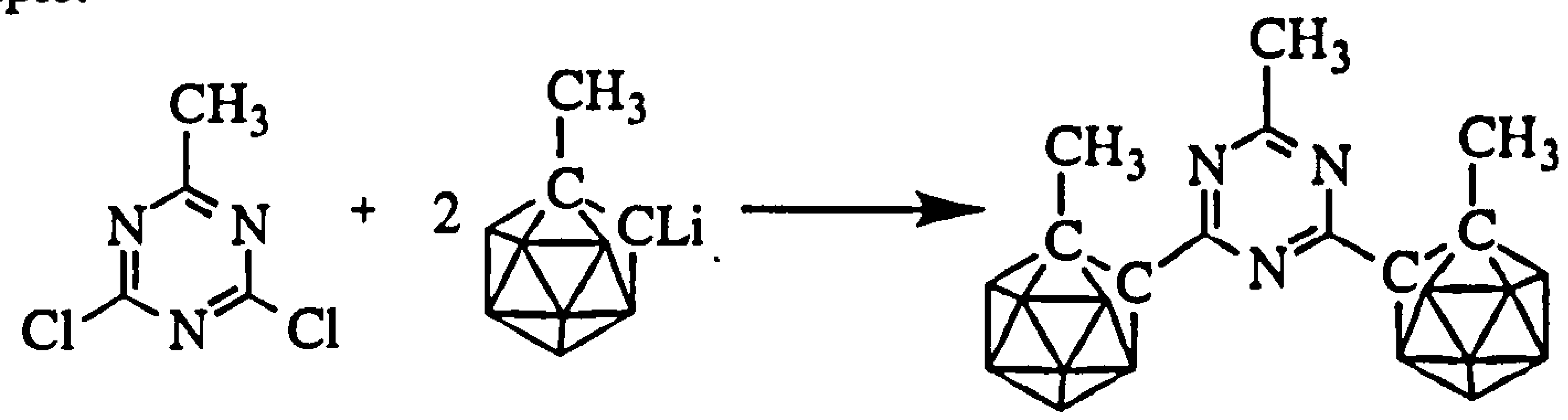

scheme 4.14: synthesis of di-carboranyl triazine derivatives

Dicarboranyl-triazines synthesised in this study were 2-methyl-4,6-di-(2'-methyl-*ortho*-carboranyl)-1,3,5-triazine and 2-methyl-4,6-di-(2'-phenyl-*ortho*-carboranyl)-1,3,5-triazine.

Although the focus of this chapter is multi-carboranyl assemblies, it was of interest to see if a mono-carboranyl triazine could be made. Using the strategy of previously substituting the triazine, the synthesis of 2,4-diethyl-6-chloro-1,3,5-triazine was attempted, with the aim of creating a dialkyl-mono-carboranyl triazine. A mixture of triazines bearing one, two and three ethyl groups was produced which were separated by fractional distillation. The yield of dialkyl product was low (31%) however, and the product decomposed with ease. Further reactions of this sort were not attempted.

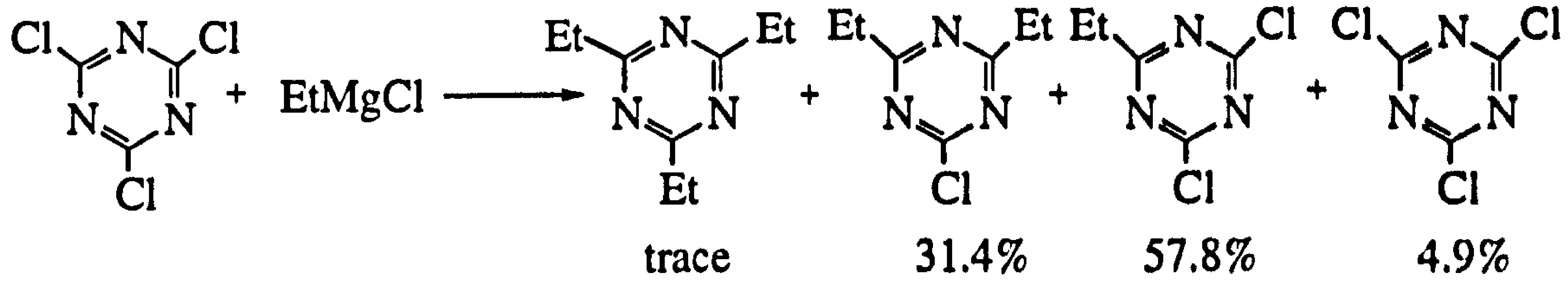

scheme 4.15: synthesis of dialkyl triazines from cyanuric chloride

An alternative method to produce mono-carboranyl-substituted di-chloro-triazines would be to first synthesise a triazinyl acetylene. Such an acetylene is attainable from the reaction between cyanuric chloride and an acetylenic Grignard reagent.[56] The unsubstituted chlorines of the triazine are, as might be expected, moisture sensitive.

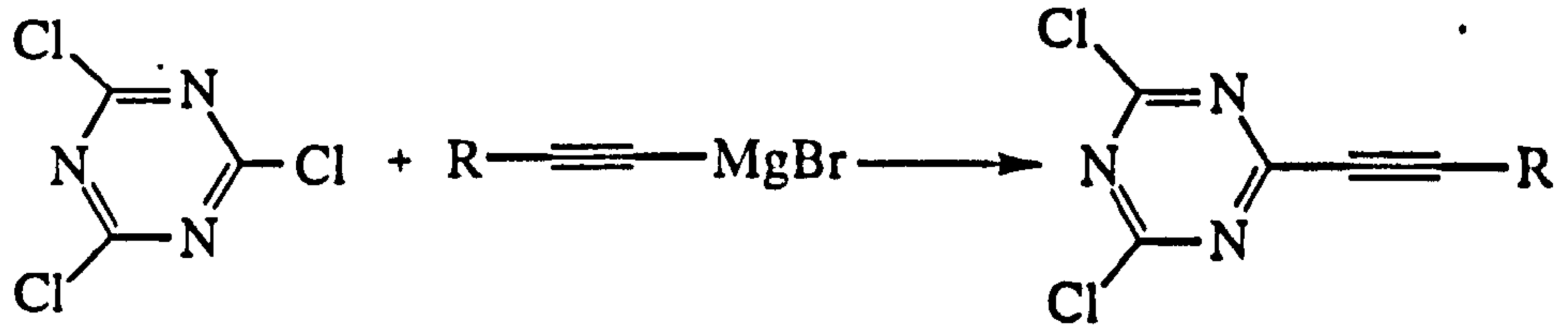

scheme 4.16: synthesis of triazine acetylenes

This could then be reacted with a decaborane adduct in much the same way as derivatised aryl-acetylenes react, to form the appropriate *ortho*-carboranyl derivative (*cf.* Chapter Two). The disadvantage of this route, however, is that it has no application for the direct synthesis of *meta*- or *para*-carboranyl analogues.

The 1-phenyl-2-(3,5-dichloro-2,4,6-triazinyl)-acetylene, synthesised in 35% yield following the above reaction scheme (R=Ph), was reacted with decaborane to give a mixture of *closo*-carboranes. The three products obtained were the 1-(3',5'-dichloro-, 1-(3'-chloro-5'-hydroxy, and 1-(3',5'-di-(hydroxy)-2',4',6'-triazinyl)-2-phenyl-*ortho*-carborane. The hydroxy products were presumably formed as a result of hydrolysis occurring during column chromatography purification on silica.

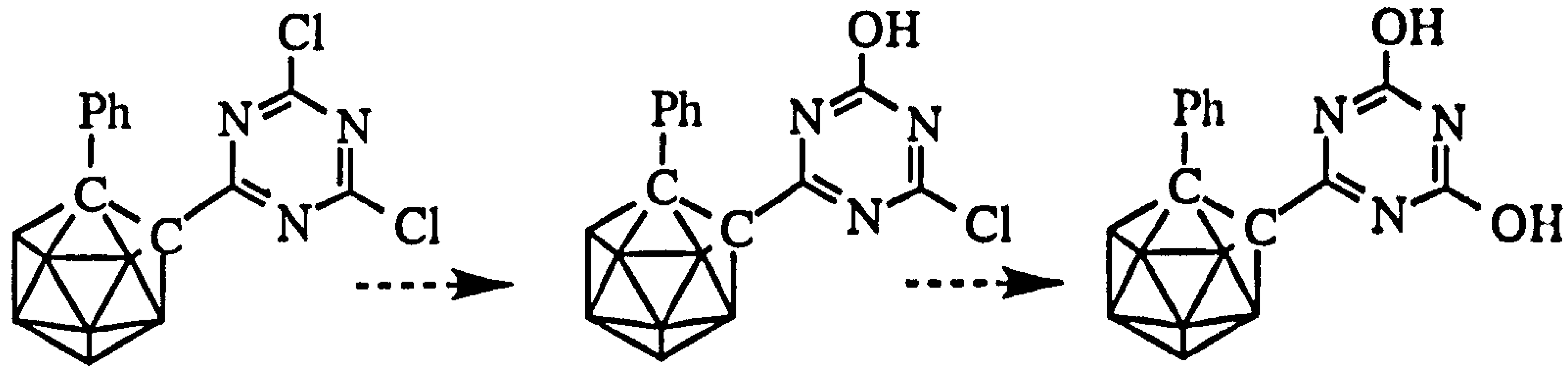

scheme 4.17: hydrolysis of triazine chlorines in a one-cage system

<u>d) Derivatisation of carboranyl triazines</u>

It was of interest to see if, once substituted onto the triazine, the carborane units could be further derivatised. Substitution of a silyl group onto the second carboranyl carbon of tri-*para*-carboranyl benzene has been achieved when the tri-carboranyl benzene was refluxed with *tert*-butyl lithium then reacted with a silyl chloride.[30] Although no attempts at lithiation with *tert*-butyl lithium were made in this current study, n-butyl lithium was found not to lithiate the second carboranyl carbon of tri-*para*-carboranyl triazine at reduced temperatures, ambient temperature or on prolonged refluxing. For this reason no further substitution was observed when the carboranyl and BuLi mixture was reacted with methyl iodide, 1-iodobutane or benzenesulfonyl chloride. As will be discussed in section 4.5.2, carboranyl triazines which have a carboranyl CH functionality are not very soluble, which was undoubtedly a factor which hindered further substitution.

To incorporate functionality into the carboranyl triazine, the carborane must be appropriately substituted before further reaction with cyanuric chloride. As well as 1-phenyl-*ortho*-, *meta*- and *para*-carboranes, and 1-methyl-*ortho*-carborane whose syntheses were described in Chapter Two, 4'-bromophenyl-*para*-carborane was also prepared and reacted successfully with cyanuric chloride.

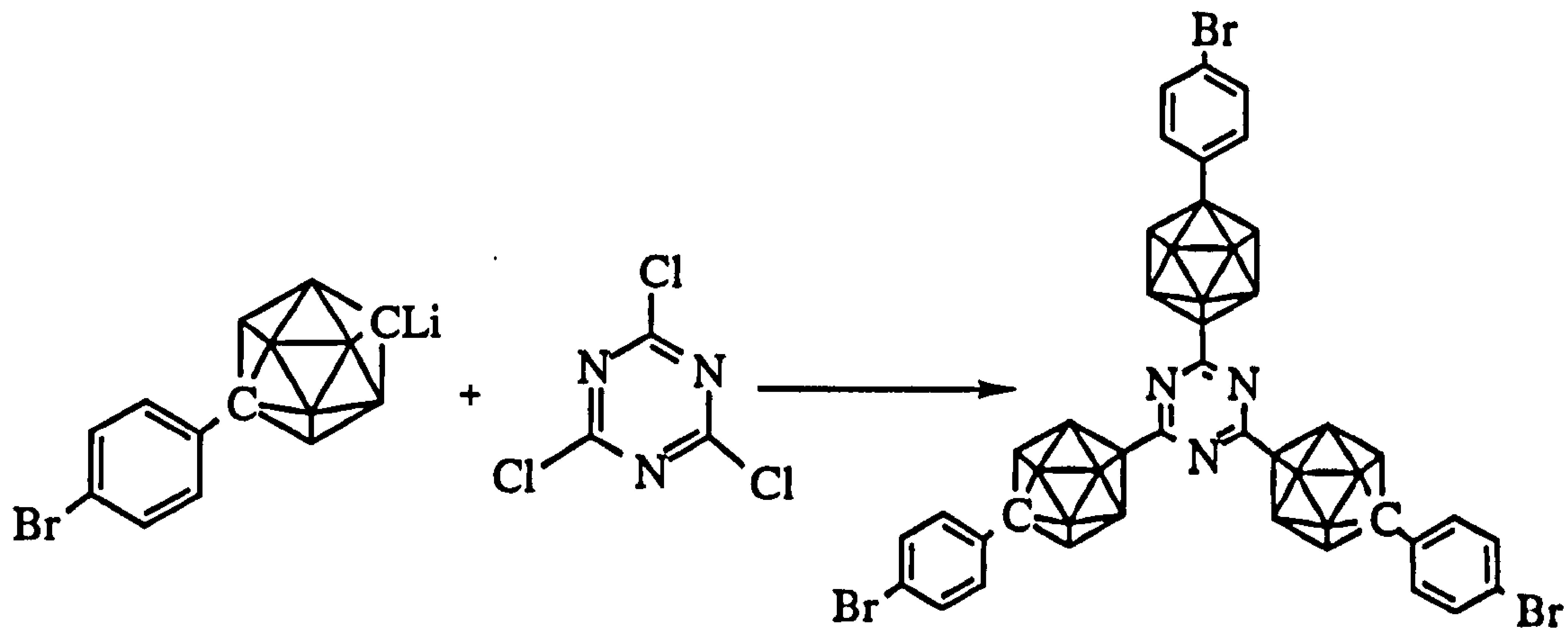

scheme 4.18: synthesis of a functionalised tri-carboranyl-triazine

This particular derivative illustrates that functionality can be incorporated into the carboranyl triazine system. Suitably derivatised, compounds of this nature could be coupled, leading to dendritic molecules.

4.5.2 Solubility And Hydrogen Bonding

It has been discovered that any 2,4,6-trisubstitued-1,3,5-triazine bearing a *meta*- or *para*-carboranyl unit where the second carboranyl C was protonated, was insoluble in common organic solvents. One possible explanation for this could be the existence of *inter*molecular N···H interactions, namely between the carboranyl C-*H*, and the triazinyl *N*, in a supramolecular hydrogen bonded architecture.

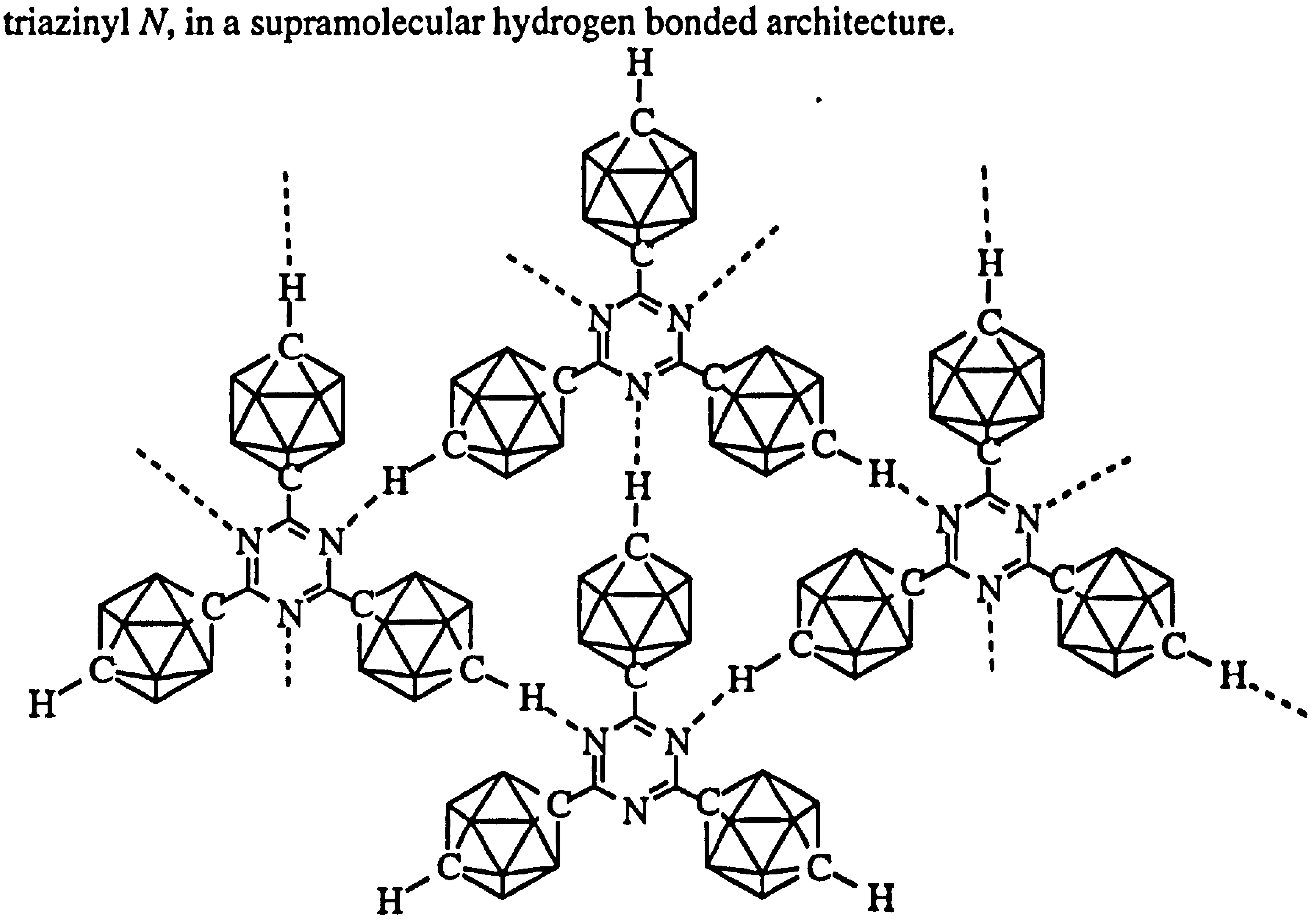

figure 4.10: Proposed hydrogen bonded sheet arrangement of 2,4,6-tri-(para-carboranyl)-1,3,5-triazine showing intermolecular N···H interactions

This insolubility was also observed in acidic and basic medium, except for the sole example of tetrabutyl ammonium fluoride solution. Solubility of the compound in F^- solution is explained through the formation of the F^- adduct of the compound, which would effectively remove the possibility of N···H intermolecular interactions.

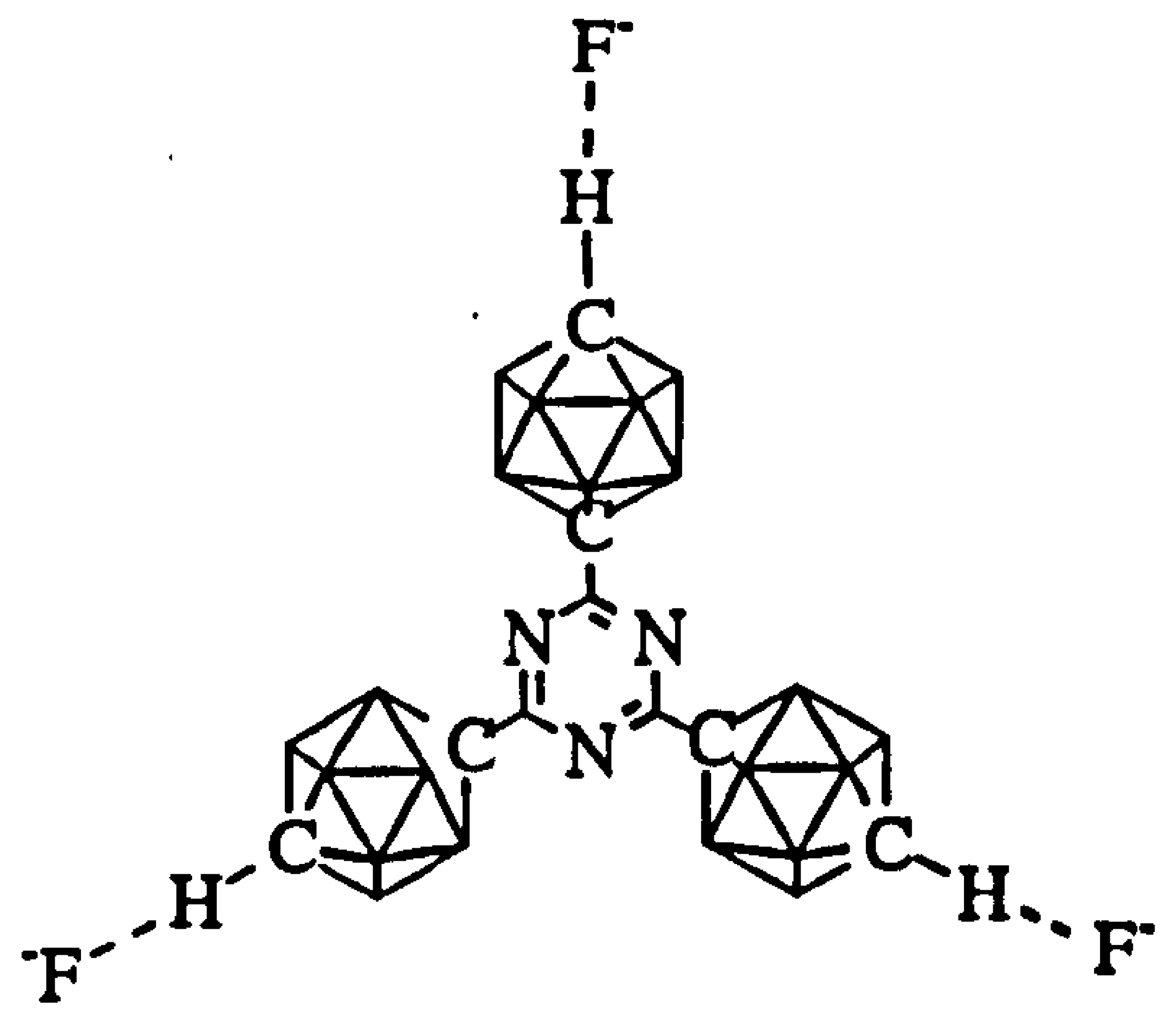

figure 4.11: soluble F^- adduct of 2,4,6-tri-(para-carboranyl)-1,3,5-triazine

To further investigate this hypothesis of intermolecular hydrogen bonding, the 2,4,6-tri-(d-*para*-carboranyl)-1,3,5-triazine was synthesised. When the infrared spectrum of 2,4,6-tri-(*para*-carboranyl)-1,3,5-triazine was examined as a KBr disc, a broad band above 3000cm^{-1} which could well be attributable to the suggested N···H intermolecular interactions, was observed, and only a weak carboranyl C-H stretch at 3064cm^{-1} was seen, suggesting this was not the predominant type of C-H stretch in this compound. The ambiguity arises, of course, from the fact that if any solvent (e.g. ether from the reaction work-up) were trapped in the triazinyl network, and the triazine effectively formed a clathrate, as triazines have been seen to do (section 4.4.1), the broad IR absorption above 3000cm^{-1} could be assigned to trapped solvent. The triazine C_3N_3 bands are at *c.*1360cm^{-1} and *c.*1530cm^{-1}.[57]

Substitution of a proton by a deuterium shifts the stretching frequency to a lower wavenumber following Hooke's Law, which correlates frequency and therefore wavenumber, to bond strength and atomic mass.[58]

$$f = \frac{1}{2\pi}\left(\frac{k}{m_1 m_2/(m_1 + m_2)}\right)^{\frac{1}{2}}$$

equation 4.1: Hooke's Law: f = frequency, k = force constant of the bond and m_1, m_2 = atomic masses

The observed carboranyl C-D frequency moved to lower wavenumber (*para*-carborane CH υ_{max}=3056cm^{-1}, deutero-*para*-carborane CD υ_{max}=2283cm^{-1}), and N···D interactions were also observed at a similarly shifted frequency. Of course, any broad bands above 3000cm^{-1} could only be attributable to trapped solvent (ether) in this instance, indicating the lack of intermolecular interactions.

Evidence from the solid state infrared spectra recorded suggested the presence of N···H and N···D intermolecular interactions, as illustrated in figure 4.12.

Comparison of the spectra of these two *para*-carboranyl triazines, synthesised from the reaction between lithio-*para*-carborane or lithio-deutero-*para*-carborane and cyanuric chloride, showed the disappearance of C-H and C-D peaks in moving from the parent carboranyl IR to the triazinyl IR spectra. Trapped solvent (Et_2O, or H_2O from KBr disc) appeared to be present in all the samples analysed, so the assignment of the band above 3000cm^{-1} could not unequivocally be assigned to N···H interactions. Ultimately though, the C-H and C-D bands had disappeared in the triazinyl products, strongly suggesting the presence of N···H and N···D intermolecular hydrogen bonding. High melting points strengthened the argument that intermolecular interactions were present.

The same phenomenon was observed for 2,4,6-tri-(*meta*-carboranyl)-1,3,5-triazine and its deuterated counterpart. In the protonated species, carboranyl BH was observed at 2604cm^{-1}, a weak CH at 3061cm^{-1} and a broad band at *c*.3419cm^{-1} suggested N···H interactions. By comparison the deutero-carboranyl analogue had a broad band at 3420cm^{-1} and a broad BH stretch at 2601 cm^{-1}. The carboranyl C-D frequency of 2287cm^{-1} seen for d-*meta*-carborane had disappeared.

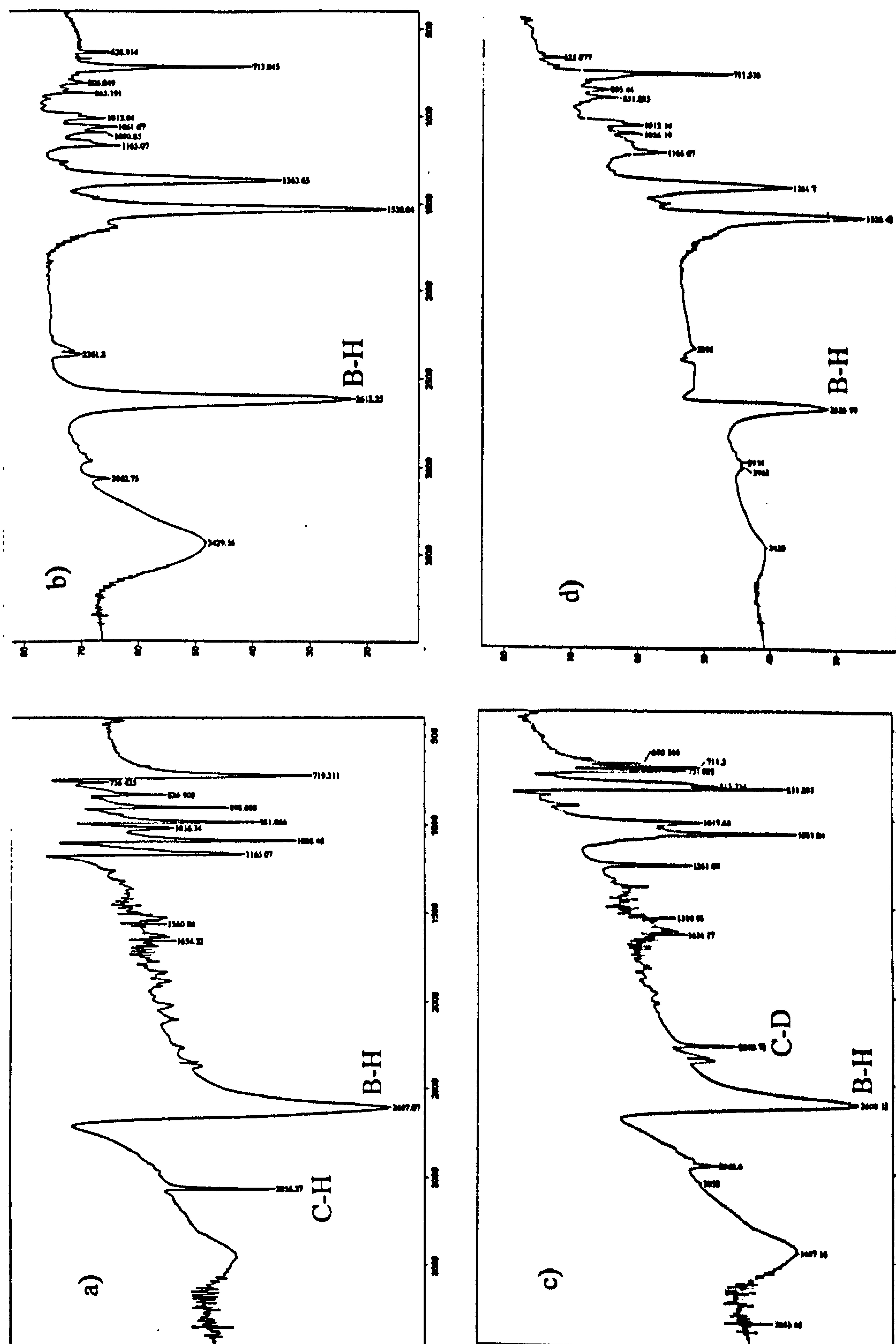

figure 4.12: IR spectra of a) para-carborane, b) 2,4,6-tri-(para-carboranyl)-1,3,5-triazine, c) deutero-para-carborane and d) 2,4,6-tri-(12'-d-para-carboranyl)-1,3,5-triazine. Samples run as KBr discs

Not unsurprisingly, no solubility problems were encountered in the *ortho*-carboranyl isomer, where the N···H interactions would be expected to be *intra*molecular.

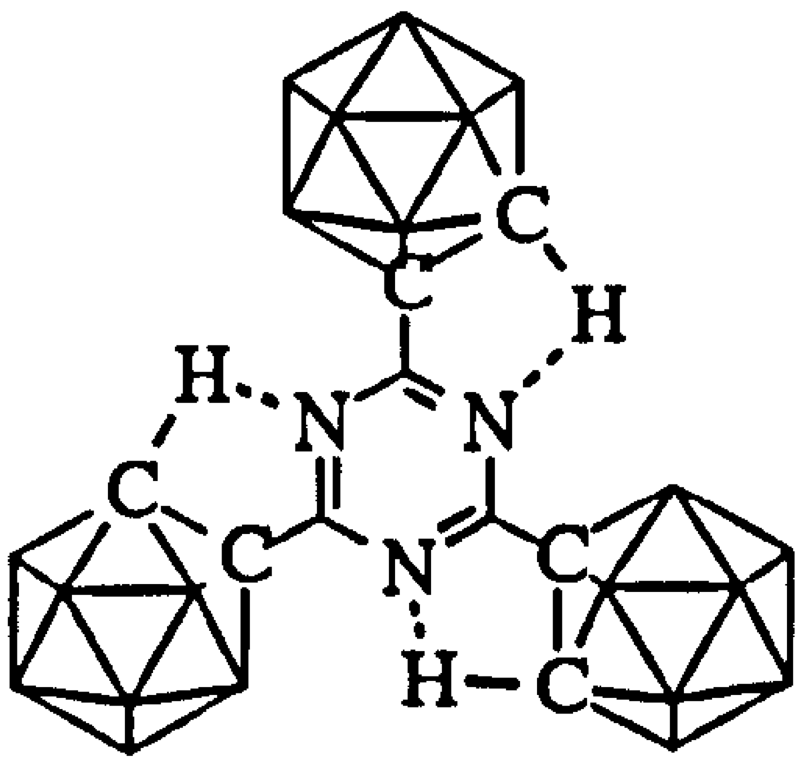

figure 4.13: intramolecular hydrogen bonding in 2,4,6-tri-(ortho-carboranyl)-1,3,5-triazine

In searching for a solution to the insolubility problem, and consequently looking at ways to confirm the presence of these intermolecular interactions, we turned to organic systems where "tails", usually aliphatic in nature, aid the solubility of a compound. The substitution of an organic substituent, be it aliphatic or aromatic in nature, rendered the triazinyl-carborane compounds soluble in common organic solvents ($CHCl_2$, $CHCl_3$, THF, alcohols) in every instance examined. The presence of the R functionality obviously removed any possibilty of N···H interactions forming, adding weight to the proposal of insolubilty in unsubstituted *meta*- and *para*-carboranyl-triazines being the result of intermolecular hydrogen bonding.

4.5.3 Structure

a) X-ray Powder Diffraction Experiments

Due to the insolubility of the *meta*- and *para*-carboranyl triazines, no crystals could be grown, however X-ray powder diffraction techniques were used to give an indication of the d-spacings between the planes which exist in the compound. In a powder sample, some of the crystallites will always be packed as to satisfy the Bragg Law, $n\lambda = 2d \sin\theta$, where n=reflection order, d=separation of the lattice planes and θ=glancing angle of diffracted X-ray, and so when X-rays are diffracted by the powder sample, a diffraction pattern emerges which can be solved to give the d-spacings of the lattice. The samples reported here were measured using Cu Kα X-rays of wavelength 154pm, so the d-spacings are calculable using the rearranged Bragg equation:

$$d = \frac{\lambda}{2 \sin \theta} = \frac{154\text{pm}}{2 \sin \theta}$$

equation 4.2: Bragg's Law

In crystalline solids, a peak is recorded for every plane in the unit cell. For 2,4,6-tri-(*para*-carboranyl)-1,3,5-triazine only one major peak was observed suggesting only one plane existed in the lattice, i.e. the compound packed in planes.

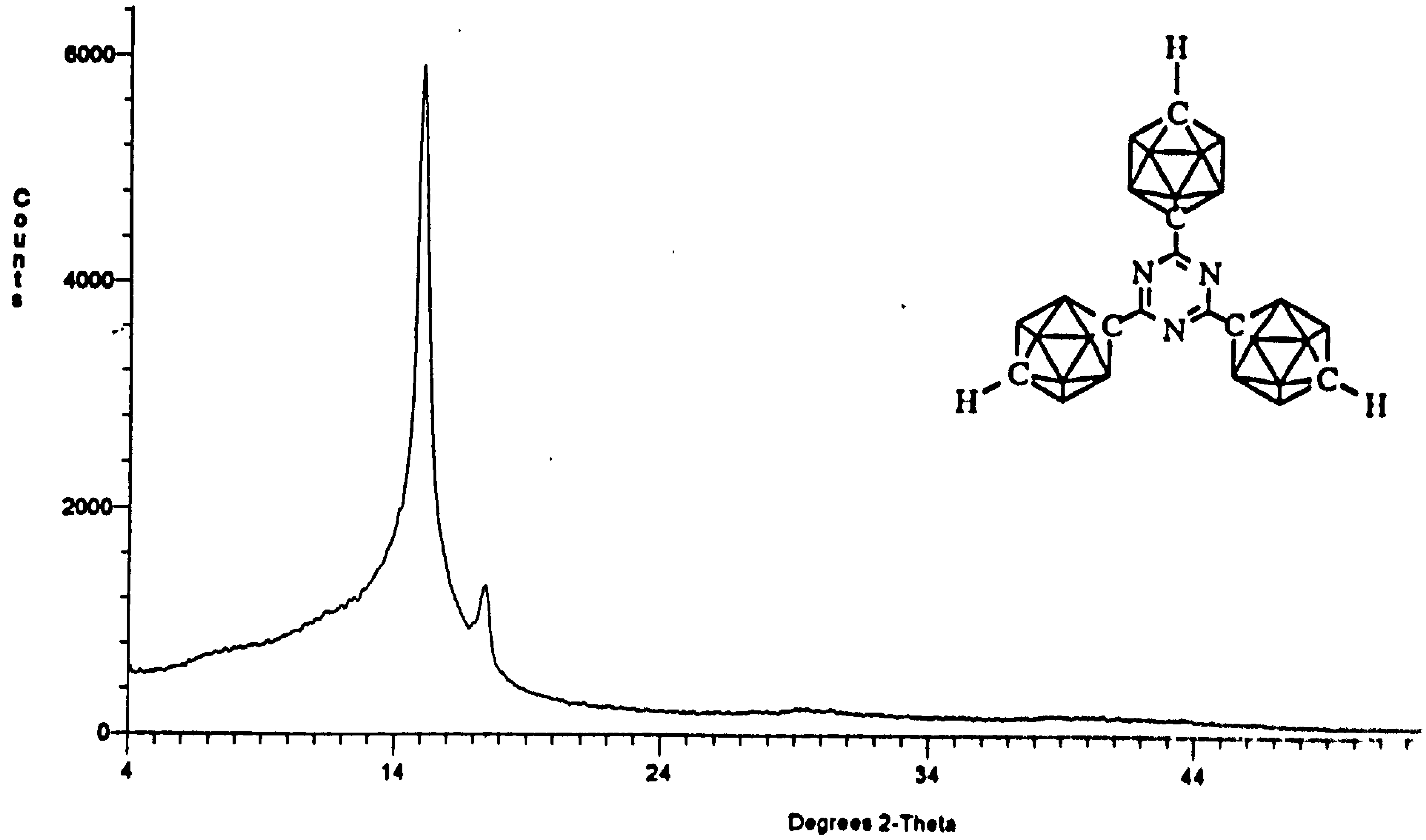

figure 4.14: X-ray powder diffraction pattern of 2,4,6-tri-(para-carboranyl)-1,3,5-triazine

This is consistent with the hypothesis expressed in the preceding section that this compound formed hydrogen bonded layers (*cf.* figure 4.10). In other triazine derivatives, N···H intermolecular interactions were observed, and have been shown to direct the compound to a planar packing arrangement.[59]

The measured diffraction angle, 2θ, of 15° gave a calculated d-spacing of 5.9Å if this was the first order diffraction (n=1 in the Bragg equation). If it were a second order diffraction (n=2), the d-spacing would be halved to 2.95Å, which was too short to accommodate the bulk of the carborane cage. (The minor peak seen here at 2θ = 17.5°, translated to a d-spacing of 5.1Å). This compares with a d-spacing of 3.35Å for graphite.[60]

The d-spacing is defined as the difference between the layers of maximum electron density. In 2,4,6-tri-(*para*-carboranyl)-1,3,5-triazine, the compound was assumed to be planar, so the plane of maximum electron density would dissect the carborane cages and triazine ring of each molecule lengthwise. There were therefore two possible packing arrangements (figure 4.15) depending on whether the bulky carborane residues were eclipsed (A) or, more plausibly, staggered (B).

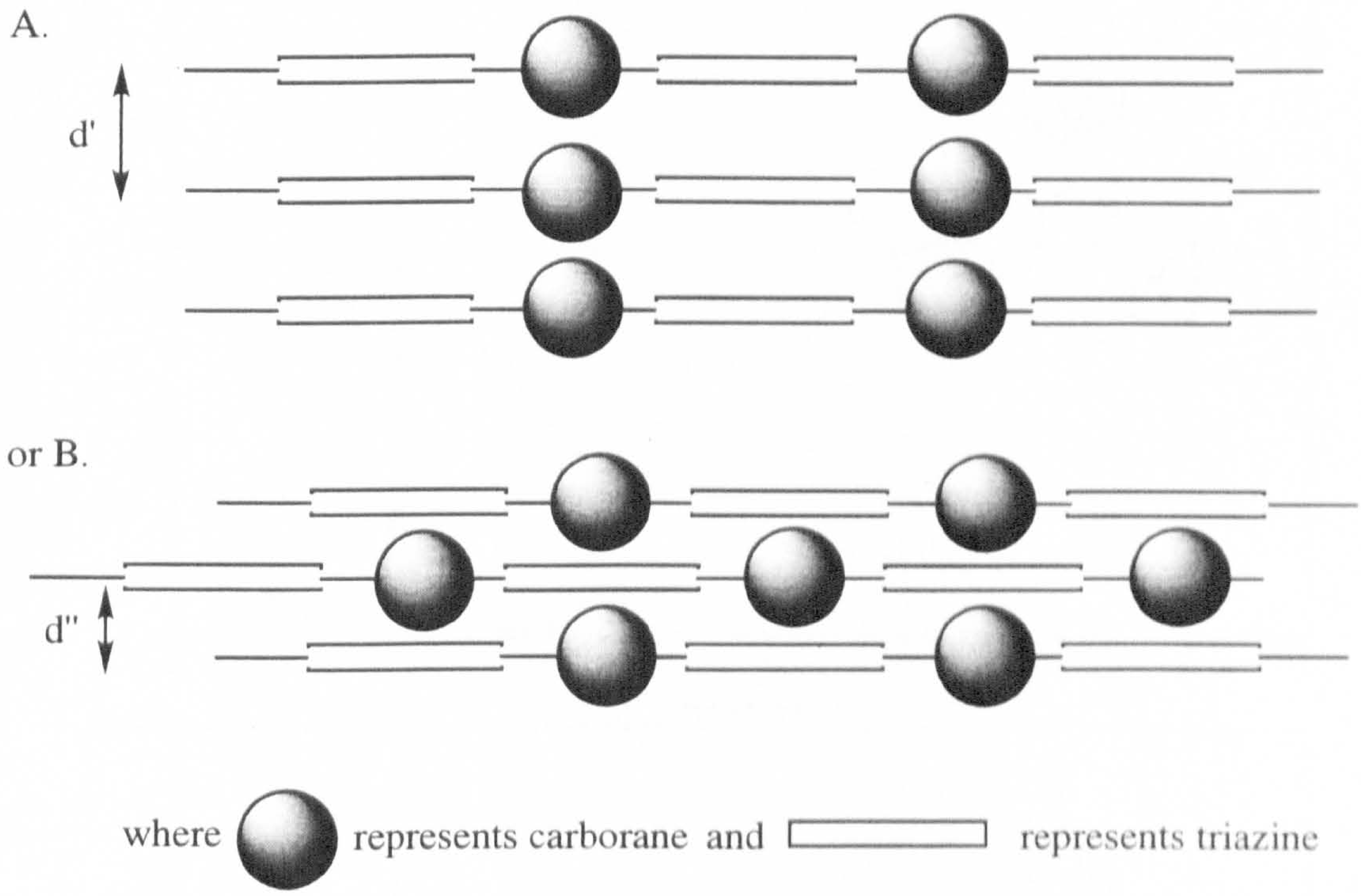

figure 4.15: possible packing arrangements of 2,4,6-tri-(para-carboranyl)-1,3,5-triazine

The crystal-structure of 1-phenyl-*para*-carborane[30] has shown the cross-cage distance of *para*-carborane (including the terminal hydrogen atoms) to be 7.3Å. The observed d-spacing of the tri-carboranyl triazine was smaller than this, so of the two packing diagrams proposed above, B was the more probable, with the tri-(carboranyl)-triazine units adopting a slipped structure where each carborane sits above a triazine ring.

2,4,6-tri-(*para*-carboranyl)-1,3,5-triazine has been shown to pack in layers which are hydrogen bonded, however, it was unknown if the observed packing pattern was a result of the intermolecular hydrogen bonding or simply due to the size and shape of the molecules. Hydrogen bonding has also been illustrated in 2,4,6-tri-(*meta*-carboranyl)-1,3,5-triazine. The powder diffraction pattern of this compound was measured and again showed a unique d-spacing of 5.9Å. For comparison, the diffraction pattern of the similarly sized and shaped 1,3,5-tri-(*para*-carboranyl)-benzene which has no potential to hydrogen bond, was recorded and shown to be identical to the triazine derivatives.

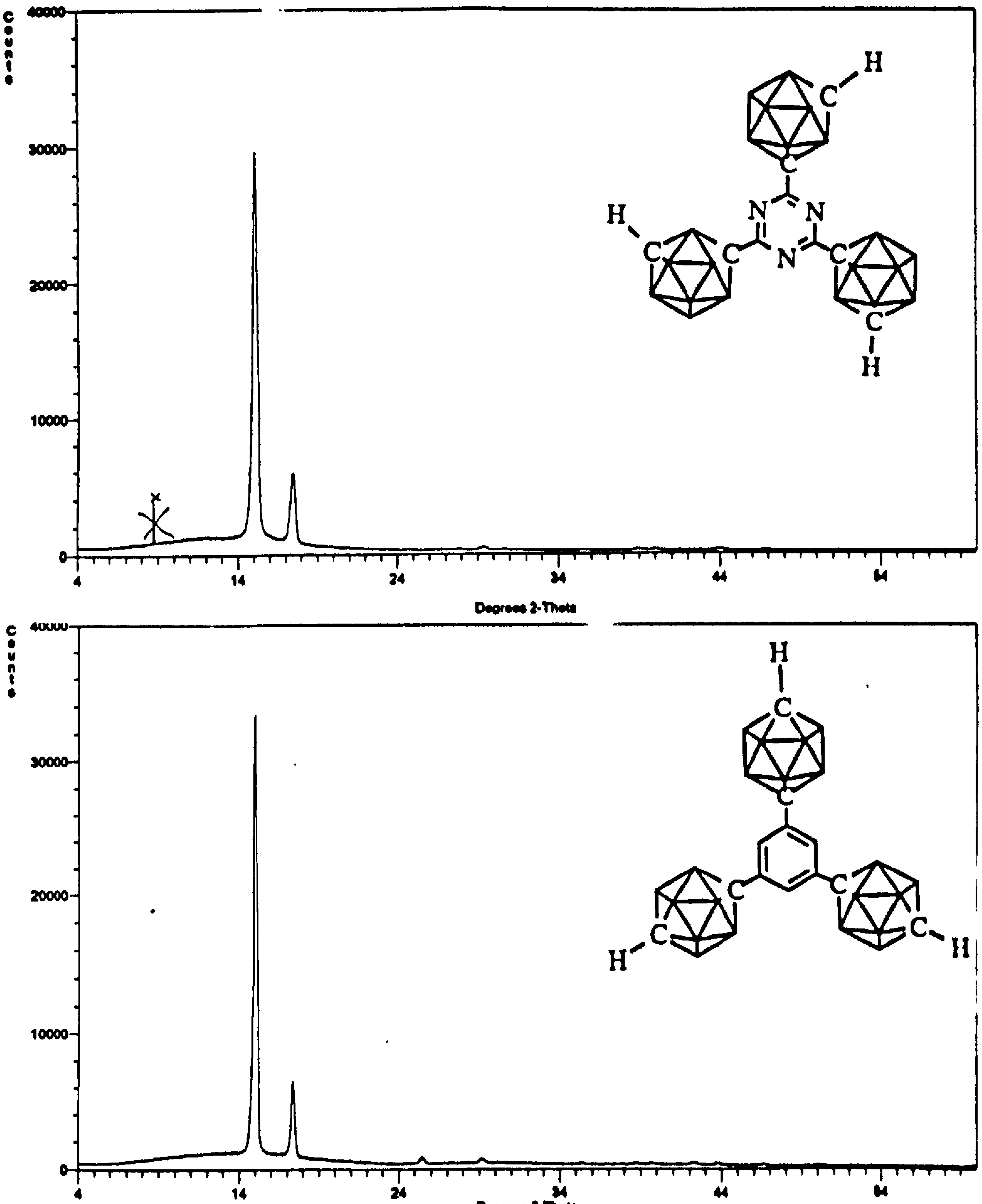

figure 4.16: X-ray powder diffraction patterns of 2,4,6-tri-(meta-carboranyl)-1,3,5-triazine (top) and 1,3,5-tri-(para-carboranyl)-benzene (bottom).

The conclusion to be drawn from this is, that although intermolecular hydrogen bonding is present in tri-carboranyl triazines where the second carboranyl carbon is protonated, the observed slipped planar packing is primarily a result of the size and shape of the molecule.

b) Structural conformations of substituted 2,4,6-tri-(carboranyl)-1,3,5-triazines

The crystal structures of 2,4,6-tri-(2'-phenyl-*ortho*-carboranyl)- and 2,4,6-tri-(12'-phenyl-*para*-carboranyl)-1,3,5-triazines have been solved from crystals grown from *ortho*-dichlorobenzene as clear colourless square platelets, and deutero-chloroform as clear colourless needles respectively. Selected information is given in the text, full crystallographic data, including all bond lengths and angles are reported in Appendix B.

i) X-ray structure of 2,4,6-tris-(2'-phenyl-*ortho*-carboranyl)-1,3,5-triazine - (I)

This compound has two possible isomers in the solid state, one in which two phenyl groups are directed upwards and one down, and the other where all three phenyl groups face upwards. Whether both isomers exist is unknown, but the structure of the latter isomer is described here. The same isomer has been solved previously for the benzene analogue, 1,3,5-tri-(2'-phenyl-*ortho*-carboranyl)-1,3,5-benzene (II), of this compound.[61]

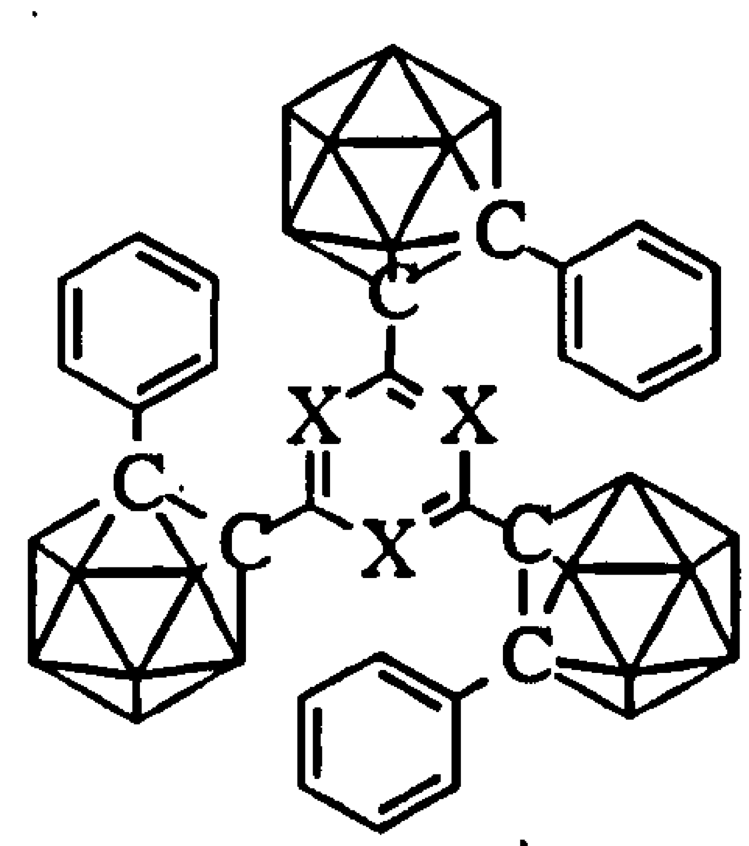

In (I), X=N
In (II), X=CH

figure 4.17: tri-(carboranyl)-triazine and benzene

This compound, like its benzene analogue, had space group R$\bar{3}$, indicative of three-fold symmetry around a screw axis and a centre of inversion. The molecule was also chiral, although for both the triazine and benzene derivatives, the same enantiomer has been isolated. All three phenyl groups face upwards, lying above and leaning in towards the plane of the central triazine ring.

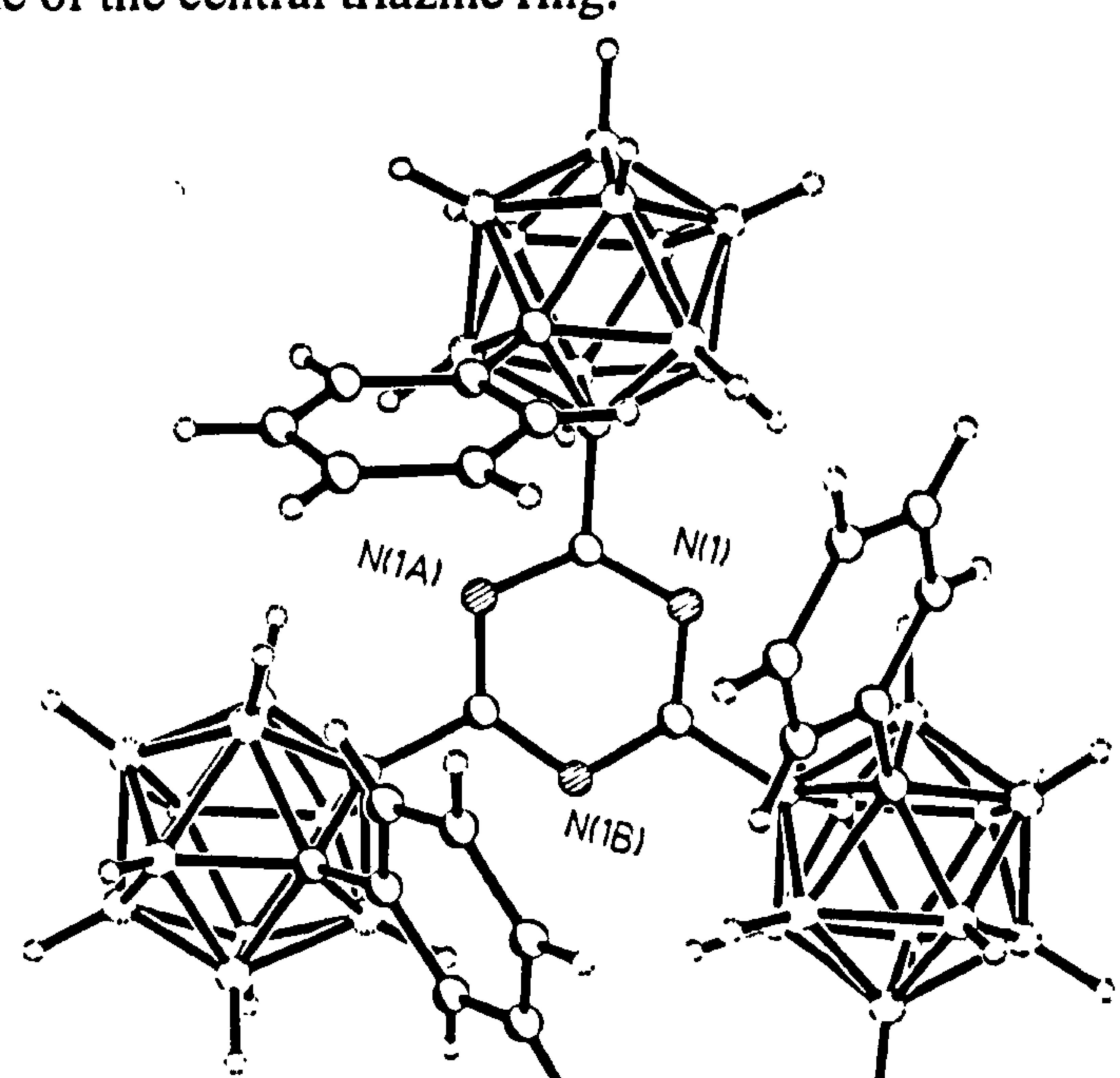

figure 4.18a: X-ray structure of 2,4,6-tri-(2'-phenyl-ortho-carboranyl)-1,3,5-triazine

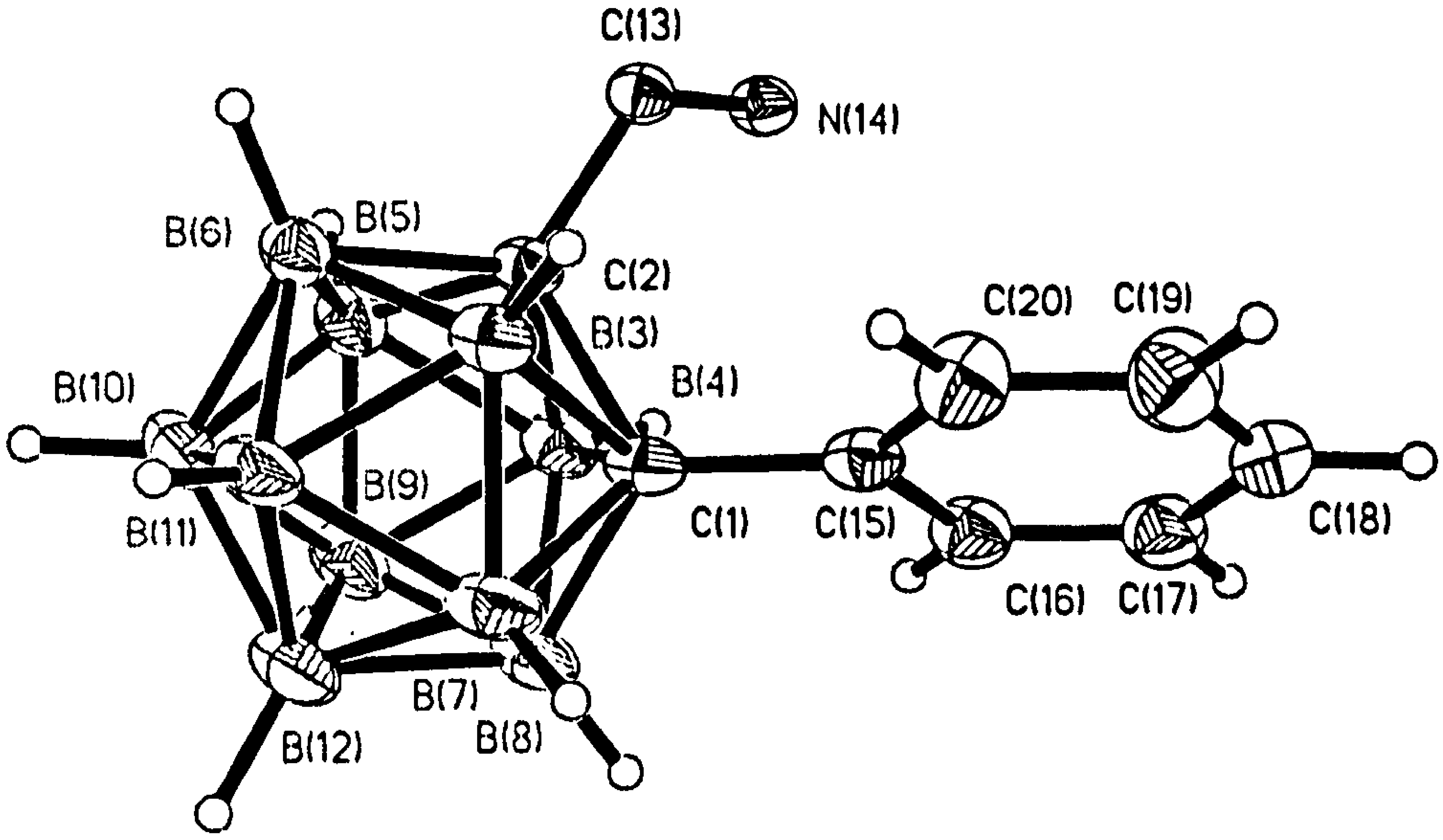

figure 4.18b: X-ray structure of 2,4,6-tri-(2'-phenyl-ortho-carboranyl)-1,3,5-triazine showing numbering scheme

	atoms	bond length/ Å	atoms	bond length/ Å
triazine ring	N(14)-C(13)	1.336(2)	N(14)-C(13)#	1.340(2)
cage - tr. / ph	C(2)-C(13)	1.510(2)	C(1)-C(15)	1.511(2)
cage C-C	C(1)-C(2)	1.686(2)		
cage C-B	C(1)-B(3)	1.758(2)	C(1)-B(4)	1.752(2)
	C(1)-B(7)	1.720(2)	C(1)-B(8)	1.718(2)
	C(2)-B(3)	1.723(2)	C(2)-B(4)	1.739(2)
	C(2)-B(5)	1.712(2)	C(2)-B(6)	1.719(2)
phenyl ring	C(15)-C(16)	1.397(2)	C(16)-C(17)	1.390(2)
	C(17)-C(18)	1.384(2)	C(18)-C(19)	1.387(2)
	C(19)-C(20)	1.392(2)	C(15)-C(20)	1.397(2)

table 4.2: selected bond lengths of 2,4,6-tri-(2'-phenyl-ortho-carboranyl)-1,3,5-triazine

atoms	bond angle / °	atoms	bond angle / °
C(13)-N(14)-C(13)#1	114.15(12)	N(14)-C(13)-N(14)#2	125.84(12)
N(14)#2-C(13)-C(2)	116.18(11)	N(14)-C(13)-C(2)	117.87(11)
C(13)-C(2)-C(1)	118.90(11)	C(2)-C(1)-C(15)	119.13(10)

table 4.3: selected bond angles for 2,4,6-tri-(2'-phenyl-ortho-carboranyl)-1,3,5-triazine

Given that the electron withdrawing influence of the carborane cage was identical on each carbon of the triazine ring, no C_3N_3 ring distortion was observed, and bond lengths within this ring were in the range 1.336(2) to 1.340(2)Å. These distances are standard for any symmetrically substituted 1,3,5-triazine.[62,63,64] The CNC internal ring angle was smaller than the NCN ring angle due to the external lone pair on the ring nitrogen. Although the bulk of the carborane cages may have been expected to cause triazine ring distortion, the angles observed were typical of symmetrically substituted 1,3,5-triazines, where the internal ring angles CNC and NCN are usually within the range 112-117° and 123-128° respectively.[62,63,64]

The carboranyl cage carbon to triazine bond length of 1.510(2) Å showed no deviation from the cage carbon to central benzene ring of (II), (1.509(3)Å). The same was true of the cage carbon to phenyl distance (1.511(2)Å cf. 1.503(3)Å for (II)), where the apparent difference is not statistically significant. The cage carbon to phenyl ring distance generally varies only slightly with a second substituent X on phenyl-*ortho*-carboranyl derivatives, with X having very little or no influence on the *exo* cage C-phenyl bond length (cf. Chapter Three and table 4.4).

Cage carbon-carbon distances, as discussed in Chapter Three, are indicative of the amount of electron density available for cage bonding. In general, if the cage is electron rich, the cage C-C distance lengthens and the cage becomes more open. Conversely, if electron density is drawn out of the cage by an *exo* substituent, the cage closes up and the cage C-C distance shortens. If each carboranyl cage of (I) were considered to be substituted with a phenyl group at position 1, and 3,5-di-(2'-phenyl-*ortho*-carboranyl)-2,4,6-triazine at position 2, comparison with compound (II) suggested compound (I) would have less electron density available for cluster bonding, as the triazine group has the greater electron withdrawing potential. This was reflected in the crystal structure, where the cage C-C distance for the triazine derivative was 1.686(2)Å, *c*.0.02Å shorter than that of compound (II) (cage C-C=1.709(3)Å). If significant, this follows the general trend of decreasing cage C-C bond length with increasing electron withdrawing potential of substituents. Unlike diphenyl-*ortho*-carborane where the cage C-C bond was lengthened as a result of steric repulsions between the two phenyl groups[65], the tri-(phenyl-*ortho*-carboranyl)-benzene and triazine derivatives were twisted so that such repulsions were minimised. Comparison with 1-phenyl-*ortho*-carborane however, where the cage C-C bond was 1.640(5)Å[66] showed there was possibly a degree of steric repulsion present which could open the cage.

compound	cage C-C distance / Å	cage C-phenyl distance / Å
o-PhCbH	1.640(5)	1.503(4)
(Ph-*o*-Cb)$_3$-C_3N_3	1.686(2)	1.511(2)
(Ph-*o*-Cb)$_3$-C_6H_3	1.709(3)	1.503(3)
o-Ph-Cb-Ph	1.733(4)	*c.* 1.5

table 4.4: cage C-C and C-Ph bond lengths for selected carborane derivatives.

Within the cage itself, the only bond found to be shortened with respect to diphenyl-*ortho*-carborane was the cage C-C distance. Distances from the triazine substituted carbon to the upper CB_4 layer were comparable with those of diphenyl-*ortho*-carborane, however, every other cage connectivity was longer. This gave a larger cage size and was consistent with the VSEPR bonding principle of less electron density forming a longer, weaker bond. Generally, there is less electron density available for cage bonding, although the electronic distribution is proposed as being such that the most density is focused on the cage carbons and the least on the antipodal atoms, resulting in very slight cage distortion.

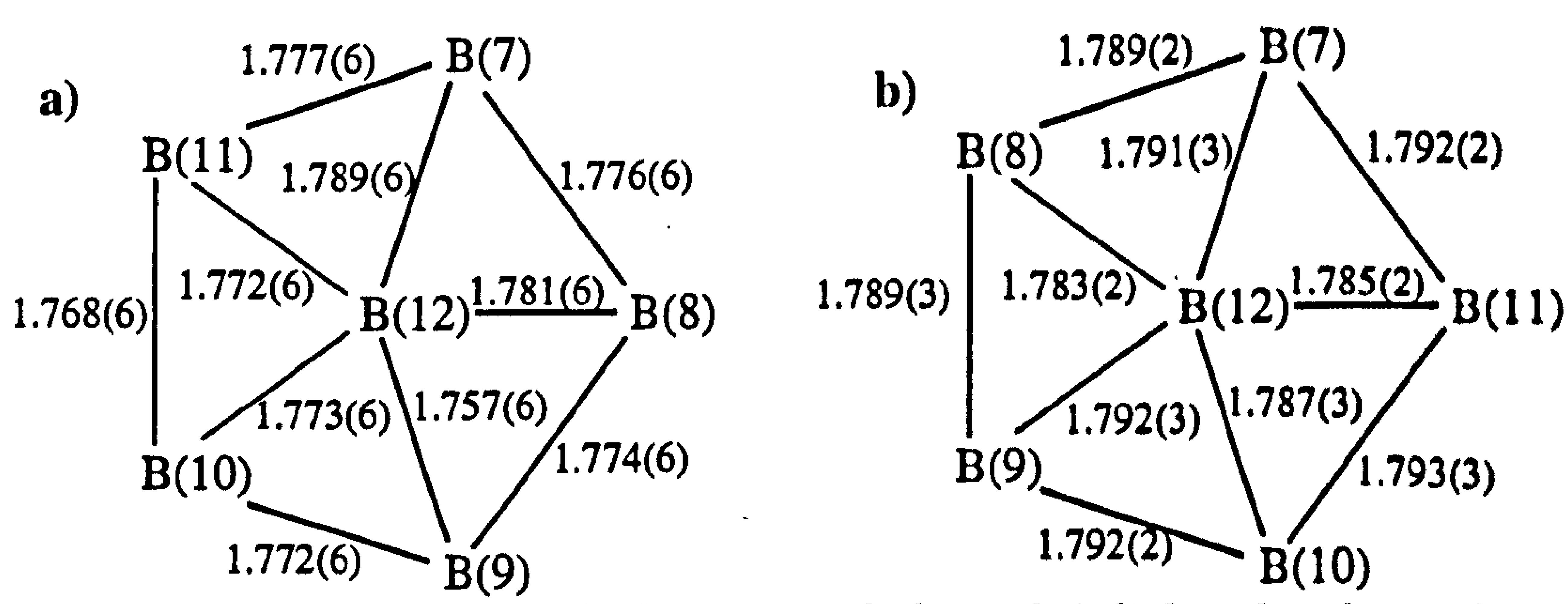

figure 4.19: representation of the lower cage halves of a) diphenyl-ortho-carborane and b) 2,4,6-tri-(2'phenyl-ortho-carboranyl)-1,3,5-triazine. The central atom is antipodal to Ph in a), and to (PhCb)$_2C_3N_3$ in b). Ph is antipodal to B(9) in a) and to B(10) in b).

Within the crystal lattice, the molecules packed in pairs with the C_3N_3 rings lying in parallel planes and with the phenyl groups of one molecule all oriented upwards, whilst those of the second molecule face down. Layers of these pairs formed stacks with the C_3N_3 rings forming a channel surrounded by phenyl-carboranyl groups.

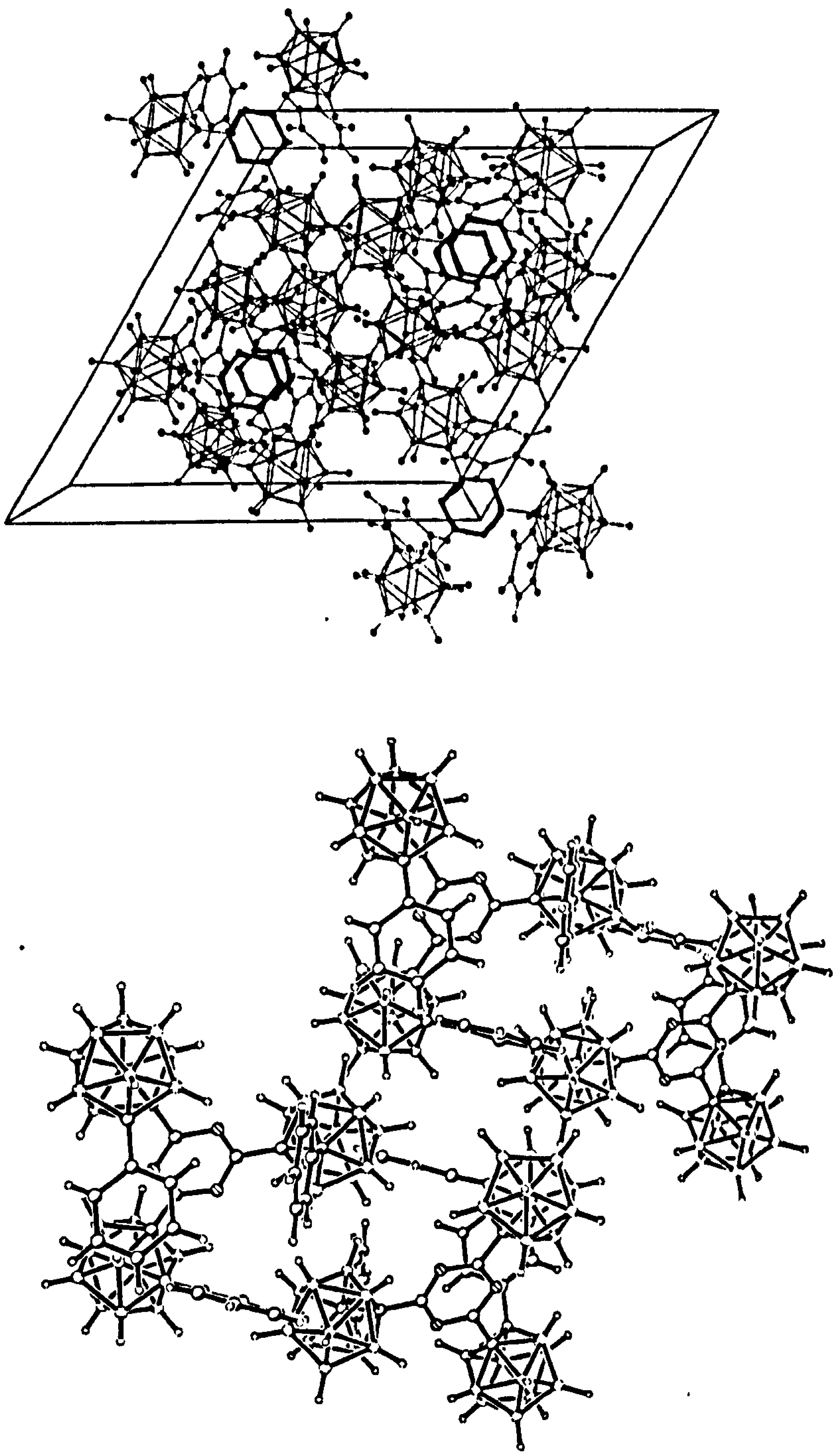

figure 4.20: packing diagrams of 2,4,6-tri-(2'-phenyl-ortho-carboranyl)-1,3,5-triazine

ii) X-ray structure of 2,4,6-tris-(12'-phenyl-*para*-carboranyl)-1,3,5-triazine-(III)

This compound did not crystallise from $CDCl_3$ as solvent, with C_{3v} symmetry as might have been expected, but instead as the $P^{-}1$ space group where one of the three phenyl groups was twisted at 90° to the other two, which lay in the plane of the C_3N_3 central ring. This configuration is often seen in molecules where a C_{3v} symmetry is possible.

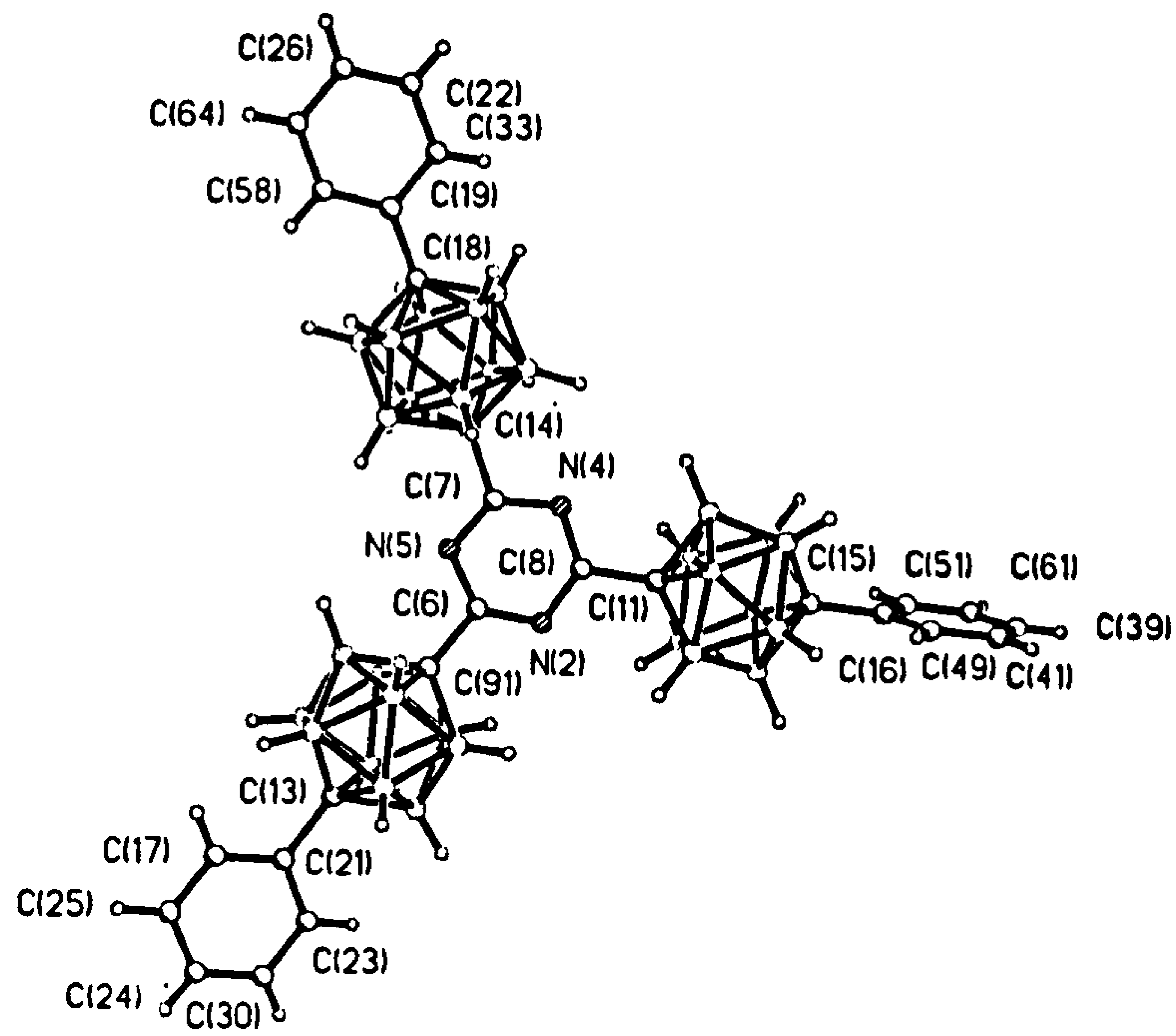

figure 4.21: crystal structure of 2,4,6-tri-(12'-phenyl-para-carboranyl)-1,3,5-triazine

	atoms	bond length/ Å	atoms	bond length/ Å
triazine ring	C(6)-N(5)	1.327(10)	N(5)-C(7)	1.333(9)
	C(7)-N(4)	1.341(9)	N(4)-C(8)	1.341(9)
	C(8)-N(2)	1.337(9)	N(2)-C(6)	1.324(10)
triazine-Cb	C(6)-C(9)	1.515(10)	C(7)-C(14)	1.507(11)
	C(8)-C(11)	1.510(10)		
Cb-Ph	C(13)-C(21)	1.524(10)	C(15)-C(16)	1.521(11)
	C(18)-C(19)	1.503(11)		
phenyl ring	Ph (⊥ to C_3N_3)	1.37	Ph (// to C_3N_3)	1.38

table 4.5: bond lengths in 2,4,6-tri-(12'-phenyl-para-carboranyl)-1,3,5-triazine

atoms	bond angle/ °	atoms	bond angle/ °
C(6)-N(5)-C(7)	113.4(7)	N(5)-C(7)-N(4)	126.3(7)
C(7)-N(4)-C(8)	113.5(6)	N(4)-C(8)-N(2)	125.8(7)
C(8)-N(2)-C(6)	113.7(7)	N(2)-C(6)-N(5)	127.2(7)

table 4.6: internal angles within the triazine ring of 2,4,6-tri-(12'-phenyl-para-carboranyl)-1,3,5-triazine

Although the three carboranyl cages were non-equivalent, all the bond lengths and angles within the C_3N_3 ring fell within standard values, although a slight ring distortion was observed due to the molecular symmetry. All cage B-B and C-B connectivities were within accepted ranges, falling in the ranges 1.746(14)Å to 1.82(2)Å and 1.686(13)Å to 1.749(13)Å respectively. No perturbations were seen in the phenyl groups either. Within experimental error, no significant differences were observed between the bond lengths of the three cages and their substituents. Crystal distortions were due in part to the solvent molecules (Et_2O, $CDCl_3$) trapped in the lattice.

In section 4.5.3a), 2,4,6-tri-(*para*-carboranyl)-1,3,5-triazine was shown, by means of X-ray powder diffraction, to pack in layers. The phenyl-*para*-carboranyl derivative also packed in sheets, with the perpendicular phenyl group slotted in between the other two phenyl-*para*-carboranyl groups of the next molecule in a head-to-tail manner. The layers above and below ran in the opposite direction.

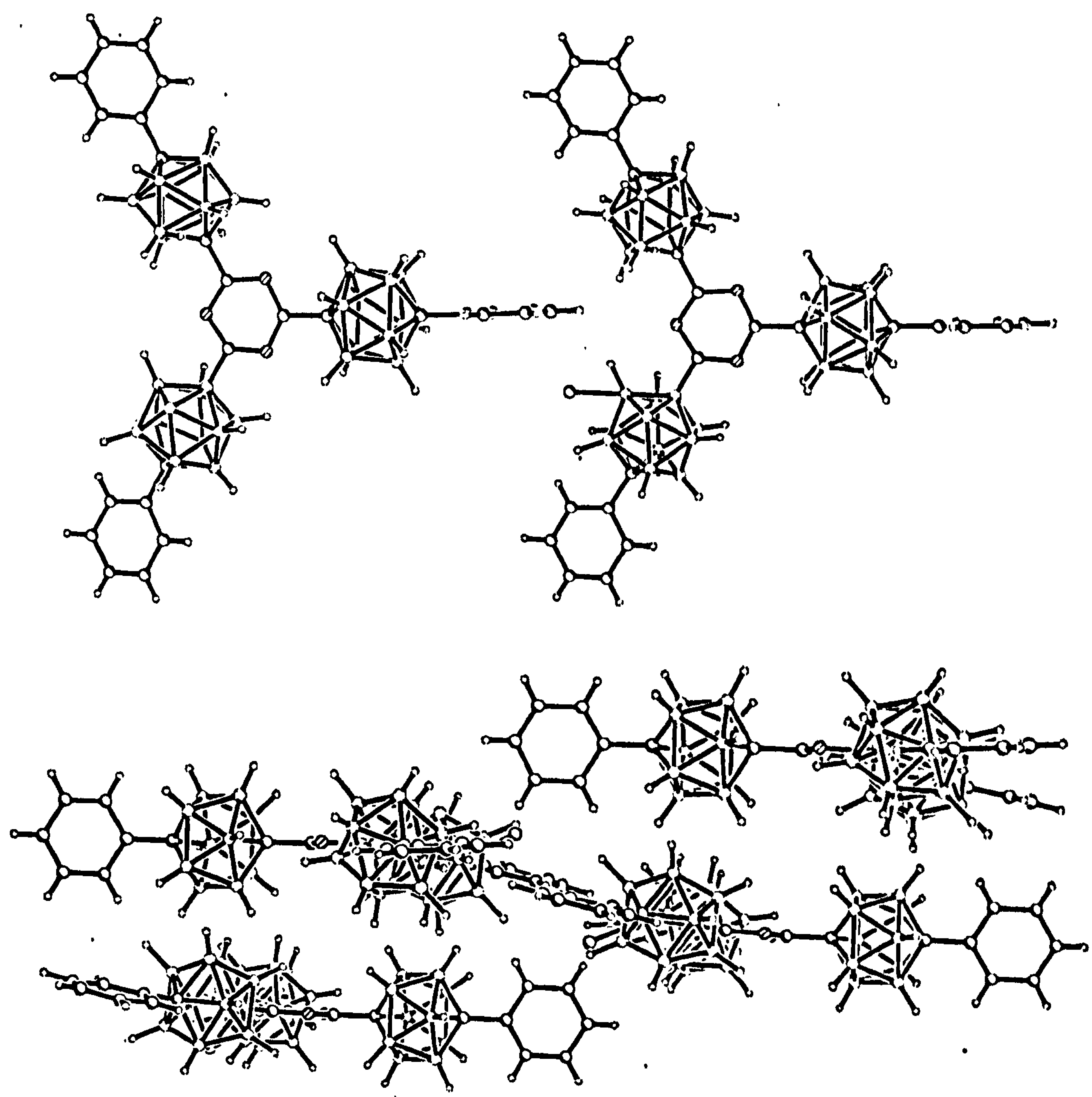

figure 4.22: packing diagrams of 2,4,6-tri-(12'-phenyl-para-carboranyl)-1,3,5-triazine

The differing electron withdrawing potentials of the two carborane isomers were not manifest in the crystal structures of the tri-(carboranyl)-triazines studied. Comparison of this structure with that of the *ortho*-isomer, showed little difference between the bond lengths and angles of the central C_3N_3 ring. This was not unsurprising as the triazine was symmetrically substituted in each example.

4.5.4 NMR Spectroscopic Studies

As explained in Chapter Three, NMR spectroscopy is an invaluable technique when seeking information on electron distribution within the carboranyl cage system. For the reason explained above, both solid and solution state FT-NMR spectroscopic techniques have been employed in the study of these multi-carboranyl triazine compounds. Although shifts in solution state NMR can be influenced by solvent effects, any possible shift effects in the compounds which will be discussed here are negligible unless stated otherwise. Solid state NMR techniques also allow the accurate and precise determination of chemical shifts and the shifts observed in solution and in solid state NMR studies are comparable. ^{1}H, $^{13}C\{^{1}H\}$, ^{13}C, $^{11}B\{^{1}H\}$, and ^{11}B studies have been conducted on the soluble and insoluble carboranyl-triazines synthesised.

a) *Ortho*-carboranes

The antipodal atoms B(9) and B(12) in *ortho*-carboranyl derivatives show the most significant changes in electronic distributions, as they are diametrically opposite the point of substitution.[67]

The structure of 2,4,6-tri-(2'-phenyl-*ortho*-carboranyl)-1,3,5-triazine was described above, and showed the bonds furthest from the carbons to be lengthened, implying that the cage electron density had become concentrated on the cage carbon atoms, and reduced on the atoms opposite the point of substitution. By $^{11}B\{^{1}H\}$ NMR spectroscopy, the atom antipodal to the di-carboranyl-triazine moiety was shown to have decreased electron density, and a shift to higher δ was observed. This was in accordance with the X-ray structure.

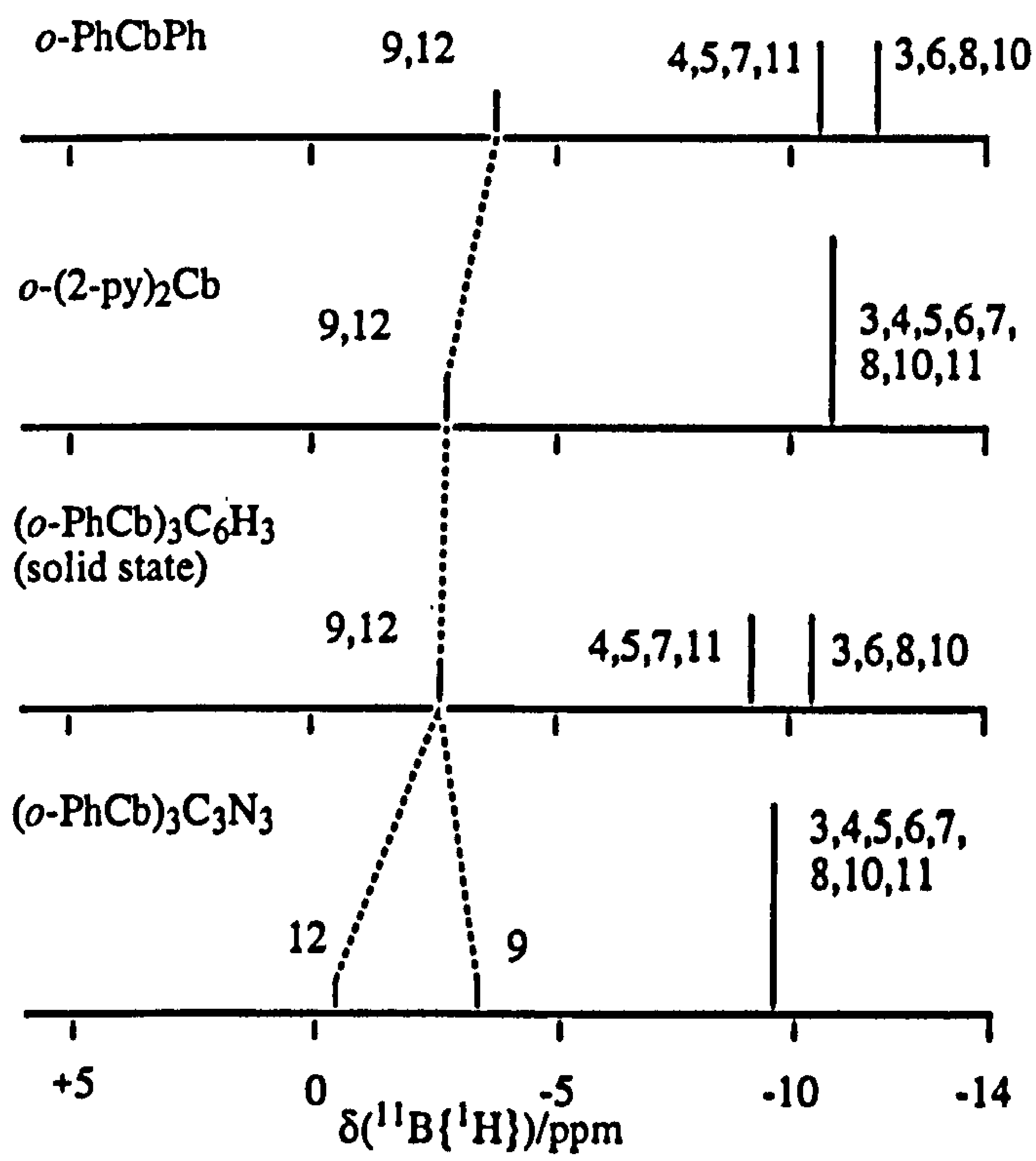

figure 4.23: $^{11}B\{^{1}H\}$ NMR spectra of disubstituted ortho-carboranyl derivatives. B(9) is antipodal to the phenyl group in the tri-carboranyl assemblies

b) *meta*-carboranes

Unfortunately, no NMR spectra of 1,3,5-tri-(*meta*-carboranyl)-benzenes were available, however a comparison of the ^{11}B NMR spectroscopic shifts of 2,4,6-tri-(*meta*-carboranyl)-1,3,5-triazine with other substituted *meta*-carboranes, illustrated that electron density was withdrawn from the cage in the triazine system. As *meta*-carboranes are less electron withdrawing than their *ortho*-analogues, the observed antipodal shift difference, (B(12)), was not so great in the *meta*-carboranes as in the *ortho*.

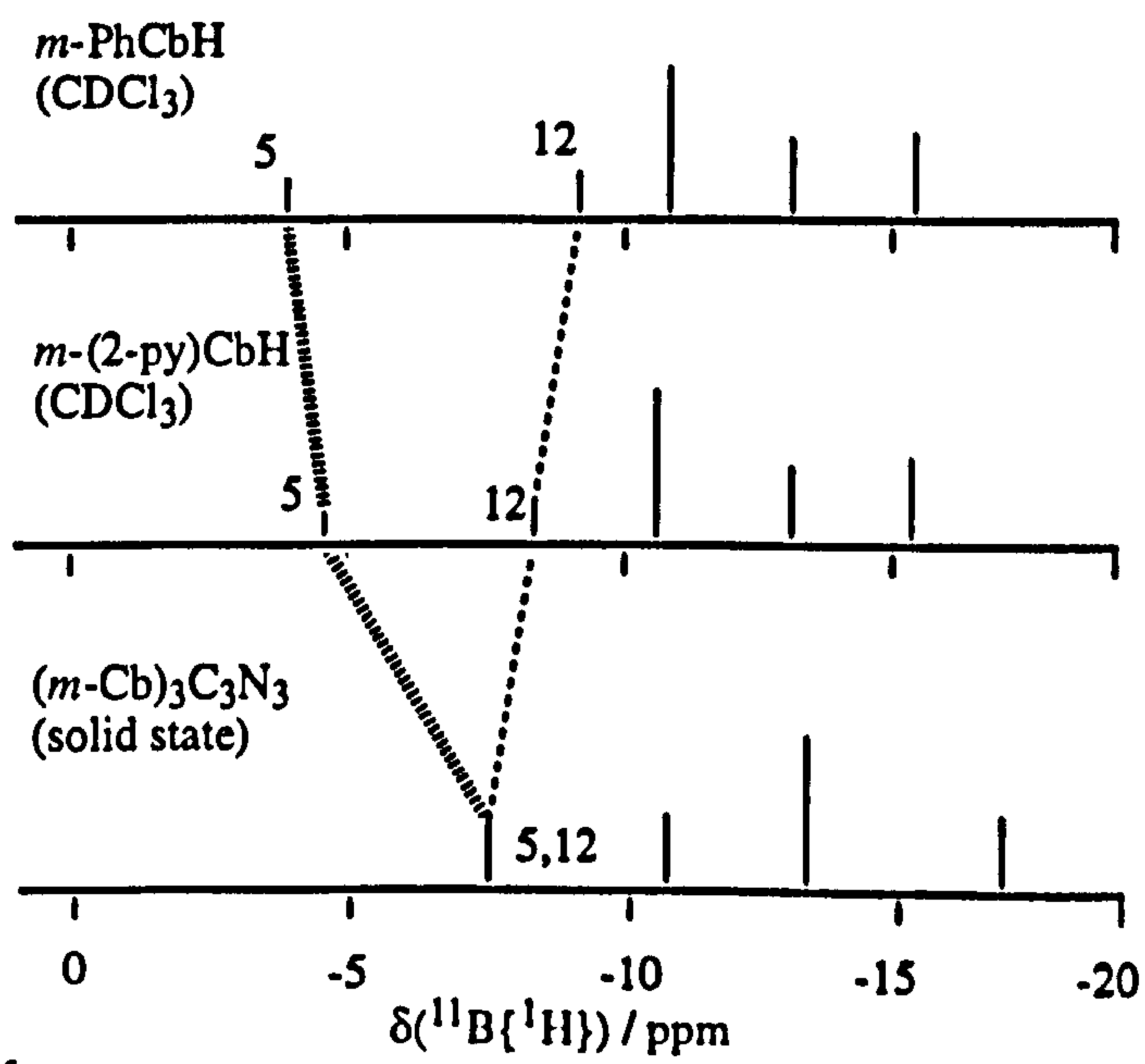

figure 4.24: $^{11}B\{^{1}H\}$ NMR spectra of meta-carborane derivatives. B(12) is antipodal to R, B(5) is the unique atom in the top carboranyl belt

c) *para*-carboranes

With *para*-carboranyl derivatives, it is no longer the boron, but the carbon atoms which are the antipodal nuclei. Electron density changes within the cage as a whole however, and information can be gleaned from both $^{13}C\{^1H\}$ and $^{11}B\{^1H\}$ NMR spectra.

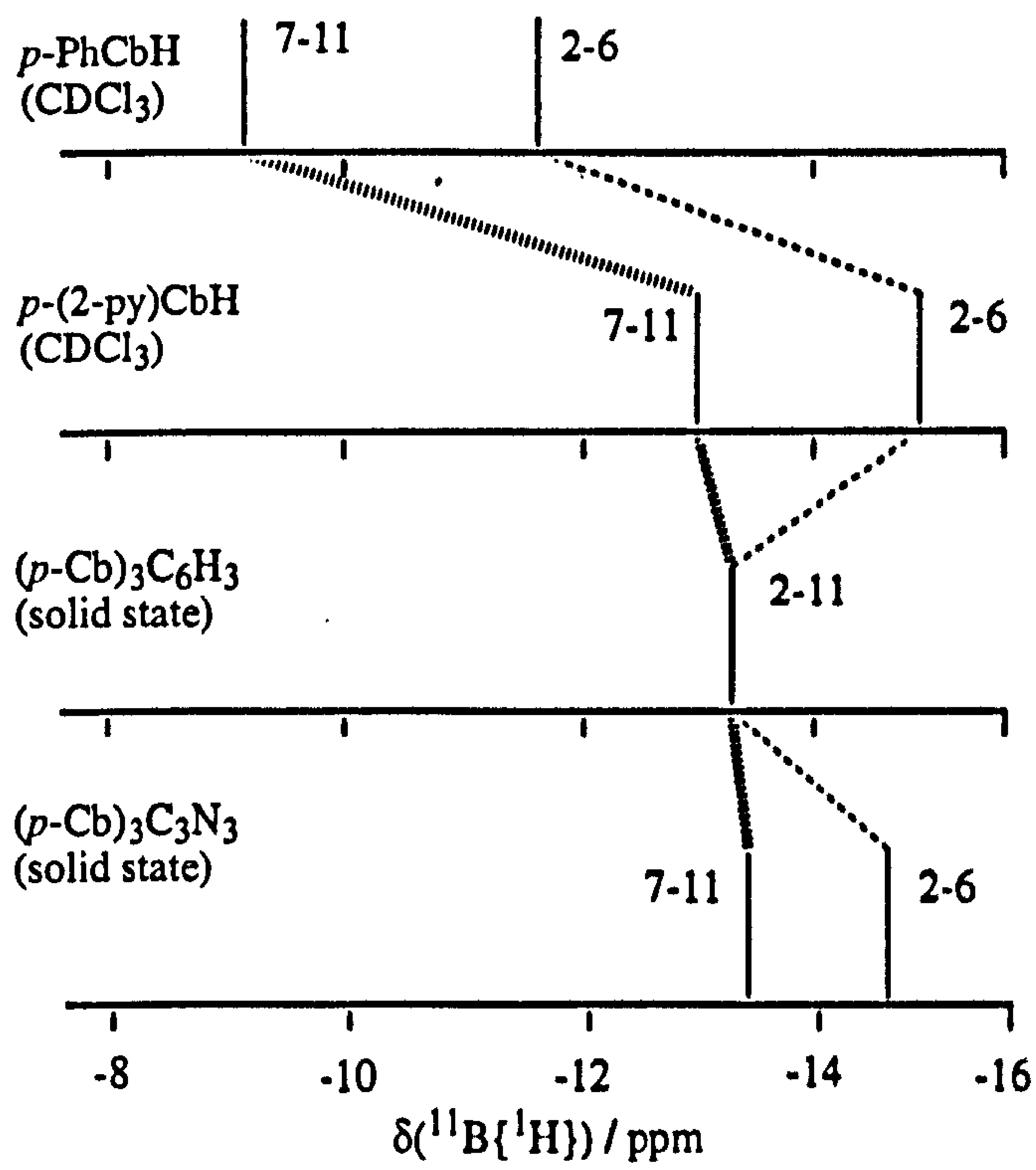

figure 4.25: $^{11}B\{^1H\}$ NMR spectra of para-carborane derivatives. B(2)-B(6) represent the boron atoms closest to the carboranyl CH unit.

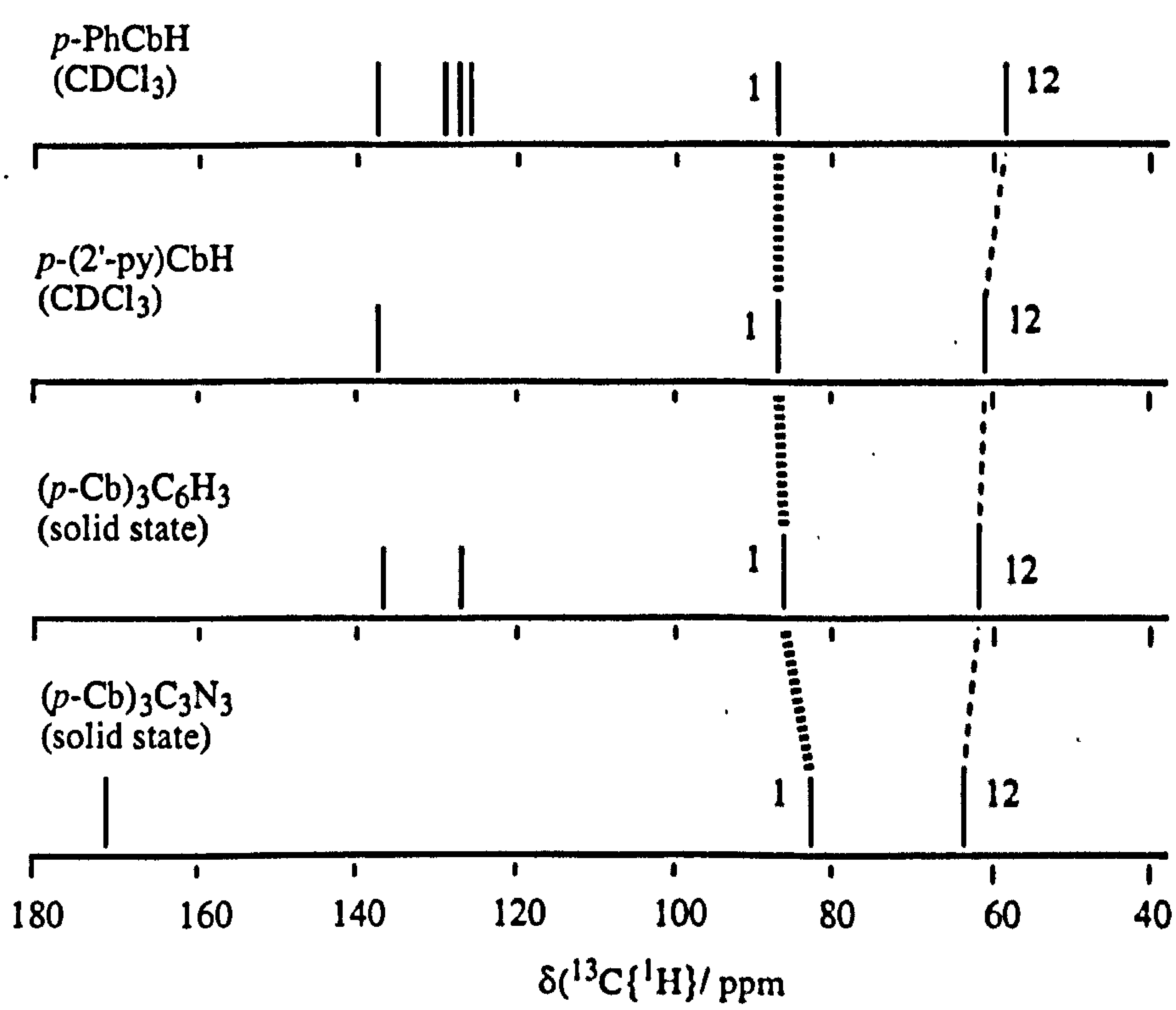

figure 4.26: $^{13}C\{^1H\}$ NMR spectra of substituted para-carboranes. 1 represents the carbon antipodal to CH, 12 represents the CH unit.

$^{11}B\{^{1}H\}$ NMR spectroscopy suggested the electron density on the boron atoms of the carborane increased as electron withdrawing substituents were introduced. The effect in 2,4,6-tri-(*para*-carboranyl)-1,3,5-triazine was comparable to that of 2'-pyridyl-*para*-carborane. The antipodal effect with the carbon atoms showed a slight upfield shift (shift to lower δ) as the carbon substituent opposite the carboranyl CH unit became more electron withdrawing, but the effect was only very small.

4.5.5 Degradation of multi-carboranyl triazines

In the chemistry of classical 1,3,5-triazines, the heterocyclic ring can be susceptible to attack by various compounds, including hydrazines,[68] which bring about either ring-degradation or ring-opening reactions. For example, if we consider the reaction of *s*-triazine with *N,N*-dimethylhydrazine[69], the ring is cleaved forming 1-formyl-2,2-dimethylhydrazine 2',2'-dimethylhydrazone.

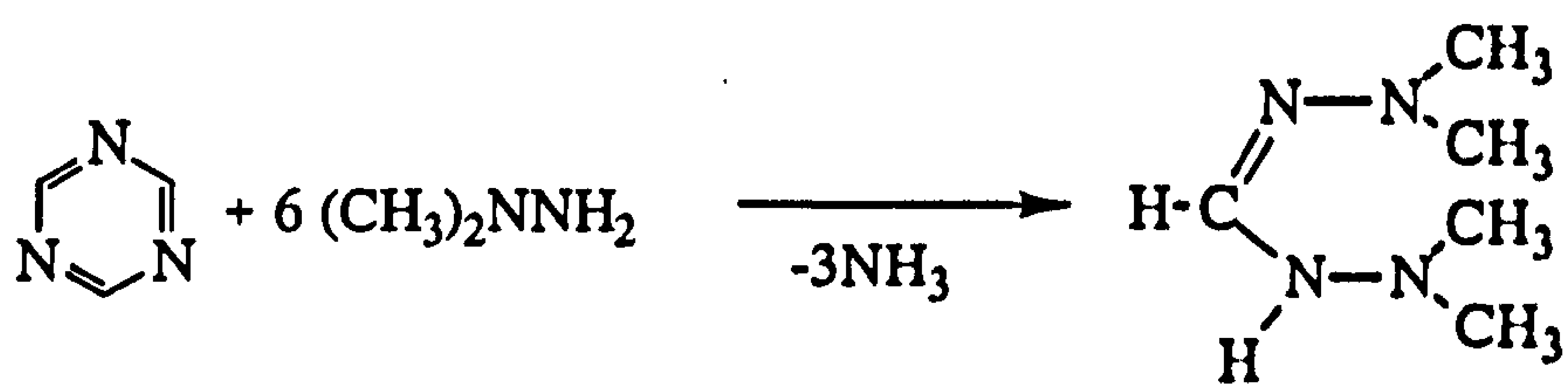

scheme 4.19: triazine ring degradation though dimethylhydrazine

Where the triazine ring was substituted, ring cleavage was observed in some cases. For example :

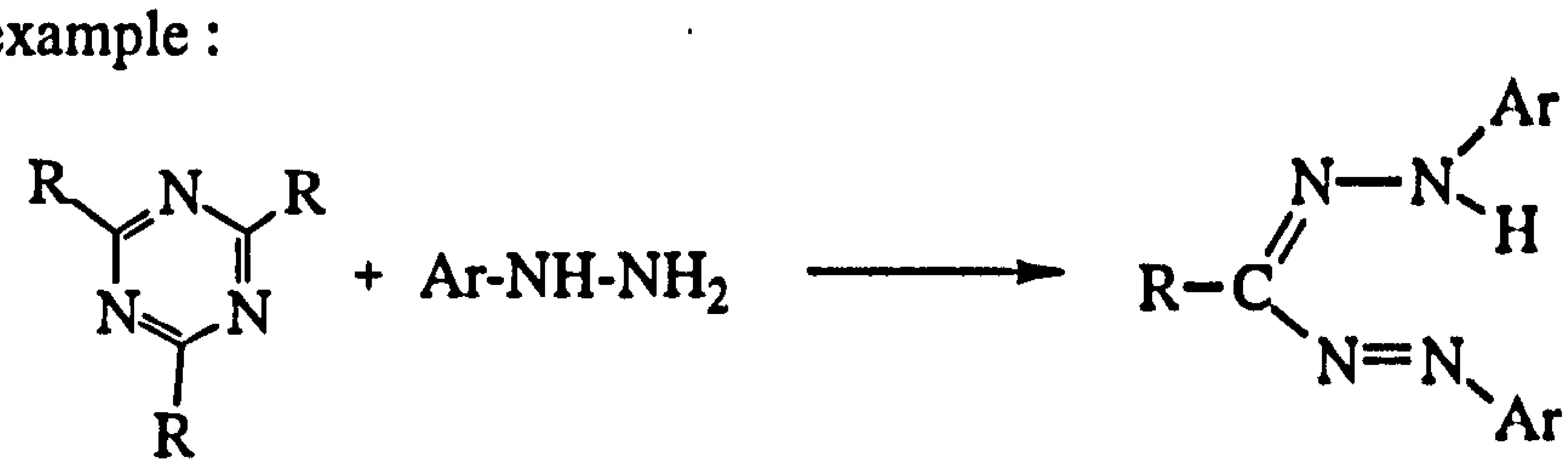

scheme 4.20: triazine ring degradation through hydrazine derivatives

To investigate the stability of the triazine ring within a carboranyl system, we proposed a series of experiments where the ring would be broken up into various substitutent parts by hydrazine derivatives. When the construction of these triazine assemblies was discussed earlier in this chapter, it was noted that if the C_3N_3 assembly were to be built from constituent parts, the initial carborane derivatives would be difficult and time consuming to prepare. These tri-carboranyl triazine assemblies have proven to be readily accessible from cyanuric chloride, however, degradation of the central C_3N_3 ring would give us an alternative preparative route to these relatively inaccessible starting materials.

If this were a viable synthetic option, the chemistry of these compounds could have been investigated more readily and, given their nature, could have led to novel polymeric and non-linear optical materials. As always however, there was an alternative possible outcome to the reaction between the tricarboranyl triazines and the hydrazine group of compounds, and that was for deboronation of the carborane cage to occur. Hydrazine is electron-rich so there was always the possibility that the carborane cage, particularly *ortho-* and to a lesser extent *meta*-carborane, would be attacked and subsequently deboronated as a result of the basicity associated with the hydrazine functionality. Deboronation was in fact the predominant result of reactions between carboranyl triazines and hydrazine derivatives, and so will be discussed with similar reactions in Chapter Five.

4.5.6 Thermal Stability of tri-carboranyl triazines

Carboranes are known to undergo thermal rearrangement to higher isomers, and reverse isomerisation from *para* to *meta* has also been reported.[70] Various mechanisms of the rearrangement mechanism have been postulated including the diamond square diamond (DSD), triangular face rotation, pentagonal pyramidal rotation and rearrangement via a 12-vertex *nido* intermediate (*c.f.* Chapter One). The aim of the present work, however, was not to investigate the mechanism of rearrangement, but to examine the thermal stability of the tri-carboranyl triazines.

Unsubstituted carboranes are known to transform to higher isomers at 723K and 893K for the *ortho* to *meta* and the *meta* to *para* conversions respectively. The first of these is quantitative, but the *meta* to *para* rearrangement is not very efficient, and a considerable degree of cage degradation also occurs. This isomerisation is also known for *bis*-carboranyl species[4], certain substituted carboranes and metallacarboranes.[71]

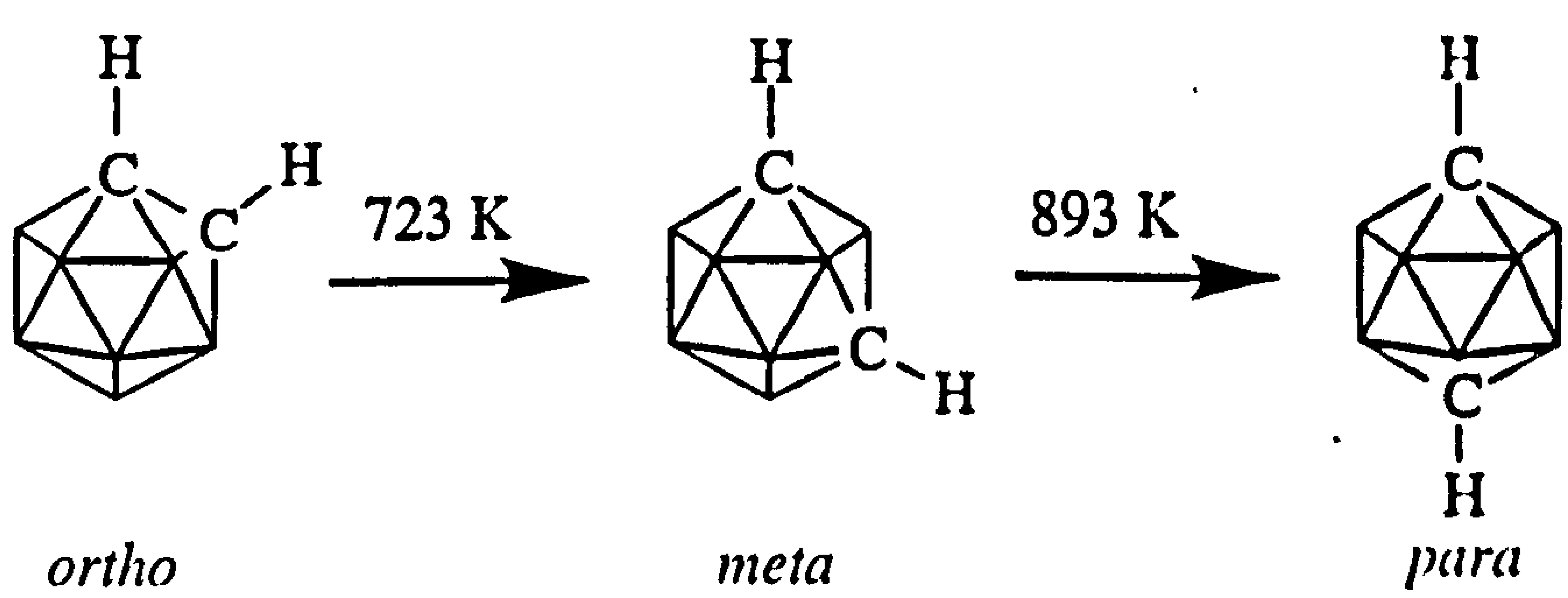

scheme 4.21: thermal isomerisation of unsubstituted carboranes

A sample of 2,4,6-tri-(2'-phenyl-*ortho*-carboranyl)-1,3,5-triazine was heated to 400°C in an evacuated Carius tube for four days. After this time, a brown glassy solid was resident on the walls of the tube together with some mushroom shaped, off-white solid deposits in the base of the tube. Each sample gave an off-white powder if ground, and both analysed as 2,4,6-tri-(2'-phenyl-*meta*-carboranyl)-1,3,5-triazine. Thermal isomerisation occurred quickly (*c.*10-15minutes) at high temperatures, and heating a sample in an evacuated flask to *c.*400°C caused the sample to sublime, melt and then isomerise in quantitative yield. Isomerisation to the *para*-derivative was not attempted.

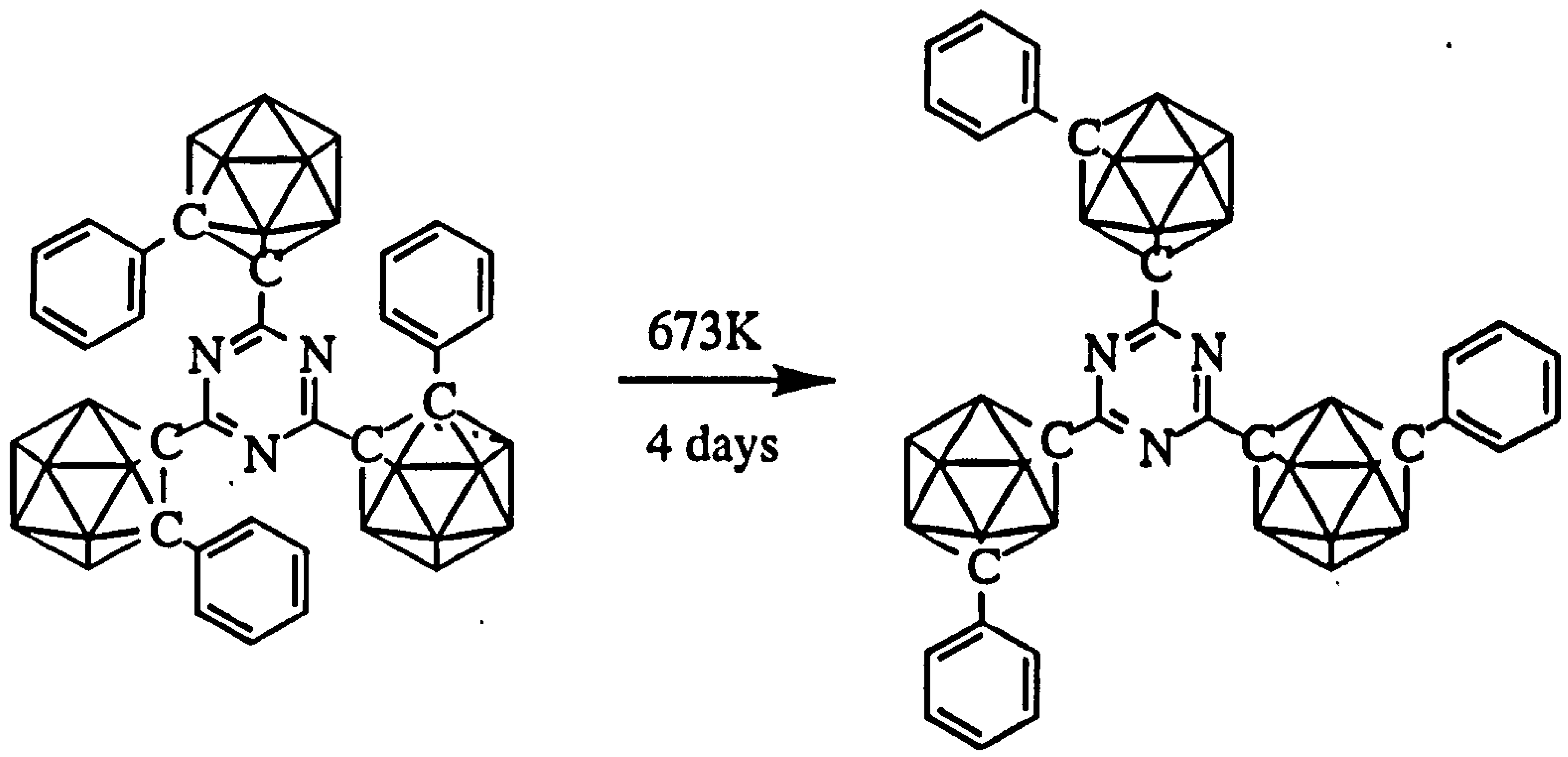

scheme 4.22: thermal isomerisation of 2,4,6-tri-(2'-phenyl-ortho-carboranyl)-1,3,5-triazine to its meta analogue

Para-carboranyl derivatives cannot be converted to a higher isomer, but are known to be thermally stable. To investigate its thermal stability, 2,4,6-tri-(*para*-carboranyl)-1,3,5-triazine, which has been shown to pack in sheets, was heated in a furnace to 1200°C under a flow of argon, to give a clear, colourless hard film on the surface of the mullite[72] boat or quartz sheet used to support the sample. On exposure to air over prolonged periods of time (*c.*3days or more), this film became opaque white and began to flake. Heating the sample to temperatures up to 800°C produced a black solid, which became grey on standing in air. Infrared spectra of the black solid showed it to contain boric acid, indicating that oxygen had not been successfully eliminated from the furnace during the heating process.

X-ray photoelectron spectroscopy (XPS) was conducted on the film produced after heating to 1200°C, as a clear, colourless film on quartz, and also as the flaked sample on quartz and on tape. The same result was obtained in each instance.

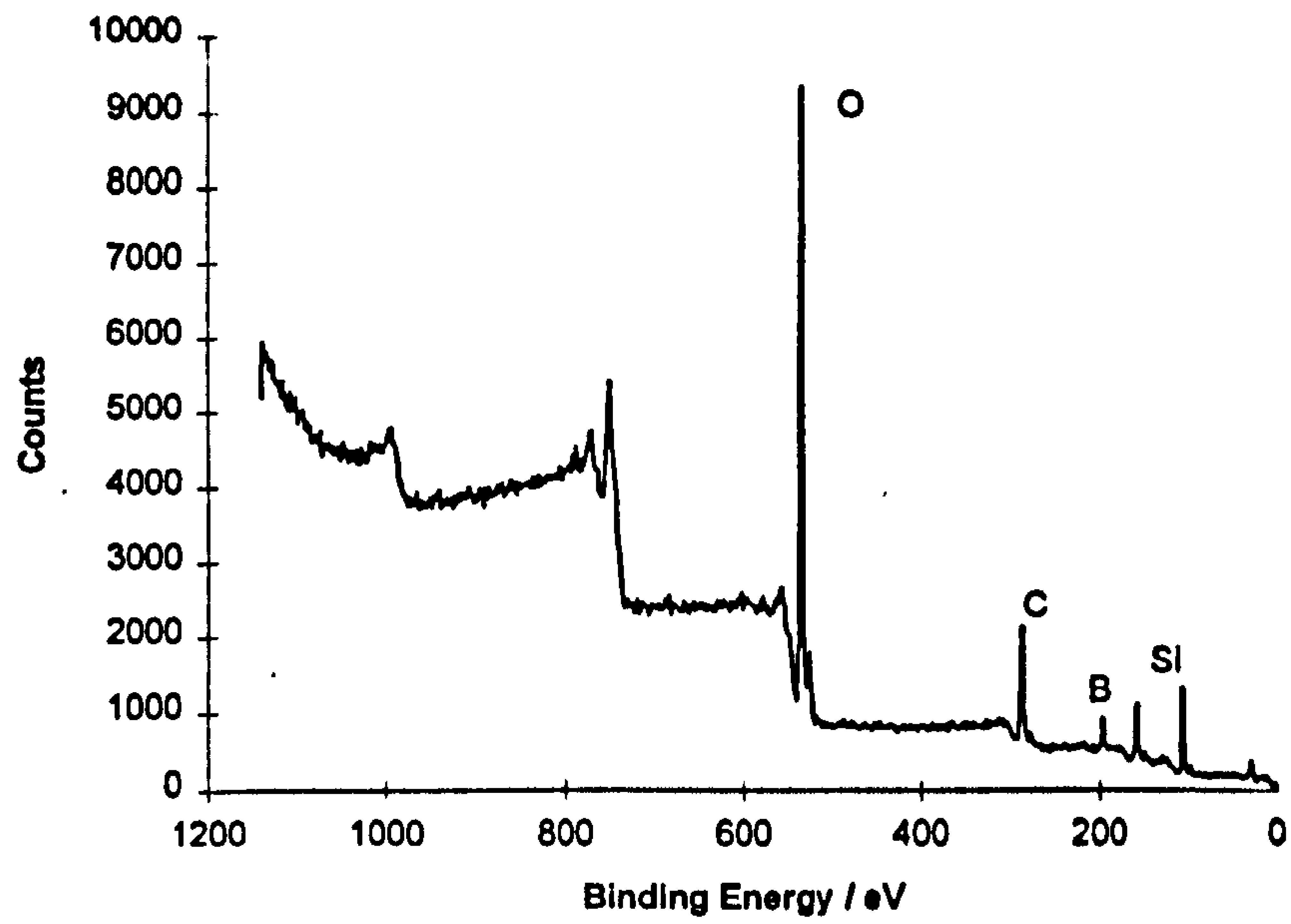

figure 4.27: XPS widescan trace of the product obtained on heating 2,4,6-tri-(para-carboranyl)-1,3,5-triazine to 1200°C

The peaks observed were attributable to oxygen (1s), carbon (1s), boron (1s) and silicon (2p). Unfortunately the elemental analysis of the product could not be accurately calculated, as it was unknown what percentage of the oxygen was attributable to the silica of the quartz plate or tape from which the measurement was recorded. The starting material contained C, H, N and B, but only C and B were seen in the final product. (Hydrogen cannot be measured by XPS.) No nitrogen was observed, indicating this had been eliminated, possibly as N_2, during the heating process.

Although prepared under a stream of argon, oxygen had obviously not been excluded, hence the large oxygen peak , and some boron oxides have probably formed. The presence of carbon suggested, however, that boron oxide was not the unique product. The carbon trace showed a "hump", indicative of bound carbon, possibly to boron. Boron was represented by a small peak.

In XPS, the peak heights are not indicative of the quantity of each element present, as various nuclei have varying sensitivities. The elemental composition of a sample can be obtained by the multiplication of peak area by the relative sensitivity. The relative sensitivities need to be calculated for each instrument, however our investigation was qualitative only. Generally sensitivities are in the order O (*c*.0.39) > C (1.00) > Si (*c*. 1.01) > B (*c*.1.96). (Carbon is given an arbitrary value of 1.00, oxygen is more sensitive, silicon and boron are less easily detected.)

This compound had all the elements present to form a ceramic material[73], although success has not been achieved here. The total exclusion of oxygen may have given a better material, and prevented the formation of boron oxides.

Experiments were also conducted on 2,4,6-tri-(*para*-carboranyl)-1,3,5-triazine at elevated temperature and pressure. Two experimental attempts were made, the first raised the temperature of the autoclave to 350°C and a pressure of 1000psi for 12hours, the second to 400°C and 900psi for 15 hours. (The melting point of the compound was 376°C.) No change in the compound was observed on either occasion. Graphite, which has a similar structure to the layered sheets of 2,4,6-tri-(*para*-carboranyl)-1,3,5-triazine is converted to diamond at 1000K and 10^4bar. If any linkage between layers of tri-carboranyl triazines were to occur, higher temperatures (presumably above the melting point of the compound) and pressures than those tried here, would be required.

4.6 EXPERIMENTAL DETAILS

Bis-ortho-carborane[1,3]

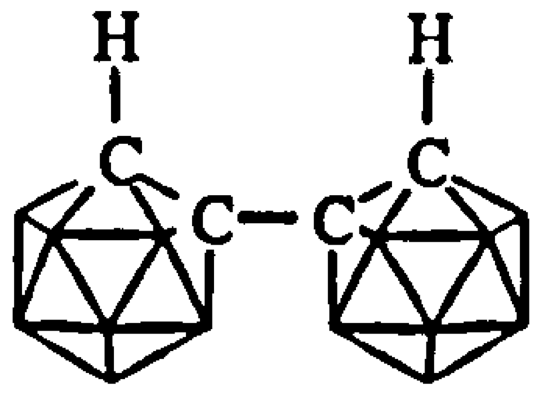

Following literature methods, decaborane DMS complex (26.84g, 0.1mol) in sodium dried toluene was reacted with diacetylene gas, produced from the hydrolysis of 1,4-dichloro-2-butyne (21.7g, 0.18mol) to give the crude product as a yellow solid. Washing with toluene and water, followed by filtration through an alumina column, left a white solid which yielded pure *bis*-carborane on recrystallisation from chloroform.

Yield: 5% *IR*: 3061 s (carboranyl C-H); 2682 m, 2647 m, 2603 s, 2580 s (carboranyl B-H); 1173 s; 1113 m; 1065 s; 1015 m; 1000 m; 905 w; 783 w; 726 s, 714 s (*bis*carboranyl stretch); 454 s cm^{-1} *m/z* (EI^+): 285 ($C_4B_{20}H_{22}$) *Elemental analysis* ($C_4B_{20}H_{22}$): C 15.74% (16.77%), H 8.01% (7.74%) *m.p.*: 320.7°C
NMR ($CDCl_3$)/ppm: ^1H: 1-4 (20H, br., carboranyl B-*H*); 3.81 (2H, carboranyl C-*H*); $^{13}C\{^1H\}$: 63.44 (d, $^1J_{C-H}$=194.5Hz, carboranyl *C*-H); 72.53 (carboranyl *C*); $^{11}B\{^1H\}$: 1.38 (2B, d, J_{BH}=153Hz), 0.71 (2B, d, J_{BH}=153Hz), -6.07 (4B, d, J_{BH}= 152Hz), -7.29 (8B, d, J_{BH}=159Hz), -9.39 (4B, d, J_{BH}=168Hz)

Reaction between di-lithio-*bis*-carborane and Dichloromethane

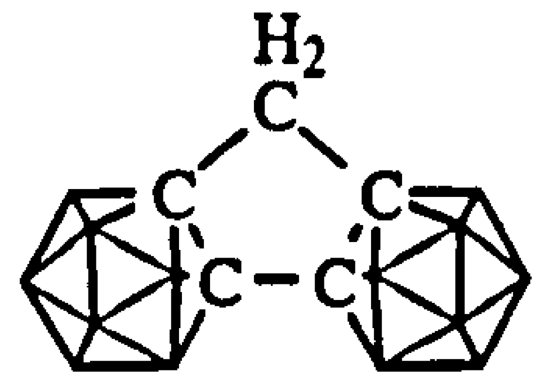

Bis-carborane (0.57g, 2mmol) was dissolved in DME (25mL) and the solution cooled to 0°C in an ice bath before the addition of a solution of n-BuLi (2.71M in hexanes, 1.5mL, 4mmol) to dilithiate the *bis*-carborane. The solution was left to warm slowly to room temperature before dry dichloromethane (0.13mL in 8.7mL DME) was added producing a dark orange solution over a period of three hours. The solution was stirred under a flow of nitrogen overnight. However, overnight the volume of solvent had dramatically decreased leaving a red air sensitive oil which analysed as the dilithium salt. The volume of solvent was increased by 25mL, a further 2mmol of dichloromethane were added and the reaction solution left to stir overnight. This did not further the reaction however, so the solution was refluxed for 24 hours. This resulted in a blood red solution from which the solvent was removed to yield a red oil.

The oil was found to be insufficiently soluble in ether, so instead was dissolved in chloroform, washed twice with distilled water (2 x 100mL) changing the red solution to yellow. The aqueous layers were reextracted with chloroform (2 x 100mL), the combined organic layers dried over anhydrous magnesium sulfate, filtered and the solvent removed leaving a brownish solid. *Bis*carborane did not run on TLC but the product showed one spot. Filtration through a silica column using 10% ethyl acetate in cyclohexane was carried out to isolate the product, and gave a white solid residue. Recrystallisation was tried (unsuccessfully) from cyclohexane but analysis of the residue suggested a bridged *bis*-carboranyl species has been formed.

<u>*Yield*</u>: 7% (crude) <u>*IR*</u>: 3061 m (carboranyl C-H); 2962 m, 2923 m, 2849 w (aliphatic C-H); 2652 m, 2580 s (carboranyl B-H); 1261 (not in *bis*-cb spec); 1097 s; 1071 s; 1019 s; 799 s (not in *bis*-Cb); 726 w, 715 m (*bis*-carboranyl doublet) cm^{-1} <u>*m/z*</u> (EI^+): 593 ($C_8B_{30}H_{32}Cl_4$), 298 ($C_5B_{20}H_{22}$, methylene-bridged-*bis*-carborane) and 286 ($C_4B_{20}H_{22}$), 139 <u>*Elemental analysis*</u> *(before recrystallisation)*($C_5B_{20}H_{12}$): C 24.70% (20.12%); H 8.24% (7.43%)

<u>*NMR*</u> ($CDCl_3$)/ppm: ^1H: 1-4 (br., carboranyl B-*H*); 2.71ppm (CH_2 bridge)

2-methyl-4,6-di-chloro-1,3,5-triazine[37]

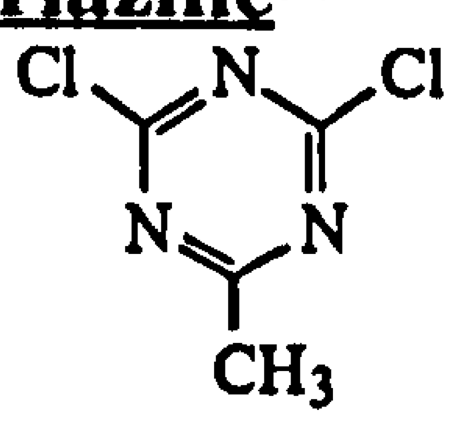

A solution of cyanuric chloride (3.69g, 20mmol) in sodium dried ether was prepared and cooled to 0°C in an ice bath before the addition of methyl magnesium bromide (3.0M in diethyl ether, 6.7mL, 20mmol). The resultant solution was allowed to warm slowly to room temperature and the yellow precipitate (MgBrCl) filtered off. The solvent was removed under reduced pressure to leave a yellow solid (3.18g) which analysed as the desired product.

Yield: 97% *IR:* 2963 w (methyl C-H); 2479 m; 2423 m; 2395 m; 2365 m; 2324 m; 2263 m; 1989 m; 1915 m; 1828 m; 1778 m; 1718 m; 1613 s (triazine CN); 1533 s; 1398 s; 1285 s; 1261 s; 1097 s; 1030 s; 999 s; 932 s; 919 s; 889 m; 883 m; 847 m; 578 m cm^{-1}
m/z (EI^+): 164 ($C_3N_3Cl_3$) *Elemental analysis* ($C_4H_3N_3Cl_2$): C 23.04% (29.30%), H 2.16% (1.84%), N 20.21% (25.63%), Cl 39.94% (43.25%) *m.p.*: 247°C

2-methyl -4,6-di-(2'-methyl-*ortho*-carboranyl)-1,3,5-triazine

1-methyl-*ortho*-carborane (0.80g, 5mmol) was dissolved in DME (25mL) and lithiated with a solution of butyl lithium (2.5M in hexanes, 2mL, 5mmol). After stirring for 20 minutes at room temperature under N_2, a cloudy, pale yellow solution was produced. This solution was cooled in an ice bath before the addition of a solution of 2-methyl-4,6-dichloro-1,3,5-triazine (0.41g, 2.5mmol) in DME (25mL) via canular transfer to give a green solution. As the solution warmed slowly to room temperature, a white precipitate (LiCl) dropped out of solution. The solution was filtered off under a dinitrogen atmosphere, giving a lime green solution which became dark red with the formation of a black oil in the base of the Schlenk tube as the solution accumulated. Agitating this solution under torchlight gave a bright orange solution. The solvent was removed under reduced pressure to leave a red oil and unreacted 1-methyl-*ortho*-carborane (0.14g) was removed by sublimation.

The remaining red oil was dissolved in diethyl ether, washed with distilled water, and the organic layer evaporated leaving an orange oil which was adsorbed onto silica and eluted with chloroform. Fractions 1-3 yielded a pale orange crystalline solid (0.75g) which analysed as the desired product.

Yield: 67% *IR*: 3062 s; 2962 s, 2919 s, 2849 s (methyl CH_3); 2593 s (carboranyl BH); 1948 w; 1853 w; 1646 m, 1625 m, 1527 s (triazine CN); 1345 m; 1262 m; 1202 w; 1096 s; 1015 s; 954 w; 938 w; 914 w; 865 m; 797 s; 720 s; 675 m; 658 m; 610 m; 586 w; 573 w; 534 w; 495 s cm^{-1} *Elemental analysis* ($C_{10}H_{29}B_{20}N_3$): C 29.69% (29.47%), H 6.99 % (7.17%), N 10.02% (10.31%)

2-methyl-4,6-di-(2'-phenyl-*ortho*-carboranyl)-1,3,5-triazine

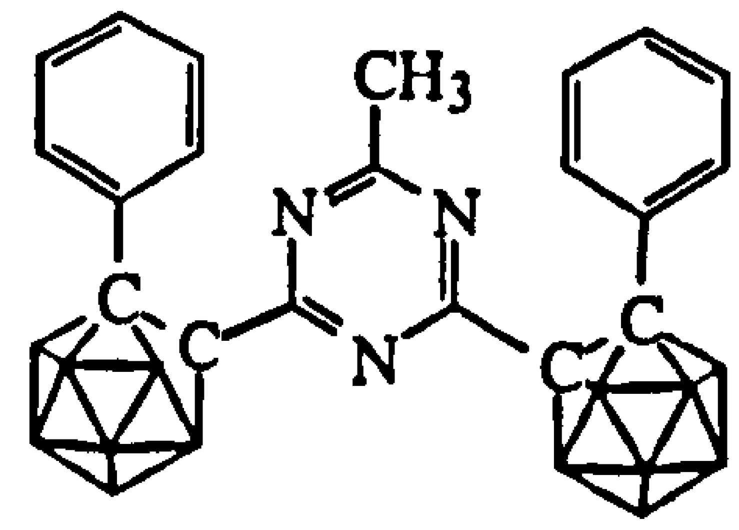

1-phenyl-*ortho*-carborane (1.10g, 5mmol) was dissolved in DME (20mL), cooled in an ice-bath, and lithiated with a solution of n-BuLi (2.5M in hexanes, 2mL, 5mmol). After 20 minutes the addition of a cooled suspension of 2-methyl-4,6-dichloro-1,3,5-triazine (0.41g, 2.5mmol) in DME (20mL) was attempted. However, the canular blocked easily so the lithiocarborane was added to the triazinyl solution giving a bright orange cloudy solution. The solution was left to stir at ambient temperature overnight, extracted with ether and washed with water. Solvent was removed from the combined organic layers to leave an orange solid, from which unreacted phenyl-*ortho*-carborane was sublimed (0.79g). Column chromatography (silica, 2:1 CH_2Cl_2:cyclohexane) of the unsublimed residue isolated the product as an orange oily solid (0.22g) in the first column fractions.

Yield: 9% *m/z* (EI^+): 549, 532 ($(PhC_2B_{10}H_{10})_3C_3N_3CH_3$), 220 ($C_6H_5CB_{10}H_{10}C$) *NMR* ($CDCl_3$)/ppm: ^1H: 7.4, 7.3 (m, phenyl CH), 4-1 (br., carboranyl BH), 2.39 (s, methyl CH_3); $^{13}C\{^1H\}$: 130.6, 128.6, 127.3 (phenyl CH), 84.5 (carboranyl C-phenyl), 80.5 (carboranyl C-triazine)

2,4-di-ethyl-6-chloro-1,3,5-triazine[50]

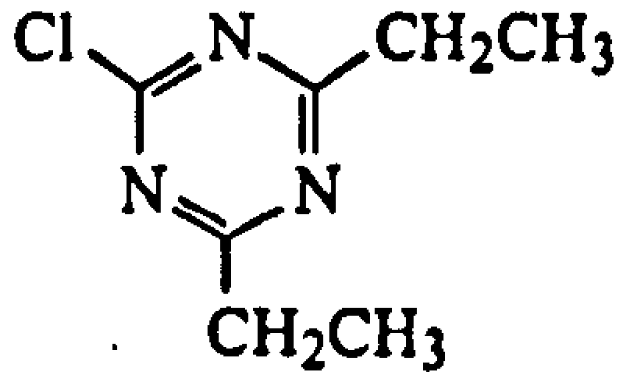

A solution of ethylmagnesium chloride in ether (23.3mL, 2M, 0.047mol) was added over a five minute period to a stirred solution of cyanuric chloride (2.15g, 0.017mol) in ethylene chloride (100mL) at *c.*-15°C. Stirring was continued at this temperature for 3 hours resulting in a dark red solution. Keeping the temperature below

-15°C, distilled water (7mL) was added dropwise. This was a vigorous reaction and the reaction solution MUST be kept cold. Anhydrous magnesium sulfate (6.5g) was added to the resultant yellow solution to form a "cake" which was left stirring overnight at room temperature. The solution was filtered and the magnesium sulfate washed with dichloromethane until the washings were colourless. The solvent was removed under reduced pressure from the filtrate leaving an orange oil which was extracted overnight into pentane using Soxhlet apparatus. The pentane was removed from the extracts leaving a yellow oil which was distilled under vacuum (55°C at 0.2mmHg) to give a cloudy yellow oil (0.33g) which analysed as a mixture of triazine products, including the desired product.

Yield: 0.10g (31.4% of distilled product), 4% *IR:* 3274; 3087; 2965 (ethyl C-H); 2183; 1948; 1712, 1632, 1536 (triazine C-N); 1378; 1306; 1257; 1161; 1107; 1068; 1003; 1003; 970; 954; 919; 886; 840; 816; 701; 525, 488, 441, 404 (C-Cl) cm^{-1}
NMR ($CDCl_3$)/ppm: ^1H: 6.13 (5H, br.), 2.90 (31H, m, ethyl CH_2), 1.76 (33H, m), 1.3 (53H, m, CH_3), 0.98(46H, m, CH_3)
GCMS: three products; mw=178, 57.8% ($C_5H_5N_3Cl_2$); mw=165, trace ($C_9H_{15}N_3$); mw=171, 31.4% ($C_7H_{10}N_3Cl$); mw=181, 4.9% (184=$C_3N_3Cl_3$)

1-phenyl-2-(3,5-di-chloro-2,4,6-triazinyl)-acetylene[56]

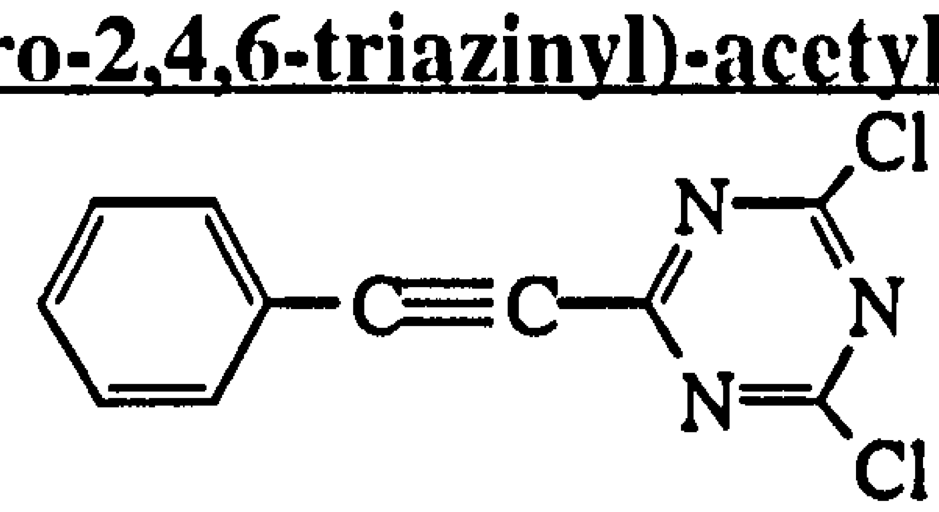

Phenylacetylene (5.5mL, 0.05mol) was added to a suspension of methylmagnesium bromide (3M in diethyl ether, 16.5mL, 0.05mol) in THF (25mL) cooled in ice. The resulting suspension was allowed to warm to room temperature. A solution of cyanuric chloride (9.22g, 0.05mol) in dry toluene (50mL) was prepared and cooled in an ice bath. The Grignard solution was poured into the cyanuric chloride solution producing a bright yellow solution instantly. The solution was warmed slowly to room temperature and with time became darker. Solvent was removed under vacuum *in situ*, the residue purified by column chromatography on silica (2:1 CH_2Cl_2:cyclohexane). The product was isolated as a yellow crystalline solid (4.21g, R_F=0.65).

Yield: 34% *IR:* 3096 w, 3064 w, 3034 w (phenyl C-H); 2964 w; 2219 s (acetylene CC); 1515 s, 1471 s, 1440 s (triazine C-N); 1403m; 1314 w; 1277 m; 1255 s; 1097 w; 1022 w; 976 w; 939 w; 901 w; 852 s; 799 s; 763 s; 679 s; 584 w; 566 m; 536 m; 507 w cm^{-1} m/z (EI^+): 284, 251 ($C_{11}H_5N_3Cl_2$), 183, 166, 153, 127, 100, 87 Elemental analysis ($C_{11}H_5N_3Cl_2$): C 41.16% (52.83%), H 2.15% (2.02%), N 16.18% (16.80%), Cl 28.48% (28.35%) m.p.: 118-123°C.

NMR($CDCl_3$)/ppm: ^{1}H: 7.69, 7.67 (2H, m, *meta* CH); 7.50, 7.41(3H, m, *ortho*, *para*-CH); $^{13}C\{^1H\}$: 170.79, 161.03 (triazinyl *C*-N); 132.48, 130.61, 127.76 (phenyl *C*-H), 118.30 (*ipso* C), 96.46, 84.69 (acetylene C)

Note - under UV compound was bright blue, as is the case for tolan derivatives PhCCPh.

reaction between 1-phenyl-2-(3,5-di-chloro-2,4,6-triazinyl)-acetylene and decaborane

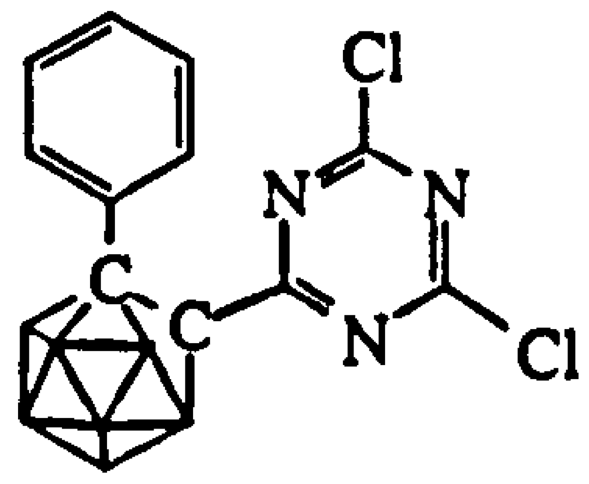

Decaborane (0.61g, 5mmol) was dissolved in acetonitrile (100mL) under a dry dinitrogen atmosphere and refluxed for three hours to give the acetonitrile adduct as a clear yellow solution. A solution of 1-phenyl-2-(3,5-dichloro-2,4,6-triazinyl)-acetylene (1.25g, 5mmol in 50mL CH_3CN) was added and the solution left to reflux for a further 3 days. Methanol (50mL) was added and the solution refluxed overnight to destroy unreacted decaborane. After cooling to room temperature, the solvent was removed *in situ* to leave an orange oil. Chromatography on silica (CH_2Cl_2:cyclohexane 1:1) yielded the product as a white crystalline solid. Analysis of this compound suggested the chlorine substituents on the triazine ring may have been hydrolysed to give the di-hydroxy derivative. Mass spectroscopy and elemental analysis showed the 2-(2'-phenyl-*ortho*-carboranyl)-4-chloro-6-hydroxy-1,3,5-triazine to be present, whilst solution state NMR suggested the compound was further hydrolysed to the di-hydroxy derivative in solution.

IR: 3094 w, 3060 w, 3010 w, 2952 w (phenyl C-H); 2650 m, 2617 s, 2597 s, 2568 s, 2554 s (carboranyl B-H); 1545 s, 1517 s (triazine CN); 1495 s; 1448 m; 1395 m; 1368 s; 1287 s; 1202 m; 1167 m; 1132 w; 1057 s; 1025 m; 931 w; 883 w; 831 m; 805 m; 770 m; 726 m; 691 s; 613 w; 583 w; 537 w; 498 w cm^{-1} m/z (EI^+): 364, 349 ($C_{11}B_{10}H_{16}N_3OCl$), 328, 313 ($C_{11}B_{10}H_{16}N_3O$) Elemental analysis

NMR/($CDCl_3$)/ppm: ^1H: 7.57 (d), 7.3 (m)(5H, phenyl C-*H*); 3.91 s (2H, s, O*H*); 4-0.8 (10H, br., carboranyl B-*H*)

2,4,6-tri-(*ortho*-carboranyl)-1,3,5-triazine

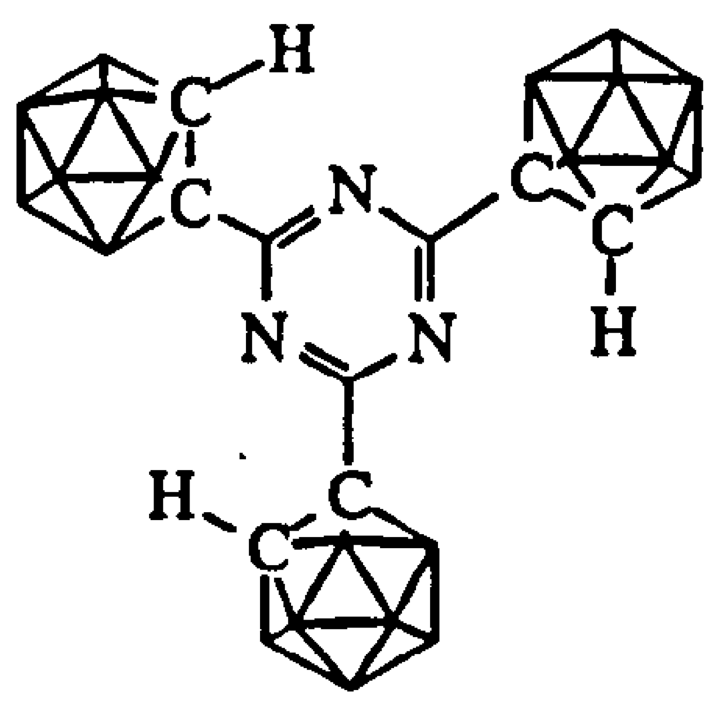

A solution of *ortho*-carborane (1.30g, 9mmol) in THF (50mL) was prepared and monolithiated with a solution of butyl lithium (2.38M in hexanes, 4mL, 9mmol) to give a clear colourless solution after 20 minutes at room temperature. This lithio-carborane solution was cooled in an ice bath before the addition of a solution of cyanuric chloride (0.55g, 3mmol in 25mL THF) via canular transfer to give a clear, deep green solution. The solvent was removed (to remove the solvent shell from LiCl) and the remaining green solid dissolved in diethyl ether (200mL), transferred to a separating funnel and washed with distilled water. The aqueous layer was re-extracted with diethyl ether, the combined organic layers dried over anhydrous magnesium sulfate, filtered and the solvent removed under reduced pressure to leave a yellow solid. Unreacted *ortho*-carborane was sublimed out (0.22g) leaving a yellow powder which was purified by column chromatography on silica (1:1 cyclohexane:dichloromethane). The named product (R_F= 0.14), was isolated as a white powder (0.22g) and the remaining products removed from the column with with ethanol.

Yield: 14% *IR:* 3069 s (carboranyl C-H); 2962 ; 2924 ; 2849 w; 2597 s (carboranyl B-H); 1531 s (triazine C-N); 1493 s ; 1456 w; 1379 s; 1261 s; 1213 w; 1101 s; 1014 s; 985; 904 w; 800 s; 713 s; 615 w cm^{-1} *m/z*(EI^+): 507 ($C_9H_{33}B_{30}N_3$); 437; 382; 366 ($C_7H_{22}B_{20}N_3$); 337; 295; 221; 209; 169; 143 ($C_2H_{11}B_{10}$) *m.p.*: >400°C
NMR ($CDCl_3$)/ppm: ^1H: 4.43 (carboranyl CH), 3.8-0.8 (br., carboranyl BH); $^{13}C\{^1H\}$: 160.41 (triazine CN), 55.11 (carboranyl CH); $^{11}B\{^1H\}$: 0.73 (2B, d, J_{BH}=149Hz), -4.84 (1B, br.), -6.13 (1B, d, J_{BH}=149Hz), -8.10 (2B, br.), -10.60 (2B, d, J_{BH}=*c*.130Hz), -11.71 (2B, d, J_{BH}=*c*.228Hz)

2,4,6-tri-(2'-methyl-*ortho*-carboranyl)-1,3,5-triazine

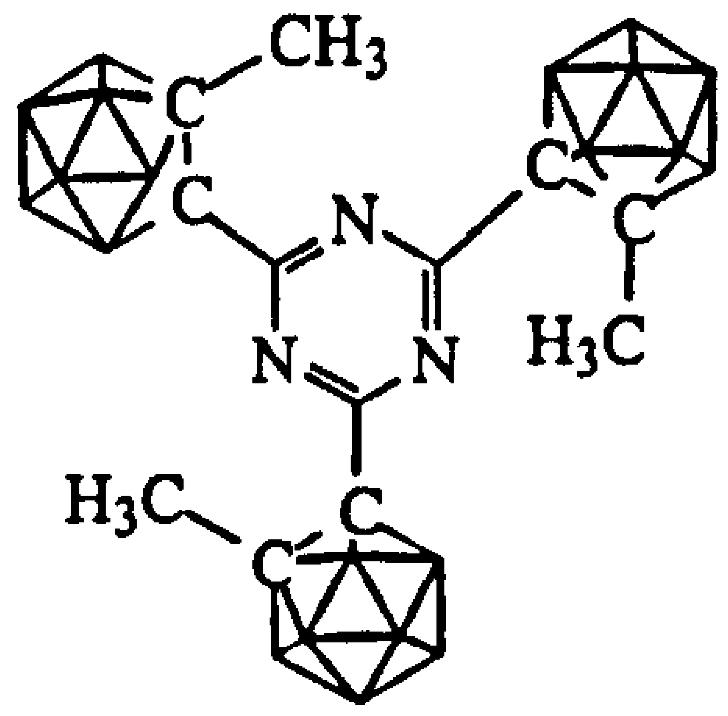

1-methyl-*ortho*-carborane (0.95g, 6mmol), dissolved in DME (30mL) and cooled to 0°C in an ice-bath, was lithiated with a solution of n-butyl lithum (2.5M in hexanes, 2.4mL, 6mmol), and combined with cyanuric chloride (0.37g, 2mmol) in DME to give a deep blue solution instantly. On warming to room temperature the solution became orange. The solution was washed with distilled water to remove LiCl, and the organic layer evaporated to leave an orange solid. This was extracted into benzene yielding an analytical sample of pure, white 2,4,6-tri-(2'-methyl-*ortho*-carboranyl)-1,3,5-triazine. It was considerably less soluble than its phenyl analogue, being soluble in boiling pyridine and sparingly soluble in chloroform and benzene.

Yield: 19% IR: 2963 s (methyl C-H); 2926 m; 2856 w; 2590 s (carboranyl B-H); 1529 s (triazine C-N); 1445 w; 1365 m; 1261 s; 1095 s; 1018 s; 856 m; 800 s; 720 m; 609 w; 468 w cm^{-1} m/z (EI$^+$): 549 ($C_{12}H_{39}B_{30}N_3$) Elemental analysis($C_{12}H_{39}B_{30}N_3$): C 27.08% (26.25%), H 7.23% (7.16%), N 6.24% (7.65%) m.p.:166-167°C
NMR (C_6D_6)/ppm: $^1H\{^{11}B\}$: 3.15 (1H, carboranyl BH), 2.90 (1H), 2.82 (2H), 2.62 (4H), 2.48 (2H), 1.35 (br.), 1.33 (br.), 1.28 (methyl C-*H*), 0.909 (br.); $^{11}B\{^1H\}$: 3.68 (1B, d, J_{BH}=147Hz, B12, antipodal to $C_3N_3(CbMe)_2$), -1.09 (1B, d, J_{BH}=155Hz, B9, antipodal to methyl), -5.55 (8B, d, J_{BH}=146.5Hz, B3-8, B10-11)

2,4,6-tri-(2'-phenyl-*ortho*-carboranyl)-1,3,5-triazine

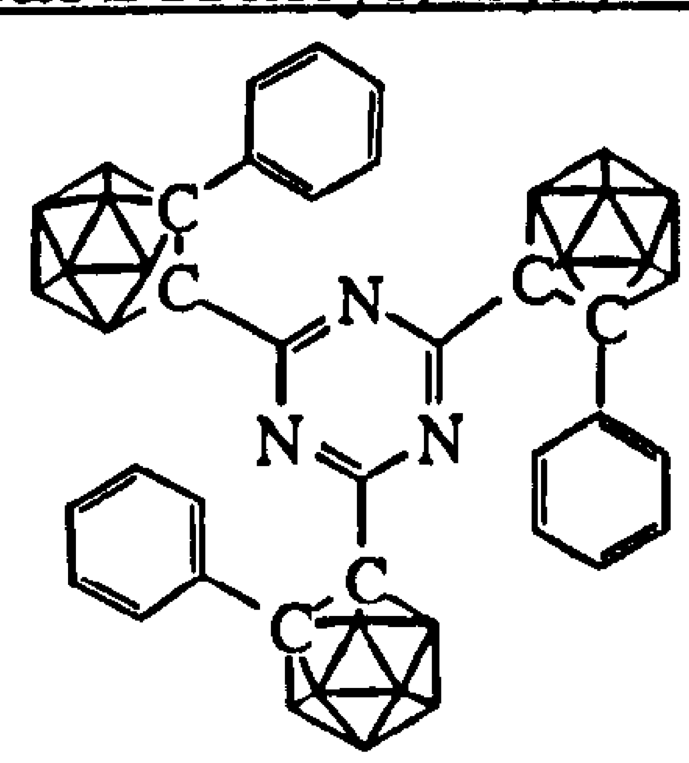

1-phenyl-*ortho*-carborane (1.32g, 6 mmol) was dissolved in DME (50mL) and lithiated with a solution of n-butyl lithium (2.38M in hexanes, 2.4mL, 6mmol). This solution of lithiocarborane was cooled in an ice-bath and a solution of cyanuric chloride (0.37g, 2mmol in 30mL DME) added via canular transfer. The reaction mixture was allowed to warm slowly to room temperature giving a white precipitate and a clear yellow solution. The precipitate was removed by filtration, washed with distilled water to remove LiCl, and the remaining solid recrystallised from *ortho*-dichlorobenzene giving clear, colourless square plate-like crystals.

Yield: 68% *IR*: 3062 m, 3044 m, 3028 m (phenyl C-H); 2666 m, 2654 s, 2633 s, 2592 s, 2576 s, 2554 s (carboranyl B-H); 1582 m, 1522 s (triazine C-N); 1446 s; 1361 s; 1250 m; 1152 m; 1107 m; 1065 s; 1024 m; 1001 m; 929 m; 887 m; 809 w; 789 m; 754 s; 729 s; 719 s; 699 m; 686 s; 610 s cm^{-1} *m/z*(EI^+): 736 ($C_{27}H_{45}B_{30}N_3$); 489 ($C_{18}H_{30}B_{20}N_2$); 244 ($C_9H_{15}B_{10}N$) *Elemental analysis*($C_{27}H_{45}B_{30}N_3$): C 43.12% (44.06%), H 6.02% (6.16%), N 5.47% (5.71%) *m.p.*: 313.5-315.5°C

NMR($CDCl_3$)/ppm: ^1H: 7.4 (1H, m, phenyl*para*CH), 7.2 (2H, m, phenyl*meta* or *ortho CH*), 7.1 (2H, m, phenyl *o* or *m* CH), 3.5-1.0 (10H, br., carboranyl B-*H*); $^1H\{^{11}B\}$: as before, with BH region 2.95 (2H, s), 2.45 (1H, s), 2.40 (1H, s), 2.30 (2H, s), 2.20 (2H, s), 1.98 (2H, s); $^{13}C\{^1H\}$: 167.16 (triazine *C*-N), 130.89, 130.42, 129.63, 128.75 (phenyl *C*-H, *ipso* C); $^{11}B\{^1H\}$: -0.33 (1B, d, J_{BH}=130Hz, antipodal to $C_3N_3(CB_{10}H_{10}CPh)_2$), -3.19 (1B, d, J_{BH}=113Hz, antipodal to phenyl), -9.93 (8B, d, J_{BH}=113Hz, B3-B8, B10-B11)

NMR(d_8 THF)/ppm: $^{13}C\{^1H\}$: 169.51 (triazine *C*-N); 133.53, 132.89, 131.79, 131.34 (phenyl *C*-H), (*ipso* C); 87.58 (carboranyl *C*-C_3N_3), 81.53 (carboranyl *C*-phenyl); $^{11}B\{^1H\}$: 4.974 (1B, antipodal to $C_3N_3(CB_{10}H_{10}CPh)_2$), 2.087 (1B, antipodal to phenyl), -4.593 (8B)

reaction between dilithio-*ortho*-carborane and cyanuric chloride (1:2 ratio)

Ortho-carborane (0.72g, 5mmol) was dissolved in DME (50mL) and dilithiated with a solution of n-BuLi (2.38M in hexanes, 5mL, 12mmol). A cloudy white solid mass formed, so toluene (25mL) was added to fluidise the solution. After 30 minutes, this solution was added to a solution of cyanuric chloride (1.94g, 11mmol) in DME (50mL) to give an orange solution and precipitate. The reaction was allowed to proceed at room temperature for *c.*1 hour, then the product was extracted into dichloromethane and ether, and washed with water. The organic layers and precipitate were combined and purification attempted by column chromatography (CH_2Cl_2). Fractions 1-3 (R_f=0.78) yielded a pale yellow carborane containing product (0.39g).

IR: 2963 w; 2606 m (carboranyl BH); 1543 s, 1509 s (triazine CN); 1263 s (carborane cage); 1097 s, 1019 s, 930 w, 849 m, 801 s, 715 w cm^{-1}

NMR ($CDCl_3$)/ppm: ^{1}H: 4-1 (br., carboranyl BH), no carboranyl CH peaks

reaction between dilithio-*meta*-carborane and cyanuric chloride (2:1 ratio)

1,7-*bis* -(3,5-di-chloro-2,4,6-triazinyl)-*meta*-carborane

Meta-carborane (0.76g, 5.3mmol) was dissolved in DME(30mL) and dilithiated with a solution of butyl lithium (2.38M in hexanes, 5mL, slight excess) to give a clear colourless solution after stirring for 20 minutes at room temperature. This solution was cooled in an ice bath, then a solution of cyanuric chloride (1.96g, 10.6mmol in 40mL DME) added via canular transfer to give an orange precipitate. The product was assumed to be air stable, so the solution was diluted with diethyl ether (50mL) and washed with distilled water. This gave a peach solid at the organic/aqueous interface which was filtered off. The solid was dried overnight under vacuum leaving a yellow insoluble solid (1.18g) which contained 1,7-*bis* -(3,5-di-chloro-2,4,6-triazinyl)-*meta*-carborane.

Yield: 81% *IR:* 3409; 3219; 2960; 2874; 2611 (carboranyl B-H); 1734; 1653; 1635; 1616; 1558, 1526 (triazine C-N); 1458; 1355; 1286; 1160; 1057; 1018; 879; 855; 813; 757; 720; 617 cm^{-1} *m.p.*: >400°C

NMR (solid state)/ppm: ^{1}H: 6.78, 4.93, 8 - 0 (br., carboranyl B-*H*); ^{13}C: 171.14 (triazine *C*-Cb), 142.20 (weak, broad - triazine *C*-Cl), 77.61 (carboranyl *C*-triazine), 56.02, 41.09, 25.98, 13.77 (all weak signals); ^{11}B: -15.41 (carboranyl *B*-H)

reaction between dilithio-*para*carborane and cyanuric chloride (1:2 ratio)

Para-carborane (0.36g, 2.5mmol) was dissolved in DME (50mL) and dilithiated with a solution of n-BuLi (2.38M in hexanes, 2.4mL, 6mmol). After 30 minutes, this solution was added to a solution of cyanuric chloride (1.06g, 6mmol) in DME (25mL) via canular transfer. Unlike other reactions between lithiocarboranes and cyanuric chloride, the reaction did not appear to be exothermic. After stirring at room temperature overnight, the compound was extracted into ether and washed with water. The product was not very soluble in ether, and a cloudy organic layer resulted. The solvent was removed to leave a pale yellow carborane containing solid (1.27g).

IR: 3124 w; 3080 w; 2961 w; 2626 s (carboranyl BH); 1718 w; 1508 s (triazine CN); 1357 s (triazine CN); 1261 s (carborane); 1166 w; 1099 m, 1059 m, 1018 m (carborane); 921 w; 850 m; 804 m; 713 m
NMR ($CDCl_3$)/ppm: ^{1}H: 4-1 (carboranyl BH)

2,4,6-tri-(*meta*-carboranyl)-1,3,5triazine*

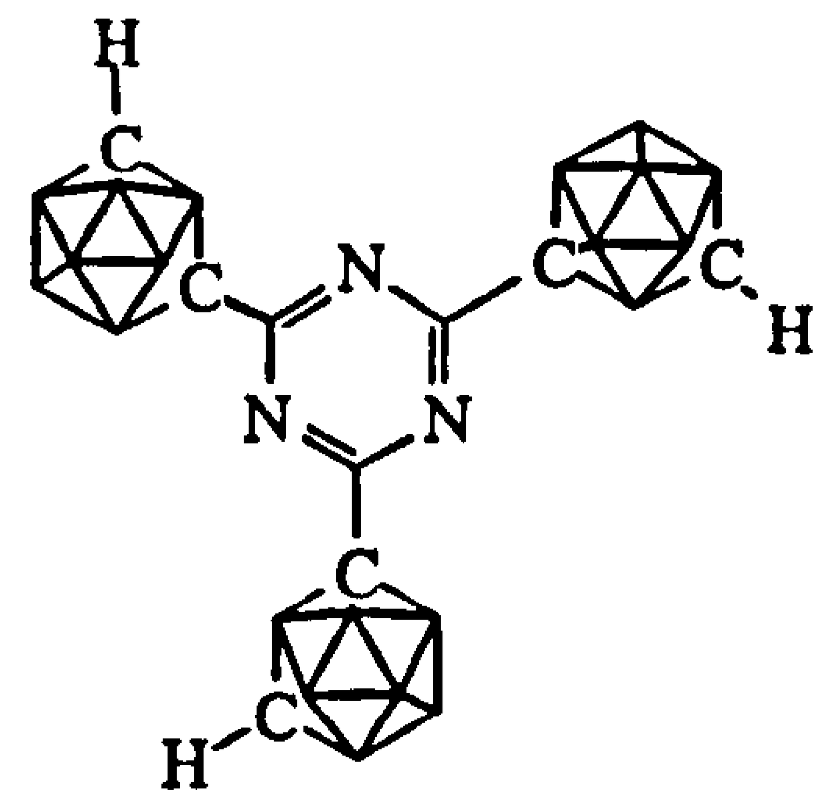

A solution of *meta*-carborane (0.58g, 4mmol) in DME (40mL) was monolithiated with a solution of n-butyl lithium (2.38M in hexanes, 2.0mL, 4.7mmol). After stirring for 20 minutes at room temperature, the solution was cooled in an ice-bath and a solution of cyanuric chloride (0.37g, 2mmol) in DME (20mL) added via canular transfer. An off-white precipitate in a clear colourless solution formed instantly. The reaction mixture was warmed to room temperature, diluted with THF and diethyl ether, then washed with distilled water to remove LiCl. The precipitate formed in the reaction was insoluble, and formed a layer at the organic/aqueous interface. The aqueous layer was isolated and discarded. The solid and the organic washings were combined and the solvents removed to leave the product as a pale yellow powder.

Yield: 90% IR: 3419 w br.; 3213 w; 3065 w (carboranyl C-H); 2961 m; 2609 s (carboranyl B-H); 1734 w; 1718 w; 1531 s (triazine CN); 1360 s; 1260 m; 1161 w; 1071 m; 1024 m; 932 w; 910 w; 879 w; 855 w; 808 m; 721 m; 691 w; 619 w; 538 w cm^{-1} m/z (EI$^+$): 507 ($C_9H_{33}N_3B_{30}$) Elemental Analysis ($C_9H_{33}B_{30}N_3$): C 23.59% (21.29%), H 5.78% (6.55%), N 8.54% (8.28%) m.p.: >400°
NMR (solid state)/ppm: ^{1}H: 4.57 (carboranyl C-*H*); 5 - 0 (br. carboranyl B-*H*); $^{13}C\{^{1}H\}$: 170.94 (triazine *C*N); 70.10 (carboranyl *C*-triazine); 55.68 (carboranyl C-H); $^{11}B\{^{1}H\}$: -7.17 (2B), -10.85 (2B), -13.51 (4B), -17.25 (2B); ^{15}N: -102.13

*Cyanuric Acid

As with the other triazinyl-carborane syntheses, the tri-substituted triazine was the favoured reaction product from the reaction between cyanuric chloride and lithio-carborane (see main text). This product was also produced when the cyanuric chloride:carborane ratio was 1:1 and 1:2. Unreacted carborane was recovered by sublimation and the cyanuric chloride converted to cyanuric acid (in equilibrium with its keto tautomer) during the aqueous work-up.

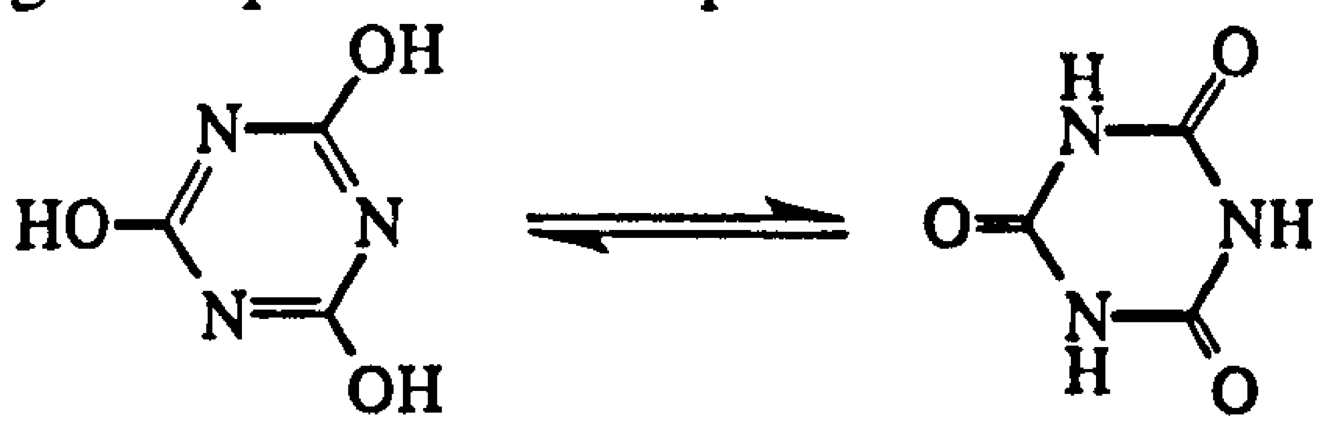

IR: 3500 - 2400 br. (OH); 1779 s, 1753 s, 1721 s (C=O), 1464 s, 1397 s (CN); 1052 m; 845 w; 773 m; 691 w; 535 s; 446 w; 411 m cm^{-1} m/z (EI+): 129 ($C_3H_3N_3O_3$) Elemental Analysis($C_3H_3N_3O_3$): C 27.01% (27.92%), H 2.48% (2.34%), N 30.74% (32.55%) m.p.: 390-392°C

1,7-di-deutero-*meta*-carborane

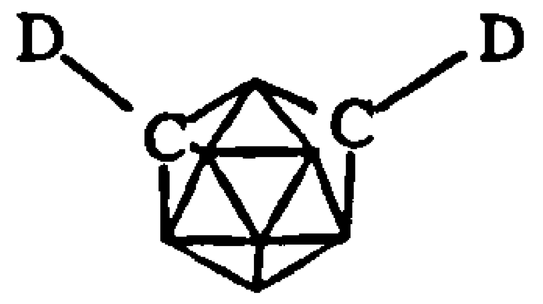

Meta-carborane (1.46g, 10mmol) was dilithiated with a solution of n-BuLi (2.59M in hexanes, 12mL, 31mmol) in ice-cooled DME (30mL). After warming to room temperature and stirring for 2 hours, a cloudy gelatinous white solution was formed. D_2O (5mL, 250mmol) was added causing the deuterated carborane to precipitate. The product was extracted into ether and washed with distilled water. The organic layer was dried over anhydrous magnesium sulfate, filtered and the solvent removed to leave the product as a white powder (1.23g).

Yield: 84% IR: 2602 s (carboranyl BH); 2287 (carboranyl CD); 1261 s; 1081 s; 1036 s; 973 s; 957 w; 941 m; 916 s; 865 w; 841 s; 802 s; 733 s; 701 s; 651 w cm^{-1} Elemental analysis($C_2H_{10}D_2B_{10}$): C 17.59% (16.44%), H 8.32% (8.21%)

2,4,6-tri-(1'-d-*meta*-carboranyl)-1,3,5-triazine

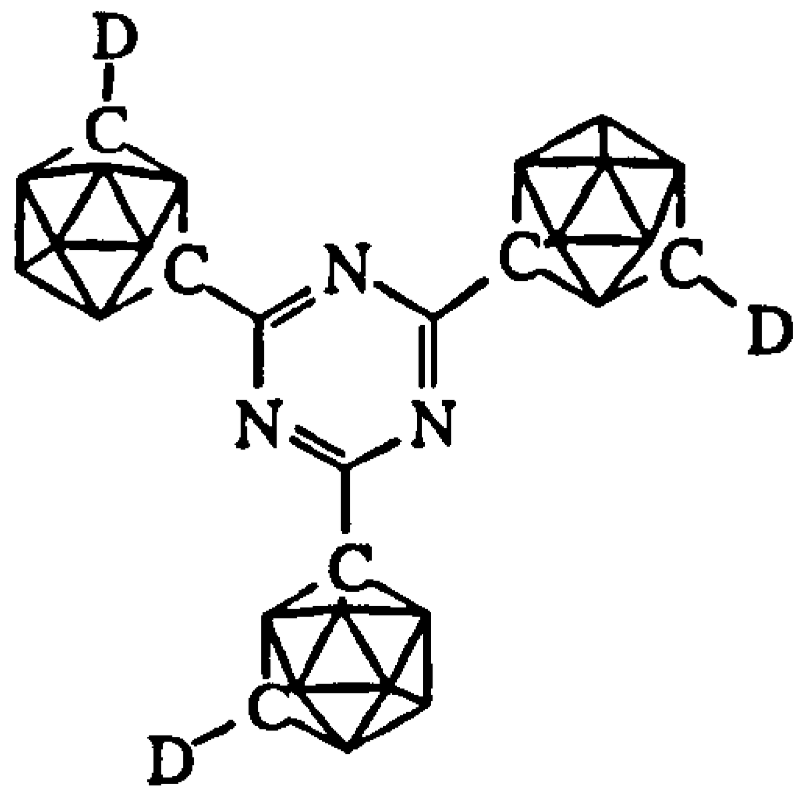

Deutero-*meta*-carborane (0.87g, 6mmol) was monolithiated in DME (40mL) with a solution of n-BuLi (2.59M in hexanes, 3.0mL, 7.8mmol) and left to equilibrate for 1 hour at room temperature. This solution was then cooled in an ice-bath and a solution of cyanuric chloride (0.38g, 2mmol) in DME (10mL) added by means of canular transfer. A bright yellow precipitate was instantly formed which became deep green at full addition of the triazine to the lithiocarborane solution. Stirring overnight at room temperature produced no change in the appearance of the solution. The solution was diluted with ether, then washed with water. The product remained as an insoluble precipitate at the interface and was isolated by filtration. Repeated washing with ether and water removed impurities to leave the product as a pale yellow solid.

Yield: 95%; *IR*: 3421 m, br. (trapped solvent); 2960 w; 2932 w, 2874 w; 2609 s (carboranyl BH); 2295 w (carboranyl CD); 1528 s, 1457 w, 1359 s (triazine CN); 1161 w; 1021 w; 855 w; 815 w; 722 m; 618 w cm^{-1} *m/z*(EI$^+$): 368 ($C_7B_{20}N_3H_{20}D_2$)

2,4,6-tri-(7'-phenyl-*meta*-carboranyl)-1,3,5-triazine

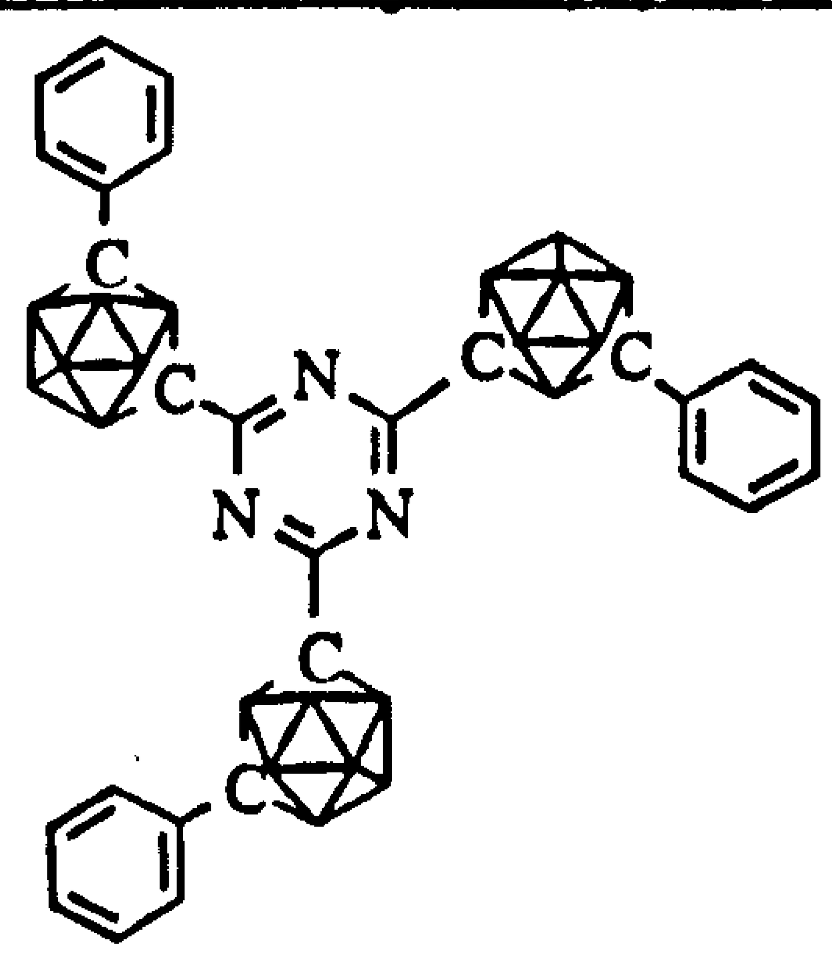

1-phenyl-*meta*-carborane (0.26g, 1.1 mmol) was dissolved in DME (40mL) and lithiated with a solution of n-butyl lithium (2.38M in hexanes, 0.6mL, 1.4mmol). This solution of lithio-carborane was then cooled in an ice-bath and a solution of cyanuric chloride (0.07g, 0.07mmol in 20mL DME) added via canular transfer. The reaction mixture was allowed to warm slowly to room temperature giving a clear green solution. On exposure to air, this became a pale yellow solution. Diethyl ether (100mL) was added to dilute the solution and the organic layer washed with distilled water to remove lithium chloride, then dried over anhydrous magnesium sulfate. Evaporation of the organic layer left a white solid which identified as the desired product.

Yield: 60%; *IR*: 3092 w, 3056 w (phenyl C-H); 2655 w, 2609 s, 2596 s, 2574 s (carboranyl B-H); 1527 s (triazine C-N); 1496 s; 1447 s; 1365 s; 1159 w; 1067 w; 1021 w; 866 w; 805 w; 742 s; 725 s; 689 s; 661 w; 611 w cm^{-1} *m/z* (EI$^+$): 735 ($C_{27}H_{45}N_3B_{30}$); 514 ($C_{19}H_{30}N_3B_{20}$); 297 ($C_{11}H_{15}N_3B_{10}$); 222 ($C_5H_{11}N_3B_{10}$); 219

($C_8H_{15}B_{10}$) Elemental analysis($C_{27}H_{45}B_{30}N_3$): C 42.75% (44.06%), H 6.32% (6.16%), N 5.24% (5.71%) m.p.: 212.2°C

NMR($CDCl_3$)/ppm: ^{1}H: 7.45 (2H, m, phenyl CH), 7.31, (3H, m, phenyl C-*H*), 4.2 - 1.1 (10H, br., carboranyl B-*H*); $^{13}C\{^1H\}$: 170.45 (triazine C); 134.61 (*ipso* C); 128.95, 128.50, 127.79 (phenyl C); 78.68, 75.43 (carboranyl C); $^{11}B\{^1H\}$: -4.12 (1B, d, J_{BH}=154Hz), -6.32 (1B, d, J_{BH}=126Hz), -10.35 (6B, d, J_{BH}=145Hz), -13.50 (2B, d, J_{BH}=163Hz)

2,4,6-tri-(*para*-carboranyl)-1,3,5-triazine*

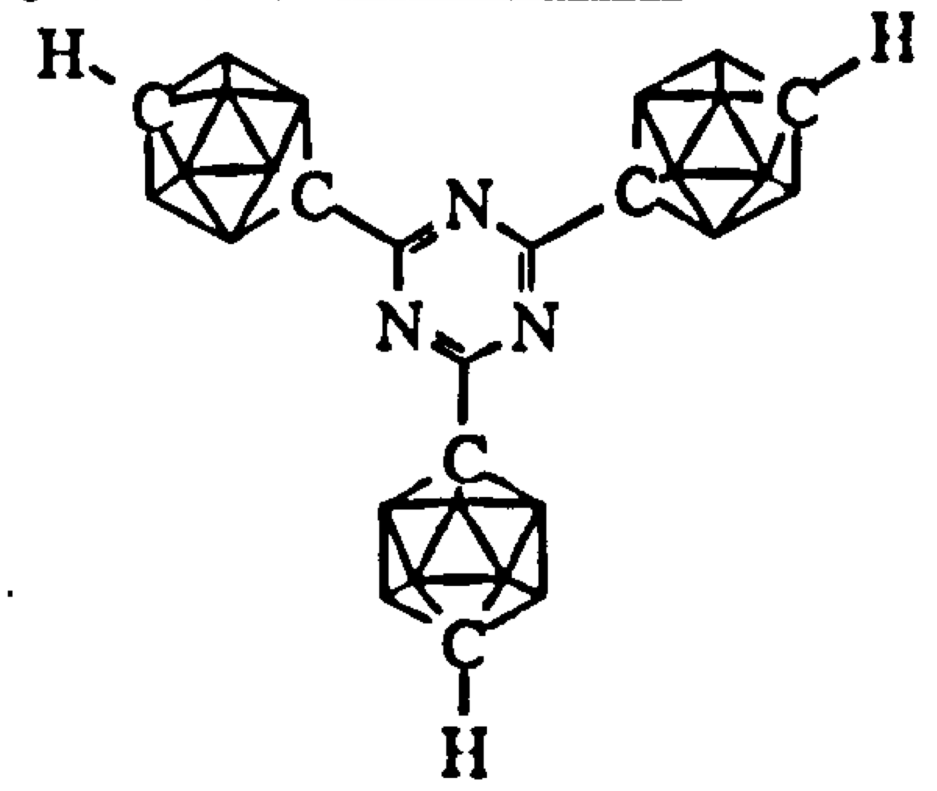

A solution of monolithio-*para*-carborane was prepared from the reaction between *para*-carborane (0.88g, 6mmol) in DME (40mL) and n-BuLi (2.38M in hexanes, 2.52mL, 6mmol). After stirring at ambient temperature for 30 minutes, the solution was cooled in an ice-bath and a solution of cyanuric chloride (0.56g, 3mmol) in DME (30mL) added via canular transfer. This immediately produced a green solution which, upon stirring, became a pale yellow solution and flocculant white solid. Once the solution had warmed to room temperature, diethyl ether (50mL) was added, and the mixture washed with distilled water. The product was present as a suspension throughout the aqueous and organic phases and was isolated by means of filtration. A white spongy solid resulted which was dried to leave a white powdery solid. This compound was insoluble in all readily available solvents.

Yield: 87% IR: 3420 br. m (trapped solvent/ N···H interactions); 3065 w (carboranyl C-H); 2614 s (carboranyl B-H); 1734 w; 1654 w; 1527 s (triazine CN); 1458 w; 1361 s; 1273 m; 1166 m; 1091 w; 1059 w; 1013 w; 712 s cm^{-1} m/z (EI$^+$): 506 ($C_9B_{30}H_{30}N_3$), 143 ($C_2B_{10}H_{11}$) Elemental analysis ($C_9H_{33}B_{30}N_3$): C 20.24% (21.32%), H 5.21% (6.56%), N 8.29% (8.54%) m.p.: 375.5°C

NMR(solid state)/ppm: ^{1}H: 4.37 (carboranyl C-*H*), 2.42 (carboranyl B-*H*); ^{13}C(protonated): 63.43 (carboranyl *C*-H); ^{13}C (non-protonated): 171.14 (triazine *C*); 82.78 (carboranyl *C*-$C_3N_3Cb_2$); ^{11}B: -13.26 (5B), -14.59 (5B)

* As noted for the instance of *meta*-carborane earlier, this product was the result of the reaction between lithiocarborane and cyanuric chloride in the ratio 1:1, 2:1 or 3:1. Lithiocarborane:cyanuric chloride used in the ratio 2:1 (as in this prep.) gives the cleanest reaction. Excess carborane was recovered by sublimation, and unused cyanuric chloride was converted to cyanuric acid.

1,12-di-deutero-*para*-carborane

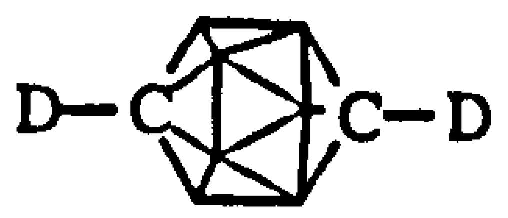

Para-carborane (1.44g, 10mmol) was dissolved in DME (60mL) and lithiated with a solution of n-BuLi (2.38M in hexanes, 9.5mL, 23mmol) giving a cloudy white suspension. After stirring at room temperature for 30minutes D_2O (2mL, 0.1mol) was added and the white precipitate which resulted extracted into diethyl ether. The organic layer was dried over anhydrous magnesium sulfate, filtered, and the solvent removed to give a white powder (1.38g).

Yield: 94% *IR*: 2606 s (carboranyl B-H); 2283 s (carboranyl C-D); 1261 s; 1083 s; 1017 s; 926 m; 866 w; 831 s; 813 s; 731 s; 711 s; 690 s cm^{-1} *m/z* (EI$^+$): 145 *m.p.*: 204-205°C *Elemental analysis* ($C_2H_{10}D_2B_{10}$) C 16.75% (16.43%), H 8.10% (6.89%)
NMR ($CDCl_3$)/ppm: $^1H\{^{11}B\}$: 2.18 (2H/D, s, carboranyl C-*D*; 3.0-1.0 ppm (10H, br., carboranyl B-*H*); $^{11}B\{^1H\}$: -11.71 (d, J_{BH}= 167Hz)

2,4,6-tri-(12'-d-*para*-carboranyl)-1,3,5-triazine

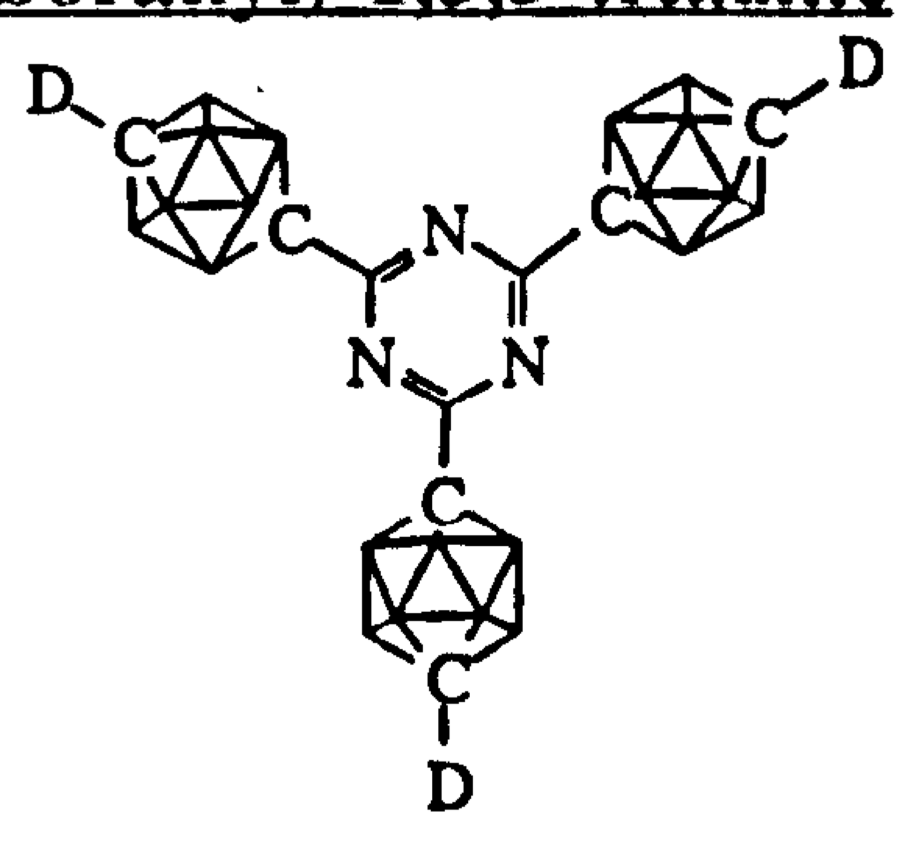

Deutero-*para*-carborane (0.44g, 3mmol) was dissolved in DME (25mL) and monolithiated with a solution on n-BuLi (2.38M in hexanes, 1.5mL, 3.6mmol). After 20 minutes equilibration at room temperature, the clear yellow solution was cooled in an ice bath and a solution of cyanuric chloride (0.20g, 1mmol) in DME (20mL) added via canular transfer. The white precipitate which formed on reaction of these two compounds was isolated by filtration, washed with distilled water to remove LiCl and then with diethyl ether to remove unreacted carborane. As with *para*-carborane, the product was a spongy solid which was dried under vacuum to give a white powdery solid. This compound was insoluble in all readily available solvents.

Yield: 115% (trapped solvent in lattice) *IR*: 3446 br. m (trapped solvent); 2963 w; 2626 s (carboranyl B-H); 2520 w (carboranyl C-D); 1559 m, 1527 s (triazine CN); 1362 s; 1261 w; 1165 w; 1109 w; 1055 w; 1013 w; 852 w; 804 w; 711 s cm^{-1}

Reaction between 2,4,6-tri-(*para*-carboranyl)-1,3,5-triazine and methyl iodide

2,4,6-tri-(*para*-carboranyl)-1,3,5-triazine (0.10g, 0.2mmol) was suspended in DME and a solution of n-BuLi (2.59M in hexanes, 0.75mL, 2mmol) added. Heating this solution to the reflux temperature for 48 hours yielded a deep orange cloudy solution. This solution was cooled to room temperature, then to 0°C before the addition of methyl iodide (0.25mL, 3.2mmol). Refluxing this solution for a further 2 days gave a pale orange cloudy solution. The solution was then diluted with dichloromethane and washed with water. The aqueous layer was isolated and the remaining residues combined and reduced to leave a sandy yellow solid. Analysis of this solid suggested the 2,4,6-tri-(*para*-carboranyl)-1,3,5-triazine was unreacted.

Reaction between 2,4,6-tri-(*para*-carboranyl)-1,3,5-triazine and 1-iodo-butane

The above reaction was repeated for 2,4,6-tri-(*para*-carboranyl)-1,3,5-triazine, lithiated with n-BuLi, and 1-iodo-butane. The carborane was recovered unreacted.

Reaction between 2,4,6-tri-(*para*-carboranyl)-1,3,5-triazine and benzenesulfonyl fluoride

2,4,6-tri-(*para*-carboranyl)-1,3,5-triazine (0.38g, 0.5mmol) was suspended in THF (35mL) and a solution of n-BuLi (2.59M in hexanes, 0.9mL, 2mmol) added. Heating this solution to the reflux temperature for 2 hours yielded a deep orange cloudy solution. Benzene sulfonyl fluoride (0.2mL, 1.9mmol) was added and the reflux continued for a further 48 hours. The final solution was pumped to dryness to remove the solvent shell from the LiCl, then suspended in dichloromethane and ether. This organic suspension was washed with water and left overnight to settle. The aqueous layer was isolated as was the solid at the interface (unreacted 2,4,6-tri-(*para*-carboranyl)-1,3,5-triazine, 0.14g) and the solvent removed from the organic layer leaving a pale yellow solid. This was also unreacted starting material.

2,4,6-tri-(12'-phenyl-*para*-carboranyl)-1,3,5-triazine

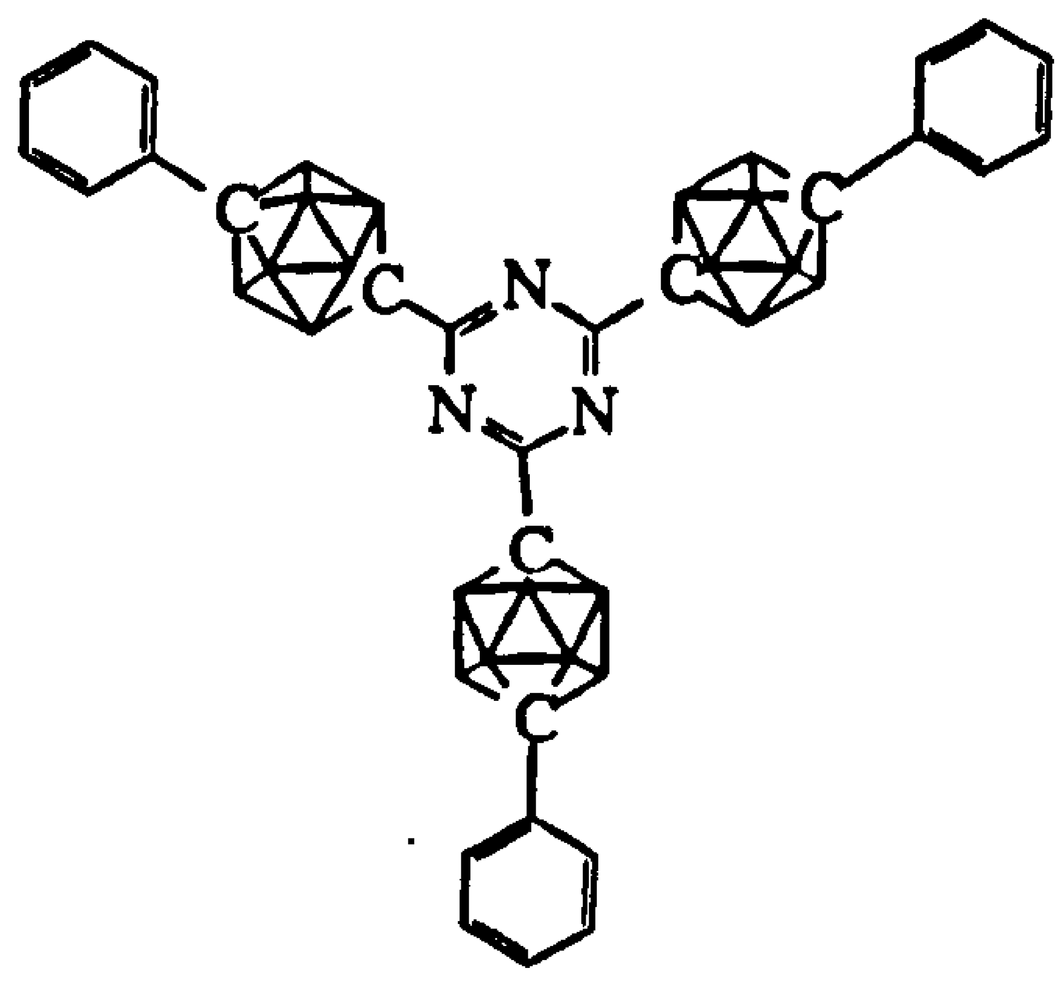

1-phenyl-*para*-carborane (0,25g, 1.1mmol) in DME (50mL) was monolithiated with a solution of n-BuLi (2.38M in hexanes, 0.6mL, 1.4mmol) to form a clear colourless solution after stirring at room temperature for 30 minutes. The solution was cooled in an ice-bath before the addition, via canular transfer, of a solution of cyanuric chloride (0.07g, 0.4mmol) in DME (10mL). The resulting clear, colourless solution was diluted with diethyl ether on warming to room temperature, washed with distilled water then the aqueous layers re-extracted with diethyl ether. The organic layers were isolated and dried over anhydrous magnesium sulfate, filtered, and the solvent removed under reduced pressure to yield the product as a white powdery solid.

Yield: 50% *IR*: 3092 w, 3062 m, 3040 w, 3026 w (phenyl C-H); 2963 s; 2924 m; 2874 m; 2814 m; 2611 s (carboranyl B-H); 1526 s (triazine C-N); 1497 s; 1447 m; 1365 s; 1261 s; 1095 s; 1021 s; 877 m; 799 s; 729 m; 705 w; 691 m; 680 m; 595 w; 492 m cm^{-1}
m/z (EI^+): 297 ($PhCB_{10}CC_3N_3$) *Elemental analysis*: C 45.16% (44.06%), H 7.04% (6.16%), N 4.21% (5.71%) *m.p.*: 135.8°C
NMR ($CDCl_3$)/ppm: ^1H: 7.27 (15H, m, phenyl CH), 4.0-1.0 (30H, br., carboranyl B-*H*); $^{13}C\{^1H\}$: 170.32 (triazine *C*-N); 135.94 (*ipso* C), 128.30, 127.86, 126.68 (phenyl *C*-H); 85.43 (carboranyl *C*-$C_3N_3(CbPh)_2$), 79.43 (carboranyl *C*- Ph); $^{11}B\{^1H\}$: -12.79 (5B, d, J_{BH}=155Hz), -13.21 (5B, d, J_{BH}=*c*.165Hz)

1-(4'-bromophenyl)-*para*-carborane and 1,12-di-(4'-bromophenyl)-*para*-carborane

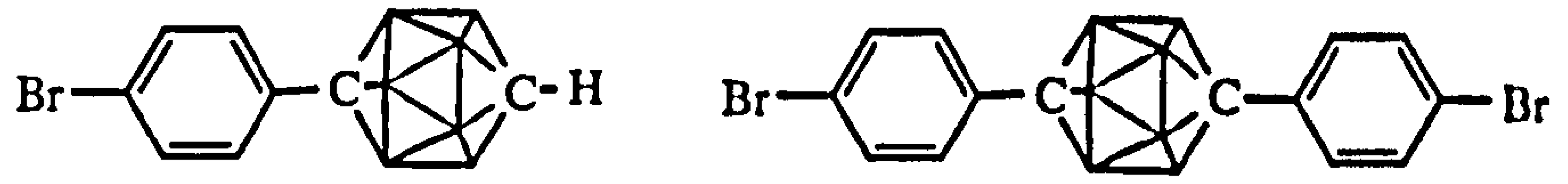

Para-carborane (2.85g, 20mmol) was dissolved in DME (100mL) and monolithiated witha a solution of n-BuLi (2.38M in hexanes, 9mL, 21mmol). After 30 minutes stirring at room temperature, pyridine (15mL) was added to the clear colourless solution, followed by CuCl (2.08g, 21mmol). The resulting solution was refluxed at

90°C for 40 minutes giving a bright orange solution. 1-bromo-4-iodobenzene (5.56g, 20mmol) was added and the solution left to reflux for a further 72 hours. After cooling to room temperature, diethyl ether (100mL) was added to the now deep pink reaction solution and the solution stirred for 4 hours to destroy the copper/pyridine complex. After filtration of this solution, the filtrate was washed with HCl (2M, 2x75mL) and distilled water (2x75mL). The aqueous layers were re-extracted with diethyl ether and the combined organic layers dried over anhydrous magnesium sulfate, filtered and the solvent removed under reduced pressure to leave an off-white solid. Unreacted *para*-carborane was removed by sublimation (59°C, dynamic vacuum) and further sublimation (70°C, dynamic vacuum) isolated the mono-substituted product (3.44g). Disubstituted product remained unsublimed, and after treating with activated charcoal, 1,12-*bis*-(4'-bromophenyl)-*para*-carborane was isolated as a pale yellow powder (0.36g).

1-(4'-bromophenyl)-para-carborane

Yield: 58% *IR:* 3058 m (carboranyl C-H); 2611 s (carboranyl B-H); 1491 m; 1395 m; 1141 w; 1089 w; 1073 m; 1009 m; 894 m; 848 m; 801 m; 737 m; 707 w; 582 w; 495 m cm^{-1} *m/z*(EI^+): 299 ($C_8H_{15}B_{10}Br$), 218 ($C_8H_{15}B_{10}$) *Elemental analysis*($C_8H_{15}B_{10}Br$): C 32.17% (32.11%), H 4.96% (5.05%), Br 27.50% (26.70%) *m.p.*: 107-108°C
NMR ($CDCl_3$)/ppm: $^1H\{^{11}B\}$: 7.4 (2H, m, phenyl CH), 7.2 (2H, m, phenyl CH), 2.92 (1H, s, carboranyl CH), 2.61 (5H, s, carboranyl BH), 2.41 (5H, s, carboranyl BH); $^{13}C\{^1H\}$: 136.5, 131.8, 129.4, 123.5, 86.1 (carboranyl C-C_6H_4Br), 60.6 (carboranyl C-H); $^{11}B\{^1H\}$: -12.71 (5H, d, J_{B-H}=164Hz), -15.21 (5H, d, J_{B-H}=166Hz)

1,12-bis-(4'bromophenyl)-para-carborane

Yield: 0.36g= 18% (based on 9mmol of 1bromo-4iodobenzene unreacted) *IR*: 3088 w, 3060 w (phenyl CH); 2963 m; 2609 s (carboranyl BH); 1903 w; 1585 w; 1508 w; 1489 s; 1395 s; 1261 s; 1189 w; 1092 s; 1071 s; 1011 s; 913 m; 893 m; 847 w; 831 s; 800 s; 749 m; 739 m; 700 m; 598 w; 491 s cm^{-1} *m/z*(EI^+): 454 ($C_{14}H_{18}B_{10}Br_2$), 299 ($C_8H_{15}B_{10}Br$), 218 ($C_8H_{15}B_{10}$)
NMR ($CDCl_3$)/ppm: $^1H\{^{11}B\}$: 7.3 (4H, m, phenyl CH), 7.1 (4H, m, phenyl CH), 2.59 (10H, s, carboranyl BH); $^{13}C\{^1H\}$: 136.0, 132.0, 129.5, 123.7, 113.4, 82.8 (weak, carboranyl C)

2,4,6-tri-(12'-(4''-bromophenyl)-*para*-carboranyl)-1,3,5-triazine

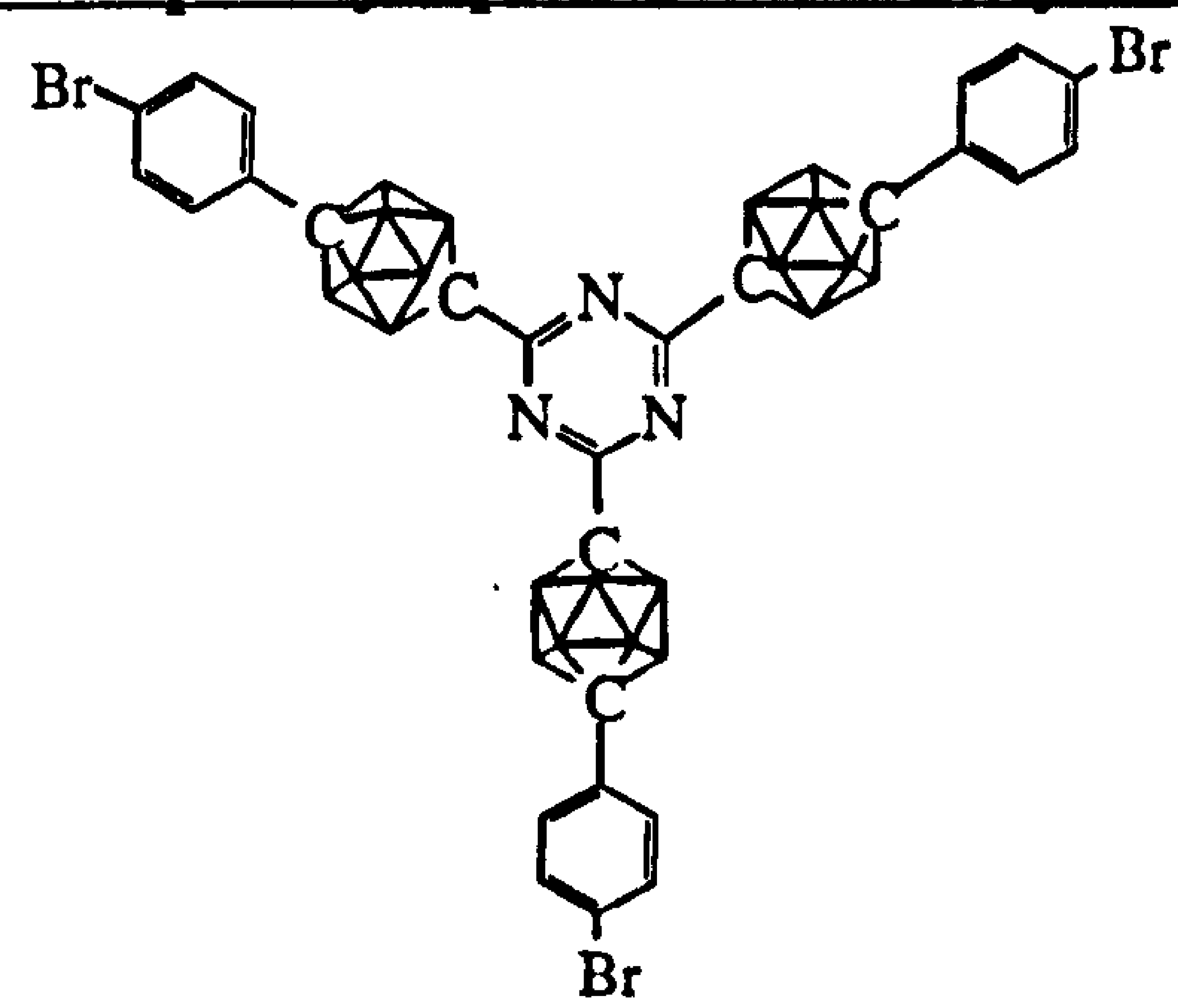

1-(4'-bromophenyl)-*para*-carborane (0.90g, 3mmol) was dissolved in DME (40mL) and lithiated with a solution of n-BuLi (2.38M in hexanes, 1.30mL, 3mmol). After 20 minutes stirring at room temperature, a solution of cyanuric chloride (0.19g, 1mmol) in DME (20mL) was added and the solution left to stir for 1 hour. The resulting solution was diluted with dichloromethane and washed with water. Removal of the solvent from the organic layer left a brown oil which, when washed with a small quantity of ethanol, yielded a pale yellow solid.

Yield: 40% *IR*: 3080 w (phenyl CH); 2963 s; 2619 s (carboranyl BH); 1528 s, 1365 s (triazine CN); 1261 s (carborane); 1097 s, 1019 s (carborane); 866 m; 800 s (C-Br?); 689 w; 499 w cm^{-1} *Elemental analysis*($C_{27}H_{42}B_{30}N_3Br_3$): C 34.46% (33.34%), H 6.74% (4.35%), N 4.38% (4.32%) *m.p.*: >400°C
NMR ($CDCl_3$)/ppm: ^{1}H: 7.32, 7.13, 7.24, 7.08 (m, phenyl CH); 3-1 (br., carboranyl BH); $^{11}B\{^1H\}$: -9.56 (5B, J_{BH}=159Hz), -9.82 (5B, J_{BH}=160Hz)

High Temperature Experiments

Thermal isomerisation of 2,4,6-tri-(2'-phenyl-*ortho*-carboranyl)-1,3,5-triazine

2,4,6-tri-(2'-phenyl-*ortho*-carboranyl)-1,3,5-triazine (0.41g,0.6mmol) was placed in an evacuated carius tube and left in a furnace (400°C) for 72 hours. The white powder was transformed to a glassy brown solid (isomerised) which lined the walls of the carius tube and pale brown "mushrooms" (mixture of *ortho* and *meta*). Powdering the "mushrooms" and heating at 400°C under vacuum with a heat gun resulted in a brown liquid which solidified to a brown glassy solid (*meta*). The glassy solid could be ground, giving a sandy white powder which was 2,4,6-tri-(7'-phenyl-*meta*-carboranyl)-1,3,5-triazine.

Yield: Sufficient heating results in 100% conversion to *meta* isomer. IR: (glassy solid) 3092 w, 3061 m, 3040 m (phenyl C-H); 2605 s, 2570 s (carboranyl B-H); 1597 w; 1582 w; 1528 s, 1495 s (triazine CN); 1447 s; 1365.74 s; 1260 m; 1191 w; 1160 w; 1067 m; 1022 m; 1003 m; 915 w; 879 w; 805 m; 742 s; 725 s; 689 s; 662 m; 624 w; 612 w cm^{-1}
NMR ($CDCl_3$)/ppm: ^1H: 7.4, 7.3 (15H, m, phenyl C-*H*); 4.2-1.2 (30H, br., carboranyl B-*H*); $^{11}B\{^1H\}$: -3.90 (1B, d, J_{BH}=*c*.150Hz), -6.45 (1B, J_{BH}=*c*.120Hz), 10.47 (6B, J_{BH}=145Hz), -13.48 (2B, J_{BH}=*c*.160Hz)

Thermal stability of 2,4,6-tri-(*para*-carboranyl)-1,3,5-triazine

Experiments were conducted under a flow of Argon using a Vecstar Horizontal Tube Furnace. Samples of 2,4,6-tri-(*para*-carboranyl)-1,3,5-triazine were placed in either a mullite ceramic boat, or alternatively on a sheet of quartz within a mullite boat and the furnace flushed with Ar for 1 hour before starting to heat the sample. Samples were heated from room temperature at a rate of 150°C/h and cooled at a rate of 300°C/h to 40°C.

Run 1: The sample (0.10g) was placed in a mullite boat and heated to 1200°C at a rate of 150°C/h from room temperature. The furnace temperature was maintained at 1200°C for 1h, then cooled to 40°C at a rate of 300°C/h. A clear, hard glassy film coated the walls of the mullite boat.

Run 2: An empty boat was subjected to the same heating/cooling cycle as before. No changes in the appearance of the boat were observed.

Run 3: Sample (0.052g) in a mullite boat was heated to 800°C and held at this temperature for one hour, before cooling. Some transparent film (as before) had formed together with some black charred solid. On standing in air for 2 days, the black solid had become silvery.

Run 4: Run 3 was repeated, but the compound held at 800°C for 4h. Less black solid, and more clear film than before is observed. No weight gain or loss was noted.

Run 5: Sample (0.0098g) was placed on a quartz plate and heated to 1200°C for 1h. A clear transparent film coated the quartz. Weight was lost from the sample (0.0039g). After 5 days, the coating turned opaque and slightly flaky.

Run 6: Sample (0.0500g) was heated in a mullite boat to 800°C for 6h. A mixture of clear film and black solid resulted. The sample had gained weight (0.0064g).

Run 7: Sample (0.0550g) was heated in a mullite boat to 1200°C for 1h. A clear colourless film resulted. Weight was lost from the sample (0.0072g).

High Pressure Experiments

Two experiments were carried out under the supervision of Mr. D. Hunter of Durham University, with 2,4,6-tri-(*para*-carboranyl)-1,3,5-triazine. In both the sample was placed inside a glass sleeve inside an autoclave under a positive nitrogen pressure.

Run 1: The sample (0.1079g) was taken to a maximum pressure of 1000psi at 350°C for 15h. The final product was slightly yellow compared to the white starting material, but no change in the compound was noted.

Run 2: Run 1 was repeated with a pressure of 900psi and a temperature of 400°C. Again, no change was observed.

X-ray Powder Diffraction Experiments

X-ray powder diffraction data on 2,4,6-tri-(*meta*-carboranyl)-1,3,5-triazine, 2,4,6-tri-(*para*-carboranyl)-1,3,5-triazine and 1,3,5-tri-(*para*-carboranyl)-benzene, were collected by Dr. Christian Lehmann of the crystallography department at Durham University.

X-ray Photoelectron Spectroscopy

XPS data on the product from heating 2,4,6-tri-(*para*-carboranyl)-1,3,5-triazine to 1200°C, was collected by Simon Hutton, working for Prof. J. Badyal at Durham University.

4.7 SUMMARY

The synthesis, properties and structures of a novel group of compounds, the mono-, di- and tri-(carboranyl)-1,3,5-triazines, has been investigated in this chapter.

The synthesis of 2,4,6-tri-(carboranyl)-1,3,5-triazines has been shown to be facile, this being the unique multi-carboranyl product from the reaction of lithio-*ortho*-, *meta*- or *para*- substituted or unsubstituted carborane with cyanuric chloride. Their synthesis has been shown to be far simpler and higher yielding than the analogous benzene derivatives, where the products are obtained from reaction of a decaborane adduct with an acetylene, or through copper or palladium catalysed coupling reactions. Di-carboranyl triazines were synthesised by first derivatising the triazine, and mono-carboranyl triazines were formed from reaction of a triazinyl-acetylene with a decaborane adduct.

In general, the carboranyl triazines were more soluble than their benzene counterparts. The only examples of insoluble compounds were where the carborane was an unsubstituted *meta-* or *para*-carborane. In these compounds, the presence of intermolecular hydrogen bonding interactions was postulated.

A structural investigation of these insoluble compounds, namely 2,4,6-tri-(*meta*- and *para*-carboranyl)-1,3,5-triazines, has shown them to pack in planes with a d-spacing of 5.9Å. The same d-spacing was observed for 1,3,5-tri-(*para*-carboranyl)-benzene, which has no potential to hydrogen bond. This suggested it was the size and shape of the molecules, and not the hydrogen bonding interactions, which directed the packing arrangement.

An X-ray crystallographic study of 2,4,6-tri-(2'-phenyl-*ortho*-carboranyl)-1,3,5-triazine has shown it to be of the same nature as the benzene analogue. Both have three-fold symmetry around a screw axis, and a centre of inversion. Crystals of the *para*-isomer reveal it to pack as interlocking molecules in a planar arrangement.

The tri-carboranyl triazines were stable compounds, both thermally and chemically. The triazine ring remained intact when the compound was reacted with hydrazine derivatives. Similar conditions were known to cleave the C_3N_3 ring in organic systems. Thermal rearrangement from 2,4,6-tri-(2'-phenyl-*ortho*-carboranyl)-1,3,5-triazine to the *meta* isomer occurred at *c.*400°C.

4.8 REFERENCES

1 J.A. Dupont, M.F. Hawthorne, J. Am. Chem. Soc., 1964, **86**, 1643

2 K.P. Callahan, M.F. Hawthorne, J. Am. Chem. Soc., 1973, **95**, 4574

3 T.E Paxson, K.P. Callahan, M.F. Hawthorne, Inorg. Chem., 1973, **12**, 708

4 V.N. Kalinin, L.I. Zakharkin, J. Gen. Chem. USSR, 1967, **37**, 2025

5 L.I. Zakharkin, A.I. Kovredov, Bull. Acad. Sci. USSR, Div. Chem. Sci., 1973, 1396

6 V.I. Stanko, Y.V. Gol'tyanin, V.A.Brattsev, J. Gen. Chem. USSR, 1967, **37**, 2247

7 W.Jiang, C.B. Knobler, C.E. Curtis, M.D. Mortimer, M.F. Hawthorne, Inorg. Chem., 1995, **34**, 3491

8 W. Jiang, I.T. Chizhevsky, M.D. Mortimer, W. Chen, C.B. Knobler, S.E. Johnson, F.A. Gomez, M.F. Hawthorne, Inorg, Chem., 1996, **35**, 5417

9 W. Clegg, W.R. Gill, J.A.H. MacBride, K. Wade, Angew. Chem., Int. Ed. Engl., 1993, **32**, 1328

10 W. Jiang, C.B. Knobler, M.F. Hawthorne, Inorg. Chem., 1996, **35**, 3056

11 D.A. Owen, M.F. Hawthorne, J. Am. Chem. Soc., 1971, **93**, 873

12 P.A. Chetcuti, W. Hofherr, A. Liégard, G. Rihs, G. Rist, Organometallics, 1995, **14**, 666

13 T.D. Getman, C.B. Knobler, M.F. Hawthorne, Inorg. Chem., 1992, **31**, 101

14 Y.-K. Yan, D.M.P. Mingos, M. Kurmoo, W.-S. Li, I.J. Scowen, M. McPartlin, A.T. Coomber, R.H. Friend, J. Chem. Soc., Dalton Trans., 1995, 2851

15 R.T. Baker, R.E. King III, C. Knobler, C.A. O'Con, M.F. Hawthorne, J. Am. Chem. Soc., 1978, **100**, 8266

16 J.A.H. MacBride, K. Wade, unpublished results

17 R. Coult, M.A. Fox, W.R. Gill, P.L. Herbertson, J.A.H. MacBride, K. Wade, J. Organometal. Chem., 1993, **462**, 19

18 D.A. Brown, H.M. Colquhoun, J.A. Daniels, J.A.H. MacBride, I.R. Stephenson, K. Wade, J. Mater. Chem., 1992, **2**, 793

19 H.M. Colquhoun, D.F. Lewis, J.A. Daniels, P.L. Herbertson, J.A.H. MacBride, I.R. Stephenson, K. Wade, Polymer, 1997, **38**, 2447

20 G.R. Newkome, C.N. Moorefield, J.M. Keith, G.R. Baker, G.H. Escamilla, Angew. Chem., Int. Ed. Engl., 1994, **33**, 666

21 D. Armspach, M. Cattalini, E.C. Constable, C.E. Housecroft, D. Phillips, Chem. Commun., 1996, 1823

22 X. Yang, C.B. Knobler. M.F. Hawthorne, J. Am. Chem. Soc., 1993, **115**, 4904

23 Z. Zheng, X. Yang, C.B. Knobler, M.F. Hawthorne, J. Am. Chem. Soc., 1993, **115**, 5320

24 W. Jiang, I.T. Chizhevsky, M.D. Mortimer, W. Chen, C.B. Knobler, M.F. Hawthorne, Inorg. Chem., 1996, **35**, 5417

25 I.T. Chizhevsky, S.E. Johnson, C.B. Knobler, F.A. Gomez, M.F. Hawthorne, J. Am. Chem. Soc., 1993, **115**, 6981

26 R.C. Haushalter, R.W. Rudolph, J. Am. Chem. Soc., 1978, **100**, 4628

27 X. Yang, Z. Zheng, C.B. Knobler, M.F. Hawthorne, J. Am. Chem. Soc., 1993, **115**, 193

28 X. Yang, W. Jang, C.B. Knobler, M.F. Hawthorne, J. Am. Chem. Soc., 1992, **114**, 9719

29 J. Müller, K. Base, T.F. Magnera, J. Michl, J. Am. Chem. Soc., 1992, **114**, 9721

30 U. Schöberl, T.F. Magnera, R.M. Harrison, F. Fleischer, J.L. Pflug, P.F.H. Schwab, X. Meng, D. Lipiak, B.C. Noll, V.S. Allured, T. Radalevige, S. Lee, J. Michl, J. Am. Chem. Soc., 1997, **119**, 3907

31 R.M. Harrison, T. Brotin, B.C. Noll, J. Michl, Organometallics, 1997, **16**, 3401

32 W.R. Gill, P.L. Herbertson, J.A.H. MacBride, K. Wade, J. Organometallic Chem., 1996, **507**, 249

33 T.G. Hibbert, K. Wade, unpublished results

34 C. Vinas, W.M. Butler, F. Teixidor, R.W. Rudolph, Inorg. Chem., 1986, **25**, 4369; F. Teixidor, R.W. Rudolph, J. Organomet. Chem., 1983, **241**, 301

35 M.F. Hawthorne, X. Yang, Z. Zheng, Pure & Appl. Chem., 1994, **66**, 245

36 T.G. Hibbert, J.A.H. MacBride, K. Wade, unpublished results

37 Comprehensive Heterocyclic Chemistry, Eds. A.J. Boulton, A. McKillop, Pergamon Press, 1984, **3**, 457-530

38 A.S. Jessiman, D.D. MacNicol, P.R. Mallinson, I. Vallance, J. Chem. Soc., Chem. Commun., 1990, 1619

39 K. Henderson, D.D. MacNicol, P.R. Mallinson, I. Vallance, Supramolecular Chem., 1995, **5**, 301

40 J.-M. Lehn, Angew. Chem. Int. Ed. Engl., 1990, **29**, 1304

41 J.P. Mathias, E.E. Simanek, G.M. Whitesides, J. Am. Chem. Soc., 1994, **116**, 4326

42 Y. Aoyama, K. Endo, T. Anzai, Y. Yamaguchi, T. Sawaki, K. Kobayashi, N. Kanehisa, H. Hashimoto, Y. Kai, H. Masuda, J. Am. Chem. Soc., 1996, **118**, 5562

43 J. Keck, H.E.A. Kramer, H. Port, T. Hirsch, P. Fischer, G. Rytz, J. Phys. Chem., 1996, **100**, 14468

44 C.-W. Chan, D.M.P. Mingos, A.J.P. White, D.J. Williams, J. Chem. Soc., Dalton Trans., 1995, 2469

45 C. Yang, X.-M. Chen, W.-H. Zhang, J. Chen, Y.-S. Yang, M.-L. Gong, J. Chem. Soc., Dalton Trans., 1996, 1767

46 H. Yonehara, W.-B. Kang, T. Kawara, C. Pac, J. Mater. Chem., 1994, **4**, 1571

47 Chemical Abstracts, **106**, 186485x; Japanese patent, Jpn. Kokai Tokkyo Koho JP, 61 258 265 [86 258 265]

48 Chemical Abstracts, **107**, 223884v; V.R. Mkrtchyan, A.F. Lunin et al., Homogeneous and Heterogeneous Catalysis, Proc. Int. Symp. Relat. Homogeneous Heterogeneous Catalysis, 5th, 1986, 617

49 E.M. Smolin, L. Rapoport, Chem. Heterocyclic Compounds, 1959, **13**, 1

50 H. Bader, E.R. Ruckel, F.X. Markley, C.G. Santangelo, P. Schickedantz, J. Org. Chem., 1965, **30**, 702

51 C. Chen, R. Dagnino Jr., J.R. McCarthy, J. Org. Chem., 1995, **60**, 8428

52 E. Degener, H.-G. Schmelzer, H. Holtschmidt, Angew. Chem., Int. Ed. Engl., 1966, 5, 960

53 H.-G. Schmelzer, E. Degener, H. Holtschmidt, Angew. Chem., Int. Ed. Engl., 1966, 5, 960-61

54 Y. Lin, T.L. Fields, V.J. Lee, S.A. Lang Jr., J. Heterocyclic Chem., 1982, **19**, 613

55 S. Horrobin, J. Chem. Soc., 1963, 4130

56 Y. Bessière-Chrétien, H. Serne, Bull. Chim. Soc. France, 1973, no. 6, 2039

57 H.F. Shurvell, Spectrochimica Acta, 1965, **21**, 2141; T.S. Hermann, Spectrochimica Acta, 1965, **21**, 663; R.D. Spencer, Spectrochimica Acta, 1965, **21**, 1543

58 W. Kemp, Organic Spectroscopy, third ed., MacMillan Education Ltd., 1991

59 G.J. Bullen, D.J. Corney, F.S. Stephens, J. Chem. Soc., Perkin Trans. 2, 1972, 642; D.S. Brown, J.D. Lee, P.R. Russell, Acta Cryst., 1976, **B32**, 2101

60 Carbon Fibres, Ed. E.A. Smith, Morgan-Grampian (Publishers) Ltd., 1970

61 P.L. Herbertson, PhD Thesis, Durham 1995

62 D. Belitskus, G.A. Jeffrey, Spectrochim. Acta, 1965, **21**, 1563

63 G.J. Bullen, D.J. Corney, F.S. Stephens, J. Chem. Soc., Perkin Trans. 2, 1972, 642

64 D.S. Brown, J.D. Lee, P.R. Russell, Acta Cryst., 1976, **B32**, 2101

65 Z.G. Lewis, A.J. Welch, Acta Cryst. 1993, **C49**, 705; This molecule has two crystal forms, the first in which the C-Ph bond length is 1.500(4)Å, and in the second 1.494(4)Å

66 P.T. Brain, J. Cowie, D.J. Donohoe, D. Hnyk, D.W.H. Rankin, D. Reed, B.D. Reid, H.E. Robertson, A.J. Welch, M. Hofmann, P.v.R. Schleyer, Inorg. Chem., 1996, **35**, 1701

67 F. Teixidor, C. Vinas, R.W. Rudolph, Inorg. Chem., 1986, **25**, 3339

68 Ch. Grundmann, A. Kreutzberger, J. Amer. Chem. Soc., 1957, **79**, 2839

69 Ch. Grundmann, Angew. Chem., Int. Ed. Engl., 1963, **2**, 309

70 L.I. Zakharkin, V.N. Kalinin, L.S. Podvisotskaya, Bull. Acad. Sci. USSR, 1967, 2212

71 D.G. Baghurst, R.C.B. Copley, H. Fleischer, D.M.P. Mingos, G.O. Kyd, L.J. Yellowlees, A.J. Welch, T.R. Spalding, D. O'Connell, J. Organometal. Chem., 1993, **447**, C14

72 Mullite, cf. Encyclopedia of Metallurgy and Materials, is a naturally occuring mineral of formula $3Al_2O_3.2SiO_2$ and is stable up to *c.* 1810°C, at which point corrundum, Al_2O_3 separates. It is also made artificially from the fusion of Al_2O_3 and SiO_2.

73 D. Byun, S-d. Hwang, P.A. Dowben, F.K. Perkins, F. Filips, N.J. Ianno, Appl. Phys. Lett., 1994, **64**, 1968; D. Bucca, T.M. Keller, J. Polymer Sci. A, Polymer Chem., 1997, **35**, 1033; S.V. Nguyen, T. Nguyen, H. Treichel, O. Spindler, J. Electrochem. Soc., 1994, **141**, 1633; A.P. Hitchcock, S.G. Urquhart, A.T. Wen, A.L.D. Kilcoyne, T. Tyliszczak, E. Rühl, N. Kosugi, J.D. Bosek, J.T. Spencer, D.N. McIlroy, P.A. Dowden, J. Phys. Chem. B, 1997, **101**, 3483; T. Komatsu, Y. Kakudate, S. Fujiwara, J. Chem. Soc., Faraday Trans., 1996, **92**, 5067

Chapter Five

Deboronation Reactions Of One And Three Cage Carborane Systems

5.1 INTRODUCTION

Chapter Five will discuss the deboronation reactions of selected one and three cage carborane derivatives from previous chapters. A survey of current methods of deboronation introduces the chapter, followed by a discussion of work relevant to this thesis. Various bases have been employed in this work, and ammonia has been shown to cause deboronation, as well as deprotonation, in carboranyl carboxylic acid derivatives. Of particular interest have been the fluoride ion deboronation reactions of hetero-aryl-*ortho*- and *meta*-carboranes. Cage fluorination has been observed at the B(2), B(3), B(8) and B(10) positions of the *nido* residues of di-(hetero-aryl)-*meta*-carboranes. Degradation reactions of tri-carboranyl-triazines are also explored, and show cage deboronation to occur in *ortho*- and *meta*-carboranes. In some instances, degradation of the C_3N_3 ring is detected, and removal of a BH vertex from a *para*-carboranyl cage is also noted.

5.2 DEBORONATION - AN OVERVIEW

Although outperforming many comparable wholly organic systems in thermal and chemical stability, carboranes do have a weakness when confronted with a strongly basic medium. In the presence of a strong nucleophile, carboranes can be deboronated, losing a BH vertex and leaving a negatively charged undecaborate anion. The BH unit that is removed is that most highly connected to the carboranyl carbon atoms as this is the most positively charged boron.

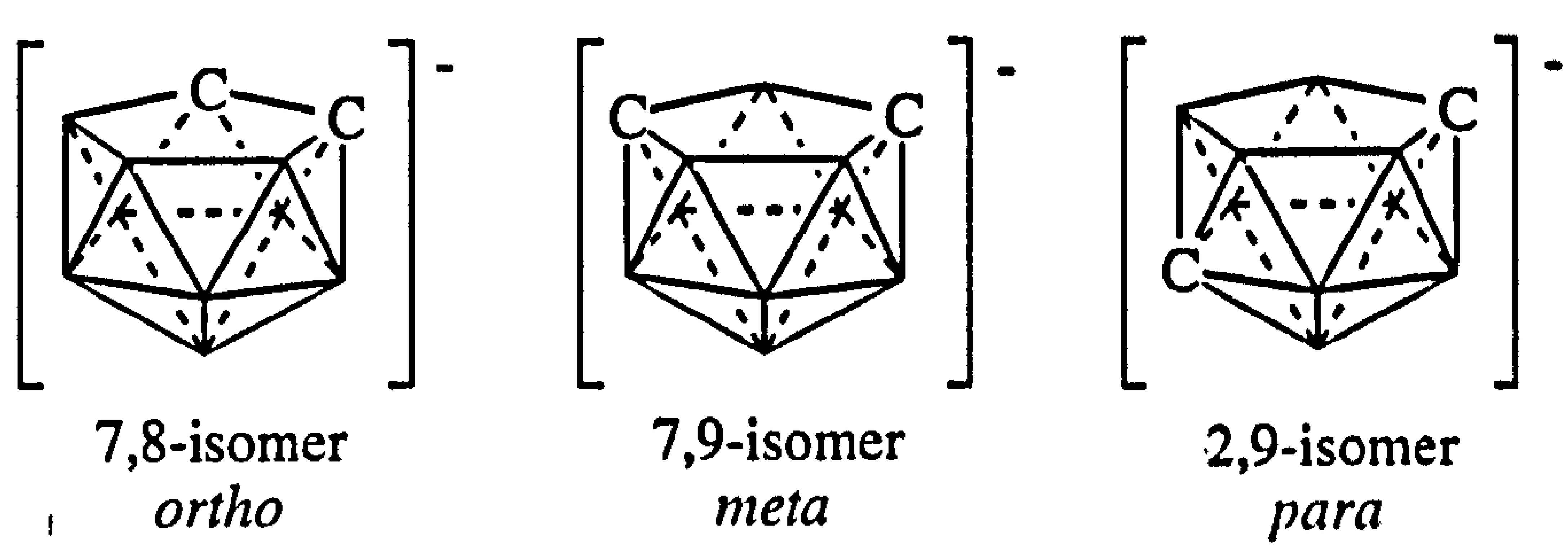

figure 5.1: nido residues of ortho-, meta- and para-carborane, $C_2B_9H_{12}^-$. An extra non-terminal hydrogen is associated with the open face in the monoanionic species.

It is commonly accepted that the *ortho*-carboranyl derivatives are by far the easiest to deboronate, followed by *meta* and that *para*-carboranyl derivatives are very resistant to degradation by base. In the *ortho*-carboranyl derivatives, two BH vertices have the same carbon connectivity (B(3) and B(6) are connected to both cage carbon atoms), and this is also true for the *meta* isomer, although the charge density on each will be slightly less given the increased C-C distance. In *para*-carborane no boron atoms are connected to both cage carbon atoms. If the ease of deboronation between isomers of the same compound is related to the carbon connectivity and to C-C distance, this logic would explain why the *ortho*-carboranes tend to deboronate most easily, followed by *meta*, and why the *para*-carboranyl derivatives give up a BH vertex rather begrudgingly, requiring harsh conditions.

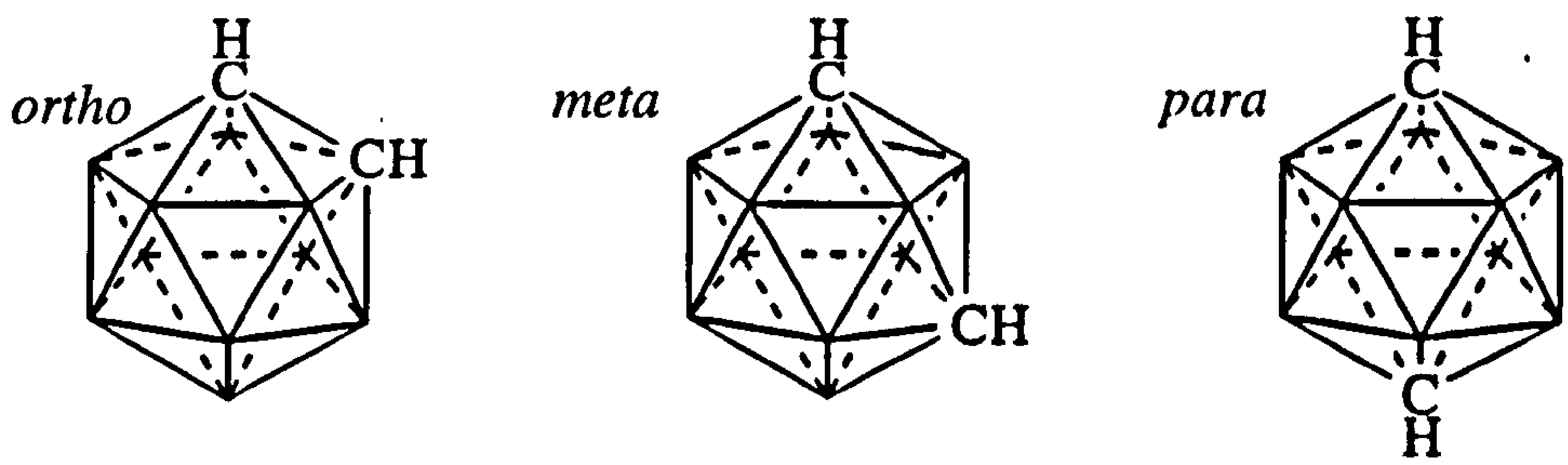

figure 5.2: carbon-carbon distance increases with higher isomerisation

In *para*-carborane, each BH unit has only one carbon connectivity, and all the BH units are identical due to the high symmetry of the compound. The carbons are more electronegative than the cage boron atoms, and no BH vertex has a higher charge concentration than another. This leaves the attacking base no preferential point of attack. There are instances where deboronation of 1,12-dicarbadodecaborane has been observed, but reports are rare.[1,2]

In the *ortho*- and *meta*-carboranyl systems, there are two possible points of attack for the nucleophile, namely the electronically equivalent B(3) and B(6) positions, causing chirality in the anions produced of carborane $RR'C_2B_{10}H_{10}$ ($R \neq R'$).[3,4] For immediate purposes, both isomers will be treated together and represented by the same schematic.

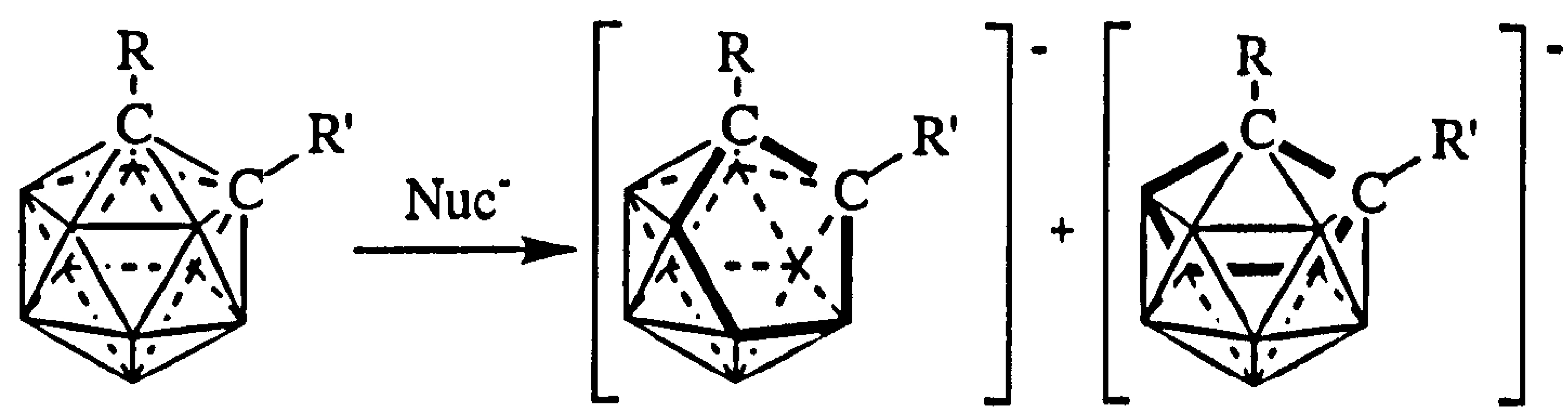

scheme 5.1: deboronation of R,R'-ortho-carborane (R≠R') leads to chirality

A variety of bases are known to effect deboronation, and some of those tried on systems studied within the scope of this thesis are described below. These methods are generally applicable to both single and multi-cage carboranyl systems.

5.2.1 Alkoxide Ion

Deboronation of *ortho* and *meta*-carboranes is achieved readily by the action of a basic alcoholic solution,[3,5] generally a methanolic or ethanolic potassium hydroxide solution. Hydrogen gas and $B(OR)_4^-$ species are produced as the reaction proceeds. Substitution of the carboranyl carbon atoms does not tend to hinder the degradation reaction, although the substituents may affect the rate of reaction as a result of their electronic influence on the cage.[6] The cations of the resulting alkali metal dicarbaundecaborate salts can be changed through simple precipitation reactions to give other salts, including caesium, rubidium, tetramethyl ammonium and thallium salts.[7,8]

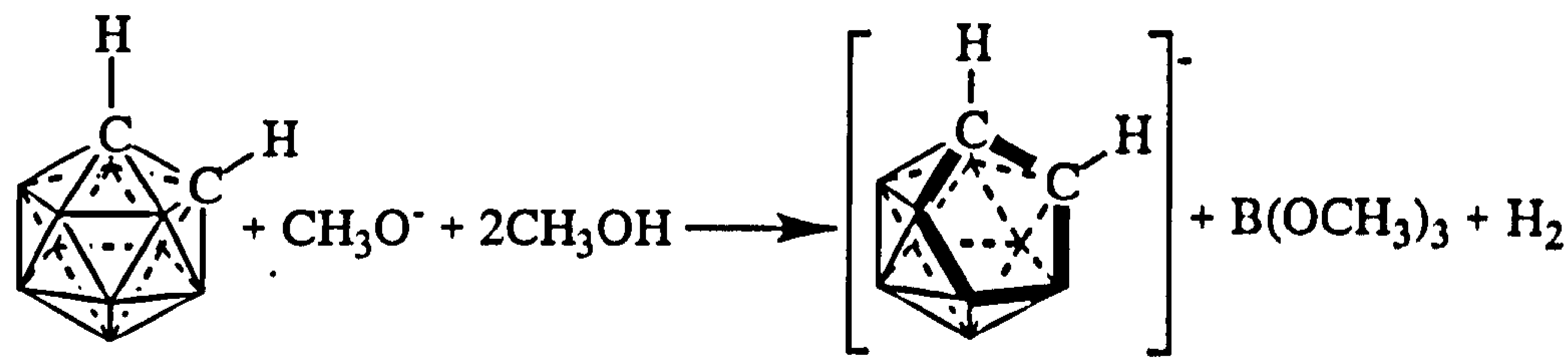

scheme 5.2: deboronation of ortho-carborane by methoxide ion

One drawback of this method of deboronation is the possibility of nucleophilic substitution on the cage boron atoms. Where it occurs, generally on conversion of *meta*-carborane derivatives to 7,9-dicarbaundecaborate anions, the substitution reaction accompanies the deboronation reaction and results in a boron atom of the lower belt (usually B(3)) being functionalised.[9] Conditions can be tempered to control this secondary reaction.

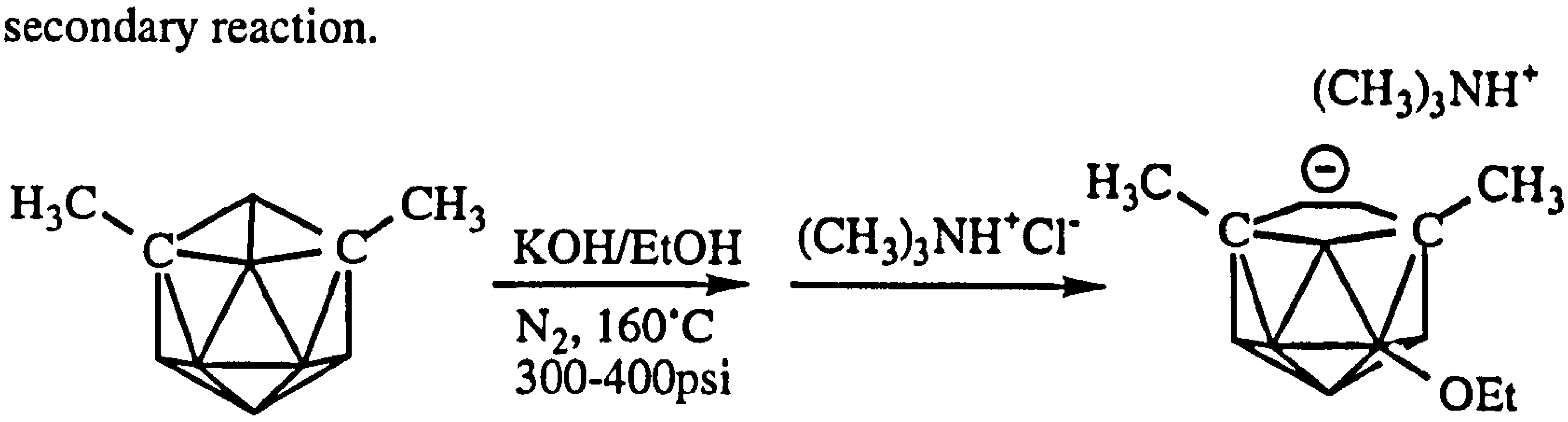

scheme 5.3: B-substitution in alkoxide deboronation reactions

There are few examples of cage degradation of the *para*-carboranyl species, however in the instances where this has been reported, the degradation has again been achieved by the action of ethanolic potassium hydroxide solution. The first report[1] observed cage degradation after six hours reflux with 20% potassium hydroxide in a propanediol solution although the yield was only 15%. A more efficient degradation, which achieved 95% conversion, was obtained through crown-ether promoted base degradation using KOH together with 18-crown-6 in refluxing benzene.[2]

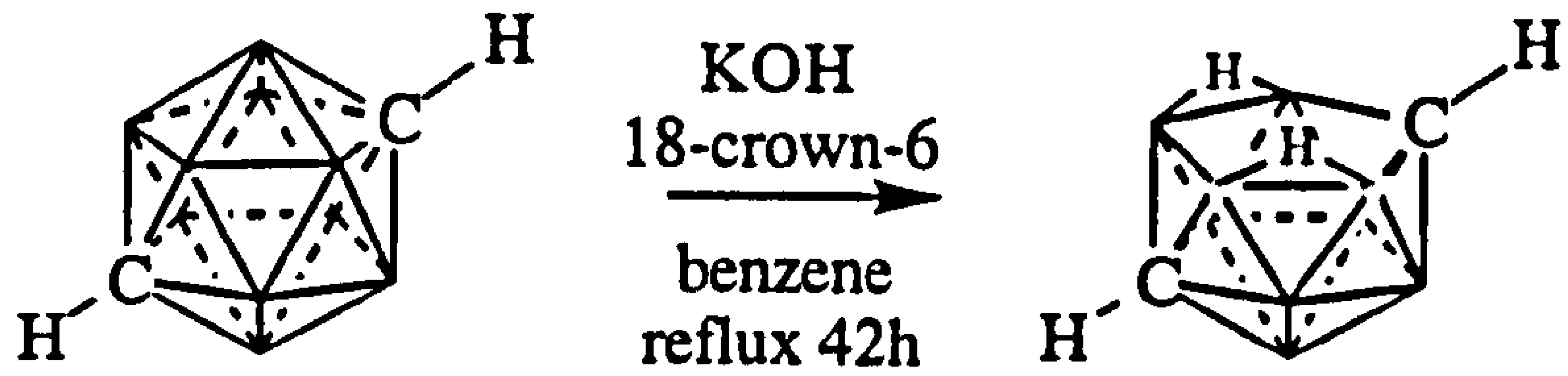

scheme 5.4: crown-ether promoted base degradation of para-carborane

5.2.2 Amine derivatives

Ammonia[10] was the first example of a nitrogen base to effect a carboranyl cage deboronation reaction. Earlier workers reported conflicting results, some reporting cage degradation, some deprotonation[11], with ammonia. Teixidor has observed that in the mercapto-carborane *o*-HS-$CB_{10}H_{10}CSH$, deboronation of the cage occurred once both SH groups had been deprotonated.[12,13,14] This progression from deprotonated to deboronated fragment explains the contradictory results of previous workers in the field.

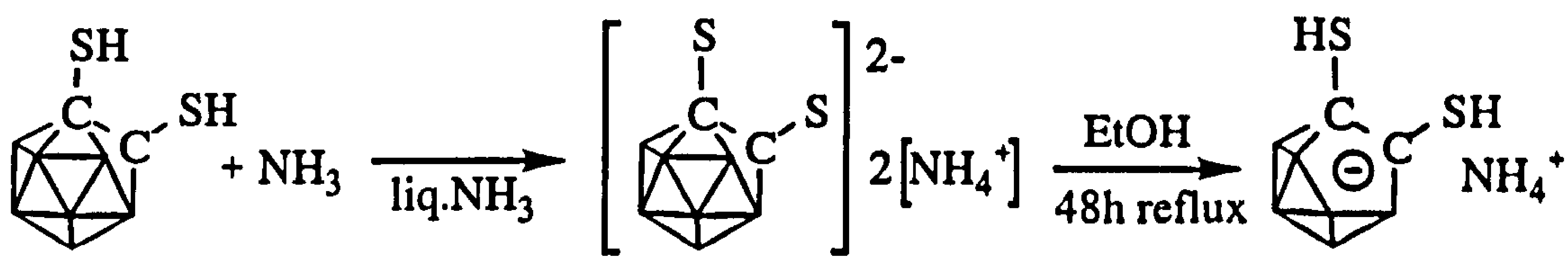

scheme 5.5: deprotonation of exo-substituents leads to deboronation in mercapto-ortho-carboranes

Hydrazine[15,16], and derivatives thereof, were also discovered to have the ability to remove a BH vertex from an icosahedral cage to leave the *nido* anion, $C_2B_9H_{11}^-$. Hydrazine is basic in nature[17], but less so than ammonia. It is in fact a bifunctional base, and in the presence of water behaves as follows:

$$N_2H_{4(aq)} + H_2O \rightleftharpoons N_2H_5^+ + OH^- \quad K_{25C}=8.5\times10^{-7}$$

$$N_2H_5^+{}_{(aq)} + H_2O \rightleftharpoons N_2H_6^{2+} + OH^- \quad K_{25C}=8.9\times10^{-16}$$

scheme 5.6: solution equilibria of hydrazine

As is evident from the above reaction schemes, two types of hydrazinium salts are possible. The $N_2H_5^+$ salts tend to be more stable in water. Degradation of the *closo*-carborane cage to the dicarbaundecaborate anion through hydrazine has been reported by several workers on *ortho*,[18] *meta*[15,16] substituted and unsubstituted isomers. In the examples of *ortho*-carborane, methyl-*ortho*-carborane, mono- and diphenyl-*ortho*-carborane and phenyl-*meta*-carborane, removal of one BH vertex was the common result when the carborane and hydrazine were refluxed together for several hours.

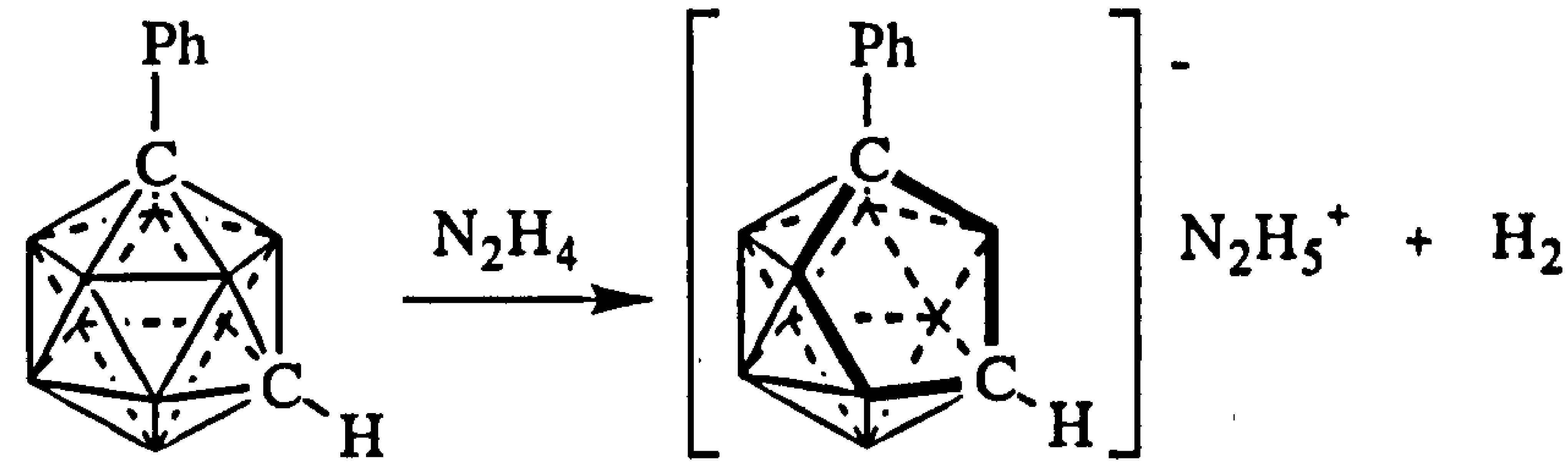

scheme 5.7: deboronation of phenyl-meta-carborane with hydrazine

Many deboronation reactions of diaryl *meta*-carboranes,[19,20] do not follow the same reaction pathway as the other carborane derivatives of the same series. The same is true of the reaction of di-phenyl-*meta*-carborane with hydrazine. When diphenyl *meta*-carborane was boiled with anhydrous hydrazine, the carborane cage underwent complete destruction.[16] The authors claimed however, that degradation of the cage could be halted at the dicarbaundecaborate anion stage when a high boiling solvent such as toluene was employed.

Amines such as piperidine and n-propylamine have been reported to form stable adducts with *ortho*-carboranyl derivatives[18] through a BN linkage with the *closo* cage (no point of substitution was proposed but B:N ratios of 10:1.5 to 10:3.3 were reported), and to undergo no reaction with *meta*-carboranes.[21] Contradictory studies[6,11] showed that these bases effected deboronation of both isomers. Other bases[22] such as pyridine and quinoline have also exhibited their potential to deboronate the *closo* icosahedral cages of *ortho* and *meta*-carboranes, and like the deboronation reaction via alkoxide ion, the reaction was first order in both the carborane and the amine.[6]

5.2.3 Fluoride Ion

Removal of a BH vertex by means of fluoride ion (from tetrabutyl ammonium fluoride) has been exploited as a means of deboronation of icosahedral carboranes over the last few years. Onak *et al.*[23] used anhydrous tetrabutyl ammonium fluoride (Bu_4NF) to effect deboronation, and reported the removal of the BH vertex to be slow but effective. Later studies[19,24,25] have exploited "wet" tetrabutyl ammonium fluoride and found the deboronation reaction to occur far more quickly under similar conditions; *ortho*-carboranyl derivatives as ever being quicker to react than their *meta*- analogues. The proposed reason for this was that water was actually involved in the deboronation reaction and that the deboronation reaction mechanism varied slightly between the *ortho-* and *meta-* deboronation reactions, although ultimately the same end-products were formed.

The deboronation reaction with fluoride ion varied slightly depending on the reactant ratios. For complete reaction of *ortho* or *meta*-carborane with fluoride ion to give the deboronated $RC_2B_{10}H_{11}^-$ residue, a 2:3 carborane:F^- ratio was found to be optimum.

$$6RC_2B_{10}H_{11} + 9F^- + 9H_2O \longrightarrow 6RC_2B_{10}H_{11}^- + 3HOBF_3^- + 6H_2 + B_3O_3(OH)_3$$

scheme 5.8: reaction of carborane with fluoride ion

Experimentation has shown that with a 1:1 ratio of carborane: fluoride ion, the reaction was slow and did not go to completion. The reaction proceeded through several stages, initially requiring two equivalents of F^- to initiate the deboronation.

$$RC_2B_{10}H_{11} + 2F^- + H_2O \longrightarrow RC_2B_{10}H_{11}^- + HOBHF_2^-$$

$$HOBHF_2^- + H_2O \longrightarrow (HO)_2BF_2^- + H_2$$

scheme 5.9: reaction stages for deboronation of ortho- and meta-carboranes with fluoride ion at a 1:1 carborane:F^-ratio

As the reaction continued, the $(HO)_2BF_2^-$ disproportionated to $HOBF_3^-$, the proportion of which decreased with time in the absence of F^- to give BF_4^- ($\delta(^{19}F)$= -150.4ppm).

$$2(HO)_2BF_2^- \longrightarrow (HO)_3BF^- + HOBF_3^- \longrightarrow (HO)_4B^- + BF_4^-$$

scheme 5.10: disproportionation of $(HO)_2BF_2^-$ to give BF_4^-

When fluoride ion was in excess, the deboronation reaction was quicker and more efficient than using the stoichiometrically required quantities. In the case of *meta*-carborane (but not *ortho*) the major fluoroborate was seen to be $(HO)_2BF_2^-$ in the initial deboronation stages (as in scheme 5.9), but as the reaction developed, the $HOBHF_2^-$, HBF_3^- and $HOBF_3^-$ species became dominant. Where there was excess fluoride ion present, an extra step involving the reaction of $HOBHF_2^-$ and F^- gave HBF_3^- ($\delta(^{19}F)$ d of q, -136.3ppm), which was then integrated into the reaction equation as:

$$RC_2B_{10}H_{11} + 3F^- + H_2O \longrightarrow RC_2B_9H_{11}^- + HBF_3^- + OH^-$$

scheme 5.11: intermediate reaction equation for deboronation of meta-carboranes with excess fluoride ion

It has been suggested that the ease of deboronation is of the same order as the Hammett acidity function of the considered compounds.[24] By this reasoning, the rate of deboronation was proposed to increase as the electron withdrawing potential of the substituent increased. No deboronations of *para* isomers with fluoride ion have been reported.

Diaryl-*meta*-carboranes, as observed for hydrazine deboronations, appear to be a special case. When 1,7-R_2-1,7-$C_2B_{10}H_{10}$ (R = phenyl, 2'-pyridyl, 4'-phenoxyphenyl or 4'-fluorophenyl) was attacked by F^- during deboronation, fluorine was seen to attach itself to the cage boron atoms on the open *nido* face, and in certain instances, with time, rearrange to appear on one of the fully enclosed cage B atoms.[19] Other workers[20] using the fluoride ion method of deboronation have not observed the presence of fluorine on the cage borons during the reaction, but by X-ray crystallography have observed the presence of a small boron-attached moiety on the open face of the compound (B(10)), assigned as a hydroxide group. The hydroxide group and fluoride group would be similar in the X-ray determination.

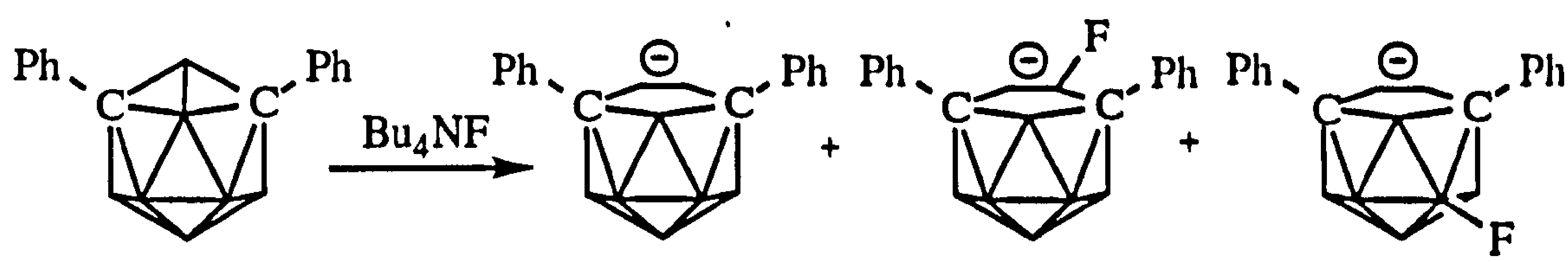

scheme 5.12: deboronation of 1,7-di-phenyl-meta-carboranewith fluoride ion

This phenomenon is not repeated in aliphatically substituted or in mixed aryl/aliphatically substituted *meta*-carboranes. B-F fluorination has been achieved by other means on other base carborane and borane systems and this has been discussed earlier with the fluorination reactions of carboranes (Chapter Two).

5.2.4 Dianionic Species

The above methodologies are ideal for creating mono-anionic *nido* species, $RR'C_2B_9H_{10}^-$. To obtain the dianionic derivatives, the *nido* species can be further reduced with an alkali metal species such as Na metal, NaH, KH or BuLi, removing the non-terminal hydrogen from the open face of the cage.[3,5] Alternatively the mono-anionic salt can be reacted with thallium acetate to yield the di-thallium salt. From this, many metallacarboranes can be produced by reaction with metal chloride to eliminate thallium chloride.[7,8]

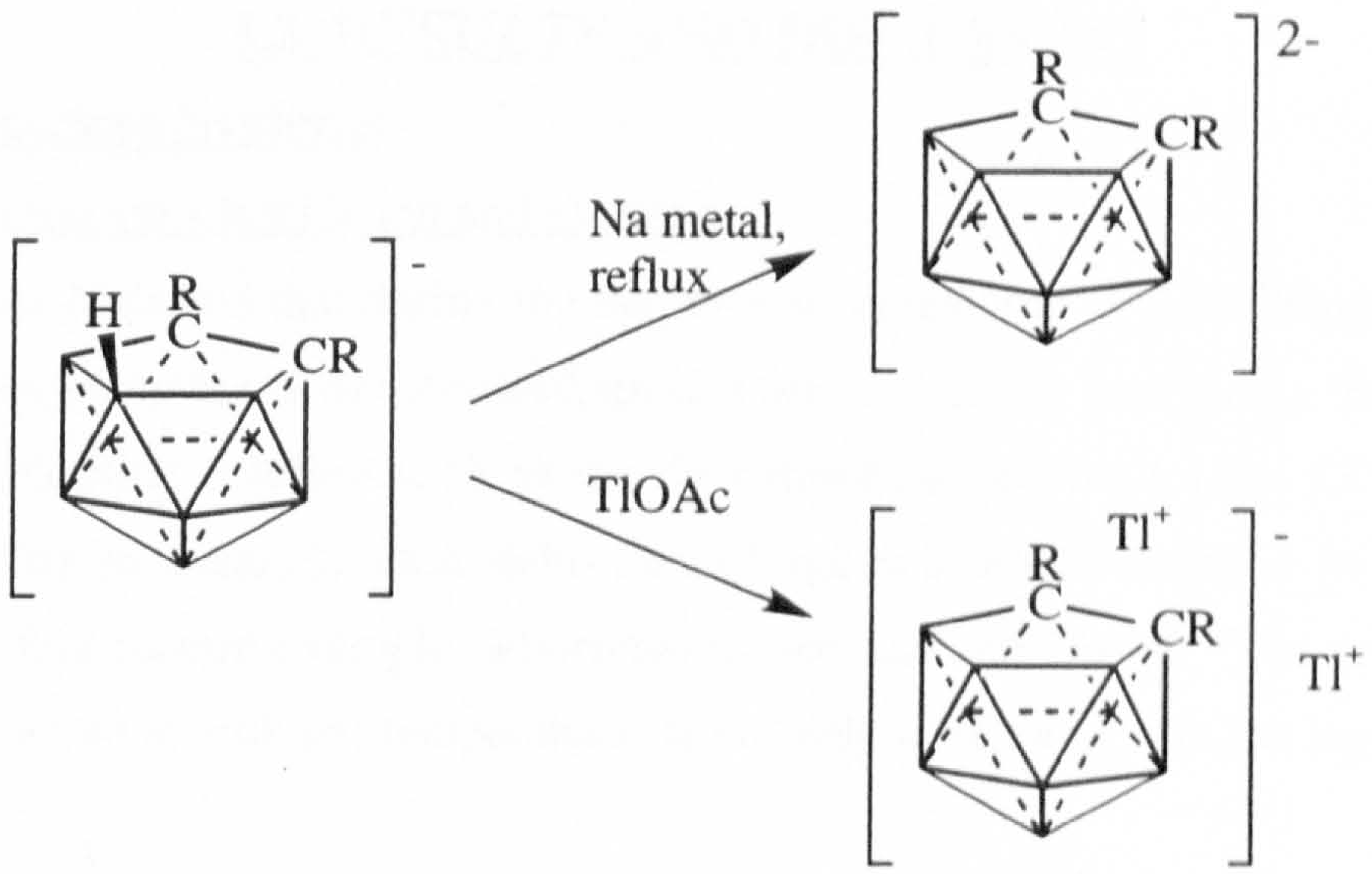

scheme 5.13: formation of the nido carboranyl dianion

5.2.5 Applications

Through deboronation of a *closo* cage, a *nido* residue which has an open face with available bonding orbitals, is formed. This opens the field of metallacarborane chemistry.[26] Non-metallic cations such as R_4N^+ have an ion pair relationship with the cage. Dicarbollide complexes, where a metal centre is complexed to dianionic *nido* residues, are similar to metallocenes in that the metal centre is co-ordinated to electron-rich five-membered rings. Some metallacarboranes have shown catalytic activity.[27] Metallacarboranes also have structural interest and many examples of metallacarboranes exist where the metal is incorporated as a cage vertex, causing distortion in the icosahedral framework.

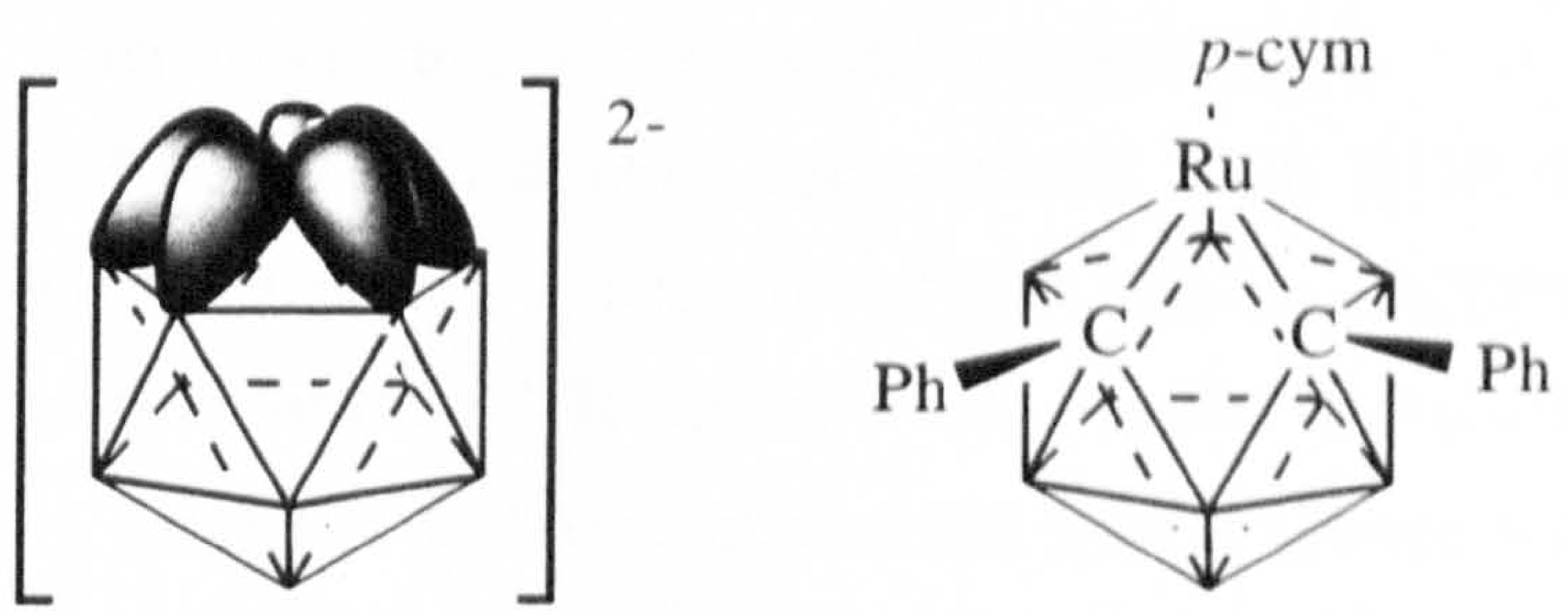

figure 5.3: bonding orbitals of the dianion $C_2B_9H_{11}^{2-}$ are oriented towards the vacant vertex. Insertion of a metal vertex can cause cage distortion. (p-cym=$CH_3C_6H_4C(CH_3)_3$)

5.3 RESULTS AND DISCUSSION

5.3.1 One-cage Systems

a) deboronation via alkoxide ion and via amines

It was observed that during the deprotonation reaction of *o*-$PhCB_{10}H_{10}CCO_2H$ with aqueous ammonia, a deboronated species was formed as well as the desired CO_2^- anion. In alkoxide solution such as the deprotonation reactions with KOH and 18-crown-6 ether in ethanol, such deboronated species would perhaps be expected, however in this current example deboronation was not anticipated. The deboronation reaction occurred at ambient temperature, apparently in tandem with the deprotonation reaction.

Reference to Teixidor's work[12,13,14] on the progressive deprotonation and deboronation reactions of mercapto-carboranes, shows the same reasoning can be postulated to explain the deboronation of *o*-$PhCB_{10}H_{10}CCO_2H$ after its initial deprotonation with ammonia. A contributing factor may also be the formation of OH^-, due to the solution equilibrium of ammonia, which could aid the deboronation reaction.

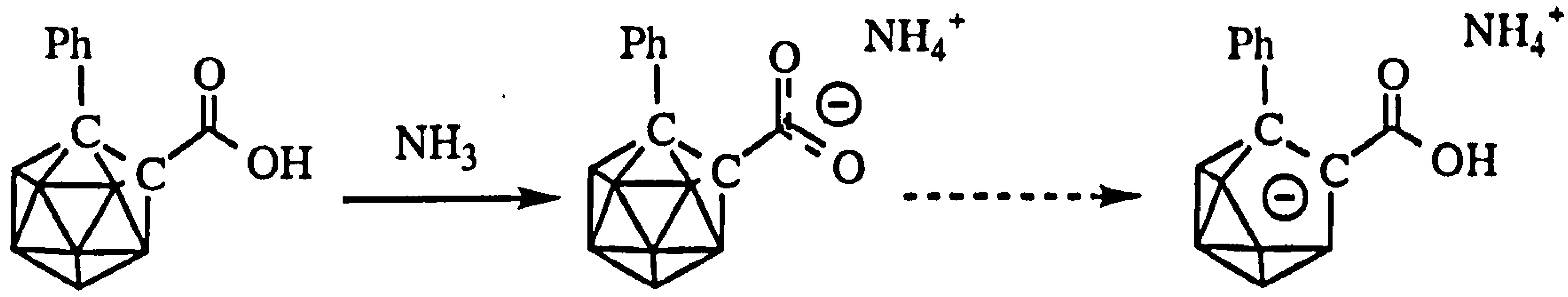

scheme 5.14: deprotonation of carboxylic acids with ammonia leads to deboronation

Deprotonation of *o*-$PhCB_{10}H_{10}CCO_2H$ by proton sponge in ether, and by KOH and 18-crown-6 ether in ethanol also gave deboronated species as minor products. *Meta*-$(HO_2C)CB_{10}H_{10}C(CO_2H)$ doubly deprotonated with KOH/18-crown-6 also became deboronated on standing in solution. NMR solutions ($CDCl_3$) became pink with time. Deboronation of the K^+/18-crown-6 salt is easily explained by the presence of alkoxide ions in solution. Deboronation of the proton sponge salts is less easily explained. In solution ($CDCl_3$, $CHCl_3$, CH_2Cl_2 and CD_3CN) all the deprotonated carboxylic acid carborane derivatives decomposed, (*meta* and *para* decomposed on diluting the reaction solutions with either CH_2Cl_2 or chloroform.) so it may be that the formation of the undecaborate anionic fragment was an intermediate before the ultimate formation of boric acid. (^{11}B NMR spectra showed a large boric acid peak at *c*.20ppm, larger than would be produced by simple deboronation.)

b) deboronation via fluoride ion

To date, fluoride ion in the form of tetrabutyl ammonium fluoride, has proven successful as a deboronating agent for a variety of aliphatically and aromatically substituted carboranes. In diaryl systems, fluorination of the cage boron atoms has also been observed as a peculiarity of this particular reagent. The present study has examined the fluoride ion deboronation reactions of 3-pyridyl- and 2-thiophenyl-*ortho*- and *meta*-carboranes, looking at the influence of heteroaryl substituents on the degradation reactions and with a particular goal of observing cage fluorination.

1,7-(2'-pyridyl)-1,7-$C_2B_{10}H_{10}$ has been shown to fluorinate during the deboronation reaction[19], however, the 3'-pyridyl substituent is significantly less electron withdrawing than either the 2'- or 4'- isomers, so it was hoped that some changes in the deboronation reaction would be manifested. The thiophenyl derivatives were chosen as a novel heteroaryl substituent for comparison.

NMR scale reactions were conducted in THF using 1-R-1,2-$C_2B_{10}H_{11}$ (R = 2'-pyridyl), 1-R-1,7-$C_2B_{10}H_{11}$ (R = 2'-pyridyl) and 1,7-R_2-1,7-$C_2B_{10}H_{10}$ (R = 2'-pyridyl or 2'-thiophenyl) with Bu_4NF in the molar ratio 5:1 (Bu_4NF:carborane), except for 1-R-1,2-$C_2B_{10}H_{11}$ (R = 2'-thiophenyl), 1-R-1,7-$C_2B_{10}H_{11}$ (R = 2'-thiophenyl) where a 1:1 ratio was used. For clarity, A refers to F^-, B to $HOBHF_2^-$, C to $(HO)_2BF_2^-$, D to $HOBF_3^-$ and E to BF_4^- in the following tables.

i) *ortho*-carboranyl derivatives

Different ratios of fluoride ion to carborane were used for each compound. It is assumed, from previous work done in this area, that the reaction will be the same for each compound at the same concentration. It has been found that for fluoride ion deboronation reactions of mono-heteroaryl-*ortho*-carboranes, the mechanism of deboronation essentially followed that predicted in earlier work.

Consider primarily the reaction between 1-(3'-pyridyl)-1,2-$C_2B_{10}H_{11}$ where the F^-:carborane ratio is 5:1. The reaction was followed by ^{19}F NMR spectroscopy.

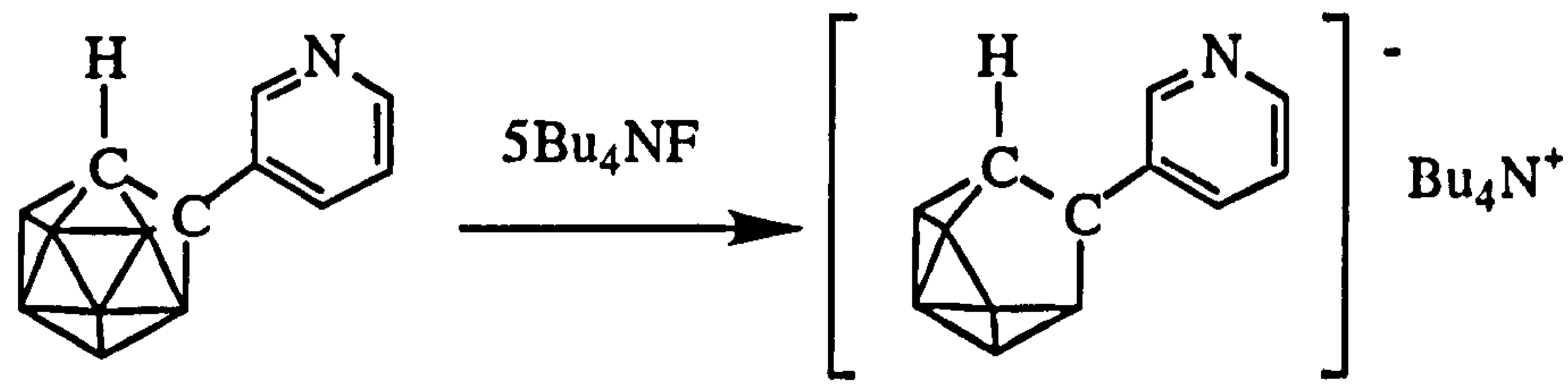

scheme 5.15: deboronation of 1-(3'-pyridyl)-ortho-carborane with excess fluoride ion

SHIFT TIME	-113.5 A	-132.3 B	-136.8 C	-143.7 D	-151.5 E
0m	100	-	-	-	-
1m	82	trace	6	-	11
2m	77	trace	5	-	17
4m	73	-	7	trace	17
6m	65	-	9	1	18
10m	63	-	10	3	18
50m	72	-	9	19	-
2h	40	-	3	15	-
14h	63	-	4	30	-
7d	62	-	3	29	-
13d	59	-	4	30	-
38d	64	-	4	29	-

table 5.1: percentages of monoboron fluorides in solution for the reaction of 1-(3'-pyridyl)-1,2-$C_2B_{10}H_{11}$ with Bu_4NF, where the F^-:carborane ratio was 5:1

As has been reported for other systems when an excess of fluoride ion was used, the initial formation of the $(HO)_2BF_2^-$ ion, together with the formation of the $HOBHF_2^-$ ion, manifested as a multiplet at -132.5ppm was observed. Unreacted F^- remained as a broad peak at -113.4ppm throughout the reaction. As time progressed, other small peaks appeared, attributable to polyborates, probably being produced as a result of reactions between the boric acid produced as the cage deboronated and the monoboron anions. After 50minutes reaction time, the $HOBF_3^-$ ion started to dominate the spectrum, and the other mono and polyborate species appeared only as minor products in the reaction.

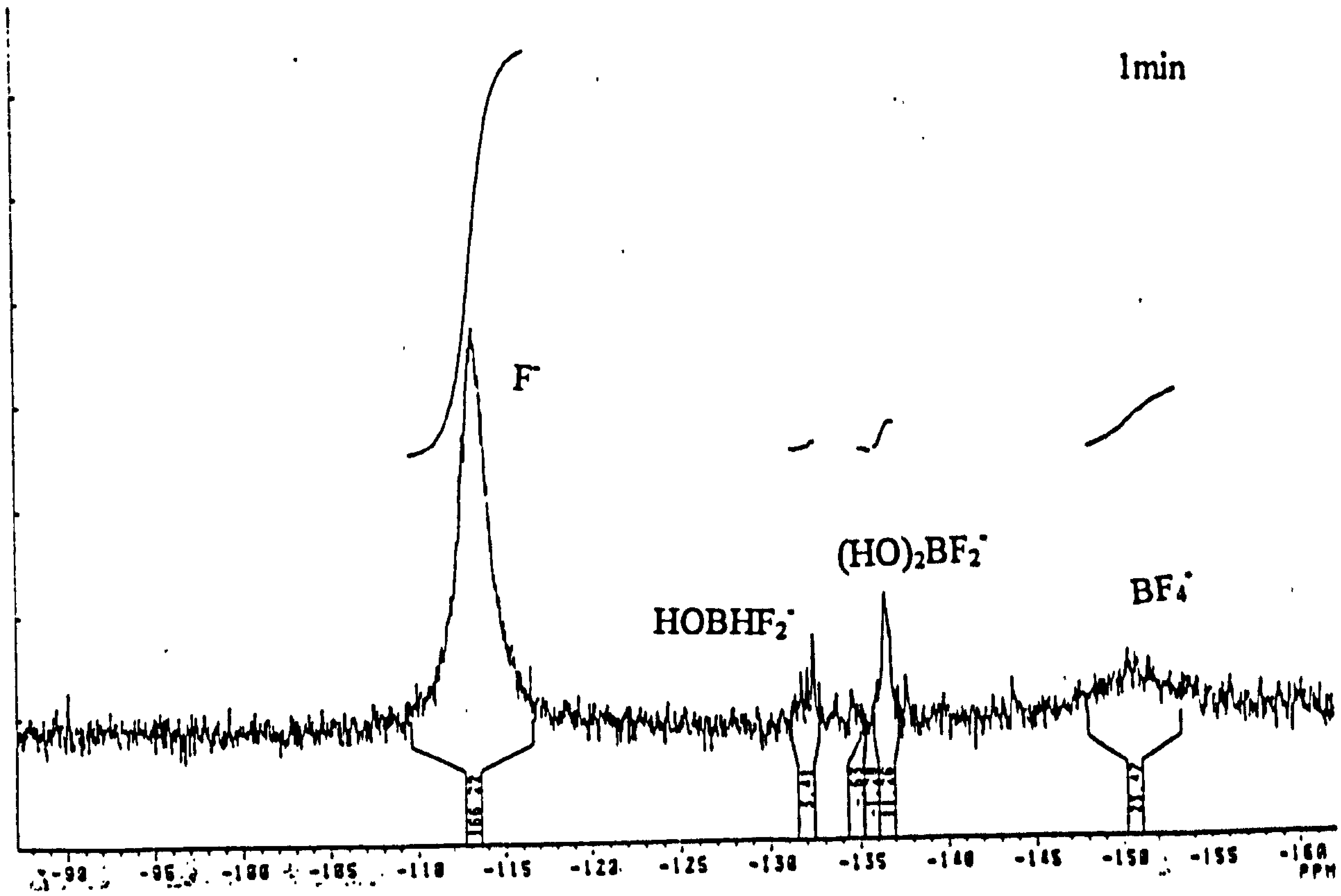
1min
F⁻
$(HO)_2BF_2^-$
$HOBHF_2^-$
BF_4^-
PPM

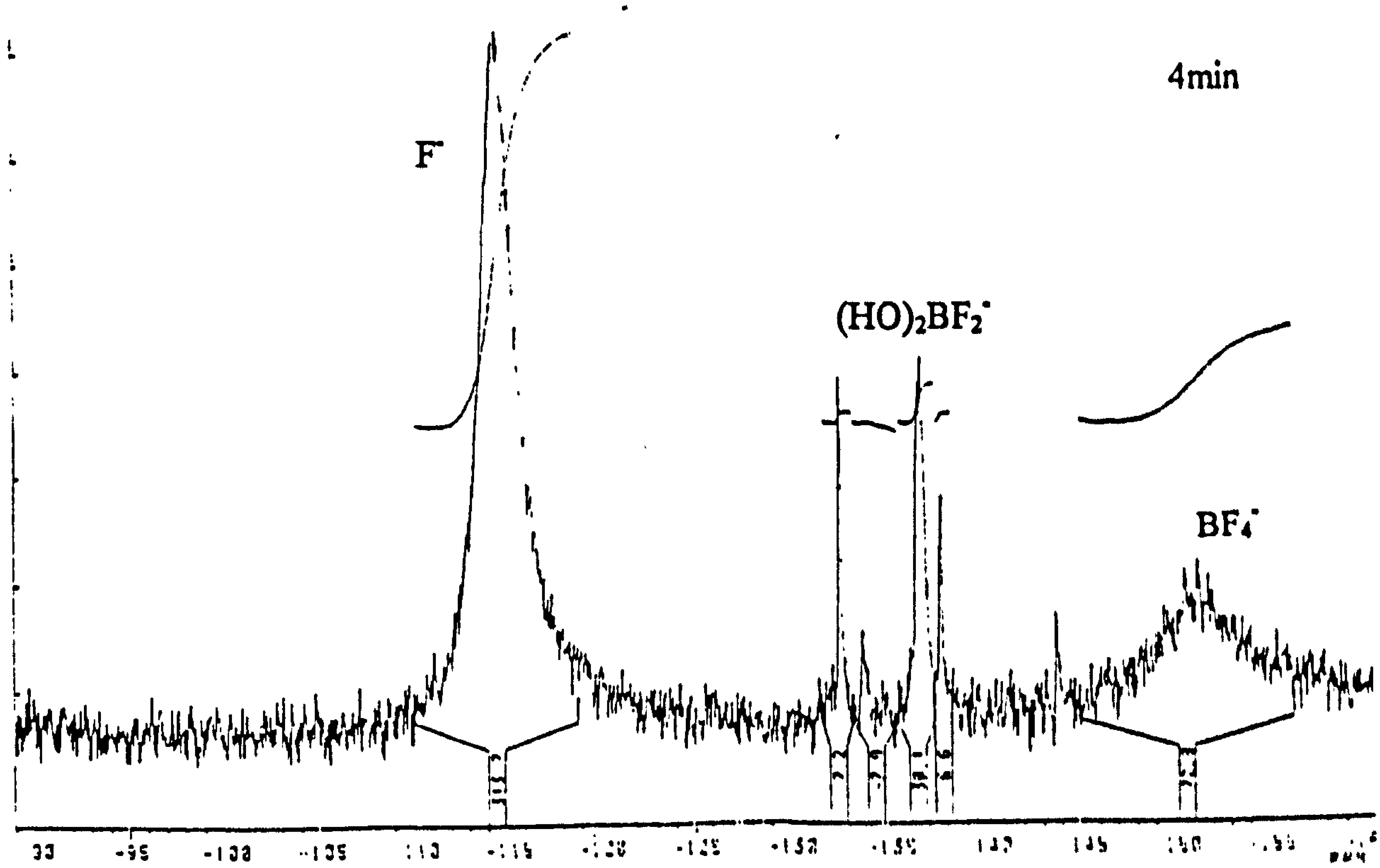
4min
F⁻
$(HO)_2BF_2^-$
BF_4^-

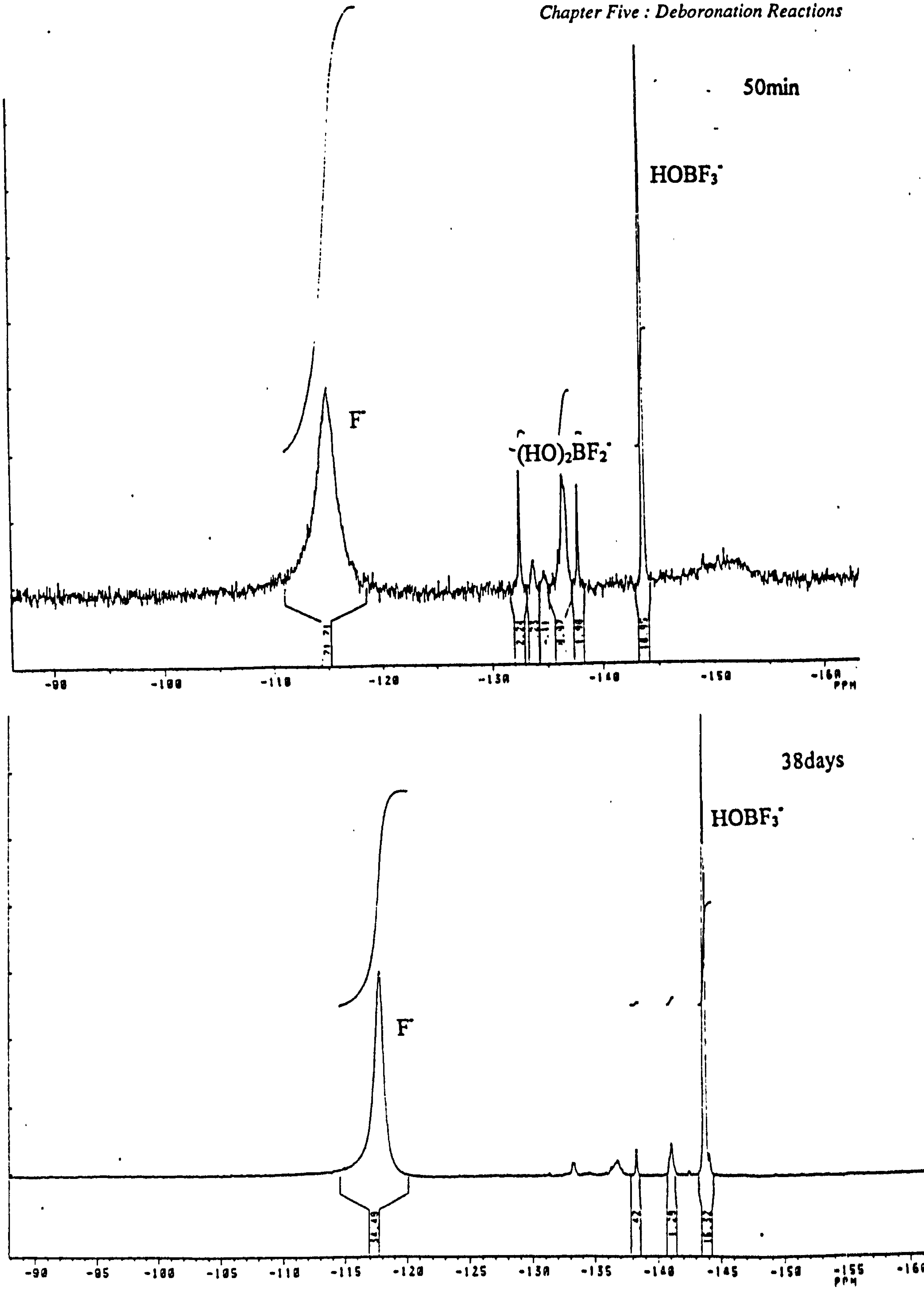

figure 5.4: ^{19}F NMR spectra following the reaction of 1-(3'-pyridyl)-ortho-carborane with Bu_4NF (1:5 ratio) in THF

For contrast, in the reaction between fluoride ion and 1-thiophenyl-*ortho*-carborane, the reactants were combined in a 1:1 ratio.

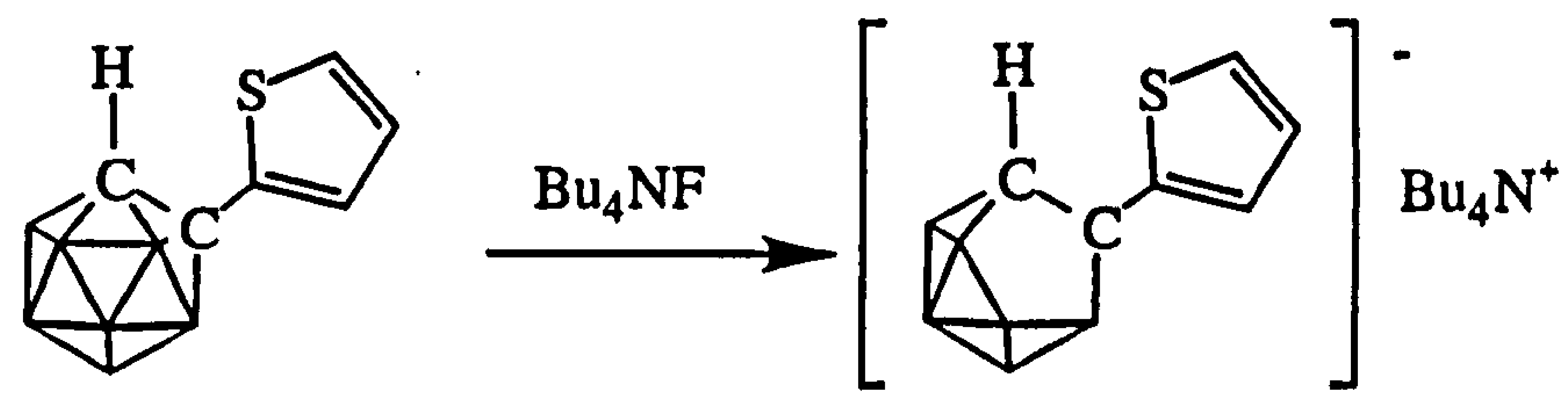

scheme 5.16: deboronation of 1-(2'-thiophenyl)-ortho-carborane with an equimolar ratio of fluoride ion

shift / time	A	-132.3 B	-137.0 C	-144.0 D	-151.4 E
0m	100				
1m	-	58	16	2	24 (br)
2m	-	64	15	4	16 (br)
5m	-	69	15	12	3 (br)
10m	-	58	7	32	-
15m	-	49	11	37	-
30m	-	39	10	49	-
60m	-	18	7	71	-
90m	-	6	6	81	-
15h	-	-	-	63	-
19d	-	-	-	-	100 (sh)
24d	-	-	-	-	76

table 5.2: percentages of monoboron fluorides in solution for the reaction of 1-(3'-thiophenyl)-1,2-$C_2B_{10}H_{11}$ with Bu_4NF, where the F^-:carborane ratio was 1:1

Upon combining the two reactants, the solution immediately turned deep yellow, and the first fluorine NMR spectrum (recorded at 1minute), showed the absence of all fluoride ion. The major product was the $HOBHF_2^-$ ion with almost equal quantities of BF_4^- and $(HO)_2BF_2^-$. As the reaction proceeded, the quantities of the products changed. Excess water in the reaction reacted with the $(HO)_2BF_2^-$ producing $HOBF_3^-$, which at 90minutes reaction time was the predominant product. After 60minutes reaction, previously unnoted peaks appeared at -139.0ppm and -144.5ppm which with time decreased and increased respectively. These were most probably polyborate materials. Also, as observed for previous fluoride ion deboronation reactions, where the carborane and Bu_4NF were in equimolar ratios, the $HOBF_3^-$ was converted to BF_4^- as the ultimate monoboron fluoride species.

ii) *meta*-carboranyl derivatives

Turning to the aryl-*meta*-carboranyl examples, there are three possible scenarios: the carborane can be 1) mono substituted, 2) R,R-disubstituted or 3) R,R'-

disubstituted. R,R' systems have not been considered here (although 2,4,6-tri-(7'-phenyl-*meta*-carboranyl)-1,3,5-triazine system is discussed in section 5.3.2b).

R-mono-substituted *meta* carboranes

The first compound to be considered was 1-(3'-pyridyl)-*meta*-carborane, reacted with a five-fold excess of Bu_4NF in THF. Again ^{19}F NMR spectroscopy was used to track the reaction.

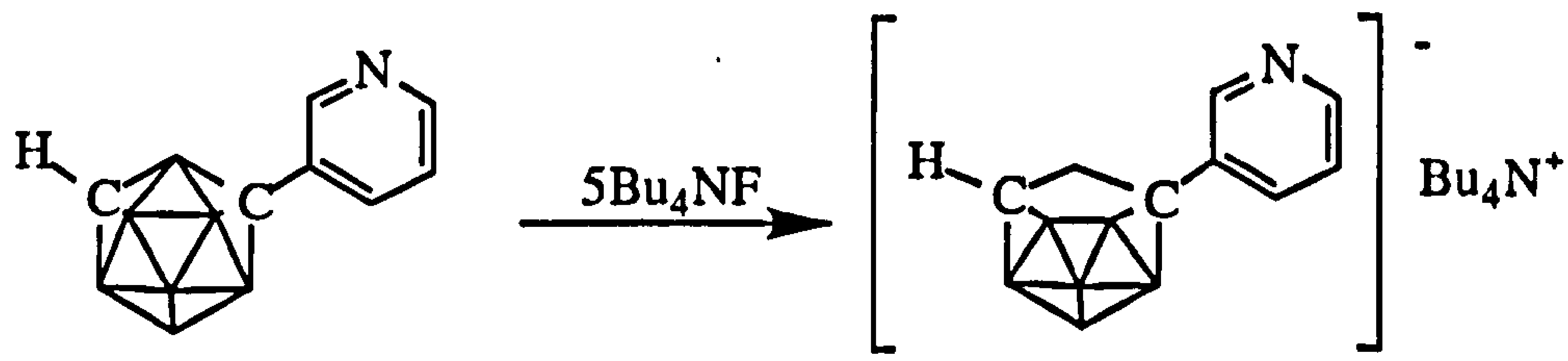

scheme 5.17: deboronation of 1-(3'-pyridyl)-meta-carborane with fluoride ion

shift time	-116.1 A	-132.2 B	-136.7 C	-143.9 D	-151.4 E
0m	100				
1m	74	15	2	-	10
2m	72	17	3	-	10
5m	68	17	4	-	11
12m	61	17	9	1	11
60m	57	-	12	18	6
13h	59	-	5	31	-
7d	48	-	8	18	-
14d	42	-	10	15	-
38d	31	-	7	16	-

table 5.3: percentages of monoboron fluorides in solution for the reaction of 1-(3'-pyridyl)-1,7-$C_2B_{10}H_{11}$ with Bu_4NF, where the F^-:carborane ratio was 5:1

As has been seen in reported reactions of this type, the initial fluoride containing monoboron product was $HOBHF_2^-$, present as a doublet of 1:1:1:1 quartets. As the reaction of side products advanced, $(HO)_2BF_2^-$ and latterly $HOBF_3^-$ became the prevailing products. ^{19}F NMR spectroscopy showed, however, that unlike previous fluoride ion deboronations of *meta*-$RC_2B_{10}H_{11}$, no HBF_3^- was present. Instead, after 38 days reaction, the mixture was composed exclusively of F^-, $(HO)_2BF_2^-$, $HOBF_3^-$, and various polyborate species ($\delta(^{19}F)$ -135.7 (br.) and -138.5 (s, sh.)).

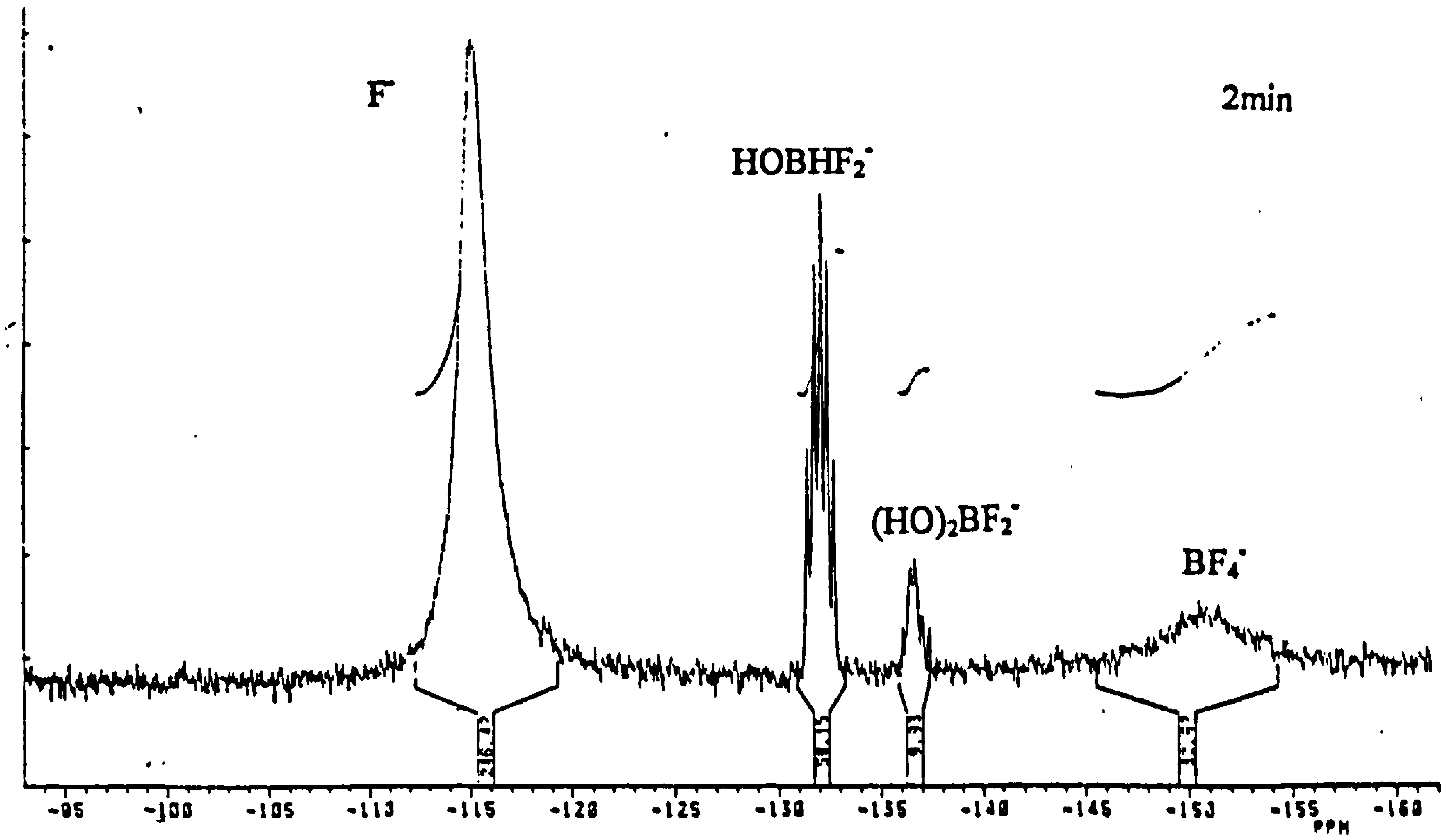

F^-
2min
$HOBHF_2^-$
$(HO)_2BF_2^-$
BF_4^-
PPM

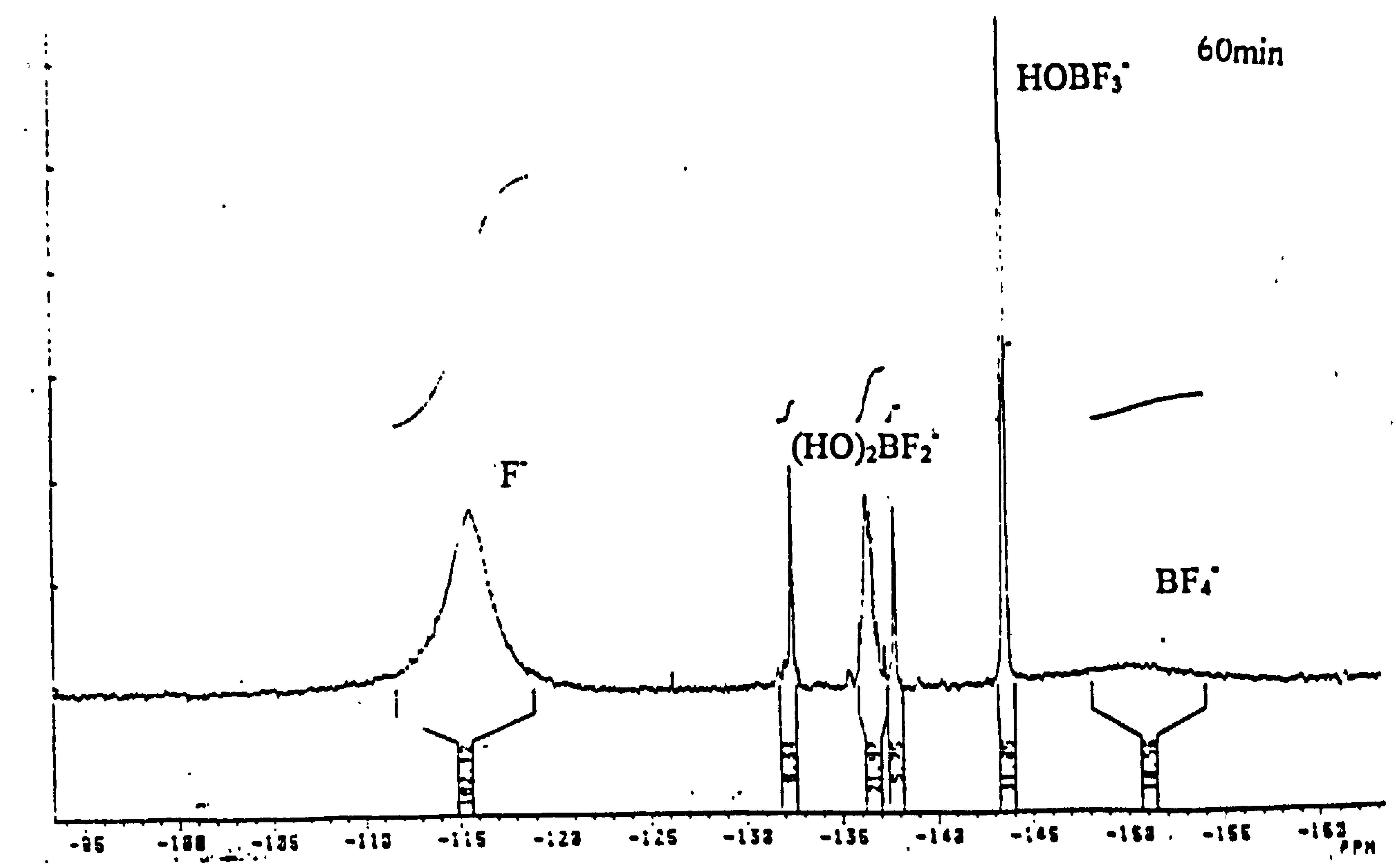

60min
$HOBF_3^-$
$(HO)_2BF_2^-$
F^-
BF_4^-
PPM

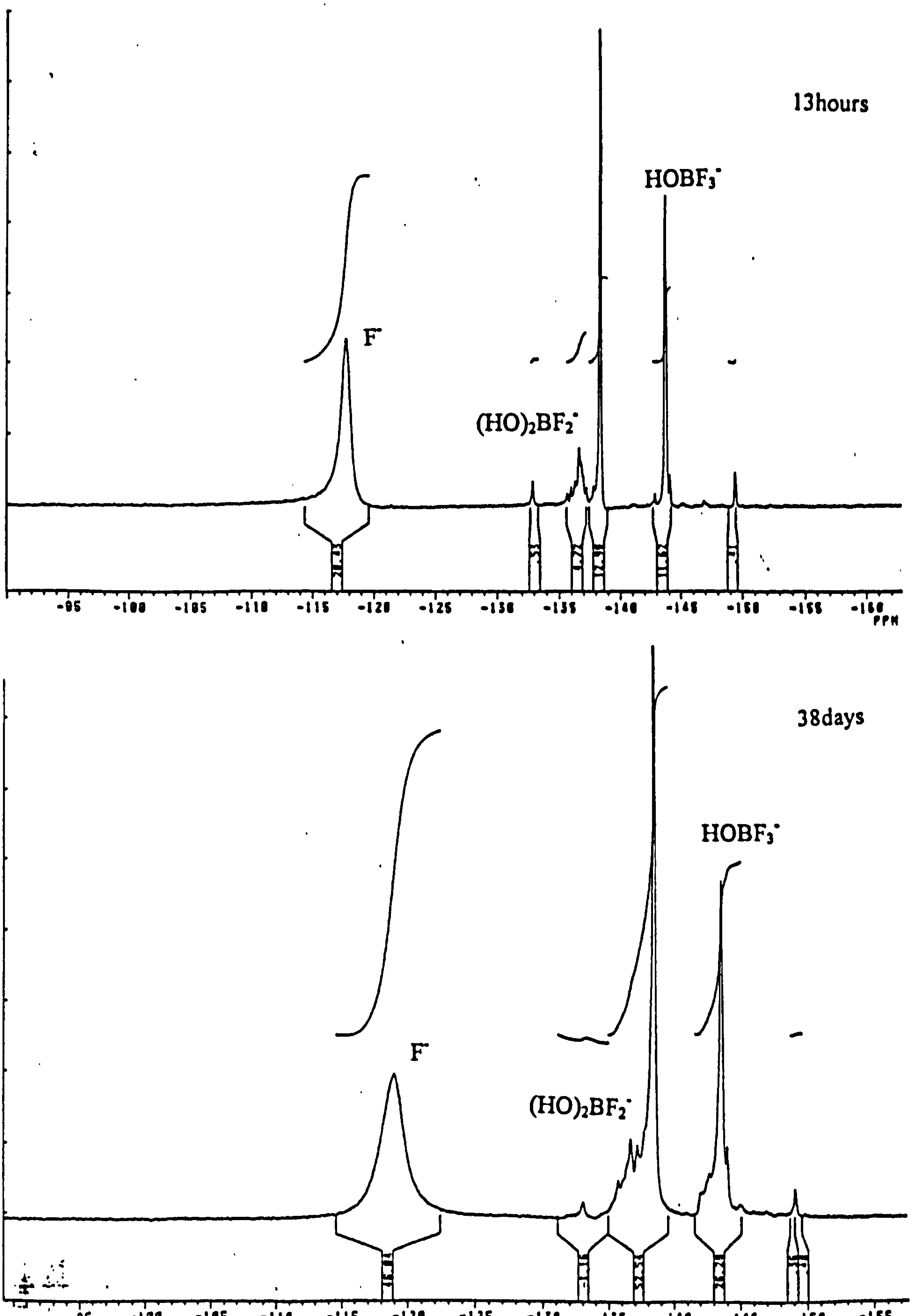

figure 5.5: ^{19}F NMR spectra from the reaction of Bu_4NF with 1-(3'-pyridyl)-meta-carborane

Degradation of *meta*-carboranes is generally slower than that of *ortho*-carboranes, and slightly more forcing conditions are required, which would favour the argument of using an excess of fluoride ion. However, for interest, a 1:1 ratio of fluoride ion (Bu_4NF) to 1-(2'-thiophenyl)-*meta*-carborane was combined, and again the reaction course monitored by ^{19}F NMR spectroscopy.

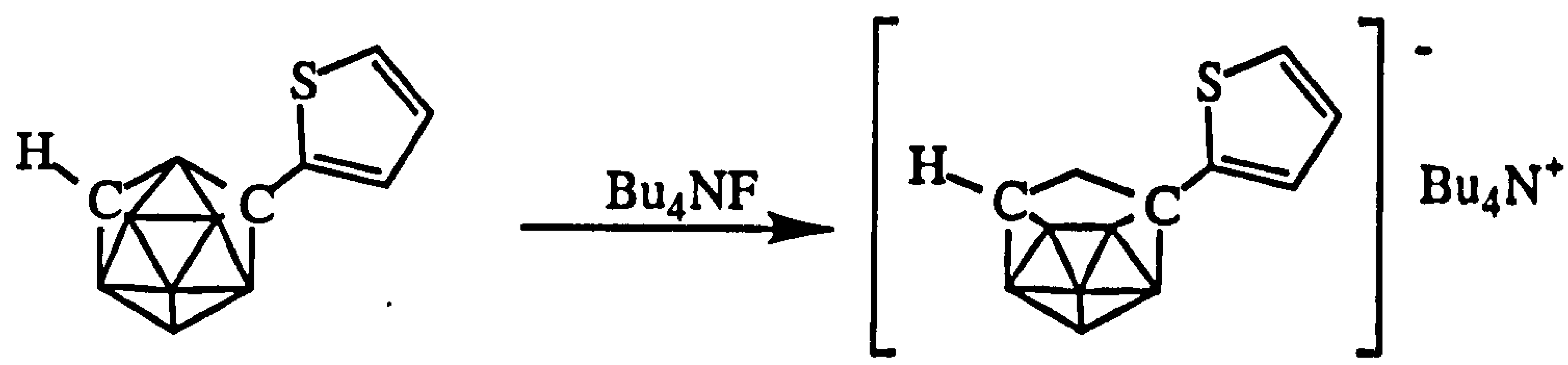

scheme 5.18: deboronation of 1-(2'-thiophenyl)-meta-carborane with fluoride ion

SHIFT TIME	-114.8 A	-132.3 B	-137.0 C	-143.9 D	-152 E
0m	100				
1m	66	22	5	-	7
3m	33	38	19	-	11
10m	19	23	29	trace	12
20m	19	14	28	9	10
30m	11	3	31	17	6
75m	8	-	24	41	-
90m	8	-	23	43	-
15.5h	-	-	-	71	-
19d	-	-	-	50	-
24d	-	-	-	60	1

table 5.4: percentages of monoboron fluorides in solution for the reaction of 1-(2'-thiophenyl)-1,7-$C_2B_{10}H_{11}$ with Bu_4NF, where the F^-:carborane ratio was 1:1

The first conclusion to be drawn was that the reaction was indeed much slower, as the fluoride ion was consumed over a much longer period of time when compared to the same reaction with the *ortho*-isomer. The first boron-fluoride product to form was $HOBHF_2^-$. With time, this was converted to $(HO)_2BF_2^-$ then ultimately to $HOBF_3^-$. Unlike the *ortho* isomer, $HOBF_3^-$ was not converted to BF_4^- in this time span, although as the reaction was generally slower, this may well have occurred with time. In common with the deboronation of 1-(3'-pyridyl)-*meta*-carborane, no HBF_3^- was observed during the course of deboronation, with polyborate and fluorinated boron species apparently being formed preferentially ($\delta(^{19}F)$ -139.1 (s, sh.) and -144.5 (s, sh.)).

Finally we look at the system which has given many curious results in the past, the diaryl *meta*-carboranes. Differences with other systems were again evident, even with respect to the di-phenyl- and di-(4'-fluorophenyl)- derivatives discussed in the literature. As stated above, two compounds were investigated, the di-(2'-thiophenyl)- and di-(3'-pyridyl)-*meta*-carboranes. The reactants were combined with a five fold excess of fluoride ion (Bu_4NF) in THF and the reaction followed by ^{19}F NMR spectroscopy. The principle markers of the reaction progress are tabulated below.

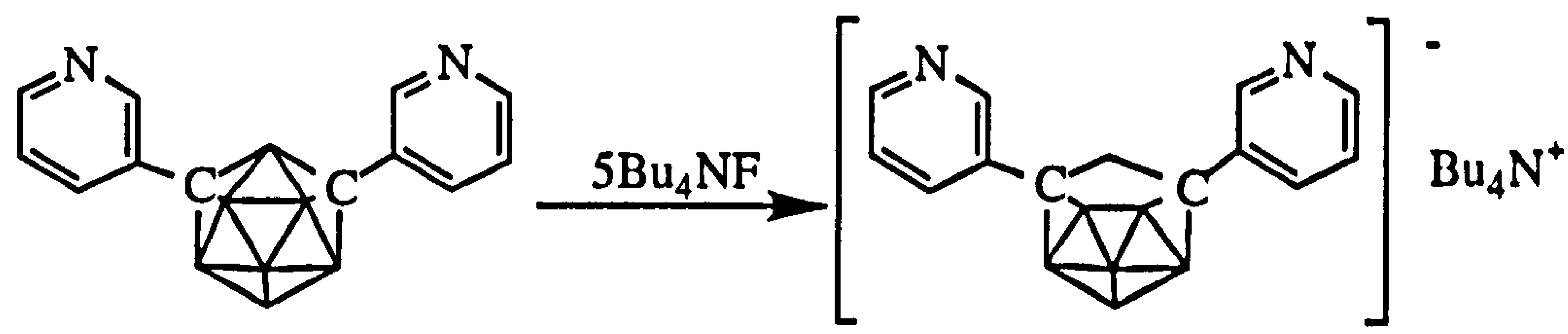

scheme 5.19: deboronation of 1,7-di-(3'-pyridyl)-meta-carborane with fluoride ion

shift time	-115.4 A	-136.8 C	-144.0 D	-150.2 E	-202.3	-209.0	-215.9	-221.5
0m	100							
1m	88	-	-	12	-	-	-	-
2m	92	-	-	8	-	-	-	-
3m	79	3	-	6	6	6	-	-
4m	79	1	-	6	8	5	-	-
5m	77	-	-	9	6	6	-	-
7m	75	1	-	9	8	6	-	-
12m	83	3	-	2	5	3	-	-
20m	76	4	-	1	7	6	-	-
35m	71	5	1	2	8	5	-	-
40m	73	5	1	1	5	4	-	-
55m	71	5	2	1	6	4	-	-
70m	70	5	2	1	5	6	-	-
90m	68	5	3	1	6	5	-	-
2h	72	2	5	-	5	6	-	-
13h	67	6	10	-	4.	4	-	-
15h	64	4	11	-	6	6	-	-
18h	67	2	12	-	6	6	-	-
19h	69	2	12	-	4	4	-	-
2d	63	2	12	-	5	5	5	2
3d	65	4	12	-	2	2	4	4
6d	66	5	12	-	-	-	5	-
7d	66	5	12	-	-	-	5	-
13d	65	9	12	-	-	-	-	-
38d	62	3	11	-	-	-	-	

table 5.5: percentages of monoboron fluorides in solution for the reaction of 1,7-di-(3'-pyridyl)-meta-carborane with Bu_4NF, where the F^-:carborane ratio was 5:1

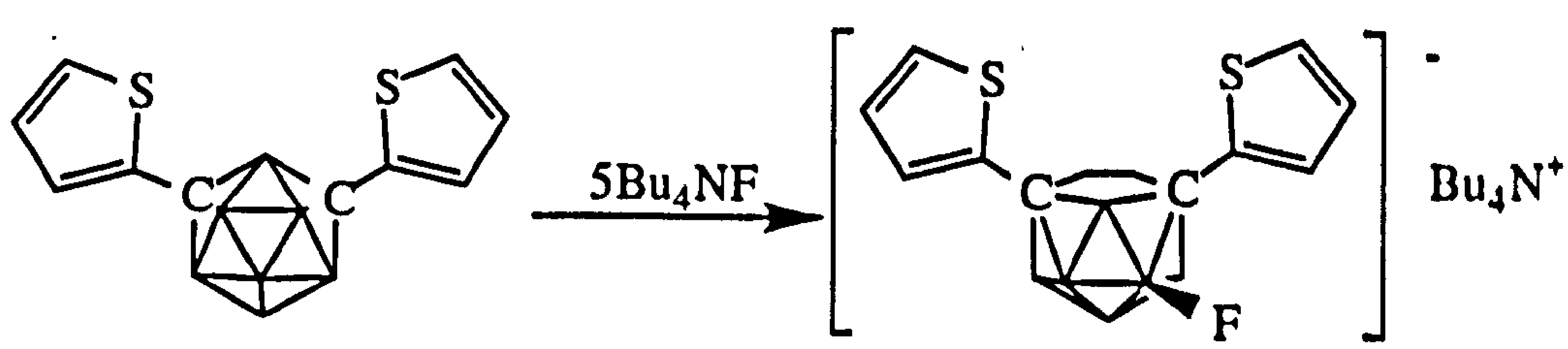

scheme 5.20: deboronation of 1,7-di-(2'-thiophenyl)-meta-carborane with fluoride ion

SHIFT TIME	-114.5 A	-132.3 B	-136.7 C	-144.0 D	-151.4 E	-202.0	-210.0	-214.9	-220.2
0m	100	-	-	-	-	-	-	-	-
1m	100	trace	-	-	trace	-	-	-	-
2m	100	trace	-	-	trace	-	-	-	-
3m	92	3	-	-	6	-	trace	-	-
4m	72	4	1	-	5	8	10	-	-
5m	78	2	1	-	4	7	7	-	-
10m	69	4	2	-	4	13	9	-	-
18m	72	1	2	1	4	12	10	-	-
25m	76	2	4	1	-	8	6	-	-
30m	72	1	5	1	-	8	6	-	-
38m	72	1	5	1	-	9	5	-	-
45m	68	1	6	1	-	9	8	-	-
60m	66	-	6	1	-	9	9	-	-
75m	66	-	6	1	-	11	6	-	-
105m	62	-	7	2	-	11	6	-	-
12.5h	51	-	3	9	-	11	7	8	-
14.5h	52	-	2	9	-	8	4	12	3
17.5h	54	-	1	11	-	5	3	12	2
18.5h	51	-	1	11	-	6	5	13	3
38h	52	-	2	11	-	6	5	13	2
62h	52	-	2	10	-	8	3	15	trace
6d	54	-	2	10	-	5	-	15	-
7d	52	-	2	9	-	7	-	15	-
9d	51	-	3	10	-	5	-	14	-
13d	48	-	3	10	-	6	-	13	-
38d	23	-	5	16	-	-	-	5	-

table 5.6: percentages of monoboron fluorides in solution for the reaction of 1,7-di-(2'-thiophenyl)-meta-carboranewith Bu_4NF,where the F^-:carborane ratio was 5:1

In both examples essentially the same reaction occurred. $HOHBF_2^-$ and BF_4^- (as a broad band) were present initially, together with some $(HO)_2BF_2^-$ but the formation of this species occurred later than in the other reactions and only really became prevalent when the $HOHBF_2^-$ and BF_4^- were consumed. In these reactions cage fluorination on the open face of the deboronated carborane ($\delta(^{19}F)$ -202ppm, -209/210ppm) accompanied the formation of these mono-boron fluorides, and this side reaction appeared to hinder the formation of the $HOBF_3^-$ species, as this only appears later on in the reaction.

The main curiosity of these particular reactions was the cage fluorination. Where cage fluorination of di-phenyl- and di-(4'-fluorophenyl)-*meta*-carboranes was seen to occur initially at the B(10) position ($\delta(^{19}F)$=*c.* -202ppm (br.,s)) with migration to the preferred B(3) position ($\delta(^{19}F)$=*c.*-215ppm (q, $^1J_{BF}$=*c.* 55Hz)), our findings indicated four positions of BF substitution, although some appeared transitory.

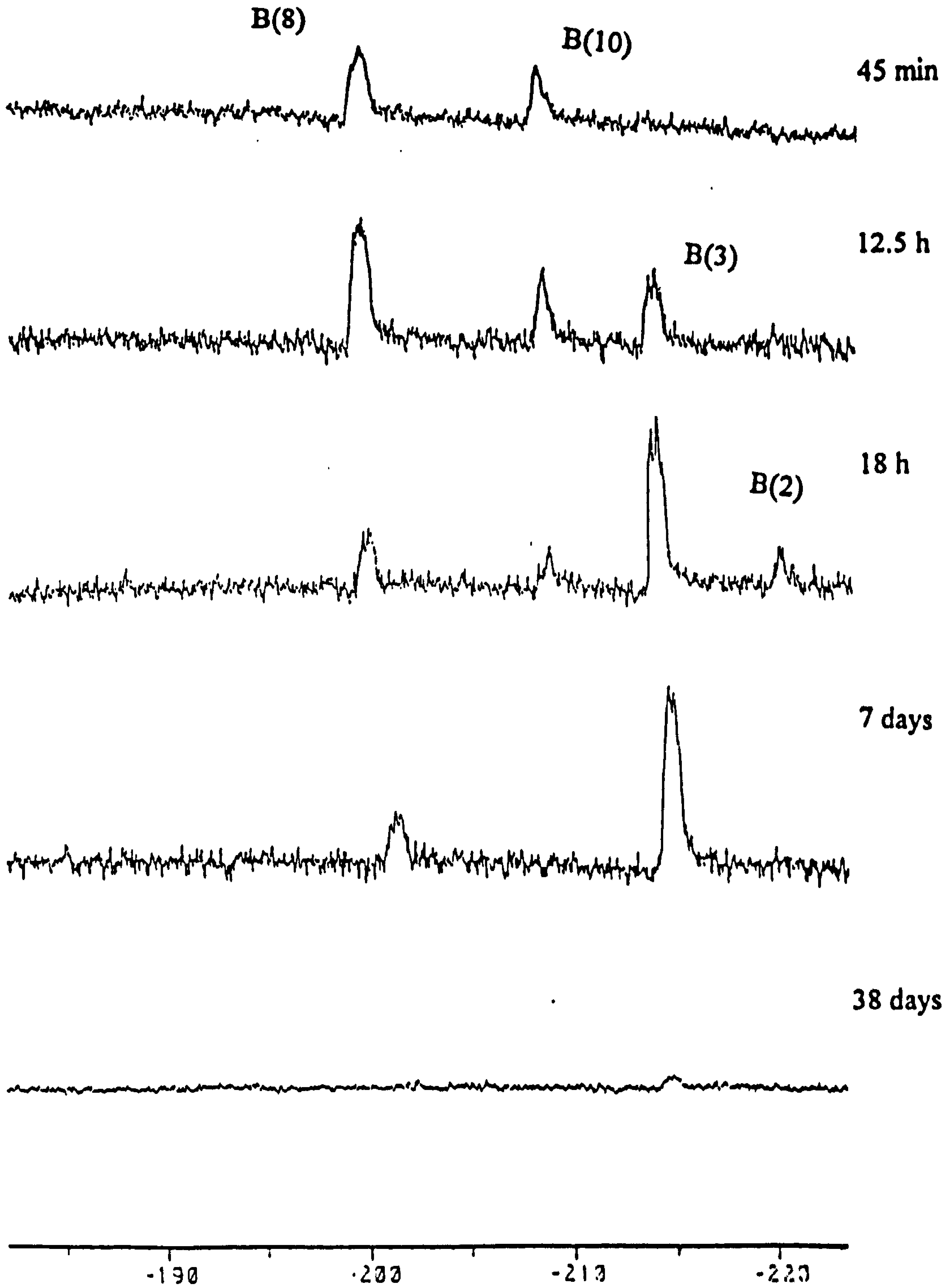

figure 5.6: [19]F NMR spectra following the deboronation reaction of 1,7-di-(2'-thiophenyl)-meta-carborane with Bu_4NF, where the F^-:carborane ratio was 5:1

The first two positions to be fluorinated were on the open face of the carborane, at B(8) and B(10), corresponding to fluorine NMR shifts of -202ppm and -210ppm ($^1J_{BF}$=*c*.55Hz) respectively, although whether one product was doubly fluorinated or if there were two distinct species in solution was unclear. Fluoride ion substitution at the B(10) position was surprising, as this position is quite hindered, particularly by the bulky heterocyclic groups, however, the product was stable in solution for a reasonable length of time in each instance.

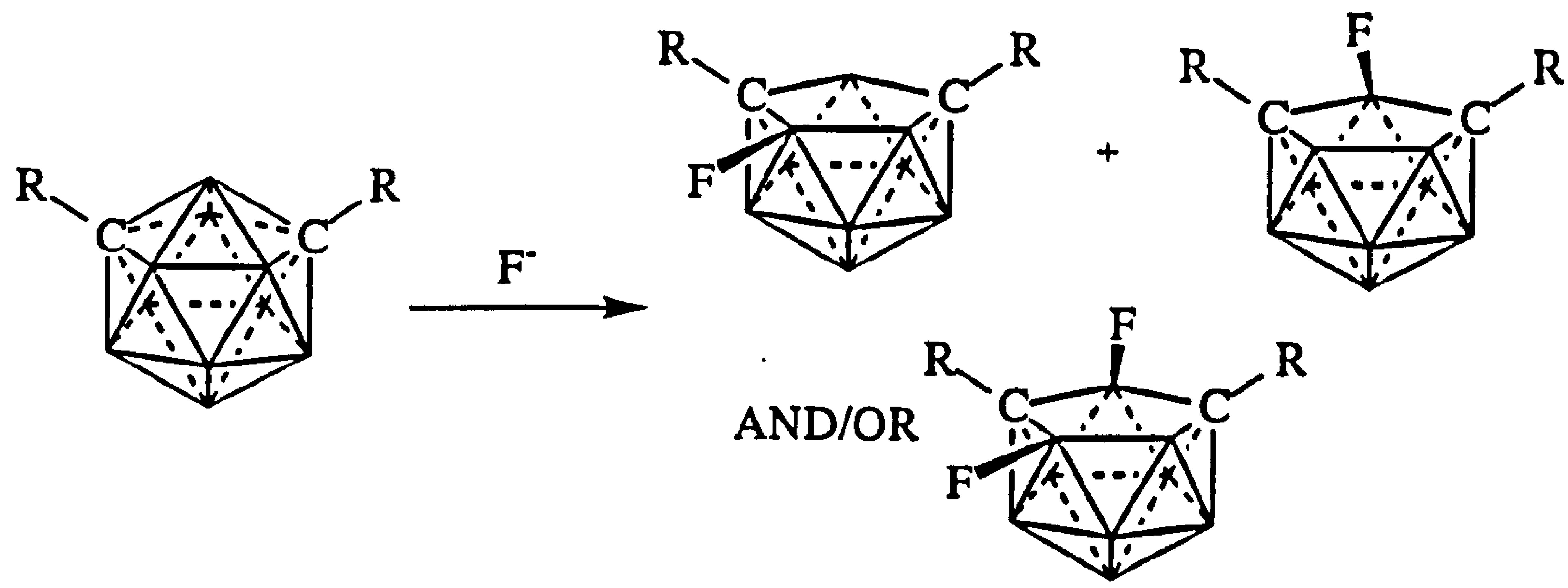

scheme 5.21: first stage of fluorination of the di-heteroaryl-meta carboranes with fluoride ion. R = 2'-thiophenyl or 3'-pyridyl

As the reaction continued, the quantities of these species decreased slightly as peaks at -215ppm and -220ppm appeared in the fluorine NMR spectra indicating the presence of fluorine on the lower carborane belt. This was where slight differences between the thiophenyl and pyridyl compounds manifested themselves. In both, the substituent at -220ppm was lost at the same time as the B(8) substituent. The major point of fluorine substitution then became B(3) in the 1,7-di-(thiophenyl)-*meta*-carborane, with the B(10) fluorine remaining attached to the cage for several days after the other fluorines were emancipated. B(3) became the only point of substitution in the di-pyridyl derivative. After an extended period of time this B(3) fluorine was also lost, leaving the dipyridyl undecaborate anion free of fluorine. (Tables 5.5 and 5.6)

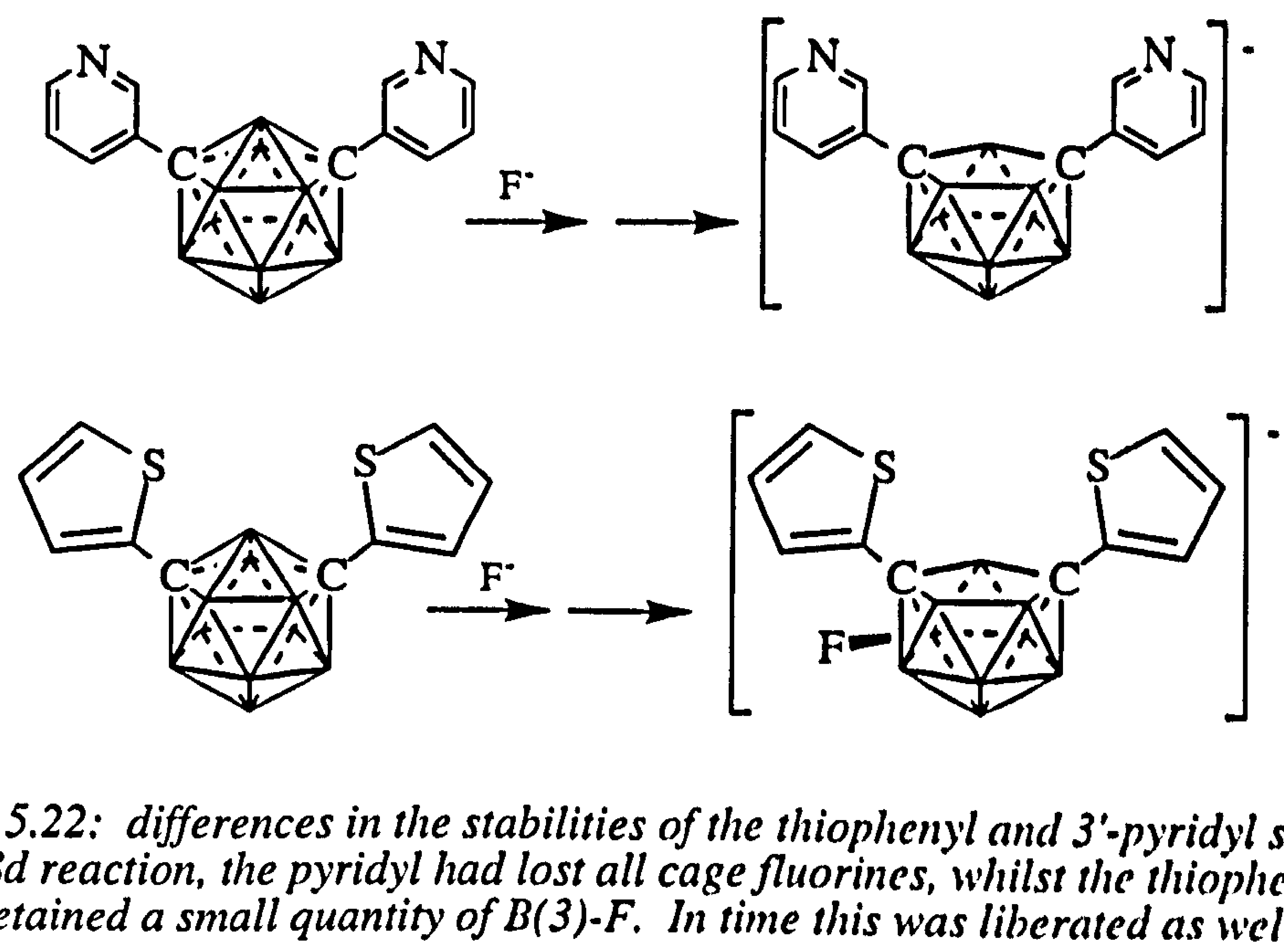

scheme 5.22: differences in the stabilities of the thiophenyl and 3'-pyridyl systems. After 38d reaction, the pyridyl had lost all cage fluorines, whilst the thiophenyl still retained a small quantity of B(3)-F. In time this was liberated as well.

The differences observed between the 3'-pyridyl and 2'-thiophenyl isomers were not major and are most likely attributable to the varying electron withdrawing powers of the substituents. The thiophenyl system possesses more electron density than the pyridyl (and also non-heterocyclic) ring systems and can therefore provide the *nido* residue with more electronic charge than the 3'-pyridyl system is able to. Perhaps for this reason, the thiophenyl B(3)-fluoro undecaborate ion was stable for longer in the reaction medium. In the 2'- and 4'-pyridyl equivalents, the proposed isomer may be more stable, given the favoured residency of the electron density of the heterocycle.

What causes the boron fluorination? If the relative electronegativities of the atoms in the *nido* cage are considered, the carbons are obviously the most δ+, followed by the borons around the open face in the order B(8) then B(10). In the lower belt, the borons with the highest carbon connectivities follow. This would imply that the primary sites of attack for the nucleophilic fluorine are the B(8) and B(10) positions. Although boron fluorination has been observed in other aryl systems, no substitution at B(8) has been noted before, implying there may also be a degree of interaction between the heterocycle and the *exo*- and bridging hydrogens of the open face, particularly in the thiophenyl example, which would leave these positions more susceptible to attack. Previous work on the 2'-pyridyl analogue noted no B(8) fluorination.

It may be that the fluorine substitution observed in the lower boron belt occurred as a result of "flipping" in the cage and by this mechanism the change from B(10) to B(3) (scheme 5.23) is easily explained.[28] The presence of both B(10) and B(3) substituted products in solution together, suggested a slow rearrangement from the B(10) to B(3) isomer. The rearrangement was quicker in the 3'-pyridyl than the 2'-thiophenyl derivative which explains the prolonged presence of B(10)-F in the ^{19}F spectra of the thiophenyl compound.

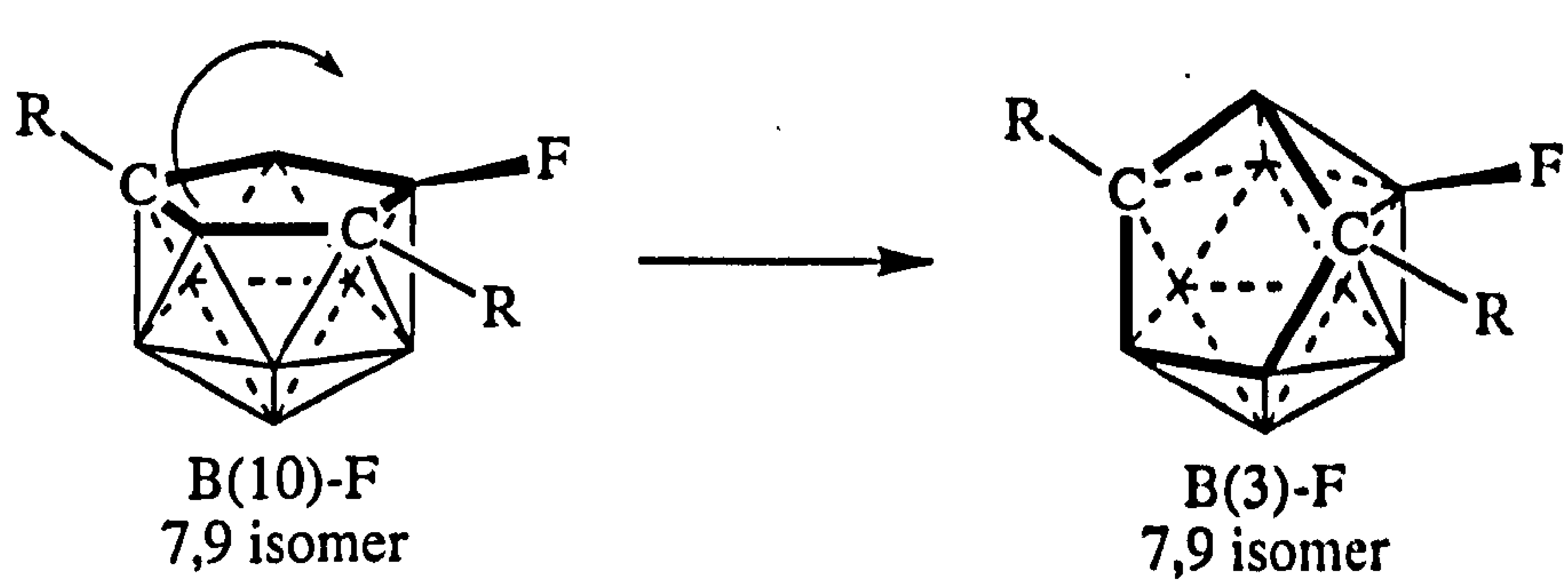

scheme 5.23: B(8) flipping mechanism

If the original *nido* cage were difluorinated in the B(8) and B(10) positions, this mechanism would result in a new B(8),B(3)-difluorinated species, which given the proximity of the fluorines would probably be unstable in this wet environment,[29] so the argument is directed in favour of two individual *nido* systems being formed initially. If this is the case, it is not unreasonable to assume that the B(8) substituted cage rearranged in a manner similar to that described above, to give rise to a species with a BF chemical shift in the observed -220ppm region.

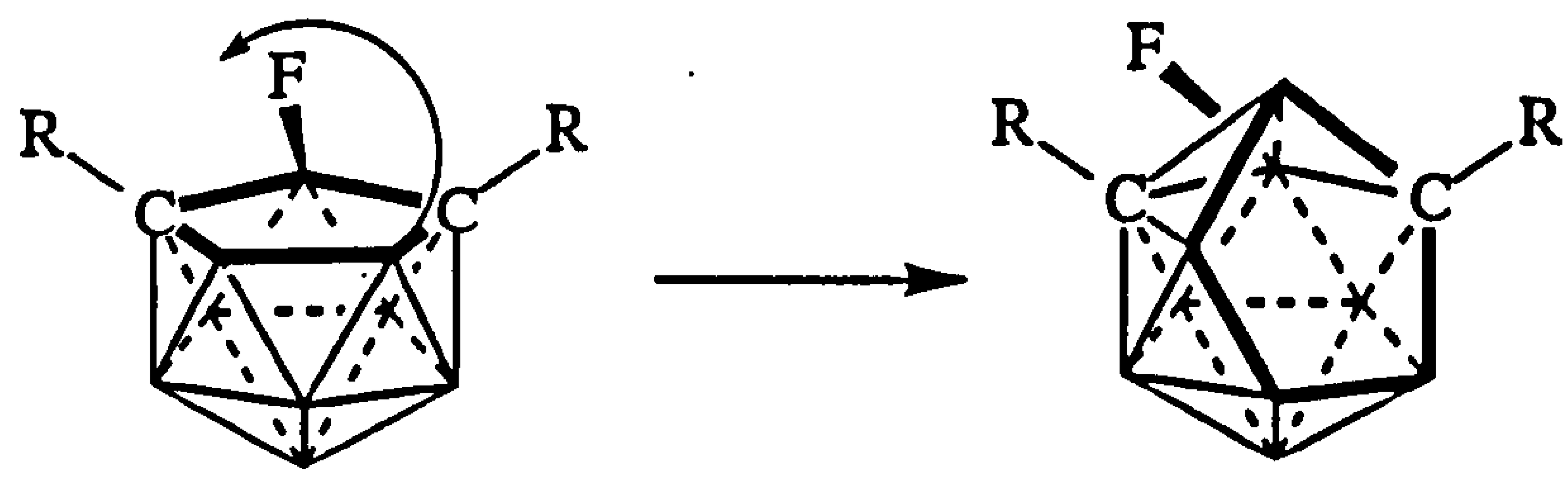

B(8)-F
7,9 isomer

B(3)-F
2,8 isomer

scheme 5.24: B(10) flipping mechanism

If the flipping mechanism postulated above is applied to this system, a *nido* cage with only one carbon on the open face is obtained in a 2,8-configuration, a rather unusual residue. (The residue expected from a deboronated *para*-carborane has a 2,9-configuration.) This gives rise to a BF species in the lower belt which fits in with the observed chemical shift value. After a period of time, this fluoro isomer was no longer present, indicating its reduced stability in this medium compared to the B(10),B(3) isomer. An alternative cage rearrangement is for the carbon to flip, however this would leave a fluorine on the cage face, and this is not consistent with the observed results.

Alternative explanations for this -220ppm fluorine NMR spectroscopic peak, include a simple migration of the fluorine to perhaps a B(2) position as observed, but not explained by other workers for an ethoxy group.[20] Further investigations regarding the boron NMR spectra of these intermediate compounds is obviously required to elucidate structural peculiarities.

Relative rates of reaction

On comparison of the deboronation reactions with fluoride ion of 3'-pyridyl- and 2'-thiophenyl *ortho-* and *meta*-carboranes, the pyridyl derivatives appeared to react more quickly. Examination of the ^{11}B NMR spectra of the final reaction solutions of these species showed that for both *ortho-* and *meta-* systems, a quantity of the unreacted *closo*-carborane was present in the thiophenyl derivative, but that the pyridyl compounds were totally converted into the undecaborate fragment after the same time period. An excess of fluoride ion has been used in both the pyridyl reactions, showing the deboronation with fluoride ion to be more efficient when an excess of F^- was employed. For the diaryl systems, the final NMR solutions showed predominantly boric acid and polyborate species, suggesting that these deboronated species were less stable than the mono-substituted derivatives.

5.3.2 Three-Cage Systems

Deboronation reactions of the tricarboranyl triazine systems are discussed in this section and comparisons drawn with the deboronations of other multi-cage systems. The methods discussed in the introduction, namely deboronation through alkoxide ion, by means of amine bases and by fluoride ion, are all applicable to multi-cage systems.

In such three cage systems there lies the possibilty that one, two or three cages may deboronate to leave the appropriate number of *nido* residues attached to the central C_3N_3 ring. Although the incorporation of potentially catalytically active metals has not been investigated, it is envisaged that the tricarboranyl triazines have the ability to hold such metals as single-cage *nido* systems do.

An alternative outcome of the reaction with a deboronating agent is that the tri-carboranyl system will prove stable to attack by base, although as the partially soluble tri-carboranyl benzene derivatives can be deboronated[30], this is unlikely. There is also the possibility that the central ring will break up. Again this is unlikely as the carboranes crowd the ring, hindering possible attack, and the C_3N_3 ring has been shown to remain intact in experiments with hydrazine derivatives (Chapter Four).

Deboronation reactions of various tri-carboranyl triazines have been attempted using all three techniques outlined in the introduction (alkoxide ion, amine base and fluoride ion). *Ortho*- and *meta*-carboranyl triazine systems have been successfully triply deboronated in all instances and no cases of one or two cage degradation have been observed. In the triply deboronated systems, as for the *closo* systems, two possible diastereomers exist. The first is where all three open cage faces are directed upwards ($\alpha\alpha\alpha$), the second where two cage faces are oriented in one direction and the third cage in the opposite direction ($\alpha\alpha\beta$).

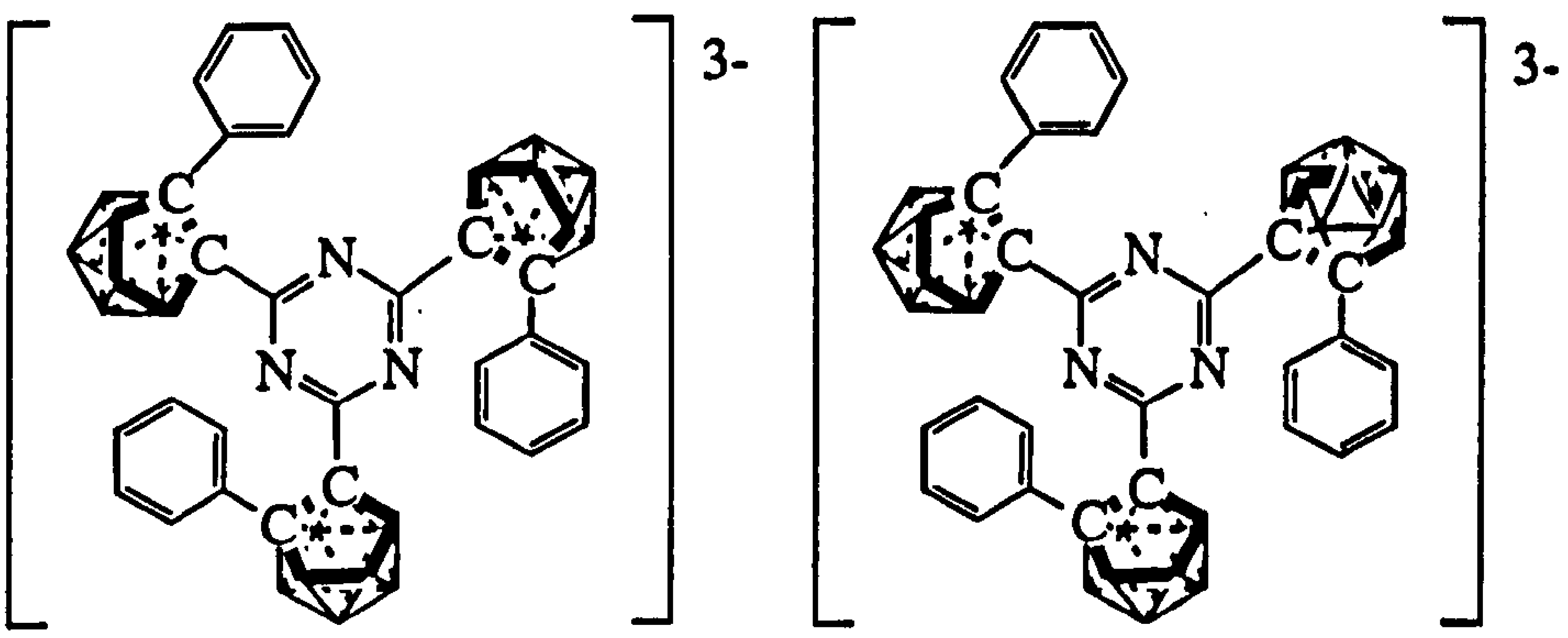

ααα ααβ

scheme 5.7: triply deboronated isomers of tri-carboranyl triazine

Deboronation of *para*-carboranyl isomers has only been noted in a few reports.[1,2] Most of the attempts at deboronation of tri-*para*-carboranyl triazines proved unsuccessful, however tri-*para*-carboranyl triazine has proven susceptible to degradation, leaving two cages intact and one deboronated. This will be discussed further in part c).

a) Degradation of tri-*ortho*-carboranyl triazines

Deboronation of 2,4,6-tri-(2'-phenyl-*ortho*-carboranyl)-1,3,5-triazine has been successfully achieved by well-known deboronation methods. Deboronation of all three cages occurred in every case and there were no instances where partial deboronation was observed. Similarly, complete cage degradation to boric acid has not been noted and the central triazine ring has remained intact.

The benzene analogue of this compound has been triply deboronated[30] by alkoxide ion and fluoride ion, and although all three cages were ultimately deboronated, deboronation took several days. By comparison, we have found that deboronation of the triazinyl compound occurred quickly and at ambient temperature, although refluxing produced a quicker reaction. This may in part be due to the increased solubility of this compound over the benzene derivative, which is only sparingly soluble.

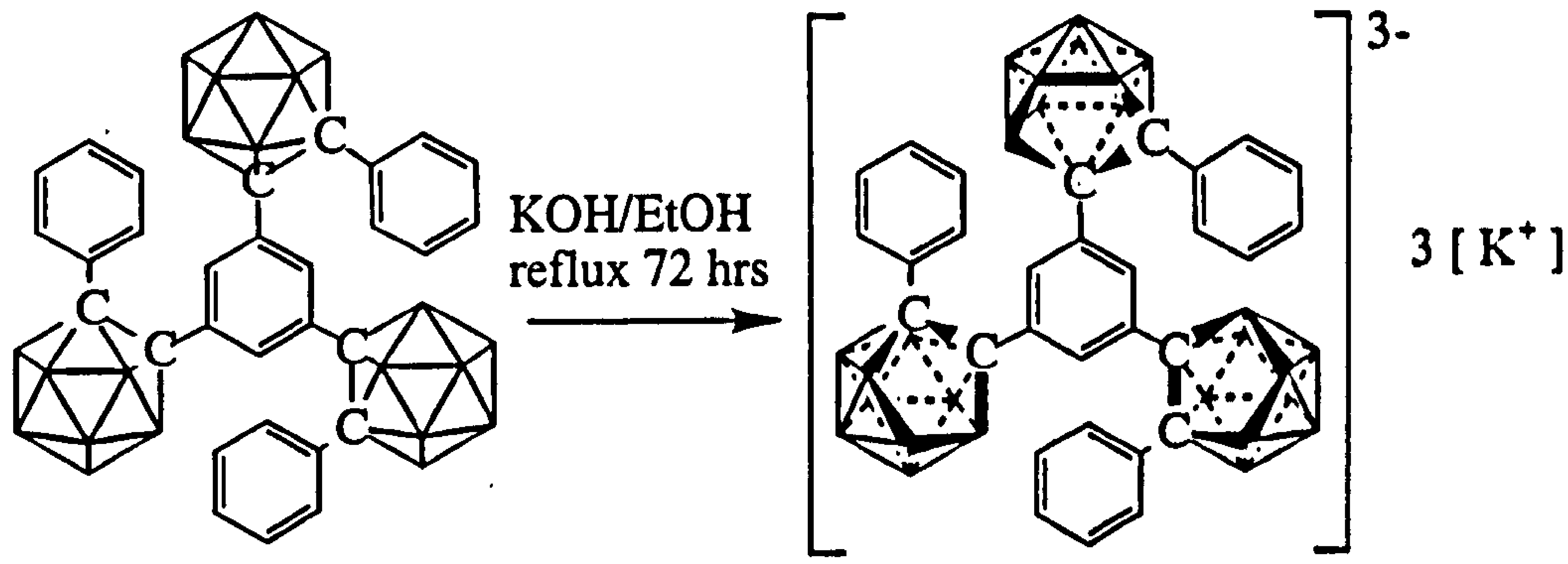

scheme 5.25: deboronation of 1,3,5-tri-(2'-phenyl-ortho-carboranyl)-benzene

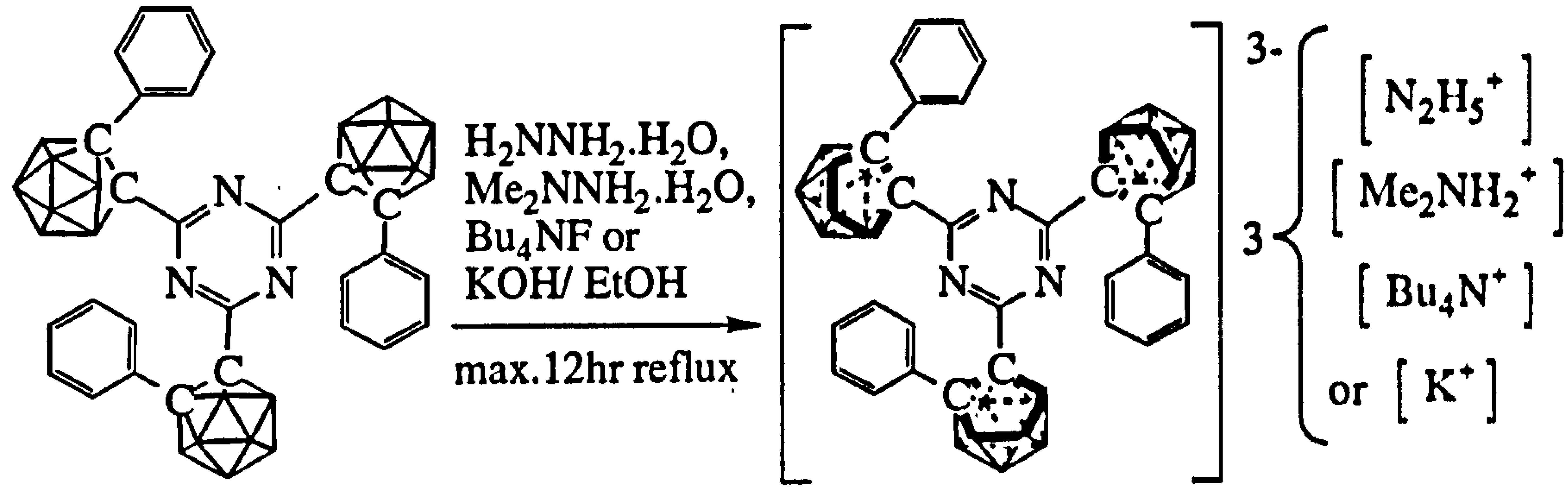

scheme 5.26: deboronation reactions of 2,4,6-tri-(2'-phenyl-ortho-carboranyl)-1,3,5-triazine

Degradation by Hydrazine Derivatives

In the experiments conducted here, deboronation was the observed result from the reaction between 2,4,6-tri-(2'-phenyl-*ortho*-carboranyl)-1,3,5-triazine and 1,1-dimethylhydrazine or hydrazine monohydrate (IR *nido* BH at 2554cm^{-1} and 2537cm^{-1} for Me_2NNH_2 and $H_2NNH_2.H_2O$ respectively). Steric factors most probably hindered the fragmentation of the triazine ring, which was protected by both the bulky three-dimensional carborane cages and also the planar phenyl groups which are free to rotate in solution. The deboronation reaction was also facile and was probably aided by the relatively large electron withdrawing influence of effectively two carborane units and a triazine unit on each cage.

Degradation by Fluoride Ion

The reaction of 2,4,6-tri-(2'-phenyl-*ortho*-carboranyl)-1,3,5-triazine with Bu_4NF in THF at room temperature caused the solution to turn blue immediately, then to clear yellow within minutes. Refluxing for three hours gave the fully deboronated product, although less time was probably required. Crystals of this compound were grown from ethanol/water but unfortunately proved to be disordered.

In the deboronated tri-carboranyl triazine compounds, as in mono-substituted or R,R'-disubstituted *ortho-* and *meta*-carboranes, there are nine different boron environments. (Unlike in the solid state, only one isomer exists in solution.)

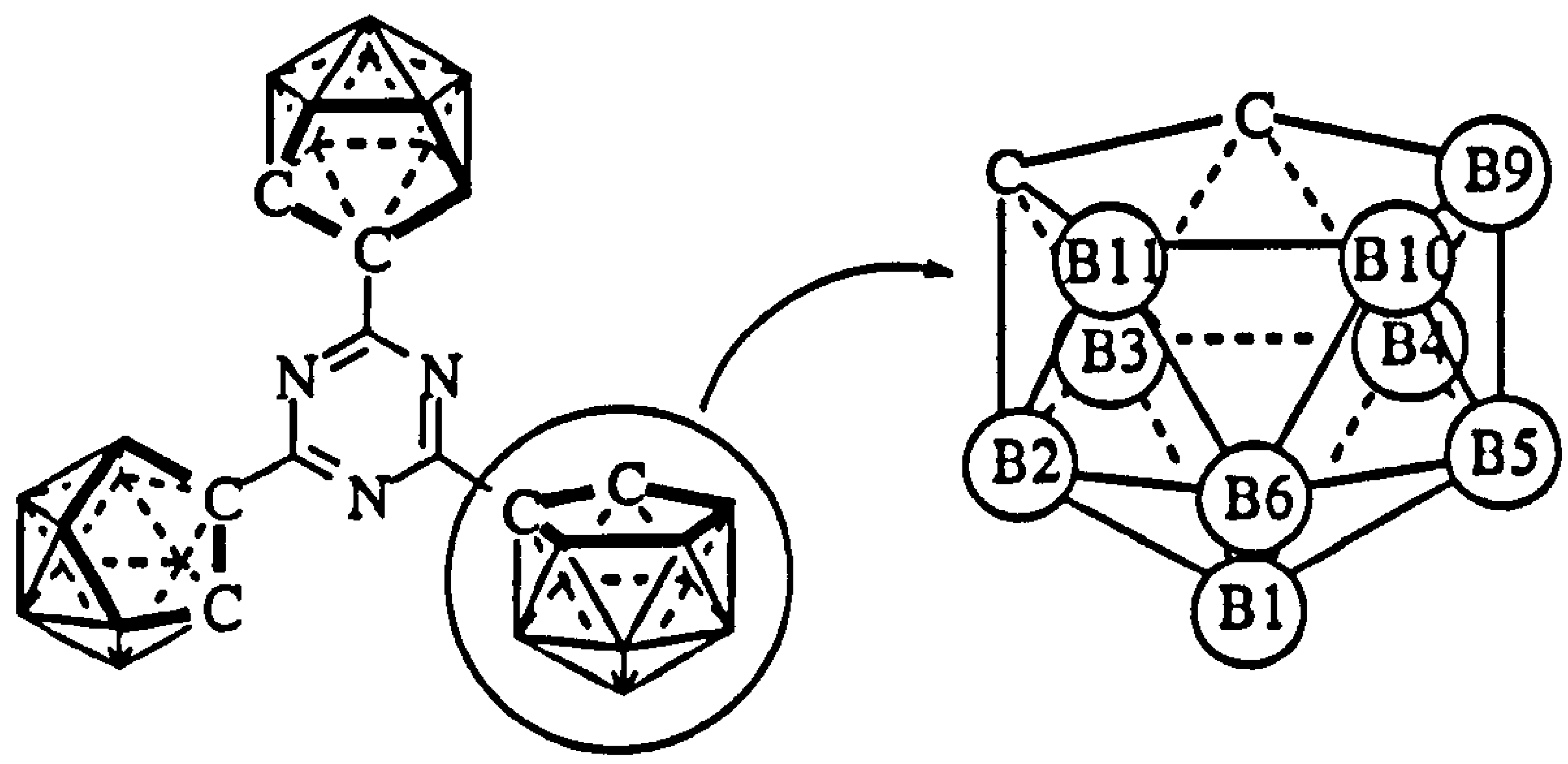

figure 5.8: triply deboronated 2,4,6-tri-(ortho-carboranyl)-1,3,5-triazines have nine different boron environments in solution

This has been well illustrated for the Bu_4N^+ salt of the triply deboronated 2,4,6-tri-(2'-phenyl-*ortho*-carboranyl)-1,3,5-triazine. 2D $^{11}B\{^1H\}$ NMR spectroscopy has been used to assign observed chemical shifts to cage vertices. Generally the peak attributable to B(10) reverts to a doublet of doublets in the ^{11}B spectra, due to splitting by the hydrogen associated with the cage open face. From this the cage connectivity can be deduced.

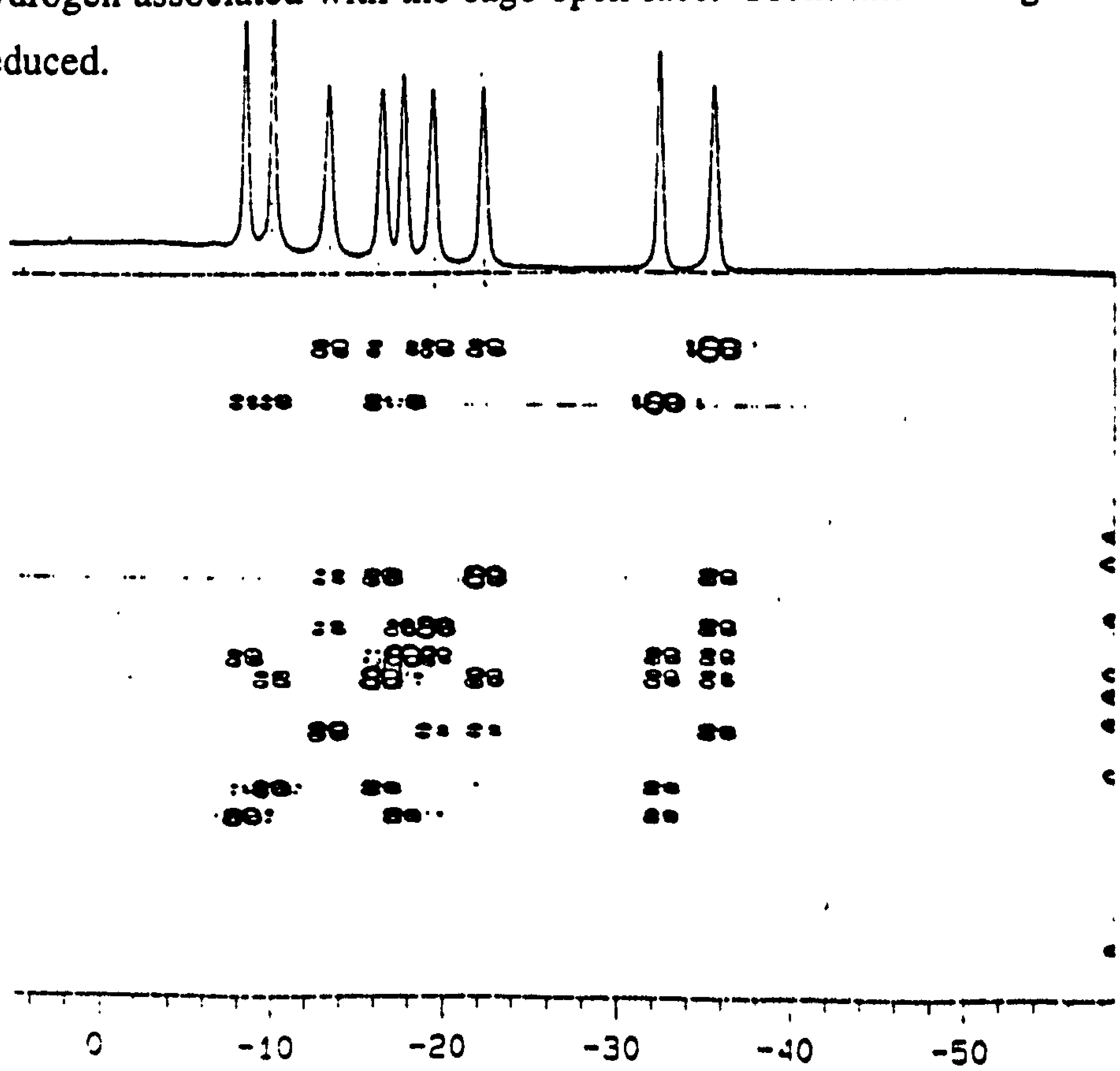

figure 5.9: $^{11}B\{^1H\}/^{11}B\{^1H\}$ cosy spectrum of the tetrabutyl ammonium salt of 2,4,6-tri-(7'-phenyl-7',8'-undecaboranyl)-1,3,5-triazine

Ambiguity arises in the assignations of B(2) and B(4), B(5) and B(6), and B(9) and B(11). From the above spectrum, these cannot be assigned with certainty although the boron with the least electron density associated with it would be expected at lower field (more positive δ). Following this reasoning, B(6) is better assigned to the lower field value of -16.33ppm as opposed to -17.57ppm as it is antipodal to the dicarboranyl-triazine substituent. Being an extremely electron withdrawing moiety, the triazinyl substituent would be expected to pull electron density away from its antipodal atom. B(5), antipodal to the phenyl group, can therefore be assigned to -17.57ppm.

Degradation with ethanolic potassium hydroxide solution

As for one-cage systems, degradation of this three cage system was readily achieved by the action of an ethanolic potassium hydroxide solution. From this triply deboronated cage system, various derivatives were prepared. The addition of an aqueous 18-crown-6 ether solution precipitated the appropriate salt as a white solid. As reported by Stone and co-workers[7], the thallium salts of *nido* cages can be prepared by reaction with thallium acetate. For the current system, this yielded the hexathallium salt as a bright yellow insoluble powder and solid state NMR spectroscopy revealed the presence of two isomers, (ααα and ααβ). The soluble PPN salt (PPN is $(Ph_3P)_2N^+$) was prepared from here by reaction with PPNCl.

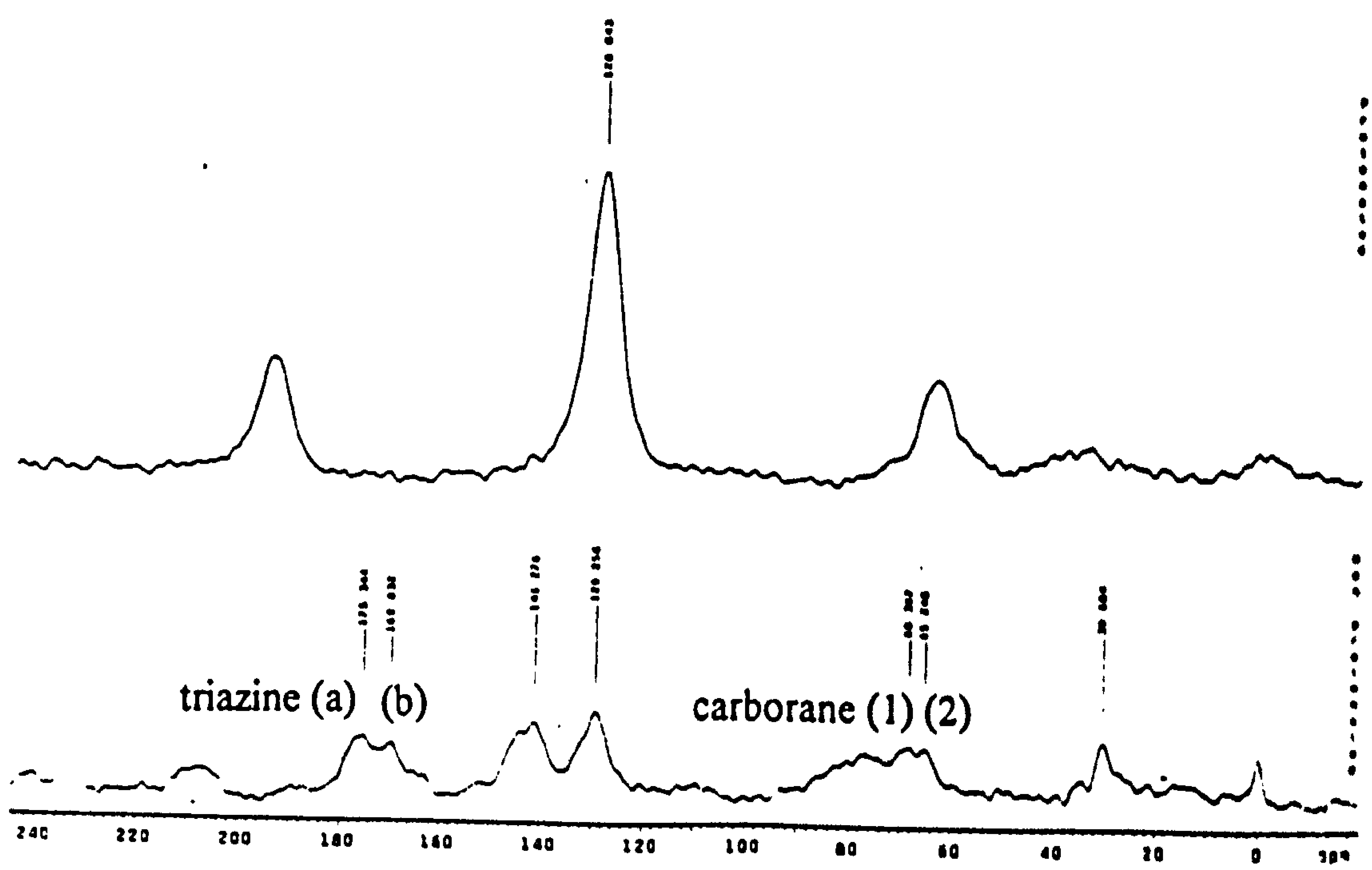

figure 5.10: solid state ^{13}C NMR shows the presence of two isomers

Preparation of the tri-ruthenium *para*-cymene salt was attempted from the hexathallium salt, but was unsuccessful. It is likely that the compound was too sterically hindered to allow the incorporation of such a large, bulky entity.

b) Degradation of tri-*meta*-carboranyl triazines

Experiments conducted on the *meta*-carboranyl triazine compounds showed deboronation to occur again, although the deboronation reaction was slower. This may be attributable to the slightly less powerful electron withdrawing ability of the *meta*-carborane unit.

Fluoride ion deboronation of 2,4,6-tri-(7'-phenyl-*meta*-carboranyl)-1,3,5-triazine was attempted on an NMR scale. The final reaction solution contained boric acid, polyborate species and unreacted starting material, but no *nido* fragments. This suggested some deboronation had occurred, then the fragments collapsed to polyborates and boric acid. The conditions were not optimised for deboronation however. Unlike fluoride ion deboronations of other diaryl *meta*-carboranes, no substitution of fluorine onto the cage was observed during the reaction period.

Reaction of the insoluble 2,4,6-tri-(*meta*-carboranyl)-1,3,5-triazine with fluoride ion (Bu_4NF) produced the soluble, triply deboronated cage system (IR 2545cm^{-1} (BH *nido*)), but no deboronation was observed on reaction with hydrazine monohydrate (IR 2606cm^{-1} (BH *closo*)).

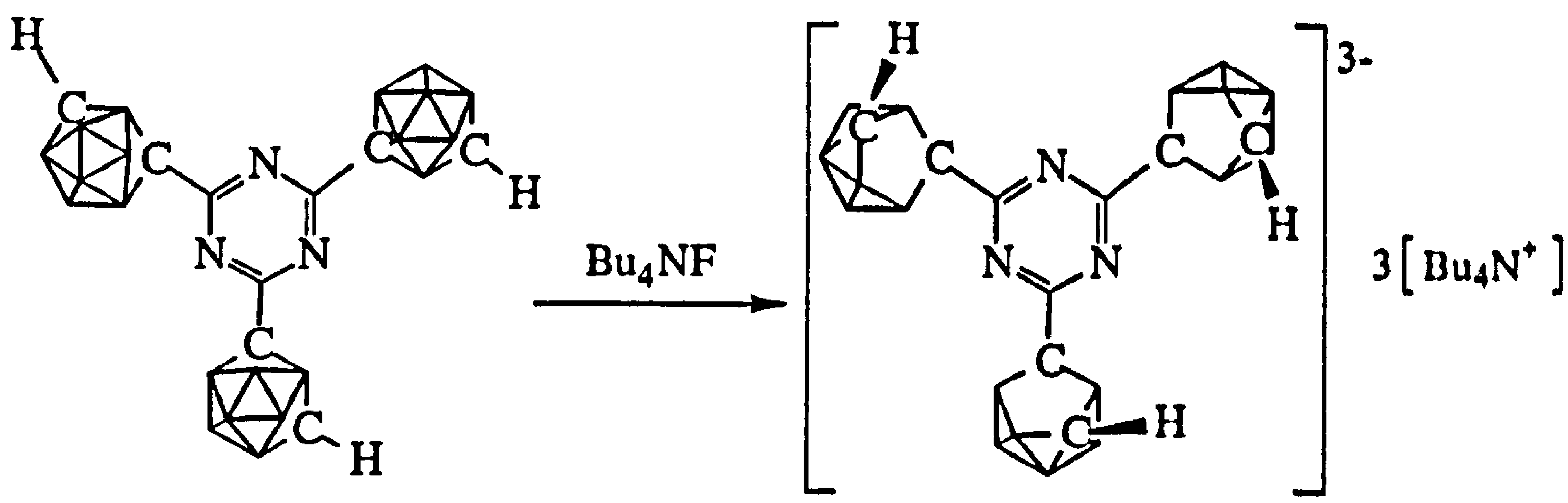

scheme 5.27: deboronation of 2,4,6-tri-(meta-carboranyl)-1,3,5-triazine

Infrared spectroscopy showed the CN stretching frequency of the triazine ring at 1534cm^{-1} as a strong sharp peak in the *closo* compound, but in the deboronated product, the CN appears as a series of broad, medium strength bands at 1540, 1508 and 1467 cm^{-1}. No change was observed in the CN stretching frequency (1537cm^{-1}) of the compound on reaction with hydrazine, showing the central ring remained intact. This shows that neither the carborane cages or the triazine ring of 2,4,6-tri-(*meta*-carboranyl)-1,3,5-triazine decomposed on reaction with hydrazine monohydrate.

c) Degradation of tri-*para*-carboranyl triazines

Little work has been published which treats the deboronation of *para*-carborane[1,2] and the use of the deboronated *para*-carborane fragments in metallo-carborane systems has not been developed. No work has been published on the deboronation of derivatised para-carboranes.

Reaction of 2,4,6-tri-(*para*-carboranyl)-1,3,5-triazines with hydrazine monohydrate gave interesting results. Deboronation through reaction with hydrazine was expected with *ortho*-carboranyl derivatives, and to a lesser extent with *meta*-derivatives, however the outcome of experiments with *para*-carboranyl derivatives was speculative. In light of the current system it was hoped that the immense electron withdrawing influence of *bis*-(*para*-carboranyl)-1,3,5-triazine on each cage may leave it suitably susceptible to attack. The alternative result, other than no reaction, was for the C_3N_3 ring to split. The *para*-carborane derivatives have the advantage over the *ortho*-carborane system in that the steric influence of the carborane substituents is reduced considerably, effectively leaving more space around the C_3N_3 unit for the relatively compact hydrazine moiety to attack. Ultimately though, the carborane units themselves are still bulky groups, so degradation of the triazine fragment remains difficult.

Several reactions between 2,4,6-tri-(*para*-carboranyl)-1,3,5-triazine and hydrazine and between 2,4,6-tri-(12'-phenyl-*para*-carboranyl)-1,3,5-triazine and hydrazine were attempted. Initially each compound was suspended or dissolved respectively in THF and stirred at room temperature with an excess of hydrazine monohydrate. No changes in either compound were noted after a two week period so both were refluxed. After refluxing overnight, no change was observed in the phenyl-*para*-carboranyl derivative and the compound was recovered unchanged from the reaction solution. The *para*-carboranyl solution had become pink after two hours reflux and remained this colour after continued reflux. (A colour change is often observed when *ortho*- and *meta*-carboranyl systems are deboronated.) The infrared spectrum of the crude product from this reaction, showed BH stretching frequencies at 2617cm^{-1} indicative of the *closo* cage and at 2549cm^{-1} indicative of a *nido* residue. (IR (*p*-$HCB_{10}H_{10}C)_3C_3N_3$ 2605cm^{-1} (*closo* BH).)

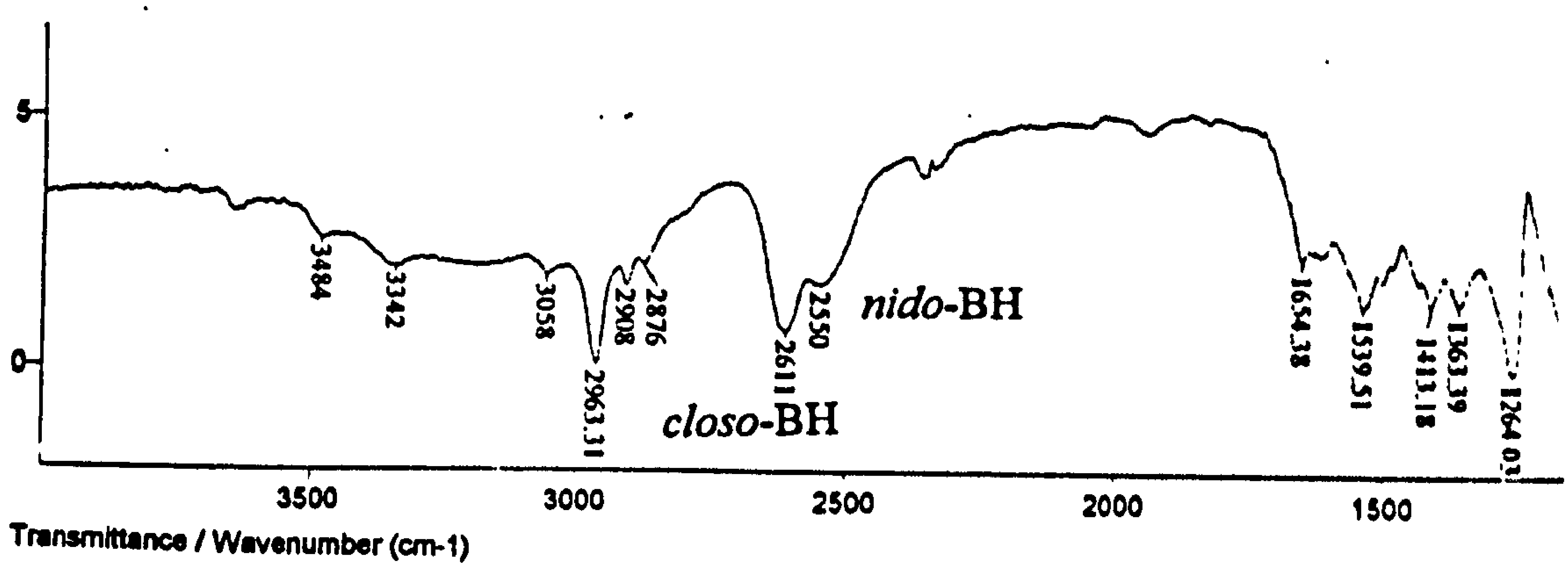

figure 5.11: infrared spectrum of partially deboronated 2,4,6-tri-(para-carboranyl)-1,3,5-triazine

The conversion of this product to the potassium 18-crown-6 ether salt was attempted as this was considered a better counterion than $N_2H_5^+$. A pale yellow oily solid resulted which again showed the IR spectroscopic bands indicative of both *closo* and *nido* fragments. Hawthorne[2] reported the BH *nido* stretch of deboronated para-carborane at 2520cm^{-1} (K^+ 18-crown-6 salt, NEt_3H salt), whilst Plesek[1] reported a value of 2590cm^{-1} (K^+ salt), closer to that of the *closo* cage.

Upon deboronation of the tri-*para*-carboranyl triazine, the compound became soluble. The parent compound was insoluble in all solvents tried, which implied the reaction product had been partially deboronated and was not a mixture of reacted and unreacted starting materials. ^{11}B NMR spectroscopy has been used to investigate the compound further.

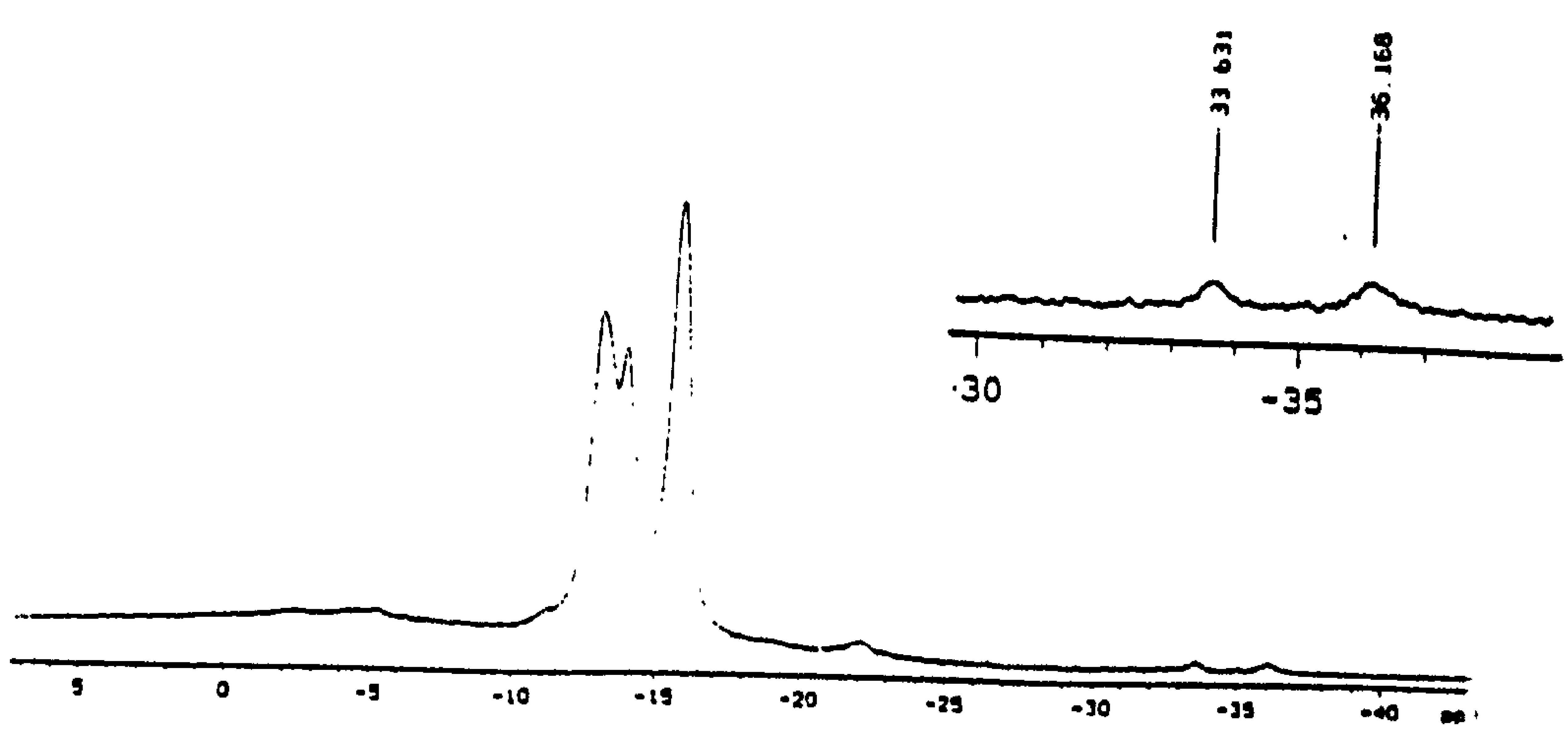

figure 5.12: $^{11}B\{^1H\}$ NMR spectrum of deboronated 2,4,6-tri-(para-carboranyl)-1,3,5-triazine

The spectrum shows three main peaks and several small peaks, all of which revert to doublets in the coupled spectrum. Solid state NMR spectroscopy gave chemical shift values of -13.26ppm and -14.59ppm for the unreacted carborane in a 1:1 ratio. If one cage of this compound were deboronated, we would expect seven resonances with relative intensities 10:10:2:2:2:2:1, for the two *closo* cages and one *nido* cage respectively.

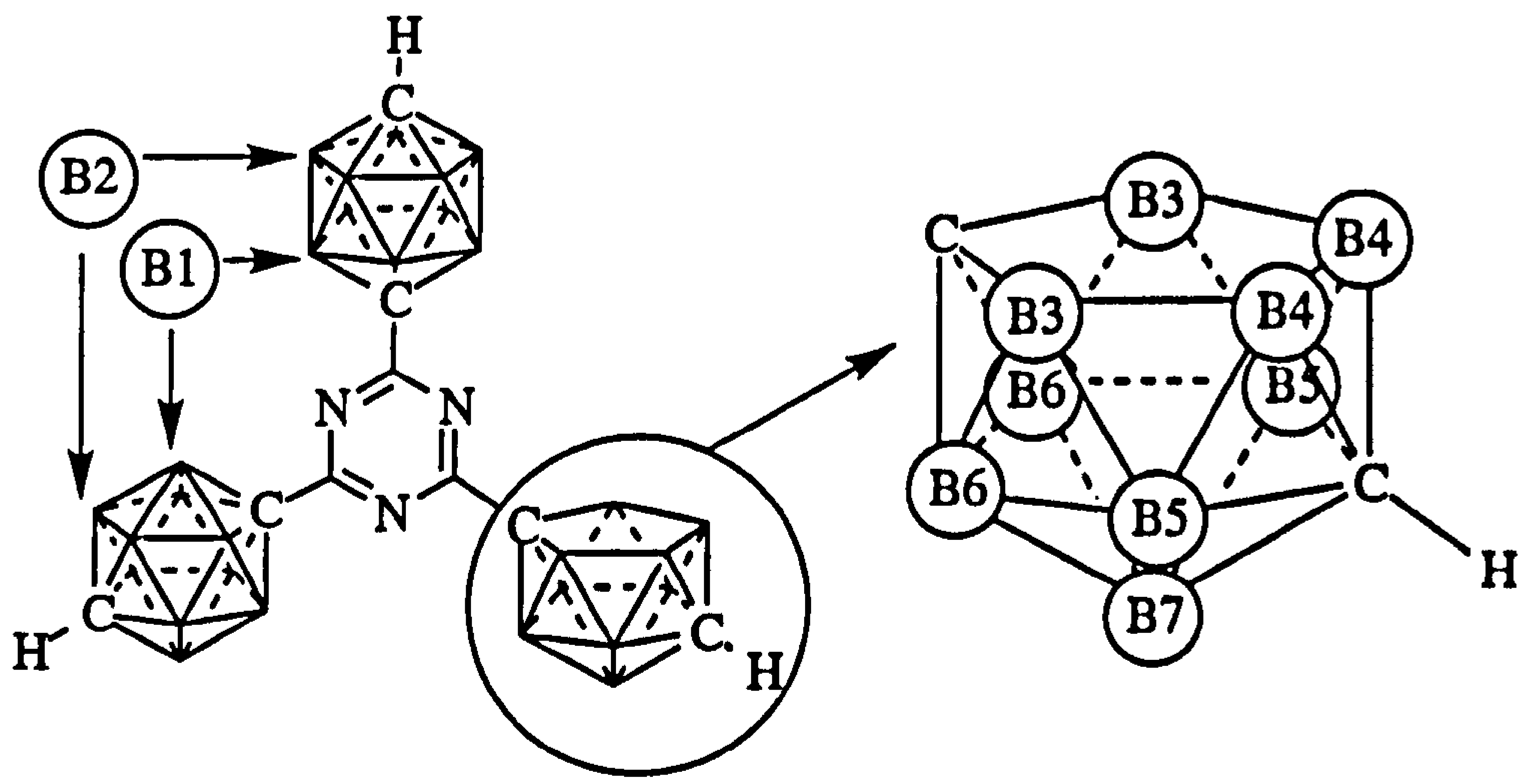

figure 5.13: seven different boron environments are created on deboronation of one cage

For deboronated para-carborane, the $^{11}B\{^1H\}$ chemical shifts are reported as -11.0 (2B), -13.2 (2B), -28.3 (1B), -29.9 (1B) and -40.4 (2B) (K^+ salt, Plesek[1]) and -13.10 (2B), -19.23 (2B), -21.58 (2B), -28.54 (2B), -42.94 (1B) (K^+ 18-crown-6 salt (d_6-acetone), Hawthorne[2]). All revert to doublets in the coupled spectra. The observed spectrum here has the three major peaks in the ratio *c.*1:1:2 (*c.*20B:20B:40B). This would suggest that the deboronated product is not unique. The peaks at -22.16, -33.63 and -36.17 are at a 5:2:2 ratio and are in accordance with the deboronated cage structure proposed above. Only a small proportion of the compound can be assumed to have deboronated given the NMR integrals, however to account for the other peaks, it is proposed that the triazine ring has degraded. Comparison of the infrared spectra of the parent and final compounds shows a shift from 1527 cm^{-1} to 1538 cm^{-1} for the CN stretch. Other stronger bands also appear at lower wavenumber.

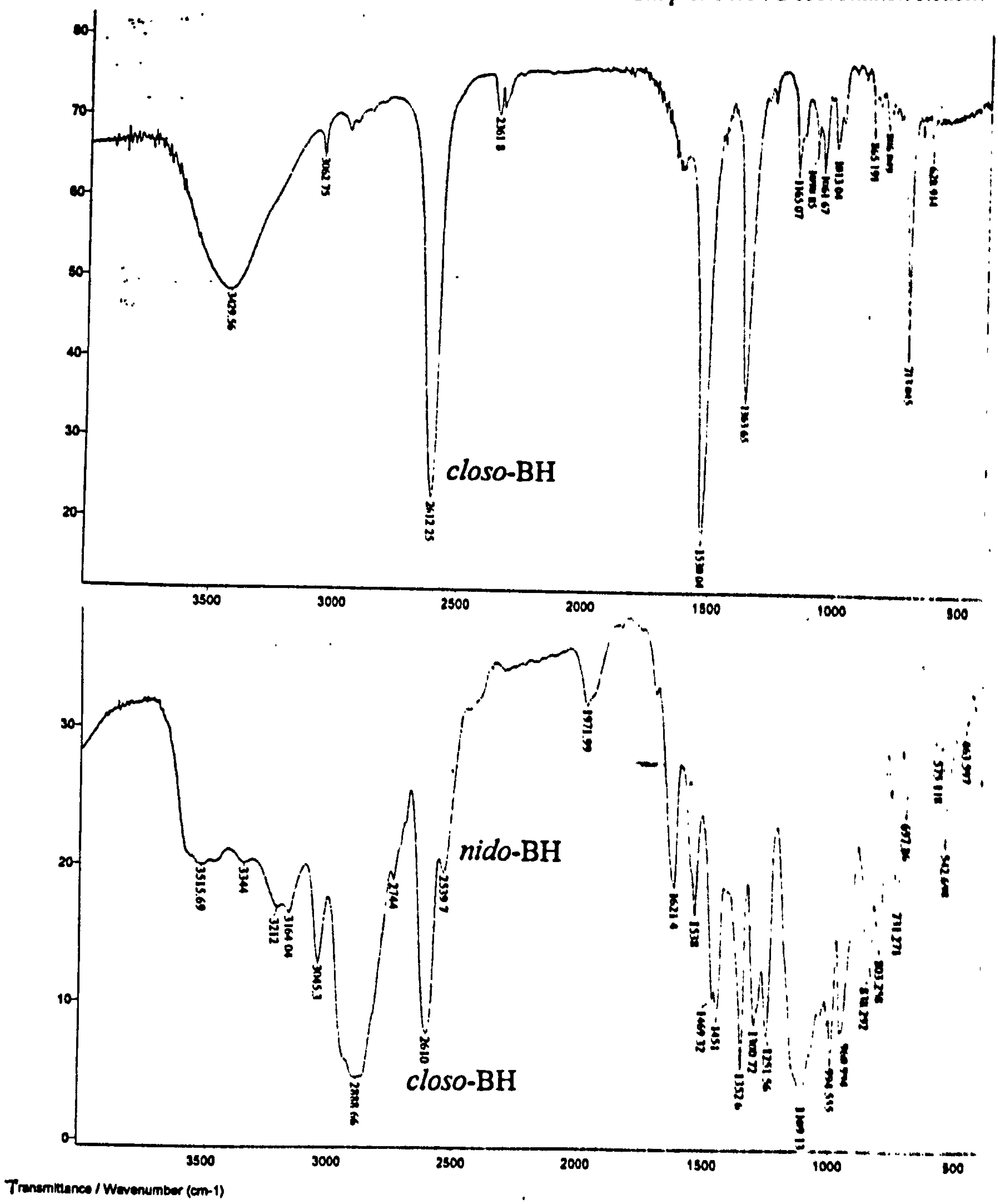

figure 5.14: infrared spectra of 2,4,6-tri-(para-carboranyl)-1,3,5-triazine (top) and the potassium 18-crown-6 ether salt of partially deboronated 2,4,6-tri-(para-carboranyl)-1,3,5-triazine

When the reaction was retried without the initial stirring period, continued reflux for up to one week failed to reproduce this result. No deboronation was observed for the 2,4,6-tri-(12'-phenyl-*para*-carboranyl)-1,3,5-triazine either.

No deboronation reactions of the above species were attempted with either alkoxide or fluoride ion. As discussed in Chapter Four, fluoride ion in solution (as Bu_4NF) dissolved 2,4,6-tri-(*para*-carboranyl)-1,3,5-triazine, and a colour change occurred. NMR spectroscopy indicated however, that no deboronation had occurred.

5.3.3 NMR effects

As discussed in earlier chapters, NMR spectroscopy (^{11}B NMR spectroscopy in particular) is indicative of changes in electron density within the carborane cage system, a shift to higher field indicating more electron density being present on the concerned vertex. When a BH vertex is removed from the cage, more electron density becomes available for cage bonding, leading to a general upfield shift for the open *nido* structure. The antipodal atoms of the cage are particularly sensitive to changes in electronic distributions, and the chemical shifts of these atoms move upfield accordingly.

Comparison of the shift values of *nido* tri-carboranyl triazine systems with those of their *closo* parents shows the cage atoms taking on distinctly different environments in moving to a *nido* system.

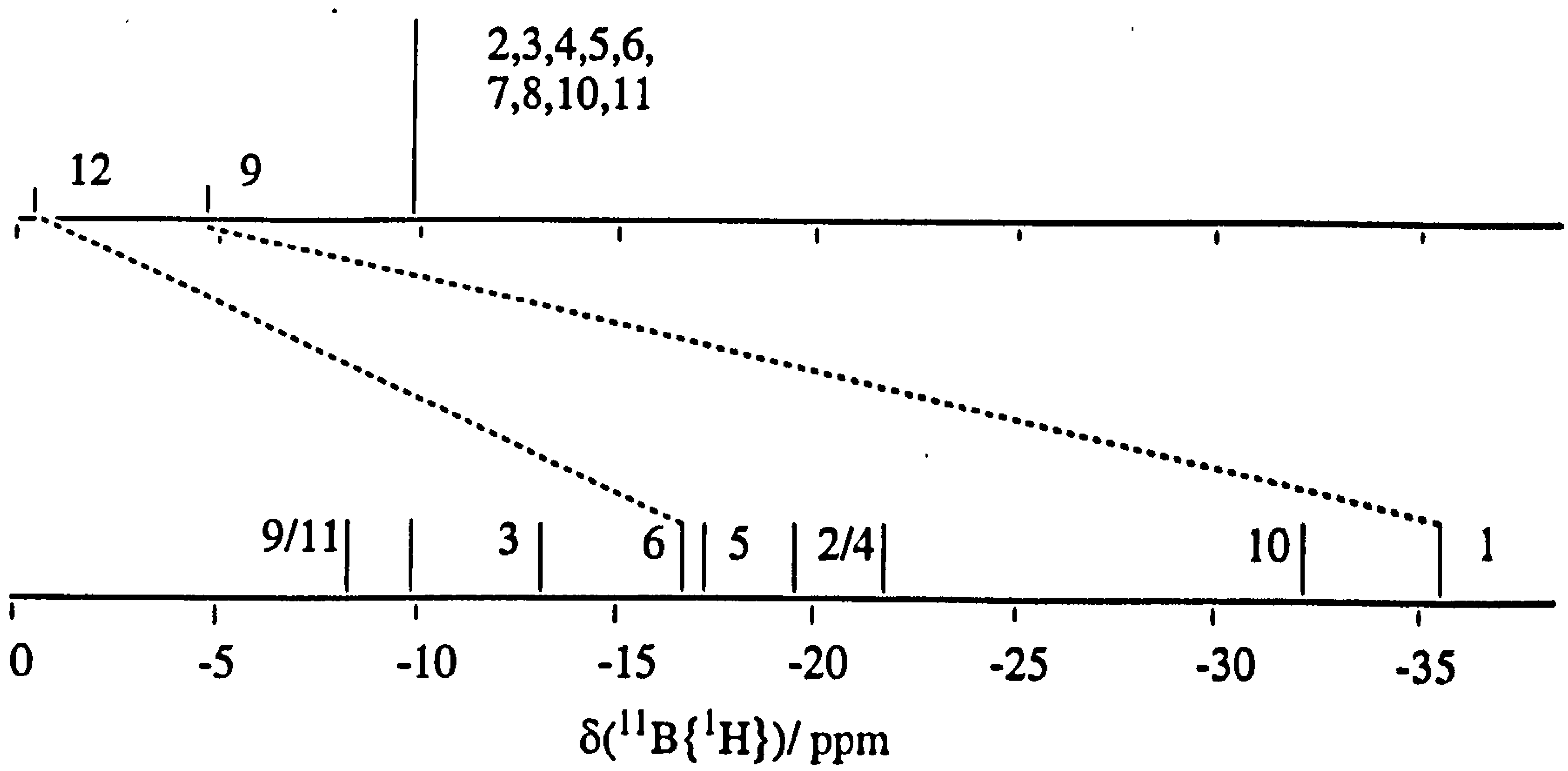

figure 5.15: representative $^{11}B\{^1H\}$ NMR spectra of 2,4,6-tri-(2'-phenyl-ortho-carboranyl)-1,3,5-triazine (top, $CDCl_3$) and its deboronated Bu_4N^+ salt (bottom, CD_3CN)

A considerable difference in chemical shift is observed between the two cage systems, particularly in the antipodal atoms, 16ppm for B(12)-B(6) and 32ppm for B(9)-B(1) (antipodal to phenyl group). It could be argued that this is due to solvent changes, however the difference is negligible as proven by the fluoride ion deboronation reaction of 2'-thiophenyl-*ortho*-carborane. Some unreacted starting material was left in the final reaction mixture (the reaction was conducted on an NMR scale, and the composition of the final reaction mixture analysed by NMR spectroscopy, *c.f.* section 5.3.1) and the chemical shift values of -1.92 (1B), -4.83 (1B), -9.29 (2B), -9.99 (4B), and -12.17 (2B) ppm in CD_3CN show little deviation from those recorded in $CDCl_3$ (-1.77 (1B), -5.02 (1B), -9.65 (2B), -10.33 (2B), -11.59 (2B), and -12.89 (2B) ppm).

This increase in cage electron density is also seen in one cage systems on creation of the *nido* residue from the *closo* parent compound. Similar shifts are observed on moving from the *closo* to *nido* residues in both 2'-thiophenyl and 3'-pyridyl-*ortho*-carboranes.

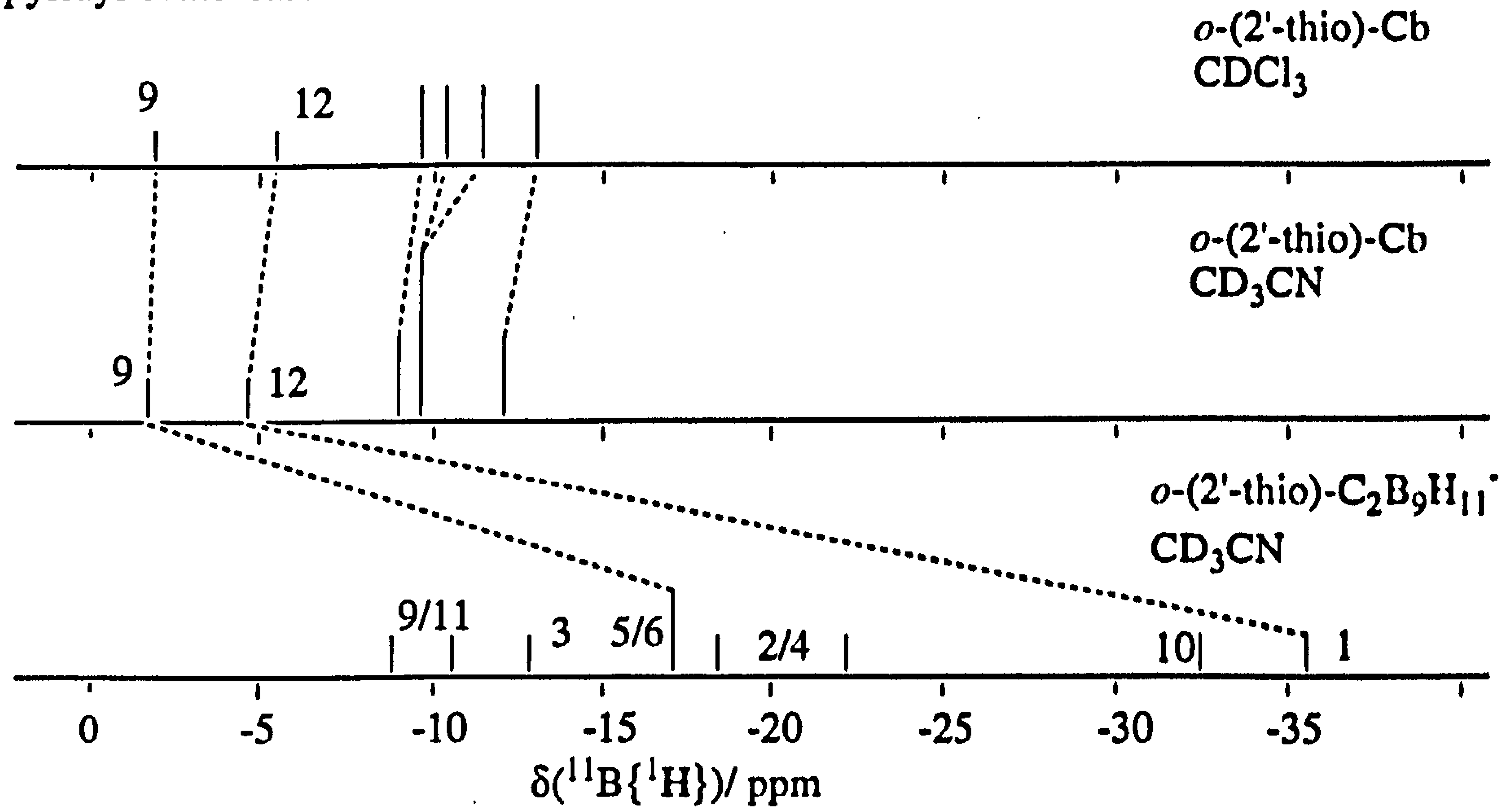

figure 5.16: representative $^{11}B\{^1H\}$ NMR spectra of 1-(2'-thiophenyl)-ortho-carborane and the deboronated 7,8-nido fragment

5.4 EXPERIMENTAL DETAILS

Many of the experiments reported here were conducted on an NMR scale and the products identified by infrared and NMR spectroscopies. No attempt was made to separate reaction products formed on an NMR scale. Tables of NMR data show the relative peak intensities of the named species at any given time in the reaction; A refers to F^-, B to $HOHBF_2^-$, C to $(HO)_2BF_2^-$, D to $(HO)BF_3^-$ and E to BF_4^-

PYRIDYL AND THIOPHENYL FLUORIDE ION DEBORONATIONS

1-(3'-pyridyl)-*ortho*-carborane

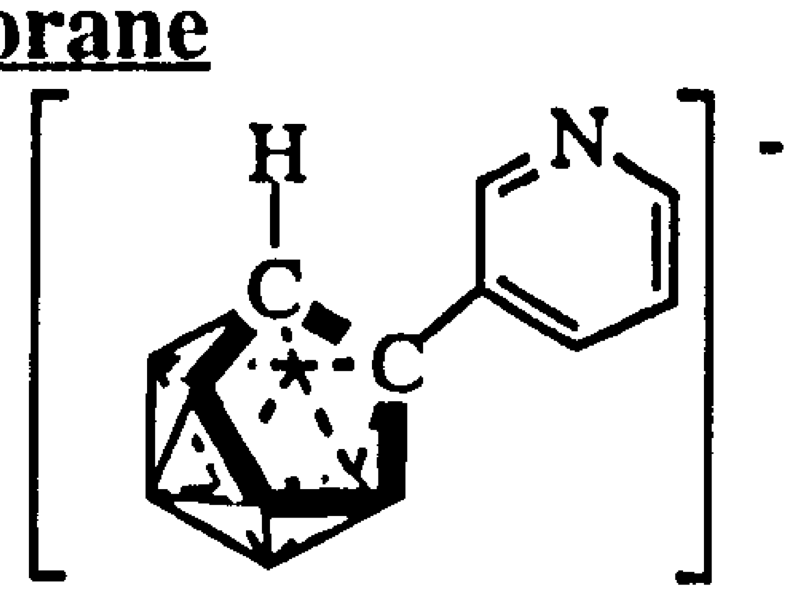

1-(3'-pyridyl)-*ortho*-carborane (0.02g, 0.1mmol) was dissolved in THF in an open 5mm NMR tube and a solution of Bu_4NF (0.16g, 0.5mmol) in THF added. The course of the reaction was monitored by ^{19}F NMR spectroscopy. Deboronated 1-(3'-pyridyl)-*ortho*-carborane was the unique carborane product.

SHIFT TIME	-113.5 A	-132.3 B	-132.5	-136.8 C	-137.7	-138.1	-141.2	-143.7 D	-151.5 E
0min	100	-	-	-	-	-	-	-	-
1min	166	1	1	12	-	-	-	-	23
2min	170	0.5	0.5	12	1	-	-	-	37
4min	314	-	7	30	7	-	-	trace	73
6min	279	-	14	40	11	-	-	6	77
10min	261	-	15	41	12	-	-	11	77
50min	72	-	2	9	2	-	-	19	?
2h	40	-	1	3	1	-	-	15	?
14h	48	-	1	3	-	1	-	23	-
7d	53	-	1	3	-	1	3	25	-
13d	44	-	1	3	-	1	3	22	-
38d	35	-	trace	2	-	0.5	1.5	16	-

final reaction solution

IR (solution): 2526 cm^{-1} (*nido* carboranyl BH)

NMR (CD_3CN): $^{11}B\{^1H\}$: 20.4 (br. s, $B(OH)_3$), 1.1 (q, BF_3 species?, J_{BF}= 16Hz), -0.05 (m, polyborate species?), -7.96 (1B, d, J_{BH}=141Hz), -9.64 (1B, d, J_{BH}=138Hz), -13.09 (1B, d, J_{BH}=159Hz), -16.53 (2B, d, J_{BH}=134Hz), -19.43 (1B, d, J_{BH}=150Hz), -21.74 (1B, d, J_{BH}=149Hz), -31.98 (1B, dd, $^1J_{BH}$=127Hz, $^2J_{BH}$=*c.* 46Hz), -35.10 (1B, d, J_{BH}=139Hz)

1-(3'-pyridyl)-*meta*-carborane

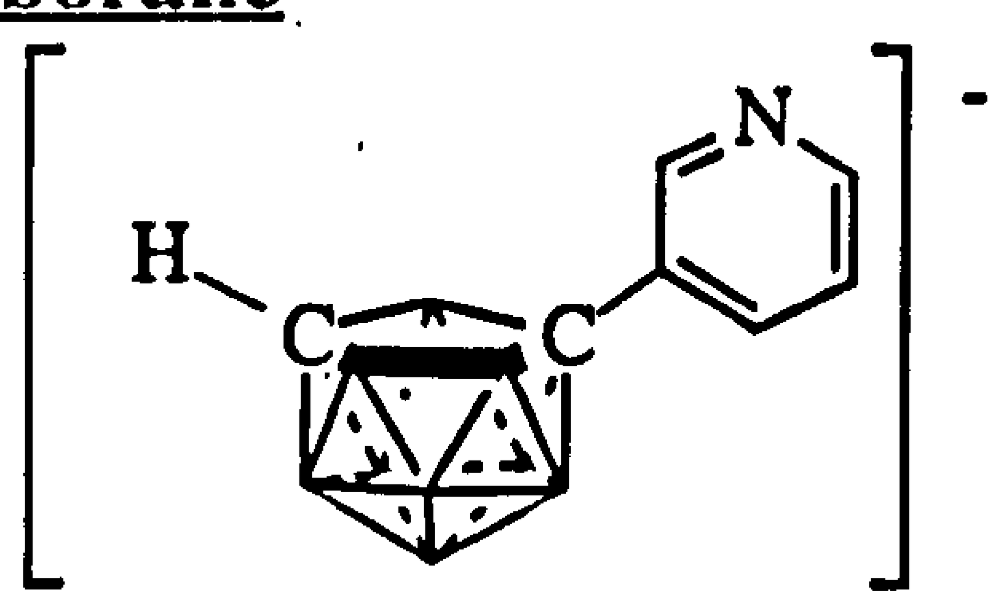

1-(3'-pyridyl)-*meta*-carborane (0.02g, 0.1mmol) and Bu_4NF (0.16g, 0.5mmol) were combined in THF in an open 5mm NMR tube and the reaction followed by ^{19}F NMR spectroscopy. Deboronated 1-(3'-pyridyl)-*meta*-carborane was the unique carborane product of this reaction.

shift time	-116.1 A	-132.2 B	-132.9	-136.7 C	-138.2	-143.9 D	-144.3	-149.7	-151.4 E
0min	100								
1min	214	43	-	5	-	-	-	-	28
2min	246	58	-	10	-	-	-	-	33
5min	257	65	-	15	-	-	-	-	42
12min	222	63	-	31	3	3	-	-	39
60min	102	-	6	22	6	32	-	-	11
13h	55	-	-	5	4	29	-	-	-
7d	29	-	1	5	13	11	1	1	-
13d	22	-	1	5	14	8	1	1	-
38d	46	-	-	10	42	24	2	1	-

final reaction solution

IR (solution): 2535 cm^{-1} (*nido* carboranyl BH)

NMR (CD_3CN): $^{11}B\{^1H\}$: 19.7 (br. s, $B(OH)_3$), 1.9 (m, polyborate, BF_3 species), -1.14 (1B, d, J_{BH}=150Hz), -3.82 (1B, d, J_{BH}=*c.* 103Hz), -4.64 (1B, d, J_{BH}=*c.* 180Hz), -17.67 (1B, d, J_{BH}=142Hz), -21.33 (3B, J_{BH}=137Hz), -29.41 (quintet, J_{BH}=32Hz), -32.35 (1B, J_{BH}= 138Hz), -35.12 (1B, d, J_{BH}=137Hz)

1,7-di-(3'-pyridyl)-*meta*-carborane

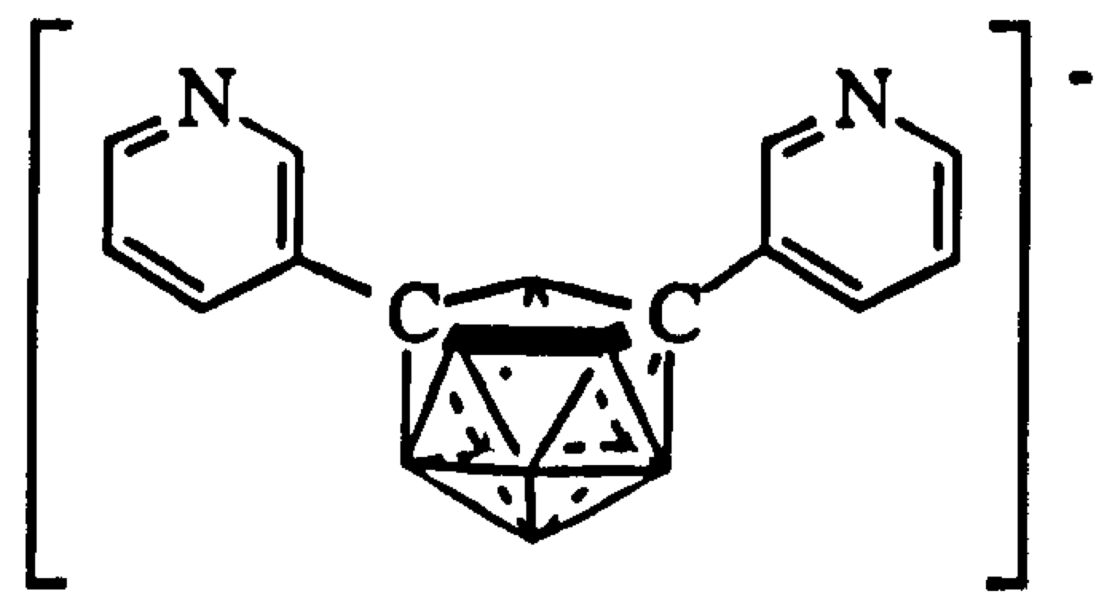

1,7-(3'-pyridyl)-*meta*-carborane (0.005g, 0.02mmol) and Bu_4NF (0.03g, 0.1mmol) were combined in an open 5mm NMR tube and the reaction followed by ^{19}F NMR spectroscopy. The compound deboronated to 1,7-di-(3'-pyridyl)-*meta*-carborane before fully degrading to boric acid.

shift time	-115.4 A	-132.3 B	-132.7	-136.8 C	-137.9	-144.0 D	-150.2 E	-202.3	-209.0	-215.9	-221.5
0min	100										
1min	72	-	-	-	-	-	10	-	-	-	-
2min	66	-	-	-	-	-	6	-	-	-	-
3min	128	-	-	5	-	-	9	10	10	-	-
4min	123	2	-	2	-	-	9	12	7	-	-
5min	120	2	-	-	1	-	14	9	10	-	-
7min	118	2	-	1	-	-	14	12	10	-	-
12min	128	3	3	5	1	-	3	7	5	-	-
20min	124	2	4	6	5	-	2	11	10	-	-
35min	121	-	5	8	11	2	3	13	8	-	-
40min	122	-	5	9	12	1	2	9	7	-	-
55min	122	-	5	9	14	3	2	10	6	-	-
70min	119	-	4	8	14	3	2	9	10	-	-
90min	120	-	5	8	15	6	2	11	9	-	-
2h	62	-	1	2	8	4	-	4	5	-	-
13h	34	-	1	3	4	5	-	2	2.3	-	-
15h	34	-	1	2	4	6	-	3	3	-	-
18h	34	-	trace	1	4	6	-	3	3	-	-
19h	34	-	trace	1	4	6	-	2	2	-	-
2d	37	-	trace	1	4	7	-	3	3	3	1
3d	37	-	trace	2	5	7	-	1	1	2	2
6d	39	-	trace	3	7	7	-	-	-	3	-
7d	39	-	trace	3	7	7	-	-	-	3	-
13d	106	-	-	15	15	19*	-	-	-	8	-
38d	61	-	-	3	23	11	-	-	-	-	-

final reaction solution

IR (solution): 2546 cm^{-1} (*nido* carboranyl BH)

NMR (CD_3CN): $^{11}B\{^1H\}$: 19.71 (br. s, $B(OH)_3$), 1.5 to -2.0 (multiplets, polyborate species), -11.73 (d, J_{BH}=102Hz), -29.49 (s, polyborate?), -32.2 (s, polyborate?), -33.91 (d, J_{BH}=*c.* 53Hz)

1-(2'-thiophenyl)-*ortho*-carborane

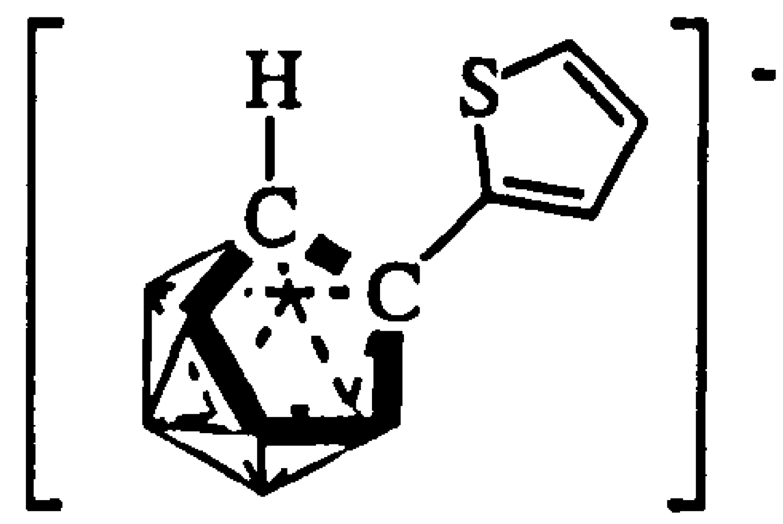

1-(2'-thiophenyl)-*ortho*-carborane (0.02g, 0.1mmol) and Bu_4NF (0.15g, 0.5mmol) were dissolved in THF (5mL) in an open NMR tube and the reaction followed by ^{19}F NMR spectroscopy. All the solid dissolved easily and H_2 was evolved. The final product was identified by IR and ^{11}B spectroscopies as a mixture of the parent compound and the deboronated species indicated above. The NMR analyses of this were recorded in CD_3CN.

shift time	A	-131.2	-132.3 B	- 135.75	-137.0 C	-139.3	-140.0	-144.0 D	-144.6	-150.1	-151.4 E
0min	100%										
1min	-	-	55	-	15	-	-	2	-	-	23(br)
2min	-	-	63	-	15	-	-	4	-	-	16(br)
5min	-	-	70	1	15	-	-	12	-	-	3(br)
10min	-	1	40	1	5	-	-	22	-	-	-
15min	-	1	45	1	10	-	-	34	-	-	-
30min	-	1	24	-	6	-	-	30	-	-	-
60min	-	-	6	-	2.5	-	1.5	24	-	-	-
90min	-	-	2	-	2	2	-	29	1	-	-
15h	-	-	-	-	-	3	-	24	11	-	-
19d	-	-	-	-	-	-	-	-	-	-	100% (sh)
24 d	-	-	-	-	-	-	-	-	-	6	19 (sh)

final reaction solution (CD_3CN)

IR (solution): 2594 (*closo* carboranyl BH), 2568, 2524 (*nido* carboranyl BH) cm^{-1}

NMR (CD_3CN)/ppm: $^{11}B\{^1H\}$: 20.3 (br. s, $B(OH)_3$), -0.81 (s), -8.45 (1B, d, J_{BH}=160Hz, B(9) or (11)), -10.60 (1B, d, J_{BH}=163Hz, B(11) or (9)), -12.78 (1B, d, J_{BH}=*c.*140Hz, B(3)), -17.11 (2B, d, J_{BH}=*c.*160Hz, B(5) and B(6)), -18.19 (1B, d, J_{BH}=*c.*140Hz, B(2) or B(4)), -22.39 (1B, d, J_{BH}=151Hz, B(4) or B(2)), -32.42 (1B, dd, $^1J_{BH}$=*c.*128Hz, $^2J_{BH}$=*c.*19Hz, B(10)), -35.32 (1B, d, J_{BH}=137Hz, B(1)) [closo species has peak values and relative intensities -1.92 (1B, d, J_{BH}=148Hz), -4.83 (1B, d, J_{BH}=147Hz), -9.29 (2B, d), -9.99 (4B, d), -12.17 (2B, d)]

1-(2'-thiophenyl)-*meta*-carborane

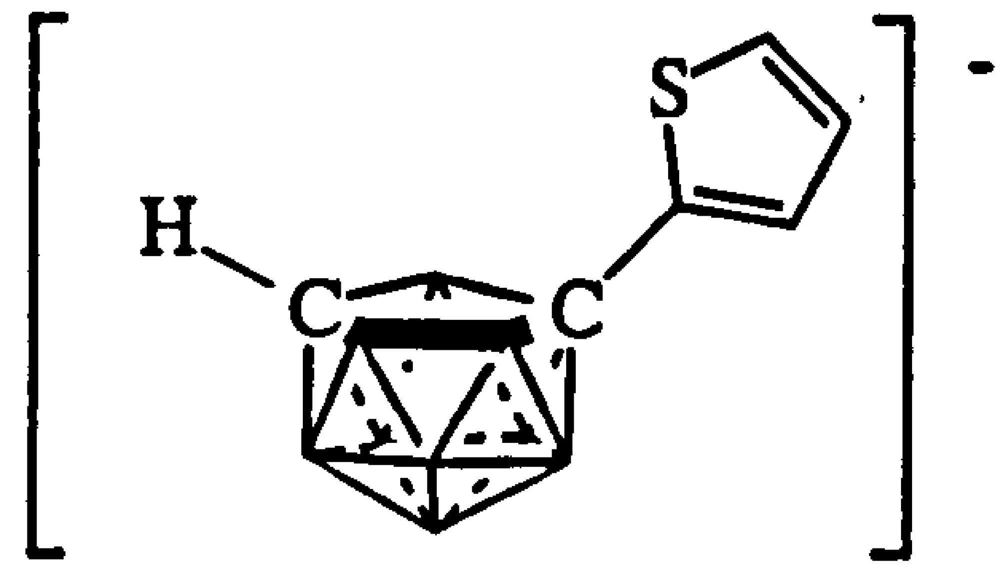

1-(2'-thiophenyl)-*meta*-carborane (0.02g, 0.1mmol) and Bu_4NF (0.15g, 0.5mmol) were dissolved in THF (5mL) in an NMR tube and the reaction followed by ^{19}F NMR spectroscopy. All the solid dissolved easily and H_2 was evolved. The final product was identified by IR and ^{11}B spectroscopies as a mixture of the parent compound and the deboronated species indicated above. The NMR analyses of this were recorded in CD_3CN.

SHIFT TIME	-114.8 A	-132.3 B ·	-132.9	-133.1	-137.0 C	-137.3	-138.2	-139.1	-143.9 D	-144.5	-149.2 (check value)	-152?? E
0min	100											
1min	118	40	-	-	9	-	-	-	-	-	-	12
3min	52	60	-	-	30	-	-	-	-	-	-	18
10min	15	18	12	-	23	-	1	-	1	-	-	9
20min	23	17	17	-	34	-	8	-	11	-	-	12
30min	12	3	25	-	34	-	10	-	19	-	-	7
75min	3	-	6	-	9	-	4	-	15	-	-	-
90min	3	-	6	-	9	-	4	-	17	-	-	-
15.5h	-	-	-	-	-	-	-	9	29	2	1	-
19d	-	-	-	-	-	-	-	11	18	7	-	-
24d	-	-	-	-	-	-	-	36	72	12	-	1

final reaction solution (CD_3CN)

IR (solution): 2603 (*closo* carboranyl BH), 2537 cm^{-1} (*nido* carboranyl BH)

NMR (CD_3CN)/ppm: $^{11}B\{^1H\}$: 19.8 (br., $B(OH)_3$), 2.1 (t, fluoroborate, J_{BF}=11Hz), 1.1 (multiplet, fluoroborate, J_{BF}=*c.* 10Hz), -3.44 (2B, d, J_{BH}=137Hz), -5.07 (1B, d, J_{BH}=150Hz), -17.13 (1B, d, J_{BH}=146Hz), -20.60 (1B, d, J_{BH}=*c.*180Hz), -21.50 (1B, d), -21.92 (1B, d), -32.74 (1B, d, J_{BH}=137Hz), -35.38 (1B, d, J_{BH}=137Hz) [*closo* species has peak values and relative intensities -0.60 (1B, d, J_{BH}=159Hz), -8.74 (1B, d, J_{BH}=*c.* 170Hz), -9.46 (2B, d), -10.47 (2B, d, J_{BH}=*c.* 150Hz), -12.92 (2B, d, J_{BH}=*c.* 170Hz), -13.94 (2B, d, J_{BH}=*c.* 180Hz)]

1,7-di-(2'-thiophenyl)-*meta*-carborane

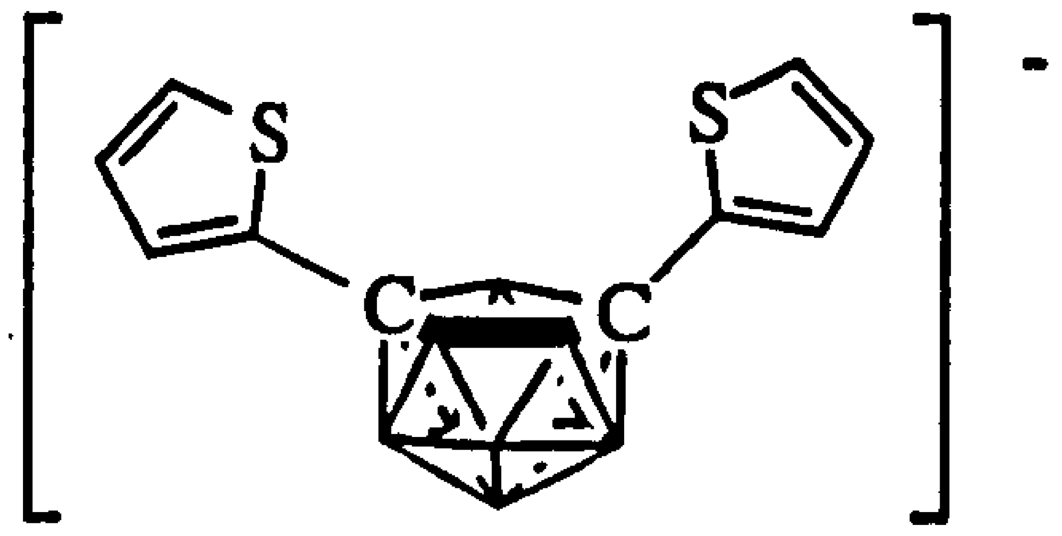

1,7-di-(2'-thiophenyl)-*meta*-carborane (0.03g, 0.1mmol) and Bu_4NF (0.16g, 0.5mmol) were dissolved in THF (5mL) in an open NMR tube and the reaction followed by ^{19}F NMR spectroscopy. All the solid dissolved easily and H_2 was evolved, slowly at first then more rapidly as the reaction proceeded. Infrared spectroscopy showed the presence of *closo* and *nido* species. On standing in solution, the compound was fully degraded to boric acid. NMR analyses were recorded in CD_3CN.

SHIFT TIME	-114.5 A	-132.3 B	-132.7	-136.7 C	-137.9	-144.0 D	-151.4 E	-202.0	-210.0	-214.9	-220.2
0min	100	-	-	-	-	-	-	-	-	-	-
1min	all	trace	-	-	-	-	trace	-	-	-	-
2min	main	trace	-	-	-	-	trace	-	-	-	-
3min	98	3	-	-	-	-	6	-	trace	-	-
4min	97	5	-	1	-	-	7	11	13	-	-
5min	96	3	-	1	-	-	5	9	9	-	-
10min	91	5	-	2	-	-	5	17	12	-	-
18min	88	1	-	2	-	1	5	14	12	-	-
25min	109	3	3	6	5	1	-	11	9	-	-
30min	111	2	4	8	6	1	-	12	10	-	-
38min	110	1	3	8	8	1	-	13	8	-	-
45min	110	1	5	9	9	1	-	14	13	-	-
60min	107	-	5	9	12	2	-	15	11	-	-
75min	105	-	3	9	14	2	-	17	9	-	-
105min	103	-	5	12	12	4	-	19	11	-	-
12.5h	51	-	1	3	9	9	-	11	7	8	-
14.5h	52	-	1	2	9	9	-	8	4	12	3
17.5h	50	-	1	1	9	10	-	5	3	11	2
18.5h	52	-	1	1	9	11	-	6	5	13	3
38h	54	-	1	2	10	11	-	6	5	13	2
62h	52	-	trace	2	10	10	-	8	3	15	trace
6d	56	-	trace	2	15	10	-	5	-	15	-
7d	53	-	trace	2	16	9	-	7	-	15	-
9d	58	-	trace	3	19	11	-	6	-	16	-
13d	107	-	trace	6	43	21	-	13	-	29	-
38d	10	-	trace	2	23	7	-	-	-	2	-

final reaction solution (CD_3CN)

IR (solution): 2682, 2656 (*closo* carboranyl BH), 2554 (*nido* carboranyl BH) cm^{-1}

NMR (CD_3CN)/ppm: $^{11}B\{^1H\}$:-19.7 (s, $B(OH)_3$), 1.5 to - 0.1 (multiplets, polyborate species), -33.59 (s, polyborate?)

DEBORONATIONS OF TRIAZINE DERIVATIVES

Deboronation of 2,4,6*tris*-(2'-phenyl-*ortho*-carboranyl) 1,3,5 triazine

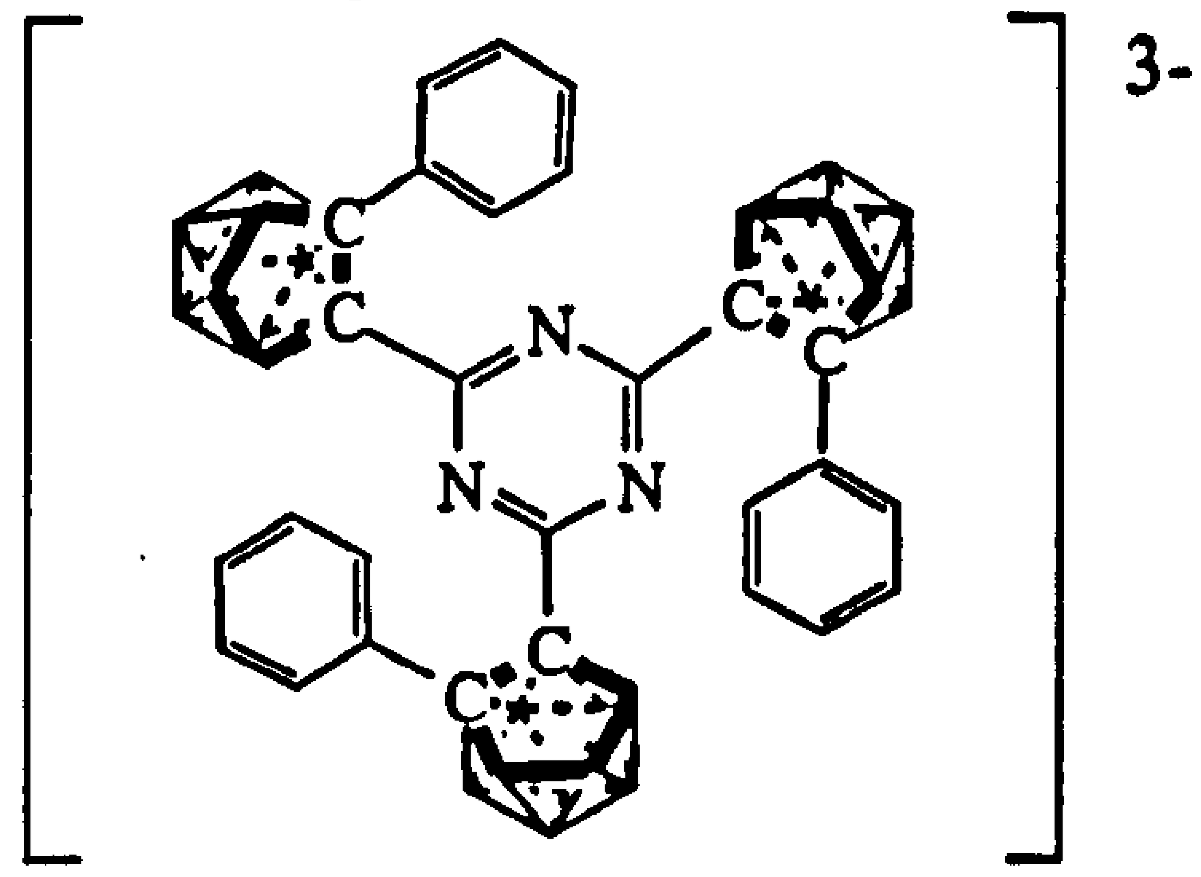

i. Preparation of the Potassium Salt

A solution of 2,4,6-tri-(2'-phenyl-*ortho*-carboranyl)-1,3,5-triazine (0.74g, 1mmol in 100mL THF) was refluxed with an ethanolic KOH solution (1.99g KOH, 35mmol in 50mL ethanol) for four hours. Each carborane cage was deboronated after this time, and the product was isolated as a yellow oil.

IR : 2532 s (carboranyl BH), 1762 m, 1678 m, 1603 s, 1560 s (CN) cm^{-1}
NMR (CD_3CN)/ppm: $^{11}B\{^1H\}$: -5.70 (3B, d, J_{BH}=136Hz), -7.31 (3B, d, J_{BH}=134Hz), -10.57 (3B, d, J_{BH}=163Hz), -13.66 (3B, d, J_{BH}=*c*.170Hz), -14.94 (3B, d, J_{BH}=148Hz), -16.54 (3B, d, J_{BH}=147Hz), -19.48 (3B, d, J_{BH}=149Hz), -29.64 (3B, dd, $^1J_{BH}$=*c*.105Hz, $^2J_{BH}$=*c*.40Hz), -32.81 (3B, d, J_{BH}=140Hz)

ii. Preparation of the Thallium salt

Thallium acetate (0.31g, 1.2mmol) was dissolved in distilled water (15mL) and added to the cooled solution of deboronated carboranyl triazine (prepared above and used without further purification). This gave a clear yellow solution. The solvent volume was reduced to *c*. 20mL and the resulting precipitate filtered off, washed with distilled water to remove unreacted thallium acetate and dried. A second crop of hexa-thallated carborane can be obtained from the mother liquor.

Yield: 0.36g, 18% IR: 3376 (br., 3600-2600, absorbed H_20); 2510 s (carboranyl B-H); 1592 w; 1526 s (triazine C-N); 1488 s; 1458 s; 1364 m; 1260 w; 1181 w; 1067 m; 1017 m; 883 w; 801 w; 759 w; 699 m cm^{-1} *Elemental analysis* ($C_{27}H_{42}N_3B_{27}Tl_6$): C 16.73% (16.80%), H 2.28% (2.35%), N 2.26% (2.18%)
NMR (solid state)/ppm: ^{13}C(protonated): 128.8 (phenyl C); ^{13}C(non-protonated): 175.34, 169.83 (triazine C, 2 isomers); 141.28, 129.26 (*ipso* C, 2 isomers); 68.31, 65.25 (carboranyl C); 30.18; ^{11}B: 11.03, 0.83, -7.42, -14.59

iii. Preparation of the Thallium-PPN salt

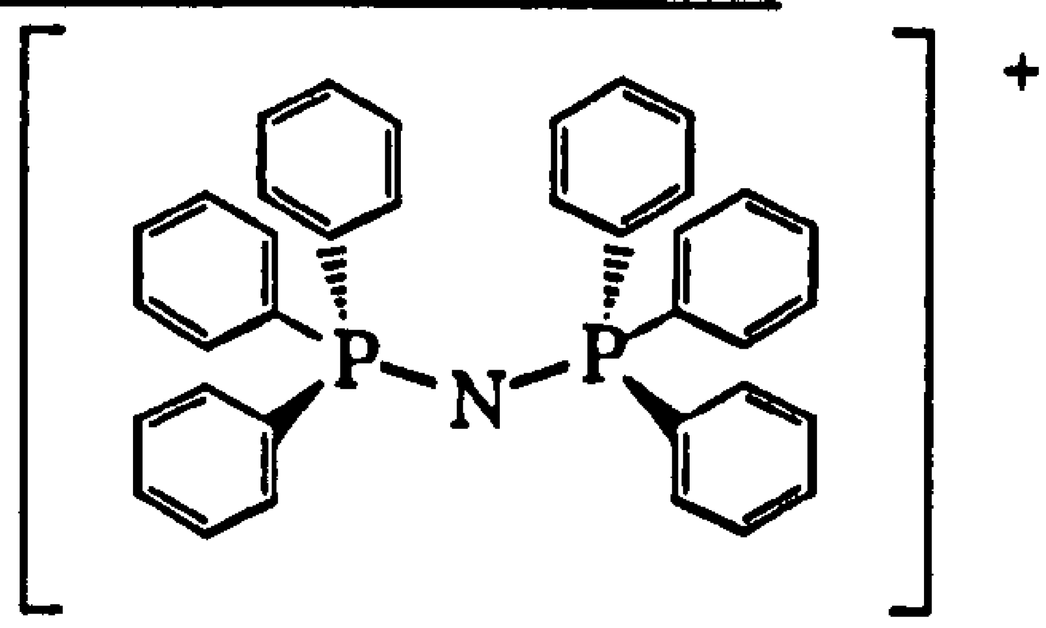

The thallium salt of 2,4,6-tri-(2'-phenyl-*ortho*-carboranyl) 1,3,5 triazine (0.19g, 0.1mmol) was suspended in acetonitrile (200mL) to give a cloudy yellow suspension. PPN chloride (0.06g, 0.1mmol) was then added and the suspension left stirring at room temperature for three hours. A white precipitate (TlCl) dropped out of solution leaving a clear yellow solution. The precipitate was removed by filtration and the solvent removed, leaving a yellow solid (0.21g).

Yield: 72% *IR*: 3404 br; 3076 w, 3054 w (phenyl CH); 2519 s (carboranyl B-H); 1684 m, 1670 m; 1522 s (CN); 1437; 1261 s; 1183 w; 1114 s; 1025; 997; 798 w; 745; 723 s; 690 s; 547 s; 533 s; 497 s cm^{-1}

NMR (CD_3CN*)/ppm: ^1H: 6.36, 6.23 (m, phenyl CH), 3.5-1.0 (carboranyl BH); $^{11}B\{^1H\}$: 20.44 (s, $B(OH)_3$), 3.49 (d, J_{BH}=*c*.170Hz), 8.31 (d, J_{BH}=*c*.120Hz), 9.98 (d, J_{BH}=*c*.120Hz), -14.33 (d, J_{BH}=169Hz), -19.25 (d, J_{BH}=*c*.180Hz), -32.23 (dd, $^1J_{BH}$=*c*.90Hz, B(10)), -34.54 (d, J_{BH}=*c*.130Hz); $^{31}P\{^1H\}$: 21.35ppm (N=*P*(Ph)$_3$)

*compound is only sparingly soluble

iv. Attempted preparation of the Ru-(*p*-cymene) salt

Hexathallium salt of 2,4,6-tri-(2'-phenyl-*ortho*-carboranyl)-1,3,5-triazine (0.20g, 0.1mmol, *c.f.* (ii) above) was suspended in CH_2Cl_2 (30mL) in a Schlenk tube, and cooled to -196°C in a liquid nitrogen bath. To this [Ru(*p*-cymene)Cl_2]$_2$ (0.032g, 0.05mmol) in CH_2Cl_2 (20mL) was added and the entire mixture frozen to -196°C. The Schlenk was evacuated, then left in the dark to warm slowly to room temperature. This resulted in a cloudy orange/brown solution. Filtration isolated an orange/red clear solution whose volume was reduced to leave a deep red oil. Prep. TLC (methanol) isolated the starting carborane. No Ru capped product was isolated.

v. Preparation of the Potassium - 18-crown-6 ether salt

The THF was removed from the deboronated carboranyl triazine solution (prepared above (i) and used without further purification) leaving an aqueous carborane-potassium salt solution. A solution of 18-crown-6 (0.93g in 20mL distilled water) was added forming a white precipitate instantly.

Yield : 40% *IR*: 3570 w; 3376 m; 3048, 3019 m (phenyl C-H); 2907 s, 2825 m, 2796 m (aliphatic C-H); 2527 s (carboranyl B-H); 1972 w; 1685 s, 1607 s (triazine C-N); 1561 s; 1520 s; 1493 m; 1472 s; 1431 m; 1351 s; 1284 s; 1261 s; 1250 s; 1104 s; 961 s; 881 w; 835 s; 801 s; 762 m; 698 m; 527 w cm^{-1} *FAB* : (FB^+) 303 (corresponds to K^+ 18-crown-6) (FB^-) 563, 524, 234 (corresponds to $PhC_2B_9H_9CN^{3-}$)

NMR ($CDCl_3$) /ppm: ^1H: 7.28, 7.12, 7.08 (15H, m, phenyl C-*H*; 3.61 (s, 18-crown-6 CH_2), 3.0- -0.5 (30H, br., carboranyl BH), -1.9 - -2.5 (br., B-*H*; $^{13}C\{^1H\}$: 127.9, 127.6, 125.3 (phenyl *C*-H), 70.7 (18-C-6, CH_2); $^{11}B\{1H\}$: -9.52 (1B), -10.84 (1B), -13.83 (1B), -16.83 (1B), -19.41 (2B), -22.91 (1B), -33.21 (1B), -36.43 (1B)

vi. Preparation of the Tetrabutyl ammonium salt (via fluoride ion deboronation)

counterion = $[(CH_3CH_2CH_2CH_2)_4N]^+$

A solution of 2,4,6-tri-(2'-phenyl-*ortho*-carboranyl)-1,3,5-triazine (0.25g, 0.34mmol) in THF (10mL) was added to a stirred solution of tetrabutyl ammonium fluoride (0.47g,1.6mmol) in THF (25mL). This instantly gave an aquamarine blue solution which changed to clear yellow within minutes. This solution was stirred at room temperature for 1.5 hours, then refluxed for a further three hours.

The solution was cooled to room temperature, diluted with dichloromethane (50mL), transferred to a separating funnel and washed with distilled water. The aqueous layers were then re-extracted with dichloromethane and the organic layers combined, dried over anhydrous magnesium sulfate, and the solvent removed under reduced pressure to leave a yellow oil which solidified on standing. This was recrystallised from ethanol yielding a bright yellow solid (first crop 0.08g). Recrystallisation of this solid from ethanol/water gave clear colourless platelets.

Yield: 17% (first crop) *IR*: 3448 br., m; 3050 w (phenyl C-H); 2961 s, 2932 s, 2874 s (butyl C-H); 2523 s (carboranyl B-H); 1591 s (C-N), 1560 m, 1482 s, 1458 s (C-N); 1381 s; 1247 w; 1153 m; 1106 s; 1026 m; 879 m; 785 m; 737 m; 703 m cm^{-1} *Elemental analysis* ($C_{27}H_{42}N_3B_{27}.3C_{16}H_{36}N$): C 56.00% (63.09%), H 10.56% (10.59%), N 5.93% (5.89%)

NMR(CD_3CN)/ppm: ^1H: 7.3 (3H, m, *para* phenyl CH), 7.2 (6H, m, phenyl CH), 7.0 (6H, m, phenyl C*H*), 3.1 (m, $[(CH_3CH_2CH_2CH_2)_4N]^+$), 1.6 (m, $[(CH_3CH_2CH_2CH_2)_4N]^+$), 1.4 (m, $[(CH_3CH_2CH_2CH_2)_4N]^+$), 1.0 (m,

[($CH_3CH_2CH_2CH_2)_4N]^+$), 3.0-0.0 (br., carboranyl B-*H*); $^{13}C\{^1H\}$: 146.3 (*ipso C* phenyl), 128.2, 127.6 (*o*, *m C* phenyl), 125.4 (*p C* phenyl), 79.2 (carboranyl C), 62.5 (carboranyl C), 59.7 ([($CH_3CH_2CH_2CH_2)_4N]^+$), 24.7 ([($CH_3CH_2CH_2CH_2)_4N]^+$), 20.5 ([($CH_3CH_2CH_2CH_2)_4N]^+$), 14.4 ([($CH_3CH_2CH_2CH_2)_4N]^+$); $^{11}B\{^1H\}$: -8.33 (3B, d, J_{BH}=139Hz, B(9) or (11)), -9.96 (3B, d, J_{BH}=133Hz, B(11) or (9)), -13.25 (3B, d, J_{BH}=154Hz, B(3)), -16.33 (3B, d, J_{BH}=130Hz, B(5) or (6)), -17.57 (3B, d, J_{BH}=142Hz, B(6) or (5)), -19.24 (3B, d, J_{BH}=150Hz, B(2) or (4)), -22.18 (3B, d, J_{BH}=150Hz, B(4) or (2)), -32.33 (3B, dd, $^1J_{BH}$=c.140Hz, $^2J_{BH}$=*c*.35Hz, B(10)), -35.50 (3B, d, J_{BH}=137Hz, B(1))

vii. Preparation of the dimethylhydrazium salt (via *N,N*-dimethylhydrazine deboronation)[31]

counterion = $[(CH_3)_2NNH_3]^+$

2,4,6-tri-(2'-phenyl-*ortho*-carboranyl)-1,3,5-triazine (0.25g, 0.34mmol) was dissolved in toluene (40mL) and the solution cooled to -78°C before the slow addition of 1,1-dimethylhydrazine monohydrate (0.15mL, 2mmol). Refluxing this solution overnight gave a clear yellow solution, however on cooling the solution to room temperature and removing the solvent, the carboranyl triazine remained unreacted. (The hydrazine was removed under the reduced pressure.) An excess of neat 1,1-dimethylhydrazine monohydrate (3mL, 40mmol) was added to the dry carborane producing an intense yellow solution which became green on standing. After stirring vigorously for 30mins at room temperature, a clear yellow solution resulted. Washing with acetonitrile precipitated out boric acid and the remaining solvent (unreacted hydrazine) was removed under dynamic vacuum to leave a yellow oil, which contained both *closo* and *nido* species.

IR: 3062 w, 3044 w, 3026 w (phenyl CH), 2666 w, 2656 m, 2633 m, 2612 s (*closo* carboranyl BH), 2592 s, 2576 s, 2554 s (*nido* carboranyl BH); 1524 s (triazine CN), 1495 s, 1447 s, 1361 s, 1261 s, 1096 s, 1021 s, 929 w, 887 w, 799 s, 755 m, 729 m, 699 m, 687 s, 666 m, 610 w cm^{-1}

NMR (CD_3CN)/ppm: $^1H\{^{11}B\}$: 7.5, 7.6, 7.3, 7.1, 7.0 (m, phenyl CH), 5.4 (s, NH), 3.56 (s, CH_3), 4.5-0.5 (br., carboranyl BH), -1.5 to -2.2 (m, carboranyl BH); $^{13}C\{^1H\}$: 162.24 (triazine CN), 141.26 (*ipso* C), 139.59, 130.47, 127.51, 126.63 (phenyl C)

viii. Preparation of the hydrazium salt (via deboronation with hydrazine monohydrate)

counterion = $[N_2H_5]^+$

2,4,6-tri-(2'phenyl-*ortho*-carboranyl)-1,3,5-triazine (0.36g, 0.5mmol) was suspended in THF (15mL) and hydrazine monohydrate (d=1.032g cm^{-1}, 1.2mL, 18mmol) added giving a clear bright yellow solution within 5minutes. A second aliquot of hydrazine (1.2mL) was added in THF (20mL) and the solution left stirring a room temperature for a further four days. The resulting pale purple solution was transferred to a separating funnel, the organic layer diluted with CH_2Cl_2 then washed with water. The organic layer was dried over anhydrous magnesium sulfate, filtered, and the solvent removed under reduced pressure leaving a yellow oil (0.58g). Recrystallisation from ethanol/water was unsuccessful.

IR (oil) - 2537 (*nido* carboranyl BH), 1697, 1650, 1610, 1556 (CN) cm^{-1}

Deboronation of 2,4,6-tri-(*meta*-carboranyl)-1,3,5-triazine with tetrabutyl ammonium fluoride

2,4,6-tri-(*meta*-carboranyl)-1,3,5-triazine (0.26g, 0.5mmol) was suspended in THF (50mL) and heated to the reflux temperature. Tetrabutyl ammonium fluoride (2.37g, 7.5mmol) in THF (25mL) was added dropwise down the condenser to the stirred suspension and the reaction mixture left to reflux for 72 hours. The resulting cloudy yellow solution was cooled to room temperature and diluted with dichloromethane (100mL). This solution was washed with distilled water (2 x 50mL) and the combined aqueous layers re-extracted with dichloromethane. Removal of the solvents from the organic layer left the product as a yellow solid (0.58g).

Yield : 97% *IR*: 2961 s, 2929 s, 2874 s (butyl C-H); 2545 s(carboranyl B-H); 1685 m; 1540 m, 1508 m, 1467 m (triazine CN), 1411 m; 1378 m; 1357 m; 1306.82 w; 1261 s; 1095 s; 1028 s; 924 w; 874 m; 803 s; 733 w cm^{-1}
NMR(CD_3CN)/ppm : ^1H: 2.5-0.0 (br., carboranyl BH), 1.82 (carboranyl CH), 0.73 (CH2), 0.33 (CH2), 0.11 (CH2), -0.28 (CH3), -1.23 (carboranyl BH); $^{13}C\{^1H\}$: 125.30 (triazine C), 78.12 (carboranyl C), 58.16 (carboranyl CH), 52.70 (CH_2), 23.21 (CH_2), 19.23 (CH_2), 12.79 (CH_3); $^{11}B\{^1H\}$(weak sample, overlapping peaks): 22.81 ($B(OH)_3$), 1.60 (d), -1.09 (d), -8.60 (d), -11.54 (d), -15.09 (d), -19.1 (d), -29.60 (d, B(10)), -32.2 (d)

ii. Reaction of 2,4,6-tri-(*meta*-carboranyl)-1,3,5-triazine with hydrazine monohydrate

2,4,6-tri-(*meta*-carboranyl)-1,3,5-triazine (0.25g, 0.5mmol) was suspended in THF (15mL) and hydrazine (1.2mL, 18mmol) added dropwise. This initially formed a deep peach suspension. A further portion of hydrazine (1.2mL, 18mmol) was added with THF (15mL) and the continued stirring of this solution at room temperature (10days) resulted in a frothy white solution. Ether was used to dilute the solution and water was added. No carborane was extracted into the ether. The cloudy aqueous layer was subsequently isolated and extracted with dichloromethane (compound was only sparingly soluble in CH_2Cl_2). Removal of the solvent left a pale yellow solid which was identified as unreacted starting material.

IR: 2606 (carboranyl BH, *closo*), 1537 (triazine CN) cm^{-1}

Deboronation of 2,4,6-tri-(7'-phenyl-*meta*-carboranyl)-1,3,5-triazine with tetrabutyl ammonium fluoride

2,4,6-tri-(7'-phenyl-*meta*-carboranyl)-1,3,5-triazine (0.04g, 0.05mol) was combined with Bu_4NF (0.05g, 1.5mmol) in THF in an open NMR tube and the progress of the reaction was followed by ^{19}F NMR spectroscopy. The final reaction solution contained a mixture of boric acid, fluorinated boron species and unreacted starting material, identified by IR and ^{11}B spectroscopies.

shift time	-115.4 A	-132.7	-136.8 C	-137.9	-138.6	-144.0 D	-150.2 E
0min	100				-		
1min	173	-	-	-	-	-	46(br)
2min	173	-	-	-	-	-	47(br)
3min	173	-	-	-	-	-	45(br)
4min	173	-	trace	-	-	trace	45(br)
5min	175	-	2	-	-	trace	47(br)
10min	173	-	4	-	-	trace	49(br)
30min	142	-	4	-	-	1	46(br)
45min	138	trace	2	trace	-	3	46(br)
60min	265	trace	11	trace	-	8	89(br)
90min	263	trace	10	trace	-	20	80(br)
2h	257	trace	10	trace	-	27	77(br)
2.5h	135	trace	5	trace	-	21	32(br)
16h	76	-	2	trace	-	28	trace (br)
19d	37	-	3	-	14	14	1(sh)
24d	139	-	10	-	56	54	2(sh)

IR: 2604 (*closo* carboranyl BH), 1656, 1562 (triazine CN) cm^{-1}

NMR (CD_3CN)/ppm: $^{11}B\{^1H\}$: 19.85 (s, $B(OH)_3$), -5.87 (br., *closo*), -10.72 (d, J_{BH}=*c.*140Hz, *closo*), -12.53 (d, J_{BH}=*c.*160Hz, *closo*)

Reaction of 2,4,6-tri-(*para*-carboranyl)-1,3,5-triazine with hydrazine monohydrate

2,4,6-tri-(*para*-carboranyl)-1,3,5triazine (0.25g, 0.5mmol) was suspended in THF(15mL) and hydrazine monohydrate (1.2mL, 18mmol) added. Initially there was no change although a small quantity of white gas was evolved. A further portion of hydrazine (1.2mL) and THF (25mL) was added and the solution left stirring at ambient temperature for two weeks with no obvious change in the appearance of the solution. The reaction solution was then refluxed overnight and upon cooling turned a pale purple colour. The solution was diluted with dichloromethane (more white gas was evolved) and washed with water. Removal of the solvent from the isolated organic layer left a pale pink sticky solid, the infrared spectrum of which suggested a certain degree of deboronation had occurred. (The suggested product has one cage deboronated with the remaining two cages remaining intact.)

IR : 2617 (*closo* BH), 2549 (*nido* BH), 1654, 1539 (triazine CN) cm^{-1}

This solid was dissolved in THF (25mL), more hydrazine (2.5mL) added and the solution refluxed for a further 20hours before being worked up as before - no change in the product was observed.

Conversion to potassium 18-crown-6 salt

The solid was dissolved in 1:1 EtOH:CH_2Cl_2 and potassium hydroxide (0.10g, 1.5mmol) in EtOH (25mL) added dropwise turning the solution from yellow to cloudy white. 18-crown-6 ether (0.40g, 1.5mmol) in ethanol (10mL) was then added with stirring producing a slightly cloudy solution. Removal of the solvent under reduced pressure left a red oil. The addition of water then ethanol resulted in a clear yellow solution, which left a yellow solid once the solvents were removed. Extraction of this solid into dichloromethane gave a pale yellow oily solid (the aqueous layer was cloudy white). IR spectroscopy showed this to contain the same carborane bands as before.

IR: 2610 (*closo* carboranyl BH), 2540 (*nido* carboranyl BH), 1538 (CN) cm^{-1}

NMR (CD_3CN)/ppm: $^{11}B\{^1H\}$: -5.12 (15B, br.), -12.88 (20B, d, J_{BH}=147Hz), -13.75 (20B, d, J_{BH}=163Hz), -15.62 (40B, d, J_{BH}=*c*.170Hz), -22.17 (5B, d, J_{BH}=*c*.160Hz); -33.63 (2B, d, J_{BH}=*c*.160Hz); -36.17 (2B, d, J_{BH}=*c*.160Hz)

NOTE

The repetition of this experiment was attempted several times by the reaction of hydrazine monohydrate with the carboranyl triazine in refluxing THF. No reaction of the carborane was observed in any example.

Reaction of 2,4,6-tri-(*para*-carboranyl)-1,3,5-triazine with tetrabutyl ammonium fluoride

2,4,6-tri-(*para*-carboranyl)-1,3,5-triazine (0.14g, 0.3mmol) was suspended in THF and tetrabutyl ammonium fluoride (0.90g, 2.5mmol) added. A deep green solution formed instantly, changing to a clear deep yellow solution at 15mins., then ultimately to a clear orange solution after 1hour. ^{19}F NMR showed F^- to be present in solution. Evaporation of the THF left a deep yellow oily solid. Infrared spectroscopy shows the cages have not undergone any deboronation, suggesting the formation of the F adduct of the compound has led to the colour and solubility changes observed.

IR: 3700-2700 s, br. (H-bonding, or solvent); 2962 s; 2875 s; 2617 m (carboranyl BH, *closo*); 2193 br. m; 1652 s (triazine CN); 1556 m; 1486 m; 1382 m; 1151 m; 881 m, 739 m cm^{-1}

NMR (THF)/ppm: ^{19}F: -113.3 (F^-) {δ ^{19}F Bu_4NF = -114.4ppm}

Reaction of 2,4,6-tri-(12'-phenyl-*para*-carboranyl)-1,3,5-triazine with hydrazine monohydrate

2,4,6-tri-(12'-phenyl-*para*-carboranyl)-1,3,5-triazine (0.12g, 0.16mmol) was dissolved in THF (15mL) and hydrazine monohydrate (0.4mL, 8mmol) added giving a slightly cloudy white solution. The addition of a further portion of hydrazine (0.4mL) and THF (20mL) gave no change to the solution's appearance. Stirring at room temperature for two weeks left the carborane unchanged.

The reaction was repeated with the same reagent quantities with the reaction being held at the reflux temperature for two weeks. Again, the carborane remained unchanged.

5.5 SUMMARY

This chapter has discussed the degradation reactions of both one and three cage icosahedral carborane systems. Fluoride ion deboronation reactions of mono-heteroaryl *ortho*- and *meta*-carboranes (2-thiophenyl and 3-pyridyl derivatives) have been shown to be similar to those of previously studied systems (aryl and aliphatic derivatives), with an excess of F^- promoting a more efficient reaction. Fluorination of cage boron atoms (B(8), (10), (2) and (3)), has been shown to occur during the deboronation of di-heteroaryl-*meta*-carboranes. Earlier work had only observed fluorination at the B(10) and B(3) positions. Initial fluorination occurred at the B(8) and B(10) positions of the open cage face, with proposed cage rearrangements leading to the latterly formed B(2) and B(3) species. These fluorinated di-(hetero-aryl)-*meta*-carboranyl *nido* systems were less stable than their mono-substituted counterparts, and were ultimately degraded to boric acid.

Also discussed were the deboronation reactions of the tri-(carboranyl)-triazine systems introduced in Chapter Four. *Ortho*-carboranyl derivatives have been successfully degraded to the tri-*nido* system with OR^-, F^- and amine bases, as have the *meta*-carboranyl derivatives. Deboronation of a *para*-carboranyl system has been achieved by the action of hydrazine on 2,4,6-tri-(*para*-carboranyl)-1,3,5-triazine, although only one of the cages has deboronated. The 2,4,6-tri-(12'-phenyl-*para*-carboranyl)-1,3,5-triazine remained intact under identical conditions. The deboronation reactions of the 2,4,6-tri-carboranyl-1,3,5-triazines were much faster than those of the tri-carboranyl benzenes, probably as a result of the increased solubility of the triazine derivatives.

5.6 REFERENCES

1 J. Plesek, S. Hermánek, Chemistry and Industry, 1973, 381

2 D.C. Busby, M.F. Hawthorne, Inorg. Chem., 1982, 21, 4101

3 M.F. Hawthorne, D.C. Young, P.M. Garrett, D.A. Owen, S.G. Schwerin, F.N. Tebbe, P.A. Wegner, J. Amer. Chem. Soc., 1968, 90 , 862

4 J. Plesek, S. Hermanek, B. Stibr, Pure and Appl. Chem., 1991, 63, 399

5 R.A. Wiesboeck, M.F. Hawthorne, J. Amer. Chem. Soc., 1964, 86, 1642

6 L.I. Zakharkin, V.S. Kirillova, Bull. Acad. Sci. USSR, Div. Chem. Sci., 1975, 24, 2484

7 J.L. Spencer, M. Green, F.G.A. Stone, J. Chem. Soc., Chem. Commun., 1972, 1178

8 M.J. Manning, C.B. Knobler, M.F. Hawthorne, Inorg. Chem., 1991, 30, 3589

9 W.R. Pretzer, D.A. Thompson, R.W. Rudolph, Inorg. Chem., 1975, **14**, 2571; V. Chowdry, W.R. Pretzer, D.N. Rai, R.W. Rudolph, J. Am. Chem. Soc., 1973, **95**, 4560

10 L.I. Zakharkin, A.V. Grebennikov, Bull. Acad. Sci. USSR, Div. Chem. Sci., 1966, 1952

11 L.I. Zakharkin, V.I. Kalinin, Tet. Lett., 1965, **7**, 407

12 F. Teixidor, R.W. Rudolph, J. Organometal. Chem., 1983, **241**, 301

13 C. Vinas, W.M. Butler, F. Teixidor, R.W. Rudolph, Organometallics, 1984, **3**, 503

14 C. Vinas, W.M. Butler, F. Teixidor, R.W. Rudolph, Inorg. Chem., 1986, **25**, 4369

15 L.I. Zakharkin, V.N. Kalinin, J. Gen Chem. USSR, 1965, **35**, 1693

16 V.I. Stanko, V.A. Brattsev, J. Gen. Chem. USSR, 1968, **38**, 636

17 F. Cardulla, J. Chem. Educ.1983, **60**, 505

18 D. Grafstein, J. Bobinski, J. Dvorak, H. Smith, N. Schwartz, M.S. Cohen, M.M. Fein, Inorg. Chem. 1963, **2**, 1120

19 M.A. Fox, K. Wade, Polyhedron, 1997, **16**, 2517

20 A.J. Welch, A.S. Weller, J. Chem. Soc., Dalton Trans., 1997, 1205

21 D. Grafstein, J. Dvorak, Inorg. Chem., 1963, **2**, 1128

22 V.A. Brattsev, G.N. Danilova, V.I. Stanko, J. Gen. Chem. USSR, 1972, **42**, 1327

23 H. Tomita, H. Luu, T. Onak, Inorg. Chem., 1991, **30**, 812

24 M.A. Fox, W.R. Gill, P.L. Herbertson, J.A.H. MacBride, K.Wade, H.M. Colquhoun, Polyhedron, 1996, **15**, 565

25 M.A. Fox, J.A.H. MacBride, K. Wade, Polyhedron, 1997, **16**, 2499

26 A.K. Saxena, N.S. Hosmane, Chem. Rev., 1993, **93**, 1081

27 a) T.E. Paxson, M.F. Hawthorne, J. Am. Chem. Soc., 1974, **96**, 4674 b) E.L. Hoel, J. Am. Chem. Soc., 1974, **96**, 4676 c) L.I. Zakharkin, T.B. Agakhanova, J. Gen. Chem. USSR, 1977, **47**, 2191 d)L.I. Zakharkin, T.B. Agakhanova, Bull. Acad. Sci. USSR, 1978, **27**, 1900 e) E.S. Chandrasekaran, D.A. Thompson, R.W. Rudolph, Inorg. Chem., 1978, **17**, 760 f) M.F. Hawthorne *et al.*, J. Am. Chem. Soc., 1978, **100**, 8266 g) M.F. Hawthorne *et al.*, J. Am. Chem. Soc., 1984, **106**, 2965-3010

28 L.I. Zakharkin, G.G. Zhigareva, V.A. Antonovich, A.I. Yanovskii, Y.T. Struchkov, J.Gen. Chem. USSR. 1986, **56**, 1823

29 S. Kongpricha, H. Schroeder, Inorg. Chem., 1969, 8, 2449

30 K. Wade, P.L. Herbertson, J.A.H. MacBride, K. Wade, unpublished results

31 note - the aim of this experiment was to cleave the triazine ring in the manner reported in the Chapter Four; the result, however, was deboronation of the cage

Appendices

Appendix A

General Experimental Details

General Synthetic Information

Ortho, *meta*, and *para*carboranes were sublimed under dynamic vacuum before use. All reactions involving lithiation of a carborane or the formation of a Grignard intermediate were carried out under a dry dinitrogen atmosphere using oven dried glassware. n-Butyl lithium was used as supplied (Aldrich) or, after storage, standardised by titration with s-butanol in toluene with 4,5-diazaphenanthrene as indicator. 1,2-dimethoxyethane (monoglyme, DME) was dried by refluxing and distillation over potassium and storage over sodium wire. For copper coupling reactions, copper(I) chloride was purified by the method of Whitesides[1] and pyridine was dried over potassium hydroxide, vacuum transferred and stored under nitrogen. Diethyl ether and toluene, when required as dry solvents, were dried over sodium wire. Ether refers to diethyl ether, used as supplied, unless stated otherwise.

All other solvents were reagent grade unless stated otherwise and all reagents were used as supplied unless stated otherwise.

General Analytical Information

Infrared spectra were recorded as KBr discs unless stated otherwise, using a Perkin Elmer 1720X FTIR spectrometer. In experiments looking at hydrogen bonding effects, solution state infrared spectra were recorded as CCl_4 solutions in a solution cell.

Mass Spectra were performed on a VG7070E Organic Mass Spectrometer using either electrical ionisation or chemical ionisation.

Melting Points were measured in capillary tubes on an Electrothermal 9200 heating block.

Elemental Analyses were performed by the departmental microanalytical services. Numbers in parentheses indicate calculated values.

Solution State NMR spectra were recorded on a Varian VXR200 (^{1}H) or a Bruker AC250 (^{1}H 250.1MHz, ^{19}F 235.2MHz, ^{11}B 80.3MHz, ^{13}C 62.9MHz, ^{31}P 161.90MHz). A Bruker AMX500 (^{11}B 160.5MHz, ^{1}H 500.1MHz, ^{13}C 125.8MHz) was also used to measure ^{1}H{^{11}B}, ^{13}C, ^{13}C{^{1}H}, ^{11}B and ^{11}B{^{1}H} spectra and to obtain HETCOR and COSY correlation spectra. The spectra from this instrument have been stated preferentially for boron and carbon measurements. (In instances where these spectra are not reported, this is stated in the text). ^{1}H NMR spectra were referenced internally to the residual protio impurity in the NMR solvent ($CDCl_3$ 7.26ppm, C_6D_6 7.26ppm, CD_3CN 2.34 ppm, D_2O 4.8ppm). ^{13}C NMR spectra were referenced to the solvent resonance ($CDCl_3$ 77.7ppm, C_6D_6 128.0ppm, CD_3CN 118.0ppm). ^{19}F and ^{11}B NMR spectra were referenced externally to $CFCl_3$ (^{19}F 0.00ppm) and $BF_3.Et_2O$ (^{11}B 0.00ppm) respectively.

Solid state NMR spectroscopic measurements were performed by Dr. David Apperley of the Mountjoy Research Centre, Durham as finely ground powders.

1 G.M. Whitesides, J.S. Sadowski, J. Lilburn, J. Am. Chem. Soc., 1974, 96, p2829

Appendix B

Crystallographic Details

Crystal data for 1-phenyl-2-hydroxy-*ortho*-carborane

Empirical Formula	$C_8H_{17}B_{10}O_{1.5}$	
Temperature	160(2) K	
Wavelength	Mo - Kα, λ = 0.71073 Å	
Crystal System	monoclinic	
Space Group	$P2_1/n$	
Unit Cell Dimensions	a = 12.628(3) Å	α = 90°
	b = 6.804(2) Å	β = 96.97(3)°
	c = 16.020(4) Å	γ = 90°
Crystal Size	0.60 x 0.52 x 0.20 mm	
Final R indices [I>2σ(I)]	R1 = 0.0540	wR2 = 0.1325
R indices (all data)	R1 = 0.0703	wR2 = 0.1488

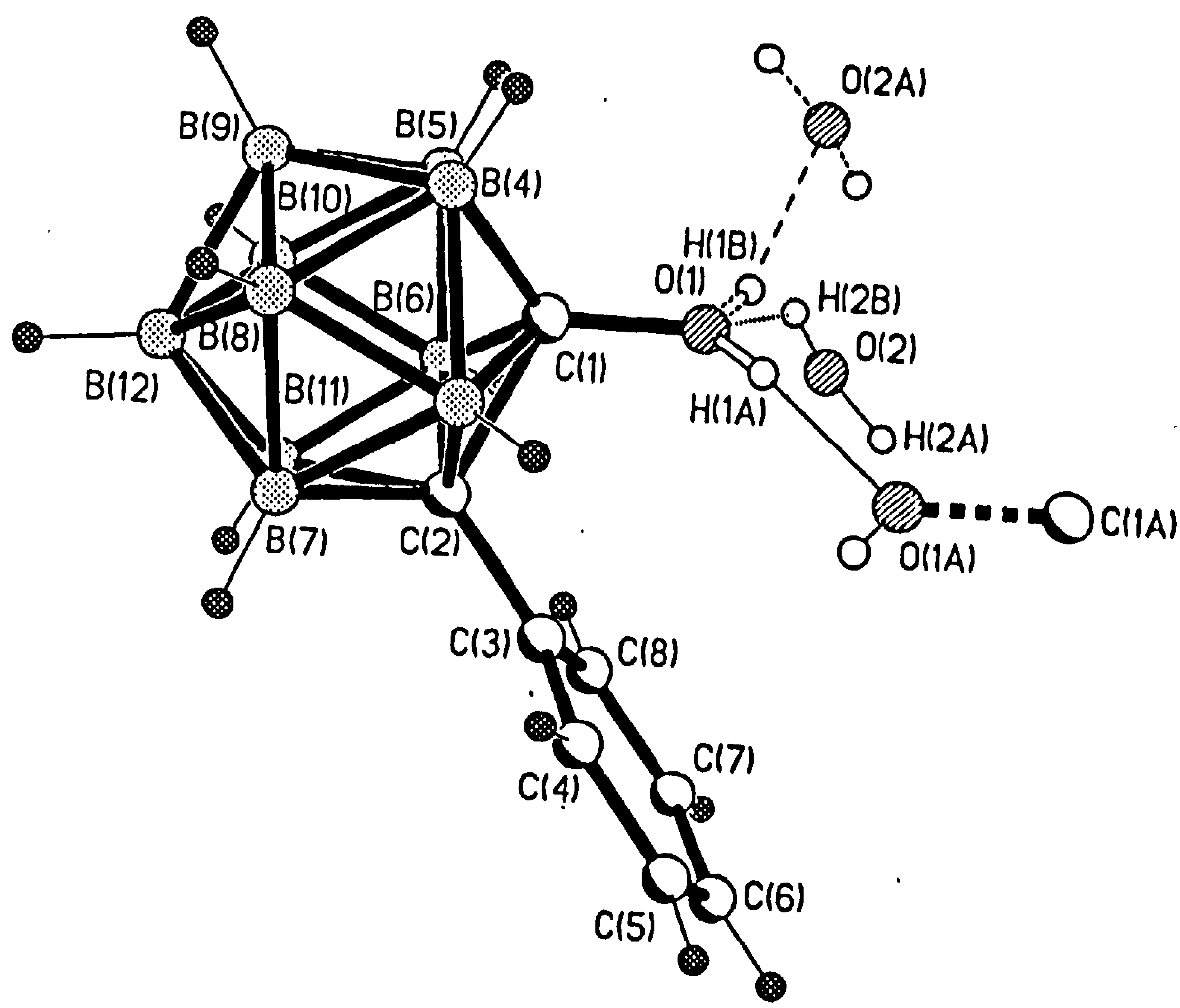

Table 2. Atomic coordinates (x 10^4) and equivalent isotropic displacement parameters ($Å^2$ x 10^3). U(eq) is defined as one third of the trace of the orthogonalized U_{ij} tensor.

	x	y	z	U(eq)
O(1)	4862.2(13)	6561(3)	4438.0(9)	33.3(4)
C(1)	4813(2)	6193(3)	3596.0(12)	25.1(5)
C(2)	5955(2)	5239(3)	3266.1(12)	22.8(5)
B(3)	4834(2)	3777(3)	3302.8(14)	24.1(5)
B(4)	3701(2)	5282(4)	3016(2)	30.6(6)
B(5)	4171(2)	7702(4)	2857(2)	31.9(6)
B(6)	5590(2)	7653(4)	3037(2)	29.1(5)
B(7)	5607(2)	3668(4)	2447.6(14)	25.3(5)
B(8)	4181(2)	3706(4)	2265(2)	28.6(5)
B(9)	3779(2)	6152(4)	1982(2)	34.1(6)
B(10)	4951(2)	7632(4)	2001(2)	33.7(6)
B(11)	6078(2)	6090(4)	2281.7(14)	28.7(5)
B(12)	4952(2)	5159(4)	1629.2(14)	28.8(5)
C(3)	6893(2)	4865(3)	3919.8(12)	25.5(5)
C(4)	7073(2)	3000(3)	4247.0(13)	32.5(5)
C(5)	7933(2)	2635(4)	4852(2)	41.0(6)
C(6)	8618(2)	4133(4)	5137.4(14)	40.3(6)
C(7)	8452(2)	5989(4)	4807(2)	42.7(6)
C(8)	7603(2)	6363(4)	4194.9(14)	36.5(6)
O(2)	5912(3)	9738(6)	5158(2)	55.9(11)

Table 3. Bond lengths (Å) and angles (°)

O(1)-H(1B)	0.80(7)	O(1)-H(1A)	0.85(6)
O(1)-C(1)	1.366(2)	C(1)-B(5)	1.697(3)
C(1)-B(4)	1.704(3)	C(1)-B(3)	1.711(3)
C(1)-B(6)	1.722(3)	C(1)-C(2)	1.723(3)
C(2)-C(3)	1.504(3)	C(2)-B(11)	1.705(3)
C(2)-B(7)	1.707(3)	C(2)-B(6)	1.734(3)
C(2)-B(3)	1.738(3)	B(3)-B(8)	1.765(3)
B(3)-B(4)	1.773(3)	B(3)-B(7)	1.778(3)
B(4)-B(8)	1.773(3)	B(4)-B(9)	1.774(4)
B(4)-B(5)	1.779(4)	B(5)-B(9)	1.776(4)
B(5)-B(6)	1.781(4)	B(5)-B(10)	1.783(4)
B(6)-B(10)	1.756(3)	B(6)-B(11)	1.777(3)
B(7)-B(12)	1.780(3)	B(7)-B(11)	1.783(3)
B(7)-B(8)	1.788(3)	B(8)-B(9)	1.783(4)
B(8)-B(12)	1.789(3)	B(9)-B(12)	1.781(3)
B(9)-B(10)	1.787(4)	B(10)-B(11)	1.782(4)
B(10)-B(12)	1.785(4)	B(11)-B(12)	1.776(3)
C(3)-C(4)	1.382(3)	C(3)-C(8)	1.394(3)
C(4)-C(5)	1.387(3)	C(5)-C(6)	1.378(4)
C(6)-C(7)	1.375(4)	C(7)-C(8)	1.387(3)
O(2)-H(2B)	0.78(6)	O(2)-H(2A)	0.80(6)
H(1B)-O(1)-C(1)	123(5)	H(1A)-O(1)-C(1)	119(5)
O(1)-C(1)-B(5)	122.6(2)	O(1)-C(1)-B(4)	122.8(2)
B(5)-C(1)-B(4)	63.09(14)	O(1)-C(1)-B(3)	116.5(2)
B(5)-C(1)-B(3)	114.3(2)	B(4)-C(1)-B(3)	62.58(13)
O(1)-C(1)-B(6)	116.6(2)	B(5)-C(1)-B(6)	62.76(14)
B(4)-C(1)-B(6)	114.2(2)	B(3)-C(1)-B(6)	112.5(2)
O(1)-C(1)-C(2)	115.6(2)	B(5)-C(1)-C(2)	111.1(2)
B(4)-C(1)-C(2)	111.1(2)	B(3)-C(1)-C(2)	60.81(12)
B(6)-C(1)-C(2)	60.42(12)	C(3)-C(2)-B(11)	123.3(2)
C(3)-C(2)-B(7)	122.5(2)	B(11)-C(2)-B(7)	63.00(13)
C(3)-C(2)-C(1)	117.9(2)	B(11)-C(2)-C(1)	109.2(2)
B(7)-C(2)-C(1)	108.9(2)	C(3)-C(2)-B(6)	118.3(2)
B(11)-C(2)-B(6)	62.22(13)	B(7)-C(2)-B(6)	113.2(2)
C(1)-C(2)-B(6)	59.77(12)	C(3)-C(2)-B(3)	117.1(2)
B(11)-C(2)-B(3)	113.1(2)	B(7)-C(2)-B(3)	62.12(13)
C(1)-C(2)-B(3)	59.25(12)	B(6)-C(2)-B(3)	110.6(2)
C(1)-B(3)-C(2)	59.94(12)	C(1)-B(3)-B(8)	105.3(2)
C(2)-B(3)-B(8)	105.8(2)	C(1)-B(3)-B(4)	58.51(13)
C(2)-B(3)-B(4)	107.2(2)	B(8)-B(3)-B(4)	60.13(13)
C(1)-B(3)-B(7)	106.2(2)	C(2)-B(3)-B(7)	58.10(12)
B(8)-B(3)-B(7)	60.64(13)	B(4)-B(3)-B(7)	109.0(2)
C(1)-B(4)-B(8)	105.3(2)	C(1)-B(4)-B(3)	58.91(12)
B(8)-B(4)-B(3)	59.70(13)	C(1)-B(4)-B(9)	104.6(2)
B(8)-B(4)-B(9)	60.36(14)	B(3)-B(4)-B(9)	107.5(2)
C(1)-B(4)-B(5)	58.28(13)	B(8)-B(4)-B(5)	108.4(2)
B(3)-B(4)-B(5)	107.4(2)	B(9)-B(4)-B(5)	59.98(14)
C(1)-B(5)-B(9)	104.8(2)	C(1)-B(5)-B(4)	58.63(13)
B(9)-B(5)-B(4)	59.85(14)	C(1)-B(5)-B(6)	59.31(13)
B(9)-B(5)-B(6)	107.2(2)	B(4)-B(5)-B(6)	107.8(2)
C(1)-B(5)-B(10)	105.0(2)	B(9)-B(5)-B(10)	60.26(14)
B(4)-B(5)-B(10)	108.1(2)	B(6)-B(5)-B(10)	59.03(14)
C(1)-B(6)-C(2)	59.81(12)	C(1)-B(6)-B(10)	105.1(2)
C(2)-B(6)-B(10)	105.8(2)	C(1)-B(6)-B(11)	106.0(2)
C(2)-B(6)-B(11)	58.09(12)	B(10)-B(6)-B(11)	60.57(14)
C(1)-B(6)-B(5)	57.94(13)	C(2)-B(6)-B(5)	106.8(2)
B(10)-B(6)-B(5)	60.56(14)	B(11)-B(6)-B(5)	109.0(2)

C(2)-B(7)-B(3)	59.78(12)	C(2)-B(7)-B(12)	105.2(2)
B(3)-B(7)-B(12)	107.1(2)	C(2)-B(7)-B(11)	58.42(12)
B(3)-B(7)-B(11)	107.5(2)	B(12)-B(7)-B(11)	59.80(13)
C(2)-B(7)-B(8)	106.1(2)	B(3)-B(7)-B(8)	59.32(13)
B(12)-B(7)-B(8)	60.19(13)	B(11)-B(7)-B(8)	108.0(2)
B(3)-B(8)-B(4)	60.17(13)	B(3)-B(8)-B(9)	107.5(2)
B(4)-B(8)-B(9)	59.85(14)	B(3)-B(8)-B(7)	60.04(12)
B(4)-B(8)-B(7)	108.5(2)	B(9)-B(8)-B(7)	107.8(2)
B(3)-B(8)-B(12)	107.3(2)	B(4)-B(8)-B(12)	107.9(2)
B(9)-B(8)-B(12)	59.82(14)	B(7)-B(8)-B(12)	59.67(13)
B(4)-B(9)-B(5)	60.17(14)	B(4)-B(9)-B(12)	108.2(2)
B(5)-B(9)-B(12)	108.2(2)	B(4)-B(9)-B(8)	59.79(14)
B(5)-B(9)-B(8)	108.1(2)	B(12)-B(9)-B(8)	60.28(14)
B(4)-B(9)-B(10)	108.2(2)	B(5)-B(9)-B(10)	60.1(2)
B(12)-B(9)-B(10)	60.03(14)	B(8)-B(9)-B(10)	108.2(2)
B(6)-B(10)-B(11)	60.29(14)	B(6)-B(10)-B(5)	60.40(14)
B(11)-B(10)-B(5)	108.7(2)	B(6)-B(10)-B(12)	107.7(2)
B(11)-B(10)-B(12)	59.74(14)	B(5)-B(10)-B(12)	107.7(2)
B(6)-B(10)-B(9)	107.8(2)	B(11)-B(10)-B(9)	107.9(2)
B(5)-B(10)-B(9)	59.66(14)	B(12)-B(10)-B(9)	59.83(14)
C(2)-B(11)-B(12)	105.5(2)	C(2)-B(11)-B(6)	59.69(13)
B(12)-B(11)-B(6)	107.2(2)	C(2)-B(11)-B(10)	105.9(2)
B(12)-B(11)-B(10)	60.21(14)	B(6)-B(11)-B(10)	59.14(14)
C(2)-B(11)-B(7)	58.58(12)	B(12)-B(11)-B(7)	60.02(13)
B(6)-B(11)-B(7)	107.6(2)	B(10)-B(11)-B(7)	108.1(2)
B(11)-B(12)-B(7)	60.18(13)	B(11)-B(12)-B(9)	108.4(2)
B(7)-B(12)-B(9)	108.2(2)	B(11)-B(12)-B(10)	60.05(14)
B(7)-B(12)-B(10)	108.1(2)	B(9)-B(12)-B(10)	60.14(14)
B(11)-B(12)-B(8)	108.3(2)	B(7)-B(12)-B(8)	60.14(13)
B(9)-B(12)-B(8)	59.90(14)	B(10)-B(12)-B(8)	108.0(2)
C(4)-C(3)-C(8)	118.8(2)	C(4)-C(3)-C(2)	120.0(2)
C(8)-C(3)-C(2)	121.2(2)	C(3)-C(4)-C(5)	120.6(2)
C(6)-C(5)-C(4)	120.4(2)	C(7)-C(6)-C(5)	119.5(2)
C(6)-C(7)-C(8)	120.6(2)	C(7)-C(8)-C(3)	120.2(2)
H(2B)-O(2)-H(2A)	138(10)		

Table 4. Anisotropic displacement parameters ($Å^2 \times 10^3$)
The anisotropic displacement factor exponent takes the form:
$-2\pi^2(h^2a^{*2}U_{11} + \ldots + 2hka^*b^*U_{12})$.

	U(11)	U(22)	U(33)	U(23)	U(13)	U(12)
O(1)	43.4(9)	33.3(9)	24.4(8)	-4.9(7)	8.9(6)	3.6(8)
C(1)	28.8(10)	21.8(10)	25.1(10)	-0.9(8)	4.5(8)	2.0(9)
C(2)	24.0(10)	21.4(10)	23.4(10)	-1.3(8)	4.4(8)	-1.7(8)
B(3)	24.1(11)	20.9(11)	27.4(12)	-0.7(9)	4.2(9)	-1.9(9)
B(4)	24.3(12)	31.1(13)	36.4(13)	-0.3(11)	3.6(10)	2.1(10)
B(5)	36.0(13)	25.5(13)	32.8(13)	2.4(10)	-2.1(10)	7.5(11)
B(6)	37.5(13)	22.7(12)	26.7(12)	0.6(10)	1.8(10)	-4.8(10)
B(7)	24.8(11)	29.0(12)	21.8(11)	-5.9(9)	1.3(8)	-1.9(10)
B(8)	25.5(11)	29.8(13)	29.3(12)	-2.4(10)	-1.7(9)	-2.8(10)
B(9)	31.2(13)	35.7(14)	33.4(14)	0.0(11)	-3.5(10)	3.7(11)
B(10)	40.5(14)	28.3(13)	30.6(13)	5.1(10)	-2.5(10)	-2.8(11)
B(11)	33.0(12)	30.6(13)	22.3(11)	1.6(10)	2.9(9)	-7.3(10)
B(12)	30.7(12)	30.2(13)	24.4(12)	-1.0(10)	-1.5(9)	-2.0(10)
C(3)	23.4(10)	31.8(11)	21.4(10)	-1.8(9)	3.2(7)	-0.1(9)
C(4)	35.1(12)	30.1(12)	30.4(11)	-3.6(9)	-3.5(9)	1.5(10)
C(5)	43.8(13)	40.2(14)	36.6(13)	-0.5(11)	-5.2(10)	10.2(11)
C(6)	30.8(11)	58(2)	29.7(12)	-4.1(11)	-6.6(9)	6.3(11)
C(7)	33.6(12)	54(2)	37.7(13)	-5.7(12)	-5.6(10)	-10.6(12)
C(8)	34.4(12)	37.3(13)	36.3(12)	2.5(10)	-1.6(9)	-8.0(10)
O(2)	68(3)	57(3)	42(2)	9(2)	5(2)	-19(2)

Table 5. Hydrogen atom coordinates ($\times 10^4$) and isotropic displacement parameters ($Å^2 \times 10^3$)

	x	y	z	U
H(1A)	4885(56)	5601(95)	4778(39)	67
H(1B)	4812(51)	7645(109)	4623(40)	67
H(3)	4809(2)	2525(3)	3753.9(14)	29
H(4)	2922(2)	5011(4)	3263(2)	37
H(5)	3701(2)	9030(4)	3001(2)	38
H(6)	6059(2)	8946(4)	3312(2)	35
H(7)	6079(2)	2332(4)	2320.0(14)	30
H(8)	3714(2)	2394(4)	2010(2)	34
H(9)	3046(2)	6460(4)	1534(2)	41
H(10)	4991(2)	8921(4)	1571(2)	40
H(11)	6863(2)	6356(4)	2043.0(14)	34
H(12)	4990(2)	4810(4)	950.2(14)	35
H(4A)	6605(2)	1958(3)	4055.9(13)	39
H(5A)	8050(2)	1345(4)	5071(2)	49
H(6A)	9199(2)	3886(4)	5558.4(14)	48
H(7A)	8924(2)	7024(4)	5001(2)	51
H(8A)	7505(2)	7643(4)	3962.1(14)	44
H(2A)	6312(63)	9406(132)	5556(45)	112
H(2B)	5382(49)	9362(132)	4905(54)	112

Crystal data for 1-phenyl-2-carboxy-*ortho*-carborane

Empirical Formula	$C_9H_{16}B_{10}O_2$	
Temperature	293 K	
Wavelength	Cu - Kα, λ= 1.54178Å	
Crystal System	monoclinic	
Space Group	$P2_1/n$ (Alt. $P2_1/c$)	
Unit Cell Dimensions	a = 12.349(1) Å	α = 90°
	b = 13.272(1) Å	β = 90.632(8)°
	c = 18.408(2)	γ = 90°
Crystal Size	0.33 x 0.20 x 0.20 mm	
Final R indices [I>2σ(I)]		
R indices (all data)		

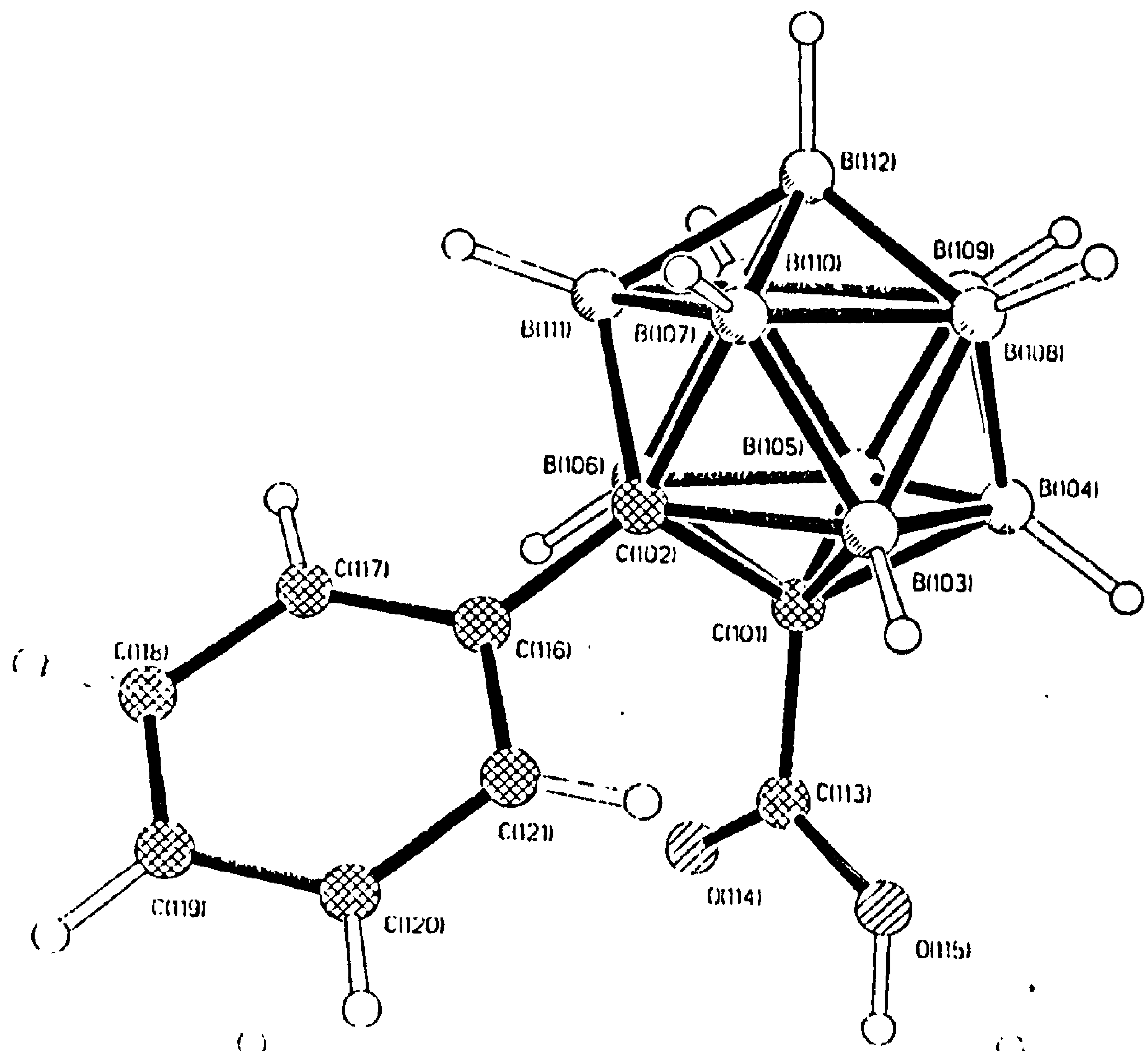

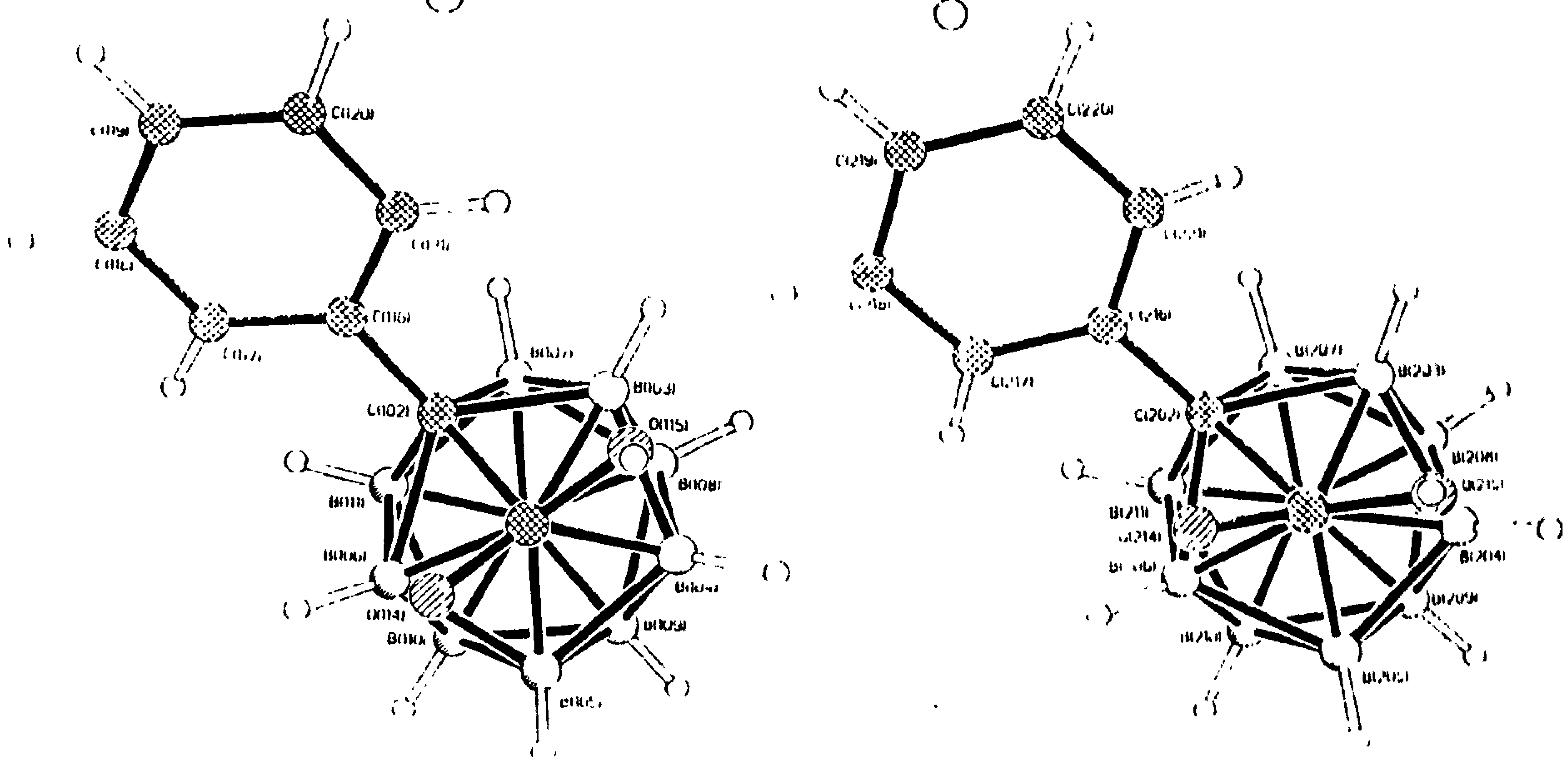

Table 2 Fractional atomic co-ordinates and equivalent isotropic ADP's (Å^2) for the non-hydrogen atoms of $C_9H_{16}B_{10}O_2$.

Atom	x	y	z	U(eq)
C(101)	0.3321(2)	0.6488(2)	0.3990(1)	0.0529
C(102)	0.2028(2)	0.6154(2)	0.3841(1)	0.0507
B(103)	0.2314(3)	0.7181(2)	0.4402(2)	0.0593
B(104)	0.3479(3)	0.7762(3)	0.4023(2)	0.0670
B(105)	0.3881(3)	0.7047(3)	0.3249(2)	0.0685
B(106)	0.2977(2)	0.6011(3)	0.3145(2)	0.0581
B(107)	0.1271(3)	0.7222(3)	0.3739(2)	0.0646
B(108)	0.2173(3)	0.8247(3)	0.3839(2)	0.0720
B(109)	0.3140(3)	0.8163(3)	0.3136(2)	0.0747
B(110)	0.2820(3)	0.7092(3)	0.2599(2)	0.0743
B(111)	0.1664(3)	0.6509(3)	0.2977(2)	0.0628
B(112)	0.1774(3)	0.7837(3)	0.2956(2)	0.0747
C(113)	0.4017(2)	0.5805(2)	0.4456(1)	0.0563
O(114)	0.4483(2)	0.5092(2)	0.4182(1)	0.0825
O(115)	0.4083(2)	0.6057(2)	0.5124(1)	0.0766
C(116)	0.1622(2)	0.5193(2)	0.4177(1)	0.0465
C(117)	0.1271(2)	0.4422(2)	0.3730(2)	0.0649
C(118)	0.0868(2)	0.3538(2)	0.4015(2)	0.0718
C(119)	0.0823(2)	0.3410(2)	0.4752(2)	0.0644
C(120)	0.1166(2)	0.4165(2)	0.5204(2)	0.0618
C(121)	0.1560(2)	0.5057(2)	0.4925(1)	0.0547
C(201)	0.6660(2)	0.4942(2)	0.1483(1)	0.0507
C(202)	0.7861(2)	0.4340(2)	0.1397(1)	0.0485
B(203)	0.7820(3)	0.5659(2)	0.1485(2)	0.0589
B(204)	0.6740(3)	0.5920(3)	0.2078(2)	0.0648
B(205)	0.6118(3)	0.4765(3)	0.2317(2)	0.0698
B(206)	0.6816(2)	0.3770(2)	0.1865(2)	0.0564
B(207)	0.8782(3)	0.4908(3)	0.1966(2)	0.0616
B(208)	0.8088(3)	0.5890(3)	0.2411(2)	0.0700
B(209)	0.7038(3)	0.5349(3)	0.2926(2)	0.0752
B(210)	0.7082(3)	0.4018(3)	0.2789(2)	0.0727
B(211)	0.8162(3)	0.3756(2)	0.2197(2)	0.0595
B(212)	0.8296(3)	0.4725(3)	0.2850(2)	0.0706
C(213)	0.5940(2)	0.4972(2)	0.0815(1)	0.0549
O(214)	0.5719(2)	0.4230(1)	0.0479(1)	0.0750
O(215)	0.5593(2)	0.5850(2)	0.0661(1)	0.0820
C(216)	0.8178(2)	0.3890(2)	0.0679(1)	0.0538
C(217)	0.8163(2)	0.2857(2)	0.0594(2)	0.0706
C(218)	0.8480(3)	0.2427(3)	-0.0055(2)	0.0872
C(219)	0.8802(3)	0.3010(5)	-0.0619(2)	0.0986
C(220)	0.8818(4)	0.4017(5)	-0.0533(2)	0.1168
C(221)	0.8508(3)	0.4466(3)	0.0110(2)	0.0899

Table 3 Fractional atomic co-ordinates and isotropic ADP's (Å^2) for the hydrogen atoms of $C_9H_{16}B_{10}O_2$.

Atom	x	y	z	U(iso)
H(103)	0.220(2)	0.710(2)	0.498(1)	0.0711
H(104)	0.411(2)	0.806(2)	0.443(1)	0.0805
H(105)	0.464(2)	0.687(2)	0.319(1)	0.0822
H(106)	0.323(2)	0.522(2)	0.301(1)	0.0698
H(107)	0.045(2)	0.718(2)	0.392(1)	0.0776
H(108)	0.189(2)	0.896(2)	0.410(1)	0.0864
H(109)	0.349(2)	0.883(2)	0.292(1)	0.0897
H(110)	0.298(2)	0.703(2)	0.204(2)	0.0892
H(111)	0.110(2)	0.602(2)	0.268(1)	0.0754
H(112)	0.120(2)	0.828(2)	0.263(2)	0.0897
H(115)	0.458(2)	0.565(2)	0.539(2)	0.0920
H(117)	0.129(2)	0.446(2)	0.322(2)	0.0778
H(118)	0.064(2)	0.303(2)	0.368(2)	0.0861
H(119)	0.058(2)	0.278(2)	0.496(1)	0.0773
H(120)	0.111(2)	0.406(2)	0.572(1)	0.0742
H(121)	0.177(2)	0.560(2)	0.523(1)	0.0657
H(203)	0.800(2)	0.610(2)	0.100(1)	0.0707
H(204)	0.628(2)	0.657(2)	0.193(1)	0.0777
H(205)	0.526(2)	0.471(2)	0.231(1)	0.0838
H(206)	0.642(2)	0.315(2)	0.161(1)	0.0677
H(207)	0.961(2)	0.491(2)	0.175(1)	0.0740
H(208)	0.854(2)	0.656(2)	0.257(1)	0.0840
H(209)	0.677(2)	0.569(2)	0.344(2)	0.0902
H(210)	0.679(2)	0.346(2)	0.320(1)	0.0872
H(211)	0.861(2)	0.304(2)	0.216(1)	0.0714
H(212)	0.885(2)	0.463(2)	0.330(2)	0.0848
H(215)	0.518(3)	0.585(2)	0.026(2)	0.0984
H(217)	0.793(2)	0.247(2)	0.099(2)	0.0847
H(218)	0.848(3)	0.175(3)	-0.010(2)	0.1047
H(219)	0.899(3)	0.271(3)	-0.107(2)	0.1183
H(220)	0.900(3)	0.448(3)	-0.090(2)	0.1403
H(221)	0.863(3)	0.513(3)	0.017(2)	0.1079

Table 4 Anisotropic ADP's ($Å^2$) for $C_9H_{16}B_{10}O_2$.

Atom	U_{11}	U_{22}	U_{33}	U_{23}	U_{13}	U_{12}
C(101)	0.045(1)	0.063(2)	0.055(1)	0.011(1)	-0.005(1)	-0.003(1)
C(102)	0.042(1)	0.065(2)	0.048(1)	0.006(1)	-0.002(1)	0.002(1)
B(103)	0.067(2)	0.053(2)	0.060(2)	0.005(2)	0.002(2)	0.002(2)
B(104)	0.065(2)	0.069(2)	0.075(2)	0.020(2)	-0.009(2)	-0.010(2)
B(105)	0.053(2)	0.093(3)	0.073(2)	0.026(2)	0.005(2)	-0.008(2)
B(106)	0.052(2)	0.087(2)	0.045(2)	0.008(2)	0.003(1)	-0.003(2)
B(107)	0.051(2)	0.072(2)	0.080(2)	0.019(2)	-0.002(2)	0.009(2)
B(108)	0.074(2)	0.060(2)	0.093(2)	0.022(2)	-0.003(2)	0.002(2)
B(109)	0.077(2)	0.084(3)	0.086(3)	0.040(2)	-0.004(2)	-0.015(2)
B(110)	0.079(2)	0.105(3)	0.057(2)	0.027(2)	-0.002(2)	-0.009(2)
B(111)	0.058(2)	0.089(2)	0.053(2)	0.018(2)	-0.009(2)	-0.001(2)
B(112)	0.073(2)	0.089(3)	0.084(2)	0.038(2)	-0.015(2)	0.000(2)
C(113)	0.046(1)	0.072(2)	0.056(2)	0.006(1)	-0.005(1)	-0.002(1)
O(114)	0.093(1)	0.098(2)	0.077(1)	-0.005(1)	-0.022(1)	0.036(1)
O(115)	0.083(1)	0.103(2)	0.063(1)	0.008(1)	-0.022(1)	0.020(1)
C(116)	0.039(1)	0.056(2)	0.046(1)	0.002(1)	0.001(1)	0.004(1)
C(117)	0.074(2)	0.072(2)	0.053(2)	-0.007(2)	0.008(1)	-0.008(2)
C(118)	0.080(2)	0.066(2)	0.076(2)	-0.017(2)	0.010(2)	-0.009(2)
C(119)	0.072(2)	0.052(2)	0.076(2)	0.004(2)	0.015(1)	-0.004(1)
C(120)	0.075(2)	0.061(2)	0.054(2)	0.008(1)	0.006(1)	-0.007(2)
C(121)	0.059(2)	0.058(2)	0.049(1)	-0.001(1)	0.001(1)	-0.004(1)
C(201)	0.048(1)	0.046(1)	0.065(2)	-0.008(1)	-0.013(1)	0.007(1)
C(202)	0.047(1)	0.044(1)	0.057(1)	0.000(1)	-0.012(1)	0.000(1)
B(203)	0.065(2)	0.046(2)	0.079(2)	0.002(2)	-0.022(2)	-0.009(2)
B(204)	0.071(2)	0.059(2)	0.083(2)	-0.022(2)	-0.026(2)	0.016(2)
B(205)	0.063(2)	0.079(2)	0.071(2)	-0.015(2)	-0.004(2)	0.004(2)
B(206)	0.060(2)	0.051(2)	0.059(2)	-0.001(1)	-0.000(2)	-0.005(1)
B(207)	0.051(2)	0.069(2)	0.076(2)	-0.008(2)	-0.020(2)	-0.002(2)
B(208)	0.081(2)	0.065(2)	0.086(2)	-0.019(2)	-0.035(2)	0.002(2)
B(209)	0.082(3)	0.090(3)	0.066(2)	-0.025(2)	-0.013(2)	0.012(2)
B(210)	0.092(3)	0.075(2)	0.056(2)	-0.003(2)	-0.004(2)	0.002(2)
B(211)	0.072(2)	0.057(2)	0.058(2)	0.002(2)	-0.017(2)	0.014(2)
B(212)	0.078(2)	0.081(2)	0.066(2)	-0.012(2)	-0.026(2)	0.012(2)
C(213)	0.053(1)	0.049(2)	0.073(2)	-0.008(1)	-0.018(1)	0.010(1)
O(214)	0.107(2)	0.059(1)	0.107(2)	-0.022(1)	-0.062(1)	0.017(1)
O(215)	0.141(2)	0.061(1)	0.122(2)	-0.016(1)	-0.086(2)	0.026(1)
C(216)	0.047(1)	0.061(2)	0.057(2)	-0.001(1)	-0.009(1)	0.000(1)
C(217)	0.068(2)	0.069(2)	0.078(2)	-0.014(2)	0.002(2)	0.002(2)
C(218)	0.076(2)	0.105(3)	0.102(3)	-0.043(3)	0.003(2)	0.004(2)
C(219)	0.084(3)	0.174(5)	0.075(3)	-0.038(3)	0.001(2)	0.008(3)
C(220)	0.165(4)	0.150(5)	0.069(3)	0.010(3)	0.025(2)	-0.003(4)
C(221)	0.126(3)	0.089(2)	0.068(2)	0.011(2)	0.013(2)	-0.004(2)

Table 5 Interatomic distances (Å) for the non-hydrogen atoms of $C_9H_{16}B_{10}O_2$.

Atoms	Distance	Atoms	Distance
C(101) - C(102)	1.677(3)	C(201) - C(202)	1.693(3)
C(101) - B(103)	1.729(4)	C(201) - B(203)	1.719(4)
C(101) - B(104)	1.703(4)	C(201) - B(204)	1.700(4)
C(101) - B(105)	1.706(4)	C(201) - B(205)	1.698(4)
C(101) - B(106)	1.727(4)	C(201) - B(206)	1.717(4)
C(101) - C(113)	1.510(3)	C(201) - C(213)	1.510(4)
C(102) - B(103)	1.745(4)	C(202) - B(203)	1.759(4)
C(102) - B(106)	1.755(4)	C(202) - B(206)	1.734(4)
C(102) - B(107)	1.708(4)	C(202) - B(207)	1.713(4)
C(102) - B(111)	1.713(4)	C(202) - B(211)	1.703(4)
C(102) - C(116)	1.505(3)	C(202) - C(216)	1.505(3)
B(103) - B(104)	1.782(5)	B(203) - B(204)	1.766(5)
B(103) - B(107)	1.766(4)	B(203) - B(207)	1.781(4)
B(103) - B(108)	1.762(4)	B(203) - B(208)	1.760(5)
B(104) - B(105)	1.787(5)	B(204) - B(205)	1.772(5)
B(104) - B(108)	1.766(5)	B(204) - B(208)	1.767(5)
B(104) - B(109)	1.764(5)	B(204) - B(209)	1.770(5)
B(105) - B(106)	1.780(5)	B(205) - B(206)	1.787(5)
B(105) - B(109)	1.752(5)	B(205) - B(209)	1.766(5)
B(105) - B(110)	1.766(5)	B(205) - B(210)	1.770(5)
B(106) - B(110)	1.762(5)	B(206) - B(210)	1.761(4)
B(106) - B(111)	1.774(5)	B(206) - B(211)	1.766(4)
B(107) - B(108)	1.767(5)	B(207) - B(208)	1.767(5)
B(107) - B(111)	1.765(5)	B(207) - B(211)	1.764(5)
B(107) - B(112)	1.775(5)	B(207) - B(212)	1.757(5)
B(108) - B(109)	1.774(5)	B(208) - B(209)	1.767(6)
B(108) - B(112)	1.780(6)	B(208) - B(212)	1.763(5)
B(109) - B(110)	1.773(6)	B(209) - B(210)	1.785(5)
B(109) - B(112)	1.770(5)	B(209) - B(212)	1.768(5)
B(110) - B(111)	1.773(5)	B(210) - B(211)	1.766(5)
B(110) - B(112)	1.760(6)	B(210) - B(212)	1.771(5)
B(111) - B(112)	1.768(5)	B(211) - B(212)	1.766(5)
C(113) - O(114)	1.219(3)	C(213) - O(214)	1.194(3)
C(113) - O(115)	1.277(3)	C(213) - O(215)	1.272(3)
C(116) - C(117)	1.380(3)	C(216) - C(217)	1.380(4)
C(116) - C(121)	1.391(3)	C(216) - C(221)	1.364(4)
C(117) - C(118)	1.380(4)	C(217) - C(218)	1.384(4)
C(118) - C(119)	1.370(4)	C(218) - C(219)	1.357(6)
C(119) - C(120)	1.367(4)	C(219) - C(220)	1.346(6)
C(120) - C(121)	1.381(4)	C(220) - C(221)	1.382(6)

Table 6 Interatomic distances (Å) to the hydrogen atoms of $C_9H_{16}B_{10}O_2$.

Atoms	Distance	Atoms	Distance
B(103) - H(103)	1.07(2)	B(203) - H(203)	1.09(2)
B(104) - H(104)	1.14(3)	B(204) - H(204)	1.06(3)
B(105) - H(105)	0.97(3)	B(205) - H(205)	1.06(3)
B(106) - H(106)	1.12(2)	B(206) - H(206)	1.06(2)
B(107) - H(107)	1.07(3)	B(207) - H(207)	1.10(3)
B(108) - H(108)	1.12(3)	B(208) - H(208)	1.09(3)
B(109) - H(109)	1.07(3)	B(209) - H(209)	1.11(3)
B(110) - H(110)	1.05(3)	B(210) - H(210)	1.12(3)
B(111) - H(111)	1.10(3)	B(211) - H(211)	1.11(3)
B(112) - H(112)	1.09(3)	B(212) - H(212)	1.07(3)
O(115) - H(115)	0.95(3)	O(215) - H(215)	0.90(3)
C(117) - H(117)	0.95(3)	C(217) - H(217)	0.94(3)
C(118) - H(118)	0.96(3)	C(218) - H(218)	0.90(3)
C(119) - H(119)	0.97(3)	C(219) - H(219)	0.96(4)
C(120) - H(120)	0.96(3)	C(220) - H(220)	0.94(4)
C(121) - H(121)	0.95(2)	C(221) - H(221)	0.90(3)

Table 7 Interatomic angles (°) for the non-hydrogen atoms of $C_9H_{16}B_{10}O_2$.

Atoms	Angle	Atoms	Angle
C(102) - C(101) - B(103)	61.6(2)	C(202) - C(201) - B(203)	62.1(1)
C(102) - C(101) - B(104)	112.2(2)	C(202) - C(201) - B(204)	112.1(2)
B(103) - C(101) - B(104)	62.6(2)	B(203) - C(201) - B(204)	62.2(2)
C(102) - C(101) - B(105)	112.2(2)	C(202) - C(201) - B(205)	112.0(2)
B(103) - C(101) - B(105)	114.8(2)	B(203) - C(201) - B(205)	114.3(2)
B(104) - C(101) - B(105)	63.2(2)	B(204) - C(201) - B(205)	62.9(2)
C(102) - C(101) - B(106)	62.0(1)	C(202) - C(201) - B(206)	61.1(1)
B(103) - C(101) - B(106)	114.8(2)	B(203) - C(201) - B(206)	114.3(2)
B(104) - C(101) - B(106)	115.0(2)	B(204) - C(201) - B(206)	115.0(2)
B(105) - C(101) - B(106)	62.4(2)	B(205) - C(201) - B(206)	63.1(2)
C(102) - C(101) - C(113)	118.0(2)	C(202) - C(201) - C(213)	116.4(2)
B(103) - C(101) - C(113)	118.6(2)	B(203) - C(201) - C(213)	118.0(2)
B(104) - C(101) - C(113)	120.7(2)	B(204) - C(201) - C(213)	122.3(2)
B(105) - C(101) - C(113)	118.8(2)	B(205) - C(201) - C(213)	120.3(2)
B(106) - C(101) - C(113)	115.1(2)	B(206) - C(201) - C(213)	114.8(2)
C(101) - C(102) - B(103)	60.7(2)	C(201) - C(202) - B(203)	59.7(2)
C(101) - C(102) - B(106)	60.4(1)	C(201) - C(202) - B(206)	60.1(1)
B(103) - C(102) - B(106)	112.6(2)	B(203) - C(202) - B(206)	111.5(2)
C(101) - C(102) - B(107)	108.5(2)	C(201) - C(202) - B(207)	108.2(2)
B(103) - C(102) - B(107)	61.5(2)	B(203) - C(202) - B(207)	61.7(2)
B(106) - C(102) - B(107)	112.3(2)	B(206) - C(202) - B(207)	112.4(2)
C(101) - C(102) - B(111)	108.6(2)	C(201) - C(202) - B(211)	108.5(2)
B(103) - C(102) - B(111)	112.6(2)	B(203) - C(202) - B(211)	112.3(2)
B(106) - C(102) - B(111)	61.5(2)	B(206) - C(202) - B(211)	61.8(2)
B(107) - C(102) - B(111)	62.1(2)	B(207) - C(202) - B(211)	62.2(2)
C(101) - C(102) - C(116)	118.5(2)	C(201) - C(202) - C(216)	120.4(2)
B(103) - C(102) - C(116)	119.0(2)	B(203) - C(202) - C(216)	119.0(2)
B(106) - C(102) - C(116)	115.9(2)	B(206) - C(202) - C(216)	117.7(2)
B(107) - C(102) - C(116)	124.3(2)	B(207) - C(202) - C(216)	122.3(2)
B(111) - C(102) - C(116)	121.9(2)	B(211) - C(202) - C(216)	121.5(2)
C(101) - B(103) - C(102)	57.7(1)	C(201) - B(203) - C(202)	58.2(1)
C(101) - B(103) - B(104)	58.0(2)	C(201) - B(203) - B(204)	58.4(2)
C(102) - B(103) - B(104)	105.4(2)	C(202) - B(203) - B(204)	105.9(2)
C(101) - B(103) - B(107)	103.6(2)	C(201) - B(203) - B(207)	104.0(2)
C(102) - B(103) - B(107)	58.2(2)	C(202) - B(203) - B(207)	57.9(2)
B(104) - B(103) - B(107)	107.6(2)	B(204) - B(203) - B(207)	107.8(2)
C(101) - B(103) - B(108)	103.6(2)	C(201) - B(203) - B(208)	104.2(2)
C(102) - B(103) - B(108)	105.1(2)	C(202) - B(203) - B(208)	104.9(2)
B(104) - B(103) - B(108)	59.8(2)	B(204) - B(203) - B(208)	60.1(2)
B(107) - B(103) - B(108)	60.1(2)	B(207) - B(203) - B(208)	59.9(2)
C(101) - B(104) - B(103)	59.4(2)	C(201) - B(204) - B(203)	59.4(2)
C(101) - B(104) - B(105)	58.5(2)	C(201) - B(204) - B(205)	58.5(2)
B(103) - B(104) - B(105)	108.4(2)	B(203) - B(204) - B(205)	108.5(2)
C(101) - B(104) - B(108)	104.5(2)	C(201) - B(204) - B(208)	104.7(2)
B(103) - B(104) - B(108)	59.5(2)	B(203) - B(204) - B(208)	59.7(2)
B(105) - B(104) - B(108)	107.5(3)	B(205) - B(204) - B(208)	107.7(3)
C(101) - B(104) - B(109)	103.9(3)	C(201) - B(204) - B(209)	104.6(2)
B(103) - B(104) - B(109)	108.0(2)	B(203) - B(204) - B(209)	108.1(2)
B(105) - B(104) - B(109)	59.1(2)	B(205) - B(204) - B(209)	59.8(2)

Table 7 Cont.

Atoms	Angle
B(108) - B(104) - B(109)	60.3(2)
C(101) - B(105) - B(104)	58.3(2)
C(101) - B(105) - B(106)	59.4(2)
B(104) - B(105) - B(106)	108.4(2)
C(101) - B(105) - B(109)	104.3(2)
B(104) - B(105) - B(109)	59.8(2)
B(106) - B(105) - B(109)	108.3(2)
C(101) - B(105) - B(110)	104.6(2)
B(104) - B(105) - B(110)	108.2(3)
B(106) - B(105) - B(110)	59.6(2)
B(109) - B(105) - B(110)	60.5(2)
C(101) - B(106) - C(102)	57.6(1)
C(101) - B(106) - B(105)	58.2(2)
C(102) - B(106) - B(105)	105.2(2)
C(101) - B(106) - B(110)	103.9(2)
C(102) - B(106) - B(110)	105.0(2)
B(105) - B(106) - B(110)	59.8(2)
C(101) - B(106) - B(111)	103.6(2)
C(102) - B(106) - B(111)	58.1(2)
B(105) - B(106) - B(111)	107.6(3)
B(110) - B(106) - B(111)	60.2(2)
C(102) - B(107) - B(103)	60.3(2)
C(102) - B(107) - B(108)	106.5(2)
B(103) - B(107) - B(108)	59.8(2)
C(102) - B(107) - B(111)	59.1(2)
B(103) - B(107) - B(111)	109.1(2)
B(108) - B(107) - B(111)	108.5(3)
C(102) - B(107) - B(112)	105.9(2)
B(103) - B(107) - B(112)	108.5(2)
B(108) - B(107) - B(112)	60.3(2)
B(111) - B(107) - B(112)	59.9(2)
B(103) - B(108) - B(104)	60.7(2)
B(103) - B(108) - B(107)	60.0(2)
B(104) - B(108) - B(107)	108.2(2)
B(103) - B(108) - B(109)	108.4(3)
B(104) - B(108) - B(109)	59.8(2)
B(107) - B(108) - B(109)	107.7(3)
B(103) - B(108) - B(112)	108.4(3)
B(104) - B(108) - B(112)	107.9(3)
B(107) - B(108) - B(112)	60.0(2)
B(109) - B(108) - B(112)	59.7(2)
B(104) - B(109) - B(105)	61.1(2)
B(104) - B(109) - B(108)	59.9(2)
B(105) - B(109) - B(108)	108.8(2)
B(104) - B(109) - B(110)	108.9(3)
B(105) - B(109) - B(110)	60.1(2)
B(108) - B(109) - B(110)	108.1(3)
B(104) - B(109) - B(112)	108.4(2)
B(105) - B(109) - B(112)	108.1(3)

Atoms	Angle
B(208) - B(204) - B(209)	59.9(2)
C(201) - B(205) - B(204)	58.6(2)
C(201) - B(205) - B(206)	59.0(2)
B(204) - B(205) - B(206)	108.1(2)
C(201) - B(205) - B(209)	104.8(3)
B(204) - B(205) - B(209)	60.0(2)
B(206) - B(205) - B(209)	108.0(3)
C(201) - B(205) - B(210)	104.6(2)
B(204) - B(205) - B(210)	108.3(3)
B(206) - B(205) - B(210)	59.3(2)
B(209) - B(205) - B(210)	60.6(2)
C(201) - B(206) - C(202)	58.8(1)
C(201) - B(206) - B(205)	57.9(2)
C(202) - B(206) - B(205)	105.9(2)
C(201) - B(206) - B(210)	104.2(2)
C(202) - B(206) - B(210)	105.5(2)
B(205) - B(206) - B(210)	59.8(2)
C(201) - B(206) - B(211)	104.6(2)
C(202) - B(206) - B(211)	58.2(2)
B(205) - B(206) - B(211)	107.7(2)
B(210) - B(206) - B(211)	60.1(2)
C(202) - B(207) - B(203)	60.4(2)
C(202) - B(207) - B(208)	106.6(2)
B(203) - B(207) - B(208)	59.5(2)
C(202) - B(207) - B(211)	58.6(2)
B(203) - B(207) - B(211)	108.4(2)
B(208) - B(207) - B(211)	108.3(3)
C(202) - B(207) - B(212)	105.9(2)
B(203) - B(207) - B(212)	107.8(3)
B(208) - B(207) - B(212)	60.0(2)
B(211) - B(207) - B(212)	60.2(2)
B(203) - B(208) - B(204)	60.1(2)
B(203) - B(208) - B(207)	60.7(2)
B(204) - B(208) - B(207)	108.4(2)
B(203) - B(208) - B(209)	108.5(2)
B(204) - B(208) - B(209)	60.1(2)
B(207) - B(208) - B(209)	108.1(3)
B(203) - B(208) - B(212)	108.4(2)
B(204) - B(208) - B(212)	108.1(3)
B(207) - B(208) - B(212)	59.7(2)
B(209) - B(208) - B(212)	60.1(2)
B(204) - B(209) - B(205)	60.2(2)
B(204) - B(209) - B(208)	59.9(2)
B(205) - B(209) - B(208)	108.0(3)
B(204) - B(209) - B(210)	107.8(2)
B(205) - B(209) - B(210)	59.8(2)
B(208) - B(209) - B(210)	107.6(3)
B(204) - B(209) - B(212)	107.8(3)
B(205) - B(209) - B(212)	107.7(2)

Table 7 Cont.

Atoms	Angle	Atoms	Angle
B(108) - B(109) - B(112)	60.3(2)	B(208) - B(209) - B(212)	59.8(2)
B(110) - B(109) - B(112)	59.6(2)	B(210) - B(209) - B(212)	59.8(2)
B(105) - B(110) - B(106)	60.6(2)	B(205) - B(210) - B(206)	60.8(2)
B(105) - B(110) - B(109)	59.3(2)	B(205) - B(210) - B(209)	59.6(2)
B(106) - B(110) - B(109)	108.2(2)	B(206) - B(210) - B(209)	108.4(2)
B(105) - B(110) - B(111)	108.2(2)	B(205) - B(210) - B(211)	108.4(2)
B(106) - B(110) - B(111)	60.2(2)	B(206) - B(210) - B(211)	60.1(2)
B(109) - B(110) - B(111)	107.8(3)	B(209) - B(210) - B(211)	107.8(3)
B(105) - B(110) - B(112)	108.0(3)	B(205) - B(210) - B(212)	107.4(3)
B(106) - B(110) - B(112)	108.7(2)	B(206) - B(210) - B(212)	108.0(3)
B(109) - B(110) - B(112)	60.1(2)	B(209) - B(210) - B(212)	59.6(2)
B(111) - B(110) - B(112)	60.0(2)	B(211) - B(210) - B(212)	59.9(2)
C(102) - B(111) - B(106)	60.4(2)	C(202) - B(211) - B(206)	60.0(2)
C(102) - B(111) - B(107)	58.8(2)	C(202) - B(211) - B(207)	59.2(2)
B(106) - B(111) - B(107)	108.7(2)	B(206) - B(211) - B(207)	108.5(2)
C(102) - B(111) - B(110)	106.3(2)	C(202) - B(211) - B(210)	106.6(2)
B(106) - B(111) - B(110)	59.6(2)	B(206) - B(211) - B(210)	59.8(2)
B(107) - B(111) - B(110)	107.9(3)	B(207) - B(211) - B(210)	108.1(2)
C(102) - B(111) - B(112)	106.0(2)	C(202) - B(211) - B(212)	106.0(2)
B(106) - B(111) - B(112)	107.8(3)	B(206) - B(211) - B(212)	108.0(2)
B(107) - B(111) - B(112)	60.3(2)	B(207) - B(211) - B(212)	59.7(2)
B(110) - B(111) - B(112)	59.6(2)	B(210) - B(211) - B(212)	60.2(2)
B(107) - B(112) - B(108)	59.6(2)	B(207) - B(212) - B(208)	60.3(2)
B(107) - B(112) - B(109)	107.5(2)	B(207) - B(212) - B(209)	108.6(3)
B(108) - B(112) - B(109)	60.0(2)	B(208) - B(212) - B(209)	60.1(2)
B(107) - B(112) - B(110)	108.1(2)	B(207) - B(212) - B(210)	108.2(2)
B(108) - B(112) - B(110)	108.4(3)	B(208) - B(212) - B(210)	108.4(2)
B(109) - B(112) - B(110)	60.3(2)	B(209) - B(212) - B(210)	60.6(2)
B(107) - B(112) - B(111)	59.8(2)	B(207) - B(212) - B(211)	60.1(2)
B(108) - B(112) - B(111)	107.8(2)	B(208) - B(212) - B(211)	108.4(2)
B(109) - B(112) - B(111)	108.2(3)	B(209) - B(212) - B(211)	108.6(2)
B(110) - B(112) - B(111)	60.4(2)	B(210) - B(212) - B(211)	59.9(2)
C(101) - C(113) - O(114)	120.0(2)	C(201) - C(213) - O(214)	122.0(2)
C(101) - C(113) - O(115)	114.8(3)	C(201) - C(213) - O(215)	113.6(2)
O(114) - C(113) - O(115)	125.2(3)	O(214) - C(213) - O(215)	124.4(2)
C(102) - C(116) - C(117)	119.2(2)	C(202) - C(216) - C(217)	119.4(2)
C(102) - C(116) - C(121)	122.6(2)	C(202) - C(216) - C(221)	122.3(3)
C(117) - C(116) - C(121)	118.2(2)	C(217) - C(216) - C(221)	118.2(3)
C(116) - C(117) - C(118)	121.1(3)	C(216) - C(217) - C(218)	120.3(3)
C(117) - C(118) - C(119)	120.0(3)	C(217) - C(218) - C(219)	120.8(4)
C(118) - C(119) - C(120)	119.7(3)	C(218) - C(219) - C(220)	118.7(4)
C(119) - C(120) - C(121)	120.7(3)	C(219) - C(220) - C(221)	121.7(4)
C(116) - C(121) - C(120)	120.2(2)	C(216) - C(221) - C(220)	120.3(4)

Table 8 Interatomic angles (°) to the hydrogen atoms of $C_9H_{16}B_{10}O_2$.

Atoms	Angle	Atoms	Angle
C(101) - B(103) - H(103)	118.7(13)	C(201) - B(203) - H(203)	118.2(13)
C(102) - B(103) - H(103)	118.8(13)	C(202) - B(203) - H(203)	116.5(13)
B(104) - B(103) - H(103)	122.6(13)	B(204) - B(203) - H(203)	124.5(13)
B(107) - B(103) - H(103)	125.9(13)	B(207) - B(203) - H(203)	124.2(13)
B(108) - B(103) - H(103)	130.2(14)	B(208) - B(203) - H(203)	131.5(13)
C(101) - B(104) - H(104)	116.4(13)	C(201) - B(204) - H(204)	115.3(14)
B(103) - B(104) - H(104)	116.4(13)	B(203) - B(204) - H(204)	114.1(14)
B(105) - B(104) - H(104)	120.6(13)	B(205) - B(204) - H(204)	121.8(14)
B(108) - B(104) - H(104)	128.0(13)	B(208) - B(204) - H(204)	127.3(14)
B(109) - B(104) - H(104)	130.7(13)	B(209) - B(204) - H(204)	132.3(14)
C(101) - B(105) - H(105)	112.6(16)	C(201) - B(205) - H(205)	114.2(15)
B(104) - B(105) - H(105)	119.6(16)	B(204) - B(205) - H(205)	119.8(15)
B(106) - B(105) - H(105)	113.9(17)	B(206) - B(205) - H(205)	115.5(15)
B(109) - B(105) - H(105)	133.8(17)	B(209) - B(205) - H(205)	132.0(15)
B(110) - B(105) - H(105)	129.8(17)	B(210) - B(205) - H(205)	128.9(15)
C(101) - B(106) - H(106)	118.0(13)	C(201) - B(206) - H(206)	118.4(13)
C(102) - B(106) - H(106)	116.9(13)	C(202) - B(206) - H(206)	117.8(13)
B(105) - B(106) - H(106)	124.4(13)	B(205) - B(206) - H(206)	123.5(13)
B(110) - B(106) - H(106)	131.7(13)	B(210) - B(206) - H(206)	130.2(13)
B(111) - B(106) - H(106)	124.8(13)	B(211) - B(206) - H(206)	124.9(13)
C(102) - B(107) - H(107)	116.3(14)	C(202) - B(207) - H(207)	113.7(13)
B(103) - B(107) - H(107)	118.2(14)	B(203) - B(207) - H(207)	116.1(13)
B(108) - B(107) - H(107)	127.3(14)	B(208) - B(207) - H(207)	128.2(13)
B(111) - B(107) - H(107)	119.1(14)	B(211) - B(207) - H(207)	120.0(13)
B(112) - B(107) - H(107)	127.9(14)	B(212) - B(207) - H(207)	131.1(13)
B(103) - B(108) - H(108)	117.1(14)	B(203) - B(208) - H(208)	119.6(14)
B(104) - B(108) - H(108)	120.8(14)	B(204) - B(208) - H(208)	123.5(14)
B(107) - B(108) - H(108)	119.9(14)	B(207) - B(208) - H(208)	118.7(14)
B(109) - B(108) - H(108)	125.5(14)	B(209) - B(208) - H(208)	124.2(14)
B(112) - B(108) - H(108)	124.7(14)	B(212) - B(208) - H(208)	121.5(14)
B(104) - B(109) - H(109)	120.4(15)	B(204) - B(209) - H(209)	121.5(15)
B(105) - B(109) - H(109)	122.4(15)	B(205) - B(209) - H(209)	122.0(15)
B(108) - B(109) - H(109)	119.9(15)	B(208) - B(209) - H(209)	121.4(15)
B(110) - B(109) - H(109)	123.1(15)	B(210) - B(209) - H(209)	122.3(15)
B(112) - B(109) - H(109)	121.4(15)	B(212) - B(209) - H(209)	121.9(14)
B(105) - B(110) - H(110)	121.0(15)	B(205) - B(210) - H(210)	118.8(14)
B(106) - B(110) - H(110)	118.0(16)	B(206) - B(210) - H(210)	117.8(14)
B(109) - B(110) - H(110)	124.7(15)	B(209) - B(210) - H(210)	123.5(14)
B(111) - B(110) - H(110)	120.4(15)	B(211) - B(210) - H(210)	122.3(14)
B(112) - B(110) - H(110)	123.9(15)	B(212) - B(210) - H(210)	126.0(14)
C(102) - B(111) - H(111)	117.2(13)	C(202) - B(211) - H(211)	116.5(13)
B(106) - B(111) - H(111)	116.2(13)	B(206) - B(211) - H(211)	117.4(13)
B(107) - B(111) - H(111)	122.2(13)	B(207) - B(211) - H(211)	120.9(13)
B(110) - B(111) - H(111)	125.2(13)	B(210) - B(211) - H(211)	126.2(13)
B(112) - B(111) - H(111)	129.0(13)	B(212) - B(211) - H(211)	128.7(12)
B(107) - B(112) - H(112)	117.2(15)	B(207) - B(212) - H(212)	120.5(15)
B(108) - B(112) - H(112)	120.4(15)	B(208) - B(212) - H(212)	122.9(14)
B(109) - B(112) - H(112)	125.8(15)	B(209) - B(212) - H(212)	123.1(14)
B(110) - B(112) - H(112)	125.0(15)	B(210) - B(212) - H(212)	121.2(15)

Table 8 Cont.

Atoms	Angle	Atoms	Angle
B(111) - B(112) - H(112)	119.8(15)	B(211) - B(212) - H(212)	119.5(14)
C(113) - O(115) - H(115)	112.3(18)	C(213) - O(215) - H(215)	111.8(20)
C(116) - C(117) - H(117)	122.7(17)	C(216) - C(217) - H(217)	116.9(18)
C(118) - C(117) - H(117)	116.1(17)	C(218) - C(217) - H(217)	122.7(18)
C(117) - C(118) - H(118)	117.6(17)	C(217) - C(218) - H(218)	119.7(23)
C(119) - C(118) - H(118)	122.3(17)	C(219) - C(218) - H(218)	119.5(23)
C(118) - C(119) - H(119)	120.9(15)	C(218) - C(219) - H(219)	120.6(22)
C(120) - C(119) - H(119)	119.3(15)	C(220) - C(219) - H(219)	120.7(22)
C(119) - C(120) - H(120)	117.6(16)	C(219) - C(220) - H(220)	124.8(26)
C(121) - C(120) - H(120)	121.7(16)	C(221) - C(220) - H(220)	113.5(26)
C(116) - C(121) - H(121)	118.2(15)	C(216) - C(221) - H(221)	119.9(24)
C(120) - C(121) - H(121)	121.6(15)	C(220) - C(221) - H(221)	119.1(24)

Crystal data for 1-fluoro-12-(phenylsulfonyl)-*para*-carborane

Empirical Formula	$C_8H_{15}B_{10}FO_2S$	
Temperature	293(2) K	
Wavelength	0.71073 Å	
Crystal System	monoclinic	
Space Group	C2/c	
Unit Cell Dimensions	a = 37.836(3) Å	$\alpha = 90^\circ$
	b = 6.6744(6) Å	$\beta = 103.4810(10)^\circ$
	c = 12.2240(10) Å	$\gamma = 90^\circ$
Final R indices [$I>2\sigma(I)$]	R1 = 0.0568	wR2 = 0.1511
R indices (all data)	R1 = 0.0611	wR2 = 0.1564

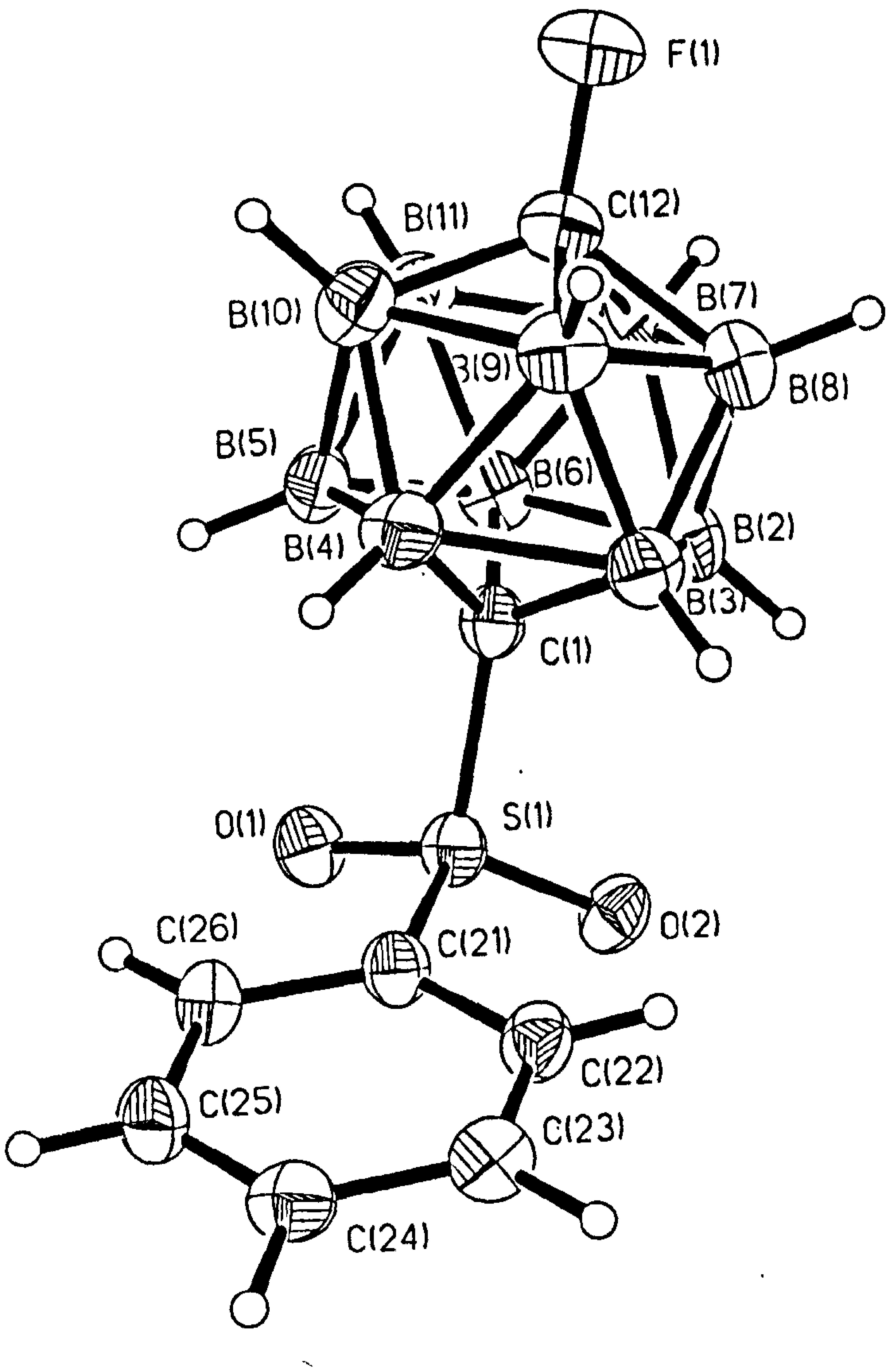

Table 2. Atomic coordinates (x 10^4) and equivalent isotropic displacement parameters (A^2 x 10^3). U(eq) is defined as one third of the trace of the orthogonalized Uij tensor.

	x	y	z	U(eq)
S(1)	3288(1)	1165(1)	9402(1)	29(1)
F(1)	4922(1)	3457(3)	11029(2)	49(1)
C(24)	2766(1)	4735(5)	6317(3)	34(1)
C(25)	2895(1)	2822(5)	6203(2)	35(1)
C(21)	3099(1)	2596(4)	8201(2)	28(1)
C(22)	2974(1)	4514(5)	8332(3)	31(1)
C(23)	2808(1)	5599(5)	7385(2)	33(1)
C(26)	3067(1)	1724(5)	7143(2)	31(1)
C(12)	4564(1)	2979(5)	10663(3)	37(1)
B(4)	3975(1)	3016(6)	8892(3)	34(1)
B(2)	3909(1)	2733(6)	11215(3)	36(1)
C(1)	3763(1)	1916(4)	9839(2)	28(1)
B(7)	4360(1)	1887(6)	11614(3)	40(1)
B(6)	4029(1)	314(5)	10785(3)	36(1)
B(3)	3871(1)	4401(5)	10044(3)	34(1)
B(5)	4071(1)	480(5)	9353(3)	34(1)
B(10)	4425(1)	2175(6)	9310(3)	40(1)
B(8)	4263(1)	4411(6)	11153(3)	39(1)
B(9)	4304(1)	4594(6)	9734(3)	37(1)
O(1)	3286(1)	-907(3)	9087(2)	35(1)
O(2)	3119(1)	1756(3)	10292(2)	35(1)
B(11)	4460(1)	488(6)	10474(3)	39(1)

Table 3. Bond lengths [A] and angles [deg]

S(1)-O(1)	1.435(2)
S(1)-O(2)	1.441(2)
S(1)-C(21)	1.758(3)
S(1)-C(1)	1.821(3)
F(1)-C(12)	1.364(3)
C(24)-C(25)	1.385(4)
C(24)-C(23)	1.402(4)
C(24)-H(24)	1.04(3)
C(25)-C(26)	1.391(4)
C(25)-H(25)	0.92(4)
C(21)-C(22)	1.387(4)
C(21)-C(26)	1.397(4)
C(22)-C(23)	1.385(4)
C(22)-H(22)	0.92(3)
C(23)-H(23)	1.06(3)
C(26)-H(26)	0.98(3)
C(12)-B(8)	1.699(5)
C(12)-B(10)	1.701(5)
C(12)-B(7)	1.702(5)
C(12)-B(9)	1.703(5)
C(12)-B(11)	1.712(5)
B(4)-C(1)	1.719(4)
B(4)-B(10)	1.751(5)
B(4)-B(9)	1.766(5)
B(4)-B(5)	1.794(5)
B(4)-B(3)	1.803(5)
B(4)-H(4)	1.08(3)
B(2)-C(1)	1.732(4)
B(2)-B(7)	1.756(5)
B(2)-B(8)	1.761(5)
B(2)-B(6)	1.789(5)
B(2)-B(3)	1.793(5)
B(2)-H(2)	1.10(3)
C(1)-B(3)	1.713(4)
C(1)-B(6)	1.719(4)
C(1)-B(5)	1.719(4)
B(7)-B(6)	1.762(5)
B(7)-B(8)	1.788(5)
B(7)-B(11)	1.790(5)
B(7)-H(7)	1.05(4)
B(6)-B(11)	1.763(5)
B(6)-B(5)	1.798(5)
B(6)-H(6)	1.04(3)
B(3)-B(8)	1.759(5)
B(3)-B(9)	1.769(5)
B(3)-H(3)	1.01(3)
B(5)-B(11)	1.762(5)
B(5)-B(10)	1.764(5)
B(5)-H(5)	1.07(3)
B(10)-B(9)	1.788(5)
B(10)-B(11)	1.795(5)
B(10)-H(10)	1.06(4)
B(8)-B(9)	1.782(5)
B(8)-H(8)	1.04(4)
B(9)-H(9)	1.08(3)
B(11)-H(11)	1.05(4)
O(1)-S(1)-O(2)	119.39(13)
O(1)-S(1)-C(21)	108.91(13)
O(2)-S(1)-C(21)	108.41(13)
O(1)-S(1)-C(1)	106.68(13)
O(2)-S(1)-C(1)	106.59(13)
C(21)-S(1)-C(1)	106.09(13)
C(25)-C(24)-C(23)	120.4(3)

C(23)-C(24)-H(24)	120(2)
C(24)-C(25)-C(26)	120.7(3)
C(24)-C(25)-H(25)	119(2)
C(26)-C(25)-H(25)	120(2)
C(22)-C(21)-C(26)	122.2(3)
C(22)-C(21)-S(1)	119.2(2)
C(26)-C(21)-S(1)	118.5(2)
C(23)-C(22)-C(21)	119.1(3)
C(23)-C(22)-H(22)	120(2)
C(21)-C(22)-H(22)	121(2)
C(22)-C(23)-C(24)	119.6(3)
C(22)-C(23)-H(23)	124(2)
C(24)-C(23)-H(23)	116(2)
C(25)-C(26)-C(21)	117.9(3)
C(25)-C(26)-H(26)	120(2)
C(21)-C(26)-H(26)	122(2)
F(1)-C(12)-B(8)	116.8(3)
F(1)-C(12)-B(10)	116.7(3)
B(8)-C(12)-B(10)	116.1(2)
F(1)-C(12)-B(7)	116.8(2)
B(8)-C(12)-B(7)	63.4(2)
B(10)-C(12)-B(7)	116.3(3)
F(1)-C(12)-B(9)	116.5(3)
B(8)-C(12)-B(9)	63.2(2)
B(10)-C(12)-B(9)	63.4(2)
B(7)-C(12)-B(9)	116.3(2)
F(1)-C(12)-B(11)	116.8(2)
B(8)-C(12)-B(11)	116.3(3)
B(10)-C(12)-B(11)	63.5(2)
B(7)-C(12)-B(11)	63.3(2)
B(9)-C(12)-B(11)	116.5(2)
C(1)-B(4)-B(10)	104.0(2)
C(1)-B(4)-B(9)	103.8(2)
B(10)-B(4)-B(9)	61.1(2)
C(1)-B(4)-B(5)	58.5(2)
B(10)-B(4)-B(5)	59.6(2)
B(9)-B(4)-B(5)	108.5(2)
C(1)-B(4)-B(3)	58.1(2)
B(10)-B(4)-B(3)	108.1(2)
B(9)-B(4)-B(3)	59.4(2)
B(5)-B(4)-B(3)	107.7(2)
C(1)-B(4)-H(4)	121(2)
B(10)-B(4)-H(4)	125(2)
B(9)-B(4)-H(4)	126(2)
B(5)-B(4)-H(4)	120(2)
B(3)-B(4)-H(4)	121(2)
C(1)-B(2)-B(7)	103.8(2)
C(1)-B(2)-B(8)	103.4(2)
B(7)-B(2)-B(8)	61.1(2)
C(1)-B(2)-B(6)	58.4(2)
B(7)-B(2)-B(6)	59.6(2)
B(8)-B(2)-B(6)	108.2(3)
C(1)-B(2)-B(3)	58.1(2)
B(7)-B(2)-B(3)	108.2(3)
B(8)-B(2)-B(3)	59.3(2)
B(6)-B(2)-B(3)	107.7(2)
C(1)-B(2)-H(2)	121(2)
B(7)-B(2)-H(2)	129(2)
B(8)-B(2)-H(2)	124(2)
B(6)-B(2)-H(2)	124(2)
B(3)-B(2)-H(2)	116(2)
B(3)-C(1)-B(6)	114.9(2)
B(3)-C(1)-B(5)	115.6(2)
B(6)-C(1)-B(5)	63.1(2)
B(3)-C(1)-B(4)	63.4(2)
B(6)-C(1)-B(4)	115.2(2)
B(5)-C(1)-B(4)	62.9(2)

B(6)-C(1)-B(2)	62.4(2)
B(5)-C(1)-B(2)	115.0(2)
B(4)-C(1)-B(2)	115.2(2)
B(3)-C(1)-S(1)	119.7(2)
B(6)-C(1)-S(1)	114.2(2)
B(5)-C(1)-S(1)	116.6(2)
B(4)-C(1)-S(1)	120.3(2)
B(2)-C(1)-S(1)	116.1(2)
C(12)-B(7)-B(2)	103.8(2)
C(12)-B(7)-B(6)	103.7(2)
B(2)-B(7)-B(6)	61.1(2)
C(12)-B(7)-B(8)	58.2(2)
B(2)-B(7)-B(8)	59.6(2)
B(6)-B(7)-B(8)	108.2(2)
C(12)-B(7)-B(11)	58.6(2)
B(2)-B(7)-B(11)	108.7(2)
B(6)-B(7)-B(11)	59.5(2)
B(8)-B(7)-B(11)	108.1(2)
C(12)-B(7)-H(7)	118(2)
B(2)-B(7)-H(7)	130(2)
B(6)-B(7)-H(7)	127(2)
B(8)-B(7)-H(7)	120(2)
B(11)-B(7)-H(7)	117(2)
C(1)-B(6)-B(7)	104.1(2)
C(1)-B(6)-B(11)	103.9(2)
B(7)-B(6)-B(11)	61.0(2)
C(1)-B(6)-B(2)	59.2(2)
B(7)-B(6)-B(2)	59.3(2)
B(11)-B(6)-B(2)	108.4(3)
C(1)-B(6)-B(5)	58.5(2)
B(7)-B(6)-B(5)	108.1(3)
B(11)-B(6)-B(5)	59.3(2)
B(2)-B(6)-B(5)	108.5(2)
C(1)-B(6)-H(6)	121(2)
B(7)-B(6)-H(6)	126(2)
B(11)-B(6)-H(6)	126(2)
B(2)-B(6)-H(6)	120(2)
B(5)-B(6)-H(6)	120(2)
C(1)-B(3)-B(8)	104.2(2)
C(1)-B(3)-B(9)	103.9(2)
B(8)-B(3)-B(9)	60.7(2)
C(1)-B(3)-B(2)	59.2(2)
B(8)-B(3)-B(2)	59.4(2)
B(9)-B(3)-B(2)	108.1(3)
C(1)-B(3)-B(4)	58.5(2)
B(8)-B(3)-B(4)	107.8(3)
B(9)-B(3)-B(4)	59.2(2)
B(2)-B(3)-B(4)	108.3(2)
C(1)-B(3)-H(3)	123(2)
B(8)-B(3)-H(3)	125(2)
B(9)-B(3)-H(3)	124(2)
B(2)-B(3)-H(3)	121(2)
B(4)-B(3)-H(3)	120(2)
C(1)-B(5)-B(11)	104.0(2)
C(1)-B(5)-B(10)	103.5(2)
B(11)-B(5)-B(10)	61.2(2)
C(1)-B(5)-B(4)	58.5(2)
B(11)-B(5)-B(4)	108.2(3)
B(10)-B(5)-B(4)	59.0(2)
C(1)-B(5)-B(6)	58.5(2)
B(11)-B(5)-B(6)	59.4(2)
B(10)-B(5)-B(6)	108.0(3)
B(4)-B(5)-B(6)	107.8(2)
C(1)-B(5)-H(5)	120(2)
B(11)-B(5)-H(5)	127(2)
B(10)-B(5)-H(5)	127(2)
B(4)-B(5)-H(5)	120(2)

C(12)-B(10)-B(4)	103.9(2)
C(12)-B(10)-B(5)	103.7(2)
B(4)-B(10)-B(5)	61.4(2)
C(12)-B(10)-B(9)	58.4(2)
B(4)-B(10)-B(9)	59.8(2)
B(5)-B(10)-B(9)	108.8(3)
C(12)-B(10)-B(11)	58.6(2)
B(4)-B(10)-B(11)	108.6(3)
B(5)-B(10)-B(11)	59.4(2)
B(9)-B(10)-B(11)	108.3(3)
C(12)-B(10)-H(10)	121(2)
B(4)-B(10)-H(10)	127(2)
B(5)-B(10)-H(10)	124(2)
B(9)-B(10)-H(10)	121(2)
B(11)-B(10)-H(10)	118(2)
C(12)-B(8)-B(3)	103.9(2)
C(12)-B(8)-B(2)	103.7(3)
B(3)-B(8)-B(2)	61.3(2)
C(12)-B(8)-B(9)	58.5(2)
B(3)-B(8)-B(9)	59.9(2)
B(2)-B(8)-B(9)	109.0(3)
C(12)-B(8)-B(7)	58.4(2)
B(3)-B(8)-B(7)	108.3(3)
B(2)-B(8)-B(7)	59.3(2)
B(9)-B(8)-B(7)	108.3(3)
C(12)-B(8)-H(8)	121(2)
B(3)-B(8)-H(8)	126(2)
B(2)-B(8)-H(8)	126(2)
B(9)-B(8)-H(8)	120(2)
B(7)-B(8)-H(8)	120(2)
C(12)-B(9)-B(4)	103.3(2)
C(12)-B(9)-B(3)	103.3(2)
B(4)-B(9)-B(3)	61.3(2)
C(12)-B(9)-B(8)	58.3(2)
B(4)-B(9)-B(8)	108.5(3)
B(3)-B(9)-B(8)	59.4(2)
C(12)-B(9)-B(10)	58.3(2)
B(4)-B(9)-B(10)	59.1(2)
B(3)-B(9)-B(10)	108.0(3)
B(8)-B(9)-B(10)	107.8(3)
C(12)-B(9)-H(9)	120(2)
B(4)-B(9)-H(9)	126(2)
B(3)-B(9)-H(9)	128(2)
B(8)-B(9)-H(9)	121(2)
B(10)-B(9)-H(9)	118(2)
C(12)-B(11)-B(5)	103.4(2)
C(12)-B(11)-B(6)	103.2(2)
B(5)-B(11)-B(6)	61.3(2)
C(12)-B(11)-B(7)	58.1(2)
B(5)-B(11)-B(7)	108.4(3)
B(6)-B(11)-B(7)	59.4(2)
C(12)-B(11)-B(10)	58.0(2)
B(5)-B(11)-B(10)	59.4(2)
B(6)-B(11)-B(10)	108.1(3)
B(7)-B(11)-B(10)	107.5(3)
C(12)-B(11)-H(11)	120(2)
B(5)-B(11)-H(11)	128(2)
B(6)-B(11)-H(11)	127(2)
B(7)-B(11)-H(11)	119(2)
B(10)-B(11)-H(11)	120(2)

Table 4. Anisotropic displacement parameters (A^2 x 10^3)
The anisotropic displacement factor exponent takes the form:
-2 pi^2 [h^2 a*^2 U11 + ... + 2 h k a* b* U12]

	U11	U22	U33	U23	U13	U12
S(1)	34(1)	28(1)	26(1)	1(1)	10(1)	-1(1)
F(1)	34(1)	56(1)	53(1)	5(1)	3(1)	-5(1)
C(24)	31(2)	39(2)	32(2)	5(1)	9(1)	0(1)
C(25)	39(2)	43(2)	24(1)	-3(1)	9(1)	0(1)
C(21)	32(2)	29(2)	24(1)	0(1)	7(1)	0(1)
C(22)	32(2)	33(2)	31(2)	-3(1)	12(1)	-2(1)
C(23)	35(2)	30(2)	35(2)	4(1)	10(1)	0(1)
C(26)	37(2)	29(2)	27(1)	-3(1)	11(1)	0(1)
C(12)	31(2)	39(2)	38(2)	2(1)	4(1)	0(1)
B(4)	35(2)	40(2)	30(2)	6(2)	11(1)	-2(2)
B(2)	45(2)	40(2)	23(2)	-3(1)	7(1)	-3(2)
C(1)	34(2)	27(2)	23(1)	1(1)	9(1)	0(1)
B(7)	45(2)	43(2)	29(2)	3(2)	3(2)	-3(2)
B(6)	43(2)	31(2)	32(2)	5(1)	7(2)	0(2)
B(3)	37(2)	24(2)	39(2)	1(1)	9(2)	0(2)
B(5)	38(2)	36(2)	31(2)	-4(2)	11(1)	5(2)
B(10)	41(2)	44(2)	38(2)	-1(2)	15(2)	3(2)
B(8)	45(2)	37(2)	34(2)	-6(2)	8(2)	-3(2)
B(9)	35(2)	35(2)	41(2)	7(2)	9(2)	0(2)
O(1)	43(1)	26(1)	37(1)	-1(1)	8(1)	-3(1)
O(2)	38(1)	42(1)	30(1)	2(1)	19(1)	2(1)
B(11)	37(2)	34(2)	46(2)	1(2)	8(2)	6(2)

Table 5. Hydrogen coordinates (x 10^4) and isotropic displacement parameters (A^2 x 10^3)

	x	y	z	U(eq)
H(24)	2621(9)	5503(50)	5612(27)	40
H(25)	2861(9)	2268(54)	5500(29)	42
H(22)	3011(9)	5095(50)	9036(29)	37
H(23)	2724(9)	7114(52)	7406(26)	40
H(26)	3151(9)	355(52)	7050(26)	37
H(4)	3830(9)	3304(48)	8033(28)	41
H(2)	3713(9)	2977(51)	11740(27)	43
H(7)	4522(9)	1590(50)	12421(30)	47
H(6)	3918(9)	-972(53)	11055(28)	43
H(3)	3681(9)	5499(51)	9892(27)	40
H(5)	3978(9)	-735(53)	8783(28)	41
H(10)	4611(9)	2008(52)	8788(29)	48
H(8)	4353(9)	5585(55)	11707(29)	47
H(9)	4425(9)	5899(53)	9441(28)	44
H(11)	4670(9)	-587(54)	10650(29)	47

Crystal data for 1-(3'-pyridyl)-*ortho*-carborane

Empirical Formula	$C_7H_{15}B_{10}N$	
Temperature	150(2) K	
Wavelength	0.71073 Å	
Crystal System		
Space Group	P-1	
Unit Cell Dimensions	a = 7.23850(10) Å	α = 100.0530(10)°
	b = 7.69990(10) Å	β = 92.3030(10)°
	c = 11.1977(2) Å	γ = 90.5720(10)°
Final R indices [I>2σ(I)]	R1 = 0.0454	wR2 = 0.1190
R indices (all data)	R1 = 0.0583	wR2 = 0.1315

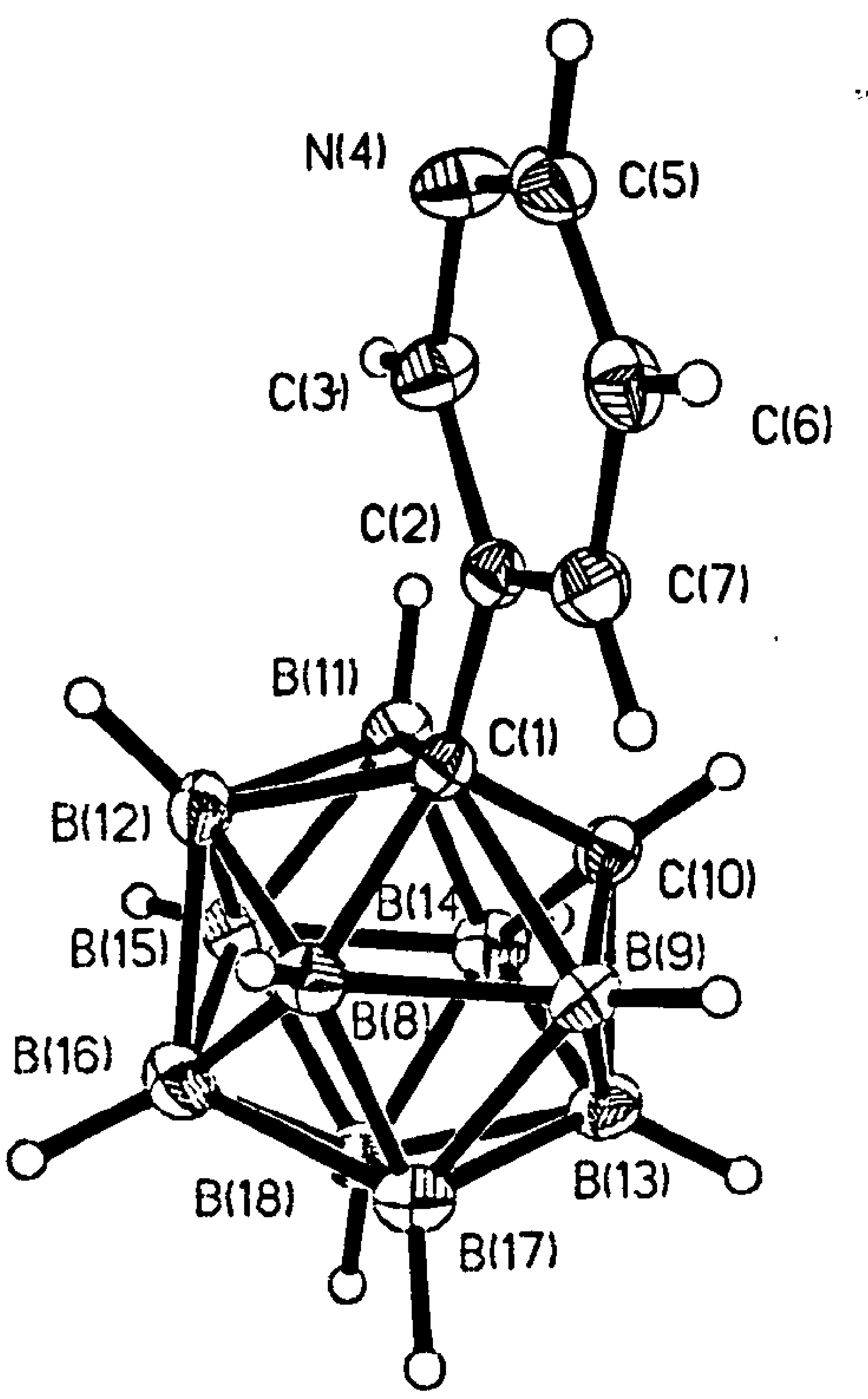

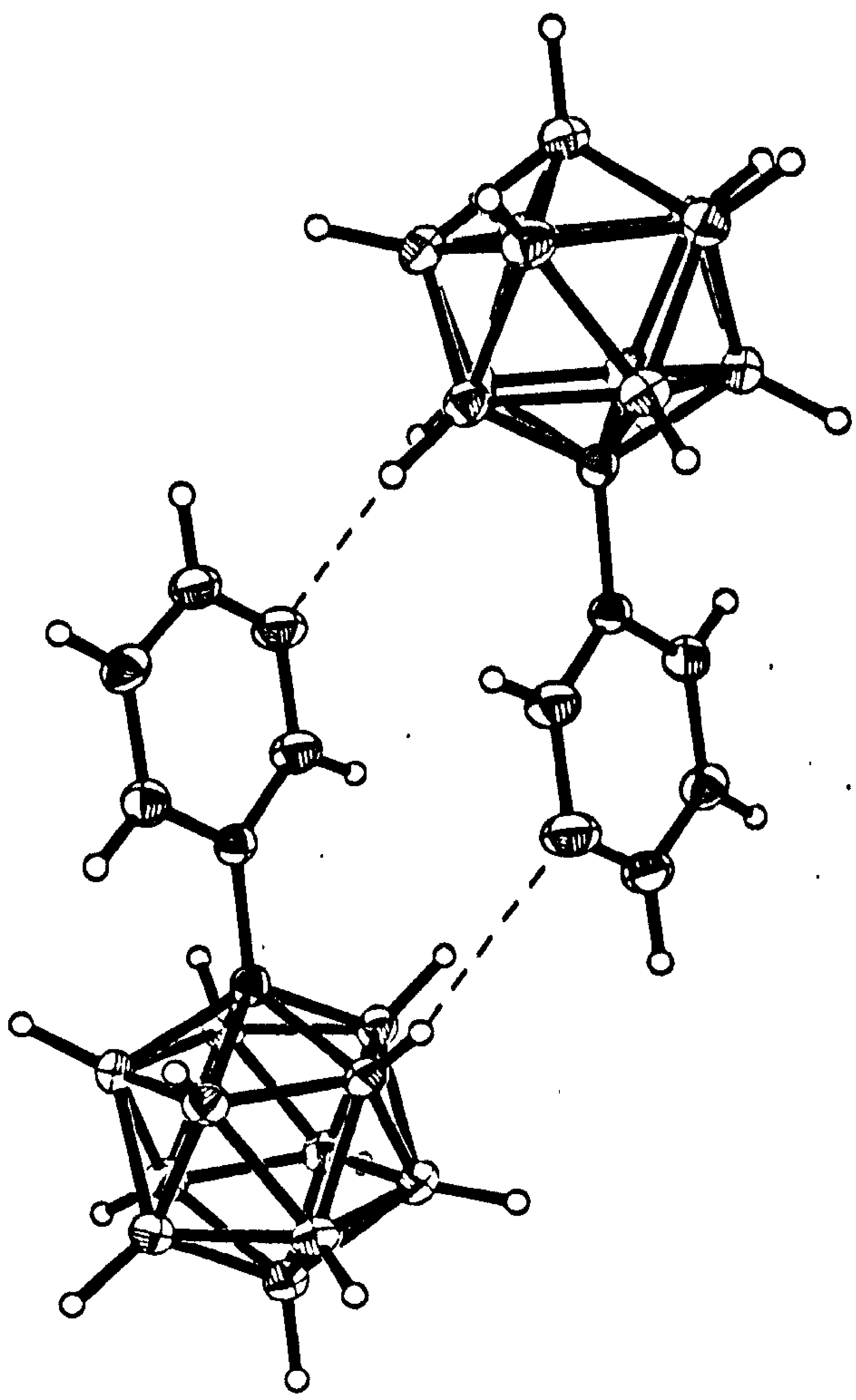

Table 2. Atomic coordinates (x 10^4) and equivalent isotropic displacement parameters (A^2 x 10^3). U(eq) is defined as one third of the trace of the orthogonalized Uij tensor.

	x	y	z	U(eq)
C(2)	4708(2)	4341(2)	1908(1)	19(1)
C(1)	6147(2)	3169(1)	2357(1)	18(1)
C(10)	8341(2)	3286(2)	1985(1)	21(1)
N(4)	2262(2)	4693(2)	442(1)	31(1)
C(7)	4273(2)	5947(2)	2604(1)	24(1)
C(3)	3656(2)	3773(2)	837(1)	26(1)
C(6)	2826(2)	6911(2)	2210(1)	26(1)
C(5)	1864(2)	6233(2)	1137(1)	27(1)
B(8)	6054(2)	2728(2)	3806(1)	22(1)
B(16)	7037(2)	608(2)	3739(1)	25(1)
B(17)	8396(2)	2555(2)	4309(1)	24(1)
B(14)	9380(2)	1287(2)	1839(1)	24(1)
B(12)	5588(2)	1053(2)	2504(1)	22(1)
B(13)	9842(2)	2964(2)	3135(1)	24(1)
B(15)	7642(2)	-171(2)	2202(1)	25(1)
B(9)	7796(2)	4184(2)	3440(1)	21(1)
B(11)	7035(2)	1462(2)	1335(1)	22(1)
B(18)	9379(2)	758(2)	3326(1)	25(1)

Table 4. Bond lengths [A] and angles [deg]

C(2)-C(7)	1.388(2)
C(2)-C(3)	1.395(2)
C(2)-C(1)	1.512(2)
C(1)-C(10)	1.664(2)
C(1)-B(12)	1.711(2)
C(1)-B(8)	1.718(2)
C(1)-B(11)	1.733(2)
C(1)-B(9)	1.744(2)
C(10)-B(13)	1.704(2)
C(10)-B(14)	1.704(2)
C(10)-B(9)	1.718(2)
C(10)-B(11)	1.719(2)
N(4)-C(5)	1.340(2)
N(4)-C(3)	1.343(2)
C(7)-C(6)	1.391(2)
C(6)-C(5)	1.381(2)
B(8)-B(16)	1.778(2)
B(8)-B(17)	1.779(2)
B(8)-B(9)	1.786(2)
B(8)-B(12)	1.788(2)
B(16)-B(18)	1.783(2)
B(16)-B(12)	1.785(2)
B(16)-B(17)	1.791(2)
B(16)-B(15)	1.794(2)
B(17)-B(9)	1.765(2)
B(17)-B(13)	1.781(2)
B(17)-B(18)	1.784(2)
B(14)-B(11)	1.781(2)
B(14)-B(18)	1.782(2)
B(14)-B(15)	1.783(2)
B(14)-B(13)	1.784(2)
B(12)-B(11)	1.777(2)
B(12)-B(15)	1.781(2)
B(13)-B(9)	1.774(2)
B(13)-B(18)	1.779(2)
B(15)-B(11)	1.767(2)
B(15)-B(18)	1.794(2)
C(7)-C(2)-C(3)	117.72(11)
C(7)-C(2)-C(1)	120.95(10)
C(3)-C(2)-C(1)	121.07(11)
C(2)-C(1)-C(10)	120.80(9)
C(2)-C(1)-B(12)	120.55(9)
C(10)-C(1)-B(12)	109.90(9)
C(2)-C(1)-B(8)	119.36(9)
C(10)-C(1)-B(8)	109.68(9)
B(12)-C(1)-B(8)	62.84(7)
C(2)-C(1)-B(11)	118.98(9)
C(10)-C(1)-B(11)	60.79(7)
B(12)-C(1)-B(11)	62.12(7)
B(8)-C(1)-B(11)	113.64(9)
C(2)-C(1)-B(9)	117.02(9)
C(10)-C(1)-B(9)	60.49(7)
B(12)-C(1)-B(9)	113.70(9)
B(8)-C(1)-B(9)	62.11(7)
B(11)-C(1)-B(9)	112.95(9)
C(1)-C(10)-B(13)	112.12(9)
C(1)-C(10)-B(14)	111.98(9)
B(13)-C(10)-B(14)	63.10(8)
C(1)-C(10)-B(9)	62.07(7)
B(13)-C(10)-B(9)	62.45(8)
B(14)-C(10)-B(9)	114.88(9)
C(1)-C(10)-B(11)	61.59(7)
B(13)-C(10)-B(11)	115.01(9)
B(14)-C(10)-B(11)	62.69(8)
B(9)-C(10)-B(11)	114.96(9)

C(2)-C(7)-C(6)	119.15(11)
N(4)-C(3)-C(2)	123.79(12)
C(5)-C(6)-C(7)	118.72(12)
N(4)-C(5)-C(6)	123.44(11)
C(1)-B(8)-B(16)	105.13(9)
C(1)-B(8)-B(17)	105.44(9)
B(16)-B(8)-B(17)	60.47(8)
C(1)-B(8)-B(9)	59.65(7)
B(16)-B(8)-B(9)	107.89(9)
B(17)-B(8)-B(9)	59.34(8)
C(1)-B(8)-B(12)	58.40(7)
B(16)-B(8)-B(12)	60.07(8)
B(17)-B(8)-B(12)	108.32(9)
B(9)-B(8)-B(12)	108.09(9)
B(8)-B(16)-B(18)	107.76(10)
B(8)-B(16)-B(12)	60.23(7)
B(18)-B(16)-B(12)	107.81(9)
B(8)-B(16)-B(17)	59.77(8)
B(18)-B(16)-B(17)	59.89(8)
B(12)-B(16)-B(17)	107.90(9)
B(8)-B(16)-B(15)	107.96(9)
B(18)-B(16)-B(15)	60.19(8)
B(12)-B(16)-B(15)	59.68(8)
B(17)-B(16)-B(15)	108.02(10)
B(9)-B(17)-B(8)	60.54(8)
B(9)-B(17)-B(13)	60.04(8)
B(8)-B(17)-B(13)	108.24(9)
B(9)-B(17)-B(18)	107.99(10)
B(8)-B(17)-B(18)	107.69(10)
B(13)-B(17)-B(18)	59.86(8)
B(9)-B(17)-B(16)	108.27(9)
B(8)-B(17)-B(16)	59.76(8)
B(13)-B(17)-B(16)	107.85(10)
B(18)-B(17)-B(16)	59.83(8)
C(10)-B(14)-B(11)	59.06(7)
C(10)-B(14)-B(18)	104.17(9)
B(11)-B(14)-B(18)	107.74(9)
C(10)-B(14)-B(15)	104.51(9)
B(11)-B(14)-B(15)	59.42(8)
B(18)-B(14)-B(15)	60.41(8)
C(10)-B(14)-B(13)	58.44(7)
B(11)-B(14)-B(13)	108.21(9)
B(18)-B(14)-B(13)	59.86(8)
B(15)-B(14)-B(13)	108.34(10)
C(1)-B(12)-B(11)	59.52(7)
C(1)-B(12)-B(15)	105.52(9)
B(11)-B(12)-B(15)	59.54(8)
C(1)-B(12)-B(16)	105.13(9)
B(11)-B(12)-B(16)	107.95(9)
B(15)-B(12)-B(16)	60.42(8)
C(1)-B(12)-B(8)	58.76(7)
B(11)-B(12)-B(8)	108.22(9)
B(15)-B(12)-B(8)	108.13(9)
B(16)-B(12)-B(8)	59.71(8)
C(10)-B(13)-B(9)	59.14(7)
C(10)-B(13)-B(18)	104.30(10)
B(9)-B(13)-B(18)	107.80(10)
C(10)-B(13)-B(17)	104.48(9)
B(9)-B(13)-B(17)	59.51(8)
B(18)-B(13)-B(17)	60.15(8)
C(10)-B(13)-B(14)	58.45(7)
B(9)-B(13)-B(14)	108.33(9)
B(18)-B(13)-B(14)	60.02(8)
B(17)-B(13)-B(14)	108.19(10)
B(11)-B(15)-B(12)	60.12(8)
B(11)-B(15)-B(14)	60.22(8)
B(12)-B(15)-B(14)	108.05(9)
B(11)-B(15)-B(18)	107.85(10)
B(12)-B(15)-B(18)	107.51(10)

B(11)-B(15)-B(16)	107.99(10)
B(12)-B(15)-B(16)	59.90(8)
B(14)-B(15)-B(16)	107.61(10)
B(18)-B(15)-B(16)	59.60(8)
C(10)-B(9)-C(1)	57.45(7)
C(10)-B(9)-B(17)	104.64(9)
C(1)-B(9)-B(17)	104.96(9)
C(10)-B(9)-B(13)	58.41(7)
C(1)-B(9)-B(13)	105.18(9)
B(17)-B(9)-B(13)	60.45(8)
C(10)-B(9)-B(8)	104.20(9)
C(1)-B(9)-B(8)	58.24(7)
B(17)-B(9)-B(8)	60.12(8)
B(13)-B(9)-B(8)	108.24(9)
C(10)-B(11)-C(1)	57.62(7)
C(10)-B(11)-B(15)	104.61(9)
C(1)-B(11)-B(15)	105.23(9)
C(10)-B(11)-B(12)	104.42(9)
C(1)-B(11)-B(12)	58.36(7)
B(15)-B(11)-B(12)	60.34(8)
C(10)-B(11)-B(14)	58.25(7)
C(1)-B(11)-B(14)	105.24(9)
B(15)-B(11)-B(14)	60.36(8)
B(12)-B(11)-B(14)	108.33(9)
B(13)-B(18)-B(14)	60.13(8)
B(13)-B(18)-B(16)	108.32(10)
B(14)-B(18)-B(16)	108.17(9)
B(13)-B(18)-B(17)	59.99(8)
B(14)-B(18)-B(17)	108.15(10)
B(16)-B(18)-B(17)	60.28(8)
B(13)-B(18)-B(15)	108.09(10)
B(14)-B(18)-B(15)	59.84(8)
B(16)-B(18)-B(15)	60.21(8)
B(17)-B(18)-B(15)	108.35(10)

Crystal data for 2,4,6-tri-(2'-phenyl-*ortho*-carboranyl)-1,3,5-triazine

Empirical Formula	$C_{27}H_{45}B_{30}N_3$	
Temperature	150(2) K	
Wavelength	0.71073 Å	
Crystal System	trigonal	
Space Group	R-3	
Unit Cell Dimensions	a = 19.8157(14) Å	α = 90°
	b = 19.8157(10) Å	β = 90°
	c = 18.1595(14) Å	γ = 120°
Crystal Size	0.4 x 0.35 x 0.35 mm	
Final R indices [I>2σ(I)]	R1 = 0.0433	wR2 = 0.1053
R indices (all data)	R1 = 0.0618	wR2 = 0.1411

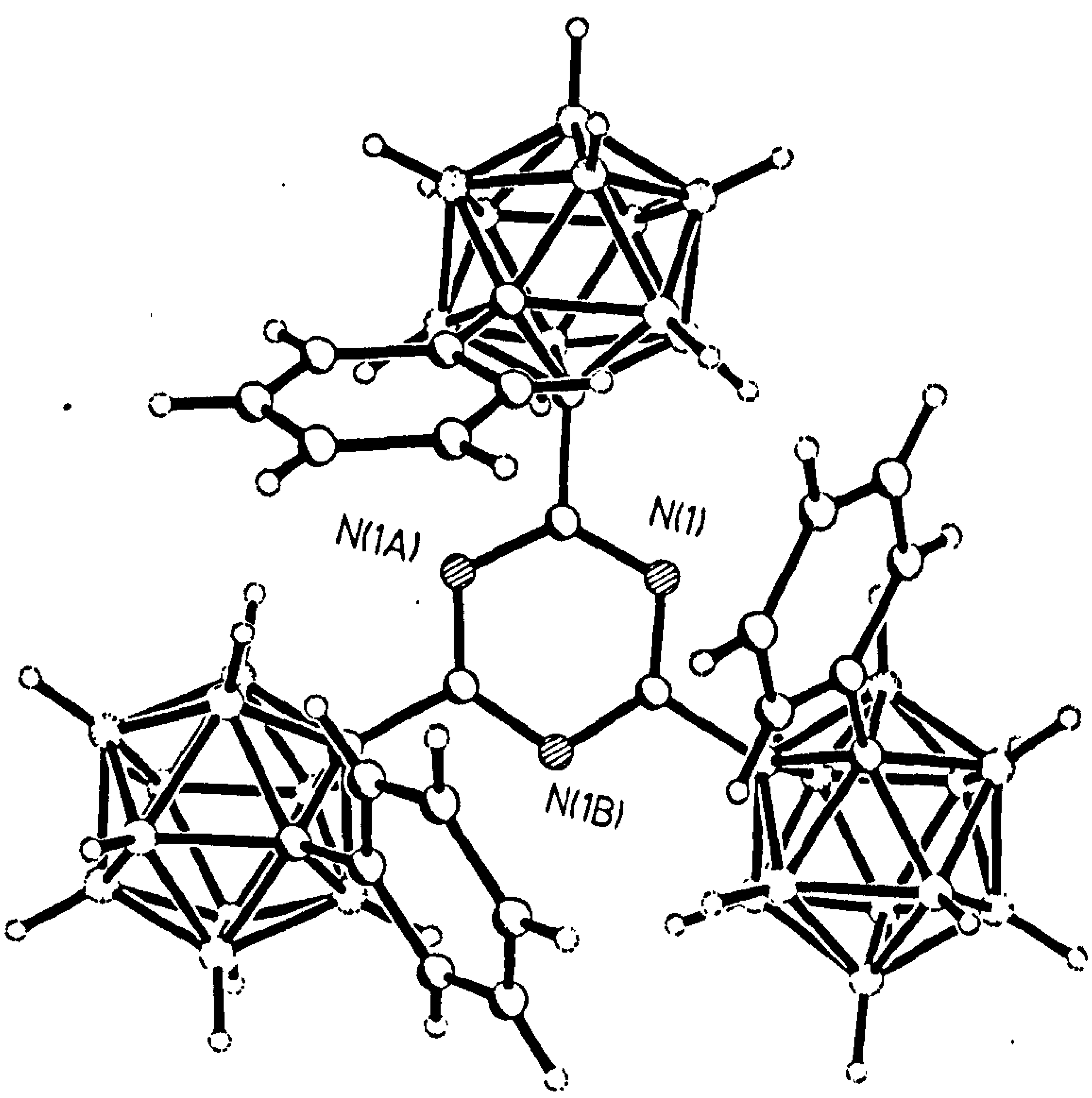

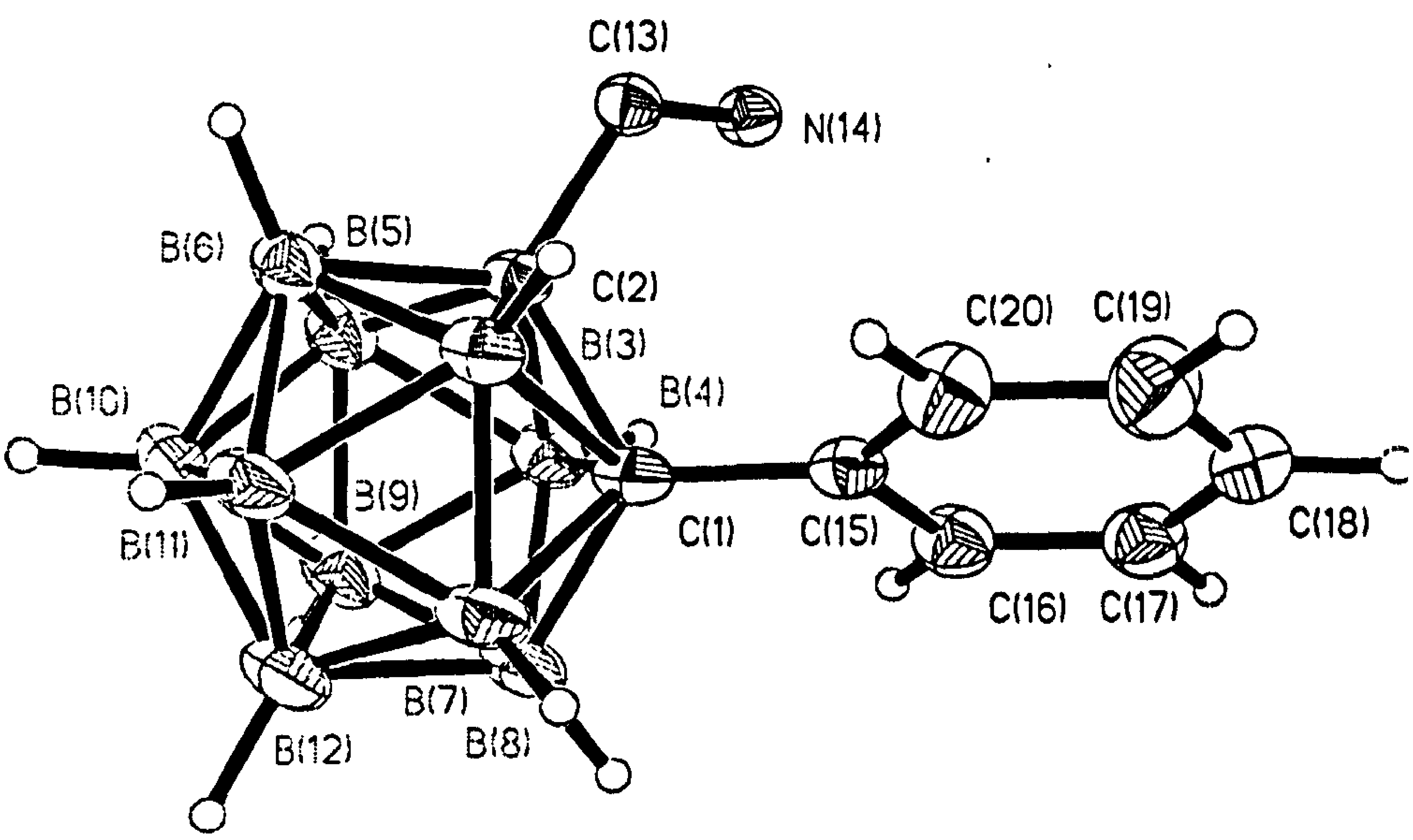

Table 2. Atomic coordinates (x 10^4) and equivalent isotropic displacement parameters (A^2 x 10^3). U(eq) is defined as one third of the trace of the orthogonalized Uij tensor.

	x	y	z	U(eq)
N(14)	108(1)	742(1)	3394(1)	23(1)
C(2)	-1298(1)	210(1)	3463(1)	22(1)
C(13)	-597(1)	104(1)	3399(1)	21(1)
C(15)	-935(1)	977(1)	2129(1)	26(1)
C(1)	-1479(1)	677(1)	2783(1)	25(1)
C(16)	-388(1)	1770(1)	2072(1)	32(1)
B(6)	-2142(1)	-511(1)	3855(1)	27(1)
C(17)	105(1)	2055(1)	1466(1)	37(1)
B(4)	-1119(1)	1150(1)	3627(1)	27(1)
B(11)	-2903(1)	-461(1)	3380(1)	33(1)
C(20)	-980(1)	480(1)	1561(1)	37(1)
B(5)	-1546(1)	401(1)	4309(1)	29(1)
B(3)	-2075(1)	-337(1)	2889(1)	26(1)
B(7)	-2469(1)	282(1)	2690(1)	32(1)
B(10)	-2577(1)	-6(1)	4263(1)	35(1)
C(18)	63(1)	1559(1)	908(1)	37(1)
B(8)	-1884(1)	1193(1)	3149(1)	32(1)
B(9)	-1945(1)	1018(1)	4119(1)	36(1)
C(19)	-481(1)	771(1)	959(1)	43(1)
B(12)	-2785(1)	481(1)	3546(1)	38(1)

Table 4. Bond lengths [A] and angles [deg]

N(14)-C(13)	1.336(2)
N(14)-C(13)#1	1.340(2)
C(2)-C(13)	1.510(2)
C(2)-C(1)	1.686(2)
C(2)-B(5)	1.712(2)
C(2)-B(6)	1.719(2)
C(2)-B(3)	1.723(2)
C(2)-B(4)	1.739(2)
C(13)-N(14)#2	1.340(2)
C(15)-C(16)	1.397(2)
C(15)-C(20)	1.397(2)
C(15)-C(1)	1.511(2)
C(1)-B(8)	1.718(2)
C(1)-B(7)	1.720(2)
C(1)-B(4)	1.752(2)
C(1)-B(3)	1.758(2)
C(16)-C(17)	1.390(2)
B(6)-B(10)	1.776(2)
B(6)-B(3)	1.780(2)
B(6)-B(11)	1.783(2)
B(6)-B(5)	1.791(2)
C(17)-C(18)	1.384(2)
B(4)-B(9)	1.766(2)
B(4)-B(8)	1.785(2)
B(4)-B(5)	1.788(2)
B(11)-B(3)	1.773(2)
B(11)-B(12)	1.785(2)
B(11)-B(7)	1.792(3)
B(11)-B(10)	1.793(3)
C(20)-C(19)	1.392(2)
B(5)-B(10)	1.783(2)
B(5)-B(9)	1.790(2)
B(3)-B(7)	1.789(2)
B(7)-B(8)	1.789(2)
B(7)-B(12)	1.791(3)
B(10)-B(12)	1.787(3)
B(10)-B(9)	1.792(2)
C(18)-C(19)	1.387(2)
B(8)-B(12)	1.783(2)
B(8)-B(9)	1.789(3)
B(9)-B(12)	1.792(3)
C(13)-N(14)-C(13)#1	114.15(12)
C(13)-C(2)-C(1)	118.90(11)
C(13)-C(2)-B(5)	119.11(11)
C(1)-C(2)-B(5)	111.86(10)
C(13)-C(2)-B(6)	119.76(11)
C(1)-C(2)-B(6)	111.92(10)
B(5)-C(2)-B(6)	62.93(9)
C(13)-C(2)-B(3)	117.49(10)
C(1)-C(2)-B(3)	62.11(8)
B(5)-C(2)-B(3)	114.60(10)
B(6)-C(2)-B(3)	62.27(9)
C(13)-C(2)-B(4)	117.01(10)
C(1)-C(2)-B(4)	61.52(8)
B(5)-C(2)-B(4)	62.39(9)
B(6)-C(2)-B(4)	114.32(10)
B(3)-C(2)-B(4)	114.60(10)
N(14)-C(13)-N(14)#2	125.84(12)
N(14)-C(13)-C(2)	117.87(11)
N(14)#2-C(13)-C(2)	116.18(11)
C(16)-C(15)-C(20)	118.58(14)
C(16)-C(15)-C(1)	120.09(13)
C(20)-C(15)-C(1)	121.31(13)
C(15)-C(1)-C(2)	119.13(10)
C(15)-C(1)-B(8)	121.47(11)

C(15)-C(1)-B(7)	121.94(12)
C(2)-C(1)-B(7)	109.28(11)
B(8)-C(1)-B(7)	62.73(9)
C(15)-C(1)-B(4)	117.21(11)
C(2)-C(1)-B(4)	60.74(8)
B(8)-C(1)-B(4)	61.90(9)
B(7)-C(1)-B(4)	113.29(11)
C(15)-C(1)-B(3)	118.43(11)
C(2)-C(1)-B(3)	59.97(8)
B(8)-C(1)-B(3)	112.95(11)
B(7)-C(1)-B(3)	61.89(9)
B(4)-C(1)-B(3)	112.14(11)
C(17)-C(16)-C(15)	120.52(14)
C(2)-B(6)-B(10)	104.41(11)
C(2)-B(6)-B(3)	58.96(8)
B(10)-B(6)-B(3)	108.17(12)
C(2)-B(6)-B(11)	104.64(11)
B(10)-B(6)-B(11)	60.51(10)
B(3)-B(6)-B(11)	59.71(9)
C(2)-B(6)-B(5)	58.35(8)
B(10)-B(6)-B(5)	59.97(9)
B(3)-B(6)-B(5)	108.10(11)
B(11)-B(6)-B(5)	108.35(11)
C(18)-C(17)-C(16)	120.7(2)
C(2)-B(4)-C(1)	57.74(8)
C(2)-B(4)-B(9)	104.52(11)
C(1)-B(4)-B(9)	105.35(11)
C(2)-B(4)-B(8)	104.16(10)
C(1)-B(4)-B(8)	58.12(9)
B(9)-B(4)-B(8)	60.48(10)
C(2)-B(4)-B(5)	58.07(8)
C(1)-B(4)-B(5)	105.33(10)
B(9)-B(4)-B(5)	60.48(10)
B(8)-B(4)-B(5)	108.39(11)
B(3)-B(11)-B(6)	60.06(9)
B(3)-B(11)-B(12)	108.12(11)
B(6)-B(11)-B(12)	107.72(12)
B(3)-B(11)-B(7)	60.23(9)
B(6)-B(11)-B(7)	108.19(11)
B(12)-B(11)-B(7)	60.09(10)
B(3)-B(11)-B(10)	107.70(11)
B(6)-B(11)-B(10)	59.57(9)
B(12)-B(11)-B(10)	59.93(11)
B(7)-B(11)-B(10)	107.97(12)
C(19)-C(20)-C(15)	120.4(2)
C(2)-B(5)-B(10)	104.42(11)
C(2)-B(5)-B(4)	59.54(8)
B(10)-B(5)-B(4)	107.65(12)
C(2)-B(5)-B(9)	104.63(12)
B(10)-B(5)-B(9)	60.22(10)
B(4)-B(5)-B(9)	59.16(9)
C(2)-B(5)-B(6)	58.72(8)
B(10)-B(5)-B(6)	59.61(9)
B(4)-B(5)-B(6)	108.56(11)
B(9)-B(5)-B(6)	107.90(12)
C(2)-B(3)-C(1)	57.92(7)
C(2)-B(3)-B(11)	104.89(11)
C(1)-B(3)-B(11)	105.08(10)
C(2)-B(3)-B(6)	58.77(8)
C(1)-B(3)-B(6)	105.77(10)
B(11)-B(3)-B(6)	60.23(10)
C(2)-B(3)-B(7)	104.52(10)
C(1)-B(3)-B(7)	57.98(8)
B(11)-B(3)-B(7)	60.40(9)
B(6)-B(3)-B(7)	108.46(12)
C(1)-B(7)-B(3)	60.12(8)
C(1)-B(7)-B(8)	58.60(8)
B(3)-B(7)-B(8)	108.20(11)
C(1)-B(7)-B(12)	105.03(12)

B(8)-B(7)-B(12)	59.73(10)
C(1)-B(7)-B(11)	105.94(11)
B(3)-B(7)-B(11)	59.37(9)
B(8)-B(7)-B(11)	107.78(13)
B(12)-B(7)-B(11)	59.76(10)
B(6)-B(10)-B(5)	60.42(9)
B(6)-B(10)-B(12)	107.90(13)
B(5)-B(10)-B(12)	108.10(12)
B(6)-B(10)-B(9)	108.44(11)
B(5)-B(10)-B(9)	60.09(10)
B(12)-B(10)-B(9)	60.10(10)
B(6)-B(10)-B(11)	59.92(9)
B(5)-B(10)-B(11)	108.24(12)
B(12)-B(10)-B(11)	59.80(10)
B(9)-B(10)-B(11)	108.09(13)
C(17)-C(18)-C(19)	119.2(2)
C(1)-B(8)-B(12)	105.43(11)
C(1)-B(8)-B(4)	59.98(8)
B(12)-B(8)-B(4)	107.65(13)
C(1)-B(8)-B(9)	105.81(11)
B(12)-B(8)-B(9)	60.25(11)
B(4)-B(8)-B(9)	59.23(10)
C(1)-B(8)-B(7)	58.66(8)
B(12)-B(8)-B(7)	60.17(10)
B(4)-B(8)-B(7)	108.44(11)
B(9)-B(8)-B(7)	108.44(12)
B(4)-B(9)-B(8)	60.29(10)
B(4)-B(9)-B(5)	60.36(9)
B(8)-B(9)-B(5)	108.14(11)
B(4)-B(9)-B(12)	108.07(13)
B(8)-B(9)-B(12)	59.72(11)
B(5)-B(9)-B(12)	107.55(12)
B(4)-B(9)-B(10)	108.18(11)
B(8)-B(9)-B(10)	107.71(13)
B(5)-B(9)-B(10)	59.69(10)
B(12)-B(9)-B(10)	59.80(11)
C(18)-C(19)-C(20)	120.6(2)
B(8)-B(12)-B(11)	108.39(12)
B(8)-B(12)-B(10)	108.20(12)
B(11)-B(12)-B(10)	60.27(10)
B(8)-B(12)-B(7)	60.10(10)
B(11)-B(12)-B(7)	60.15(10)
B(10)-B(12)-B(7)	108.29(12)
B(8)-B(12)-B(9)	60.03(10)
B(11)-B(12)-B(9)	108.47(12)
B(10)-B(12)-B(9)	60.10(11)
B(7)-B(12)-B(9)	108.21(11)

Symmetry transformations used to generate equivalent atoms:
#1 -x+y,-x,z   #2 -y,x-y,z

Crystal data for 2,4,6-tri-(12'-phenyl-*para*-carboranyl)-1,3,5-triazine

Empirical Formula	$C_{25}H_{45}B_{30}N_3$	
Temperature	293(2) K	
Wavelength	0.71073 Å	
Crystal System		
Space Group	P-1	
Unit Cell Dimensions	a = 7.2452(3) Å	α = 78.063(2)°
	b = 15.9567(6) Å	β = 80.499(2)°
	c = 20.9322(8) Å	γ = 81.549(2)°
Final R indices [I>2σ(I)]	R1 = 0.2201	wR2 = 0.3616
R indices (all data)	r1 = 0.4027	wR2 = 0.5224

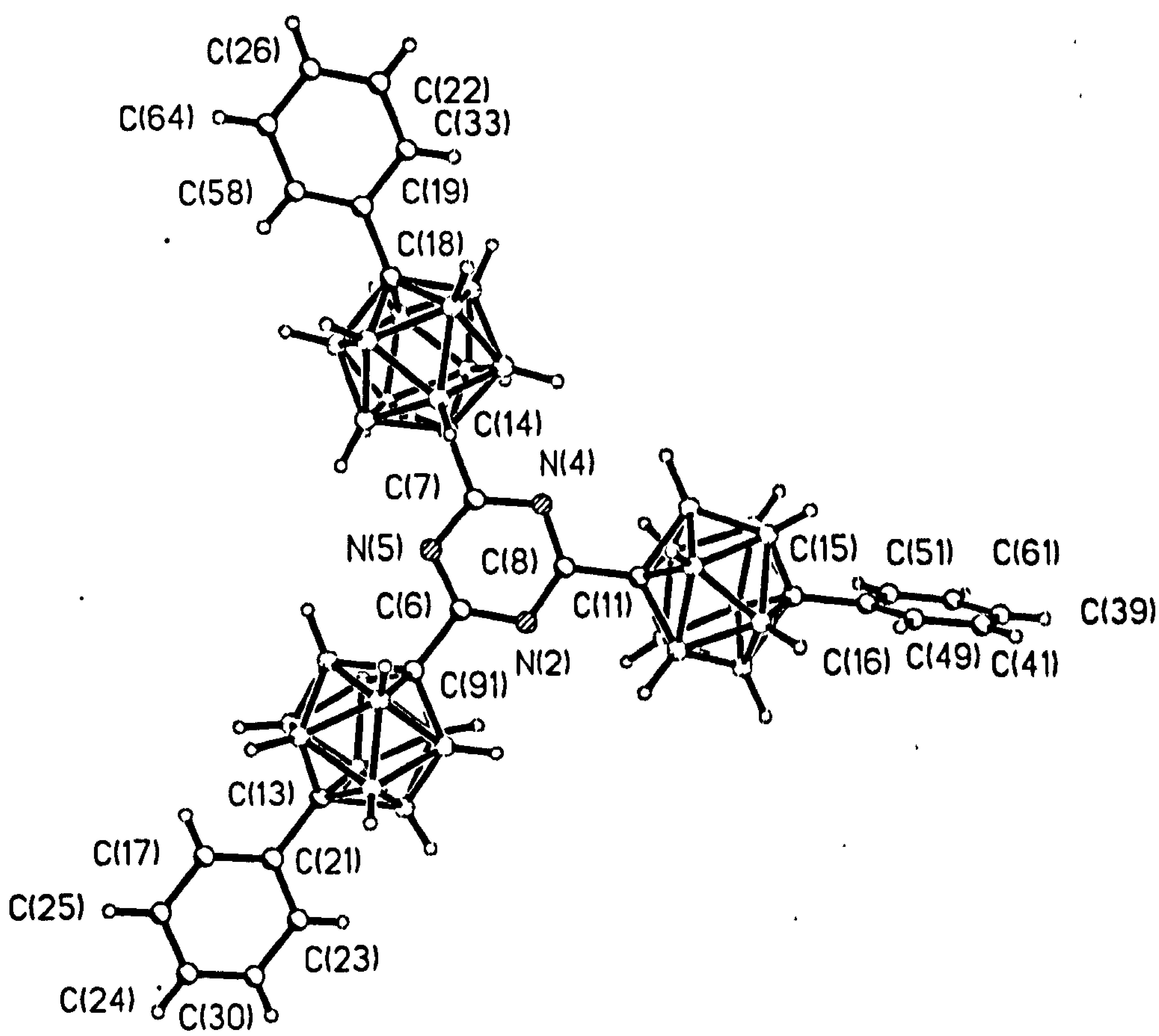

displacement parameters (A^2 x 10^3). U(eq) is defined as one third of the trace of the orthogonalized Uij tensor.

	x	y	z	U(eq)
N(2)	16269(9)	9327(4)	3142(3)	33(2)
N(4)	14816(9)	9638(4)	2164(3)	31(2)
N(5)	14979(10)	8221(4)	2817(3)	34(2)
C(6)	15857(11)	8528(5)	3212(4)	29(2)
C(7)	14474(11)	8811(5)	2306(4)	28(2)
C(8)	15721(12)	9854(5)	2604(4)	30(2)
C(9)	16372(12)	7898(5)	3821(4)	30(2)
C(11)	16083(11)	10784(5)	2498(4)	29(2)
C(13)	17452(12)	6649(5)	5100(4)	32(2)
C(14)	13401(12)	8557(5)	1832(4)	27(2)
C(15)	16767(12)	12720(5)	2268(4)	32(2)
C(16)	17116(12)	13660(5)	2144(4)	31(2)
C(17)	17323(12)	5222(5)	5911(4)	37(2)
C(18)	11153(12)	8004(5)	866(4)	34(2)
C(19)	10049(12)	7736(5)	409(4)	32(2)
C(21)	17942(12)	6028(5)	5723(4)	34(2)
C(22)	8207(14)	8092(6)	-496(4)	50(3)
C(23)	19173(12)	6241(6)	6102(4)	42(2)
C(24)	18995(13)	4877(6)	6841(4)	43(2)
C(25)	17828(14)	4658(6)	6460(4)	46(3)
C(26)	7962(13)	7257(6)	-451(4)	40(2)
B(27)	14723(15)	12477(7)	2065(5)	36(3)
B(28)	14156(15)	11537(6)	2627(5)	36(2)
B(29)	17767(14)	11145(6)	1857(5)	29(2)
C(30)	19699(15)	5663(6)	6657(5)	55(3)
B(31)	18678(16)	11957(6)	2139(5)	34(2)
B(32)	17537(15)	12017(6)	2951(5)	33(2)
C(33)	9239(13)	8346(6)	-83(4)	46(2)
B(34)	15043(16)	12338(6)	2902(5)	36(2)
B(35)	17590(14)	6227(7)	4395(5)	35(2)
B(36)	15331(16)	11479(6)	1816(5)	39(3)
B(37)	16945(15)	12238(6)	1591(5)	33(2)
B(38)	19234(15)	6941(7)	4477(5)	39(3)
C(39)	17708(14)	15393(7)	1886(5)	49(3)
B(40)	15812(16)	6854(6)	3975(5)	38(3)
C(41)	16190(15)	15120(6)	2304(5)	54(3)
B(42)	18187(15)	7085(6)	3741(5)	38(3)
B(43)	15365(15)	6571(6)	4824(5)	34(2)
B(44)	18429(15)	7985(6)	4096(5)	33(2)
B(45)	18118(15)	11004(6)	2707(5)	33(2)
B(46)	15872(15)	11252(7)	3187(5)	37(2)
B(47)	16214(16)	8321(7)	4531(5)	39(3)
B(48)	12196(17)	8927(8)	618(5)	48(3)
C(49)	15867(15)	14253(6)	2440(5)	54(3)
B(50)	17987(15)	7674(7)	4968(5)	38(3)
C(51)	18660(15)	13947(6)	1723(5)	54(3)
B(52)	14599(16)	7628(7)	4441(5)	40(3)
B(53)	15589(16)	7471(7)	5173(5)	41(3)
B(54)	12138(16)	9338(7)	1341(6)	43(3)
B(55)	11004(17)	8636(9)	2012(6)	51(3)
B(56)	13550(16)	7910(10)	710(6)	59(4)
B(57)	10196(17)	8856(8)	1240(6)	47(3)
C(58)	9792(20)	6902(7)	438(5)	89(5)
B(59)	10332(19)	7802(9)	1704(5)	54(4)
B(60)	12397(23)	7223(8)	1375(7)	72(5)
C(61)	18939(16)	14805(6)	1604(6)	67(3)
B(62)	14201(18)	8761(9)	1018(5)	54(4)
B(63)	14362(21)	7680(8)	1471(7)	65(5)
C(64)	8744(21)	6658(7)	16(6)	98(5)
B(66)	12338(20)	7627(9)	2088(6)	61(4)

C(5X)	8256(13)	9813(6)	5893(5)	28(2)
C(6X)	23865(8)	14695(3)	869(3)	2(1)
C(7X)	8289(73)	9839(32)	5793(25)	343(23)
C(3XB)	11955(16)	9612(8)	5072(6)	57(3)
C(41X)	25487(47)	14990(23)	361(15)	152(12)
C(42X)	26929(37)	14295(17)	104(13)	79(9)
C(43X)	25702(11)	14393(5)	497(4)	23(2)
C(44X)	27393(13)	14408(6)	-26(4)	16(2)
C(47X)	9845(30)	10307(13)	5212(10)	80(6)
C(46X)	11189(18)	9513(9)	5516(6)	51(3)
C(45X)	11022(190)	3019(82)	6705(62)	511(75)

Table 4. Bond lengths [A] and angles [deg]

N(2)-C(6)	1.324(10)
N(2)-C(8)	1.337(9)
N(4)-C(8)	1.341(9)
N(4)-C(7)	1.341(9)
N(5)-C(6)	1.327(10)
N(5)-C(7)	1.333(9)
C(6)-C(9)	1.515(10)
C(7)-C(14)	1.507(11)
C(8)-C(11)	1.510(10)
C(9)-B(52)	1.703(13)
C(9)-B(44)	1.717(13)
C(9)-B(42)	1.719(13)
C(9)-B(40)	1.725(12)
C(9)-B(47)	1.735(13)
C(11)-B(45)	1.707(12)
C(11)-B(29)	1.723(12)
C(11)-B(28)	1.726(13)
C(11)-B(46)	1.730(13)
C(11)-B(36)	1.730(12)
C(13)-C(21)	1.524(10)
C(13)-B(50)	1.693(13)
C(13)-B(38)	1.719(13)
C(13)-B(35)	1.727(13)
C(13)-B(43)	1.734(12)
C(13)-B(53)	1.749(13)
C(14)-B(62)	1.686(13)
C(14)-B(54)	1.700(12)
C(14)-B(55)	1.71(2)
C(14)-B(66)	1.719(14)
C(14)-B(63)	1.729(14)
C(15)-C(16)	1.521(11)
C(15)-B(27)	1.724(13)
C(15)-B(37)	1.726(12)
C(15)-B(31)	1.729(13)
C(15)-B(34)	1.741(13)
C(15)-B(32)	1.741(12)
C(16)-C(51)	1.376(12)
C(16)-C(49)	1.380(12)
C(17)-C(25)	1.371(11)
C(17)-C(21)	1.384(11)
C(18)-C(19)	1.503(11)
C(18)-B(48)	1.700(13)
C(18)-B(56)	1.703(14)
C(18)-B(57)	1.711(14)
C(18)-B(60)	1.714(14)
C(18)-B(59)	1.735(13)
C(19)-C(58)	1.359(12)
C(19)-C(33)	1.403(11)
C(21)-C(23)	1.405(11)
C(22)-C(26)	1.352(12)
C(22)-C(33)	1.386(12)
C(23)-C(30)	1.396(11)
C(24)-C(25)	1.377(12)
C(24)-C(30)	1.380(12)
C(26)-C(64)	1.353(12)
B(27)-B(36)	1.75(2)
B(27)-B(28)	1.759(14)
B(27)-B(34)	1.770(14)
B(27)-B(37)	1.78(2)
B(28)-B(34)	1.746(14)
B(28)-B(36)	1.78(2)
B(28)-B(46)	1.795(14)
B(29)-B(37)	1.763(13)
B(29)-B(36)	1.78(2)
B(29)-B(31)	1.779(14)
B(29)-B(45)	1.802(13)

B(31)-B(32)	1.778(14)
B(31)-B(37)	1.787(14)
B(32)-B(45)	1.767(13)
B(32)-B(46)	1.782(14)
B(32)-B(34)	1.82(2)
B(34)-B(46)	1.762(14)
B(35)-B(40)	1.751(14)
B(35)-B(42)	1.773(14)
B(35)-B(43)	1.78(2)
B(35)-B(38)	1.81(2)
B(36)-B(37)	1.75(2)
B(38)-B(44)	1.752(13)
B(38)-B(50)	1.77(2)
B(38)-B(42)	1.785(14)
C(39)-C(61)	1.353(13)
C(39)-C(41)	1.353(13)
B(40)-B(43)	1.729(14)
B(40)-B(52)	1.77(2)
B(40)-B(42)	1.78(2)
C(41)-C(49)	1.399(12)
B(42)-C(45X)#1	1.04(13)
B(42)-B(44)	1.79(2)
B(43)-B(52)	1.763(14)
B(43)-B(53)	1.78(2)
B(44)-B(47)	1.78(2)
B(44)-B(50)	1.777(14)
B(45)-B(46)	1.80(2)
B(47)-B(53)	1.75(2)
B(47)-B(50)	1.778(14)
B(47)-B(52)	1.78(2)
B(48)-B(62)	1.75(2)
B(48)-B(56)	1.76(2)
B(48)-B(54)	1.76(2)
B(48)-B(57)	1.78(2)
B(50)-B(53)	1.78(2)
C(51)-C(61)	1.379(12)
B(52)-B(53)	1.75(2)
B(54)-B(62)	1.75(2)
B(54)-B(57)	1.76(2)
B(54)-B(55)	1.77(2)
B(55)-B(66)	1.74(2)
B(55)-B(59)	1.75(2)
B(55)-B(57)	1.76(2)
B(56)-B(63)	1.74(2)
B(56)-B(60)	1.76(2)
B(56)-B(62)	1.77(2)
B(57)-B(59)	1.76(2)
C(58)-C(64)	1.398(13)
B(59)-B(66)	1.73(2)
B(59)-B(60)	1.76(2)
B(60)-B(66)	1.74(2)
B(60)-B(63)	1.75(2)
B(62)-B(63)	1.79(2)
B(63)-B(66)	1.79(2)
C(3X)-C(46X)	.55(2)
C(3X)-C(3XB)	.76(2)
C(3X)-C(47X)#2	1.63(2)
C(3X)-C(47X)	1.88(3)
C(5X)-C(47X)	1.80(2)
C(6X)-C(41X)	1.51(3)
C(6X)-C(43X)	1.494(10)
C(7X)-C(47X)	1.65(5)
C(7X)-C(3XB)#2	1.87(5)
C(3XB)-C(46X)	1.00(2)
C(3XB)-C(47X)#2	1.50(2)
C(3XB)-C(47X)	1.77(2)
C(3XB)-C(7X)#2	1.87(5)
C(41X)-C(43X)	.93(3)
C(41X)-C(42X)	1.53(4)

C(42X)-C(43X)	1.12(3)
C(43X)-C(44X)	1.501(13)
C(47X)-C(47X)#2	1.42(4)
C(47X)-C(3XB)#2	1.50(2)
C(47X)-C(46X)	1.57(2)
C(47X)-C(3X)#2	1.63(2)
C(47X)-C(46X)#2	1.76(2)
C(46X)-C(47X)#2	1.76(2)
C(45X)-B(42)#1	1.04(13)
C(6)-N(2)-C(8)	113.7(7)
C(8)-N(4)-C(7)	113.5(6)
C(6)-N(5)-C(7)	113.4(7)
N(2)-C(6)-N(5)	127.2(7)
N(2)-C(6)-C(9)	117.0(7)
N(5)-C(6)-C(9)	115.7(7)
N(5)-C(7)-N(4)	126.3(7)
N(5)-C(7)-C(14)	118.9(7)
N(4)-C(7)-C(14)	114.7(7)
N(2)-C(8)-N(4)	125.8(7)
N(2)-C(8)-C(11)	117.2(7)
N(4)-C(8)-C(11)	117.0(6)
C(6)-C(9)-B(52)	117.8(7)
C(6)-C(9)-B(44)	117.6(7)
B(52)-C(9)-B(44)	113.5(6)
C(6)-C(9)-B(42)	119.3(7)
B(52)-C(9)-B(42)	114.3(7)
B(44)-C(9)-B(42)	62.8(6)
C(6)-C(9)-B(40)	120.6(7)
B(52)-C(9)-B(40)	62.3(6)
B(44)-C(9)-B(40)	113.3(6)
B(42)-C(9)-B(40)	62.2(6)
C(6)-C(9)-B(47)	116.3(7)
B(52)-C(9)-B(47)	62.3(6)
B(44)-C(9)-B(47)	62.0(6)
B(42)-C(9)-B(47)	114.1(7)
B(40)-C(9)-B(47)	113.3(7)
C(8)-C(11)-B(45)	118.5(6)
C(8)-C(11)-B(29)	117.9(7)
B(45)-C(11)-B(29)	63.4(5)
C(8)-C(11)-B(28)	117.1(7)
B(45)-C(11)-B(28)	114.8(6)
B(29)-C(11)-B(28)	114.1(6)
C(8)-C(11)-B(46)	117.8(7)
B(45)-C(11)-B(46)	63.2(6)
B(29)-C(11)-B(46)	115.5(7)
B(28)-C(11)-B(46)	62.6(6)
C(8)-C(11)-B(36)	117.6(6)
B(45)-C(11)-B(36)	114.3(7)
B(29)-C(11)-B(36)	62.0(5)
B(28)-C(11)-B(36)	62.1(6)
B(46)-C(11)-B(36)	114.0(7)
C(21)-C(13)-B(50)	119.0(7)
C(21)-C(13)-B(38)	119.1(7)
B(50)-C(13)-B(38)	62.4(6)
C(21)-C(13)-B(35)	117.5(7)
B(50)-C(13)-B(35)	114.8(6)
B(38)-C(13)-B(35)	63.5(6)
C(21)-C(13)-B(43)	117.7(7)
B(50)-C(13)-B(43)	113.2(6)
B(38)-C(13)-B(43)	113.8(6)
B(35)-C(13)-B(43)	61.9(6)
C(21)-C(13)-B(53)	118.6(7)
B(50)-C(13)-B(53)	62.2(6)
B(38)-C(13)-B(53)	113.3(7)
B(35)-C(13)-B(53)	113.0(6)
B(43)-C(13)-B(53)	61.4(6)
C(7)-C(14)-B(62)	119.1(7)
C(7)-C(14)-B(54)	119.2(7)

C(7)-C(14)-B(55)	117.6(7)
B(62)-C(14)-B(55)	114.1(7)
B(54)-C(14)-B(55)	62.7(7)
C(7)-C(14)-B(66)	117.7(7)
B(62)-C(14)-B(66)	114.0(8)
B(54)-C(14)-B(66)	112.8(7)
B(55)-C(14)-B(66)	61.2(7)
C(7)-C(14)-B(63)	118.2(7)
B(62)-C(14)-B(63)	63.1(7)
B(54)-C(14)-B(63)	113.9(7)
B(55)-C(14)-B(63)	113.4(8)
B(66)-C(14)-B(63)	62.4(9)
C(16)-C(15)-B(27)	118.5(7)
C(16)-C(15)-B(37)	117.6(7)
B(27)-C(15)-B(37)	62.1(6)
C(16)-C(15)-B(31)	118.0(7)
B(27)-C(15)-B(31)	113.3(7)
B(37)-C(15)-B(31)	62.3(5)
C(16)-C(15)-B(34)	119.9(7)
B(27)-C(15)-B(34)	61.4(5)
B(37)-C(15)-B(34)	112.6(7)
B(31)-C(15)-B(34)	113.2(6)
C(16)-C(15)-B(32)	119.3(6)
B(27)-C(15)-B(32)	113.4(7)
B(37)-C(15)-B(32)	113.0(6)
B(31)-C(15)-B(32)	61.6(5)
B(34)-C(15)-B(32)	62.9(5)
C(51)-C(16)-C(49)	118.2(8)
C(51)-C(16)-C(15)	121.1(8)
C(49)-C(16)-C(15)	120.7(8)
C(25)-C(17)-C(21)	121.7(8)
C(19)-C(18)-B(48)	119.3(7)
C(19)-C(18)-B(56)	119.9(7)
B(48)-C(18)-B(56)	62.3(7)
C(19)-C(18)-B(57)	118.4(7)
B(48)-C(18)-B(57)	63.0(7)
B(56)-C(18)-B(57)	113.3(7)
C(19)-C(18)-B(60)	119.0(7)
B(48)-C(18)-B(60)	113.0(8)
B(56)-C(18)-B(60)	61.9(8)
B(57)-C(18)-B(60)	111.8(7)
C(19)-C(18)-B(59)	117.8(7)
B(48)-C(18)-B(59)	113.2(7)
B(56)-C(18)-B(59)	112.4(7)
B(57)-C(18)-B(59)	61.3(7)
B(60)-C(18)-B(59)	61.2(8)
C(58)-C(19)-C(33)	116.1(8)
C(58)-C(19)-C(18)	122.8(8)
C(33)-C(19)-C(18)	121.1(8)
C(17)-C(21)-C(23)	117.6(7)
C(17)-C(21)-C(13)	122.3(7)
C(23)-C(21)-C(13)	120.0(8)
C(26)-C(22)-C(33)	122.0(9)
C(30)-C(23)-C(21)	120.6(9)
C(25)-C(24)-C(30)	119.6(8)
C(17)-C(25)-C(24)	120.6(9)
C(22)-C(26)-C(64)	118.4(8)
C(15)-B(27)-B(36)	105.1(7)
C(15)-B(27)-B(28)	105.6(6)
B(36)-B(27)-B(28)	61.1(6)
C(15)-B(27)-B(34)	59.8(5)
B(36)-B(27)-B(34)	108.3(7)
B(28)-B(27)-B(34)	59.3(6)
C(15)-B(27)-B(37)	59.0(5)
B(36)-B(27)-B(37)	59.3(6)
B(28)-B(27)-B(37)	108.5(7)
B(34)-B(27)-B(37)	108.7(7)
C(11)-B(28)-B(34)	104.5(7)
C(11)-B(28)-B(27)	104.5(7)

C(11)-B(28)-B(36)	59.1(5)
B(34)-B(28)-B(36)	107.9(8)
B(27)-B(28)-B(36)	59.2(6)
C(11)-B(28)-B(46)	58.8(5)
B(34)-B(28)-B(46)	59.7(5)
B(27)-B(28)-B(46)	108.3(7)
B(36)-B(28)-B(46)	108.4(7)
C(11)-B(29)-B(37)	104.4(7)
C(11)-B(29)-B(36)	59.2(5)
B(37)-B(29)-B(36)	59.1(5)
C(11)-B(29)-B(31)	103.7(7)
B(37)-B(29)-B(31)	60.6(5)
B(36)-B(29)-B(31)	107.4(7)
C(11)-B(29)-B(45)	57.9(5)
B(37)-B(29)-B(45)	107.9(7)
B(36)-B(29)-B(45)	107.5(7)
B(31)-B(29)-B(45)	59.5(5)
C(24)-C(30)-C(23)	119.9(9)
C(15)-B(31)-B(45)	105.2(7)
C(15)-B(31)-B(32)	59.5(5)
B(45)-B(31)-B(32)	59.6(5)
C(15)-B(31)-B(29)	104.9(7)
B(45)-B(31)-B(29)	60.9(5)
B(32)-B(31)-B(29)	108.6(7)
C(15)-B(31)-B(37)	58.8(5)
B(45)-B(31)-B(37)	107.9(7)
B(32)-B(31)-B(37)	108.4(7)
B(29)-B(31)-B(37)	59.3(5)
C(15)-B(32)-B(45)	105.2(6)
C(15)-B(32)-B(31)	58.8(5)
B(45)-B(32)-B(31)	60.2(5)
C(15)-B(32)-B(46)	104.7(7)
B(45)-B(32)-B(46)	61.0(6)
B(31)-B(32)-B(46)	108.9(7)
C(15)-B(32)-B(34)	58.5(5)
B(45)-B(32)-B(34)	107.2(7)
B(31)-B(32)-B(34)	107.3(7)
B(46)-B(32)-B(34)	58.6(6)
C(22)-C(33)-C(19)	120.4(9)
C(15)-B(34)-B(28)	105.4(7)
C(15)-B(34)-B(46)	105.5(7)
B(28)-B(34)-B(46)	61.5(6)
C(15)-B(34)-B(27)	58.8(5)
B(28)-B(34)-B(27)	60.0(6)
B(46)-B(34)-B(27)	109.3(7)
C(15)-B(34)-B(32)	58.5(5)
B(28)-B(34)-B(32)	108.5(7)
B(46)-B(34)-B(32)	59.7(6)
B(27)-B(34)-B(32)	107.6(7)
C(13)-B(35)-B(40)	104.4(7)
C(13)-B(35)-B(42)	104.4(7)
B(40)-B(35)-B(42)	60.7(6)
C(13)-B(35)-B(43)	59.2(5)
B(40)-B(35)-B(43)	58.6(6)
B(42)-B(35)-B(43)	107.2(7)
C(13)-B(35)-B(38)	58.0(5)
B(40)-B(35)-B(38)	107.7(7)
B(42)-B(35)-B(38)	59.7(5)
B(43)-B(35)-B(38)	107.1(7)
C(11)-B(36)-B(37)	104.7(7)
C(11)-B(36)-B(27)	104.7(7)
B(37)-B(36)-B(27)	61.2(6)
C(11)-B(36)-B(29)	58.8(5)
B(37)-B(36)-B(29)	60.0(6)
B(27)-B(36)-B(29)	109.1(7)
C(11)-B(36)-B(28)	58.8(5)
B(37)-B(36)-B(28)	108.8(7)
B(27)-B(36)-B(28)	59.7(6)
B(29)-B(36)-B(28)	108.7(7)

C(15)-B(37)-B(29)	105.8(6)
B(36)-B(37)-B(29)	60.9(6)
C(15)-B(37)-B(27)	58.9(5)
B(36)-B(37)-B(27)	59.5(6)
B(29)-B(37)-B(27)	108.4(7)
C(15)-B(37)-B(31)	58.9(5)
B(36)-B(37)-B(31)	108.5(7)
B(29)-B(37)-B(31)	60.2(5)
B(27)-B(37)-B(31)	108.0(7)
C(13)-B(38)-B(44)	104.8(7)
C(13)-B(38)-B(50)	58.1(6)
B(44)-B(38)-B(50)	60.7(6)
C(13)-B(38)-B(42)	104.2(7)
B(44)-B(38)-B(42)	60.8(5)
B(50)-B(38)-B(42)	108.7(7)
C(13)-B(38)-B(35)	58.4(5)
B(44)-B(38)-B(35)	107.6(7)
B(50)-B(38)-B(35)	107.1(8)
B(42)-B(38)-B(35)	59.0(5)
C(61)-C(39)-C(41)	118.5(10)
C(9)-B(40)-B(43)	105.2(7)
C(9)-B(40)-B(35)	105.6(7)
B(43)-B(40)-B(35)	61.6(6)
C(9)-B(40)-B(52)	58.2(5)
B(43)-B(40)-B(52)	60.4(6)
B(35)-B(40)-B(52)	109.7(7)
C(9)-B(40)-B(42)	58.7(6)
B(43)-B(40)-B(42)	109.2(7)
B(35)-B(40)-B(42)	60.3(6)
B(52)-B(40)-B(42)	107.9(8)
C(39)-C(41)-C(49)	121.3(9)
C(45X)#1-B(42)-C(9)	125(7)
C(45X)#1-B(42)-B(35)	122(7)
C(9)-B(42)-B(35)	104.9(8)
C(45X)#1-B(42)-B(40)	123(8)
C(9)-B(42)-B(40)	59.1(5)
B(35)-B(42)-B(40)	59.0(6)
C(45X)#1-B(42)-B(38)	122(8)
C(9)-B(42)-B(38)	104.3(7)
B(35)-B(42)-B(38)	61.3(6)
B(40)-B(42)-B(38)	107.7(8)
C(45X)#1-B(42)-B(44)	121(7)
C(9)-B(42)-B(44)	58.6(5)
B(35)-B(42)-B(44)	107.8(7)
B(40)-B(42)-B(44)	107.3(8)
B(38)-B(42)-B(44)	58.7(6)
B(40)-B(43)-C(13)	105.0(7)
B(40)-B(43)-B(52)	61.1(6)
C(13)-B(43)-B(52)	105.2(7)
B(40)-B(43)-B(53)	108.7(7)
C(13)-B(43)-B(53)	59.7(5)
B(52)-B(43)-B(53)	59.3(6)
B(40)-B(43)-B(35)	59.8(6)
C(13)-B(43)-B(35)	58.8(5)
B(52)-B(43)-B(35)	108.8(7)
B(53)-B(43)-B(35)	109.1(7)
C(9)-B(44)-B(38)	105.8(7)
C(9)-B(44)-B(47)	59.5(5)
B(38)-B(44)-B(47)	109.0(7)
C(9)-B(44)-B(50)	105.2(7)
B(38)-B(44)-B(50)	60.1(6)
B(47)-B(44)-B(50)	60.0(6)
C(9)-B(44)-B(42)	58.7(5)
B(38)-B(44)-B(42)	60.5(6)
B(47)-B(44)-B(42)	108.8(8)
B(50)-B(44)-B(42)	108.1(7)
C(11)-B(45)-B(32)	104.9(7)
C(11)-B(45)-B(31)	104.4(7)
B(32)-B(45)-B(31)	60.2(5)

B(32)-B(45)-B(46)	59.9(6)
B(31)-B(45)-B(46)	108.0(7)
C(11)-B(45)-B(29)	58.7(5)
B(32)-B(45)-B(29)	108.0(7)
B(31)-B(45)-B(29)	59.6(5)
B(46)-B(45)-B(29)	108.2(7)
C(11)-B(46)-B(34)	103.6(7)
C(11)-B(46)-B(32)	103.3(7)
B(34)-B(46)-B(32)	61.7(6)
C(11)-B(46)-B(28)	58.6(5)
B(34)-B(46)-B(28)	58.8(6)
B(32)-B(46)-B(28)	107.9(7)
C(11)-B(46)-B(45)	57.8(5)
B(34)-B(46)-B(45)	108.1(7)
B(32)-B(46)-B(45)	59.1(6)
B(28)-B(46)-B(45)	107.1(7)
C(9)-B(47)-B(53)	104.1(7)
C(9)-B(47)-B(44)	58.5(5)
B(53)-B(47)-B(44)	108.2(8)
C(9)-B(47)-B(50)	104.4(7)
B(53)-B(47)-B(50)	60.5(6)
B(44)-B(47)-B(50)	60.0(6)
C(9)-B(47)-B(52)	58.0(5)
B(53)-B(47)-B(52)	59.5(6)
B(44)-B(47)-B(52)	107.0(7)
B(50)-B(47)-B(52)	107.4(8)
C(18)-B(48)-B(62)	106.0(8)
C(18)-B(48)-B(56)	58.9(6)
B(62)-B(48)-B(56)	60.4(7)
C(18)-B(48)-B(54)	105.4(7)
B(62)-B(48)-B(54)	59.6(6)
B(56)-B(48)-B(54)	107.7(7)
C(18)-B(48)-B(57)	58.8(6)
B(62)-B(48)-B(57)	107.3(7)
B(56)-B(48)-B(57)	107.3(8)
B(54)-B(48)-B(57)	59.6(6)
C(16)-C(49)-C(41)	119.7(9)
C(13)-B(50)-B(38)	59.6(6)
C(13)-B(50)-B(47)	106.0(7)
B(38)-B(50)-B(47)	108.3(7)
C(13)-B(50)-B(44)	104.8(7)
B(38)-B(50)-B(44)	59.3(5)
B(47)-B(50)-B(44)	60.0(6)
C(13)-B(50)-B(53)	60.4(6)
B(38)-B(50)-B(53)	109.6(8)
B(47)-B(50)-B(53)	59.1(6)
B(44)-B(50)-B(53)	107.1(7)
C(16)-C(51)-C(61)	120.5(9)
C(9)-B(52)-B(53)	105.6(8)
C(9)-B(52)-B(43)	104.7(8)
B(53)-B(52)-B(43)	60.8(6)
C(9)-B(52)-B(40)	59.5(6)
B(53)-B(52)-B(40)	107.8(8)
B(43)-B(52)-B(40)	58.5(6)
C(9)-B(52)-B(47)	59.7(5)
B(53)-B(52)-B(47)	59.6(6)
B(43)-B(52)-B(47)	108.1(8)
B(40)-B(52)-B(47)	108.9(8)
C(13)-B(53)-B(52)	104.9(7)
C(13)-B(53)-B(47)	104.5(8)
B(52)-B(53)-B(47)	60.9(6)
C(13)-B(53)-B(43)	58.9(5)
B(52)-B(53)-B(43)	59.9(6)
B(47)-B(53)-B(43)	108.6(7)
C(13)-B(53)-B(50)	57.3(6)
B(52)-B(53)-B(50)	108.5(8)
B(47)-B(53)-B(50)	60.4(6)
B(43)-B(53)-B(50)	107.0(8)
C(14)-B(54)-B(62)	58.5(6)

B(62)-B(54)-B(57)	108.5(8)
C(14)-B(54)-B(48)	104.8(8)
B(62)-B(54)-B(48)	60.0(7)
B(57)-B(54)-B(48)	60.7(6)
C(14)-B(54)-B(55)	58.9(6)
B(62)-B(54)-B(55)	108.0(8)
B(57)-B(54)-B(55)	59.8(6)
B(48)-B(54)-B(55)	108.3(8)
C(14)-B(55)-B(66)	59.7(6)
C(14)-B(55)-B(59)	105.4(8)
B(66)-B(55)-B(59)	59.5(7)
C(14)-B(55)-B(57)	104.7(8)
B(66)-B(55)-B(57)	107.5(8)
B(59)-B(55)-B(57)	60.0(6)
C(14)-B(55)-B(54)	58.5(6)
B(66)-B(55)-B(54)	108.2(9)
B(59)-B(55)-B(54)	108.0(8)
B(57)-B(55)-B(54)	59.8(7)
C(18)-B(56)-B(63)	106.7(9)
C(18)-B(56)-B(48)	58.8(6)
B(63)-B(56)-B(48)	109.4(8)
C(18)-B(56)-B(60)	59.3(7)
B(63)-B(56)-B(60)	60.0(8)
B(48)-B(56)-B(60)	108.0(9)
C(18)-B(56)-B(62)	105.2(8)
B(63)-B(56)-B(62)	61.2(7)
B(48)-B(56)-B(62)	59.6(7)
B(60)-B(56)-B(62)	108.1(8)
C(18)-B(57)-B(59)	60.0(6)
C(18)-B(57)-B(55)	105.9(8)
B(59)-B(57)-B(55)	59.8(7)
C(18)-B(57)-B(54)	105.0(8)
B(59)-B(57)-B(54)	108.4(8)
B(55)-B(57)-B(54)	60.4(6)
C(18)-B(57)-B(48)	58.2(6)
B(59)-B(57)-B(48)	108.3(8)
B(55)-B(57)-B(48)	108.0(8)
B(54)-B(57)-B(48)	59.7(7)
C(19)-C(58)-C(64)	122.6(10)
C(18)-B(59)-B(66)	104.9(9)
C(18)-B(59)-B(55)	105.1(8)
B(66)-B(59)-B(55)	60.0(7)
C(18)-B(59)-B(60)	58.8(6)
B(66)-B(59)-B(60)	59.6(8)
B(55)-B(59)-B(60)	107.5(9)
C(18)-B(59)-B(57)	58.6(6)
B(66)-B(59)-B(57)	108.0(8)
B(55)-B(59)-B(57)	60.2(7)
B(60)-B(59)-B(57)	107.6(9)
C(18)-B(60)-B(66)	105.8(9)
C(18)-B(60)-B(63)	105.7(9)
B(66)-B(60)-B(63)	61.7(8)
C(18)-B(60)-B(59)	60.0(6)
B(66)-B(60)-B(59)	59.6(8)
B(63)-B(60)-B(59)	109.6(9)
C(18)-B(60)-B(56)	58.7(6)
B(66)-B(60)-B(56)	108.4(9)
B(63)-B(60)-B(56)	59.4(8)
B(59)-B(60)-B(56)	108.8(9)
C(39)-C(61)-C(51)	121.7(10)
C(14)-B(62)-B(54)	59.3(6)
C(14)-B(62)-B(48)	105.8(8)
B(54)-B(62)-B(48)	60.4(7)
C(14)-B(62)-B(56)	104.6(8)
B(54)-B(62)-B(56)	107.9(8)
B(48)-B(62)-B(56)	59.9(7)
C(14)-B(62)-B(63)	59.7(6)
B(54)-B(62)-B(63)	108.8(9)
B(48)-B(62)-B(63)	107.5(8)

C(14)-B(63)-B(56)	104.1(8)
C(14)-B(63)-B(60)	103.9(10)
B(56)-B(63)-B(60)	60.6(7)
C(14)-B(63)-B(66)	58.5(7)
B(56)-B(63)-B(66)	107.1(9)
B(60)-B(63)-B(66)	58.8(8)
C(14)-B(63)-B(62)	57.3(6)
B(56)-B(63)-B(62)	60.2(7)
B(60)-B(63)-B(62)	107.7(8)
B(66)-B(63)-B(62)	106.1(9)
C(26)-C(64)-C(58)	120.3(10)
C(14)-B(66)-B(60)	104.9(9)
C(14)-B(66)-B(59)	105.8(8)
B(60)-B(66)-B(59)	60.8(7)
C(14)-B(66)-B(55)	59.1(6)
B(60)-B(66)-B(55)	108.9(8)
B(59)-B(66)-B(55)	60.6(7)
C(14)-B(66)-B(63)	59.1(7)
B(60)-B(66)-B(63)	59.5(8)
B(59)-B(66)-B(63)	108.9(8)
B(55)-B(66)-B(63)	108.9(9)
C(46X)-C(3X)-C(3XB)	98(3)
C(46X)-C(3X)-C(47X)#2	94(3)
C(3XB)-C(3X)-C(47X)#2	66(2)
C(46X)-C(3X)-C(47X)	49(2)
C(3XB)-C(3X)-C(47X)	70(2)
C(47X)#2-C(3X)-C(47X)	47.2(12)
C(41X)-C(6X)-C(43X)	36.2(13)
C(47X)-C(7X)-C(3XB)#2	50(2)
C(3X)-C(3XB)-C(46X)	33(2)
C(3X)-C(3XB)-C(47X)#2	86(2)
C(46X)-C(3XB)-C(47X)#2	87.4(13)
C(3X)-C(3XB)-C(47X)	86(2)
C(46X)-C(3XB)-C(47X)	61.8(11)
C(47X)#2-C(3XB)-C(47X)	50.8(12)
C(3X)-C(3XB)-C(7X)#2	142(3)
C(46X)-C(3XB)-C(7X)#2	140(2)
C(47X)#2-C(3XB)-C(7X)#2	58(2)
C(47X)-C(3XB)-C(7X)#2	80(2)
C(43X)-C(41X)-C(6X)	71(2)
C(43X)-C(41X)-C(42X)	47(2)
C(6X)-C(41X)-C(42X)	117(3)
C(43X)-C(41X)-C(44X)	60(2)
C(6X)-C(41X)-C(44X)	131(2)
C(42X)-C(41X)-C(44X)	13.5(11)
C(43X)-C(42X)-C(41X)	38(2)
C(41X)-C(43X)-C(42X)	96(2)
C(41X)-C(43X)-C(44X)	87(2)
C(42X)-C(43X)-C(44X)	9(2)
C(41X)-C(43X)-C(6X)	73(2)
C(42X)-C(43X)-C(6X)	165(2)
C(44X)-C(43X)-C(6X)	159.1(7)
C(43X)-C(44X)-C(41X)	32.6(11)
C(47X)#2-C(47X)-C(3XB)#2	75(2)
C(47X)#2-C(47X)-C(46X)	72(2)
C(3XB)#2-C(47X)-C(46X)	133(2)
C(47X)#2-C(47X)-C(3X)#2	76(2)
C(3XB)#2-C(47X)-C(3X)#2	27.5(7)
C(46X)-C(47X)-C(3X)#2	147.2(14)
C(47X)#2-C(47X)-C(7X)	99(3)
C(3XB)#2-C(47X)-C(7X)	73(2)
C(46X)-C(47X)-C(7X)	82(2)
C(3X)#2-C(47X)-C(7X)	99(2)
C(47X)#2-C(47X)-C(46X)#2	57.9(14)
C(3XB)#2-C(47X)-C(46X)#2	34.4(7)
C(46X)-C(47X)-C(46X)#2	129.8(12)
C(3X)#2-C(47X)-C(46X)#2	18.2(7)
C(7X)-C(47X)-C(46X)#2	105(2)
C(47X)#2-C(47X)-C(3XB)	54.6(14)

C(46X)-C(47X)-C(3XB)	34.0(7)
C(3X)#2-C(47X)-C(3XB)	123.4(13)
C(7X)-C(47X)-C(3XB)	112(2)
C(46X)#2-C(47X)-C(3XB)	105.7(11)
C(47X)#2-C(47X)-C(5X)	102(2)
C(3XB)#2-C(47X)-C(5X)	76.7(11)
C(46X)-C(47X)-C(5X)	79.5(11)
C(3X)#2-C(47X)-C(5X)	103.3(13)
C(7X)-C(47X)-C(5X)	5(2)
C(46X)#2-C(47X)-C(5X)	109.4(12)
C(3XB)-C(47X)-C(5X)	111.3(12)
C(47X)#2-C(47X)-C(3X)	57.2(14)
C(3XB)#2-C(47X)-C(3X)	124.6(13)
C(46X)-C(47X)-C(3X)	15.3(7)
C(3X)#2-C(47X)-C(3X)	132.8(12)
C(7X)-C(47X)-C(3X)	89(2)
C(46X)#2-C(47X)-C(3X)	114.9(11)
C(3XB)-C(47X)-C(3X)	23.6(6)
C(5X)-C(47X)-C(3X)	87.6(11)
C(3X)-C(46X)-C(3XB)	49(2)
C(3X)-C(46X)-C(47X)	116(3)
C(3XB)-C(46X)-C(47X)	84.2(14)
C(3X)-C(46X)-C(47X)#2	68(2)
C(3XB)-C(46X)-C(47X)#2	58.2(11)
C(47X)-C(46X)-C(47X)#2	50.2(12)

Symmetry transformations used to generate equivalent atoms:
#1 -x+3,-y+1,-z+1 #2 -x+2,-y+2,-z+1

Appendix C

Conferences, Courses and Colloquia

Lecture Courses

"Organometallic Chemistry" - Prof. D. Parker, Prof. V.C. Gibson

"Polymer Synthesis" - Prof. W.J. Feast

"Introduction to NMR spectroscopy" - Dr. A. Kenwright

Conferences and Symposia

* poster, † paper

06/04/95	North East Universities Graduate Symposium, University of Durham
10-13/04/95	Royal Society of Chemistry AGM, Herriot-Watt University, Edinburgh *
11-13/09/95	Intraboron 15 Devonshire Hall, University of Leeds †
02/04/96	North East Universities Graduate Symposium University of Sunderland
14-18/07/96	Imeboron IX Ruprecht-Karls-Universität, Heidelberg, Germany *
18-20/09/96	Intraboron 16 Van Mildert College, University of Durham †
05/02/97	Scottish Dalton Meeting Edinburgh University
07/04/97	North East Universities Graduate Symposium University of Newcastle
01-03/09/97	Intraboron 17 Firbush Point Field Centre, University of Edinburgh †

University of Durham
Colloquia, Lectures and Seminars from Invited Speakers

Only lectures attended by the author are shown.

1994 - 1995 (August 1 - July 31)

October 5	Prof. N. L. Owen, Brigham Young University, Utah, USA Determining Molecular Structure - the INADEQUATE NMR way
October 19	Prof. N. Bartlett, University of California Some Aspects of Ag(II) and Ag(III) Chemistry
November 2	Dr P. G. Edwards, University of Wales, Cardiff The Manipulation of Electronic and Structural Diversity in Metal Complexes - New Ligands
November 9	Dr G. Hogarth, University College, London New Vistas in Metal-imido Chemistry
November 23	Dr J. M. J. Williams, University of Loughborough New Approaches to Asymmetric Catalysis
January 11	Prof. P. Parsons, University of Reading Applications of Tandem Reactions in Organic Synthesis
February 1	Dr T. Cosgrove, Bristol University Polymers do it at Interfaces
February 8	Dr D. O'Hare, Oxford University Synthesis and Solid-state Properties of Poly-, Oligo- and Multidecker Metallocenes
February 22	Prof. E. Schaumann, University of Clausthal Silicon- and Sulphur-mediated Ring-opening Reactions of Epoxide
March 1	Dr M. Rosseinsky, Oxford University Fullerene Intercalation Chemistry
April 26	Dr M. Schroder, University of Edinburgh

Redox-active Macrocyclic Complexes : Rings, Stacks and Liquid Crystals

May 4 — Prof. A. J. Kresge, University of Toronto
The Ingold Lecture Reactive Intermediates : Carboxylic-acid Enols and Other Unstable Species

<u>1995 - 1996 (August 1 - July 31)</u>

October 11 — Prof. P. Lugar, Frei Univ Berlin, FRG
Low Temperature Crystallography

October 13 — Prof. R. Schmutzler, Univ Braunschweig, FRG.
Calixarene-Phosphorus Chemistry: A New Dimension in Phosphorus Chemistry

October 25 — Dr.D.Martin Davies, University of Northumbria
Chemical reactions in organised systems.

November 15 — Dr Andrea Sella, UCL, London
Chemistry of Lanthanides with Polypyrazoylborate Ligands

November 17 — Prof. David Bergbreiter, Texas A&M, USA
Design of Smart Catalysts, Substrates and Surfaces from Simple Polymers

November 22 — Prof. I Soutar, Lancaster University
A Water of Glass? Luminescence Studies of Water-Soluble Polymers.

November 29 — Prof. Dennis Tuck, University of Windsor, Ontario, Canada
New Indium Coordination Chemistry

January 10 — Dr Bill Henderson, Waikato University, NZ
Electrospray Mass Spectrometry - a new sporting technique

February 12 — Dr Paul Pringle, University of Bristol
Catalytic Self-Replication of Phosphines on Platinum(O)

February 28 — Prof. E. W. Randall, Queen Mary & Westfield College
New Perspectives in NMR Imaging

1996 - 1997 (August 1 - July 31)

October 9	Professor G. Bowmaker, University Aukland, NZ Coordination and Materials Chemistry of the Group 11 and Group 12 Metals : Some Recent Vibrational and Solid State NMR Studies
October 29	Professor D. M. Knight, Department of Philosophy, University of Durham. The Purpose of Experiment - A Look at Davy and Faraday
November 6	Dr Melinda Duer, Chemistry Department, Cambridge Solid-state NMR Studies of Organic Solid to Liquid-crystalline Phase Transitions
November 13	Dr G. Resnati, Milan Perfluorinated Oxaziridines: Mild Yet Powerful Oxidising Agents
November 18	Professor G. A. Olah, University of Southern California, USA Crossing Conventional Lines in my Chemistry of the Elements
November 19	Professor R. E. Grigg, University of Leeds Assembly of Complex Molecules by Palladium-Catalysed Queueing Processes
November 27	Dr Richard Templer, Imperial College, London Molecular Tubes and Sponges
December 3	Professor D. Phillips, Imperial College, London "A Little Light Relief" -
January 16	Dr Sally Brooker, University of Otago, NZ Macrocycles: Exciting yet Controlled Thiolate Coordination Chemistry
January 21	Mr D. Rudge, Zeneca Pharmaceuticals High Speed Automation of Chemical Reactions
January 22	Dr Neil Cooley, BP Chemicals, Sunbury Synthesis and Properties of Alternating Polyketones

February 4 — Dr A. J. Banister, University of Durham
From Runways to Non-metallic Metals - A New Chemistry Based on Sulphur

February 18 — Professor Sir James Black, Foundation/King's College London
My Dialogues with Medicinal Chemists

February 26 — Dr Tony Ryan, UMIST
Making Hairpins from Rings and Chains

March 4 — Professor C. W. Rees, Imperial College
Some Very Heterocyclic Chemistry

March 11 — Dr A. D. Taylor, ISIS Facility, Rutherford Appleton Laboratory
Expanding the Frontiers of Neutron Scattering